GEOLOGICAL SURVEY OF CANADA
COMMISSION GÉOLOGIQUE DU CANADA

CURRENT RESEARCH 1994-D

EASTERN CANADA AND NATIONAL AND GENERAL PROGRAMS

RECHERCHES EN COURS 1994-D

EST DU CANADA ET PROGRAMMES NATIONAUX ET GÉNÉRAUX

1994

Natural Resources Canada | Ressources naturelles Canada

Canada

NOTICE TO LIBRARIANS AND INDEXERS

The Geological Survey's Current Research series contains many reports comparable in scope and subject matter to those appearing in scientific journals and other serials. Most contributions to Current Research include an abstract and bibliographic citation. It is hoped that these will assist you in cataloguing and indexing these reports and that this will result in a still wider dissemination of the results of the Geological Survey's research activities.

AVIS AUX BIBLIOTHÉCAIRES ET PRÉPARATEURS D'INDEX

La série Recherches en cours de la Commission géologique contient plusieurs rapports dont la portée et la nature sont comparables à ceux qui paraissent dans les revues scientifiques et autres périodiques. La plupart des articles publiés dans Recherches en cours sont accompagnés d'un résumé et d'une bibliographie, ce qui vous permettra, on l'espère, de cataloguer et d'indexer ces rapports, d'où une meilleure diffusion des résultats de recherche de la Commission géologique.

GEOLOGICAL SURVEY OF CANADA
COMMISSION GÉOLOGIQUE DU CANADA

CURRENT RESEARCH 1994-D

EASTERN CANADA AND NATIONAL AND GENERAL PROGRAMS

RECHERCHES EN COURS 1994-D

EST DU CANADA ET PROGRAMMES NATIONAUX ET GÉNÉRAUX

1994

Available in Canada through
authorized bookstore agents and other bookstores

or by mail from

Canada Communication Group - Publishing
Ottawa, Canada K1A 0S9

and from

Geological Survey of Canada offices:

601 Booth Street
Ottawa, Canada K1A 0E8

3303-33rd Street N.W.,
Calgary, Alberta T2L 2A7

100 West Pender Street
Vancouver, B.C. V6B 1R8

A deposit copy of this publication is also available for reference
in public libraries across Canada

Cat. No. M44-1994/4
ISBN 0-660-58988-5

Price subject to change without notice

Cover description

Bioherm of the Middle Windsor Group (Early Carboniferous), Cape Dauphin section, Cape Breton Island. See paper by Lavoie, p. 79-88. (photo by D. Lavoie. GSC 1993-305C)

Description de la photo couverture

Bioherme dans la partie intermédiaire du Groupe de Windsor (Carbonifère précoce), coupe du cap Dauphin, île du Cap-Breton. Voir l'article de Lavoie, p. 79-88. (photo de D. Lavoie, GSC 1993-305C)

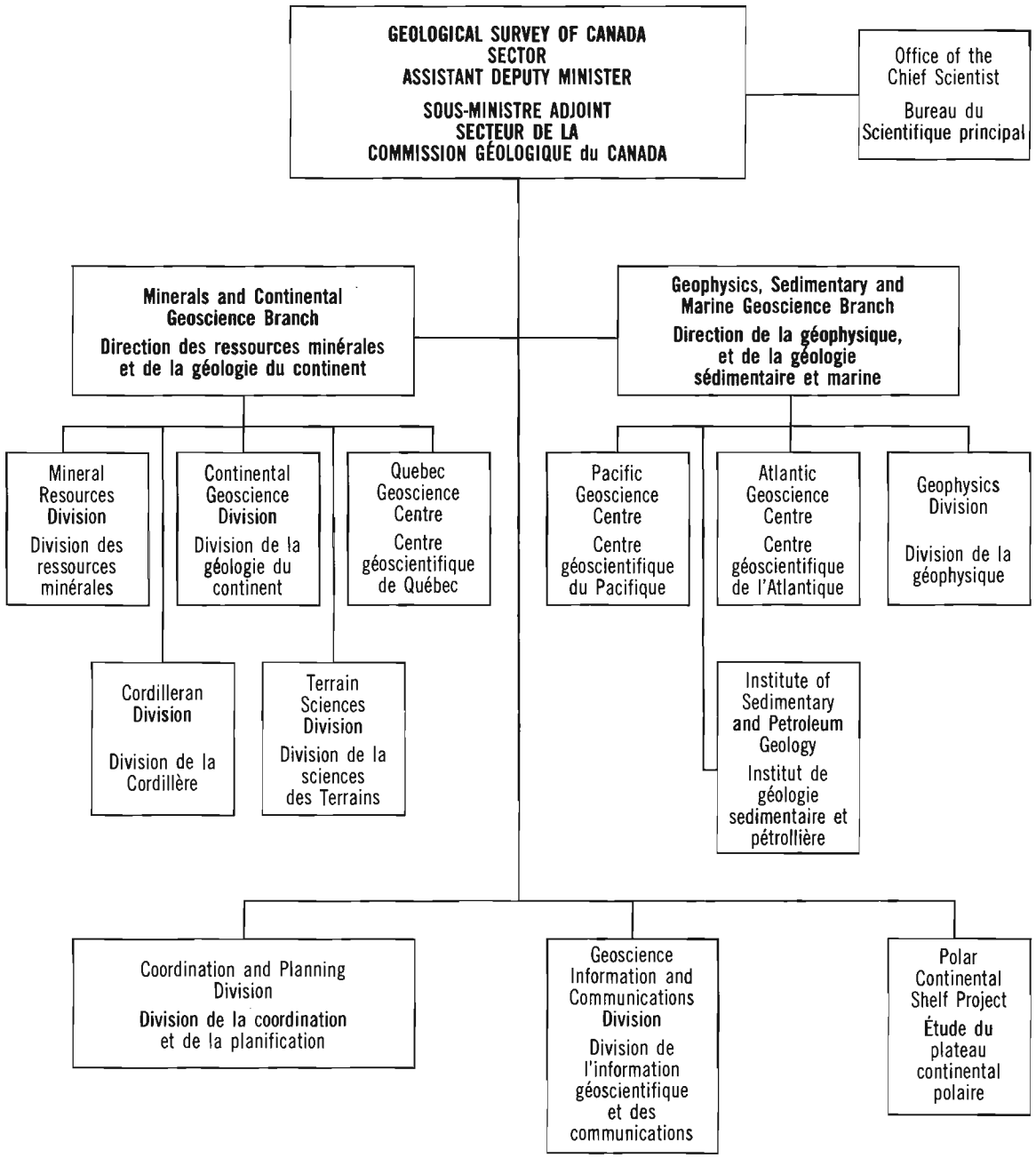
GEOLOGICAL SURVEY OF CANADA
SECTOR
ASSISTANT DEPUTY MINISTER
SOUS-MINISTRE ADJOINT
SECTEUR DE LA
COMMISSION GÉOLOGIQUE du CANADA
Office of the Chief Scientist
Bureau du Scientifique principal
Minerals and Continental Geoscience Branch
Direction des ressources minérales et de la géologie du continent
Geophysics, Sedimentary and Marine Geoscience Branch
Direction de la géophysique, et de la géologie sédimentaire et marine
Mineral Resources Division
Division des ressources minérales
Continental Geoscience Division
Division de la géologie du continent
Quebec Geoscience Centre
Centre géoscientifique de Québec
Pacific Geoscience Centre
Centre géoscientifique du Pacifique
Atlantic Geoscience Centre
Centre géoscientifique de l'Atlantique
Geophysics Division
Division de la géophysique
Cordilleran Division
Division de la Cordillère
Terrain Sciences Division
Division de la sciences des Terrains
Institute of Sedimentary and Petroleum Geology
Institut de géologie sedimentaire et pétrollière
Coordination and Planning Division
Division de la coordination et de la planification
Geoscience Information and Communications Division
Division de l'information géoscientifique et des communications
Polar Continental Shelf Project
Étude du plateau continental polaire

Separates

A limited number of separates of the papers that appear in this volume are available by direct request to the individual authors. The addresses of the Geological Survey of Canada offices follow:

601 Booth Street
OTTAWA, Ontario
K1A 0E8
(FAX: 613-996-9990)

Institute of Sedimentary and Petroleum Geology
3303-33rd Street N.W.
CALGARY, Alberta
T2L 2A7
(FAX: 403-292-5377)

Cordilleran Division
100 West Pender Street
VANCOUVER, B.C.
V6B 1R8
(FAX: 604-666-1124)

Pacific Geoscience Centre
P.O. Box 6000
9860 Saanich Road
SIDNEY, B.C.
V8L 4B2
(Fax: 604-363-6565)

Atlantic Geoscience Centre
Bedford Institute of Oceanography
P.O. Box 1006
DARTMOUTH, N.S.
B2Y 4A2
(FAX: 902-426-2256)

Québec Geoscience Centre
2700, rue Einstein
C.P. 7500
Ste-Foy (Québec)
G1V 4C7
(FAX: 418-654-2615)

When no location accompanies an author's name in the title of a paper, the Ottawa address should be used.

Tirés à part

On peut obtenir un nombre limité de «tirés à part» des articles qui paraissent dans cette publication en s'adressant directement à chaque auteur. Les adresses des différents bureaux de la Commission géologique du Canada sont les suivantes:

601, rue Booth
OTTAWA, Ontario
K1A 0E8
(facsimilé : 613-996-9990)

Institut de géologie sédimentaire et pétrolière
3303-33rd St. N.W.,
CALGARY, Alberta
T2L 2A7
(facsimilé : 403-292-5377)

Division de la Cordillère
100 West Pender Street
VANCOUVER, British Columbia
V6B 1R8
(facsimilé : 604-666-1124)

Centre géoscientifique du Pacifique
P.O. Box 6000
9860 Saanich Road
SIDNEY, British Columbia
V8L 4B2
(facsimilé : 604-363-6565)

Centre géoscientifique de l'Atlantique
Institut océanographique Bedford
B.P. 1006
DARTMOUTH, Nova Scotia
B2Y 4A2
(facsimilé : 902-426-2256)

Centre géoscientifique de Québec
2700, rue Einstein
C.P. 7500
Ste-Foy (Québec)
G1V 4C7
(facsimilé : 418-654-2615)

Lorsque l'adresse de l'auteur ne figure pas sous le titre d'un document, on doit alors utiliser l'adresse d'Ottawa.

Contents

Cenozoic foraminiferal assemblages of the Hibernia area, Grand Banks of Newfoundland, and paleoecological implications

F.C. Thomas
Atlantic Geoscience Centre, Dartmouth

Thomas, F.C., 1994: Cenozoic foraminiferal assemblages of the Hibernia area, Grand Banks of Newfoundland, and paleoecological implications; in Current Research 1994-D; Geological Survey of Canada, p. 1-12.

Abstract: Cuttings samples from Cenozoic sections of six Hibernia field wells (Hibernia B-08, G-55, I-46, J-34, K-18, and O-35) have been analyzed for shelly microfossil content. The results indicate the presence of benthic foraminiferal zones representing Eocene to Miocene sedimentation in most wells, and Paleocene levels in deeper sites.

During the Eocene, all sites experienced a change in benthic foraminiferal faunas from a primarily agglutinated assemblage to a calcareous one. At most sites, the latter continued with some alteration through the Oligocene. Miocene assemblages show inter-site variations, probably related to environmental differences.

Certain regional events such as an abundance of calcareous "balls", peaks of pyritized diatoms, and widespread microfossil pyritization are correlatable within these wells and to certain other sites in the Jeanne d'Arc Basin.

The relative thicknesses of series as defined by benthic foraminiferal zones tend to suggest constant sedimentation rates through the Tertiary intervals of these wells.

Résumé : Dans des échantillons de déblais de forage, recueillis dans les successions cénozoïques de six puits du champ pétrolifère d'Hibernia (Hibernia B-08, G-55,I-46, J-34, K-18 et O-35), on a analysé les microfossiles à coquille présents. Les résultats indiquent l'existence de zones de foraminifères benthiques qui représentent la sédimentation de l'Éocène au Miocène dans la plupart des puits, et des niveaux du Paléocène dans les sites plus profonds.

À l'Éocène, tous les sites ont connu une modification des faunes de foraminifères benthiques, dans lesquelles une association de foraminifères principalement constituée d'individus à test agglutiné a fait place à une association de foraminifères à test calcaire. Dans la plupart des sites, celle-ci a continué à exister avec quelques modifications tout au long de l'Oligocène. Les associations du Miocène montrent des variations d'un site à l'autre, probablement dues à des différences environnementales.

Certains phénomènes régionaux tels que l'abondance de «boulets» calcareux, les maximums d'abondance de diatomées pyritisées, et la pyritisation étendue des microfossiles, se laissent corréler dans ces puits et avec certains autres sites du bassin de Jeanne d'Arc.

Les épaisseurs relatives des séries telles que définies en fonction des zones de foraminifères benthiques semblent indiquer que les vitesses de sédimentation ont été uniformes tout au long des intervalles du Tertiaire étudiés dans ces puits.

INTRODUCTION

The giant Hibernia oil field, discovered in 1979, is located in the western central portion of the Jeanne d'Arc Basin in the northeastern part of the Grand Banks of Newfoundland. The Jeanne d'Arc is a failed rift basin having its origins in early Mesozoic tectonic events (McAlpine, 1990).

The economic possibilities of the Hibernia field have driven an array of geological/geophysical studies of the region, centred mostly on the Cretaceous oil-bearing strata. Recent work on modelling the Mesozoic sedimentation of the whole Basin (Williamson, 1992; Williamson et al., 1993) has, however, demanded better constraints on the timing and relative rates of sedimentary input during the Cenozoic, as they have impacted the basin's later hydrocarbon generation, maturation, and migration history. Results reported here represent preliminary findings and have yet to be put into a context that includes regional seismic and sequence correlations to be reported later.

The Hibernia field, with its relatively closely spaced wells (Fig. 1), provides in its foraminiferal assemblages a detailed view of the Cenozoic sedimentary/paleoceanographic history of the immediate area, which, in time, may prove to be applicable to the rest of the Basin. Table 1 provides names, locations, and some technical data on the wells used in this study. All six are officially known as Mobil et al. Hibernia ..., but for purposes of this study will be referred to by their alphanumeric suffixes. The numerous seismic lines run in the Jeanne d'Arc Basin reveal nearly flat-lying, laterally continuous reflectors with a slight eastward dip in the Cenozoic rocks. These attest to the tectonically quiescent and stable history of the region since the end of the Cretaceous (McAlpine, 1990).

Coeval foraminiferal assemblages from six wells in the Hibernia field show variations in content, diversity, and even diagenetic effects such as pyritization, all of which may yield clues to the changing benthic environments since the end of the Mesozoic.

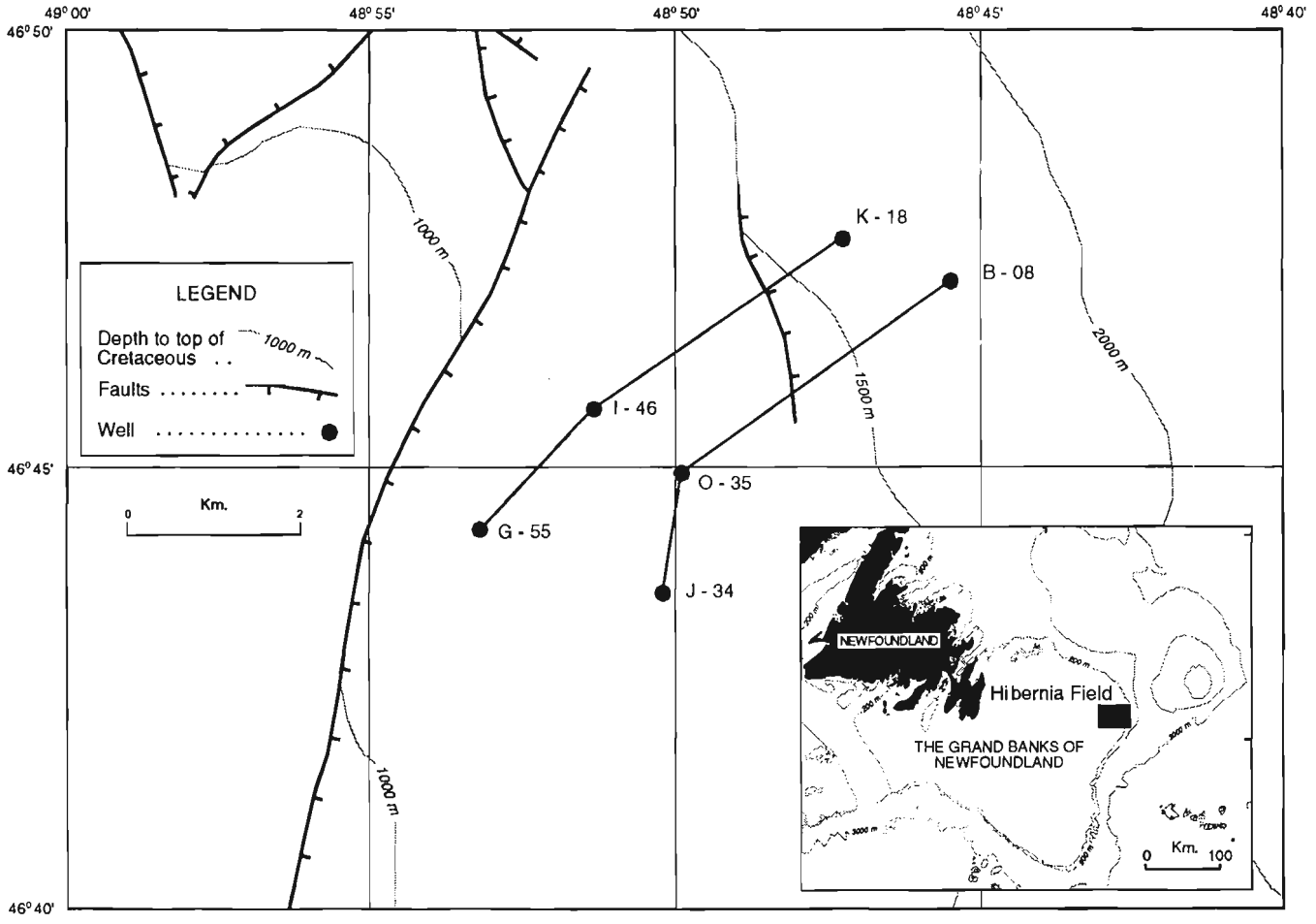

Figure 1. *Location map of Grand Banks area showing Hibernia Field, locations of six Hibernia wells, and two transects. Contours (in metres) of present depth to top of Cretaceous are also indicated.*

Table 1. Hibernia field wells, locations, datums (Rotary table height) and water depths, both in metres

Well	Latitude (N)	Longitude (W)	Datum	Water Depth
B-08	46.47'06.36"	48.45'29.87"	25.9	82.9
G-55	46.44'17.02"	48.53'10.75"	29.7	76.5
I-46	46.45'40.74"	48.51'17.20"	33.2	78.7
J-34	46.43'33.84"	48.50'13.00"	29.0	78.3
K-18	46.47'34.69"	48.47'17.05"	29.7	78.3
O-35	46.44'54.92"	48.49'53.74"	24.4	79.6

Technical data on these and other wells in the Jeanne d'Arc Basin are provided in Canada-Newfoundland Offshore Petroleum Board (1990).

MATERIALS AND METHODS

Suites of ditch cuttings samples from each of the six wells were the raw material for this study. These consisted of composite samples usually derived from a ten-metre interval. Usually, 20 or 30 m (occasionally 50 m) gaps separated adjacent samples, but in the bottom portion of B-08, these gaps were filled with supplementary samples. A list of the samples used is provided in Table 2.

Ditch cuttings sampling started in all wells just below the bottom of the surface casing, and this level varied among the wells, in some cases entirely missing the Upper Miocene strata.

The samples consisted mostly of mudstones, siltstones, and shales, with small amounts of sandstone in some locations. All were disaggregated using the "Industrial Soap" method described by Thomas and Murney (1985). Similar quantities of material >125 μm were then hand-picked for shelly microfossils. By keeping the amounts of picked material reasonably similar, comparisons of sample-to-sample faunal richness were more realistic. The resulting slides are thus a semi-quantitative representation of the microfossil assemblages in the samples. A list of all microfossils formally or informally designated, noted in any of the wells is provided in the Appendix. They total some 200 species of Cenozoic foraminifera and 20 non-foraminiferal taxa.

As usual with cuttings samples, downhole contamination by younger fossils (caving) renders only stratigraphic tops or last occurrences useful for age determination. Long-ranging species persisting downhole through long sections were regarded as in place in lower levels only if their styles of preservation (colour, texture) continued to match that of the in situ fauna. In the same way, reworked specimens of these or other forms can usually be identified by staining and/or higher grades of abrasional wear on the tests.

Age determinations for these analyses are based on the quantitatively-derived zonation of Gradstein and Agterberg (1982). Their document, based on suites of mostly cuttings samples from nearly two dozen wells in the eastern Canadian offshore area, incorporates benthic and planktic foraminifera as well as several non-protozoan taxa which occur regularly in the region. This is particularly useful in the present study, since the planktic foraminifera used in the more traditional zonal schemes are found only sporadically in the Cenozoic sections of the Hibernia wells.

Results – Cenozoic foraminiferal assemblages of the Hibernia area

Micropaleontological analysis and inter-well comparisons of coeval sections of the six wells has provided, within the constraints of sampling, an overview of the types of microfaunal assemblages extant in the area from the Paleocene to the Late Miocene. For purposes of these comparisons, the six wells can be viewed as two roughly parallel three-well transects (Fig. 1) trending northeastwards from near the high forming the western perimeter of the basin (Bonavista Platform) towards its depocenter some 60 km away. Also shown in Figure 1 are depth contours to the present top of Cretaceous rock (T. Edwards, Norcen, pers. comm., 1992) reflecting a gradual increase in depth towards the northeast end of the transects.

Furthermore, these transect comparisons aid in extrapolating probable ages of sections in some wells which were otherwise too poor in in situ fauna to confidently assign ages.

AREAL DISTRIBUTION OF BENTHIC FAUNAS

Paleocene

Good diagnostic Paleocene foraminifera are found in only one site, B-08. There, a few specimens of *Morozovella pseudobulloides* and *Gavelinella beccariiformis* are found in otherwise impoverished faunas. In K-18 there occurs a single

Table 2. List of Hibernia wells and samples used. Depths are in metres.

B-08	G-55	I-46	J-34	K-18	O-35
540-550	540-550	490-500	430-440	920-930	520-530
570-580	570-580	530-540	470-480	950-960	550-560
600-610	600-610	570-580	510-520	980-990	580-590
630-640	650-660	610-620	550-560	1005-1015	610-620
660-670	680-690	650-660	590-600	1035-1045	640-650
690-700	710-720	690-700	630-640	1065-1075	670-680
720-730	740-750	730-740	670-680	1095-1105	700-710
750-760	770-780	770-780	710-720	1125-1135	730-740
780-790	800-810	810-820	750-760	1155-1165	760-770
810-820	830-840	850-860	790-800	1185-1195	790-800
840-850	860-870	890-900	830-840	1215-1225	820-830
870-880	890-900	930-940	870-880	1245-1255	850-860
900-910	990-1000	970-980	910-920	1275-1285	880-890
930-940	1020-1030	1010-1020	950-960	1305-1315	910-920
960-970	1050-1060	1050-1060	990-1000	1335-1345	940-950
990-1000	1085-1090	1090-1100	1035-1045	1365-1375	970-980
1020-1030	1115-1120	1130-1140	1075-1085	1395-1405	1000-1010
1045-1055	1140-1150	1170-1180	1115-1125	1425-1435	1030-1040
1105-1115	1170-1180	1200-1210	1155-1165	1455-1465	1060-1070
1135-1145	1220-1230	1240-1250	1190-1200	1485-1495	1090-1100
1165-1175	1250-1260	1280-1290	1230-1240	1515-1525	1120-1130
1195-1205	1280-1290	1320-1330	1270-1280	1545-1555	1150-1160
1225-1235	1310-1320	1360-1370	1310-1320	1575-1585	1180-1190
1255-1265	1370-1380	1400-1410	1350-1360	1605-1615	1210-1220
1285-1295		1440-1450	1390-1400	1635-1645	1235-1245
1315-1325			1430-1440		1265-1275
1345-1355			1470-1480		1295-1305

poorly preserved gavelinellid probably representing the Paleocene *Gavelinella beccariiformis* and a few specimens of *Spiroplectammina navarroana*, a form often associated with Paleocene and Early Eocene assemblages in some other northern East Coast wells (Gradstein and Kaminski, 1989). The two middle wells in the transects (I-46 and O-35), contain intervals of indeterminate age between clearly Lower Eocene and Cretaceous levels. O-35 contains small numbers of reworked Late Cretaceous foraminifera in this apocryphal interval. A similar situation occurs in the two most updip wells, G-55 and J-34, with Early Eocene faunas separated from clearly Late Cretaceous material by a few samples containing mostly a confusing mixture of (?) reworked Cretaceous fossils and caved younger taxa. Again, there may have been Paleocene deposition, but these impoverished assemblages contain no clear indicators for this epoch.

Eocene

The Early Eocene (Gradstein and Agterberg's so-called Megaspore sp.1 Zone) is recognized in all six wells by an abundance of rough-surfaced, discoid to spheroidal "balls" of unknown origin. These are approximately 200 μ m in diameter, slightly effervescent in 10% HCl, and make up the largest part of the assemblages in G-55, I-46, J-34, and K-18, sections otherwise very poor in microfossils. In 0-35 and B-08 a few Early Eocene benthic markers such as *Bulimina midwayensis* and *Nodosaria* cf. *pozoensis* provide firm age tie-points for this somewhat enigmatic benthic event.

The lower Middle Eocene, corresponding to Gradstein and Agterberg's *Spiroplectammina spectabilis* Zone, is easily recognized in all wells by relatively large numbers of the nominate taxon. Also common are *Haplophragmoides walteri*,

B-08	G-55	I-46	J-34	K-18	O-35
1375-1385					1325-1335
1405-1415					1355-1365
1435-1445					1385-1395
1465-1475					1415-1425
1495-1505					1445-1455
1525-1535					1475-1485
1565-1575					1505-1515
1595-1605					1535-1545
1610					1570-1580
1620					1600-1610
1625-1635					1630-1640
1630					1660-1670
1640					1690-1700
1650					1720-1730
1655-1665					
1660					
1670					
1680					
1685-1695					
1690					
1700					
1710					
1715-1725					
1720					
1730					
1740					
1745-1755					

Haplophragmoides kirki, and unidentified *Recurvoides* spp. The assemblage is always largely agglutinated, and sometimes exclusively so. In upper levels of this zone, numbers of large, robust taxa such as *Cyclammina* spp., *Bathysiphon discreta* gr., and *Ammodiscus latus* are also commonly encountered, but these probably represent caved material from overlying strata. Some of the more widespread calcareous benthics occurring in this zone are *Cibicidoides* aff. *subspiratus, Cibicidoides tuxpamensis, Eponides plummerae, Stilostomella* cf. *aculeata*, and *Stilostomella midwayensis*. In K-18 and B-08 (again, the more basinward sites), planktics are somewhat more common, though never constituting more than a small proportion of the total assemblage.

Overlying this in all sites is a section encompassing the entire Upper Eocene and upper half of the Middle Eocene termed by Gradstein and Agterberg the *Cyclammina amplectens* – Pteropod sp.1 Zone. In the near absence of planktic foraminifera in these sites, it is not possible to further subdivide this interval. While this zone is easily recognizable in all wells, certain events within this interval are restricted to some sites.

All six wells contain mostly agglutinated assemblages in the lower portions of this zone, although the relative richness of the fauna at each site varies widely. The most common genera are *Cyclammina* (including *Reticulophragmium* spp.), *Haplophragmoides*, and *Recurvoides*. Unknown proportions of these groups may in fact be caved from higher levels within the zone, where these species tend to dominate richer associations. In the deeper sites, B-08 and K-18, relatively large numbers of the pyritized frustules of the diatom genus *Coscinodiscus* spp. appear in these presumably upper Middle Eocene layers.

Pyritization of internal casts of foraminifera, and pyrite cylinders are seen in most sites to some extent near the middle of this zonal section. Oddly, the most northern well, K-18, contains the least replacement pyrite (except for diatom frustules), and the specimens of the nominate taxa Pteropod sp.1 (= *Limacina canadensis*) are in their original aragonitic form, rather than as the pyritized internal casts usually seen.

The uppermost part of this zone, representing probably latest Eocene deposition, contains a mixed foraminiferal suite composed of mostly calcareous species, with greatest abundances and diversities in the deeper sites, and correspondingly poorer assemblages at the shallower ones. Common species

in this zone include *Ammodiscus latus, Bathysiphon* cf. *discreta, Bulimina cooperensis, Cibicidoides eocaenus, Cibicidoides* cf. *laurisae, Cyclammina placenta*, and *Lenticulina* cf. *whitei*, to name a few. In terms of sheer numbers, the various *Cibicidoides* forms are probably the single most common genus.

Oligocene

Gradstein and Agterberg's (1982) *Turrilina alsatica* Zone is recognizable by the presence of at least small numbers of the nominate species in five of the wells. No single genus seems to strongly predominate at any site, although some samples contain numerous large Lenticulinids. Other widespread genera are *Biloculina, Ceratobulimina, Cibicidoides, Cornuspira, Gyroidina, Hoeglundina, Melonis, Nodosaria, Oridorsalis, Pullenia, Quinqueloculina, Stilostomella, Uvigerina*, and *Vaginulinopsis*. Small agglutinated components in many samples include representatives of *Bathysiphon, Eggerella*, and *Karreriella*. Large numbers of *Spiroplectammina carinata* are presumably caved from overlying Miocene levels. Planktic foraminifera are virtually absent in all wells.

I-46 contains a section of indeterminate age between identifiable Miocene and Eocene intervals which could represent, at least in part, Oligocene deposition. The generally poor assemblages feature several species correlatable to, though not exclusive to, Oligocene sections in the other sites. Interestingly, a few reworked Paleocene and Eocene taxa are present suggesting an updip erosional source, along with some pyritized tubes and casts. These latter also appear in small numbers in B-08, the well furthest from I-46, suggesting more localized events than the mid-Eocene pyritization event.

Miocene

The Early/Middle Miocene *Spiroplectammina carinata* Zone of Gradstein and Agterberg (1982) is clearly delineated in all wells by large numbers of the nominate form. Also common are Lenticulinids representing several species, *Cibicidoides, Quinqueloculina*, and *Hoeglundina* in the deeper sites, among others, almost all calcareous except for *Spiroplectammina carinata*. The single most remarkable Miocene event is an apparently short-lived abundance of the so-called *Uvigerina* cf. *miozea-nuttalli*, described informally by Thomas (1988). This appears in only one or two samples in four of the six wells; B-08, I-46, J-34, and O-35. These include one of the two "deep" sites, one "shallow", and both intermediate ones.

The Late Miocene *Asterigerina gurichi* Zone is represented by impoverished faunas containing a few specimens of the nominate taxon along with occasional specimens of *Cibicides, Lenticulina*, and a few other forms. This assemblage is only encountered in the three wells of the eastern transect: B-08, J-34, and O-35.

DISCUSSION

Benthic events and assemblages

In spite of the attendant downhole "slurring" of the fossil record due to sampling inaccuracies inherent in the drilling process, a number of discrete benthic events and gradual changes in assemblages can be documented in the Cenozoic history of the Hibernia area.

The presence of a Paleocene interval in B-08, and probably K-18, is probably related to the fact that these are the two easternmost (basinward) sites, presumably with the deepest water during this epoch, and therefore with the best chance of providing a suitable habitat for our Paleocene markers, which are either deep-water benthics or planktic forms. The two "intermediate" wells in the transects, I-46 and O-35, and the two "shallowest" sites, G-55 and J-34, all contain intervals of indeterminate age which could contain levels of Paleocene deposition, but in situ microfossil assemblages are very poor, containing no diagnostic markers. This is itself anomalous, since under normal hydrographic and sedimentary conditions, a better-developed Paleocene fauna should have been established at even the "shallower" sites, given the probably bathyal water depth at the time. The small numbers of presumably reworked Cretaceous microfossils in G-55 and J-34 suggest an updip source of eroding Mesozoic clastics in the area at the time.

The enigmatic "balls" so prevalent in the basal Eocene of the Hibernia area and some other sites in the Jeanne d'Arc Basin (F.M. Gradstein, pers. comm., 1991), are the single most distinguishing feature of this interval. In bright light some appear to possess an internal structure reminiscent of certain radiolarians, including some Paleocene species recently documented from DSDP Site 384, some 700 km to the south (Nishimura, 1992). At other times, they have been informally referred to as "algal balls", but their actual provenance has never been determined and may, indeed, be mineral rather than organic. Their reaction to HCl suggests at least some calcareous content, which could support either theory.

The peak in pyritized diatom abundance seen in the deeper sites B-08 and K-18 in the lower part of the *Cyclammina amplectens* – Pteropod sp.1 zone correlates to similar peaks in Middle and Lower Eocene levels in other Grand Banks and Labrador Sea sites documented elsewhere (Thomas and Gradstein, 1981).

Pyritization of internal casts of foraminiferal tests and pyrite cylinders are present in most sites near the middle of the Middle/Late Eocene zone (the Middle/Late Eocene boundary?) and may reflect either an oceanographic event such as a sudden influx or generation of corrosive bottom waters or a diagenetic process. Where this occurs, normally preserved calcareous foraminifera and even agglutinated taxa are much less common. It is possible that a cleaner, more discrete sampling method would sharpen the vertical boundaries of this event into a more clearly correlatable horizon.

The general progression of a succession of primarily agglutinated faunas up through the Eocene at all sites to the establishment of a mostly calcareous benthic assemblage probably reflects changing parameters of the bottom water as the sites shallowed due to the steady infilling of the basin. There does not seem to be a great deal of difference in the actual composition of this fauna between the "shallow" and "deep" ends of the transects, though the latter seem to exhibit a greater diversity of relatively rare taxa. Given the fairly slight present differences in depth to the top of the Eocene, the presence of a more or less uniform benthic assemblage in all sites does not seem unreasonable.

In the Oligocene of B-08, and the indeterminate but possibly Oligocene interval of I-46, small numbers of pyritized cylinders and casts occur, along with a few pyritized diatoms, similar to those in the Eocene. These diatoms also occur in the Oligocene of G-55 and probably correspond to the secondary peak of these forms in the Lower Miocene/Oligocene previously reported in several northern Grand Banks wells (Thomas and Gradstein, 1981). There is a somewhat greater inter-well variety of the benthic assemblages in the Oligocene compared to the Eocene, probably a function of closer proximity to the landmass to the west with lessening water depth. In general, the deeper sites tend to have richer, more diverse faunas than the shallower ones, including a few agglutinated species such as *Cyclammina placenta* and *Bathysiphon discreta* gr.

The Lower/Middle Miocene assemblage at most sites appears to be more or less a continuation of the mixed Oligocene suite, except for the disappearance of *Turrilina*

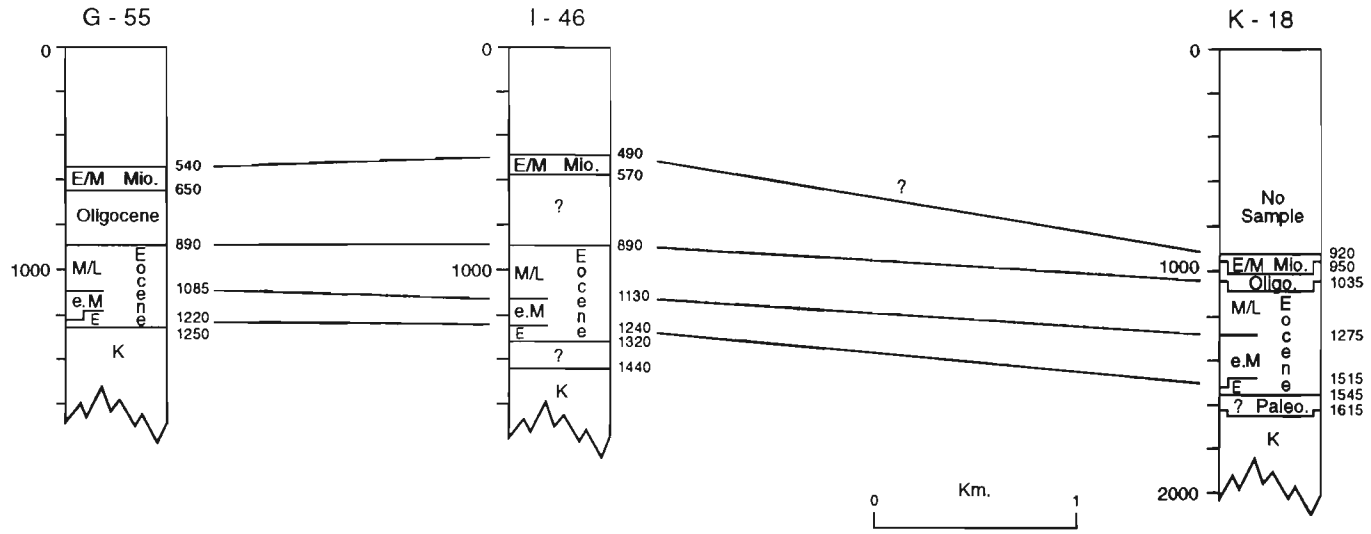

Figure 2a. *Correlation chart of eastern transect G-55 - I-46 - K-18. Depth scale in metres.*

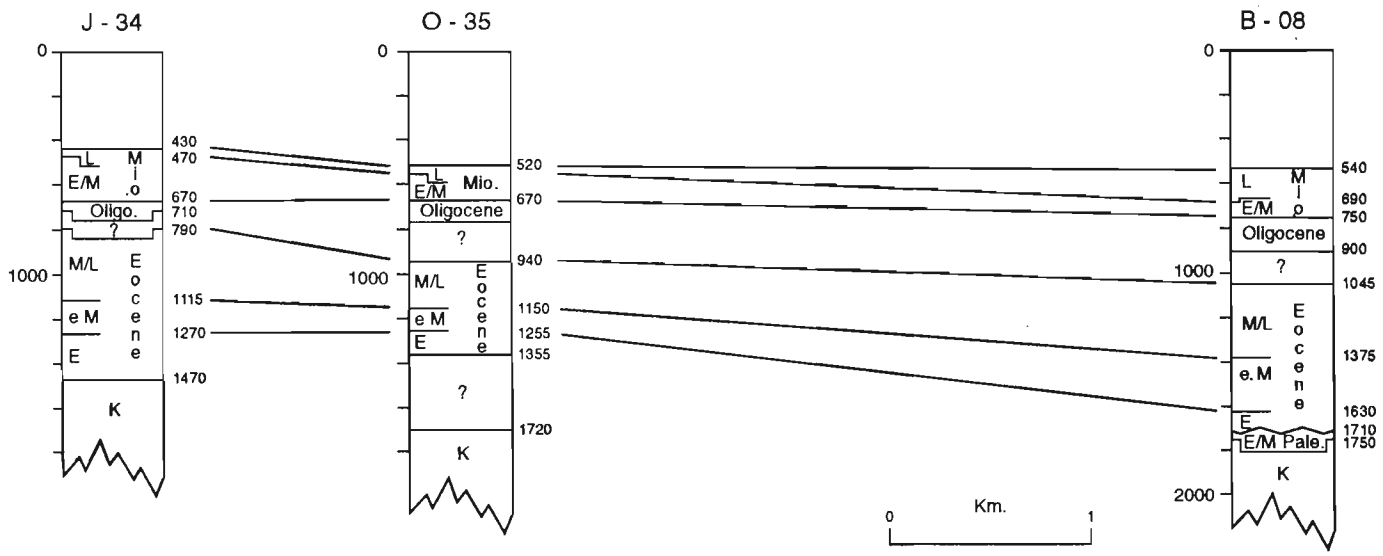

Figure 2b. *Correlation chart of western transect J-34 - O-35 - B-08. Depth scale in metres.*

alsatica and the appearance of large numbers of in situ *Spiroplectammina carinata*. Important components, in most sites except B-08, are Lenticulinids. Several species of these occur.

The distribution of the *Uvigerina* assemblage is puzzling, but may be related to sampling procedures. Since the *Uvigerina*-bed is demonstrably thin, it may lie in the gaps between successive samples in the other two wells. In the four wells in which it is present, it is at the top of the zone (i.e., it appears simultaneously with *Spiroplectammina carinata*) in B-08, but below the top of *Spiroplectammina carinata* in the other three. Its variable position within the zone may well be a product of sampling, or could be a function of the species' environmental preference, or may even indicate a lateral migration of this assemblage through time.

Similarly, the areal distribution of the Late Miocene *Asterigerina* Zone may be a function of sampling, with the collection of ditch cuttings samples beginning, perhaps, just below that interval.

Cenozoic sedimentation history of the Hibernia area

When the six wells are arranged in two transects (Fig. 2a, b) they provide, within the constraints of sampling, information as to the relative rates of sedimentation in this part of the Jeanne d'Arc Basin during the Cenozoic.

Paleocene deposition is apparently restricted to the deep sites B-08 and (probably) K-18, where relatively thin layers occur. The intermediate sites I-46 and O-35 may contain some Paleocene in sustantially thick units of indeterminate age. In the shallower sites the Paleocene is absent.

The three zones representing Eocene sedimentation (Middle/Late, early Middle, and Early) are clearly identifiable in all wells, and their relative thicknesses appear to generally conform to the relative sizes of the time intervals which they represent. The Middle/Late Eocene zone is roughly equivalent to the combined thicknesses of the other two zones, indicating reasonably constant rates of sedimentation throughout the Eocene. The two deepest sites appear to have slightly thicker Eocene sections than most others, although the indeterminate strata bracketing the Eocene top and bottom in the two intermediate wells may represent at least some Eocene deposition. If an oceanographic event such as a change in watermass characteristics did produce the "pyritization event" near the Middle/Late Eocene boundary, it does not appear to have resulted in a significant break in sedimentation or an erosional event.

The Oligocene, recognizable in all wells but I-46, appears somewhat thinner in most sites than an epoch of its duration relative to the Eocene would produce, but again, underlying strata of indeterminate age may represent in part Oligocene deposition, which would then suggest a rate of deposition not dissimilar to that of the Eocene.

The Miocene sections, probably truncated by lack of sample in the western transect, vary somewhat in thickness, but in general seem to suggest a continuation of the same rate of accumulation as was prevalent in the underlying sections.

At this stage in the research of the Cenozoic of this area, backstripping of overburden and decompaction studies have not been completed, so more succinct information on the sedimentation history is not yet available.

FUTURE WORK

It is intended to input this and other new data on the Hibernia field into basin modelling work and describe resulting effects on the generation of hydrocarbons and overpressures within Hibernia's drainage area.

Further future work will incorporate a detailed comparison of the micropaleontological data with existing palynological studies of the area and to tie the resulting synthesis into local seismic coverage.

CONCLUSIONS

A study of benthic foraminiferal assemblages in the Cenozoic sections of six wells of the Hibernia field permits a biostratigraphic study of age-depth relationships and changing benthic associations in the study area, and provides evidence of oceanographic or diagenetic events. The principal findings of this study are:

1. Paleocene deposition in the field is only demonstrable at the deep site B-08, and probably also occurred at K-18. It is unrecognizable, if present, at the shallower sites.
2. The Lower Eocene "balls" event in other northern Grand Banks area wells is clearly recognized in all six sites.
3. A minor abundance peak of pyritized diatoms in the lower Middle Eocene of some wells appears to correlate with a similar event previously described from northern Grand Banks and Labrador Sea wells.
4. A "pyritization event" around the Middle/Upper Eocene boundary in most sites may be the result of an oceanographic event, but apparently did not produce a disruption in sedimentation.
5. The predominantly agglutinated benthic foraminiferal assemblages of the Lower and Middle Eocene are replaced in the uppermost Eocene by largely calcareous assemblages.
6. The Oligocene, where recognizable, contains a mixed benthic foraminiferal assemblage, predominantly calcareous in nature. In some sites another "pyritization" event appears to have taken place, and numbers of pyritized diatoms correlate to a second peak documented in other northern East Coast wells.
7. The Lower/Middle Miocene is recognized in all wells, containing a largely mixed calcareous assemblage.
8. The Upper Miocene is absent in some sites, probably not having been sampled.

9. The relative thicknesses of the Eocene zones and Oligocene zone generally suggest similar and more or less constant rates of sediment accumulation at all the sites during those two epochs, within the constraints of the sampling procedure. Insufficient data are available to similarly quantify Paleocene and Miocene deposition.

ACKNOWLEDGMENTS

Many thanks to A.C. Grant and M.A. Williamson for critically reviewing the manuscript. Thanks also to P.S. Parks for preparing the figures and N. Koziel for word processing.

REFERENCES

Canada-Newfoundland Offshore Petroleum Board
1990: Schedule of Wells Newfoundland Offshore Area; CNOPB, St. John's, Newfoundland.

Gradstein, F.M. and Agterberg, F.P.
1982: Models of Cenozoic Foraminiferal Stratigraphy – Northwestern Atlantic Margin; in Quantitative Stratigraphic Correlation (ed.) J.M. Cubitt and R.A. Reyment; John Wiley & Sons, Ltd., Chichester, U.K., p. 119-173.

Gradstein, F.M. and Kaminski, M.A.
1989: Taxonomy and biostratigraphy of new and emended species of Cenozoic deep-water agglutinated foraminifera from the Labrador and North Seas; Micropaleontology, v. 35, no. 1, p. 72-92.

McAlpine, K.D.
1990: Mesozoic stratigraphy, sedimentary evolution, and petroleum potential of the Jeanne d'Arc Basin, Grand Banks of Newfoundland; Geological Survey of Canada, Paper 89-17, 50 p.

Nishimura, A.
1992: Paleocene radiolarian biostratigraphy in the northwest Atlantic at Site 384, Leg 43, of the Deep Sea Drilling Project; Micropaleontology, v. 38, no. 4, p. 317-362.

Thomas, F.C.
1988: Taxonomy and stratigraphy of selected Cenozoic benthic foraminifera, Canadian Atlantic margin; Micropaleontology, v. 34, no. 1, p. 67-82.

Thomas, F.C. and Gradstein, F.M.
1981: Tertiary subsurface correlations using pyritized diatoms, offshore Eastern Canada; in Current Research, Part B; Geological Survey of Canada, Paper 81-1B, p. 17-23.

Thomas, F.C. and Murney, M.G.
1985: Techniques for extraction of Foraminifers and Ostracodes from sediment samples; Canadian Technical Report of Hydrography and Ocean Sciences, no. 54, 24 p.

Williamson, M.A.
1992: The subsidence, compaction, thermal and maturation history of the Egret Member source rock, Jeanne d'Arc Basin, offshore Newfoundland; Bulletin of Canadian Petroleum Geology, v. 40, no. 2, p. 136-150.

Williamson, M.A., Katsube, J., Huang, Z., Fowler, M., McAlpine, K.D., Thomas, F.C., Fensome, R.A., and Avery, M.P.
1993: Hydrocarbon charge history of east coast offshore basins: modelling geological uncertainty; in Current Research, Part E; Geological Survey of Canada, Paper 93-1E, p. 299-306.

Geological Survey of Canada Projects 850055, 920058, 710065

APPENDIX

List of foraminiferal species and other taxa formally or informally designated, encountered in Hibernia wells. Numbered species, unless otherwise indicated, refer to types in the Canadian Atlantic Margin Reference Collection, Atlantic Geoscience Centre.

Cenozoic Foraminifera

Acarinina densa (Cushman)
Alabamina scitula Bandy
Alabamina sp.
Ammobaculites sp.
Ammodiscus latus Grzybowski
Ammodiscus planus Loeblich
Ammomarginulina aubertae Gradstein and Kaminski
Ammosphaeroidina pseudopauciloculata (Mjatliuk)
Anomalina grosserugosa (Gumbel)
Anomalina sp.
Anomalina cf. *spissiformis* Cushman and Stainforth
Anomalinoides acuta (Plummer)
Anomalinoides aff. *rubiginosus* (Cushman)
Astacolus sp.
Asterigerina gurichi (Franke)
Bathysiphon aff. *brosgei* (Tappan)
Bathysiphon discreta gr. (Brady)
Biloculina sp.
Bolivina dilatata (Reuss)
Bolivina sp.
Buccella cf. *tenerrima* (Bandy)
Bulimina alazanensis (Cushman)
Bulimina bradburyi (Martin)
Bulimina cooperensis (Cushman)
Bulimina midwayensis (Cushman and Parker)
Bulimina cf. *semicostata* Nuttall
Bulimina spp.
Bulimina trigonalis Ten Dam
Buliminella elegantissima (d'Orbigny)
Cassidulinoides sp.
Cassigerinella aff. *chipolensis* (Cushman and Ponton)
Catapsydrax aff. *dissimilis* (Cushman and Bermudez)
Ceratobulimina contraria (Reuss)
Ceratocancris sp.1
Chilostomella oolina Schwager
Cibicides cf. *lobatulus* (Walker and Jacob)
Cibicidoides eocaenus (Gumbel)
Cibicidoides havanensis (Cushman and Bermudez)
Cibicidoides cf. *laurisae* (Mallory)
Cibicidoides cf. *mexicanus* (Nuttall)
Cibicidoides pachyderma (Rzehak)
Cibicidoides praemundulus Berggren and Miller
Cibicidoides sp.2 Tjalsma and Lohmann
Cibicidoides sp.14 van Morkhoven et al.
Cibicidoides spp.
Cibicidoides aff. *subspiratus* (Nuttall)
Cibicidoides truncanus (Gumbel)
Cibicidoides aff. *tuxpamensis* (Cole)
Cibicidoides cf. *ungerianus* (d'Orbigny)
Cornuspira sp. "*punctate*"
Cornuspira involvens Reuss
Cribrostomoides sp.
Cribrostomoides subglobosus (Sars)
Cyclammina cancellata Brady
Cyclammina placenta (Reuss)
Cyclammina rotundidorsata (Hantken)
Cyclammina sp.
Cystammina pauciloculata (Brady)
Dentalina sp.
Dorothia sp.2
Dorothia cf. *trochoides* (Marsson)
Eggerella bradyi (Cushman)
Eggerella sp.
Epistomina eocaenica Cushman and Hanna
Eponides plummerae Cushman
Fissurina marginata (Walker and Boys)
Fissurina sp.
Frondicularia cf. *budensis* (Hantken)
Gaudryina laevigata Franke
Gaudryina pyramidata Cushman
Gaudryina sp.
Gavelinella cf. *beccariiformis* (White)
Gavelinella cf. *capitata* (Gumbel)
Gavelinella danica (Brotzen)
Gavelinella micra (Bermudez)
Globigerina bulloides d'Orbigny/*praebulloides* Blow gr.
Globigerina eocaena Gumbel
Globigerina aff. *linaperta* Finlay
Globigerina ouachitaensis Howe and Wallace
Globigerina cf. *selli* (Borsetti)
Globigerina aff. *senni* (Beckmann)
Globigerina sp.
Globigerina cf. *yeguaensis* Weinzierl and Applin
Globigerinoides sp.
Globigerinoides cf. *trilobus* (Reuss)
Globobulimina ovata (d'Orbigny)
Globocassidulina subglobosa (Brady)
Globoquadrina venezuelana (Hedberg)
Globorotalia fohsi peripheroronda Blow and Banner
Globorotalia opima gr. Bolli
Globulina gibba d'Orbigny
Glomospira corona Cushman and Jarvis
Guttulina problema d'Orbigny
Guttulina sp.
Gyroidina girardana (Reuss)
Gyroidina octocamerata Cushman and Hanna
Gyroidina primitiva Hofker
Gyroidina soldanii d'Orbigny
Gyroidina soldanii mamillata (Andreae)
Gyroidina sp.

Gyroidina cf. *subangulata* (Plummer)
Gyroidinoides globosus (Hagenow)
Gyroidinoides sp.
Haplophragmoides excavatus (Cushman)
Haplophragmoides kirki Wickenden
Haplophragmoides retroseptus (Grzybowski)
Haplophragmoides spp.
Haplophragmoides walteri (Grzybowski)
Hoeglundina elegans (d'Orbigny)
Hormosina sp.
Kalamopsis sp.
Karreriella bradyi (Cushman)
Karreriella cf. *conversa* Grzybowski
Karreriella subglabra (Gumbel)
Lagena spp.
Lenticulina aff. *alatolimbata* (Gumbel)
Lenticulina calcar (Linne)
Lenticulina depressa (Asano)
Lenticulina iota (Cushman)
Lenticulina spp.
Lenticulina cf. *whitei* Tjalsma and Lohmann
Marginulina aff. *bachei* Bailey
Marginulina sp.
Marginulina sp.10
Martinotiella nodulosa (Cushman)
Martinotiella sp.
Melonis barleeanum (Williamson)
Melonis aff. *pompilioides* (Fichtel and Moll)
Morozovella pseudobulloides (Plummer)
Morozovella sp.
Neoeponides hillebrandti Fisher
Nodosaria cf. *elegantissima* Hantken
Nodosaria cf. *pozoensis* Berry
Nodosaria sp.4
Nodosaria sp.5
Nodosaria sp.12
Nodosaria sp.20
Oolina sp.
Oridorsalis tener (Brady)
Oridorsalis umbonatus (Reuss)
Orthomorphina sp.
Osangularia expansa (Toulmin)
Osangularia sp.
Parafrondicularia cf. *miocenica* (Cushman)
Pararotalia sp.2
Planulina cf. *costata* (Hantken)
Plectofrondicularia cf. *paucicostata* Cushman and Jarvis
Plectofrondicularia aff. *vaughani* Cushman
Polymorphina sp.
Pseudoglandulina humilis (Roemer)
Pseudohastigerina micra (Cole)
Pseudohastigerina wilcoxensis (Cushman and Ponton)
Pseudopolymorphina cf. *novangliae* (Cushman)
Pullenia bulloides Parker and Jones
Pullenia cf. *eocaenica* Cushman and Siegfus
Pullenia quinqueloba (Reuss)
Pyrgo bulloides (d'Orbigny)
Pyrulina sp.
Quinqueloculina sp.
Quinqueloculina cf. *stalkeri* Loeblich and Tappan
Quinqueloculina cf. *triloculiniformis* McLean
Recurvoides spp.
Reophax sp.
Reticulophragmium amplectens (Grzybowski)
Rhizammina sp.
Saccamina sp.
Sigmoilina sp.
Sigmomorphina cf. *vaughani* Cushman and Ozawa
Siphonina advena Cushman
Sphaeroidina bulloides d'Orbigny
Spirillina sp.
Spiroloculina cf. *canaliculata* d'Orbigny
Spiroplectammina carinata (d'Orbigny)
Spiroplectammina dentata (Alth)
Spiroplectammina navarroana Cushman
Spiroplectammina spectabilis (Grzybowski)
Stetsonia sp.
Stilostomella aculeata (Cushman and Jarvis)
Stilostomella cf. *midwayensis* (Cushman and Todd)
Stilostomella spp.
Stilostomella cf. *subspinosus* Cushman
Subbotina frontosa (Subbotina)
Textularia agglutinans d'Orbigny
Tosaia cf. *hanzawai* Takayanagi
Trifarina cf. *angulosa* (Williamson)
Trifarina fluens (Todd)
Trochammina aff. *globigeriniformis* Parker and Jones
Trochammina sp.
Turrilina alsatica Andreae
Turrilina robertsi (Howe and Ellis)
Uvigerina cf. *batjesi* Kaasschieter
Uvigerina cf. *havanensis* Cushman and Bermudez
Uvigerina mexicana Nuttall
Uvigerina miozea-nuttalli gr. Thomas
Uvigerina proboscidea Schwager
Uvigerina sp.
Uvigerina spinicostata Cushman and Jarvis
Vaginulinopsis decorata (Reuss)
Vaginulinopsis sp.
Valvulineria petrolei (Andreae)
Verneuilina sp.

Reworked Cretaceous Foraminifera

Gaudryina sp.
Gavelinella minima (Vieaux)
Globotruncana fornicata Plummer
Hedbergella cf. *delrioensis* (Carsey)
Heterohelix aff. *globulosa* (Ehrenberg)

Other taxa

"Balls"

Appendix (cont.)

Bryozoa
Coscinodiscus sp.1 Thomas and Gradstein (diatom)
Coscinodiscus sp.2 Thomas and Gradstein
Coscinodiscus sp.3 Thomas and Gradstein
Coscinodiscus sp.4 Thomas and Gradstein
Coscinodiscus spp.
Echinoderm fragments
Fish otoliths
Fish teeth
Limacina canadensis Hodgkinson, Garvie and Be (pteropod)
Limacina planispiralis Hodgkinson, Garvie and Be
Megaspore sp.
Mollusc fragments (bivalve and gastropod)
Ostracodes
Pyrite tubes
Scaphopod "corrugated"
Scaphopod "fluted"
Scaphopod sp.1
Selachian denticles

A preliminary interpretation of glacial history derived from glacial striations, central Newfoundland[1]

R.A. Klassen
Terrain Sciences Division

Klassen, R.A., 1994: A preliminary interpretation of glacial history derived from glacial striations, central Newfoundland; in Current Research 1994-D; Geological Survey of Canada, p. 13-22.

Abstract: In central Newfoundland, striations and indicator erratics define four distinct glacial flow events. During the oldest, ice flow was regionally southward to southeastward from the Topsails Plateau, initially defining radial flow across NTS map areas 12A/10 and 16, and later more southward. The dispersal centre was located either on the Topsails Plateau or north of it. Subsequent to that event, ice flow was regionally northeastward, curving around the eastern Topsails Plateau and, within map areas 12H/1 and parts of 12A/16, it later shifted more northward towards the heads of coastal inlets. North of Buchans townsite, the last ice flow was northward and southward from an apparent ice divide, although ice-marginal landforms indicate that the last ice margin retreated southward from Hinds Lake, and eastward and northward towards the Topsails Plateau. Within Red Indian Lake, P-forms indicate subglacial erosion by meltwater flowing towards the southwest and northeast.

Résumé : Dans le centre de Terre-Neuve, les stries et les traînées de blocs indicateurs permettent d'établir l'existence de quatre écoulements glaciaires distincts. Pendant l'événement le plus ancien, les glaces s'écoulaient régionalement, à partir du plateau Topsails, dans une direction sud à sud-sud-est, définissant initialement un écoulement radial dans les régions cartographiques 12A/10 et 16 du SNRC, et qui, plus tard, a adopté une direction plus proche du sud. Le centre de dispersion se trouvait sur le plateau Topsails ou au nord de celui-ci. Après ce premier événement, l'écoulement glaciaire était dirigé régionalement vers le nord-est, s'incurvant autour de la bordure orientale du plateau Topsails, puis, plus tard, adoptant une direction plus rapprochée du nord dans la région de la carte 12H/1 et d'une partie de la carte 12A/16, en se dirigeant vers la tête d'inlets côtiers. Au nord de la ville de Buchans, le dernier écoulement glaciaire était dirigé à la fois vers le nord et vers le sud à partir d'une ligne de partage glaciaire apparente; des modelés de marge glaciaire indiquent toutefois que la dernière marge glaciaire s'est retirée vers le sud depuis le lac Hinds, puis en direction de l'est et du nord, vers le plateau Topsails. Dans le lac Red Indian, des formes en P indiquent une érosion sous-glaciaire par des eaux de fonte s'écoulant vers le sud-est et le nord-est.

[1] Contribution to Canada-Newfoundland Cooperation Agreement on Mineral Development (1990-1994), a subsidiary agreement under the Canada-Newfoundland Economic and Regional Development Agreement.

INTRODUCTION

During 1991 and 1992, the Quaternary geology, glacial history, and drift composition of central Newfoundland were studied to define a geological framework for mineral exploration by drift prospecting (Fig. 1). Within that area, mineral exploration has been focused on volcanic rocks of the Buchans and Roberts Arm Groups north of Red Indian Lake, and Victoria Lake Group to the south. Until recent time, a major lead-zinc mining operation was located at Buchans, and mineralized showings occur elsewhere in the area that are currently under active investigation. Exploration, however, has been hampered by varied, complex directions of ice flow and glacial transport, and by thick surficial deposits. Despite these difficulties, several discoveries have been facilitated by boulder tracing and drift prospecting. For example, tracing mineralized boulders found in surficial deposits during the early 1920s lead to the discovery of the Buchans orebodies (Neary, 1981). To assist mineral exploration, detailed studies of ice flow indicators, of surficial deposits and stratigraphy, and of till composition and glacial transport history were undertaken. This summary report describes the dominant ice flow patterns within NTS map areas 12A/10, 12A/15, 12A16, and 12H/1, and presents a preliminary reconstruction of glacial history.

PREVIOUS WORK

In central Newfoundland, varied directions and ages of ice flow have been defined based on glacial striations and streamlined landforms, and on crosscutting relationships among them. The geological record, however, has proven to be complex, and conclusions regarding glacial history have been inconsistent and contradictory. Landforms shown on the Glacial Map of Canada (Prest et al., 1969) define major ice flow towards the northeast and the southwest across central Newfoundland, with other flow directions indicated by isolated striations. Across the Buchans area, northwest-southeast trends are evident on radar images (Graham and Grant, 1991). Among earlier workers, a detailed record of glacial striations within the study area is given by Murray (1955) who described ice flow in the area south of Red Indian Lake through his own observations and those of other exploration geologists. Based on the distribution of granitic erratics, he defined the principal direction of ice flow and glacial transport toward the northeast. Elsewhere within the study area, striation records show marked variations in ice flow directions in the western part of the study area near Buchans, adjacent to Red Indian Lake, and in the southwestern part of the Lake Ambrose map area (12A/10) (Grant and Tucker, 1976; Sparkes, 1985).

Stratigraphic sequences comprising two compositionally distinct tills are exposed within the Oriental Pit at Buchans, and in borrow pits south of Red Indian Lake (Mihychuk, 1985; Sparkes, 1985). Within the Oriental Pit (Fig. 1), the sequence includes: a) an older lodgment till that contains Buchans Group volcanic rock, and was likely deposited from ice flowing northeastward, and b) a younger granitic till deposited from ice flowing southwestward (Sparkes, 1985).

Through the work of Sparkes (1985, 1987) and of Vanderveer and Sparkes (1982), the following sequence of ice flow events is proposed, from oldest to youngest:

1. Early regional flow toward the south (160-190°) originating from north of Red Indian Lake. This event is associated with a compact grey till in the Tulks River valley, and could be pre-Wisconsinan in age.

2. Formation of a glacial lake, informally named glacial lake Shanadithit (Mihychuk, 1985), that extended to 59 m above the present level of Red Indian Lake (Vanderveer and Sparkes, 1982), and formed either during the retreat of the southward flowing glacial ice, or during a later advance from a centre near Hinds Lake (Vanderveer and Sparkes, 1982). Pollen in the lake sediments (unpublished analyses, Royal Ontario Museum) indicates the glacial lake could be associated with an interglacial or interstadial period.

3. Renewed glaciation, with ice flow originating from several dispersal centres. Ice flow was directed northeastward and southeastward from a centre located between Victoria Lake (12A/7) and Lake Ambrose (12A/10), and there is indication of topographic control on the ice in some areas. At the same time ice flowed south to southwest from a centre near Hinds Lake and occupied Red Indian Lake (Sparkes, 1984). The northeastward ice flow deposited a lower grey till at the Oriental Pit at Buchans. A red granitic till that overlies the grey till was deposited by later southwestward flowing ice (Sparkes, 1985). Water discharge from Red Indian Lake was to the southwest, in contrast to modern flow which is by way of Exploits River to the east.

The orientation and location of ice marginal landforms and glaciofluvial deposits, indicate that during deglaciation ice receded toward an ice divide arcing across the central part of the island, and later split into separate, shrinking ice caps, one of which was last located within Red Indian Lake basin (Grant, 1974). Landforms outline the successive margins of an ice lobe retreating northeastward within the lake basin, southward from Hinds Lake, and eastward toward the Topsails Plateau (Grant, 1975). According to Grant, final disintegration of the ice was within Red Indian Lake basin. This general model of deglacial history is supported by the conclusions of Lundqvist (1965) and St. Croix and Taylor (1991), which are based on striations mapped in north central and northeastern Newfoundland, and by the work reported here.

Drift prospecting activities near Buchans have been summarized by James and Perkins (1981) who identified three ice flow directions including "... a dominant ice movement from the northeast, a prominent movement from the northwest, and an obscure movement from the west-southwest", from oldest to youngest (James and Perkins, 1981: p. 281). They found a prominent zone of zinc enrichment that defines a glacial dispersal train extending more than 8 km southwest of Buchans. Mineralized erratics of Buchans–type ore occur both within that dispersal train southwest of their source, and 10 to 20 km east and northeast of it (e. g. James and Perkins, 1981).

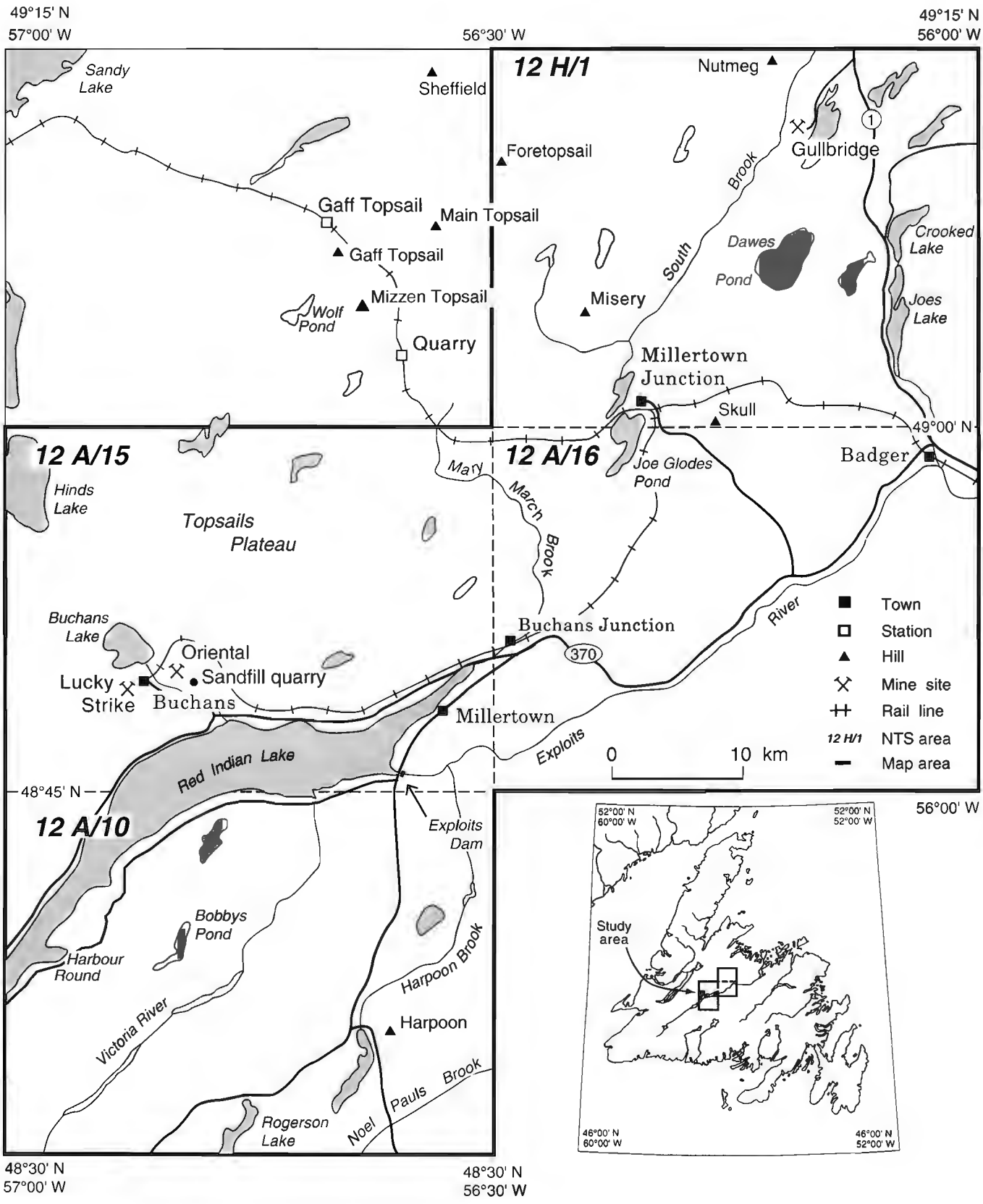

Figure 1. *Location map of study area, including Lake Ambrose (12A/10), Buchans (12A/15), Badger (12A/16), and Dawes Pond (12H/1) NTS map areas.*

METHODS

Striations

At more than 200 sites throughout the study area, striations and other ice flow marks on bedrock were mapped to determine ice flow history. Where geological criteria at a site allowed, trend, sense of ice flow, and relative age of striations were determined (e.g. Prest, 1983). Buried surfaces around the margins of outcrop were excavated and washed to expose striations on 'lee' surfaces sheltered from later flow(s). Relative ages of striations are determined from crosscutting relations among striations and from the positions of striations with regard to slope aspect (Fig. 2). Striations on uppermost, exposed 'stoss' faces are 'youngest', whereas those on 'lee' faces on the margins of outcrop are either 'older' or 'oldest' in a sequence of two or more striation sets. Few striations were found on outcrop of the Topsails Plateau because exposed surfaces of the intrusive rocks that form the Plateau have been weathered and because extensive organic bog deposits cover most of the Plateau.

Indicator erratics

To determine distances and directions of glacial transport associated with distinct ice flow events, indicator erratics derived from lithologically distinct sources were mapped. They include pink, medium grained granite lacking metamorphic fabric and derived from the Topsails Plateau (Fig. 3a), and red micaceous sandstone derived from bedrock underlying Red Indian Lake (Fig. 3b). Pink granitic erratics could also have been derived from bedrock sources to the south of the Lake Ambrose map area (NTS 12A/10). As shown (Fig. 3a), granitic erratics are interpreted to have been derived from bedrock of the Topsails Plateau because there is no striation data to indicate that there was northward ice flow from southern sources. Red micaceous sandstone in drift defines a glacial dispersal train extending more than 30 km northeast of Red Indian Lake to the area of Skull Hill. Some of the sandstone could be derived from small, unmapped outliers in bedrock along the path of that dispersal train (D. Evans, pers. comm., 1993). The extent of glacial dispersal and relative abundance of sandstone in drift indicates that bedrock underlying Red Indian Lake is the principal source of the dispersal train.

RESULTS AND INTERPRETATIONS

Constraints of the interpretation of striations

Interpretation of the erosional record in terms of ice flow events can be difficult. At any outcrop site striations may not record all ice flow events that affected the area, and evidence for the determination of relative ages may not be present. Within the area of study, the expression of different striation sets can also vary depending on the thickness and extent of ice and the erosional vigour of ice flow that produced them, and the geological substrate upon which they are expressed. Finally, ice flow events of different ages that have similar trends can be difficult to distinguish using striations alone. Despite the geological constraints on the interpretation of the erosional record, and the apparent complexity of the striation record (Fig. 4), coherent patterns of ice flow can be identified and a sequence of ice flow events can be defined.

A summary of ice flow events in central Newfoundland is given in Figure 5, and it is based on the combined evidence of striations and glacial dispersal of indicator erratics. For

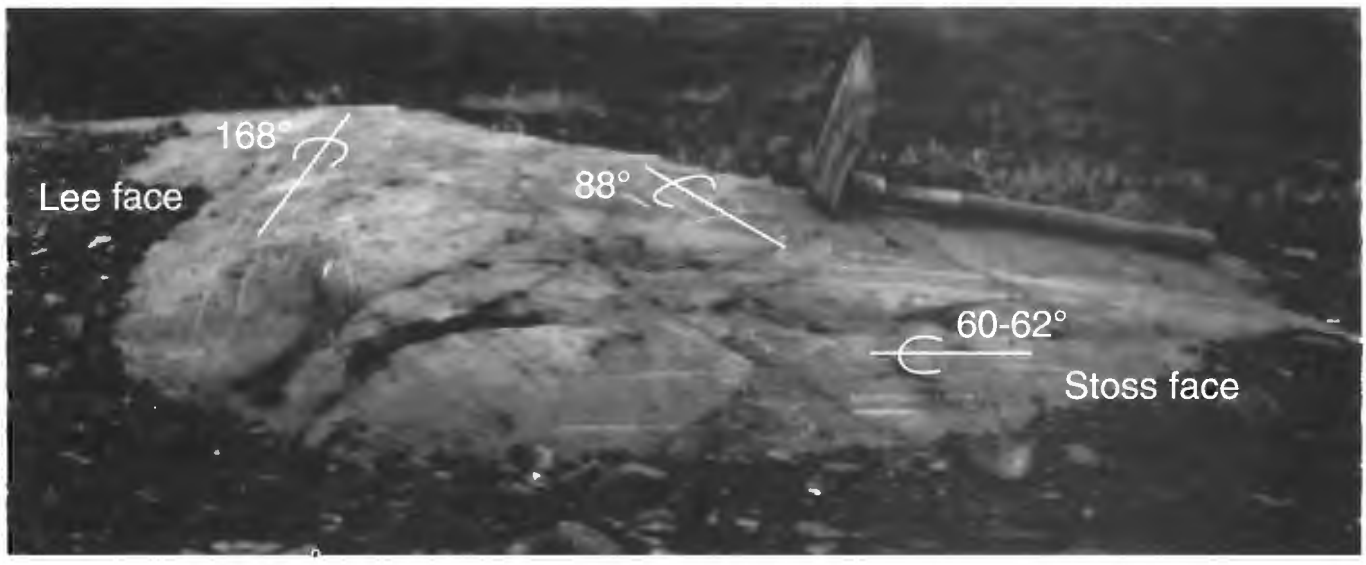

Figure 2. *Depending on slope aspect and exposure to ice flow, striated surfaces record different ice flow events. Here, the sequence of ice flow events was initially southward (168°) across the lee face (event I), later northeastward (60-62°) across the stoss face (event II), and finally eastward (88°), as recorded by crosscutting striations on the stoss face (event IV). Ice flow events are described later in this report. (GSC 1992-300E)*

convenience, the events are named here by Roman Numerals from oldest (I) to youngest (IV). In the absence of other geological evidence (e.g. stratigraphic) that would support a more complex interpretation, crossing sets of striations divergent by <15° and consistently expressed on outcrop are associated with one ice flow event. The shifts in ice flow that they represent are designated by lower case letters as part of one event (e.g. Ia, Ib). As shown (Fig. 5), arrows defining a glacial event reflect the areal extent of the striation record that defines the event.

For central Newfoundland, the interpretation of striations in terms of ice flow history that is given in this report differs from those of other workers (e.g. Sparkes, 1985; Vanderveer and Sparkes, 1982). It identifies ice flow events having similar flow trends, and those parts of the study area that they affected. Correlations with glacial events outside the study area (e.g. Batterson and Taylor, 1990; Batterson and Vatcher, 1992; Batterson and McGrath, 1993; St. Croix and Taylor, 1991) are based chiefly on the regional consistency in striation trends and the relative effects of topography on ice flow. Late glacial ice flow events associated with either a thin ice cap or several remnant ice caps can be characterized by marked local variation in ice flow direction, and are not necessarily contemporaneous. Thus, except in a general sense there is no basis for correlation among those events based on the striation record alone.

Summary of ice flow events

Event Ia, b

As summarized in Figure 5, the oldest ice flow, event Ia, was divergent southward to southeastward from the Topsails Plateau across most of the region, although the striation record for this event is best developed within the Lake Ambrose map area (12A/10). There (map area 12A/10), granitic erratics derived from bedrock underlying the Topsails Plateau are widely distributed, and they are evidence for southward glacial transport of several tens of kilometres by regional southward flow of event I (Fig. 3a). The consistency of striation trends and distance of glacial transport indicate that the ice was of significant extent and thickness. The dispersal centre associated with it could have been located either on or north of the Topsails Plateau. During event Ib, ice flow shifted more southward.

Within the Buchans (12A/15) and Dawes Pond (12H/1) map areas no evidence for event I is known, although it is presumed to have affected that area because of the regional extent of the striation record and southward glacial dispersal of granitic erratics derived from the Topsails Plateau. Striations on the plateau are few because exposed bedrock is readily weathered, and because bog and organic deposits are extensive. If the Topsails Plateau was the location of an ice divide, a striation record of Event I may not ever have been well developed.

Event IIa, b

During event IIa, the region was crossed by northeastward flowing ice. Event IIa is defined by the most prominent and widespread striation record, and by northeast glacial transport of red micaceous sandstone tens of kilometres from their source across the southern margin of Topsails Plateau as far as Skull Hill near Millertown Junction. Event IIa ice flow was topographically affected by the Topsails Plateau. As ice flowed northeastward past the plateau's eastern margin in the Dawes Pond map area (12H/1), it diverged north northeastward and northward (Fig. 5).

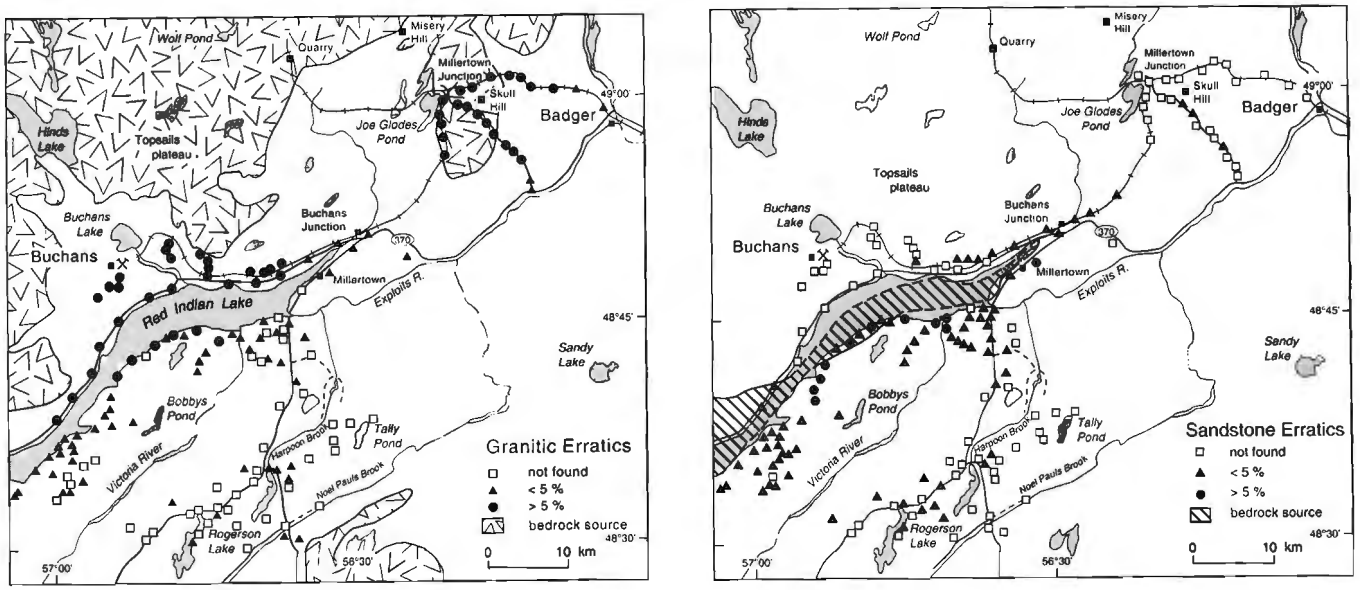

*Figure 3. Distribution of indicator erratics in drift: **a)** red granite derived from the Topsails Plateau, north of Red Indian Lake; and **b)** red micaceous sandstone derived from bedrock underlying and adjacent to Red Indian Lake.*

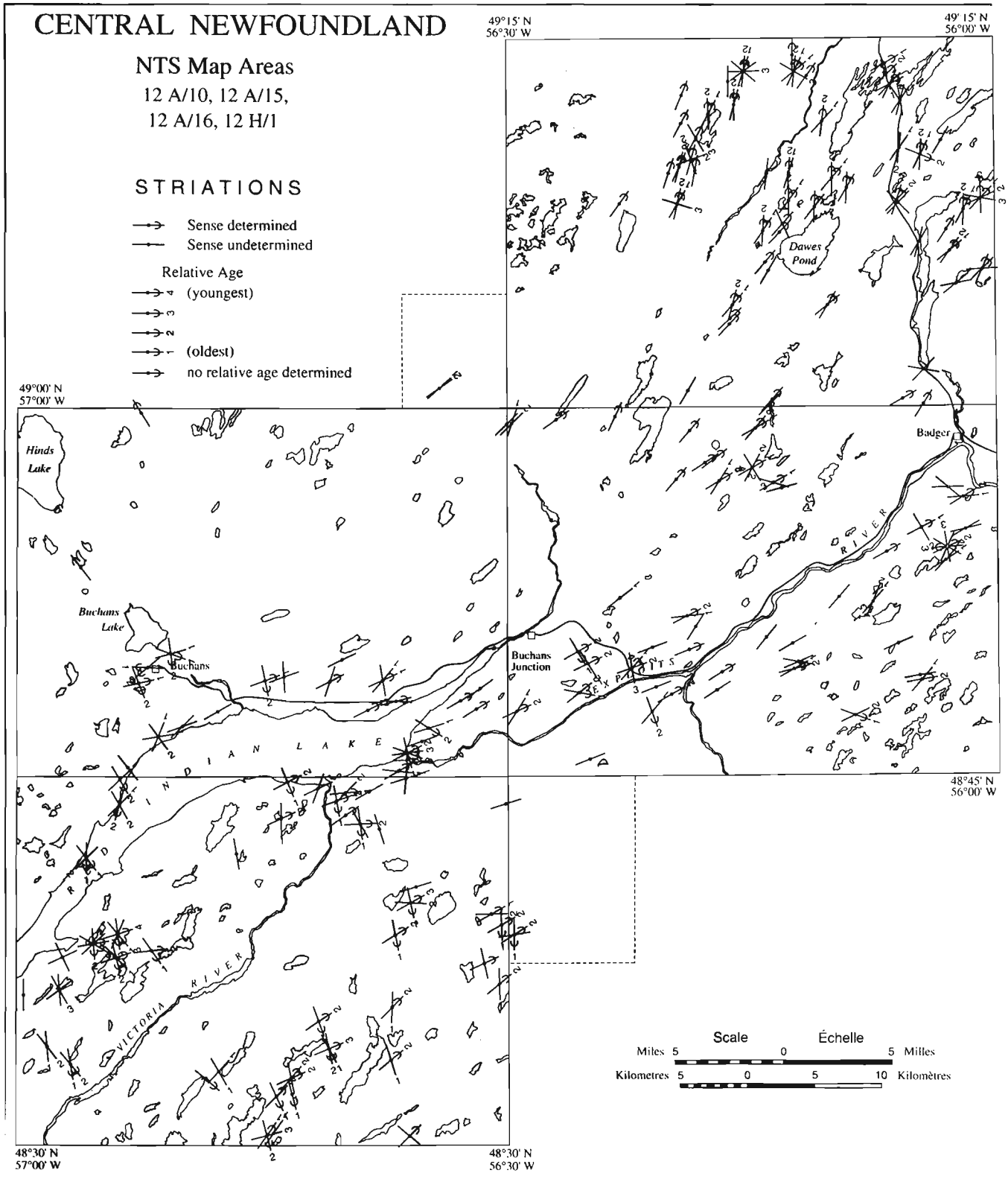

Figure 4. *Striation map of study area, based on representative sites.*

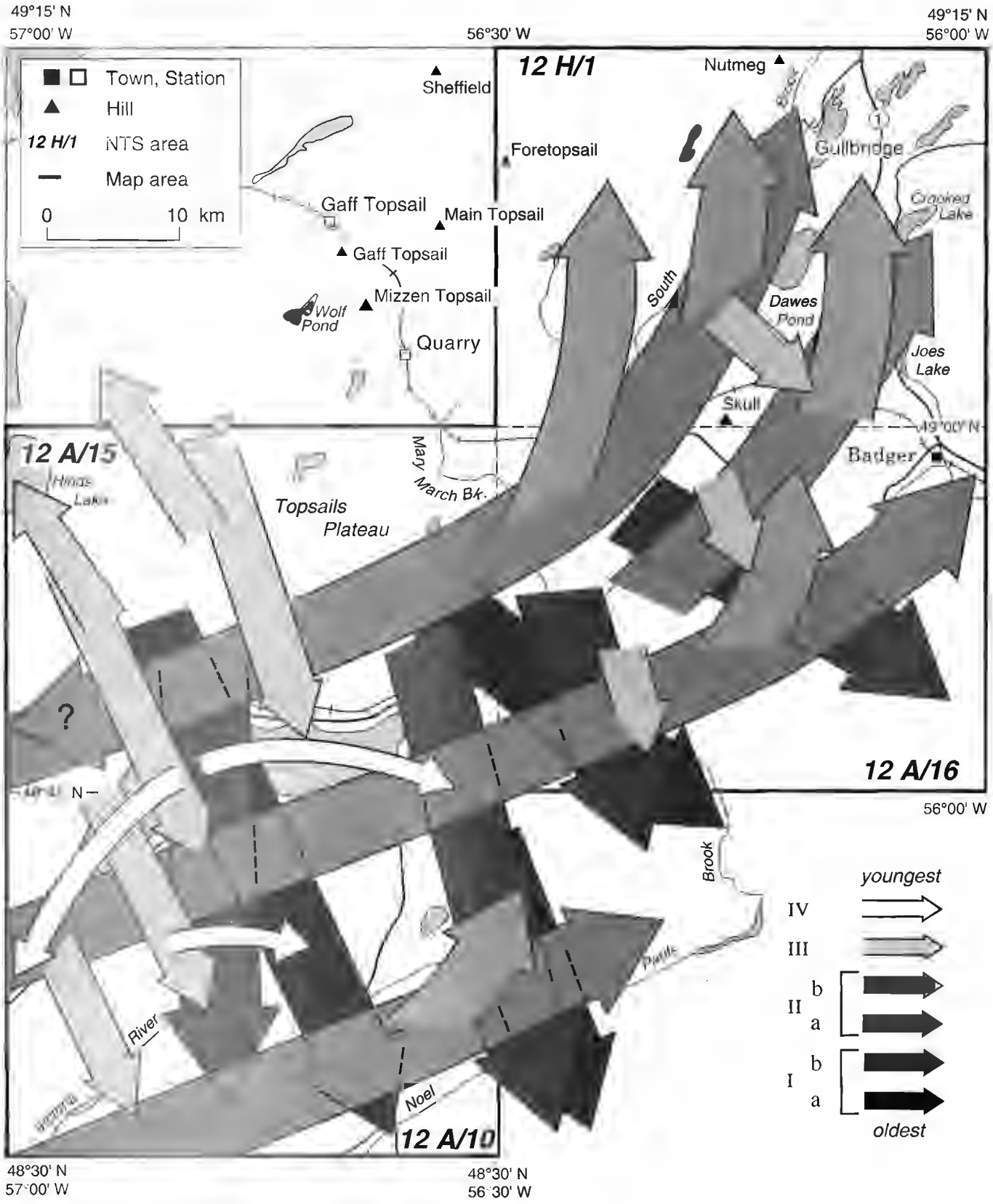

Figure 5. *Summary map of ice flow directions interpreted from striations and indicator erratics.*

Within the Dawes Pond map area (12H/1), during event IIb there was a marked northwards shift in ice flow that is possibly the result of a late glacial 'drawdown' toward major bays on the northern coast near Springdale (e.g. Liverman et al., 1991).

At outcrop scale, particularly within Lake Ambrose map area (12A/10), the erosional record of event IIa ice flow is largely confined to the stoss sides of outcrop, whereas lee sides remain either 'untouched', or nearly so (Fig. 2). The preferential occurrence of striations on stoss faces indicates flow separation at the base of the ice, with cavities forming in the 'lee' of bedrock obstructions. The erosional evidence is consistent with a relatively thin ice sheet during event II. At small scales (<1 m), selective erosion of 'stoss' bedrock surfaces, and the accompanying preservation of 'lee' faces, could be significant to mineral exploration and modelling of glacial dispersal. At one site south of Red Indian Lake, within the Lake Ambrose map area (12A/10), older bedrock surfaces crossed by south-trending striations (event I) are iron stained and contrast with younger surfaces bearing younger northeast trending striations (event II) that are glacially polished. Where the two sets of striations cross an unstained surface, the northeast-trending striations are fresh and unweathered, whereas the base of south-trending, older striations is stained indicating that staining occurred prior to the younger erosional event.

Across the study area, the relative effects of the two ice flow events (I and II) on drift composition vary. Within the Buchans (12A/15) and Badger (12A/16) map areas, drift composition is related largely to the effects northeast-flowing ice (e.g. Murray, 1955). Within the Lake Ambrose map area (12A/10) to the south, drift composition reflects the older southward ice flow of event Ia, b, although it could have been modified by later northeastward-flowing ice of event II.

Beneath a thick sequence of Quaternary sediments exposed at the Lucky Strike mine at Buchans (Fig. 1), a single striation site indicates ice flow toward 290°, and later 227°. The striations are the only known evidence for either westward or southwestward flow that could be related to a prominent southwest-oriented dispersal train of zinc in till and erratics of Buchans-type ore (James and Perkins, 1981). The significance of the westward and southwestward flow record is not well understood. In Figure 5, westward and southwestward ice flow defined by those striations is associated with event II, and is portrayed as a local reversal in ice flow. If the mineralized erratics are derived from outcropping ore at Buchans, then southwest ice flow could be more significant to reconstructions of ice flow history in central Newfoundland than described here.

Event III

In the west-central part of the study area, ice flow was again southward from the Topsails Plateau toward Red Indian Lake. Cross-cutting striations north of Red Indian Lake clearly demonstrate that this southward flow event is younger than event II, and is distinct from earlier southward flow of event I. Ice appears to have crossed Red Indian Lake, flowing southward across the western part of the Lake Ambrose map area. Event III is interpreted be the result of local ice flow, in part originating on the Topsails Plateau.

Northward ice flow toward Hinds Lake during late glacial time is indicated by the shape and slope of ice marginal landforms across hillsides north of Buchans and by striations at one site near Hinds Lake. As shown in Figure 5, that ice flow is interpreted as part of event III, and an ice divide associated with northward ice flow is located in the valley between Buchans and Hinds Lake.

As noted by Grant (1975), during the last phase of the last glaciation, the ice margin retreated eastward and northward within valleys towards a remnant ice cap on the Topsails Plateau. In the Badger (12A/16) and Dawes Pond (12H/1) map areas, minor, faint striations that occur only on the uppermost surfaces of outcrop define late glacial, southeastward ice flow. They are associated with flow from a remnant ice cap on the plateau, and as such are associated with event III.

Event IV

Within and adjacent to Red Indian Lake, the last phase of ice flow was along the axis of the lake towards the northeast and southwest outwards from a dispersal centre in Red Indian Lake at the approximate longitude of Buchans. It is defined by striations and by prominent P-Forms on shoreline outcrops. The record indicates glaciofluvial erosion at the base of the ice cap, and that ice flow likely occurred during late glacial time in association with a glacial remnant within Red Indian Lake basin. In drift on hillsides along the southern shore of Red Indian Lake, red micaceous sandstone is abundant, and it could relate either to this last phase of ice flow along the axis of the lake, or to earlier northeast flow associated with event II.

Correlations

East of the study area, Event I is likely correlated with the east-southeast 'first ice-flow event' described by St. Croix and Taylor (1991) because it appears to be the extension of the southeast flow trends of event I across the Badger map area (12A/16). To the west, in the Grand Lake valley north of Hinds Lake (Fig. 1), the oldest regional ice flow is westward to northwestward from a source on the Topsails Plateau (Batterson and Taylor, 1990; Batterson and Vatcher, 1992; Batterson and McGrath, 1993). Those ice flow trends are consistent with either event I or event III, although the regional character of flow would indicate correlation with event I.

Event II is likely correlated with the 'second ice-flow event' associated with north-northeast trending striations described by St. Croix and Taylor (1991). According to them, "The broad coverage and consistency of the north-northeast ice flow indicates a possible ice-divide, directly south of the area..." (St. Croix and Taylor, 1991, p. 64). The axis of their proposed ice divide trends nearly east-west south of Red Indian Lake. Its configuration and location, however, are not consistent with the well defined northeast ice flow trends associated with event II within the study area.

The 'third ice-flow event' recorded by St. Croix and Taylor (1991) is defined by northeast striations that crosscut earlier, north-northeast flow. According to them, "This third flow represents either two separate, but local ice-flow events or two contemporaneous ice flows across the area." (St. Croix and Taylor, 1991, p. 65). Their third ice flow event likely relates to late glacial drawdown toward Notre Dame Bay, and is thus equivalent to event IIb.

Correlation of either event III or IV with youngest striations mapped outside the study area is difficult. Late glacial events could have only local significance either within the context of a thinning ice cap or as part of separate, remnant ice caps, and may have occurred late during deglaciation. In the Grand Lake valley, youngest flow trends are topographically directed generally southwestward along the axis of the valley, and they are associated with a relatively thin ice-mass (Batterson and Taylor, 1990). They could be associated with late glacial event III, with ice flowing generally northwestward from Hinds Lake feeding glacier ice confined within Grand Lake valley.

Implications for ice cap reconstructions

Although the erosional record of ice flow constitutes an important basis for ice sheet reconstructions, the depositional history recorded in stratigraphic sections (e.g. Sparkes, 1985), is critical to the interpretation of non-glacial events and to the character of ice flow defined by striations. Due to an absence of buried organic materials, there is no radiocarbon basis for dating the glacial events described here, and stratigraphic evidence in mine exposures and borrow pits (e.g. Sparkes, 1985; Vanderveer and Sparkes, 1982) is limited. Based on a few poorly preserved pollen grains within sub-till lake sediments, Sparkes (1985) speculated that early southward flow (i.e. event I) could be pre-Wisconsinan.

Differential staining of surfaces striated by different ice flow events occurs in the Lake Ambrose map area (12A/10), and similar observations have been reported elsewhere in Newfoundland, and the maritime region of Canada (Grant, 1989). Grant (1989) speculated that the iron stain is indicative of chemical weathering during ice-free periods. Thus a non-glacial interval could separate events I and II. The consistency of trends recorded by event I and II striations indicates that both events are associated with extensive ice cover, and thus a non-glacial event separating those events would indicate significant change in the Newfoundland ice cap.

The divergence of ice flow from the eastern margin of Topsails Plateau indicates flow within the ice cap during event II was topographically affected, and that ice flowing across from the plateau was insufficient to prevent ice flowing northeastward across its southern margin from diverging north northeastward and northward around the eastern margin of the plateau. There is approximately 200 m difference in elevation between the plateau surface and the central and eastern parts of the Dawes Pond map area. The topographic effects indicate that event II is likely associated with an island-centred ice cap of limited overall thickness.

The interpretations presented in this report are consistent with the glacial model suggested by Grant (1974) that depicts an evolution from a Newfoundland ice sheet, perhaps one characterized by separate domes, to multiple separate remnant ice caps during deglaciation. As shown by Grant (1974, Fig. 1, p. 216), one remnant ice cap was likely located over the Topsails Plateau.

ACKNOWLEDGMENTS

P.J. Henderson (in 1991) and F.J. Thompson (in 1992) made significant contributions through mapping indicator erratics and measuring striations, and this report is based in part on their fieldwork and discussions with them. E. Shilts and A. Jones, and J. Rutherford, C. Johns, and C. O'Hara are thanked for their enthusiastic work as field assistants during the summers of 1991 and 1992, respectively. The manuscript was reviewed by B. McClenaghan.

REFERENCES

Batterson, M. and McGrath, B.
1993: Quaternary geology of the Deer Lake and Pasadena map areas (NTS 12H/3 and 12H/4); in Current Research; Newfoundland Department of Mines and Energy, Geological Survey Branch, Report 93-1, p. 103-112.

Batterson, M.J. and Taylor, D.M.
1990: Glacial history of the Humber River basin; in Current Research; Newfoundland Department of Mines and Energy, Report 90-1, p. 1-6.

Batterson, M.J. and Vatcher, S.V.
1992: Quaternary geology of the Corner Brook-Pasadena area (NTS 12A/13 and 12H/4); in Current Research; Newfoundland Department of Mines and Energy, Geological Survey Branch, Report 92-1, p. 1-12.

Graham, D.F. and Grant, D.R.
1991: A test of airborne, side-looking synthetic-aperture radar in central Newfoundland for geological reconnaissance; Canadian Journal of Earth Sciences, v. 28, p. 257-265.

Grant, D.R.
1974: Prospecting in central Newfoundland and the theory of multiple shrinking ice caps; in Report of Activities; Geological Survey of Canada, Paper 74-1, Part B, p. 215-216.
1975: Surficial geology of Red Indian Lake map-area, Newfoundland-A preliminary interpretation; in Report of Activities; Geological Survey of Canada, Paper 75-1, Part B, p. 111-112.
1989: Quaternary geology of the Atlantic Appalachian region of Canada; Chapter 5 in Quaternary Geology of Canada and Greenland, R.J. Fulton (ed.); Geological Survey of Canada, Geology of Canada, no.1, p. 393-440.

Grant D.R. and Tucker, C.M.
1976: Preliminary results of terrain mapping and base metal analysis of till in the Red Indian Lake and Gander Lake map-areas of central Newfoundland; in Report of Activities, Part A; Geological Survey of Canada, Paper 76-1A, p.283-285.

James, L.D. and Perkins, E.W.
1981: Glacial dispersion from sulphide mineralization, Buchans area, Newfoundland; in The Buchans Orebodies: Fifty Years of Geology and Mining, (ed.) E.A. Swanson, D.F. Strong, and J.G. Thurlow; Geological Association of Canada, Special Paper 22, p. 269-283.

Liverman, D.G.E., Scott, S., and Vatcher, H.
1991: Quaternary geology of the Springdale map area (12H/8); in Current Research; Newfoundland Department of Mines and Energy, Geological Survey Branch, Report 91-1, p. 29-44.

Lundqvist, J.
1965: Glacial geology in northeastern Newfoundland; Geologiska Foreningen i Stockholm Forhandlingar, v. 87, p. 285-306.

Mihychuck, M.
1985: Drift prospecting in the Victoria and Tally Pond areas, central Newfoundland; in Current Research; Newfoundland Department of Mines and Energy, Report 85-1. p. 99-104.
Murray, R.C.
1955: Directions of glacier ice motion in south-central Newfoundland; Journal of Geology, v. 63, p. 268-274.
Neary, G.
1981: Mining history of the Buchans area; in The Buchans Orebodies: Fifty Years of Geology and Mining, (ed.) E.A. Swanson, D.F. Strong, and J.G. Thurlow; Geological Association of Canada, Special Paper 22, p. 1-64.
Prest, V.K.
1983: Canada's Heritage of Glacial Features; Geological Survey of Canada, Miscellaneous Report 28, 119 p.
Prest, V.K., Grant, D.R., and Rampton, V.N.
1969: Glacial Map of Canada, Geological Survey of Canada, Map 1253A.
St. Croix, L. and Taylor, D.M.
1990: Ice flow in north-central Newfoundland; in Current Research; Newfoundland Department of Mines and Energy, Geological Survey Branch, Report 90-1, p. 85-88.
1991: Regional striation survey and deglacial history of the Notre Dame Bay area Newfoundland; in Current Research; Newfoundland Department of Mines and Energy, Geological Survey Branch, Report 91-1, p. 61-68.
Sparkes, B.G.
1984: Surficial and glacial geology, central Newfoundland, including geochemistry of till samples Victoria Lake (12A/6), Snowshoe Pond (12A/7), Star Lake (12a/11); Mineral Development Division, Newfoundland Department of Mines and Energy, Open File 12A (347), 11 p. and appendix.
1985: Quaternary mapping, Central Volcanic Belt; in Current Research; Newfoundland Department of Mines and Energy, Geological Survey Branch, Report 85-1, p. 94-98.
1987: Glacial geology and till geochemistry of the Buchans (12A/15) map area, Newfoundland; Mineral Development Division, Newfoundland Department of Mines and Energy, Open File 12A/15 (396), 11 p.
Vanderveer, D.G. and Sparkes, B.G.
1982: Regional Quaternary mapping-an aid to mineral Exploration in west-central Newfoundland; Prospecting in Areas of Glaciated Terrain, (ed.) P.H. Davenport; Canadian Institute of Mining, Geology Division Publication, p. 284-299.

Geological Survey of Canada Project 910002

The Dunnage Melange, Newfoundland, revisited

Harold Williams[1]
Continental Geoscience Division

Williams, H., 1994: The Dunnage Melange, Newfoundland, revisited; in Current Research 1994-D; Geological Survey of Canada, p. 23-31.

Abstract: Most of the northeast portion of the Dunnage Melange was remapped in 1993 and relationships examined elsewhere. In the northeast, the Dunnage Melange occupies an overturned anticline, thrust modified along its northwest overturned limb and truncated to the southeast by the Reach Fault.

The variety of blocks within the mélange and proportions of lithologies are different than the kinds of rocks and their proportions in nearby groups. A variety of structures from disrupted greywacke beds to psammites and disaggregated schists all formed in the mélange. Bedded sections within the mélange contain recycled disaggregated greywacke blocks. The mélange was also the locus of Ordovician intrusions, some with intricate and ambiguous intrusive relations.

The regional chaos is largely olistostromal, overprinted by a variety of tectonic and intrusive effects. These effects are illustrated in superb exposures and their understanding is key to the structural evolution and plate tectonic setting of the Dunnage Melange.

Résumé : La majeure partie du secteur nord-est du Mélange de Dunnage a été recartographiée en 1993 et l'auteur en a examiné ailleurs les liens avec les roches encaissantes. Au nord-est, le Mélange de Dunnage occupe un anticlinal déversé, modifié par un charriage survenu sur son flanc déversé vers le nord-ouest, et tronqué au sud-est par la faille de Reach.

Les divers types de blocs du mélange et les proportions des lithologies diffèrent par rapport aux types de roches et à leurs proportions dans les groupes proches. Diverses structures allant de couches de grauwacke fragmentées à des psammites et à des schistes désagrégés, se sont toutes formées dans le mélange. Les intervalles stratifiés à l'intérieur du mélange contiennent des blocs recyclés de grauwacke désagrégé. Le mélange a également été un lieu préférentiel de mise en place d'intrusions à l'Ordovicien, dont certaines montrent entre elles des relations compliquées et ambiguës.

Cette accumulation chaotique de blocs d'étendue régionale constitue en grande partie un olistostrome, auquel se sont superposés divers effets tectoniques et intrusifs. Ces effets ont laissé leur trace dans de superbes affleurements et il est essentiel de les comprendre afin expliquer l'évolution structurale du Mélange de Dunnage et de définir le milieu que celui-ci occupe dans le cadre de la tectonique globale.

[1] Department of Earth Sciences, Memorial University of Newfoundland, St. John's, Newfoundland A1B 3X5

INTRODUCTION

The Dunnage Melange is the most distinctive feature of the central belt of the Newfoundland Appalachians, from which the Dunnage Zone takes its name. Its resistive blocks, up to a kilometre or more in diameter, are expressed as islands, shoals, or sunkers in the coastal region and as inland knolls. Its shaly matrix is recessive but forms wide shoreline benches. Because of its morphological expression and coastal setting, the Dunnage Melange is superbly exposed at low tide and is easy to access.

Since its discovery in the early 1960s, the Dunnage Melange has been included in many plate-tectonic models (see Hibbard and Williams, 1979 for review). Its internal makeup has been viewed both as olistostromal (e.g., Hibbard and Williams, 1979) and tectonic (e.g., Karlstrom et al., 1982). Its regional setting has been interpreted as linked to nearby groups (Horne, 1969, 1970; Kay, 1976; Hibbard and Williams, 1979; Wasowski and Jacobi, 1985) or a suspect terrane (Elliott et al., 1991; Lafrance and Williams, 1992). Internally, it shows all the complications of olistostromal and tectonic processes. An Ordovician age of formation is indicated by fossil ages of blocks and matrix, lack of younger components, and isotopic ages of intrusions that cut the mélange.

In 1993, 1:50 000 mapping in the Comfort Cove (2E/7) and Twillingate (2E/10) areas provided an opportunity to re-examine the Dunnage Melange and reassess its salient features.

NATURE OF DUNNAGE BOUNDARIES AND STRUCTURAL SETTING

Along its southeast margin, the Dunnage Melange is bounded by the Reach Fault or truncated by the Loon Bay Batholith (Fig. 1). At its southwest termination between Thwart Island and Lewisporte just west of Figure 1 (Hibbard and Williams, 1979; O'Brien, 1993), the New Bay Formation of the Early and Middle Ordovician Exploits Group faces northeastward toward the Dunnage Melange. The boundary has been interpreted as conformable (Hibbard and Williams, 1979) or faulted (O'Brien, 1993). Gabbro sills, so common in the New Bay Formation cut the Dunnage Melange, thus establishing an intrusive link.

Along its northwest boundary from Cheneyville to Farmers Island (Fig. 1), Middle Ordovician to Silurian sedimentary rocks (Dildo sequence of Kay, 1976) dip southeast and face northwest away from the mélange. The boundary here has also been interpreted as conformable (Horne, 1969, 1970; Hibbard and Williams, 1979) and faulted (Kay, 1976; Lorenz, 1984a; van der Pluijm, 1986; Elliott et al. 1991; Lafrance and Williams, 1992). The different interpretations are somewhat dependent upon where the boundary is drawn. For example, some workers located the boundary south of the conglomerates at Cheneyville (Dean and Strong, 1975; Kay, 1976; van der Pluijm, 1986) and it has been placed farther south on Coaker Island (Lorenz, 1984a) beneath shales that resemble the base of the Dildo sequence. Along the southeast shore of New World Island (Fig. 1), the boundary is commonly marked by disrupted black graptolitic shales, like those at Joe Whites Cove, and conglomerates and buff limestones and shales, like those at Cheneyville (Fig. 1). Volcanic blocks in black shale occur north of Cheneyville, exposed at low tide on the south side of the cove west of Cheneyville. The north-facing Cheneyville section, previously regarded as the base of the Dildo sequence is actually within the Dunnage Melange rather than an unconformable or faulted cover. Nearby at Coaker Island and islands and shoals to the west, bedded sections of black and grey shales alternate with mélange. All may be part of a conformable northwest-facing stratigraphic section or the alternations may represent structural repetition of mélange and cover rocks. Clasts of Coaker Porphyry, which cuts the Dunnage Melange, were reported in Cheneyville conglomerates (Kay, 1976). A few of the porphyry clasts resemble the Coaker Porphyry but many more are atypical and of unknown provenance. This important sedimentary relationship requires further confirmation.

At the east end of Dildo Run Provincial Park, intensely cleaved Caradocian shales of the Dildo sequence, Dark Hole Formation (Horne, 1969), dip gently southeast below mafic volcanic rocks regarded as blocks in the Dunnage Melange. This indicates that the Dunnage Melange is thrust northwestward above the Dildo sequence as suggested by van der Pluijm (1986). Northwest thrusting agrees with the structural style of most Ordovician-Silurian sequences at New World Island that dip southeast and face northwest, and with the style of northwest overturned regional folds at Pikes Arm (Arnott et al., 1985), Port Albert Peninsula, and Change Islands (Williams, 1993). Before thrusting, the Dunnage-Dark Hole boundary was probably stratigraphic because the Caradocian Dark Hole Formation and overlying greywackes at New World Island are traceable southwestward into the same units at the stratigraphic top of the Exploits Group, which itself had an earlier intrusive link with the Dunnage Melange (Hibbard and Williams, 1979).

Correlation of the Dildo sequence with similar rocks east of the Reach Fault at Port Albert Peninsula (Karlstrom et al., 1982; Williams, 1993) indicates that the northeastern portion of the Dunnage Melange occupies an overturned anticline, thrust modified along its northwest overturned limb and truncated to the southeast by the Reach Fault.

In the southeast at southern Chapel Island, a thick section of coarse greywackes and conglomerates, Chapel formation (Lorenz, 1984a), is exposed on a logging road. The section is steeply-dipping, southeast-facing and apparently conformable above mélange. A wide sill of fine grained Coaker Porphyry separates the greywackes and conglomerates from shales with coticules farther south, which are in turn truncated by the Loon Bay Batholith. Other southeast-facing bedded sections occur along the southeast side of the mélange at the east shore of Chapel Island, Holmes Point, and Newmans Point of Boyds Cove. These southeast-facing sections on its southeast side complement the northwest-facing sections within the mélange on its northwest side at Cheneyville and western Coaker Island, thus supporting an anticlinal structure.

The Boyds Cove Complex (Kay, 1976) at Holmes Point and northeastward is a combination of fine grained Coaker Porphyry and Silurian sandstones and volcanic rocks, baked

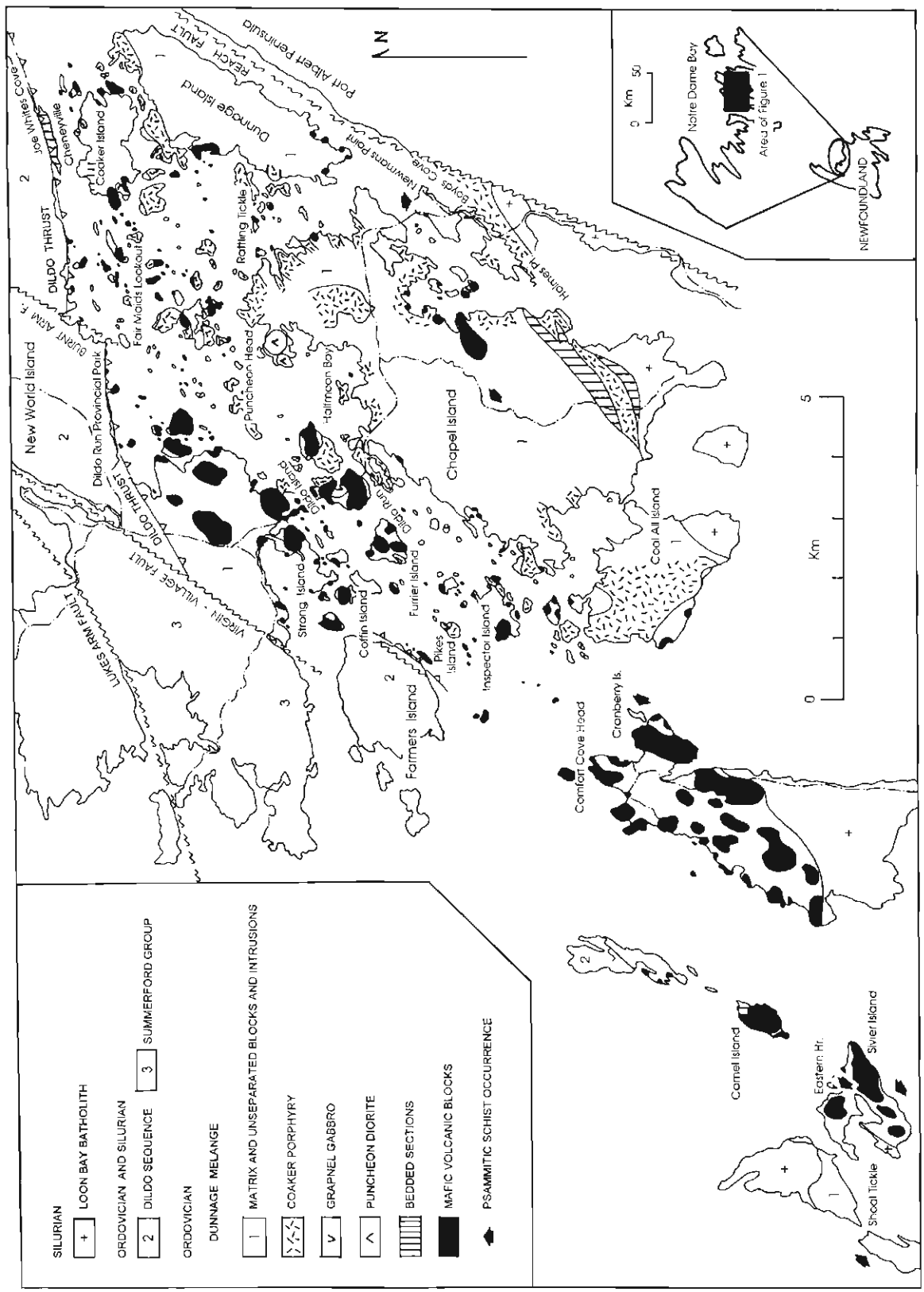

Figure 1. General geology of the Dunnage Melange.

by the Loon Bay Batholith and broken by the Reach Fault (Williams, 1993). The Holmes Point Fault (Kay, 1976) is a minor splay of the Reach Fault that is not traceable to nearby Chapel Island.

The thickness and subsurface geometry of the Dunnage Melange remain unknown. Mélange is absent a few kilometres northwest of its boundary in Ordovician stratigraphic sections, and nothing comparable in scale to the Dunnage Melange occurs immediately east of the Reach Fault, although there are small occurrences of mélange beneath Siluran cover rocks at Stoneville and Dog Bay Point and larger occurrences at Gander Bay and Carmanville (Williams et al., 1991; Williams, 1992, 1993; Currie, 1993).

DUNNAGE MELANGE ROCK TYPES

The most obvious components of the Dunnage Melange are large round blocks of mafic volcanic rocks with fragmental rocks (Fig. 2) more abundant than pillow lavas (Fig. 3). Grey limestone is a common associate of the mafic volcanic rocks. Volcanic blocks shown separately in Figure 1 have dimensions exceeding 50 m and some are a kilometre across. Quartz greywackes, commonly micaceous, are the second most abundant rock type. Greywacke occurs in large, discrete blocks but more commonly as broken formations or as ellipsoidal blocks surrounded by resistant masses of smaller disaggregated blocks. Other important components of the Dunnage Melange are silicic volcanic rocks, limestones, conglomerates, cherts, and psammitic schists. Minor oddities are coarse fragmental mafic volcanic rocks with cobbles and boulders of gabbro and granodiorite near the boat launch of Dildo Island, mixtite with sparse well-rounded cobbles of quartzite and limestone (Fig. 4), and a block of massive ferrugenous manganiferous chert that contains an impressive exploration shaft at northwest Chapel Island. Serpentinites, ultramafic rocks, or other ophiolitic components are absent.

The Dunnage Melange also has bedded sections: volcanic rocks, limestone, black shale, and shales with coticules at Camel Island; conglomerate, greywacke, and siltstone at Cheneyville, Rattling Tickle, and Newmans Point; grey chert and black argillite at northeast Coffin Island; and black and grey shales and green shales and siltstones at western Coaker Island and nearby islands to the west. Camel Island has the thickest intact section, exposed along its eastern side. Limestones toward the south are overlain by tuffs and shales with coticule layers and wisps, followed northward by two distinctive volcanic units with metre-scale limestone blocks, in turn followed by more shales with coticule (Fig. 5). This is one of the few places where the coticule rocks of eastern Notre Dame Bay are clearly within a stratigraphic association. Conglomerates at Newmans Point are polymictic with granitoid clasts and synsedimentary ripups of coarse greywacke and dark siltstone. Thin bedded siltstones are conformable within a conglomerate occurrence at the extreme northeast tip of Newmans Point, and the siltstones contain a round resistive block of disaggregated greywacke. It is uncertain whether the bedded section of southern Chapel Island is within the mélange or a stratigraphic cover. It too contains clasts of cleaved and disaggregated psammitic rocks.

Figure 2. *Volcanic breccia in the Dunnage Melange, Strong Island.*

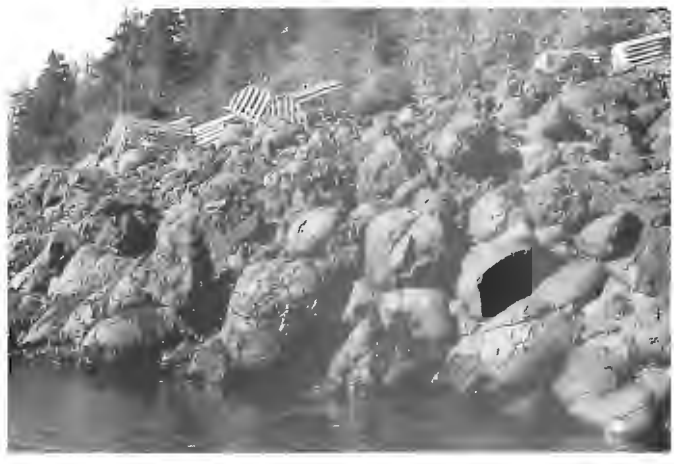

Figure 3. *Pillow lava in a 1 km block southwest of Comfort Cove Head. Limestone fills pillow intersticies.*

Figure 4. *Mixtite with rounded quartzite clasts (white) and limestone clasts (smaller, grey), northwest shore of Strong Island.*

The matrix of the mélange is black, grey, green, and locally red shales with streaky layers of former beds and recumbent folds of bedding and cleavage. Matrix shales alternate with pebbly black shales that are mixed with disaggregated greywackes, combinations of which also form a matrix surrounding some volcanic blocks.

Many of the blocks can be matched with nearby rocks of the Exploits and Summerford groups to the northwest (Hibbard and Williams, 1979), and some volcanic breccias resemble the Loon Harbour volcanics to the southeast (Currie, 1994); however, the variety of blocks is far greater in the mélange and some are of unknown provenance, such as a volcanic block containing fossiliferous Middle Cambrian limestone at southeast Dunnage Island (Kay and Eldridge, 1968), mafic volcanic breccias with granitoid and gabbroic clasts, mixtite, and ferruginous manganiferous chert. The proportions of lithologies in the mélange are different than those in nearby groups (i.e., the abundance of greywackes and black and green shales in the mélange compared to nearby groups).

Disregarding intrusive rocks, equant blocks greater than 5 m diameter make up about 25% of the mélange, blocks from 0.5 m to 5 m make up another 20%, cobbly to pebbly sandstone 20%, and bedded sections and matrix the remainder.

INTERNAL FEATURES OF THE DUNNAGE MELANGE

The internal chaos of the Dunnage Melange defines it as a mappable unit distinct from surrounding rocks. The chaos results from processes that range from syndepositional soft rock deformation to penetrative shearing with the development of cleavages and schistosities, to brittle breakup or disaggregation of tough greywackes and psammitic schists. These structures are all thought to be Ordovician because they are restricted to the Dunnage Melange, and the Coaker Porphyry, dated at 467 ± 5 Ma (Elliott et al., 1991), cuts mélange as well as the bedded section at southern Chapel Island that contains intraformational deformed psammitic clasts. An ubiquitous northeast-trending, southeast-dipping cleavage is equated with cleavage in adjacent Silurian rocks and development of the regional Dunnage anticline.

The first order chaotic style of the mélange is attributed to soft rock deformation and olistostromal effects as the variety of blocks and matrices cannot be equated with a known stratigraphic section, and the largest discrete blocks are equidimensional, lack peripheral cleavage, and are surrounded by shales without intense shearing. Internally, bouldery to pebbly mudstones are also olistostromal, but breakup and disaggregation of tough greywackes and cleaved or schistose rocks are tectonic.

Local, internal cleavage and schistosity are most obvious in greywackes. Some blocks show internal gradations from massive greywacke to cleaved greywacke (Fig. 6) or to kinked psammitic schist (Fig. 7). Single exposures show variations from bedded sections or slightly disrupted angular beds in shale (Fig. 8), zones of disaggregaed greywacke with

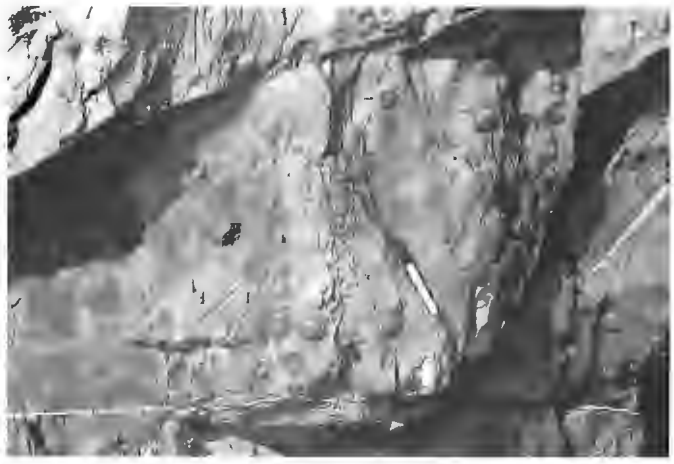

Figure 5. *Coticule nodules in shale, northeast end of Camel Island.*

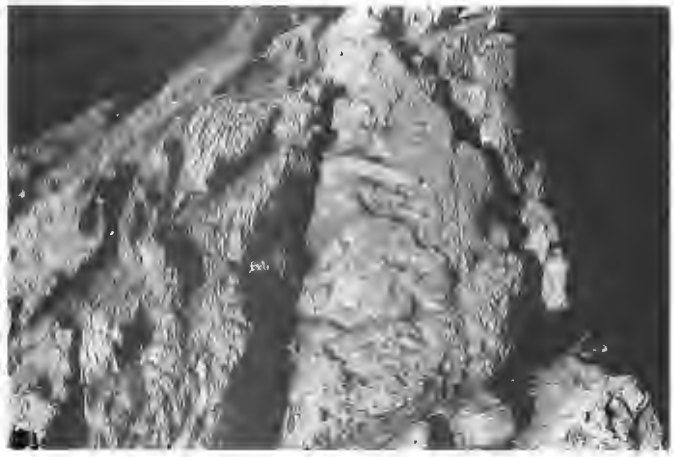

Figure 6. *Massive greywacke (right) gradational with cleaved greywacke (left); small volcanic island northeast of Furrier Island.*

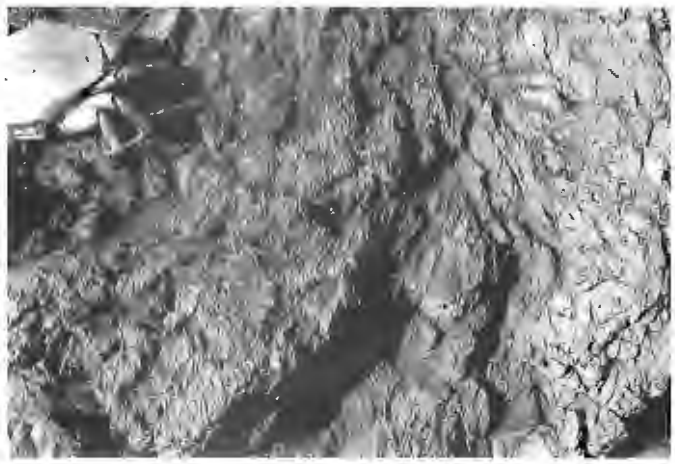

Figure 7. *Kinked psammitic schist within disaggregated greywacke mélange, same outcrop as Figure 6.*

abraded rounded blocks in a sandy matrix of smaller clasts (Fig. 9), to zones of sheared greywacke with disoriented schistose clasts in a cleaved sandy matrix (Fig. 10). Examples of these variations at southwest Dunnage Island are gradational, but in other places zones of sheared greywacke with cleaved clasts are in sharp contact with slightly disrupted bedded greywackes and siltstones, such as at the northwest shore of Inspector Island, or with thin bedded cherts and argillites, such as at the northeast end of Coffin Island, implying tectonic juxtapositioning of the structurally contrasting rocks. Brecciation or tectonic disaggregation affects all varieties of greywackes, and it is especially evident at the peripheries of massive larger blocks and as zones affecting already cleaved greywackes.

The most deformed rocks are psammitic schists with quartz plates, veins, and stringers (Fig. 11). Schistosity is everywhere discontinuous, either folded and truncated by later shears or truncated by zones of brecciation (Fig. 12).

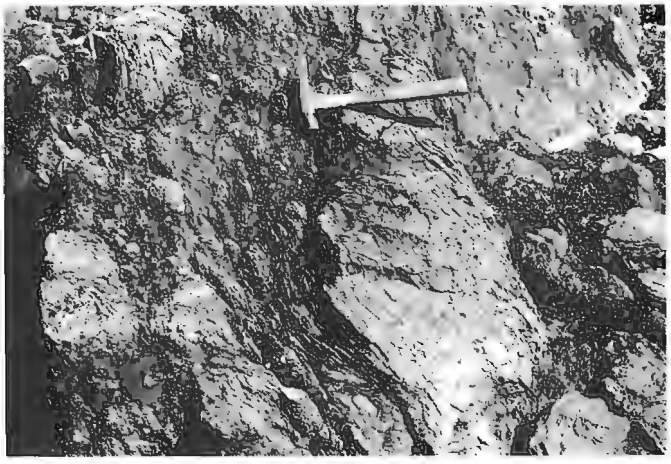

Figure 10. *Sheared greywacke breccia containing cleaved or schistose greywacke clasts, southwest end of Dunnage Island.*

Figure 8. *Slightly disrupted greywacke beds in shale, southwest end of Dunnage Island.*

Figure 11. *Disaggregated psammitic schist within Dunnage Melange at the southeast side of Sivier Island.*

Figure 9. *Disaggregated greywacke gradational with disrupted greywacke beds at southwest end of Dunnage Island.*

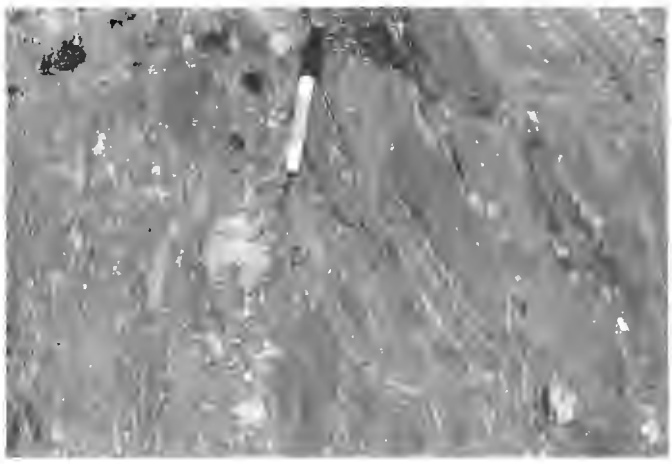

Figure 12. *Psammitic schist (right) crossed by a zone of disaggregated psammite and quartz clasts (left), Eastern Harbour of Sivier Island.*

Psammitic schists occur as blocks of 1 m or less in shaly mélange matrix but most occurrences are larger and tens of metres across. The larger occurrences are juxtaposed with pebbly mudstones or shales with marked structural contrast. A psammitic schistose block with extensive internal brecciation and trains of smaller clasts in a black shale matrix occurs at Newmans Point. Larger areas of pasmmitic schist occur just southwest of Shoal Tickle, at Eastern Harbour of Sivier Islands and along the southeast shore of Sivier Island, at Cranberry Island southeast of Comfort Cove Head, and on the logging road of central Chapel Island. The locus of these major occurrences is a narrow zone crossing the interior of the mélange in a northeast direction.

INTRUSIVE ROCKS

The Dunnage Melange is host to a variety of intrusions. The most voluminous is the Coaker Porphyry, which is unique to the northeast portion of the mélange where it comprises about a third of the outcrop area (Fig. 1). The Coaker Porphyry cuts small mafic intrusions, such as the Puncheon Diorite (Kay, 1976; Lorenz, 1984a) at Puncheon Head, and it may be coeval with others, such as the Grapnel Gabbro (Hibbard, 1976; Lorenz, 1984a) of Pikes Island. The Puncheon Diorite occurs in at least two nested stocks that have coarse grained, relatively felsic interiors and finer grained mafic exteriors. Northeast-trending and southeast-dipping mafic dykes cut the Coaker Porphyry and mélange. These are especially numerous between Inspector Island and Dildo Run and along the shoreline of nearby Chapel Island. The Loon Bay Batholith, dated at 408 ± 2 Ma (Elliott et al., 1991), cuts the Coaker Porphyry at southern Chapel Island and Coal All Island. Absence of mafic dykes within the batholith compared to nearby mélange suggests the dykes are older, and this is supported by their scarcity or absence in adjacent Middle Ordovician and Silurian formations. Relationships of gabbro sills at the southwest portion of the mélange to the Coaker Porphyry and other intrusions in the northeast are unknown. The gabbro sills in the southwest are interpreted as Ordovician as they are mainly confined to the New Bay Formation of the Exploits Group and they do not cut Caradocian black shales or higher units.

The Coaker Porphyry is of special interest because of its abundance and localization within the mélange, its Ordovician age, its xenoliths and mineralogy, and its spectacular interactions with surrounding shales (Lorenz, 1984a, b). The porphyry occurs as numerous small intrusions from a few kilometres to a few metres wide. The larger occurrences are weakly elongate in a northeast direction but contacts are irregular in detail with porphyry-mélange alternations. The porphyry cuts blocks and matrix of the Dunnage Melange but it is mainly hosted by matrix shales. Medium grained varieties have dense square feldspar phenocrysts and sparse to abundant mafic and ultramafic inclusions from 1-30 cm diameter. These inclusions are rounded, some mafic types are unaltered, but ultramafic types have pronounced reaction rims and radiating textures. Locally as at Halfmoon Bay and northeast Coaker Island, anhedral to euhedral red garnets, some more than 1 cm diameter, are common. Fine grained varieties are flow banded, commonly with a platy parting parallel to flow bands. Euhedral muscovite phenocrysts are present in the fine grained Coaker Porphyry at northeast Inspector Island.

The medium grained varieties occur in massive rounded stocks without significant chilling at their margins and sharp intrusive contacts with negligible to narrow metamorphic aureoles. The fine grained varieties occur as lenticular bodies, lobes, and bulbous masses that resemble giant pillows. Well-preserved intrusive surfaces are billowy and cracked (Fig. 13) to corrigated and fluted, with lobate terminations of lenticular bodies (Fig. 14). These features suggest intrusion into soft muds (Hibbard and Williams, 1979; Lorenz, 1984a, b). Complex interlayering and commingling with shale and pebbly shale is another less common feature of fine grained Coaker Porphyry (Fig. 15). This has been attributed also to magma

Figure 13. *Billowy, cracked surface of a small Coaker intrusion near boat launch of Dildo Island. Coil of rope in lower left lies on shale at intusive contact.*

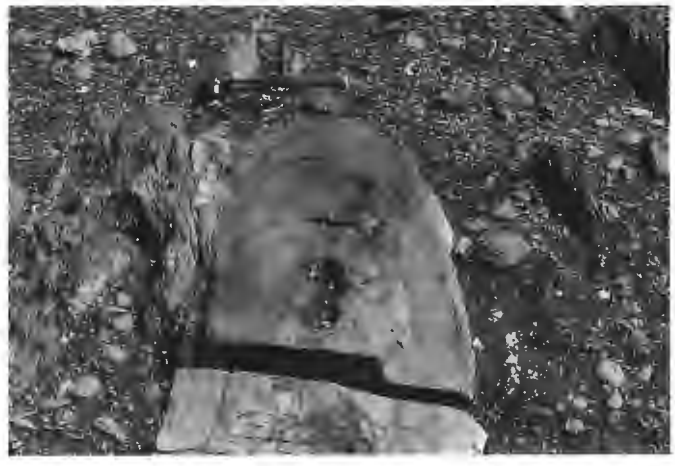

Figure 14. *Lobate termination of lenticular body of Coaker Porphyry, north end of Fair Maids Lookout.*

Figure 15. Interlayering and intricate commingling of Coaker Porphyry (light grey) and black shale (dark grey), Halfmoon Bay.

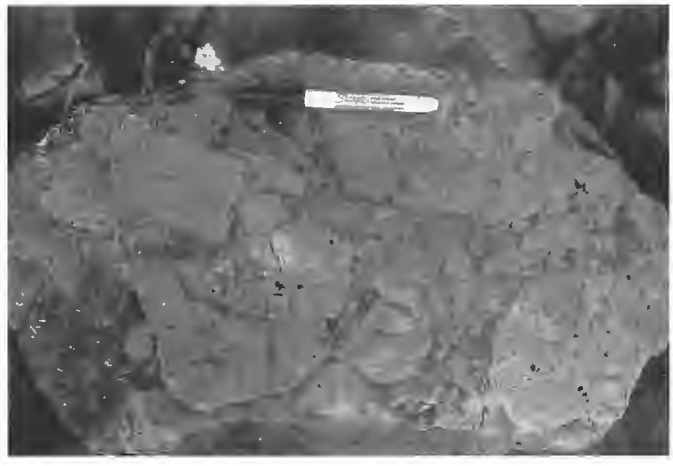

Figure 16. Breccia of fine grained Coaker Porphyry and shale at southwest Chapel Island.

injection into soft mud (Hibbard and Williams, 1979; Lorenz, 1984a, b), but it may be the result of remobilization of pebbly shale to fill gaps and intersticies of folded platy porphyry. The latter interpretation is supported by the fact that intricate interlayering only occurs where the fine grained Coaker Porphyry has open to tight folds of platy parting. Pebbly shales also occur as dykes that cut the Coaker Porphyry, blocks and matrix of nearby mélange, and cleavage in the mélange (Williams et al., 1988). Coaker Porphyry breccia with a black shale matrix (Fig. 16), interpreted as peperite or mud-magma explosive breccia (Lorenz, 1984a), is also probably the result of pebbly shale injection. The example at southwest Chapel Island is cut by a northeast-trending mafic dyke, setting an upper limit to this phase of activity.

The largest stock of uniformly coarse porphyritic Coaker occurs at Coal All Island, suggesting the deepest level of emplacement toward the southwest. However, there are many textural variations and no systematic patterns exist.

The Coaker Porphyry is interpreted as a peraluminous S-type rhyodacite that formed from partial melting of a metasedimentary source (Lorenz, 1984a). Older mafic intrusions such as the New Bay gabbro sills, Puncheon Diorite, Grapnel Gabbro, and later northeast-trending mafic dykes are not genetically related to the Coaker Porphyry. They are interpreted as within-plate tholeiites of an undepleted mantle source (Lorenz, 1984a).

CONCLUDING REMARKS

Relationships of the Dunnage Melange to surrounding rocks are still debatable and its internal complexities are far greater than envisaged in previous studies. Timing of commencement and termination are still unknown and parts of the mélange have a lively history of deformation, sedimentation, and continuing deformation and assembly of mélange components.

Links with the Exploits and Summerford groups apparently negate the idea that the mélange is a suspect terrane, but it is much more complicated than a simple slump and distal equivalent of the Exploits and Summerford groups. There is also little doubt of combined olistostromal and tectonic processes involved in mélange formation. Since the mélange is the locus for tectonic and intrusive effects, it is difficult to understand how such effects could be localized at a particular stratigraphic level without affecting underlying rocks.

If Coaker clasts occur in Cheneyville conglomerates and if the conglomerates are entrained within the mélange, the Coaker must also have been involved in late stages of mélange entrainment. Yet intrusive contacts of the Coaker Porphyry with surrounding rocks are intact, and there are no clear examples of Coaker blocks or clasts within the mélange.

Mafic-ultramafic inclusions within the Coaker Porphyry suggest an ophiolitic layer between its metasedimentary source rocks and the surface. The numerous intrusions within the confines of the mélange imply deep connections and that the mélange was not entirely controlled by surficial processes.

The structural styles of many torn up components and disrupted beds within the mélange are extensional and an extensional regime is also indicated by the quantity and frequency of intrusions into the mélange.

Compared to other mélanges in Newfoundland, the Dunnage is much thicker, more polymictic, has more internal structural complications, had a more prolonged evolution, and was the locus of contemporary intrusions. Regardless of its setting and controls, the Dunnage Melange is the best exposed in the Appalachian Orogen and its wave-washed outcrops contain important facts about the processes of mélange development, such as recycling of intraformational schistose rocks, causes of disaggregation, mechanics of mud-magma relationships, and the properties of fluidized muds and their interaction with resistant igneous rocks. A knowledge and understanding of these processes may be the most important lessons from the Dunnage Melange. Like other

mélanges, its tectonic message is undoubtedly profound but that message awaits further studies and resolution of the myriad of internal problems.

All previous workers correlated the Dunnage Melange with the Carmanville Melange to the east, mainly because they have similar volcanic and sedimentary blocks and matrices and both are associated with coticule-bearing shales and siltstones (Williams, 1992). Recognition of widespread psammitic schist occurrences within the Dunnage Melange is another link with the Carmanville Melange. The metamorphic rocks are interpreted as intraformational in the Carmanville example (Williams et al., 1991) and this is supported by relations within the Dunnage Melange, implying similar internal processes of deformation, disaggregation, and recycling.

Correlating the Dunnage and Carmanville mélanges places the Dunnage Melange on the eastern side of Iapetus and favours a back-arc setting with respect to an Exploits arc to the west. Formation of the Dunnage Melange is coeval, at least in part, with the destruction of the Laurentian margin of Iapetus and with the interaction of the Exploits Subzone with the Gander Zone. Thus it formed in an extensional setting at a time when Iapetus was contracting.

ACKNOWLEDGMENTS

This work was conducted through a contract with the Department of Energy, Mines and Resources. I wish to thank K.L. Currie for his support, companionship, and discussions in the field, and Charles Conway for reproducing Figure 1. K.L. Currie and C.R. van Staal are also thanked for reviewing the manuscript.

REFERENCES

Arnott, R.J., McKerrow, W.S., and Cocks, L.R.M.
1985: The tectonics and depositional history of the Ordovician and Silurian rocks of Notre Dame Bay, Newfoundland; Canadian Journal of Earth Sciences, v. 22, p. 607-618.

Currie, K.L.
1992: A new look at Gander-Dunnage relations in Carmanville map-area, Newfoundland; in Current Research, Part D; Geological Survey of Canada, Paper 92-1D, p. 27-33.
1993: Ordovician-Silurian stratigraphy between Gander Bay and Birchy Bay, Newfoundland; in Current Research, Part D; Geological Survey of Canada, Paper 93-1D, p. 11-18.
1994: Reconsidering parts of Comfort Cove and Gander River map areas, Dunnage Zone of Newfoundland; in Current Research 1994-D; Geological Survey of Canada.

Dean, P.L. and Strong, D.F.
1975: Twillingate, Newfoundland; Mineral Development Division, Newfoundland Department of Mines and Energy, scale 1:50 000, map and marginal notes.

Elliott, C.G., Dunning, G.R., and Williams, P.F.
1991: New U-Pb zircon age constraints on the timing of deformation in north-central Newfoundland and implications for early Paleozoic Appalachian orogenesis; Geological Society of America, Bulletin, v. 103, p. 125-135.

Hibbard, J.P.
1976: The southwest portion of the Dunnage Melange and its relationships to nearby groups; M.Sc. thesis, Memorial University of Newfoundland, St. John's, Newfoundland, 131 p.

Hibbard, J.P. and Williams, H.
1979: The regional setting of the Dunnage Melange in the Newfoundland Appalachians; American Journal of Science, v. 279, p. 993-1021.

Horne, G.S.
1969: Early Ordovician chaotic deposits in the Central Volcanic Belt of northeast Newfoundland; Geological Society of America, Bulletin, v. 80, p. 2451-2464.
1970: Complex volcanic-sedimentary patterns in the Magog Belt of northeastern Newfoundland; Geological Society of America, Bulletin, v. 81, p. 1767-1788.

Karlstrom, K.E., van der Pluijm, B.A., and Williams, P.F.
1982: Structural interpretation of the eastern Notre Dame Bay area, Newfoundland: regional post-Middle Silurian thrusting and asymmetrical folding; Canadian Journal of Earth Sciences, v. 19, p. 2325-2341.

Kay, M.
1976: Dunnage Melange and subduction of the Protoacadic Ocean, northeast Newfoundland; Geological Society of America, Special Paper 175, 49 p.

Kay, M. and Eldredge, N.
1968: Cambrian trilobites in central Newfoundland volcanic belt; Geological Magazine, v. 105, no. 4, p. 372-377.

Lafrance, B. and Williams, P.F.
1992: Silurian deformation in eastern Notre Dame Bay, Newfoundland; Canadian Journal of Earth Sciences, v. 29, p. 1899-1914.

Lorenz, B.E.
1984a: A study of the igneous intrusive rocks of the Dunnage Melange, Newfoundland; Ph.D. thesis, Memorial University of Newfoundland, St. John's, Canada, 220 p.
1984b: Mud-magma interactions in the Dunnage Melange, Newfoundland; in Marginal Basin Geology, (ed.) E.P. Kokelaar and M.F. Howells; Geological Society, Special Publication, no. 16, p. 271-277.

O'Brien, B.H.
1993: Geology of the region around Lewisporte (parts of 2E/2,3,6,7), north-central Newfoundland; Geological Survey Branch, Department of Mines and Energy, Map 92-25.

van der Pluijm, B.A.
1986: Geology of eastern New World Island, Newfoundland: an accretionary terrane in the northeastern Appalachians; Geological Society of America, Bulletin, v. 97, p. 932-945.

Wasowski, J.J. and Jacobi, R.D.
1985: Geochemistry and tectonic significance of the mafic volcanic blocks in the Dunnage melange, north central Nrewfoundland; Canadian Journal of Earth Sciences, v. 22, p. 1248-1256.

Williams, H.
1992: Melanges and coticule occurrences in the northeast Exploits Subzone, Newfoundland; in Current Research, Part D; Geological Survey of Canada, Paper 92-1D, p. 121-127.
1993: Stratigraphy and structure of the Botwood Belt and definition of the Dog Bay Line in northeastern Newfoundland; in Current Research, Part D; Geological Survey of Canada, Paper 93-1D, p. 19-27.

Williams, H., Piasecki, M.A.J., and Johnston, D.
1991: The Carmanville Melange and Dunnage-Gander relationships in northeast Newfoundland; in Current Research, Part D; Geological Survey of Canada, Paper 91-1D, p. 15-23.

Williams, P.F., Elliott, C.G., and Lafrance, B.
1988: Structural geology and melanges of eastern Notre Dame Bay, Newfoundland; Geological Association of Canada, Field Trip Guidebook, Trip B2, 60 p.

Geological Survey of Canada Project 730044

Reconsidering parts of Comfort Cove and Gander River map areas, Dunnage Zone of Newfoundland

K.L. Currie
Continental Geoscience Division

Currie, K.L., 1994: Reconsidering parts of Comfort Cove and Gander River map areas, Dunnage Zone of Newfoundland; in Current Research 1994-D; Geological Survey of Canada, p. 33-40.

Abstract: The map area consists of five regions: (i) east of Dog Bay Line, underlain by Ordovician Hamilton Sound Group and disconformably overlying Silurian Indian Islands Group, (ii) Dog Bay Line-Reach Fault region, characterised by Duder complex of intensely cleaved sedimentary rocks containing large blocks of mafic igneous rocks, (iii) northeast Bay of Exploits underlain by Dunnage Melange, (iv) Indian Arm-Loon Bay region underlain by Loon Bay batholith, and (v) Campbellton-Long Pond region underlain by mid-Ordovician to Silurian turbidites and volcanic rocks. Silurian and Devonian rocks (Ten Mile sandstone, Loon Bay batholith) link the regions. Loon Bay batholith comprises two plutons originating from different sources than felsic igneous rocks of Dunnage Melange, and marks a structural boundary against which the melange is truncated and strata of the Campbellton-Long Pond region are warped. Mid-Ordovician obduction and rifting, followed by Silurian subduction could explain the observations.

Résumé : Cette région cartographique comprend cinq secteurs : (i) la région à l'est de la ligne de Dog Bay, occupée par le Groupe de Hamilton Sound (Ordovicien) que surmonte en disconformité le Groupe d'Indian Islands (Silurien), (ii) le secteur compris entre la ligne de Dog Bay et la faille de Reach, renfermant le complexe de Duder, composé de roches sédimentaires clivées contenant de gros blocs de roches ignées mafiques, (iii) la région au nord-est de la baie d'Exploits, où affleure le Mélange de Dunnage, (iv) le secteur du bras Indian et de la baie Loon, qu'occupe le batholite de Loon Bay et (v) la région de Campbellton et de Long Pond qui se compose de turbidites et de roches volcaniques qui s'échelonnent de l'Ordovicien moyen au Silurien. Des roches du Silurien et du Dévonien (grès de Ten Mile, batholite de Loon Bay) établissent un lien entre ces régions. Le batholite de Loon Bay englobe deux plutons, issus de sources différentes de celles des roches ignées felsiques du Mélange de Dunnage, et marque une importante limite structurale au niveau de laquelle le mélange est tronqué, et le long de laquelle les unitées de la région de Campbellton et Long Pond sont déviées. Un épisode d'obduction et de rifting à l'Ordovicien moyen suivi d'une période de subduction au Silurien pourraient expliquer ces observations.

INTRODUCTION

The Dunnage Zone of Newfoundland has played a key role in understanding ancient orogens since Dewey and Bird (1971) modelled ophiolitic allochthons of western Newfoundland as remnants of the oceanic Dunnage Zone expelled during mid-Ordovician plate collision. This model rested on classic coastal exposures of the Dunnage Zone around Bay of Exploits. New mapping further south showed that parts of the Dunnage Zone formed after emplacement of the allochthons (Colman-Sadd et al., 1992; Swinden et al., 1990), and that climactic deformation and plutonism occurred in Silurian time (Dunning et al, 1990). Correlation with the Bay of Exploits region proved difficult, due to lack of detailed mapping inland of the well-known coastal exposures. However inland mapping is now practicable because of the extensive network of forest access roads. Mapping of Comfort Cove map area (2E/7) which contains Dunnage Island after which the zone was named, was completed during 1993, and work on the Gander River map area (2E/2) was commenced.

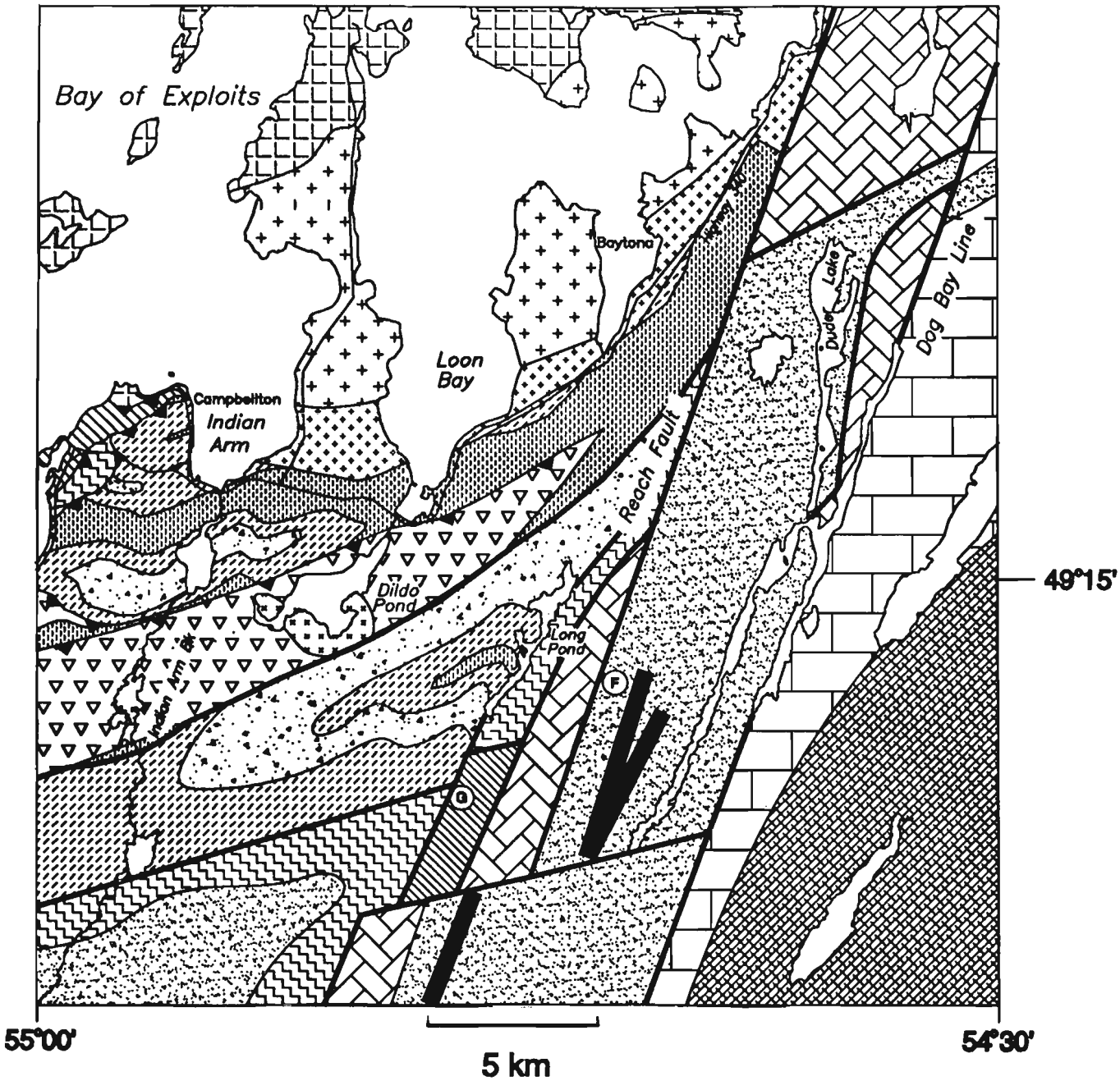

Figure 1. Geological map of parts of the Comfort Cove (NTS 2E/7) and Gander River (2E/8) map areas, northeast Newfoundland.

PREVOUS WORK

Important references on the geology of the Bay of Exploits region go back 60 years (Heyl, 1936; Espenshade, 1937; Twenhofel and Shrock, 1937), but current stratigraphic ideas are based on the mapping of H. Williams (1964), as revised by O'Brien (1992, 1993), Currie (1992, 1993), and H.Williams (1992,1993). Comfort Cove map area was mapped by Patrick (1956), based mainly on coastal exposures. Parts of Gander River map area were mapped by Blackwood (1982) and by Evans et al. (1992), but this area has received relatively little attention, in part because of a paucity of outcrop.

GEOLOGICAL SUMMARY

The region mapped falls into five sub-areas (Fig. 1), namely (i) east of the Dog Bay Line, (ii) between the Dog Bay Line and the Reach Fault, (iii) the Bay of Exploits region, (iv) the Indian Arm-Loon Bay region and (v) the Campbellton-Long Pond region. Each of these regions exhibits distinctive stratigraphy as summarized in Table 1. The region east of the Dog Bay Line comprises the Indian Islands terrane (Williams et al., in press), including the Ordovician Hamilton Sound Group and the disconformably overlying Silurian Indian Islands Group, which were described last year (Currie, 1993). Between the Dog Bay Line and Reach Fault, much of the area is underlain by Duder complex (previously termed Duder group by Currie, 1993) consisting of intensely cleaved sedimentary rocks containing large blocks of mafic igneous rocks. The Duder complex appears to be conformably overlain by the upper Ordovician to lower Silurian Badger and Botwood groups described by Williams et al. (in press). The northwestern part of the mapped area, comprising islands in the Bay of Exploits, is underlain by the celebrated Dunnage Melange, a mass of regional extent, including important igneous units, whose relations to surrounding sequences are uncertain and controversial. The mélange is separated from sequences to the south and east by the Loon Bay batholith, a composite mass comprising at least two plutons, which appears to mark a major structural inflection in this region. South of the Loon Bay batholith the region between Campbellton and Long Pond contains the extension of folded and thrust mid-Ordovician to Silurian turbidites and volcanogenic strata mapped by O'Brien (1993). This belt is truncated by the Reach Fault.

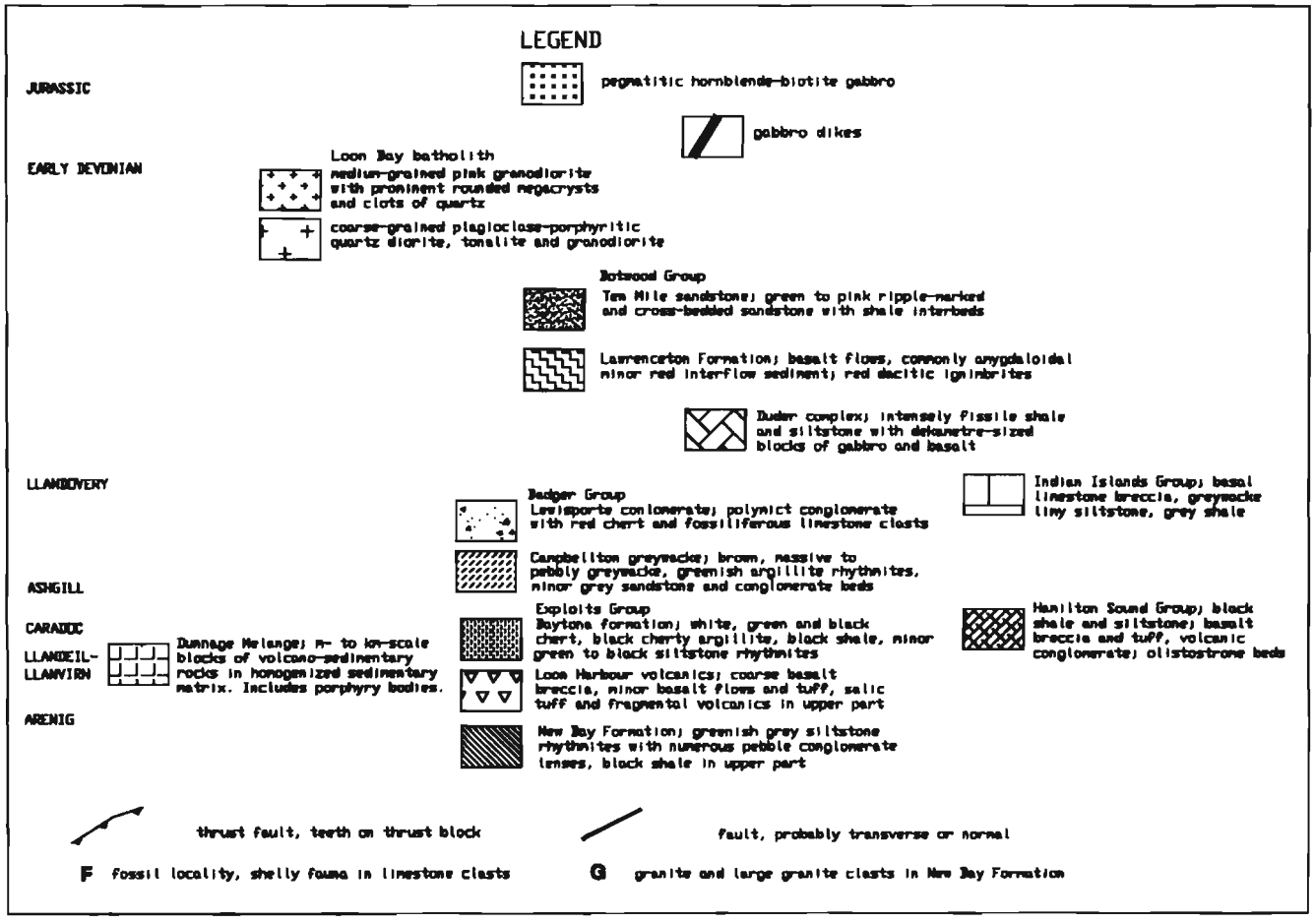

DESCRIPTION OF UNITS

East of the Dog Bay Line, a Silurian terrane boundary, the Hamilton Sound and Indian Islands groups were described by Currie (1993), Williams (1993) and Williams et al. (in press). Between the Dog Bay Line and the Reach Fault, much of the region is underlain by highly cleaved black to grey siltstone and shale with tectonic inclusions of mafic dykes and lavas. These rocks were initially referred to as Duder group (Currie, 1993), but further examination suggests that a variety of components have been tectonically mixed together. The name Duder group is therefore abandoned in favour of Duder complex. The matrix of the Duder complex consists of black and grey shale and siltstone. In the western part of the belt these rocks are so intensely cleaved and sheared that bedding is visible only in enclaves a few centimetres across. A section of 2.5 km of "paper schist" is exposed on a woods road commencing near grid reference 674717. Because of its extremely cleaved nature, outcrop of this material is rare, but material turned up in spoil pits on woods roads suggests that it underlies the western two-thirds of the Duder complex. Within about 1.5 km of the Dog Bay Line the cleavage is less intense and the rocks can be identified as a sequence of greenish black, fine grained greywacke, locally with graded beds containing feldspar debris, pale greenish grey sandstone and siltstone, locally crossbedded, pebble conglomerate intervals up to 5 m thick, and black turbiditic siltstone-shale rhythmites. This sequence is isoclinally folded on a scale of a few hundred metres. These strata resemble the Arenig New Bay Formation west of Campbellton. A small enclave of rhythmically bedded siltstone with chert lenses and rhyolite fragments east of Long Pond (gridref 623574) and surrounding homogenized siltstone resembles the Baytona formation and Campbellton greywacke west of Long Pond.

The matrix contains scattered blocks of gabbro, pillow lava and pillow breccia. Mafic volcanic rocks occur as rare hillocks up to a few tens of metres across consisting of pillow

Table 1. Geological subdivision and correlation chart for the Comfort Cove-Gander River area.

	S.New World Island	Bay of Exploits	Campbellton-Long Pond area	Reach Fault-Dog Bay Line	East of Dog Bay Line
Jurassic			Dildo Pond Gabbro		
Silurian					
		Loon Bay batholith		gabbro	Fogo batholith
			BOTWOOD GROUP	BOTWOOD GP.	INDIAN ISLANDS GP.
Wenlock			Ten Mile sandstone	Ten Mile Ss	Centennial red sandstone
			Lawrenceton volcanics	Lawrenceton Fm.	Horwood shale
	BADGER GROUP		BADGER GROUP	BADGER GP.	Charles Cove siltstone
Llandovery	Goldson red massive conglomerate		Lewisporte conglomerate	Stoneville Fm.	Seal Island limestone breccia
			Campbellton greywacke	Sawmill shale, olistostromes	
Ordovician					
Ashgill	Milliners Arm green conglomerate				
	Sansom greywacke,		Baytona chert and		
Caradoc	shale, turbidites		black shale		
					HAMILTON SOUND GP.
	Dark Hole Fm.				Carmanville Melange
	black shale and chert	gabbroic dikes		Duder complex	Main Point black shale
				(age unknown)	Noggin Cove volcanics
Llandeilo	Cobbs Arm limestone	Coaker porphyry	Loon Harbour volcanics		DAVIDSVILLE GP.
	(includes older rocks)	porphyritic rhyolite			Round Pond siltstone-shale
		Dunnage Melange			Barrys Ponds conglomerate
Llanvirn	Summerford "Group"	olistostromal and			
	mafic volcanics and	tectonic melange			
Arenig	associated limestone		New Bay Fm.,siltstone,shale	New Bay Fm.?	Gander River complex,
	(includes rocks as	mafic volcanics			utramafics, volcanics
Tremadoc	old as Tremadoc)	in the melange	trondhjemite		trondhjemite

The Loon Bay batholith forms a pin between the Cambellton -Long Pond region and the Dunnage Melange, since it intrudes both.

lava, pillow breccia, and interstitial chert and limestone. Gabbro forms hillocks as much as 200 m long by 50 m wide concentrated in a roughly linear zone extending north-nothneast from Duder Lake. Churchill and Evans (1992) considered these masses to be dykes, and some occurrences preserve coarse centres and finer grained rims, but no intrusive contacts have been found, even in drill core (D.T.W. Evans, pers. comm., 1993), no hornfels occurs in the country rocks, despite the size of some of the bodies, and where outcrop is complete gabbro forms boudins in a sedimentary matrix (Currie, 1993). These observations indicate that the blocks are tectonic inclusions. Rare plagioclase porphyry dykes cut both foliation and mafic blocks. These porpyhry dykes resemble those cutting the Exploits Group to the west which are truncated and hornfelsed by the Loon Bay batholith.

The source of the mafic igneous rocks is not known. The volcanic rocks do not resemble the Loon Harbour volcanics of the Exploits Group (which contain no limestone or chert) but do resemble the older Tea Arm volcanics (compare O'Brien, 1993). The gabbro could be correlative to intrusive rocks of similar age in the New Bay Formation, or to younger gabbro cutting the Silurian Ten Mile sandstone. These observations suggest that the Duder complex could represent a tectonically homogenized Exploits Group.

Along the north boundary of the map area, the Duder complex is overlain by the Badger and Botwood groups as described last year (Williams, 1993, Williams et al., in press). These rocks are also strongly cleaved, but the degree of deformation is quantitatively less than that in the Duder complex. Farther south, a single outcrop of Badger Group conglomerate with fossiliferous limestone clasts occurs at gridref 637548 surrounded by Ten Mile sandstone. No stratigraphic contact between Ten Mile sandstone and older units has been found but the large discrepancy between isoclinal folding and strong cleavage in the older rocks and generally open folding with weak cleavage in the Ten Mile sandstone implies a major unconformity. The Ten Mile sandstone crosses the Dog Bay Line, as hypothesized last year (Currie, 1993), and must be younger, at least in part, than the Wenlock fossils reported from the underlying Charles Cove Formation of the Indian Islands Group (Wu, 1979). The Ten Mile sandstone is cut by large north-northeast trending dykes of gabbro, one of which near gridref 628508 appears to be more than 500 m thick.

A region more than 50 km in length and 10 km wide, including the myriad of islands in northeastern Bay of Exploits, is underlain by the Dunnage Melange, a unit lacking regional coherent stratigraphy whose thickness and internal structure are unknown. The mélange has been restudied by Williams (1994) whose work emphasized that (1) formation involved both olistostromal and tectonic events, (2) mélange does not extend in the subsurface much beyond its surface exposure, (3) many of the blocks in the melange cannot be correlated with strata now surrounding the mélange, and (4) the mélange contains a unique igneous suite (Coaker porphyry and mafic dykes).

Loon Bay and Indian Arm are underlain by the Loon Bay batholith, a northeast- trending lens of granitoid rocks 25 km long and up to 15 km wide which bounds most of the southern edge of the Dunnage Melange and joins the Long Island batholith (O'Brien, 1993) at the western edge of the map area to form a continuous belt of granitoid rocks more than 50 km long. The Loon Bay batholith consists of a southeastern marginal biotite granodiorite to quartz monzonite with prominent quartz, and a main pluton varying from coarse foliated biotite-hornblende diorite on the southeast to massive, medium grained tonalite to granodiorite on the northwest. A screen of hornfelsed sedimentary rocks, well exposed in the village of Birchy Bay, separates the two plutons except at the northeast extremity where the quartz-prominent pluton cuts and fractures the main pluton. The quartz-prominent phase commonly weathers to a surface studded with centimetre-size raised, polycrystalline, round to irregular quartz masses. The main pluton is plagioclase-phenocrystic, and the more mafic phases contain ovoid or irregular masses of plagioclase up to 2 cm across. Most of the original hornblende has been coated with, or converted to, biotite. Neither pluton contains prominent pegmatitic phases, and both are surrounded by a hornfels aureole 100-200 m wide locally containing andalusite spots up to 2 mm in diameter. These observations suggest the pluton was hot and dry when emplaced.

A dyke correlated to the Loon Bay batholith was dated at 408±2 Ma by U-Pb zircon (Elliot et al., 1991). The batholith intrudes both the Dunnage Melange and Exploits Group, demonstrating that these units were juxtaposed at that time. Extensive fracturing and patchy foliation, both cataclastic and due to alignment of phenocrysts, of the main pluton suggest late tectonic emplacement.

The region south of the Loon Bay batholith and west of the Reach Fault is underlain by mid-Ordovician to lower Silurian strata correlative to those described by O'Brien (1993) farther west. He divided strata older than the early Silurian Botwood Group into (in order of decreasing age) Tea Arm volcanics, New Bay Formation, Loon Harbour volcanics, Strong Island chert, Luscombe Shale, Campbellton greywacke, and Lewisporte conglomerate. In the region mapped this year the Tea Arm volcanics do not outcrop. The Strong Island chert and Luscombe shale cannot be consistently distinguished, and have therefore been combined into the informal Baytona formation. O'Brien (1993) proposed no group names, but the four older formations clearly belong to the Exploits Group, whereas the Campbellton greywacke and Lewisporte conglomerate belong to the Badger Group as defined by Williams et al. (in press).

The New Bay Formation outcrops on the western edge of the map area, southwest of Long Pond, and possibly within the Duder complex east of Duder Lake. The lowest exposed strata consist of fine grained turbiditic grey siltstone and sandstone with beds of conglomerate up to 2 m thick containing sparse siltstone and rare granitoid pebbles. The upper part of the formation comprises fine grained greenish turbidites laminated on centimetre scale and thinly laminated black

shale. Southwest of Long Pond (gridref 577514) a small area of intensely fractured pink trondhjemite occurs within the New Bay Formation (locality G of Fig. 1). The conglomerate outcrop adjacent to this exposure contains boulders of trondhjemite up to 40 cm across, and conglomerate lenses within 2 km contain pebbles to cobbles of this lithology. These relations imply an unconformiy between the trondhjemite and New Bay Formation. Gabbro sills, typical of the lower part of the New Bay Formation, were not observed in the map area.

The Loon Harbour volcanics, named by Kay (1975), consist mainly of basaltic rocks, but significant amounts of salic volcanic rocks and fine greywacke occur in the upper part. Spectacular volcanic breccias consisting of angular basalt blocks up to 20 cm on a side with vesicular cores and thin glassy rinds comprise much of the formation southwest of Dildo Pond. Massive basalt and pillow breccia are present in lesser amount. Northeast of Dildo Pond, finer fragmentals are more common, interspersed with almost massive, deep green greywacke, presumed to be derived from the basalt. More silicic fragmental volcanic rocks and minor rhyolite occur at the top of the unit from Indian Arm Brook to east of Loon Bay.

The Baytona formation, named after the settlement of Baytona, is here defined to include strata between the Loon Harbour volcanics and the Campbellton greywacke. The type section, along a diversion canal of Indian Arm Brook at Campbellton, consists mainly of chert, commonly in beds 2 to 5 cm thick, but finely laminated internally. The base of this section is faulted off, but the loss of section is believed to be minimal. The lower part of the section contains rhyolite and silicified tuff. A vesicular basaltic flow is present on the east side of Loon Bay. The upper part of the section contains black shale, locally pyritiferous and/or manganiferous, and siliceous argillite in interbeds from a few millemetres to 2 m thick. S.H. Williams (1993) has shown these interbeds are of late Caradoc (clingani) age at Campbellton. A sharp but conformable contact between black chert and Campbellton greywacke (Badger Group) is exposed on the shore behind the old mill at Campbelton. The Baytona formation is about 300 m thick.

The Campbellton greywacke typically consists of massive brown greywacke, locally pebbly, in beds up to 3 m thick. Where well exposed, the greywacke can be seen to form ovoid lenses a few metres to tens of metres in length, embedded in thinly bedded grey-green homogeneous turbiditic siltstone. Bedding can only be seen in the greywacke where pebbly beds, commonly graded, are present. These pebbly beds grade to conglomerate.

The Lewisporte conglomerate varies from greenish grey pebbly conglomerate with packed, imbricate pebbles, to massive boulder conglomerate. The conglomerate is locally clast-supported, but commonly is matrix supported. The sub-rounded to well-rounded clasts consist mainly of siltstone, gabbroic to granitoid plutonic rocks and shale rip-ups, but red chert and limestone clasts form a distinctive though minor component. The presence of fossiliferous limestone pebbles typifies Badger Group conglomerates throughout the Bay of Exploits region.

The Lawrenceton Formation of the Botwood Group outcrops in two fault-bounded slices, one on highway 340 west of Campbellton, the other a northeast-trending slice on the southern margin of the mapped area. Both consist mainly of amygdaloidal basalt, with local red-stained flow tops and thin red interflow sediment. Rhyolite and rhyolitic tuff occur in this unit southwest of Long Pond. Most outcrops of Lawrenceton Formation exhibit little penetrative deformation, but the slice west of Campbellton is strongly deformed.

Ripple-marked red siltstone occurs as a separate imbricate of the northern slice of Lawrenceton Formation, and outcrops sparingly over a considerable area in the southwest corner of the mapped area. These rocks are identical in lithology and structural style (relatively open folding) to the Wenlock or younger Ten Mile sandstone overlying the Duder complex. However they were correlated with the Llandovery Wigwam Formation by O'Brien (1993). Two red sandstone units of slightly differing ages may be present, or the unit may be diachronous.

An intrusion of undeformed pegmatitic hornblende-biotite-gabbro about 2 km in diameter underlies much of Dildo Pond. Strong and Harris (1974) deduced that this unusual alkaline rock was of Jurassic age, and correlative to the sparse lamprophyre dykes occurring throughout the northeastern Dunnage Zone.

STRUCTURAL GEOLOGY

Each of the five subregions described above has a distinct structural style. The Indian Islands terrane is dominated by north-northeast-trending isoclinal, upright to slightly eastward overturned folds. These folds probably represent at least a second phase of deformation, and the northeastern part of the terrane, east of the map area, was further complexly deformed (Piasecki, 1992). Between the Dog Bay Line and the Reach Fault, the Botwood and Badger groups exhibit north-northeast-trending isoclinal folds overturned to the northwest. These groups are also affected by the intense north- to north-northwest trending cleavage of the Duder complex. The structure of the Dunnage Melange is little known, although Williams (1994) presented further evidence that it is broadly antiformal. The matrix and most blocks exhibit a late northeast-trending, southeast-dipping cleavage at a high angle to cleavage east of the Reach Fault. The Loon Bay batholith exhibits patchy internal foliation trending northeast and dipping steeply and the margins of the batholith are extensively sheared and fractured. These structural trends parallel those in the Dunnage Melange, but contrast with trends to the south where the Exploits and Badger groups display east-northeast-trending isoclinal folds with axial planes vertical or slightly overturned to the north. The wavelength of the folds is commonly a few hundred metres, as demonstrated by the spacing of cores of Lewisporte conglomerate. These folds are dextrally kinked about axes plunging about 40 to 50° toward 230°, resulting in a generally east-west trend of units. The whole sequence has been thrust to the north along faults which have themselves been folded (O'Brien, 1993). Many of these faults have only small stratigraphic

displacement, and may be a result of competency contrasts between units. However the larger faults cut out much of the section and are clearly major structures. A fault bounding the southern belt of Lawrenceton Formation appears to be offset 5 km on the Reach fault, a late sinistral feature (Williams et al., in press) which in the vicinity of Long Pond splays from a single well-defined break into a horsetailing series of faults, some of which are dextrally offset by east-northeast-trending faults.

DISCUSSION

Virtually all workers since Williams (1964) have assumed that a single stratigraphic column is applicable to the region mapped this year. Table 1 shows that any simplified stratigraphic column such as that proposed by Dean (1978) must encounter problems. West of the Dog Bay Line, a Silurian terrane boundary separating diverse early to mid-Silurian stratigraphies, regions exhibit gross similarities in stratigraphy but notable differences in detail. Just north of the mag-area Southern New World Island, according to Lafrance and Williams (1992), is characterized by the sequence Summerford volcanics-Cobbs Arm limestone-Dark Hole shale-Sansom greywacke-green Milliners Arm conglomerate-red Goldson conglomerate. In a simplified stratigraphy, rhythmically bedded turbidites of the Sansom Formation should be equivalent to almost massive Campbellton greywacke. There is no equivalent on New World Island for the chert-dominated Baytona formation, and the mafic volcanic-limestone assemblages of southern New World Island do not correlate well with either the Loon Harbour volcanics, which lack limestone, or the older Tea Arm volcanics which fall in a time interval (Arenig) not represented by fossils from New World Island. The most reliable stratigraphic link between the Campbellton-Long Pond, Dog Bay Line-Reach Fault and southern New World Island regions is conglomerate of the Badger Group with fossiliferous limestone clasts, but the source(s) of these clasts is competely unknown.

The Dunnage Melange, an element which cannot be accomodated in any simplified stratigraphy, appears to be a depocentre of Llandeilo or older age into which material slid from both northeast and southwest (Hibbard and Williams, 1979; O'Brien, 1993; Williams, 1994). The mélange appears to be restricted essentially to its present outcrop area and was associated with shallow igneous activity (Lorenz, 1984), suggesting an original tensional, rather than subduction-related, setting which has not been significantly imbricated with its surroundings by subsequent thrusting. Igneous activity in the mélange may be roughly correlative with coeval non-arc volcanism in the surrounding regions.

The Loon Bay batholith marks a major structural element in this region, defined by a 70° deflection in strike around the south side of the batholith. The calc-alkaline composition and foliated structure of the batholith suggest a subduction-related source unrelated to the peraluminous, almost massive igneous rocks of the Dunnage Melange. Development of the intense cleavage which characterizes the Duder Group extended at least into Silurian time, since it affects the Silurian Botwood Group and may truncate the early Devonian Loon Bay batholith along the Reach Fault. However the quantitatively more intense cleavage in pre-Silurian strata suggests that development of the cleavage began in pre-Silurin time.

A model which could accommodate these observations includes early Ordovician southeast-directed thrusts and ophiolite obduction (Colman-Sadd et al., 1992), which have been repeatedly postulated but not demonstrated in the Bay of Exploits region (compare Lafrance and Williams, 1992 with Currie and Williams, 1993). Mid-Ordovician rifting to produce mélange sedimentation into pull-apart basins with accompanying non-arc igneous activity seems to be indicated. The ubiquitous west-verging late Ordovician-early Silurian folds and thrusts could be due to relatively minor, oblique, east-dipping subduction following a polarity flip. The Reach Fault-Dog Bay Line region would then represent an escape structure translated northward to accommodate this subduction. Such a model could explain why pre-Silurian units such as the Dunnage Melange and Loon Harbour volcanics have correlatives east of the Dog Bay Line (Carmanville Melange, Noggin Cove Formation, Currie, 1992; Johnston, 1992), and why some of the sources of the Dunnage Melange have disappeared. All models, however, remain speculative until supported by further mapping.

ACKNOWLEDGMENTS

I am indebted to my co-worker Hank Williams of Memorial University whose encyclopedic knowledge of central Newfoundland geology made the project possible, and whose inimitable style and panache have made it a pleasure. The meticulous mapping of Brien O'Brien of the Newfoundland Geological Surveys Branch now forms the basis for all serious work on the stratified rocks of the southern Bay of Exploits, and he shared his expertise freely. Dave Evans of the Geological Surveys Branch freely shared his knowledge of the Gander River sheet with me.

REFERENCES

Blackwood, R.F.
1982: Geology of the Gander Lake (2D/15) and Gander River (2E/2) area; Newfoundland Mineral Development Division Report 82-4, 56 p.

Churchill, R.A. and Evans, D.T.W.
1992: Geology and gold mineralization of the Duder Lake gold showings, eastern Notre Dame Bay, Newfoundland; Newfoundland Geological Surveys Branch Report 92-1, p. 211-220.

Colman-Sadd, S.P., Dunning, G.R., and Dec, T.
1992: Dunnage-Gander relationships and Ordovician orogeny in central Newfoundland: a sediment provenance and U/Pb age study; American Journal of Science v. 292, p. 317-355.

Currie, K.L.
1992: A new look at Gander-Dunnage relations in Carmanville map-area, Newfoundland; in Current Research, Part D; Geological Survey of Canada, Paper 92-1D, p. 27-33.
1993: Ordovician-Silurian stratigraphy between Gander Bay and Birchy Bay, Newfoundland; in Current Research, Part D; Geological Survey of Canada, Paper 93-1D, p. 11-18.

Currie, K.L. and Williams, H.
1993: Silurian deformation in eastern Notre Dame Bay, Newfoundland – discussion; Canadan Journal of Earth Sciences, v. 29, p. 1547-1549.

Dean, P.L.
1978: The volcanic stratigraphy and metallogeny of Notre Dame Bay, Newfoundland; M.Sc. thesis, Memorial university of Newfoundland, St. John's, Newfoundland, 205 p.
Dewey, J.F. and Bird, J.M.
1971: Origin and emplacement of the ophiolite suite: Appalachian ophiolites in Newfoundland; Journal of Geophysical Research, v. 76, p. 3179-3206.
Dunning, G.R., O'Brien, S.J., Colman-Sadd, S.P., Blackwood, R.F., Dickson, L.W., O'Neill, P.P., and Krogh, T.E.
1990: Silurian Orogeny in the Newfoundland Appalachians; Journal of Geology, v. 98, p.895-913.
Elliot, C.G., Dunning, G.R., and Williams, P.F.
1991: New U-Pb zircon age constraints on the timing of deformation in north-central Newfoundland and implications for early Paleozoic Appalachian orogenesis; Geological Society of America Bulletin, v. 103, p. 125-135.
Espenshade, G.H.
1937: Geology and mineral deposits of the Pilleys Island area; Newfoundland Department of Natural Resources, Geological Section, Bulletin 6, 56 p.
Evans, D.T.W., Hayes, J.P., and Blackwood, R.F.
1992: Gander River, Newfoundland; Newfoundland Geological Surveys, Branch Map 92-21.
Heyl, G.R.
1936: Geology and Mineral resources of the Bay of Exploits area; Newfoundland Department of Natural Resources, Geological Section, Bulletin 3, 55 p.
Hibbard, J. and Williams, H.
1979: Regional setting of the Dunnage Melange in the Newfoundland Appalachians; American Journal of Science, v. 279, p. 993-1021.
Johnston, D.
1992: The Noggin Cove Formation, Carmanville map-area, northeast Newfoundland; a back-arc volcanic complex; in Current Research, Part E; Geological Survey of Canada, Paper 92-1E, p. 27-36.
Kay, M.
1975: Campbellton sequence: manganiferous beds adjoining the Dunnage Melange, northeastern Newfoundland; Geological Society of America, Bulletin, v. 86, p. 105-108.
Lafrance, B. and Williams, P.F.
1992: Silurian deformation in eastern Notre Dame Bay, Newfoundland; Canadian Journal of Earth Sciences, v. 29, p. 1899-1914.
Lorenz,B.E.
1984: A study of the igneous intrusive rocks of the Dunnage Melange, Newfoundland; Ph.D. thesis, Memorial University of Newfoundland, Saint John's, Newfoundland, 220 p.
O'Brien, B.H.
1993: A mappers guide to Notre Dame Bay's folded thrusts: evolution and regional development; Newfoundland Geological Survey, Report 93-1, p. 279-292.
Patrick, T.O.H.
1956: Comfort Cove, Newfoundland; Geological Survey of Canada, Paper 55-31.
Piasecki, M.A.J.
1992: Tectonics across the Gander-Dunnage boundary in northeastern Newfoundland; in Current Research, Part E; Geological Survey of Canada, Paper 92-1E, p. 259-268.
Strong, D.F. and Harris, A.
1974: The geology of Mesozoic alkaline intrusives of central Newfoundland; Canadian Journal of Earth Sciences, v. 11, p. 1208-1219.
Swinden, H.S., Jenner, G.A., Fryer, B.J., Hertogen, J., and Roddick, J.C.
1990: Petrogenesis and paleotectonic history of the Wild Bight Group, an Ordovician rifted island arc in central Newfoundland; Contributions to Mineralogy and Petrology, v. 105, p. 219-241.
Twenhofel, W.H. and Shrock, R.R.
1937: Silurian strata of Notre Dame Bay and Exploits Valley, Newfoundland; Geological Society of America, Bulletin, v. 48, p. 1743-1772.
Williams, H.
1964: Botwood, Newfoundland; Geological Survey of Canada, Map 60-1963.
1992: Melanges and coticule occurrences in the northeast Exploits Subzone, Newfoundland; in Current Research, Part D; Geological Survey of Canada, Paper 92-1D, p. 121-127.
1993: Stratigraphy and structure of the Botwood Belt and definition of the Dog Bay Line in northeastern Newfoundland; in Current Research, Part D; Geological Survey of Canada, Paper 93-1D, p. 19-27.
Williams, H., Currie, K.L., and Piasecki, M.A.J.
in press: The Dog Bay Line – a Silurian terrane boundary in northeast Newfoundland; Canadian Journal of Earth Sciences, v. 29.
Williams, S.H.
1993: More Ordovician and Silurian graptolites from the Exploits Zone; Newfoundland Geological Surveys Branch, Report 93-1, p. 311-316.
Wu, T.W.
1979: Structural, stratigraphic and geochemical studies in the Horwood Peninsula-Gander Bay area, northeastern Newfoundland; M.Sc. thesis, Brock University, Saint Catherines, Ontario, 185 p.

Geological Survey of Canada Project 730044

Paleontological evidence for marine influence during deposition of the Westphalian Coal Measures in the Gulf of St. Lawrence-Sydney Basin region, Atlantic Canada

W.G. Wightman[1], A.C. Grant, and T.A. Rehill[2]
Atlantic Geoscience Centre, Dartmouth

Wightman, W.G., Grant, A.C., and Rehill, T.A., 1994: Paleontological evidence for marine influence during deposition of the Westphalian Coal Measures in the Gulf of St. Lawrence-Sydney Basin region, Atlantic Canada; in Current Research 1994-D; Geological Survey of Canada, p. 41-50.

Abstract: Coal Measures penetrated by oil and gas exploration wells in Gulf of St. Lawrence – Sydney Basin are a regionally mappable seismic facies. The broad extent of this seismic facies has prompted the speculation that it reflects cyclothem deposition, analogous to cyclothem deposits of the Illinois Basin and Mid-Continent Basin region of the United States. This implies that the depositional cycles included periods of marine incursion. Evidence for such incursions, in the form of agglutinated foraminifera assemblages, has been reported from coal-bearing strata of the Sydney Basin, Cape Breton Island. Similar assemblages have now been found in two offshore wells in the Gulf of St. Lawrence. This discovery supports arguments for cyclothymic deposition, enhances the possibility of marine source rocks for hydrocarbon generation, and underlines the need for review of the paleogeographic and depositional history of the Central Maritimes Basin.

Résumé : Les couches de charbon traversées par des puits d'exploration du pétrole et du gaz, dans le golfe du Saint-Laurent et le bassin de Sydney, représentent un faciès sismique cartographiable à l'échelle régionale. En raison de la vaste étendue de ce faciès sismique, on a formulé l'hypothèse selon laquelle il représenterait le dépôt de cyclothèmes analogues à ceux du bassin de l'Illinois et de la région du bassin médio-continental des États-Unis. Ceci signifie que les cycles de sédimentation comprenaient des périodes d'incursion des eaux marines. Les preuves de ces incursions, soit la présence d'associations de foraminifères à test aggluiné, ont été signalées dans les strates houillères du bassin de Sydney, dans l'île du Cap-Breton. Des associations semblables ont été observées dans deux puits extracôtiers du golfe du Saint-Laurent. Cette découverte appuie l'hypothèse du dépôt de cyclothèmes, augmente la possibilité de la présence de roches mères marines capables de former des hydrocarbures, et souligne le besoin de réviser l'évolution paléogéographique et sédimentaire de la partie centrale du bassin des Maritimes.

[1] Paleotec Geological Consulting, 2375 Moran St., Halifax, Nova Scotia B3K 4K1
[2] Department of Geology, Dalhousie University, Halifax, Nova Scotia B3H 3J5

INTRODUCTION

The Gulf of St. Lawrence – Sydney Basin region includes Prince Edward Island and the offshore part of the Permo-Carboniferous Maritimes Basin of Atlantic Canada (Fig. 1). In assessing the offshore extent of the late Westphalian to Stephanian (Fig. 2) coal seams formerly mined in the Mabou and Inverness coalfields, western Cape Breton island, Hacquebard (1986) examined five oil and gas exploratory wells in the Gulf of St. Lawrence (Fig. 3). Four distinctive coal-bearing zones were recognized that could be traced over distances of up to 240 km and correlated with onshore sections. The coal zones were named after intervals of coal seams found in the Sydney Mines Formation of the Sydney coalfield (Fig. 3), and dated by Barss and Hacquebard's (1967) spore zones of the Pictou Group (Fig. 2). Hacquebard (1986) and Hacquebard et al. (1989) interpreted the Mabou and Inverness coalfields to be part of a much larger basin, and defined the Gulf of St. Lawrence Carboniferous Coal Basin as the largest coal basin in eastern Canada.

Based on interpretation of industry seismic data (Fig. 4), Grant and Moir (1992) showed that the coal occurrences in the exploratory wells coincide with a "Coal Measures" seismic facies mappable over a large portion of the Gulf of St. Lawrence – Sydney Basin region (Fig. 5). They inferred the original extent of Coal Measures deposition to be over 100 000 km^2. Grant (in press) compared the depositional extent of this seismic facies to that of cyclothem deposition in the Illinois Basin and Mid-Continent Basin region of the United States.

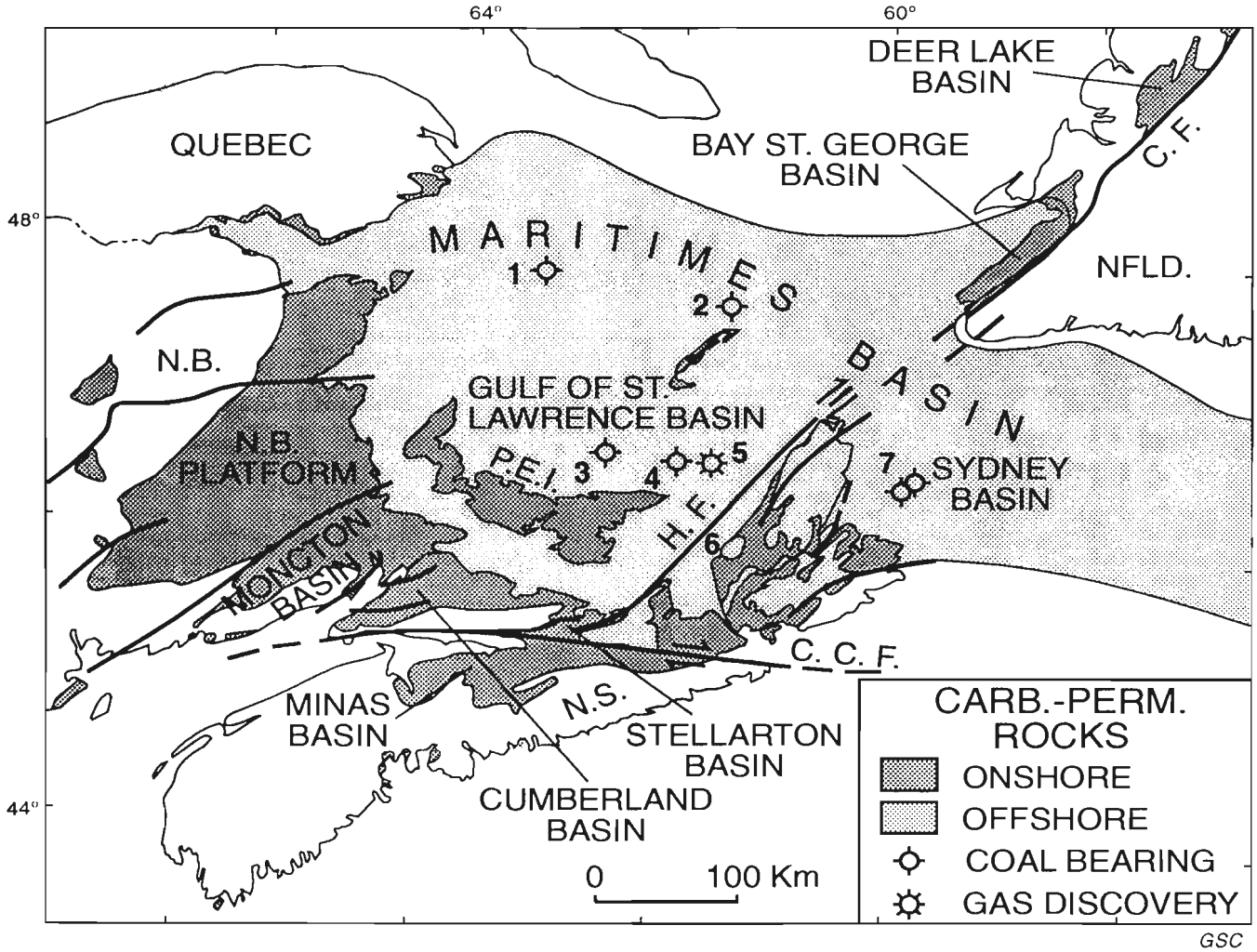

Figure 1. *Distribution of Carboniferous and Permian rocks (shaded) in the Maritimes Basin of Atlantic Canada. Major faults: C.F. – Cabot Fault; C.C.F. – Cobequid-Chedabucto Fault; H.F. – Hollow Fault. Numbers denote well locations offshore and coalfields on land referred to in text: 1 – Bradelle L-49 well; 2 – Brion Island No. 1 well; 3 – Cable Head E-95 well; 4 – Beaton Point F-70 well; 5 – East Point E-49 well; 6 – Mabou-Inverness coalfield; 7 – Sydney coalfield on land to south-southwest. After Gibling et al. (1992).*

The Sydney Mines Formation of the Sydney Basin coalfield has traditionally been thought to have been deposited in a freshwater setting. However, documentation of cyclothymic stratal patterns (Bird, 1987), and preliminary identification of agglutinated foraminifera (Thibideau and Medioli, 1986), suggested a marine influence during deposition. Gibling and Bird (1990) and Gibling (1992) subsequently documented eleven complete cyclothems within the Sydney Mines Formation. Wightman et al. (1992, 1993, in press) have reported on the agglutinated foraminifera and thecamoebian assemblages within these cyclothems, and identified various levels of marine influence during deposition.

The presence of marine strata in the Upper Carboniferous of the Maritimes Basin would have implications for marine source rock distribution and reservoir depositional models. Therefore, the Geological Survey of Canada issued a contract (Wightman, 1993, No. 23420-3-Co69/01-OSC) to examine cuttings from exploratory wells in the Gulf of St. Lawrence region for the presence of similar agglutinated foraminifera and thecamoebian assemblages. Although this work is still in progress, preliminary results indicate the occurrence of such assemblages in the Bradelle L-49 and East Point E-49 wells (Fig. 1, 3, 5). This paper documents the distribution of the assemblages in these wells, and comments on their significance.

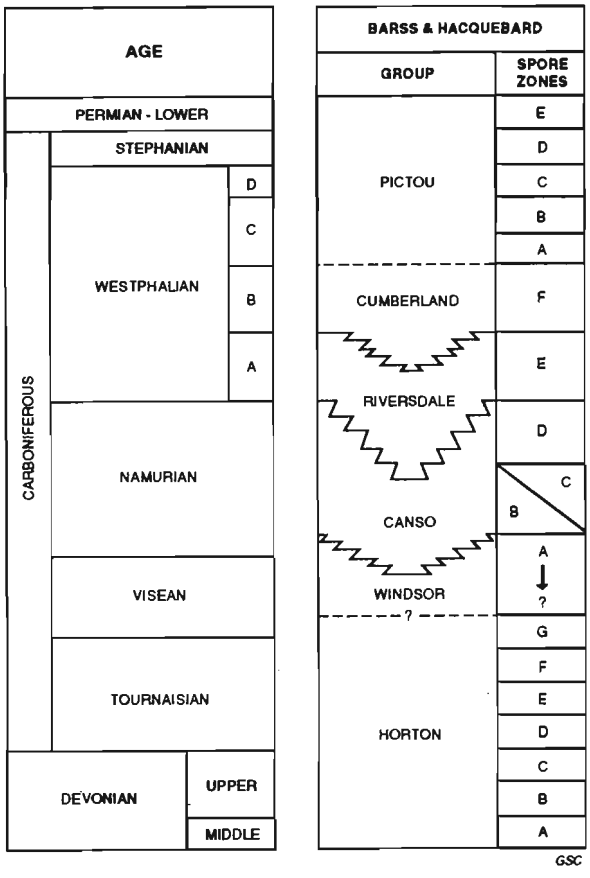

Figure 2. Stratigraphic subdivisions and age of Upper Paleozoic rocks in eastern Canada, after Hacquebard et al. (1989).

MATERIALS AND METHODS

Rotary cuttings from the Gulf of St. Lawrence wells are stored in the Nova Scotia Offshore Petroleum Board facilities, Dartmouth, Nova Scotia. Samples of approximately 20 g were collected every 3 m, and combined every 30 m, resulting in a 200 g sample for each 30 m interval. Allowing for intervals for which no samples were available, this resulted in a total of 17 samples for the 1033-1966 m interval in the Bradelle L-49 well, and 13 samples for the 2179-2813 m interval in the East Point E-49 well. These intervals correspond to the approximate position of the coal-bearing strata identified in the wells by Hacquebard (1986), and the Coal Measures seismic facies mapped by Grant and Moir (1992). The advantage of our sampling strategy is that it allows for a rapid appraisal of the microfossil characteristics of each well. The main drawback is that if nine of the ten samples collected for each 30 m interval are barren of microfossils, any microfossils in the tenth sample will be diluted by a factor of ten.

Samples from the Bradelle L-49 well were washed through a 63 μm wet sieve to remove the clay, and then oven dried. A portion of each washed sample was put aside for immediate examination, while the remainder of the sample was processed using the industrial detergent method described by Wightman et al. (in press). Comparison of the portions of the samples that had been washed only with water to the portions treated with industrial detergent showed that no significant advantage was to be gained from use of the latter method. This is probably because drilling had ground the strata sufficiently to release the microfossils through mechanical breakdown of the rock. The samples from the East Point E-49 well were consequently not treated with industrial detergent. A small (approximately 10 g) portion of the coarse (>1.0 mm) fraction of the water-washed samples from both wells was also treated with sodium hypochlorite, using the method described by Wightman et al. (in press). This method of treatment is the most effective way of releasing agglutinated foraminifera from carbonaceous shales and siltstones, and gave good results in this study.

Washed residues were sieved into >63 μm, >125 μm, >250 μm and >500 μm size fractions, and each of these was systematically examined by sprinkling an even, light coating of the residue over a 5 cm x 10 cm picking tray. All foraminifera and thecamoebians were picked from two such picking tray spreads for each size fraction. Because of poor preservation, specimens were examined under both reflected light, and transmitted light with glycerin. Photomicrographs of the best specimens were taken with the environmental scanning electron microscope unit at the Atlantic Geoscience Centre.

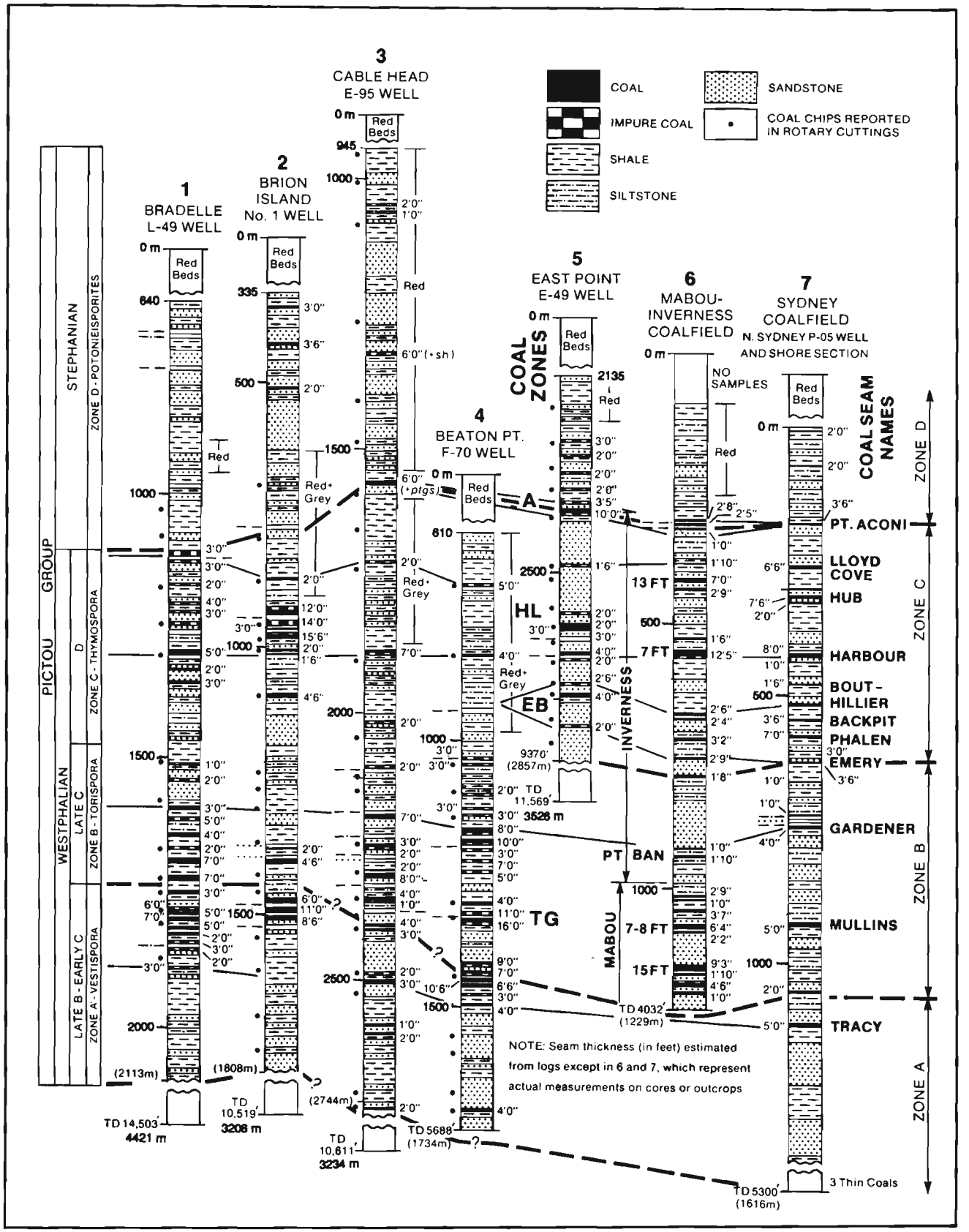

Figure 3. Logs of wells in the Gulf of St. Lawrence region with correlations of coal-bearing strata to coalfields on Cape Breton Island (locations in Fig. 1). After Hacquebard (1986).

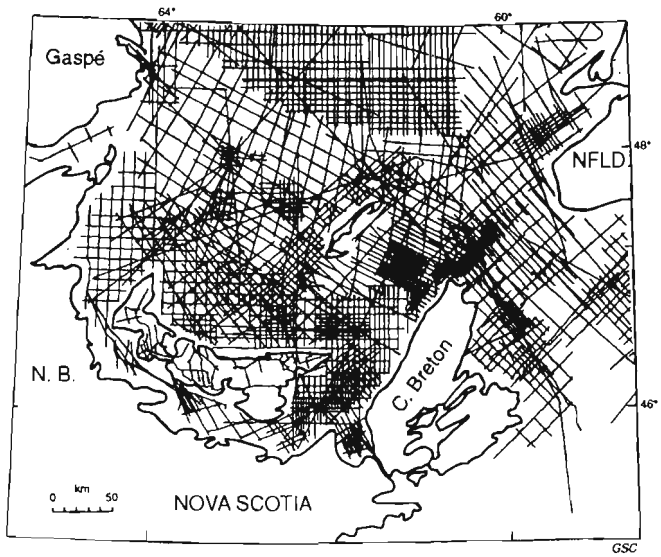

Figure 4. Map showing location of industry seismic lines in the Gulf of Saint Lawrence and on Prince Edward Island. From Grant and Moir (1992).

RESULTS

As discussed above, our sampling strategy enables a rapid overview of the wells to determine if there were marine influences during deposition. Although the results represent an average of each 30 m interval, broader distribution patterns of the agglutinated foraminifera and thecamoebians both downhole and between the two wells are apparent. Agglutinated foraminifera and thecamoebians were identified at all intervals in both wells, with the exception of the 1033-1064 m interval in the Bradelle L-49 well. Variations in the thecamoebian and agglutinated foraminiferal components picked from each interval are plotted in percentage diagrams, together with lithology types (Fig. 6, 7). Lithology types are based on grain counts of the same intervals.

In both wells, the agglutinated foraminifera are dominated by the genera *Trochammina*, *Ammotium* and *Ammobaculites*. The morphological variants within these groups (Plate 1) are similar to those observed in the Sydney Coalfield (Wightman et al., 1993, in press) and the Illinois Basin (Devera et al., 1993). Other groups found include biserial morphotypes and uniserial forms that may include *Reophax*, although the

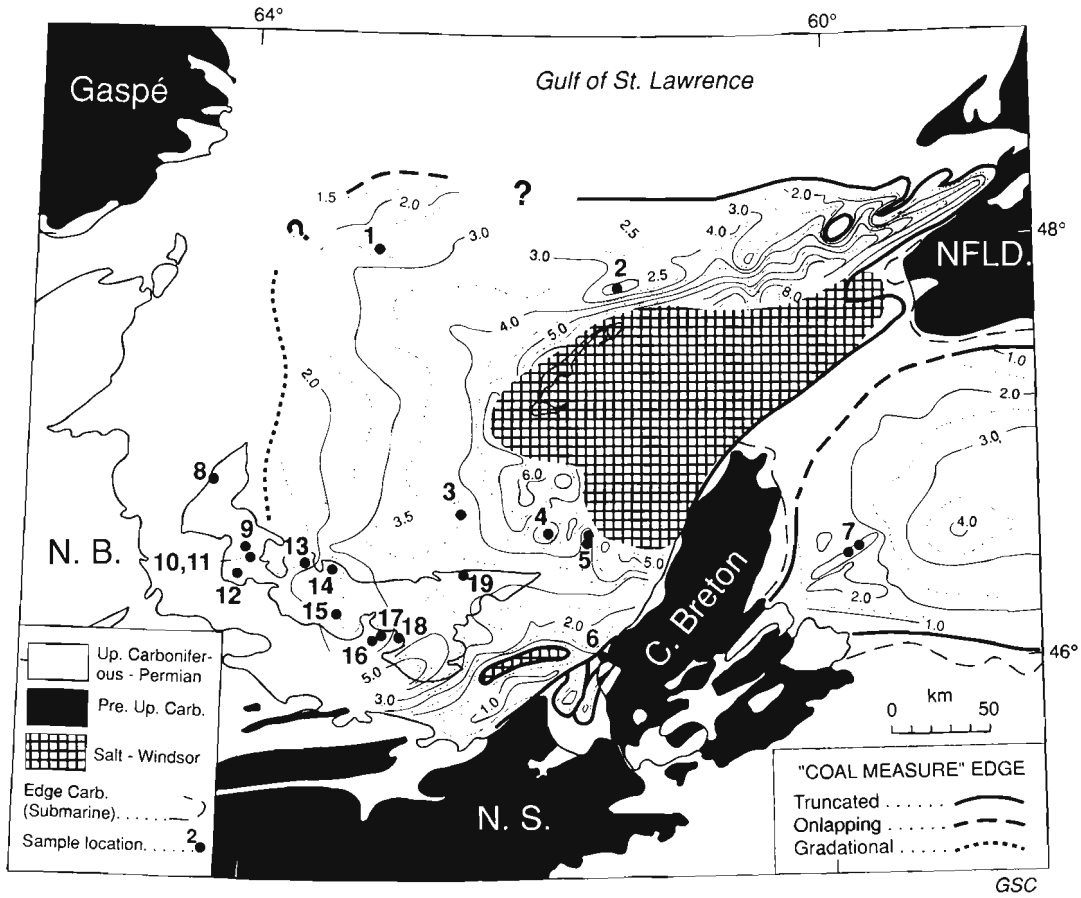

Figure 5. Map of the present extent and depth of the Coal Measures seismic facies, contour interval 0.5 km, derived from interpretation of industry seismic data (Fig. 4). Areas of evaporite tectonism indicated by cross hatching. Numbers denote well locations and coal mining areas; 1-7 are identified in Figure 1 caption. After Grant and Moir (1992).

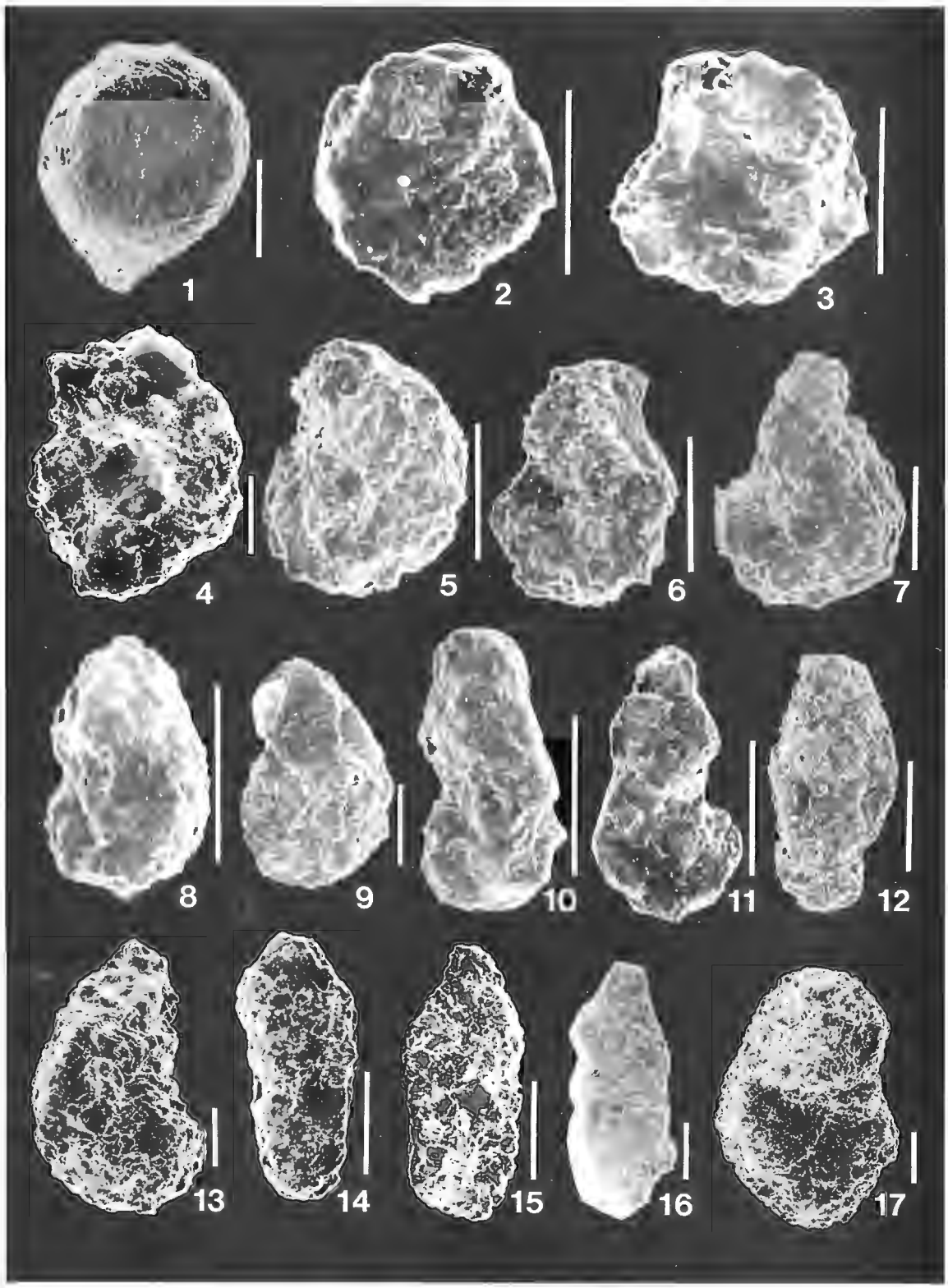

PLATE 1

number of specimens is small and the preservation too poor to make accurate identifications. The thecamoebians are of the spherical morphotypes (comparable to recent *Difflugia* and *Centropyxis*), also reported from the Sydney Coalfield (Wightman et al., in press).

In the Bradelle L-49 well, the proportion of thecamoebians in the interval sampled increases downhole to the point where they dominate over the agglutinated foraminiferal groups at intervals below 1829 m. *Trochammina* is dominant over the other groups of agglutinated foraminifera and is generally more abundant in the shallower part of the sample interval. *Ammotium* is represented by low numbers of individuals that occur sporadically in the samples. *Ammobaculites* occurs in more samples than *Ammotium*, and is generally more abundant. Biserial forms occur in low abundances in the 1576-1589 m, 1722-1750 m and 1905-1932 m intervals. Lithologically, grey siltstone is the dominant clast type in the Bradelle L-49 well samples. Red siltstone occurs in equal proportion to the grey siltstone in the upper 91 m of the sample interval, but declines thereafter. The proportion of coal is often highest within the deeper intervals. Sandstone occurs sporadically in most samples, and is more common in the upper part of the sample interval. Limestone clasts occur in the 1661-1719 m interval only.

With the exception of the 2301-2329 m and 2362-2390 m intervals in the East Point E-49 well, agglutinated foraminifera are dominant over the thecamoebians. The uncoiling morphotypes *Ammotium* and *Ammobaculites* represent a greater proportion of the fauna in the sampled interval in this well than in the Bradelle L-49 well, and combined, they dominate the assemblages in the 2332-2359 m and 2786-2813 m intervals. As with the Bradelle L-49 samples, *Ammobaculites* occurs

PLATE 1

Scale bar = 100 μm

Figure 1. Thecamoebian, spherical form with a short spine, comparable to the modern genus *Centropyxis*. Bradelle L-49 well, 1244-1274 m.

Figures 2, 3. *Trochammina* spp. East Point E-49 well, 2301-2329 m (specimen 2); 2591-2618 m (specimen 3).

Figures 4-11. *Ammobaculites* spp. **4**: specimen with well developed coil. Uncoiled portion broken off. East Point E-49 well, 2210-2237 m. **5**: Showing well developed coil. Bradelle L-49 well, 1417-1445 m. **6, 7:** large coiled variants that have retained part of their uncoiled portions. Bradelle L-49 well, 1661-1689 m (specimen 6), 1094-1125 m (specimen 7). **8, 9:** smaller coiled variants. East Point E-49 well, 2484-2512 m (specimen 8), 2179-2207 m (specimen 9). **10, 11:** Specimens with well developed uncoiled portions. Note the preservation of the terminal aperture on specimen 11. East Point E-49 well, 2707-2734 m (specimen 10), 2591-2618 m (specimen 11).

Figures 12-16. *Ammotium* spp. **12**: Small coiled variant, Bradelle L-49 well, 1094-1122 m. **13**: Large coiled variant composed of fine sand grains. East Point E-49 well, 2240-2268 m. **14-16:** small coiled variants with typical form of aperture that is drawn out on a short neck. Specimen 16 displays well preserved lobate lateral margins. East Point E-49 well, 2646-2673 m (specimen 14), 2362-2390 m (specimen 15), Bradelle L-49 well, 1094-1122 m (specimen 16).

Figure 17. Agglutinated foraminifera of uncertain affinity. The aperture, which has been infilled, appears as a circular depression on the face of the final chamber. Bradelle L-49 well, 1661-1689 m.

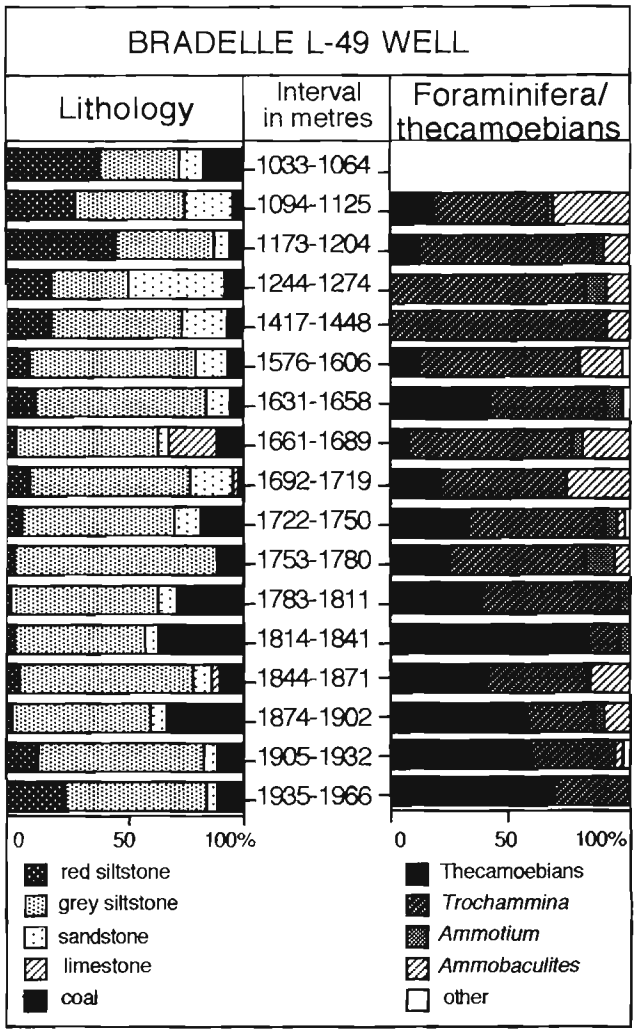

Figure 6. *Percentage diagrams of lithological clasts and agglutinated foraminifera and thecamoebians in the intervals examined in the Bradelle L-49 well.*

more frequently than *Ammotium*, and is usually more abundant. *Trochammina* is present in all intervals and typically comprises 30 to 70% of the fauna. Other types of agglutinated foraminifera, including biserial forms and possible *Reophax*, occur in the 2484-2588 m and 2646-2673 m intervals in moderate proportions. In comparison with the Bradelle L-49 well, the East Point E-49 sample interval is lithologically more sandy. Sandstone is the dominant lithology through most of the samples, and increases in its proportion downhole to compose as much as 80% of the clasts. Red siltstone is most abundant in the upper 61 m of the sample interval, but decreases downhole. Grey siltstone occurs in moderate proportions (<25% of the clasts) through most of the samples, whereas coal is present in small proportions (<15%) at depths below 2271 m. A small amount of limestone was observed in the 2240-2268 m interval.

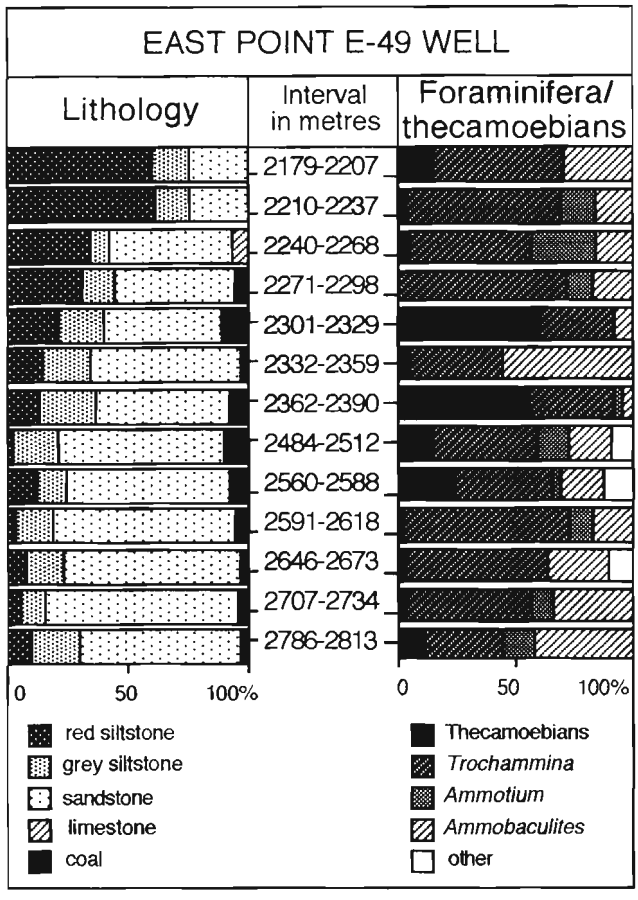

Figure 7. *Percentage diagrams of lithological clasts and agglutinated foraminifera and thecamoebians in the intervals examined in the East Point E-49 well.*

DISCUSSION

Paleoenvironmental interpretation

The distribution of agglutinated foraminifera and thecamoebian assemblages in the Bradelle L-49 and East Point E-49 wells can be compared with the distribution of similar assemblages in coastal outcrop sections of Westphalian to Stephanian age in the Sydney Basin, Nova Scotia, examined in detail by Wightman et al. (1993, in press). Direct comparison may also be made with the modern distributions of agglutinated assemblages in marginal marine and coastal settings, since the foraminiferal faunas in these environments have evolved little, if at all, and have occupied the same ecological niches for the past 300 Ma (Wightman et al., 1993).

Bradelle L-49 well

The gradual increase in thecamoebians downhole in the Bradelle L-49 well suggests an overall increase in freshwater depositional settings with depth, based on the predominance of thecamoebians in freshwater environments today (Medioli and Scott, 1983). Carboniferous thecamoebian and agglutinated foraminiferal assemblages are, in many cases, mutually exclusive in coal bearing strata from the Sydney Basin, indicating the two groups occupied separate niches in adjacent (freshwater and brackish) environments (Wightman et al., in press).

Brackish water environments are also evident in the Bradelle L-49 well, based on the agglutinated foraminiferal assemblages dominated by *Trochammina*. The 1935-1966 m interval, characterized by thecamoebians and *Trochammina*, suggests restricted high marsh environments may have fluctuated with freshwater environments at the terrestrial extreme of tidal influence within an upper estuarine setting. A similar interpretation has been made for alternation of thecamoebian and *Trochammina* assemblages preserved in the seat earth beneath the Point Aconi coal seam in the Sydney Coalfield (Wightman et al., in press). *Trochammina* dominates higher elevations in modern salt marshes (Scott et al., 1991), but is also found in association with *Ammotium*, *Ammobaculites* and other agglutinants in lower marsh or estuarine environments (Ellison and Nichols, 1976; Scott et al., 1991).

The association of *Ammotium* and *Ammobaculites* in many of the sample intervals of the Bradelle L-49 well suggests middle or lower estuarine deposition. This is supported by the presence of biserial foraminifera, normally associated with more open marine environments and subject to reworking into shallower areas.

East Point E-49 well

The greater abundance of *Ammotium* and *Ammobaculites* in the East Point E-49 samples suggests deposition was under more of a marine influence than the sampled interval in the Bradelle L-49 well. This interpretation is supported by larger proportions of biserial and other forms in three of the intervals. Although thecamoebians are present, there is no obvious trend that would indicate an overall change in depositional environments up- or downhole. The dominance of thecamoebians in the 2301-2329 m and 2362-2390 m intervals suggests, however, a greater freshwater influence during these two episodes.

Regional implications

Within a regional context, the sampled strata of the Bradelle L-49 well were likely to have been deposited in an uppermost estuarine setting, at the terrestrial extreme of tidal influence. The general dominance of finer sediments in this section supports our interpretation of an uppermost estuarine mudflat paleoenvironment, with adjacent freshwater coal-forming swamps and marshes. The sampled strata of the East Point E-49 well, in contrast, were probably deposited in a middle to lower estuarine environment. The dominantly sandy character of the samples accords with this interpretation.

Following Hacquebard's (1986) correlation of the main coal-bearing strata in the Gulf of St. Lawrence and Sydney Basins, the 1033-1448 m interval in the Bradelle L-49 well would correlate with the 2484-2813 m interval in the East Point E-49 well, and would represent all but the lowest (Emery) coal seam of the Sydney Mines Formation of the Sydney Coalfield (Barss and Hacquebard's (1967) Spore Zone C). Gibling (1992) recognized eleven cyclothems within the Sydney Mines Formation, and assuming Hacquebard's (1986) correlations to be correct, we anticipate the cyclothems to be present within the above intervals in the Bradelle L-49 and East Point E-49 wells. Work currently being undertaken by T.A. Rehill (Dalhousie University, Ph.D. thesis) on the downhole characteristics of these two wells will evaluate the existing correlations between the wells, and will help to evaluate the role of cyclothymic deposition in the Maritimes Basin.

The agglutinated foraminifera and thecamoebian assemblages of the Gulf of St. Lawrence are closely similar to those documented from the cyclothems of the Sydney Coalfield (Wightman et al., 1993, in press). Several distinctive paleoenvironments, related to the varying degrees of marine influence associated with cyclothem development have been recognized on the basis of their agglutinated foraminifera and thecamoebian assemblages (Gibling and Wightman, in prep.) The assemblages identified in the Bradelle L-49 and East Point E-49 wells undoubtedly represent the combination of several distinct paleoenvironments that would have developed as a result of varying marine influences during cyclothymic deposition.

CONCLUSIONS

The discovery of agglutinated foraminifera assemblages in offshore wells in the Gulf of St. Lawrence supports the argument that the regionally extensive Coal Measures seismic facies reflects cyclothymic deposition, including phases of marine incursion. A marine component in this facies enhances the possibility of marine source rocks for hydrocarbon generation, with potential for oil as well as gas resources related to the Coal Measures facies. These new findings highlight the need for further research on the paleogeographic and depositional history of the Gulf of St. Lawrence region of the Maritimes Basin, and for review of the hydrocarbon potential of this region.

ACKNOWLEDGMENTS

Research is supported by contract No. 23420-3-C069/01-OSC awarded to W.G. Wightman, and T.A. Rehill is funded by a NSERC Grant (through M. Gibling), by Dalhousie University's Industry Research Associate Scheme, and the Geological Survey of Canada's Hydrocarbon Charge Modelling Project. We are grateful to the Nova Scotia Offshore Petroleum Board for providing sample material. Thanks are due Patricia Stoffyn for her assistance with the E.S.E.M., Arthur Jackson for extensive help with seismic data, and Gary Grant for the illustrations. This work has benefitted from discussions with Martin Gibling, Franco Medioli and Dave Scott. Peter Hacquebard and Mark Williamson are thanked for their comments as reviewers.

REFERENCES

Barss, M.S. and Hacquebard, P.A.
1967: Age and the stratigraphy of the Pictou Group in the Maritime Provinces as revealed by fossil spores; Geological Association of Canada, Special paper 4, p. 267-282.

Bird, D.J.
1987: The depositional environment of the Late Carboniferous, coal-bearing Sydney Mines Formation, Point Aconi area, Cape Breton Island, Nova Scotia; M.Sc. thesis, Dalhousie University, 343 p.

Devera, J., Staub, J., Kvale, E., Eble, C., Nelson, J., Dimichele, W., and Wightman, W.G.
1993: Tidally influenced depositional settings in the Tradewater Formation (Westphalian B, C, and D), Illinois Basin, U.S.A; in Carboniferous to Jurassic Pangea: A global view of environments and resources; Canadian Society of Petroleum Geologists, Program and Abstracts, p. 74.

Ellison, R.L. and Nichols, M.M.
1976: Modern and Holocene foraminifera in the Chesapeake Bay region; in First International Symposium on Benthonic foraminifera of the continental margins, Part A, Ecology and Biology; Maritime Sediments, Special Publication 1, p. 131-151.

Gibling, M.R.
1992: Late Carboniferous alluvial paleovalleys in the Sydney basin of Nova Scotia; Geological Association of Canada, Abstracts, v. 17, p. A39-40.

Gibling, M.R. and Bird, D.J.
1990: Late Carboniferous cyclothems in the Sydney Coalfield; Nova Scotia Department of Mines and Energy, Report 90-3, p. 39.

Gibling, M.R., Calder, J.H., Ryan, R., van de Poll, H.W., and Yeo, G.M.
1992: Late Carboniferous and Early Permian drainage patterns in Atlantic Canada; Canadian Journal of Earth Sciences, v. 29, p. 338-352.

Grant, A.C.
In press: Aspects of seismic character and extent of Upper Carboniferous Coal Measures, Gulf of St. Lawrence and Sydney Basins; Paleogeography, Paleoclimatology, Paleoecology.

Grant, A.C. and Moir, P.N.
1992: Observations on coalbed methane potential, Prince Edward Island; in Current Research, Part E; Geological Survey of Canada, Paper 92-1E, p. 267-278.

Hacquebard, P.A.
1986: The Gulf of St. Lawrence Carboniferous Basin; the largest coalfield of eastern Canada; Bulletin of Canadian Institute of Mining and Metallurgy, v. 79, p. 67-78.

Hacquebard, P.A., Gillis, K.S., and Bromley, D.S.
1989: Re-evaluation of the coal resources of Western Cape Breton Island; Nova Scotia Department of Mines and Energy, Paper 89-3, 47 p.

Medioli, F.S. and Scott, D.B.
1983: Holocene Arcellacea (Thecamoebians) from eastern Canada; Cushman Foundation for Foraminiferal Research, Special Publication 21, 63 p.

Scott, D.B., Suter, J.R., and Kosters, E.C.
1991: Marsh foraminifera and arcellaceans of the lower Mississippi Delta: Controls on spatial distributions; Micropalaeontology, v. 37, p. 373-392.

Thibaudeau, S.A. and Medioli, F.S.
1986: Carboniferous thecamoebian and marsh foraminifera: New stratigraphic tools for ancient paralic deposits; Geological Society of America Abstracts with Programs, v. 18, p. 771.

Wightman, W.G., Scott, D.B., Medioli, F.S., and Gibling, M.R.
1992: Upper Pennsylvanian agglutinated foraminifers from the Cape Breton coalfield, Nova Scotia: Their use in the determination of brackish-marine depositional environments; Geological Association of Canada Annual Meeting, Abstracts, v. 17, p. A117.

Wightman, W.G., Scott, D.B., Medioli, F.S., and Gibling, M.R.
1993: Carboniferous marsh foraminifera from coal-bearing strata of the Sydney Basin, Nova Scotia: A new tool for identifying paralic coal-forming environments; Geology, v. 21, p. 631-634.

Wightman, W.G., Scott, D.B., Medioli, F.S., and Gibling, M.R.
In press: Agglutinated foraminifera and thecamoebians from the late Carboniferous Sydney Coalfield, Nova Scotia: Paleoecology, paleoenvironments and paleogeographical implications; Paleogeography, Paleoclimatology, Paleoecology.

Geological Survey of Canada Project 870050

Detrital and organic facies of Upper Carboniferous strata at Mabou Mines, western Cape Breton Island, Nova Scotia[1]

M.R. Gibling[2], D.L. Marchioni[3], and W.D. Kalkreuth[4]
Atlantic Geoscience Centre

Gibling, M.R., Marchioni, D.L., and Kalkreuth, W.D., 1994: Detrital and organic facies of Upper Carboniferous strata at Mabou Mines, western Cape Breton Island, Nova Scotia; in Current Research 1994-D; Geological Survey of Canada, p. 51-56.

Abstract: The Late Carboniferous section at Mabou Mines contains thick (>125 m) fine grained intervals that include coals and canneloid shales and were deposited in mires, lakes, and on poorly drained floodplains. Coal analysis indicates that the precursor peat accumulated under conditions of high groundwater level consistent with an upper delta plain to alluvial plain setting. Thick (about 50-100 m) sandstone intervals with strongly erosional bases and multiple storeys alternate with the coal-bearing intervals and are interpreted as braided-fluvial deposits. Such a succession of thick coal-bearing and braided-fluvial intervals reflects recurrent, radical changes in depositional conditions, possibly related to activity on the adjacent Hollow Fault Zone.

Résumé : Aux mines Mabou, la succession remontant au Carbonifère tardif renferme d'épais intervalles (>125 m) de lithologies à grain fin composées de charbons et de shales riches en spores qui se sont déposés dans des fondrières, des lacs et des plaines d'inondation mal drainées. L'analyse des charbons indique que la tourbe de laquelle ils tirent leur origine s'est accumulée dans des conditions de haut niveau des eaux souterraines, conditions caractéristiques des milieux de plaine deltaïque supérieure et de plaine alluviale. D'épais intervalles (environ 50 à 100 m) de grès présentant un contact basal témoignant nettement d'une érosion et comportant plusieurs étages, alternent avec les intervalles houillers et seraient des dépôts de cours d'eau anastomosés. Une telle succession d'épais intervalles de lithologies houillères et de grès de cours d'eau anastomosés témoigne de changements radicaux et récurrents des conditions de dépôt, qui sont peut-être reliés à l'activité dans la zone de failles Hollow qui se trouve à proximité.

[1] Contribution to Canada-Nova Scotia Cooperation Agreement on Mineral Development (1992-1995), a subsidiary agreement under the Canada-Nova Scotia Economic and Regional Development Agreement.
[2] Department of Earth Sciences, Dalhousie University, Halifax, Nova Scotia B3H 3J5
[3] Petro-Logic Services, 231 - 10A St. N.W., Calgary, Alberta T2N 1W7
[4] Institute of Sedimentary and Petroleum Geology, Calgary, Alberta T2L 2A7

INTRODUCTION

The Gulf of St. Lawrence and adjacent onshore regions of the Atlantic provinces form eastern Canada's largest coal basin, about 46 000 km^2 in area (Fig. 1A). Well-log, seismic, and biostratigraphic analyses indicate that the coal-bearing interval is locally in excess of 2 km thick and includes strata as old as Westphalian A but principally of Westphalian C-D to Stephanian age (Hacquebard, 1986; Hacquebard et al., 1989; Grant and Moir, 1992). Although the strata have economic potential for nearshore coal mining (Hacquebard et al., 1989) and for coal-bed methane (Grant and Moir, 1992), little is known about the lithofacies succession of the submarine part of the coal basin.

Coal measures of the Inverness Formation, of Westphalian C-D age, that outcrop in the Mabou Mines and Inverness areas of western Cape Breton Island provide a "window" into the coal-bearing strata in the immediately adjacent offshore area. The stratigraphy, organic petrology, and sedimentology of the Mabou Mines strata (Fig. 1B) were studied by Norman (1935), Keating (1950), Hacquebard (1962, 1980, 1986, in press), Deal (1986), Dickie (1986), and Gibling and Kalkreuth (1991). The stratigraphic architecture is unusual in that thick intervals dominated by mudrocks, coal, and oil shale alternate with channel-sandstone intervals up to about 100 m thick. The intervals extend into the adjacent offshore area and may be considerably more extensive. This paper presents preliminary results of studies at Mabou Mines carried out under the current Federal-Nova Scotia Mineral Development Agreement and draws inferences about the depositional setting of the strata using information from both detrital and organic rocks.

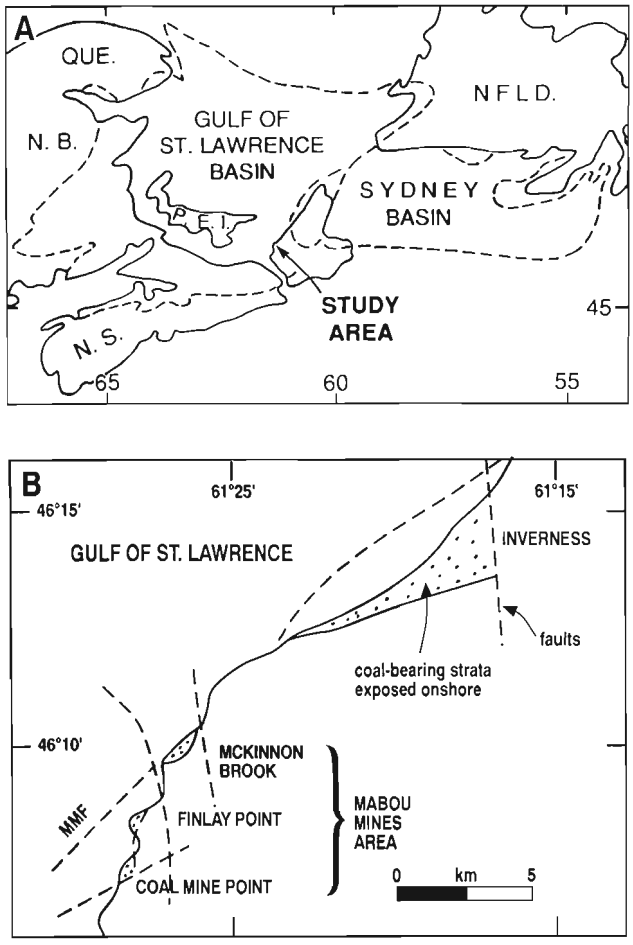

Figure 1. *A) Present-day distribution of Late Paleozoic strata (within dashed lines) in Atlantic Canada, including the Gulf of St. Lawrence and Sydney basins. Location of Mabou Mines study area is shown.* ***B)*** *Distribution of coal-bearing strata onshore at Mabou Mines and Inverness, with some major faults shown; MMF indicates the Mabou Mines Fault. Modified from Hacquebard (in press, Fig. 12).*

GEOLOGICAL SETTING AND AGE

The Inverness Formation at Mabou Mines is exposed at Coal Mine Point, Finlay Point, and McKinnon Brook (Fig. 1B). The strata rest unconformably on, or are faulted against, older Carboniferous rocks that fringe the Mabou Highlands to the east (Norman, 1935). The coal measures are strongly deformed in the onshore exposures, with steep dips and numerous faults. Hacquebard et al. (1989) showed from seismic analysis and seam correlation that a large reversed fault, the Mabou Mines Fault, lies about 1 km offshore from Finlay Point (Fig. 1B). Some of the faults are probably components of the Hollow Fault-Cabot Fault system which lies offshore western Cape Breton and was active during the Late Carboniferous (Yeo and Ruixiang, 1987; Langdon, 1993). The extensional Ainslie Detachment, mapped in western Cape Breton by Giles and Lynch (1993), was active during this period, and evaporite diapirs which are abundant under the southern Gulf of St. Lawrence were probably in early stages of development (Howie, 1988). Some of the deformation may reflect later Alleghanian or Mesozoic events, and it is at present unclear how much of the deformation at Mabou Mines was syndepositional and how much postdepositional.

Barss and Hacquebard (1967) gave a Westphalian C age to the Mabou Mines strata. Dolby (1987) assigned a late Westphalian C to early Westphalian D age, with the C-D boundary tentatively placed at about the level of the 5 Foot Seam at Coal Mine Point, below the Eagle Sandstone (Fig. 2).

STRATIGRAPHIC SECTIONS

On the south side of Coal Mine Point, 125 m of coal-bearing strata, faulted against older rocks, are overlain by the Eagle Sandstone, which is about 93 m thick (Fig. 2). This, in turn, is overlain by 68 m of coal-bearing strata capped by the Stack Sandstone, which is about 55 m thick. At Finlay Point, 20 m of coal-bearing strata, faulted at the base, are overlain by the Point Sandstone (about 90 m thick) (Deal, 1986). Predominantly sandstone strata at McKinnon Brook (Fig. 1B) are not discussed in this report.

COAL-BEARING INTERVALS

Detrital facies

Grey shale and siltstone form the bulk of the coal-bearing intervals. These fine grained strata are mainly massive but locally laminated. Roots, including *Stigmaria*, and plant fragments are present at many levels. Bivalves are common, and *Anthracomya* was identified by Keating (1950). Siderite nodules are present both scattered and in nodule-rich layers, and siderite bands up to 5 cm thick are observed.

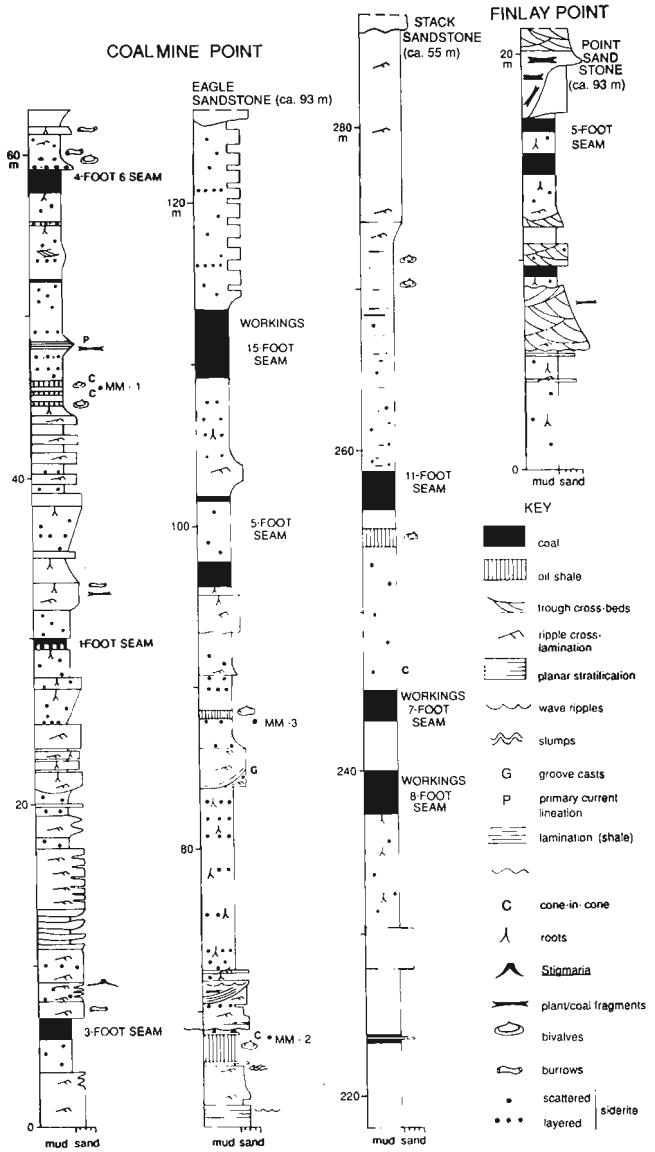

Figure 2. *Lithofacies profile for coal-bearing strata at Coal Mine Point and on the southern side of Finlay Point, Mabou Mines area. Seam names are taken from Hacquebard (1980). MM-1 to MM-3 indicates location of dark shale samples studied by Gibling and Kalkreuth (1991). Profile is based in part on sections in Deal (1986) and Dickie (1986).*

Associated sandstones, predominantly fine grained, form units a few centimetres to about 2 m thick, and are mainly restricted to the lower coal-bearing interval. The sandstone beds are commonly interbedded with shales in units up to about 10 m thick, and show current- and wave-ripple stratification and planar stratification with primary current lineation. Some sandstone beds occupy shallow scours and show groove casts on their basal, erosional surfaces. Roots, siderite nodules, and burrows are observed in some beds.

Dark, tough shale units, up to about 1 m thick, are interbedded with the grey shales or associated with some coals. Most units are rich in bivalves and ostracodes, the flattened tests of which impart a wavy stratification to the rocks. Cone-in-cone structure is present in some units. Three samples (MM-1 to MM-3; see Fig. 2 for locations) analyzed by Gibling and Kalkreuth (1991) are composed of clay minerals (illite, kaolinite, and chlorite), with quartz silt and variable amounts of shells and fine grained calcite, fish material, pyrite, siderite grains, and phosphatic nodules (possibly coprolites). One occurrence of burrows was noted in thin section. Total organic carbon content ranges from 2.3 to 13.2%. Vitrinite predominates in the organic component of two samples and sporinite in the third, with minor telalginite, cutinite, liptodetrinite, and inertinite. The organic matter is characterized as Type III, consistent with terrestrial plant sources, and the samples can be termed canneloid shales. Hutton (1987) restricted the term "oil shale" to rocks with >5 vol.% of liptinite, on which basis only sample MM-2 would be an oil shale. The samples show a modest oil and gas potential, from 2.7 to 42.6 kg of hydrocarbons per tonne of rock, and vitrinite reflectance of one sample was 0.62%Ro. Four dark shale samples analyzed by Smith and Naylor (1990) yielded similar results.

Stratal patterns are complex, but units that coarsen up from dark or grey shale to sandstone are present and locally greater than 10 m thick. The Mabou Mines strata are currently interpreted as freshwater deposits. Several shale samples disaggregated by W.G. Wightman (pers. comm., 1993) failed to yield agglutinated foraminifera. These organisms are found in abundance in coal-measure shales in the Sydney Coalfield where they are indicative of marine influence (Wightman et al., 1993).

Coals

Eight major seams are present in the Coal Mine Point section (Fig. 2), and are named based on their approximate thicknesses. An additional seam (the "New 11-Foot Seam": Hacquebard, in press) lies below the base of the exposed section. Maximum seam thickness, including partings, is 3.9 m, with six seams greater than 1.4 m thick.

The petrography and technical properties of seven Mabou Mines coals were documented in detail by Hacquebard (in press). The coals are high volatile B to C in rank with vitrinite reflectance levels of 0.6-0.7%Ro. Seam-average ash and sulphur contents range from 4.8 to 17.5% and 1.5 to 7.1%, respectively. Finely disseminated pyrite typically accounts for 50-60% of the total sulphur. Within most seams, predominantly bright coal alternates with coal that has a considerable

amount of dull coal components. Microlithotype analysis shows a predominance of the reed moor facies, with lesser proportions of open moor and forest moor facies. Small monolete miospores with sphenopsid (horsetail) affinity are present in great abundance.

As part of a regional study of Late Carboniferous coals in Atlantic Canada, six Mabou coals (the 3, 4'6", 5, 15, 7 and 8 Foot seams: Fig. 2) were sampled, and their maceral proportions were determined on full-seam composites. Five of the coals show relatively high vitrinite (72-82%), moderate inertinite (15-23%), and low liptinite (<6%) proportions on a mineral-matter-free (mmf) basis (Fig. 3). Pyrite contents are relatively low (<3.3%) and clastic mineral contents moderate (clay plus quartz up to 8%). The 5 Foot seam is unusual, with relatively lower vitrinite (62%, mmf), higher inertinite (31%, mmf), and higher clastic mineral (19%) contents. Petrographic parameters are quite variable, apart from the W/D ratio [structured vitrinite+structured inertinite/inertodetrinite+discrete macrinite+sporinite], which is moderately high (>5) in the Mabou Mines seams. On maceral-ratio diagrams (Diessel, 1986, 1992), the coals show moderate values of Gelification and Tissue Preservation Index (Fig. 4), and their plotted positions correspond to Diessel's upper delta plain to alluvial plain zone as determined for coals of the Newcastle Coal Measures, Australia. Hacquebard (in press, Fig. 17) plotted a maceral-ratio diagram for the Mabou Mines seams using ratios modified slightly from those of Diessel (1986, 1992), and obtained broadly similar results.

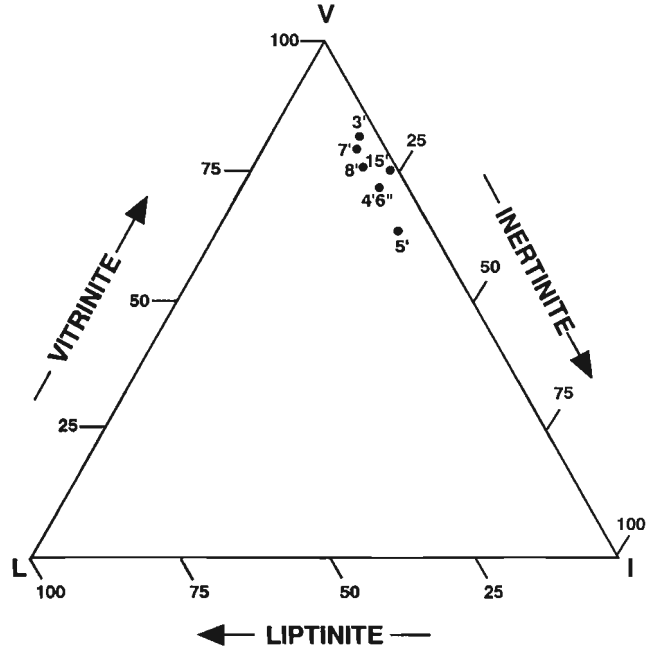

Figure 3. Ternary plot of the maceral group compositions for seams in the Mabou Mines area. See Figure 2 for stratigraphic positions of seams.

SANDSTONE INTERVALS

Preliminary study of the Eagle and Stack sandstones of the Coal Mine Point section and the Point Sandstone at Finlay Point shows that they are predominantly medium grained and trough crossbedded, with subordinate planar stratification, ripple crosslamination, planar crossbeds, and massive to convolute-stratified sandstone. The sandstone bodies are multistoried, with individual storeys separated by erosional surfaces mantled with intrabasinal mudstone, vascular plant fragments and extrabasinal clasts up to 40 cm in diameter. There is little indication of upward fining or pronounced upward succession of sedimentary structures within the storeys. Thin shales are present at a few levels within the bodies, and a thin coal associated with shale is present 38 m above the base of the Point Sandstone. Coal clasts up to 30 cm thick and 1.5 m long are present in sandstones that overlie the strongly erosional base of the Point Sandstone.

Hacquebard (1962, in press, Fig. 7) suggested from petrographic and palynological analysis that the 15 Foot seam in the Coal Mine Point section correlates with the 5 Foot Seam that underlies the Point Sandstone at Finlay Point. He also suggested, from correlation of outcrop sections and drill cores, that the 7 Foot seam correlates with the thin coal located within the Point Sandstone. These

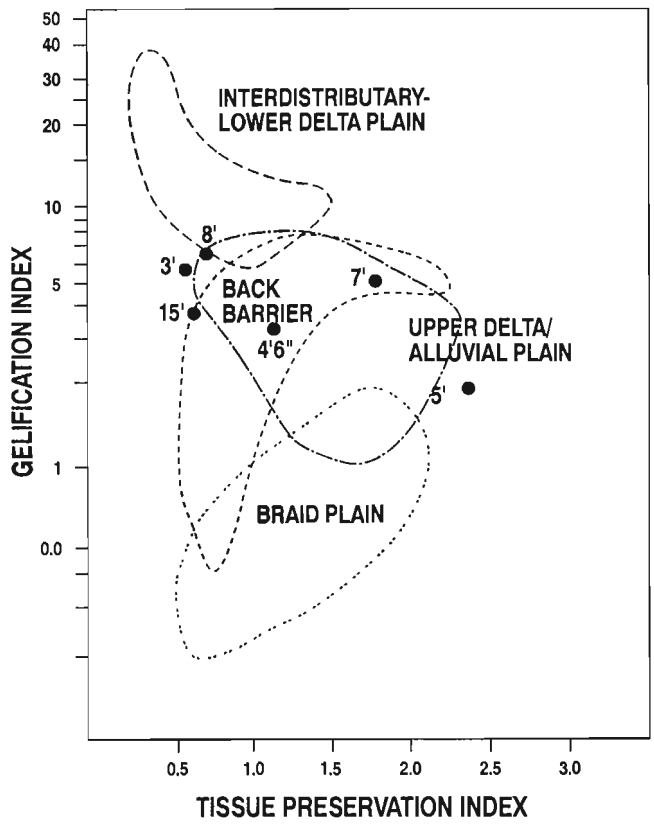

Figure 4. Maceral-ratio facies diagram for seams of the Mabou Mines area. The depositional zones were defined for the Newcastle Coal Measures (Permian) in eastern Australia (Diessel, 1986, 1992).

correlations suggest that the Eagle and Stack sandstones are locally incised and highly variable in thickness, and that they are amalgamated at Finlay Point.

DEPOSITIONAL ENVIRONMENT

The abundance of rooted grey mudstones in the coal-bearing intervals at Coal Mine and Finlay Point indicates that deposition took place on poorly drained, vegetated floodplains. Associated thin beds of ripple crosslaminated sandstone are interpreted as crevasse splays. Coarsening up (shale to sandstone) units, rooted in their upper parts, probably formed when crevasse splays or small deltas prograded into standing-water bodies. The abundant siderite is indicative of reducing conditions at shallow depths of burial. The dark shales are interpreted as lake deposits, formed where an unusually low input of siliciclastic and carbonate detritus permitted the preferential accumulation of biological materials including shells, fish bones, coprolites, spores, algae, and woody material (Gibling and Kalkreuth, 1991). The presence of *Anthracomya* and ostracodes, but the apparent absence of foraminifera suggests that standing-water bodies were fresh.

Thick bituminous coals attest to the periodic accumulation of peats tens of metres thick. The predominance of the reed-moor facies indicates that the peats accumulated under relatively high groundwater levels (Hacquebard, in press). This conclusion is supported by the abundance of palynomorphs derived from sphenopsids, a group that typically grew along lake and point-bar margins in clastic floodbasins (Scott, 1978; Dimichele and Phillips, in press). Maceral-ratio diagrams show that the Mabou Mines coals are comparable with coals from upper delta-plain to (distal) alluvial-plain strata of the Newcastle Coal Measures. These results are in accord with the prevalence of lake deposits, including canneloid shales, in the associated detrital strata. The relatively high W/D ratios indicate that clastic influxes were short-lived and did not influence mire ecology significantly. This inference is supported by the paucity of microlithotypes attributed to the open moor facies (Hacquebard, in press). The high sulphur levels of some seams and parts of seams may indicate the influence of Late Carboniferous marine waters or of sulphate derived from the underlying Windsor Group evaporites (Gibling et al., 1989).

Many of the above sediment types can be matched in the Mississippi Delta region (Coleman and Prior, 1980) where modern analogues for the Mabou Mines strata include the shallow, flood-basin lakes and mires of the Atchafalaya and Barataria basins (Kosters et al., 1987; Tye and Coleman, 1988). The coals, however, are much thicker than those that would result from lithification of the modern, thin peats.

The exceptional thickness (about 50-100 m), multistorey character, and relative uniformity of grain size and sedimentary structures of the sandstone intervals indicates that they represent the stacked deposits of low-sinuosity (braided) channels. The predominance of trough crossbeds suggests that individual channels were relatively deep and partially confined (cf. Rust and Gibling, 1990).

DISCUSSION

The abrupt alternation of thick, braided channel-belt sandstones and thick coal-bearing intervals is an unusual aspect of the Mabou Mines strata. Although some braided-fluvial systems lie adjacent to wetlands, the relative thickness of the two types of sediment body at Mabou Mines suggests that they represent successive channel-belt and wetland phases of considerable areal extent, rather than formerly coeval facies now seen in vertical succession in accord with Walther's Law. Maceral-ratio diagrams provide support for this inference because the coals plot within an upper delta plain to alluvial plain zone, rather than a braidplain zone, by comparison with the Newcastle Coal Measures. A similar alternation of facies in British coal measures was described by Haszeldine and Anderton (1980). Strong incision at the bases of some sandstone bodies is indicated by lateral variation in sand-body relationships and evidence for substantial erosion of peat. This suggests that the onset of channel-belt conditions was associated with considerable downcutting.

The cause of this alternation is speculative at present. Proximity of the strata to the Hollow Fault Zone, known to have been active elsewhere in Nova Scotia at this time, suggests that the stratal alternation had a tectonic origin. The abundance of "wet" lithotypes suggests that subsidence was rapid during formation of the coal-bearing intervals. Although a eustatic cause is also possible, marine influence has not been demonstrated to date for these strata.

As regards hydrocarbon source potential, the strata contain abundant coal and canneloid shales with Type III organic matter and moderate hydrocarbon yields on pyrolysis. Vitrinite reflectance data for the coals and oil shales (0.6-0.7% Ro) indicate that the strata are currently within the oil window and close to the window of gas generation from Type III organic matter (onset at 0.55 and 0.8% Ro, respectively, Kalkreuth and McMechan, 1988). Gas shows were noted in many wells in the Gulf of St. Lawrence area (Grant and Moir, 1992).

ACKNOWLEDGMENTS

We are grateful for financial support from the Federal - Nova Scotia Mineral Development Agreement to Gibling, and from Energy, Mines and Resources (Institute of Sedimentary and Petroleum Geology) at Calgary to Marchioni and Kalkreuth.

REFERENCES

Barss, M.S. and Hacquebard, P.A.
1967: Age and the stratigraphy of the Pictou Group in the Maritime Provinces as revealed by fossil spores; in Geology of the Atlantic Region, (ed.) E.R.W. Neale and H. Williams; Geological Association of Canada, Special Paper 4, p. 267-282.

Coleman, J.M. and Prior, D.B.
1980: Deltaic sand bodies; American Association of Petroleum Geologists Education Course Notes Series No. 15, Tulsa, Oklahoma, 171 p.

Deal, A.J.
1986: Carboniferous fluvial strata of the Inverness Formation at Finlay Point, southwest Cape Breton Island; B.Sc. Honours thesis, Dalhousie University, Halifax, Nova Scotia, 73 p.
Dickie, J.R.
1986: Upper Carboniferous fluvial sedimentation in the Gulf of St. Lawrence Coal Basin, Mabou Mines, Nova Scotia; B.Sc. Honours thesis, Dalhousie University, Halifax, Nova Scotia, 118 p.
Diessel, C.F.K.
1986: The correlation between coal facies and depositional environments; in Advances in the Study of the Sydney Basin, Proceedings 20th Symposium, University of Newcastle, New South Wales, Australia, p. 19-22.
1992: Coal-bearing depositional systems; Springer-Verlag, Berlin, 721 p.
Dimichele, W.A. and Phillips, T.L.
in press: Paleobotanical and paleoecological constraints on models of peat formation in the Late Carboniferous of Euramerica; Palaeogeography, Palaeoclimatology, Palaeoecology.
Dolby, G.
1987: Palynological analysis of samples from the Stellarton Basin, Canfield Creek and Mabou Mines, Nova Scotia; Nova Scotia Department of Natural Resources, unpublished report 87/18.
Gibling, M.R. and Kalkreuth, W.D.
1991: Petrology of selected carbonaceous limestones and shales in Late Carboniferous coal basins of Atlantic Canada; International Journal of Coal Geology, v. 17, p. 239-271.
Gibling, M.R., Zentilli, M., and McCready, R.G.L.
1989: Sulphur in Pennsylvanian coals of Atlantic Canada: geologic and isotopic evidence for a bedrock evaporite source; International Journal of Coal Geology, v. 11, p. 81-104.
Giles, P.S. and Lynch, G.
1993: Bedding-parallel faults, breccia zones, large-scale recumbent folds and basin evolution: the case for extensional tectonics in the onshore Magdalen Basin in Nova Scotia; Atlantic Geoscience Society Annual Colloquium, Program with Abstracts.
Grant, A.C. and Moir, P.N.
1992: Observations on coalbed methane potential, Prince Edward Island; in Current Research, Part E; Geological Survey of Canada, Paper 92-1E, p. 269-278.
Hacquebard, P.A.
1962: Palynological studies on some upper and lower Carboniferous strata in Nova Scotia; Proceedings, Third Coal Conference, Crystal Cliffs, Nova Scotia, p. 227-253.
1980: Geology of Carboniferous coal deposits in Nova Scotia; Field Trip Guidebook, Geological Association of Canada, Trip 7, 37 p.
1986: The Gulf of St. Lawrence Carboniferous Basin; the largest coalfield of Eastern Canada; Canadian Institute of Mining Bulletin, v. 79, p. 67-78.
in press: Petrology and facies studies of the coal seams in the Carboniferous section of the Mabou and Inverness Coalfields, Cape Breton Island, Nova Scotia, Canada; International Journal of Coal Geology.
Hacquebard, P.A., Gillis, K.S., and Bromley, D.S.
1989: Re-evaluation of the coal resources of western Cape Breton Island; Nova Scotia Department of Mines and Energy, Paper 89-3, 47 p.
Haszeldine, R.S. and Anderton, R.
1980: A braidplain facies model for the Westphalian B Coal Measures of north-east England; Nature, v. 284, p. 51-53.
Howie, R.D.
1988: Upper Paleozoic evaporites of southeastern Canada; Geological Survey of Canada, Bulletin 380, 120 p.
Hutton, A.C.
1987: Petrographic classification of oil shales; International Journal of Coal Geology, v. 8, p. 203-231.
Kalkreuth, W.D. and McMechan, M.
1988: Burial history and thermal maturity, Rocky Mountain Front Ranges, Foothills, and foreland, east-central British Columbia and adjacent Alberta, Canada; American Association of Petroleum Geologists, Bulletin, v. 72, p. 1395-1410.
Keating, B.J.
1950: Mabou coal area, Inverness County, Nova Scotia; Nova Scotia Research Foundation, Halifax, unpublished report.
Kosters, E.C., Chmura, G.L., and Bailey, A.
1987: Sedimentary and botanical factors influencing peat accumulation in the Mississippi Delta; Journal of the Geological Society, London, v. 141, p. 423-434.
Langdon, G.S.
1993: Examples of Carboniferous structural styles determined from seismic data in the Cabot Strait; Atlantic Geoscience Society Annual Colloquium, Program with Abstracts.
Norman, G.W.H.
1935: Lake Ainslie Map-area, N.S.; Geological Survey of Canada, Memoir 177, 103 p.
Rust, B.R. and Gibling, M.R.
1990: Braidplain evolution in the Pennsylvanian South Bar Formation, Sydney Basin, Nova Scotia, Canada; Journal of Sedimentary Petrology, v. 60, p. 59-72.
Scott, A.C.
1978: The ecology of Coal Measure floras from northern Britain; Proceedings of the Geologists Association, v. 90, p. 97-116.
Smith, W.D. and Naylor, R.D.
1990: Oil shale resources of Nova Scotia; Nova Scotia Department of Mines and Energy, Economic Geology Series 90-3, 73 p.
Tye, R.S. and Coleman, J.M.
1989: Depositional processes and stratigraphy of fluvially dominated lacustrine deltas: Mississippi delta plain; Journal of Sedimentary Petrology, v. 59, p. 973-996.
Wightman, W.G., Scott, D.B., Medioli, F.S., and Gibling, M.R.
1993: Carboniferous marsh foraminifera from coal-bearing strata at the Sydney basin, Nova Scotia: a new tool for identifying paralic coal-forming environments; Geology, v. 21, p. 631-634.
Yeo, G.M. and Ruixiang, G.
1987: Stellarton Graben: an Upper Carboniferous pull-apart basin in northern Nova Scotia; in Sedimentary Basins and Basin-forming Mechanisms, (ed.) C. Beaumont and A.J. Tankard; Canadian Society of Petroleum Geologists, Memoir 12, p. 299-309.

Geological Survey of Canada Project 920020

Ainslie Detachment in the Carboniferous River Denys basin of Cape Breton Island, Nova Scotia, with regional implications for Pb-Zn mineralization[1]

Greg Lynch and Harold Brisson
Quebec Geoscience Centre, Sainte-Foy

Lynch, G. and Brisson, H., 1994: Ainslie Detachment in the Carboniferous River Denys basin of Cape Breton Island, Nova Scotia, with regional implications for Pb-Zn mineralization; in Current Research 1994-D; Geological Survey of Canada, p. 57-62.

Abstract: The Visean Windsor and Namurian Mabou groups in the River Denys basin of southwest Cape Breton Island are allochthonous above the Ainslie Detachment and Macumber Formation. A ramp and flat geometry is documented; the upper flat occurs beneath the Namurian Mabou Group which has been transported down-section towards the southwest onto the basal detachment at the top of the Macumber Formation. A roll over anticline of Mabou Group and upper Windsor Group lithologies is found to the west. Movement on the detachment has stripped away thick evaporitic units of the Lower Windsor Group, effectively breaching a regional aquiclude and placing overlying carbonates onto the principal basin aquifer, creating a favourable environment for Pb-Zn mineralization. Thickness variations within coarse clastic rocks and pinch-out of the underlying Horton Group may also have focused basin fluids.

Résumé : Les groupes de Windsor (Viséen) et de Mabou (Namurien) dans le bassin de River Denys dans le sud-ouest de l'île du Cap-Breton sont allochtones au-dessus de la faille de détachement d'Ainslie et de la Formation de Macumber. Une géométrie de rampe et de plat est documentée; le plat supérieur est situé à la base du Groupe de Mabou du Namurien qui a été transporté vers le bas de la coupe, vers le sud-ouest, pour reposer directement sur la faille de détachement basale située au sommet de la Formation de Macumber. Un anticlinal de compensation dans les lithologies du Groupe de Mabou et de la partie supérieure du Groupe de Windsor se trouve à l'ouest. Le déplacement le long de la faille de détachement a entraîné la disparition d'épaisses unités évaporitiques de la partie inférieure du Groupe de Windsor, créant une brèche dans un aquiclude régional et amenant les carbonates sus-jacents en contact avec le principal aquifère du bassin, créant ainsi un milieu favorable à la minéralisation de Pb-Zn. Les variations d'épaisseur des roches clastiques grossières et la disparition en biseau du Groupe de Horton sous-jacent ont pu également concentrer les fluides du bassin.

[1] Contribution to Canada-Nova Scotia Cooperation Agreement on Mineral Development (1992-1995), a subsidiary agreement under the Canada-Nova Scotia Economic and Regional Development Agreement.

INTRODUCTION

The River Denys basin (Kelley, 1967) occurs in southwestern Cape Breton Island (Fig. 1) as part of the broader Late Devonian to Carboniferous Maritimes Basin (Howie and Barss, 1975). From southwest to northeast the basin is approximately 50 km long. However, the present limits of the basin are the products of folding and erosion, and do not define the primary outlines of a depositional sub-basin to the Maritimes Basin. The Maritimes Basin is defined by five major groups including the Tournaisian Horton Group, the Visean Windsor Group, the Namurian Mabou Group, the Westphalian Cumberland Group, and the Westphalian to Permian Pictou Group (Howie and Barss, 1975; Ryan et al., 1991). The sedimentary succession reflects postorogenic extension (Horton Group), regional subsidence and marine invasion (Windsor Group), and late dominantly nonmarine clastic sedimentation (Mabou, Cumberland, and Pictou groups). Three of these groups, the Horton, Windsor, and Mabou groups are found in the River Denys basin.

Carbonate hosted Pb-Zn mineralization in the Windsor Group occurs within the River Denys basin at the Jubilee deposit northeast of the present study area (Hein et al. 1993; Paradis et al., 1993). Galena and sphalerite are found in breccia at the top of the Macumber Formation, at a structural and stratigraphic level coincident with the Ainslie Detachment (Lynch and Giles, 1993). The detachment is a low-angle extensional fault which is stratigraphically controlled by the contact between carbonates of the underlying Macumber Formation and a thick overlying evaporitic succession. Extensional tectonics are inferred by the significant stratigraphic gaps which are reported for the Windsor Group in the River Denys basin (Kelley, 1967) and regionally within the Maritimes Basin (Howie and Barss, 1975). Metallogenic models propose that regional fluid flow and Pb-Zn mineralization were controlled by the impervious evaporite cap of the lower Windsor Group above a permeable aquifer consisting of the basal carbonate to the lower Windsor Group and clastic rocks from the underlying Horton Group (Ravenhurst et al, 1989). The study area also encompasses important reserves of industrial minerals including potash, as well as a producing gypsum mine.

This paper focuses on the structural history of Carboniferous rocks in the River Denys basin and to the west along coastal sections within the Whycocomagh 1:50 000 map sheet (NTS 11F/14) (Fig. 2). Particular attention is given to the characterization of the Ainslie Detachment, and the implications for metallogenic models and Pb-Zn mineralization are investigated.

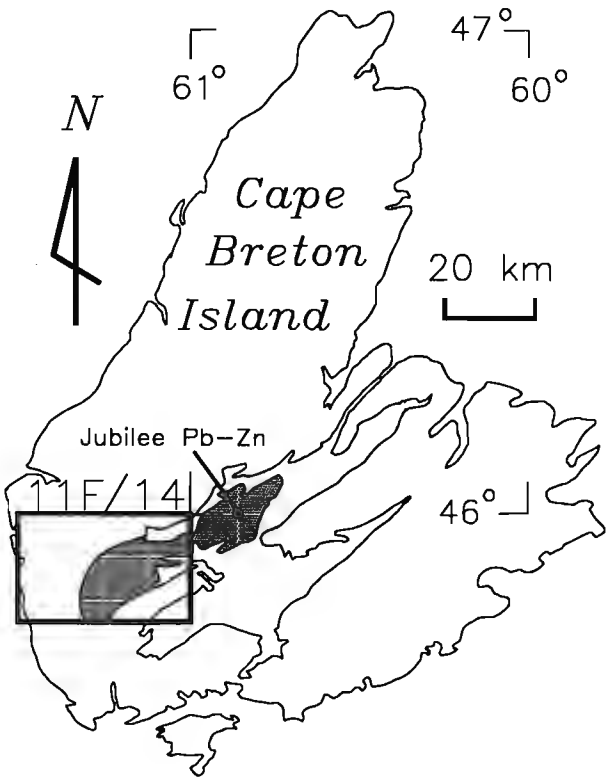

Figure 1. Location map of the study area in Cape Breton Island, showing NTS mapsheet 11F/14, and location of Jubilee Pb-Zn deposit. Stippled pattern outlines River Denys basin.

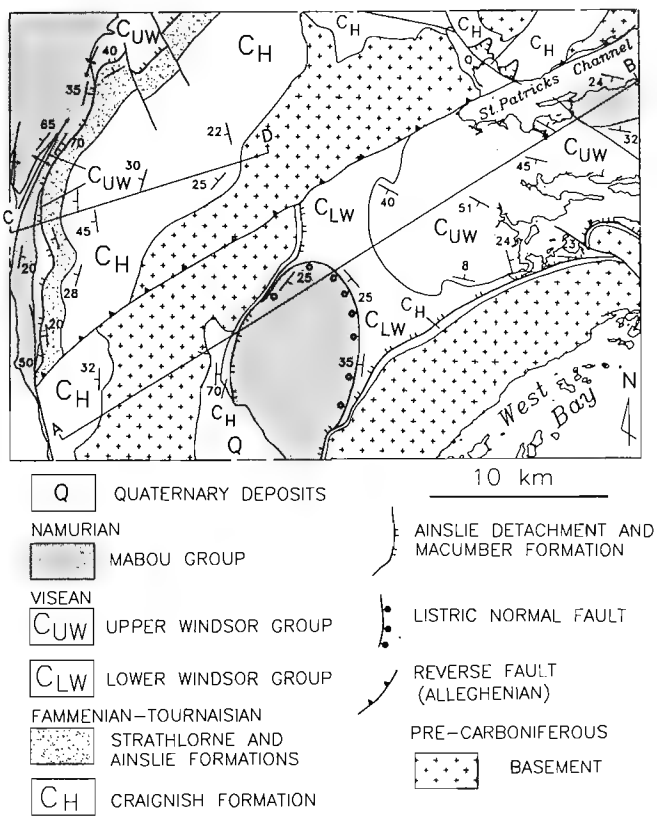

Figure 2. Geological map of the Whycocomagh map sheet (11F/14) (modified from Kelley, 1967) showing surface trace of the Ainslie Detachment. Stratigraphic position of the Macumber Formation equals the trace of the Ainslie Detachment.

BASIN GEOLOGY

Horton Group

The Horton Group is dominated by clastic rocks of Late Devonian (Fammenian) to Carboniferous (Tournaisian) age (Hamblin and Rust, 1989). Conglomerates rest unconformably on basement rocks at several localities. Basement rocks are described by Kelley (1967), Hill (1990), Raeside (1990), and Sangster et al. (1990). Aside from the abundant and diverse plutonic bodies, the basement is dominated by variably metamorphosed rocks of the Precambrian George River Group (Kelley, 1967; Hill, 1990), including limestone/marble, quartzite, phyllite/schist, gneiss, and minor mafic volcanic units. Clasts within basal Horton Group conglomerates typically reflect local provenances; to the north the conglomerates are rich in rounded white quartzite clasts adjacent to the George River Group, whereas granitic clasts are more abundant in the south where the conglomerates have been deposited onto granitic rocks.

In the present study area Kelley (1967) adopted the divisions for the Horton Group of Murray (1960), consisting of the lower Craignish Formation, middle Strathlorne Formation, and upper Ainslie Formation. However Kelley (1967) noted lateral facies changes and interfingering of the Strathlorne and Ainslie Formations. Hamblin and Rust (1989) described the depositional systems for the Horton Group in western Cape Breton Island, focusing much of their study in the northwestern sector of 11F/14. The Craignish Formation features coarse to fine braidplain sediments near fault-bounded alluvial fans as well as distal mudflat/playa deposits; the Strathlorne Formation is interpreted as including lacustrine, shoreline, and fan delta facies; whereas the overlying Ainslie Formation is described as an alluvial fan, fluvial, and floodplain system (Hamblin and Rust, 1989). Facies within the Craignish and Ainslie formations have close similarities. However the Strathlorne Formation is distinguished by the presence of 10-30 cm thick limestone beds, interbedded with mudstone, redbeds, and conglomerate. The limestones are micritic and have typically been affected by dissolution and karsting. Interbedded conglomerates contain micritic limestone clasts and redbed clasts indicating erosion and cannibalization within the unit.

The thickness of the Horton Group varies greatly in the study area. In the east along the margins of the River Denys basin the Horton Group is approximately 500 m thick, whereas in the west it may be as much as 3-5 km thick. Most of the thickness increase is within the Craignish Formation. Maritimes Basin – wide facies variations within the Horton Group indicate sedimentation during active normal faulting (Hamblin and Rust, 1989), which would appear to be a necessary mechanism to accommodate such pronounced thickness variations in the study area.

Windsor Group

The Windsor Group consists of a 2-3 km thick succession of carbonates, evaporites, and siltstone with a well defined internal stratigraphy (Giles, 1981). For the purpose of this study, the group is divided into upper and lower units according to the Upper Windsor Macrofaunal and Lower Windsor Macrofaunal zonation of Bell (1929). The division is marked by the Herbert River Limestone Member (Moore, 1967), which occurs at the base of the Upper Windsor in the River Denys basin as well as along the Southwest Mabou River. The Herbert River Limestone Member is approximately 1-2 m thick, and is distinguished by the presence of solitary rugose corals and an abundance of crinoid stems. The Upper Windsor is also characterized by a predominance of grey siltstone and redbed siltstone over evaporites, as well as by distinctive carbonate members; the C1 limestone (Giles and Boehner, 1982) features an abundance of laterally linked digital stromatolites developed along bedding tops; the E1 limestone (Giles and Boehner, 1982) consists of an oolitic crosslaminated packstone with an abundance of pelecypods at the base of the limestone and brachiopods at the top. Carbonate units in the Upper Windsor are laterally extensive horizons which are useful as regional stratigraphic markers (Giles, 1981). The Herbert River Limestone, C1 limestone, and E1 limestone all outcrop in the project area.

The Lower Windsor is dominated by thick evaporite deposits of gypsum and anhydrite. Biohermal limestones are a minor component of the Lower Windsor. The bioherms are typically dolomitized forming micritic mound-like structures with an abundant pelecypods, brachiopods, and crinoids in the flanking beds. The structure is capped by high frequency peritidal carbonates showing karst dissolution, siliciclastic infills and carbonate cements (D. Lavoie, pers. comm., 1993). The Macumber Formation is a distinct 10-15 m thick limestone unit occurring as the basal carbonate to the Windsor Group; twelve localities were uncovered and investigated in the project area. The Macumber rests conformably on the Horton Group, and its lower 5-10 m are typified by laminated couplets of peloidal and micritic limestone. Both shallow marine (Schenk, 1967), and deep marine (Giles, 1981) depositional environments have been proposed for the formation, with more recently Lavoie (1994) suggesting a substorm wave base setting. The 5-10 m at the top of the formation are ubiquitously strained and recrystallized, with a well developed paper-thin laminated tectonic fabric parallel to bedding, as well as stylolitization and brecciation. The top of the Macumber Formation also contains distinct 1-5 cm boudinaged elliptical recrystallized calcite nodules, which have been interpreted as either evaporite replacement molds (Geldsetzer, 1978), or as "birds-eye" structures (Schenk, 1967); however, the origin of the nodules remains unclear because of the penetrative deformation, but the restriction of the nodules to the high strain zone allows for the possibility that they originated entirely as boudins segmented from tectonically recrystallized layers.

Mabou Group

The Visean to Namurian Mabou Group (Ryan et al., 1991), is the youngest group of rocks in the study area (Kelley, 1967), and appears to be in gradational contact with the underlying Windsor Group. Two members are recognized. The lower member is approximately 200-800 m thick, and consists of thinly bedded black mudstone, grey and red siltstone,

and subordinate 2-15 cm thick brown stromatolitic dolostone beds of likely shallow marine origin. The upper member is at least 1000 m thick and is distinguished by thinly bedded siltstone, redbeds, and arkosic sandstone with well developed climbing ripple crosslaminations. Widespread detrital coal chips, and occasional plant fossils indicate a likely terrestrial setting for the upper member, signalling a general regressive event from lower to upper members of the Mabou Group. Coal beds occur in the upper portions of the Mabou Group in the Maple Brook syncline (Kelley, 1967).

Ainslie Detachment

The Ainslie Detachment (Lynch and Giles, 1993) occurs along the top of the Macumber Formation in the River Denys basin, and to the west along the coastal exposures of the Macumber (Fig. 2 and 3). The most striking features of the detachment are the regional stratigraphic control on the fault, the stratigraphic omissions in the hanging wall of the fault, and the microtextures developed within the Macumber Formation. At the western end of the River Denys basin, a klippe of the Mabou Group is isolated on a listric normal fault which down-ramps through the Lower Windsor Group onto the top of the Macumber Formation and Ainslie Detachment (Fig. 2 and 3). The contact is exposed along River Inhabitants where bedding of the lower member of the Mabou Group parallels that of the adjacent Macumber Formation across a zone of breccia, cataclasis, and gouge. Penetrative deformation at the top of the Macumber Formation features laminated recrystallized calcmylonite. Coarse recrystallized calcite nodules comprise up to twenty per cent of the rock. The nodules have rounded to oval elongated outlines, and appear to have acted as semi-rigid bodies or augen producing symmetrical and asymmetrical shape fabrics and winged inclusions surrounded by fine grained, ductilely deformed laminated carbonate. Fluorite-calcite veins are concentrated at the top of the Macumber Formation where they crosscut the tectonic fabric and are also sheared by it. In other areas, the tectonized Macumber features small scale recumbent, isoclinal intrafolial folds. Fine grained breccia horizons occur between recrystallized laminae. Coarse breccias have clasts of calcmylonite, demonstrating a progressive evolution from ductile to brittle fault conditions.

The fact that the fault runs parallel to bedding along the base of the Mabou Group indicates that an upper flat-lying detachment was active beneath the Mabou Group before it was down-ramped along a listric normal fault onto the Ainslie Detachment. The listric fault cuts through Lower Windsor evaporites (Fig. 2). The geometric relationships between bedding and the fault provide evidence for a staircase or ramp and flat geometry.

In the western portion of the project area, the Upper Windsor and Mabou Group are juxtaposed against the Macumber Formation across the Ainslie Detachment (Fig. 2 and 3). Although cut-offs have not been directly observed, close projections of bedding in outcrops of the Upper Windsor Group onto the detachment suggest a high-angle cut-off. Folding in the hanging wall of the detachment features northeast-trending upright to overturned structures with tight to close interlimb angles (Fig. 2). Such folding is not recorded in the footwall of the detachment, in which case it is proposed that the folds are related to movement on the detachment and may have originated as roll-over structures.

An upper age limit on the Ainslie Detachment has not been established in the local study area, although faulting clearly post-dates the Namurian Mabou Group. However, to the immediate north in the region around the town of Inverness the detachment is unconformably overlain by Westphalian C clastic rocks of the Cumberland Group (P.S. Giles, pers. comm., 1993). The age of the Ainslie Detachment is thus constrained to a period in the Carboniferous between Namurian time and Wetsphalian C time.

DISCUSSION

Implications of detachment faulting for Pb-Zn mineralization

Recognition of the Ainslie Detachment locally in the River Denys basin, and regionally in the Maritimes Basin (Lynch and Giles, 1993; Lavoie, 1994) has important implications for the understanding of Pb-Zn mineralization. The Jubilee Pb-Zn deposit is located at the northeast end of the River Denys basin on the Iona Peninsula, immediately adjacent to the present study area. The deposit is stratabound to the brecciated Macumber limestone (Pembroke Breccia of Lavoie, 1994), and occurs at the same stratigraphic level as the Ainslie Detachment. Galena, sphalerite, pyrite, marcasite, chalcopyrite, and calcite occur as cavity and breccia fillings, as veins, as disseminations, or as limestone replacements (Paradis et al., 1993). Other important Pb and Pb-Zn deposits in Nova Scotia

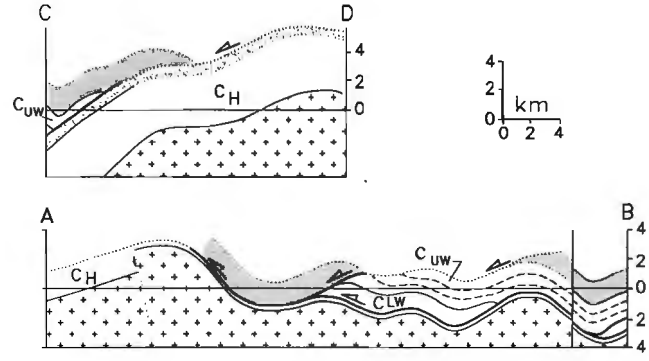

Figure 3. Cross-sections corresponding to lines A-B and C-D on Figure 2 demonstrating downward tectonic transport of Mabou Group (dark stippled pattern) onto the Ainslie Detachment and Macumber Formation (lower heavy line) at the base of the Windsor Group. Thin layer of Horton Group (C_H) is found beneath the detachment and Macumber Formation in the east. Dashed lines are bedding form-lines within Upper Windsor Group, cross pattern corresponds to basement rocks.

which occur along or immediately adjacent to the Ainslie Detachment include the Walton, Smithfield, and Pembroke occurrences (Lynch and Giles, 1993). The age of the mineralizing event has been estimated by fission track and K-Ar methods to be 300-330 Ma (Ravenhurst et al., 1989). The time interval corresponds approximately with the available age constraints for movement on the Ainslie Detachment in southwestern Cape Breton Island (post-Namurian and pre-Westphalian C). A genetic link may thus be inferred between the Ainslie Detachment and regional Pb-Zn mineralization, because of the documented spacial and temporal overlap between the two.

Ravenhurst et al. (1989) proposed that the Horton Group acted as the principal lower basin aquifer, and that the thick evaporite succession in the lower Windsor Group provided an effective seal over this aquifer channelling fluid flow (Fig. 4A). However, the Ainslie Detachment likely affected the basin hydrology in at least three ways; (1) brecciation along the detachment is interpreted to have resulted from the extensional unloading of upper units causing hydrofracturing and brecciation, effectively increasing permeability in the Macumber Formation on a regional scale; (2) fluidassisted faulting and movement on the detachment may have resulted in hydraulic pumping (Sibson, 1987), creating gradients in fluid pressure assisting fluid migration; and (3) large segments of the evaporite cap have been removed by the detachment, breaching the seal and opening the deep basin fluid system to shallow circulating surface waters and upper stratigraphic units (Fig. 4b). This last point may be of particular significance since fluid mixing has been shown to be an important mineralizing process at the Jubilee deposit (Fallara et al., 1994).

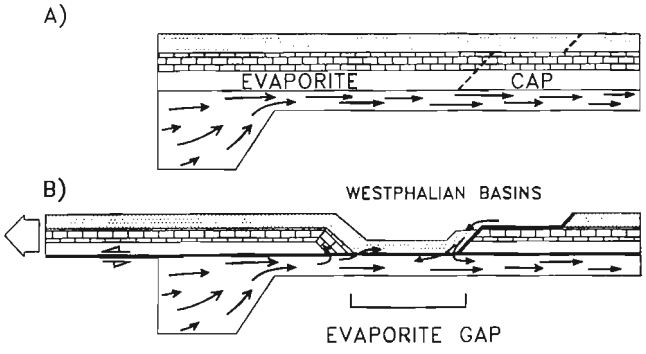

Figure 4. Diagram illustrating schematic palinspastic restoration in study area, and interpretation of basin hydrology with heavy arrows representing flow net (A) before detachment faulting with deep basin fluid flow constrained to below the evaporite cap (modified from Ravenhurst et al., 1989), and (B) after detachment faulting once the evaporite cap has been locally removed opening the system to the influence of shallow basin fluids.

ACKNOWLEDGMENTS

Acknowledgements are extended to Jacquelyn Stevens for help during fieldwork. Peter Giles and Denis Lavoie provided insight into the Carboniferous stratigraphy, and many stimulating discussions on the Ainslie Detachment. Funding was received through the Canada – Nova Scotia Cooperation Agreement on Mineral Development, project C1.101 entitled "Characterization of Major Fault Systems in Western Cape Breton Island", for which I am grateful.

REFERENCES

Bell, W.A.
1929: Horton-Windsor district, Nova Scotia; Geological Survey of Canada, Memoir 155, 268 p.

Fallara, F., Savard, M.M., Lynch, G., and Paradis, S.
1994: Preliminary geological and geochemical results in the Jubilee Pb-Zn deposit, Cape Breton Island, Nova Scotia; in Current Research 1994-D; Geological Survey of Canada.

Geldsetzer, H.H.J.
1978: The Windsor Group in Atlantic Canada – an update; in Current Research, Part C; Geological Survey of Canada, Paper 78-1C, p. 43-48.

Giles, P.S.
1981: Major transgressive-regressive cycle in middle to late Visean rocks of Nova Scotia; Nova Scotian Department of Mines and Energy, Paper 81-2, 27 p.

Giles, P.S. and Boehner, R.C.
1982: Geological map of the Shubenacadie and Musquodoboit basins, central Nova Scotia; Nova Scotia Department of Mines and Energy, Map 82-4, scale 1:50 000.

Hamblin, A.P. and Rust, B.R.
1989: Tectono-sedimentary analysis of alternate-polarity half-graben basin-fill successions: Late Devonian-Early Carboniferous Horton Group, Cape Breton Island, Nova Scotia; Basin Research, v. 2, p. 239-255.

Hein, F.J., Graves, M.C., and Ruffman, A.
1993: The Jubilee Zn-Pb deposit, Nova Scotia: the role of synsedimentary faults; in Mineral Deposit Studies in Nova Scotia, Volume 2, (ed.) A.L. Sangster; Geological Survey of Canada, Paper 91-9, p. 49-69.

Hill, J.R.
1990: A geological and geochemical study of metacarbonate rocks and contained mineral deposits, Cape Breton Island, Nova Scotia; in Mineral Deposit Studies in Nova Scotia, Volume 1, (ed.) A.L. Sangster; Geological Survey of Canada, Paper 90-8, p. 3-30.

Howie, R.D. and Barss, M.S.
1975: Upper Paleozoic rocks of the Atlantic provinces, Gulf of St. Lawrence, and adjacent continental shelf; Geological Survey of Canada, Paper 74-30, p. 35-50.

Kelley, D.G.
1967: Baddeck and Whycocomagh map-areas with emphasis on Mississippian stratigraphy of central Cape Breton Island, Nova Scotia (11K/2 and 11F/14); Geological Survey of Canada, Memoir 351, 65 p.

Lavoie, D.
1994: Lithology and preliminary paleoenvironmental interpretations of the Macumber and Pembroke formations (Windsor Group, Early Carboniferous), Nova Scotia; in Current Research 1994-D; Geological Survey of Canada.

Lynch, G. and Giles, P.S.
1993: Extensional tectonics and evolution of the Upper Devonian-Carboniferous Maritimes Basin, Nova Scotia; Geological Association of Canada Annual Meeting, Abstracts with Program, A-62.

Moore, R.G.
1967: Lithostratigraphic units in the upper part of the Windsor Group, Minas sub-basin, Nova Scotia; Geological Association of Canada, Special Paper 4, p. 245-266.

Murray, B.C.
1960: Stratigraphy of the Horton Group in parts of Nova Scotia; Nova Scotia Research Foundation, Halifax, 160 p.

Paradis, S., Savard, M., and Fallara, F.
1993: Preliminary study on diagenesis and mineralization of the Jubilee Pb-Zn deposit, Nova Scotia; in Current Research, Part D; Geological Survey of Canada, Paper 93-1D, p. 111-119.

Raeside, R.P.
1990: Low-pressure metamorphism of the Lime Hill gneissic complex, Bras d'Or Terrane, Cape Breton Island, Nova Scotia; in Mineral Deposit Studies in Nova Scotia, Volume 1, (ed.) A.L. Sangster; Geological Survey of Canada Paper 90-8, p. 67-76.

Ravenhurst, C.E., Reynolds, P.H., Zentilli, M., Krueger, H.W., and Blenkinsop, J.
1989: Formation of Carboniferous Pb-Zn and barite mineralization from basin-derived fluids, Nova Scotia, Canada; Economic Geology, v. 84, p. 1471-1488.

Ryan, R.J., Boehner, R.C., and Calder, J.H.
1991: Lithostratigraphic revisions of the Upper Carboniferous to Lower Permian strata in the Cumberland Basin, Nova Scotia and the regional implications for the Maritimes Basin in Atlantic Canada; Bulletin of Canadian Petroleum Geology, v. 39, p. 289-314.

Sangster, A.L., Justino, M.F., and Thorpe, R.I.
1990: Metallogeny of the Proterozoic marble-hosted zinc occurrences at Lime Hill and Meat Cove, Cape Breton Island, Nova Scotia; in Mineral Deposit Studies in Nova Scotia, Volume 1, (ed.) A.L. Sangster; Geological Survey of Canada Paper 90-8, p. 31-66.

Schenk, P.E.
1967: The Macumber Formation of the Maritime Provinces – a Mississippian analogue to Recent strand-line carbonates of the Persian Gulf. Journal of Sedimentary Petrology, v. 37, p. 365-376.

Sibson, R.H.
1987: Earthquake rupturing as hydrothermal mineralizing agent; Geology, v. 15, p. 751-754.

Geological Survey of Canada Project 920004

Preliminary geological and geochemical results characterizing the mineralization processes in the Jubilee Pb-Zn deposit, Cape Breton Island, Nova Scotia[1]

F. Fallara, M.M. Savard, G. Lynch, and S. Paradis
Quebec Geoscience Centre, Sainte-Foy

Fallara, F., Savard, M.M., Lynch, G., and Paradis, S., 1994: Preliminary geological and geochemical results characterizing the mineralization processes in the Jubilee Pb-Zn deposit, Cape Breton Island, Nova Scotia; in Current Research 1994-D; Geological Survey of Canada, p. 63-71.

Abstract: At the Jubilee deposit, the host Macumber Formation consists of four successive lithofacies: micritic, intramicritic, sheared and brecciated. The Pb-Zn ore minerals are always restricted to this last brecciated unit which contains fragments of sheared limestones. We interpret the sheared limestones as calcmylonite and suggest that progressive shearing resulted in brecciation of this calcmylonite.

Preliminary $\delta^{18}O$-$\delta^{13}C$ results for the carbonate units and paragenetic phases from the mine area indicate that micritic limestones were stabilized under warm, burial conditions. A biogenic carbon-rich system has influenced recrystallization of limestones during shearing, and has precipitated pre-, syn- and post-ore calcites.

The Ainslie Detachment probably provided the necessary background preparation for Pb-Zn mineralization at the deposit, by creating secondary porosity through brecciation and new channelways through faulting.

Résumé : Au gîte de Jubilee, les roches encaissantes de la Formation de Macumber ont été divisées en quatre lithofaciès successifs: micritique, intramicritique, cisaillé et bréchifié. La minéralisation en Pb-Zn est restreinte à l'unité bréchifiée qui contient des fragments de calcaire cisaillé. Ce lithofaciès est interprété comme étant une calcmylonite. La bréchification résulte de la déformation progressive du lithofaciès.

Des résultats préliminaires de $\delta^{18}O$-$\delta^{13}C$ pour les unités de carbonates et les phases paragénétiques présentes à la mine démontrent que les calcaires micritiques se sont stabilisés dans des conditions d'enfouissement relativement chaudes. Un système riche en carbone biogénique a influencé la recristallisation des calcaires durant leur cisaillement et la précipitation de calcites avant, pendant et après le processus de minéralisation.

Le détachement d'Ainslie semble avoir joué un rôle majeur dans la mise en place du Pb-Zn au gîte en créant une porosité secondaire et des systèmes de canalisation, par bréchification et formation de failles.

[1] Contribution to Canada-Nova Scotia Cooperation Agreement on Mineral Development (1992-1995), a subsidiary agreement under the Canada-Nova Scotia Economic and Regional Development Agreement.

INTRODUCTION

The Jubilee Pb-Zn deposit is situated in the vicinity of Little Narrows, on the northwestern side of the Iona Peninsula, in Cape Breton Island, Nova Scotia (Fig. 1). The deposit is a stratabound carbonate-hosted occurrence contained within the Lower Carboniferous Macumber Formation. Hein et al. (1988, 1993) and Graves et al. (1990) described the general characteristics of the deposit and suggested an intimate relationship between faulting and deposition during the accumulation of the host sediments. Paradis et al. (1993) have established the general paragenetic sequence at the deposit and in the immediate surroundings, demonstrating a relationship between brecciation, calcite cementation and mineralization. Although petrographic and isotope results for mine samples were previously reported (Ravenhurst et al., 1989; Armstrong et al., in press), detailed diagenetic and geochemical work on the Macumber Formation has never been made.

The aim of this paper is to complement the detailed petrographic and paragenetic sequence documented by Paradis et al. (1993) by presenting corresponding isotopic results ($\delta^{18}O$, $\delta^{13}C$) obtained from carbonates of the mine sequence, which lead to a preliminary characterization of the various fluid types that have affected the Macumber Formation at the Jubilee Pb-Zn deposit. Regional results will be the topic of another report. The present study is a contribution to the Nova Scotia-MDA projects on Windsor base metal deposits (Sangster-Savard-Paradis), to identify fluids responsible for Pb-Zn mineralization, and to verify the possible genetic links between the numerous base metal deposits in the River Denys, Shubenacadie, Mosquodoboit and Kennetcook sub-basins.

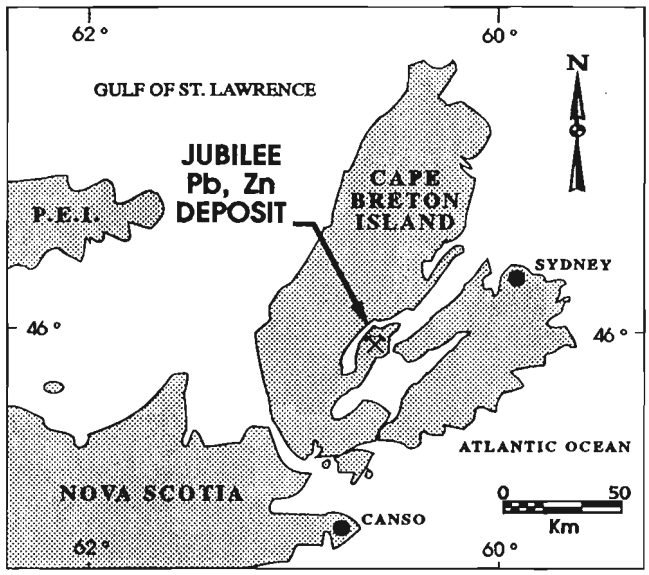

Figure 1. Location map of the Jubilee Pb-Zn deposit within Cape Breton Island, Nova Scotia.

GEOLOGICAL SETTING

The stratabound limestone-hosted Jubilee Pb-Zn deposit is located in the brecciated limestones of the Macumber Formation (Weeks, 1948) within the Windsor Group, in the Carboniferous River Denys sub-basin of the Maritimes Basin (Eastern Canada).

Faulting and rifting resulted from a post-Acadian extensional system which created the intracontinental Maritimes Basin. Thick accumulations of sediments were deposited in numerous sub-basins (Belt, 1968; Sheridan and Drake, 1968; Howie and Barss, 1975; Fralick and Schenk, 1981; Giles, 1981).

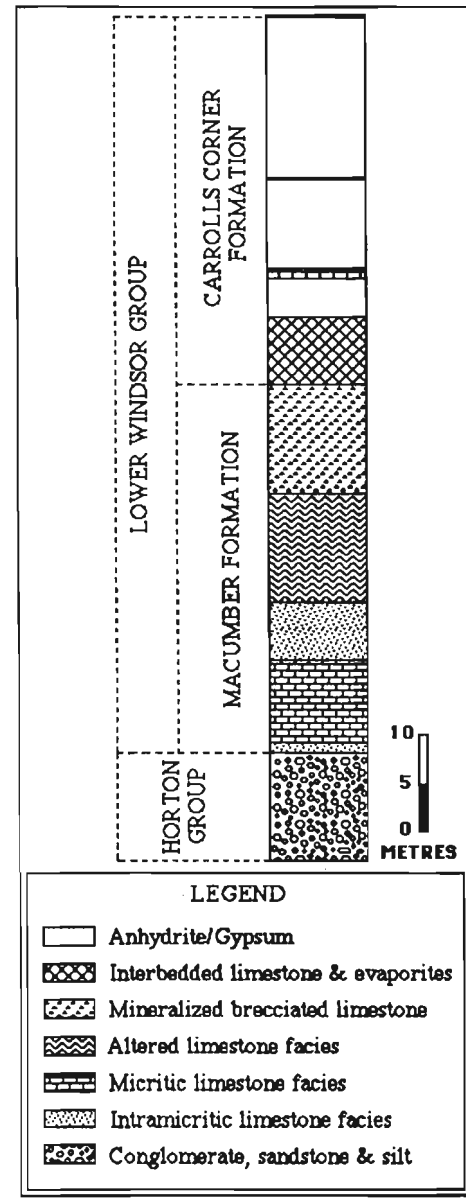

Figure 2. Stratigraphic sequence of the Lower Windsor Group at the Jubilee Pb-Zn deposit.

The Windsor Group (Bell, 1929) constitutes the first and only marine deposit in a thick continental sedimentary sequence (Giles, 1981). It is essentially composed of carbonates, evaporites and siltstones of Viséan age (348-336 Ma). The Windsor Group is underlain by the red and grey-green conglomerates, sandstones, and siltstones of Tournaisian age (360-350 Ma) of the Horton Group. In the Jubilee deposit area, the contact between the two groups is concordant and sharp. The Windsor Group is conformably to unconformably overlain by siliciclastic rocks from the Namurian Mabou Group and from the Westphalian Cumberland Group, respectively.

In Cape Breton Island, field investigations indicate that the Macumber Formation was affected by a major low-angle detachment fault, known as the Ainslie Detachment (320 Ma) (Lynch and Giles, 1993). The detachment occurs along the top of the Macumber Formation, where it is in contact with a thick evaporite succession. Lynch and Giles (1993) suggested that the carbonates of the Macumber Formation acted mainly as a continental stress guide, directing the Ainslie Detachment throughout the basin.

GEOLOGY OF THE JUBILEE DEPOSIT

The Jubilee deposit is hosted by brecciated limestones of the Macumber Formation, in the basal portion of the Windsor Group (Lower Windsor; Ravenhurst et al., 1989). The Lower Windsor sequence (Fig. 2) contains, from bottom to top, carbonates of the Macumber Formation and evaporites of the Carrolls Corner Formation (Weeks, 1948). During burial, the Macumber Formation was overlying porous rocks (Horton Group) and underlying a thick impermeable sequence of massive anhydrite. A horst with a northwestern elongation (Fig. 3), known as the "Jubilee dome" has been proposed by Graves et al. (1990). The Macumber Formation is laterally equivalent to the Gays River Formation, which is well known for its Pb-Zn Gays River deposit (Ravenhurst et al., 1989; Savard, 1991, 1992).

Sedimentary facies of the Macumber Formation

The total thickness of the Macumber Formation, including sheared and brecciated lithofacies, measured in drill cores, is approximately between 30 to 50 m thick in the area of the Jubilee deposit. The formation is subdivided into four lithofacies, in ascending order: (1) micritic, (2) intramicritic, (3) altered or sheared, and (4) brecciated. Lithofacies at the base of the Macumber Formation, i.e., the micritic and intramicritic lithofacies, are non-altered, undeformed and contain well preserved recognizable primary sedimentary structures. Lithofacies in the upper part of the formation are generally highly altered and recrystallized, and mainly comprise sheared limestones. The micritic lithofacies consists of finely laminated dark grey-brown limestones, with relatively thin beds (10-40 cm; Fig. 4). The absence of open marine fauna, bioturbation and wave-induced structures suggest a relatively deep water environment (see also Lavoie, 1994).

The intramicritic lithofacies is a finely laminated dark grey-brown limestone, thickness of beds vary from 10 to 30 cm. It contains a high percentage of sub-angular to rounded intraclasts (Fig. 5), as well as oolites, peloids, and calcimicrobe fragments (Fig. 6). The micritic and the intramicritic lithofacies alternate and the passage between the two is gradual (Fig. 7). The total thickness of these two lithofacies is between one and ten metres.

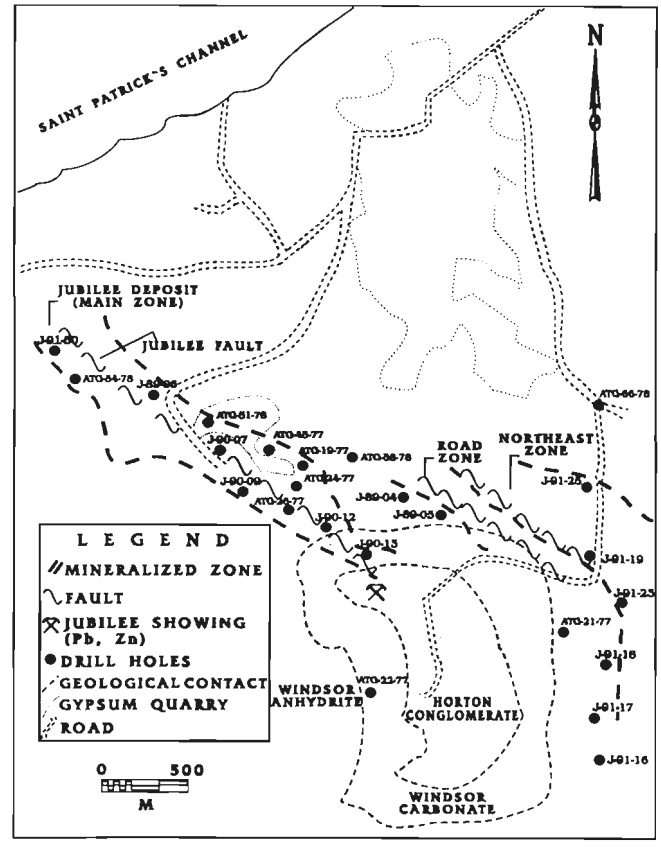

Figure 3. Geological map and location of drill holes (modified from Graham, 1979) of the Jubilee Pb-Zn deposit (after Paradis et al., 1993). Drill holes J-90 are from Falconbridge Limited, Windsor, Nova Scotia.

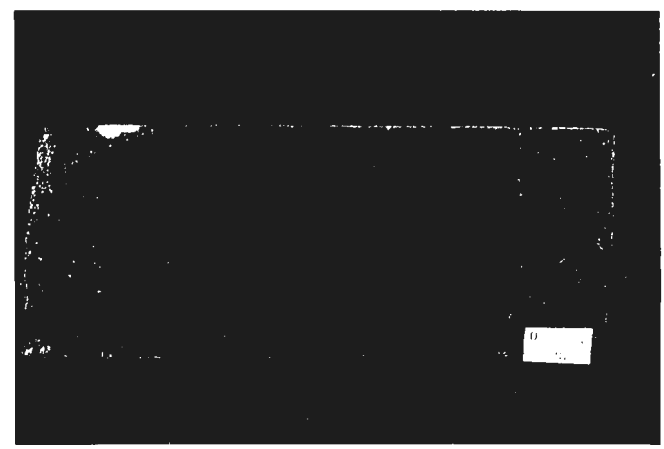

Figure 4. Polished rock slab of the fine laminated dark grey-brown limestones of the micritic lithofacies.

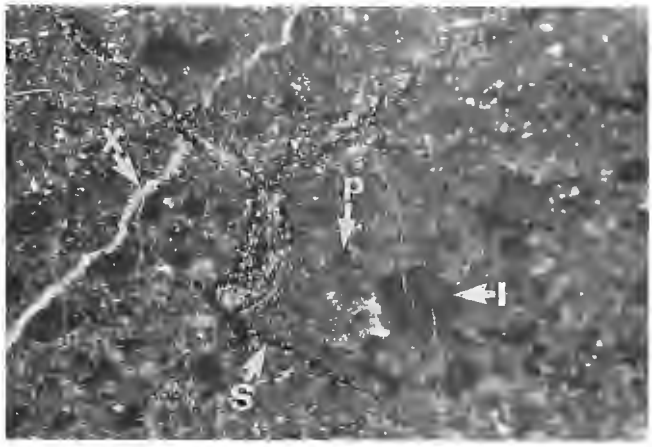

Figure 5. *Thin section of a pelsparite with peloids (p) and sub-angular to rounded intraclasts (I). Second generation stylolites (S) at angle with bedding, cuts through all the rock components and the coarse anhedral white calcite cement (X). Long dimension of photo is 4.5 mm.*

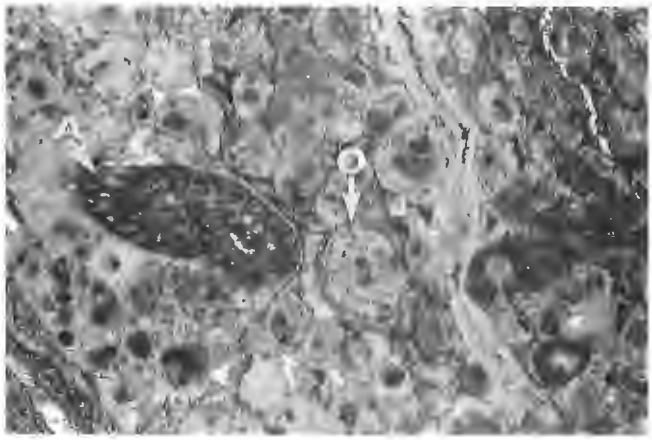

Figure 6. *Oosparite containing oolites (O) and a fragment of calcimicrobe (A). Long dimension of photo is 4.5 mm.*

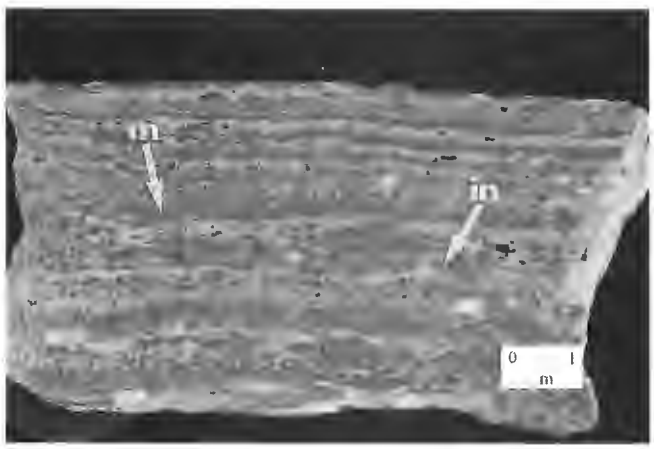

Figure 7. *Alternance of the micritic (m) and intramicritic (in) lithofacies. The passage between the two is gradual. They are non-altered, undeformed and not intensely recrystallized.*

The sheared limestones are beige and consist of millimetre- to centimetre-thick carbonate and siliclastic laminae that contain boudinaged and rotated anhydrite or calcite nodules (Fig. 8). Small scale detached and recumbent folds are contained within the sheared limestones and either overprint the tectonic fabric or are truncated by it. The total apparent thickness of the altered limestone varies from 2 to 15 m. In thin section (Fig. 9), laminae in the sheared limestones are defined by layers of very fine- to medium-grained recrystallized calcite; primary sedimentary features have been completely erased.

The brecciated facies overlaps and lies above the sheared limestones at the top of the Macumber Formation. The breccia contains limestone fragments of the Macumber Formation cemented by calcite. The fragments consist of micrite, intramicrite and sheared limestones. Locally, the breccia is mineralized therefore, it has been subdivided into mineralized

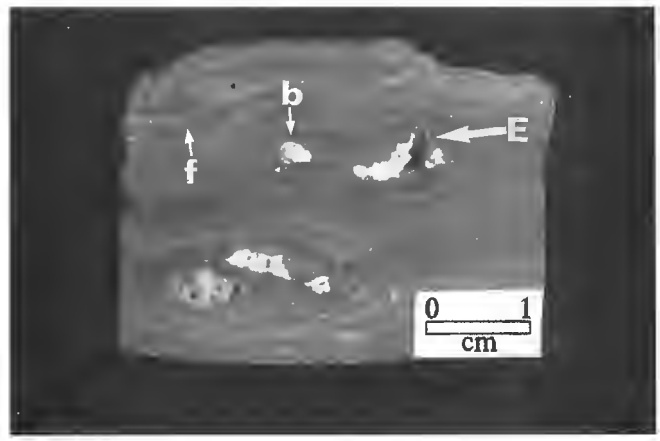

Figure 8. *Polished rock slab of the folded (f) altered and sheared limestones with boudinaged (b) and rotated evaporite casts (E). Laminated texture consists of recrystallized and strained calcite.*

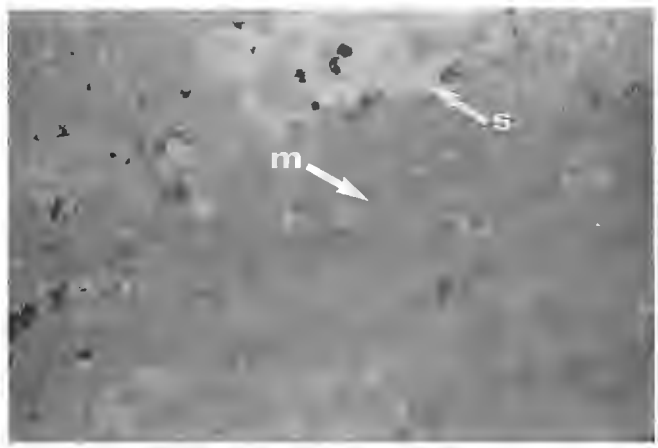

Figure 9. *Thin section of sheared and recrystallized limestones. The planar fabric is not visible at this scale, but crystal sizes and texture varies from micritic (m) to sparry (s) calcite.*

and non-mineralized types (Hein et al., 1988). The non-mineralized breccia contains small (1-3 cm) angular to subrounded limestone fragments of the Macumber Formation in a fine grained limestone matrix or calcite cement. Mainly recrystallized angular to subrounded limestone fragments (centimetre scale) of the Macumber Formation are found in the mineralized breccia, which is the main host to ore; however, some fragments having their original laminated and oolitic textures are also observed.

Sedimentary environments and alteration processes

The origin and mode of deposition of the Macumber Formation is still controversial. The top of the formation is characterized by limestones with fine penetrative planar laminites which have been interpreted over the years as either a supratidal stromatolitic marine facies (lithosome B of Schenk, 1967), as deep water marine cyanobacterian laminites (Giles and Boehner, 1982) or, alternatively, as deep lacustrine peloidal laminites (Schenk, 1992). However, based on stratigraphic and structural arguments, Lynch and Giles (1993) have interpreted the planar fabric (Fig. 10) as a tectonic laminite related to the Ainslie Detachment. Field and petrographic observations made during the course of this study suggest that tectonic origin shearing has affected the laminated lithofacies (possibly microbial dominated) in the Jubilee area.

In the lower intramicritic lithofacies, the absence of an intragranular cement and the presence of micrite and pseudosparite between oolites suggest that these particles were likely transported from a shallow intertidal environment to a relatively calm setting below wave action. This agrees with observations of oolites in current structures within the Macumber Formation elsewhere (Lavoie, pers. comm.), a feature also suggesting redeposition of oolites. There are no indications of bioturbation, only few marine organisms. Therefore, the well preserved sedimentary features in the lower member of the formation suggest below wave base resedimented carbonate deposit.

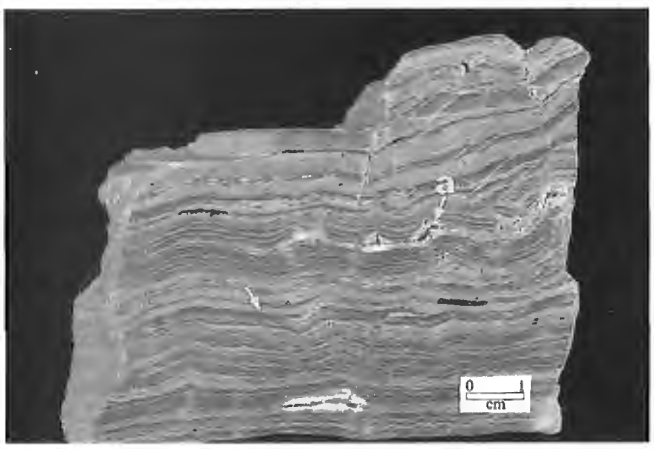

Figure 10. *Regular planar fabric (see arrow) in tectonized limestones of the Macumber Formation. These fabrics do not resemble the typical cyanobacterian laminites. Notice the empty boudinaged coarse carbonate layers (a).*

A syn-sedimentary origin has been proposed previously for the breccia (Hein et al., 1993). However, the breccia clearly post-dates tectonic fabrics produced by shearing, since sheared limestone fragments are an important component of the breccia. Consequently, the breccia is interpreted as a tectonic or fault breccia, with the fault running along the top of the Macumber Formation. Movement on the fault cannot be estimated in the immediate study area. However, the position of the fault corresponds to that of the Ainslie Detachment regionally, and as mapped to the southwest in the River Denys basin (Lynch, 1994). Penetrative recrystallization, a laminated fabric, and brecciation within the Macumber Formation are characteristic of the immediate footwall to the detachment. Brecciation appears to reflect a brittle phase within a sequence of progressive shear.

Paragenesis

The mineral paragenesis was determined in thin section by crosscutting textures and mineral overgrowths, and is consistent with the observations of Paradis et al. (1993). The paragenetic sequence related to mineralization at the Jubilee Pb-Zn deposit can be summarized as follows (Fig. 11): (1) stabilization of the micritic facies, (2) precipitation of pyrite, (3) first phase of stylolitization (parallel to bedding), (4) recrystallization by shearing or mylonitization, (5) fracturing- brecciation-dissolution, (6) brown fibrous calcite cementation, (7) precipitation of pyrite-marcasite, (8) precipitation of sphalerite and galena, (9) precipitation of chalcopyrite, (10) white coarse anhedral calcite cementation (syn to post-ore), (11) second phase of stylolitization (at angle with bedding), and (12) precipitation of barite, anhydrite and gypsum.

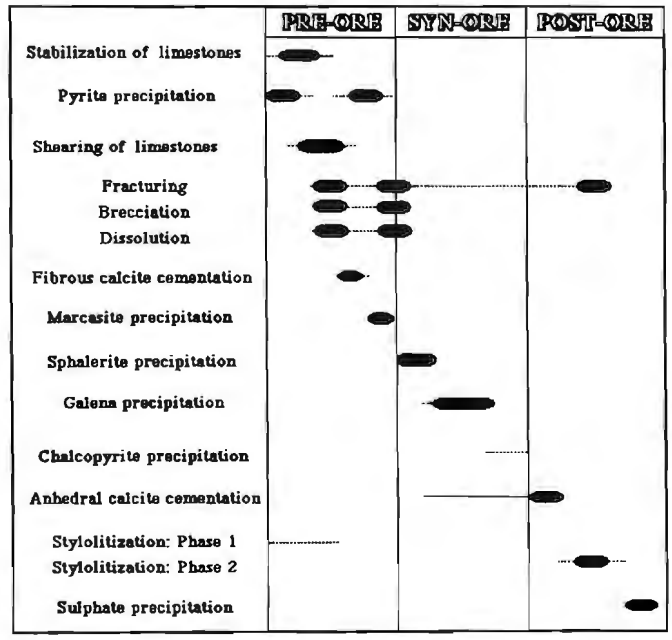

Figure 11. *Paragenetic sequence of the Jubilee Pb-Zn deposit. Stylolites 1 are parallel to bedding and Stylolites 2 are at angle with bedding. The relative chronology refers to mineralization (Py, Sph and Gn). Modified after Paradis et al. (1993).*

Stabilization (process 1) by opposition to recrystallization by shearing (process 4) refers to mineralogical transformations mediated by diagenetic waters as the sediments undergo unsuitable physico-chemical conditions for high-magnesium calcite and aragonite stability.

The first cement, the brown fibrous calcite, appears in thin (millimetre scale) isopachous layers encrusting brecciated fragments and filling empty vugs and fractures (Fig. 12). This cement is itself brecciated and fractured, indicating that cementation was co-genetic with fracturing and brecciation.

The succeeding cement consists of a white coarse anhedral calcite (Fig. 13) which fills cavities and fractures. Anhedral crystal mosaics with triple point junctions between crystals indicate that it is often recrystallized. This late cement postdates fibrous cement but is syn- to post-ore and precedes sulphate precipitation and late stylolitization.

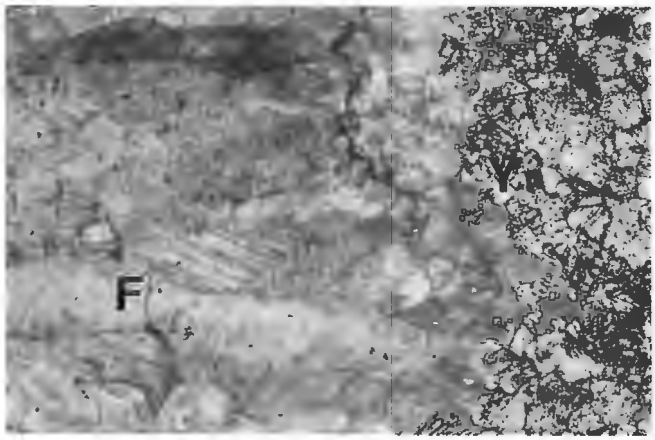

Figure 12. *Photomicrograph of a polished thin section illustrating the first cement, i.e., brown fibrous calcite cement (F) which fills the vugs and fractures. Also, a neomorphozed marine substrate can be observed (Y).*

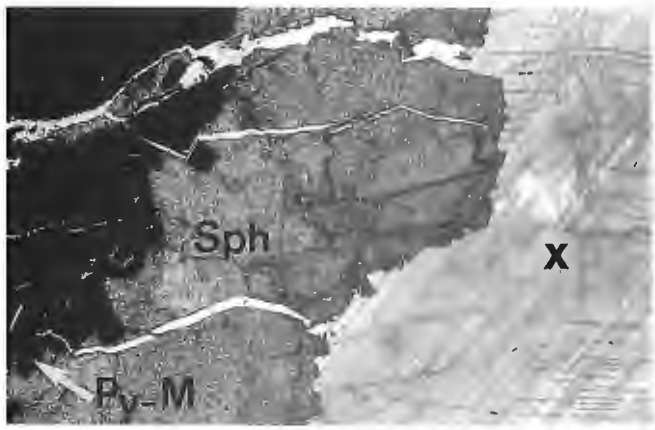

Figure 13. *The second generation of cement consists of a late recrystallized white coarse anhedral calcite (X). Notice the brecciated intergrowths of pyrite-marcasite (Py-M) and sphalerite (Sph) coated and crosscut by this late anhedral cement (X).*

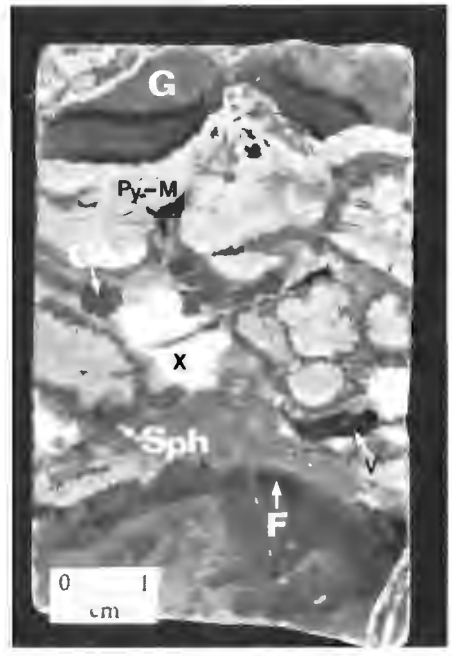

Figure 14. *Polished rock slab of the mineralized breccia illustrating the paragenetic sequence: brown fibrous calcite cement (F), intergrowths of pyrite-marcasite (Py-M), sphalerite (Sph) and galena (Gn), the late white coarse anhedral calcite (X) filling in the empty vugs (v) and fragments of the laminated limestone (G).*

The relationship between mineralization and each stage of cementation is as follows: ore minerals postdate brown fibrous calcite, but are pre- to syn-anhedral calcite (Fig. 14). Mineralization at the Jubilee deposit is epigenetic and ore minerals occur mainly as pore-filling phases, in fractures, disseminated and sometimes as replacement of limestones. Further descriptions of the sulphides are available in Paradis et al. (1993).

CARBON AND OXYGEN ISOTOPE GEOCHEMISTRY

Analytical methods

Thirty-five drill core samples from the Jubilee deposit, obtained from the Nova Scotia Department of Mines and Energy Core Storage facility in Stellarton, were analyzed to characterize the various fluid types which affected the Macumber Formation. The carbon and oxygen isotope analyses were systematically performed on micritic limestones, sheared limestones, fibrous calcite and coarse anhedral calcite cements. The CO_2 gas was extracted by reacting 5 mg of carbonate powders for twelve hours with phosphoric acid at 25°C. The liberated gas was analyzed on a VG-SIRA 12 mass spectrometer at the Laboratoire de Géochimie Isotopique (LGI) of the Quebec Geoscience Centre, Geological Survey of Canada. The results are expressed in the usual delta notation and given in per mil (‰) relative to the Peedee Belemnite standard (PDB). All values

are corrected for the presence of ^{17}O and for internal linear deviation (LGI, QGC). Precision (2σ) of the data is +/- 0.1 ‰.

Results

Isotopic ($\delta^{18}O_{PDB}$, $\delta^{13}C_{PDB}$) fields illustrated in Figure 15 belong to four different petrographic types. Non-altered micritic limestones (1) show $\delta^{18}O$ and $\delta^{13}C$-values ranging from -2.0 to -6.5 and +4.6 to -0.3 ‰, respectively. Sheared limestones (2) have more or less constant $\delta^{18}O$-values and highly variable $\delta^{13}C$-values, ranging from -2.6 to -4.8 and +4.5 to -15.2 ‰, respectively. Brownish fibrous calcite (3) shows results which cluster around -6.5 and -22.0 ‰ for $\delta^{18}O$ and $\delta^{13}C$, respectively. Results for syn- to post-ore white coarse anhedral calcite (4) range from -5.5 to -11.8 ‰ for $\delta^{18}O$ and from -10.0 to -21.3 ‰ for $\delta^{13}C$.

Characterization of pre-, syn- and post-ore fluids: interpretation

Type 1 (non-altered micritic limestones) shows a continuous depletion in $\delta^{18}O$-values, from normal marine values (-2.0 ‰) to a significantly lower value (-6.5 ‰), and relatively constant $\delta^{13}C$-values (mean value = 2.4 ‰). In stabilized micritic limestones, trends of decreasing $\delta^{18}O$ can be explained either by exchange at higher temperatures with sea-derived waters, or by exchange with ^{18}O-depleted fluids, or by a combination of both. Discrimination between the two possible exchange systems would require the use of another tracer such as the strontium isotope ratios (work in progress). However, at this stage, our preliminary interpretation of type 1 is as a burial trend; buffering of the carbon isotope ratios by *in situ* marine bicarbonates with lowering O isotope ratios could well be the result of burial stabilization, in presence of slightly modified marine waters (Moore, 1989; Banner and Hanson, 1990; Choquette and James, 1990).

The progressively lower $\delta^{13}C$-values of type 2 (sheared limestones) and the cluster obtained for type 3 (fibrous cement) form a continuous trend that likely reflects fluid-rock interactions. The highest $\delta^{13}C$-values belong to recrystallized limestones and reflect low water/rock interactions, whereas the lowest values of the trend belong to the calcite cement likely reflecting fluid values and highest water/rock ratios. The low $\delta^{13}C$-values (around -25 ‰) of the fibrous calcite strongly suggest that the carbon in the cement is derived from oxidation of organic material such as hydrocarbons (-20 to -30 ‰) or partly derived from methane (-35 to -110 ‰). In numerous thin sections, we have identified hydrocarbons in the fine limestones of the Macumber Formation. Hein et al. (1993) also observed a high quantity of hydrocarbons-bearing fluid inclusions in calcite cements from the mine area. Hence, we suggest that the ^{13}C-depleted carbon was derived from hydrocarbons.

Type 4 (coarse anhedral white calcite cement) shows a progressive decline in $\delta^{18}O$-values, either due to precipitation at increasing temperatures or to precipitation from ^{18}O-depleted waters. The low $\delta^{13}C$-values indicate that organic carbon was still abundant in the fluids. However, the values are higher than those for fibrous calcite (domain 3, Fig. 15), indicating that the fluids which precipitated late calcite (domain 4) were more strongly influenced by interaction with the carbonate host rocks, producing higher $\delta^{13}C$-values. Since the coarse calcite precipitated during and after mineralization, it most likely incorporated carbonate-derived

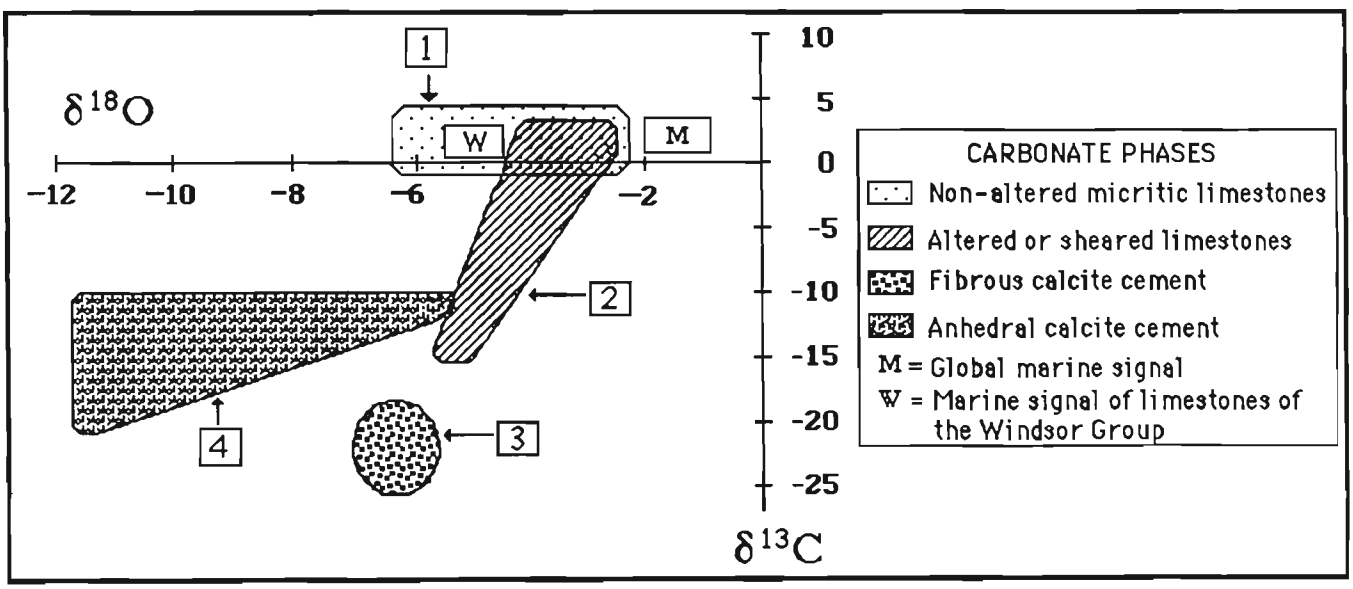

Figure 15. *$\delta^{18}O$ and $\delta^{13}C$ fields of carbonate phases from the Jubilee Pb-Zn deposit. The field identified as "M" represents the compilation of the worldwide results of the Lower Visean after Lohmann, Walker and Popp et al. (1986). "W" represents the compilation results for the Windsor limestones after Ravenhurst et al. (1987).*

bicarbonate liberated during replacement of host limestones by ore minerals (see section on Paragenesis). Final shift towards lower $\delta^{13}C$-values (left portion of domain 4) marks the return to higher water/rock interaction, i.e. ending of replacement by ore minerals and possibly ending of ore precipitation, with a carbon budget still dominated by bicarbonates derived from oxidized organic matter.

The paragenesis established for the Jubilee deposit implies that geochemical attributes of types 2 and 3 reflect immediate pre-ore conditions, and attributes of type 4 reflect, syn- to post-ore conditions. The continuous geochemical trend of these three types represents the evolution in time of the mineralizing system. As fine limestones were recrystallized and sheared (type 2), hydrocarbons were already present in the system producing lower $\delta^{13}C$-values with increasing fluid/rock ratios. During mineralization, organic matter possibly contributed to sulphate reduction, liberating H_2S for sulphide mineralization. The presence of organic matter may also have created relatively acid conditions causing dissolution and replacement of carbonates.

Mixing of metal carrying waters and hydrocarbons at Jubilee could well have been generated by the fault movements along the Ainslie Detachment. The latter certainly played a significant role in ground preparation since it is responsible for brecciation (secondary porosity) and faulting at the deposit. However, its potential role as a regional channelway remains to be fully assessed.

CONCLUSIONS

From this study, two major conclusions can be drawn from the above observations. First, preliminary stable isotope results for micritic and sheared limestones and for paragenetic calcites demonstrate that carbonate ions derived from the oxidation of hydrocarbons. Therefore, hydrocarbons played a major role in the mineralizing system, they were present before, during and after precipitation of ore minerals. Sulphide precipitation likely occurred as a result of sulphate reduction during interaction with reduced organic-rich fluids. Secondly, the Ainslie Detachment probably provided the necessary ground preparation for Pb-Zn mineralization at the Jubilee deposit. The suggestion that the Ainslie Detachment might have controlled mineralization has important implications for regional exploration guidelines.

ACKNOWLEDGMENTS

We would like to thank P. Giles and F. Hein for their help in our field work; D. Lavoie for his help on petrography and on interpretations of sedimentary features; Normand Tassé for making critical review on the manuscript; Jacquelyn Stevens for being an excellent field assistant; Harold Brisson for sharing his geological and cultural expertise; Marc Luzincourt of the Laboratoire de Géochimie Isotopique of the Quebec Geoscience Center, Geological Survey of Canada, for the isotopic analyses. Jim Langile and Don Weir of the Nova Scotia Department of Mines and Energy, at the Core Storage facility in Stellarton, for their precious help and patience; and, Falconbridge Limited for property access and drill hole maps.

REFERENCES

Armstrong, J.P., Longstaffe, F.J., and Hein, F.J.
in press: Carbon and oxygen isotope geochemistry of calcite from the Jubilee Zn-Pb deposit, Cape Breton Island.

Banner, J.L. and Hanson, G.H.
1990: Calculation of simultaneous isotopic trace element variations during water-rock interaction with applications to carbonate diagenesis; Geochimica et Cosmochimica Acta, v. 54, p. 3123-3137.

Bell, W.A.
1929: Horton-Windsor district Nova Scotia; Geological Survey of Canada, Memoir 155, 268 p.

Belt, E.S.
1968: Post-Acadian rifts and related facies, eastern Canada; in studies of Appalachian geology, Northern and Maritime, (ed.) E. Zen et al.; New York, Wiley Intersci., p. 95-113.

Choquette, P.W. and James, N.P.
1990: The deep burial environment; in Diagenesis, (ed.) I.A. Morrow and D.W. Morrow, Geoscience Canada, reprint series #4, p. 13-34.

Fralick, P.W. and Schenk, P.E.
1981: Molasse deposition and basin evolution in a wrench tectonic setting: The late Paleozoic eastern Cumberland basin, Maritime Canada; Geological Association of Canada, Special Paper 23, p. 77-97.

Giles, P.S.
1981: Major transgressive-regressive cycles in the Middle to Late Visean rocks of Nova Scotia; Department of Mines and Energy, Nova Scotia, Paper 81-2, 27 p.

Giles, P.S. and Boehner, R.C.
1982: Geological map of the Shubenacadie and Musquodoboit Basins, central Nova Scotia; Nova Scotia Department of Mines and Energy, Map 82-4, scale 1:50 000.

Graham, R.A.S.
1979: The Iona RER lead-zinc project, Nova Scotia, review of data; Report to Texas-Gulf Canada Limited, May 1979, 3 inclosures, 12 p.

Graves, M.C., Hein, F.J., and Ruffman, A.
1990: The geology of the Jubilee zinc-lead deposit, Victoria County, Cape Breton Island, Nova Scotia supplementary data; Geological Survey of Canada, Open File 2279, 80 p.

Hein, F.J., Graves, M.C., and Ruffman, A.
1988: Geology of the Jubilee Zn-Pb deposit, Victoria County, Cape Breton Island, Nova Scotia; Geological Survey of Canada, Open File 1891, 134 p.

Hein, F.J., Graves, M.C., and Ruffman, A.
1993: The Jubilee Zn-Pb deposit, Nova Scotia: the role of synsedimentary faults; Geological Survey of Canada, Paper 91-9, p. 49-69.

Howie, R.D. and Barss, M.S.
1975: Upper Paleozoic rocks of the Atlantic provinces, Gulf of St-Lawrence, and adjacent continental shelf; Geological Survey of Canada, Paper 74-30, p. 35-50.

Lavoie, D.
1994: Lithology and preliminary paleoenvironmental interpretation of the Macumber and Pembroke formations (Windsor Group, Early Carboniferous), Nova Scotia; in Current Research 1994-D, Geological Survey of Canada..

Lohmann, K.C. and Walker J.C.G.
1989: The $\delta^{18}O$ record of Phanerozoic abiotic marine calcite cements; Geophysical Research Letters, v. 16, p. 319-322.

Lynch, G.
1994: Ainslie Detachment in the Carboniferous River Denys basin of Cape Breton Island, Nova Scotia, with regional implications for Pb-Zn mineralization; in Current Research 1994-D, Geological Survey of Canada.

Lynch, G. and Giles, P.
1993: The Ainslie detachment – field evidence of carboniferous low-angle extensional faulting, Nova Scotia; Geological Association of Canada Annual Meeting, Program with Abstracts, p. 129.

Moore, C.H.
1989: Carbonate diagenesis and porosity; Development in Sedimentology 46. Elsevier, Amsterdam – Oxford – New York – Tokyo, 330 p.

Paradis, S., Savard, M., and Fallara, F.
1993: Preliminary study on diagenesis and mineralization of the Jubilee Pb-Zn deposit, Nova Scotia; in Current Research; Geological Survey of Canada, Paper 93-1D, p. 111-119.

Popp, B., Anderson, T.F. , and Sandberg, P.A.
1986: Brachiopods as indicators of original isotopic compositions in some Paleozoic limestones; Geological Society of America Bulletin, v. 97, p. 1262-1269.

Ravenhurst, C.E., Reynolds, P.H., Zentilli, M., and Akande, S.O.
1987: Isotopic constraints on the genesis of Zn-Pb mineralization at Gays River, Nova Scotia, Canada; Economic Geology, v. 82, p. 1294-1308.

Ravenhurst, C.E., Reynolds, P.H., Zentilli, M., Krueger, H.W., and Blenkinsop, J.
1989: Formation of Carboniferous Pb-Zn and Barite mineralization from basin-derived fluids, Nova Scotia; Economic Geology and the Bulletin of the Society of Economic Geologists, v. 84, no. 6, p. 1471-1488.

Savard, M.M.
1991: A preliminary report on the relationship between mineralization and carbonate diagenesis in the Gays River Formation, Nova Scotia; in Current Research, Part D; Geological Survey of Canada, Paper 91-1D, p. 147-156.

Savard, M.M. (cont.)
1992: Diagenèse pré- et post-minéralisation: implication pour le dépôt de Gays River, Nouvelle-Écosse; dans Recherche en cours, Partie E; Commission Géologique du Canada, Étude 92-1E, p. 289-298.

Schenk, P.E.
1967: The Macumber Formation of the Maritimes Provinces, Canada, a Mississippian analogue to recent strand-line carbonates of the Persian Gulf; Journal of Sedimentary Petrology, v. 37, p. 365-376.
1992: A lacustrine origine for the basal Windsor/Codroy Groups (Carboniferous) of atlantic Canada – Introducing Loch Macumber!; Geological Association of Canada, Wolfville 1992, v. 17, A99.

Sheridan, R.E. and Drake, C.L.
1968: Seaward extension of the Canadian Appalachians: Canadian Journal of Earth Sciences, v. 5, p. 337-374.

Weeks, L.J.
1948: Londonderry and Bass River map-areas, Colchester and Hants Counties, Nova Scotia; Geological Survey of Canada, Memoir 245, 86 p. 195-198.

Geological Survey of Canada Project 860018

A note on the occurrence of beryl in the Port Mouton pluton, southwestern Nova Scotia[1]

K.L. Currie and J.B.Whalen
Continental Geoscience Division

Currie, K.L. and Whalen, J.B., 1994: A note on the occurrence of beryl in the Port Mouton pluton, southwestern Nova Scotia; in Current Research 1994-D; Geological Survey of Canada, p. 73-77.

Abstract: The peraluminous, late tectonic Port Mouton pluton consists of subordinate biotite-dominant rocks ranging from tonalite to granodiorite, muscovite-dominant granodiorite and a suite of granitic pegmatite sheets and dykes related to associated major phases. Beryl occurs in tourmaline-bearing pegmatite dykes which cut other pegmatites. The biotite-dominant phase is similar to parts of the more primitive, pegmatite-absent Barrington Passage pluton. The Shelburne pluton consists mainly of biotite-dominant phases like Barrington Passage but contains a pegmatite suite. The three plutons and an associated metamorphic culmination define a post-early-Acadian thermal and structural event. Field data suggest that the Shelburne and Port Mouton plutons contain components lacking in the Barrington Passage pluton. Future work will attempt to characterize these components chemically and isotopically.

Résumé : Le pluton hyperalumineux et tarditectonique de Port Mouton se compose d'une phase subordonnée de roches à biotite dominante, dont la composition varie de la tonalite et à la granodiorite, d'une phase de granodiorite à muscovite dominante et d'une suite de feuillets et dykes de pegmatite granitique apparentés aux phases majeures associées. Du béryl est présent dans des dykes de pegmatite à tourmaline qui recoupent d'autres pegmatites. La phase à biotite dominante est semblable à des portions du pluton de Barrington Passage, plus primitif et dépourvu de pegmatites. Le pluton de Shelburne se compose principalement de phases à biotite dominante, comme le pluton de Barrington Passage, mais contient une suite pegmatitique. Les trois plutons et une culmination métamorphique associée définissent un épisode thermique et structural postérieur à l'Acadien précoce. Les données de terrain semblent indiquer que les plutons de Shelburne et Port Mouton possèdent des composants qui sont absents du pluton de Barrington Passage. Lors de travaux futurs, on s'efforcera de caractériser ces composants des points de vue chimique et isotopique.

[1] Contribution to Canada-Nova Scotia Cooperation Agreement on Mineral Development (1992-1995), a subsidiary agreement under the Canada-Nova Scotia Economic and Regional Development Agreement.

INTRODUCTION

The Meguma Zone of southern Nova Scotia (Williams, 1979) consists mainly of Cambro-Ordovician turbiditic psammite and pelite (Meguma Group) intruded by numerous Devonian peraluminous plutons, which were derived in part by melting of the host sedimentary rocks (Halliday et al., 1981). The Meguma Group comprises several mappable units (O'Brien, 1986) at generally low metamorphic grade (subgreenschist) except for narrow contact aureoles around the plutons. Plutons range in composition from tonalite through quartz monzonite to granitic aplite. Progressive enrichment of lithophile elements, particularly Sn and U, with differentiation is well known and economically important in the South Mountain Batholith (Kontak and Chatterjee, 1992), which dominates the granitoid rocks of the Meguma Zone.

In the southwestern part of the Meguma Zone, a metamorphic culmination reaching andalusite-cordierite grade (Hope et al., 1988) extends 80 km from Pubnico Harbour to Broad River (Fig. 1, 2). The rocks are folded into tight, upright, large wavelength (>1 km) almost cylindrical folds like the rest of the Meguma Zone, but isograds trend east-northeast, cutting across the north to north-northeast trend of the folds. Three plutons along the culmination exhibit progressive changes in lithology and texture from homogeneous quartz diorite, tonalite, and granodiorite in the Barrington Passage pluton to the west, through tonalite to granodiorite with abundant marginal pegmatite-aplite sheets and dykes in the Shelburne pluton, to tonalite, muscovite-biotite granite, and a maze of pegmatite pods, dykes, and sheets in the Port Mouton pluton. The last contains well-known occurrences of beryl whereas the former two do not. The present investigation examines the source and mechanism of concentration of beryl in the Port Mouton pluton.

GEOLOGICAL SETTING

The Port Mounton pluton forms a body at least 16 km in length by 8 km wide (Fig. 2) whose eastern extremitiy lies under the Atlantic Ocean. The pluton has been examined in

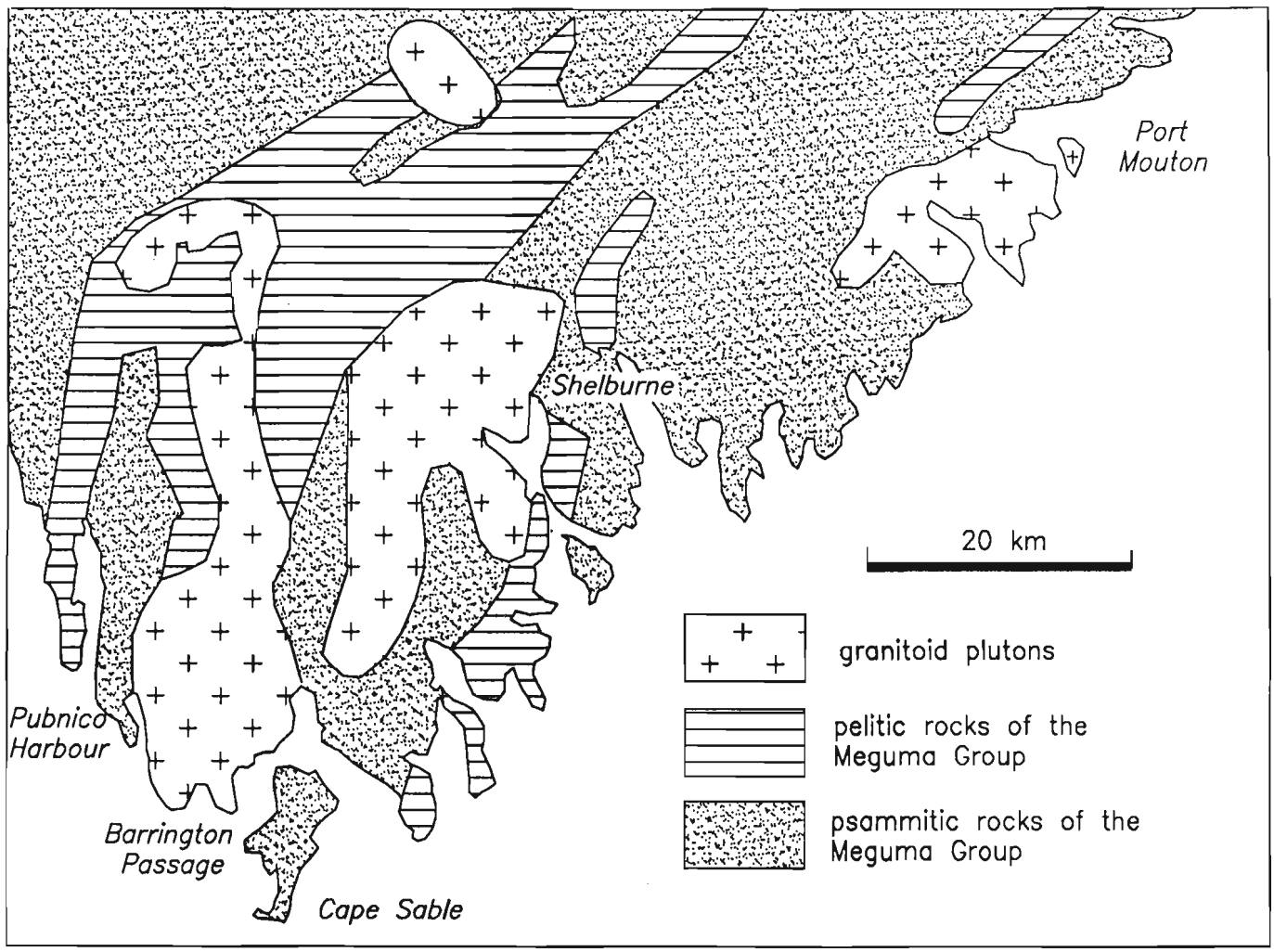

Figure 1. Geological sketch of southern Nova Scotia showing the location of the Port Mouton, Shelburne, and Barrington Passage plutons, and associated metamorphic rocks (modified after Hope et al., 1988; Rogers, 1988).

detail by Douma (1988) who distinguished nine phases. However, for the present purpose a three-fold subdivision is adequate. The oldest part of the pluton, forming the southern third, consists of medium grained, homogeneous rocks in which biotite is the dominant mafic mineral and muscovite occurs only in minor to trace amounts. The more mafic parts of this unit lack potassium feldspar (tonalite), but throughout much of the unit potassium feldspar occurs in distinctive pale buff grains and composition ranges from granodioritic to quartz monzonite. The more mafic rocks have colour indices (CI) as high as 40, while some leucocratic varieties have CI<15. Locally these extremes can be seen within a few metres of each other, although more mafic varieties tend to be concentrated toward the southern margin. The biotite-dominant phase commonly exhibits foliation trending between 120 and 140° and dipping steeply. This foliation includes both flow banding (wispy layering defined by variations in mafic mineral content), and cataclastic layering (flattened biotitic partings, incipient S-C fabric).

The northern two-thirds of the Port Mouton pluton consists of a remarkably homogeneous medium grained muscovite granite with minor amounts of biotite. This rock contains few mafic enclaves, but locally contains pegmatitic pods, dykes, and sheets described in more detail below. The muscovite granite locally exhibits a flow or cataclastic foliation striking between 40 and 70° and dipping steeply. Along the south shore of Port Mouton, flow foliation appears to pass continuously into cataclastic foliation, but more commonly the cataclastic foliation has a more northerly trend than the flow foliation. Limited data from asymmetric augen and S-C fabrics suggest the central part of the pluton moved up and eastward with respect to the margins.

The third major element of the Port Mouton pluton is a diverse suite of pegmatitic rocks. In general the pegmatites are concentrated along the margins of the pluton. Indeed the margins of the pluton are difficult to define exactly because of the large numbers of sheets and dykes of pegmatite with intervening screens of country rocks. The pegmatites fall into

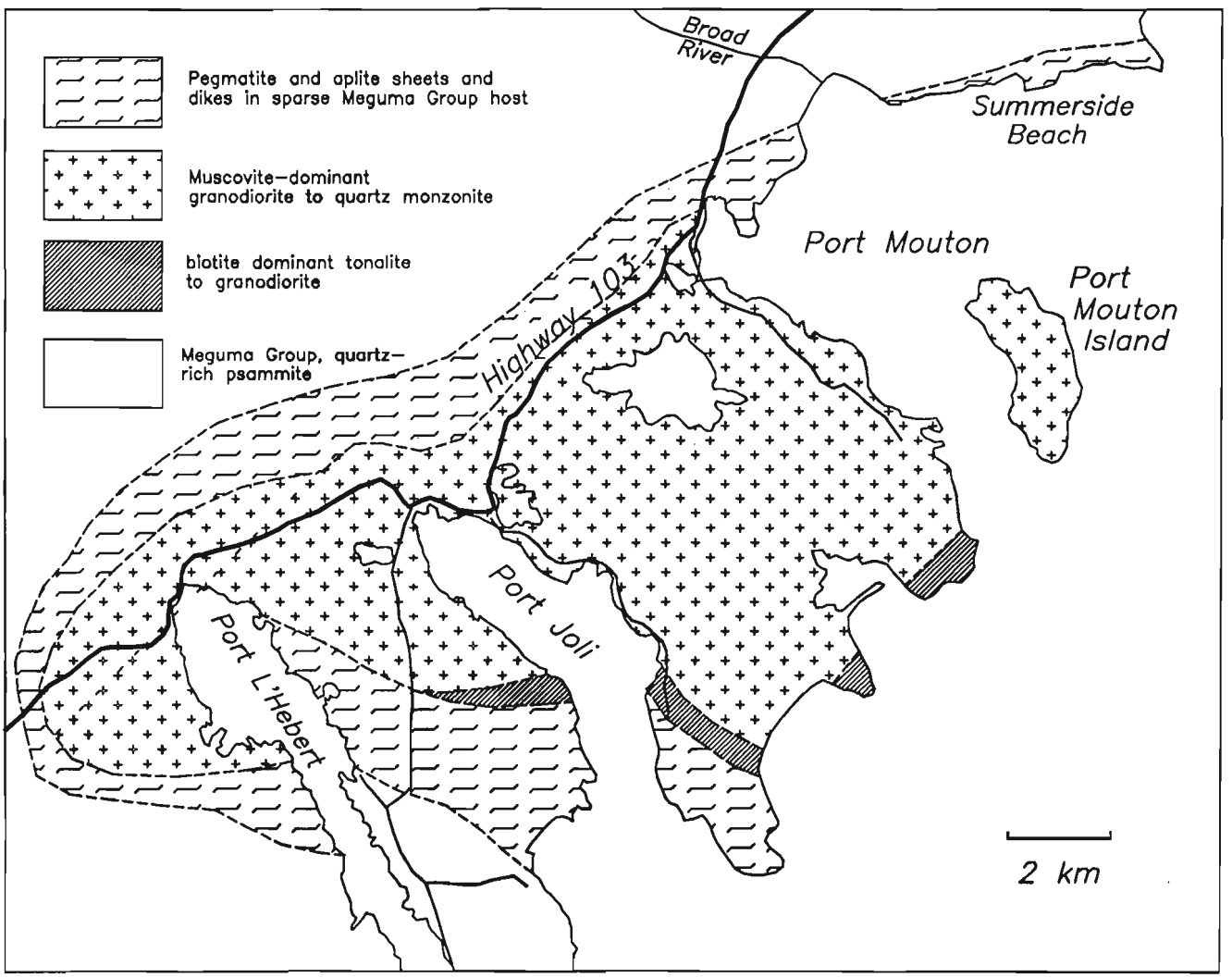

Figure 2. Geological sketch of the Port Mouton pluton (modified after Douma, 1988).

three major varieties, namely biotite-muscovite pegmatite, muscovite pegmatite, and muscovite-tourmaline pegmatite. All three types of pegmatite bodies have generally low dips, locally contain garnet, may exhibit monomineralic zones, particularly quartz cores, and commonly exhibit aplitic rims or lenses that form up to 50% of the body. Pegmatite bodies are tabular to lenticular where well exposed, and range from 10 cm to more than 10 m in thickness. Although the three varieties of pegmatite are well defined on hand specimen scale, large pegmatite bodies exhibit gradational transitions from one type to another over a scale of a few metres.

Biotite-muscovite pegmatites commonly occur in or near biotite-dominant hosts. In a few cases contacts are gradational between diffuse pegmatitic patches and finer grained host rock. Biotite tends to form elongate prisms up to 10 cm in length which locally clump into radiating sprays. Muscovite is younger than the biotite and often overgrows it, either as discrete books or as rounded overgrowths on the sprays. Garnet, where present, forms fine grained symplectic intergrowths with quartz.

Muscovite pegmatites occur with muscovite-granite, locally forming gradational patches in the granite. Muscovite books to 10 cm across are abundant, and garnet euhedra up to 2 cm across occur in the cores of the pegmatites (but not in the rims). Muscovite aplite rims and internal lenses are ubiquitous.

Muscovite-tourmaline pegmatites are more rare, and tend to be smaller than the other types. Tourmaline occurs either as euhedra up to 5 cm long, or as patches of fine grained symplectic intergrowths with quartz up to 10 cm across. Muscovite is a common but a rather sparse constituent. Garnet is erratically distributed in euhedra up to 2 cm across. Most examples of tourmaline-bearing pegmatites examined by us sharply crosscut their host, commonly other pegmatites. Beryl occurs only within the tourmaline-bearing pegmatites, in most places as small disseminated grains, although crystals up to 10 cm long have been reported from Port Mouton Island (Hope et al., 1988).

The Port Mouton pluton is emplaced mainly into psammitic rocks of the Meguma Group (Goldenville Formation, New Harbour, and West Dublin members). The fine grained quartz-plagioclase-biotite wackes of this formation are remarkably impervious to changes in metamorphic grade. Thin semi-pelitic beds and calcareous concretions show more response. Hope et al. (1988) considered that the sillimanite-grade (fibrolite) contact aureole of the Port Mouton pluton overprinted the regional andalusite-cordierite grade culmination. However pegmatites of all the varieties noted above are so common in the wall rocks of the pluton that we found it impossible to distinguish between screens and/or roof pendants and a true contact aureole. The "migmatite" reported by Douma (1988) and Hope et al. (1988) at Summerside Beach clearly consists of slightly deformed pegmatite sheets and dykes occupying rectlinear fractures in wall rocks which show no evidence of partial melting. Similar dyke and sheet complexes occur on the southwest side of the pluton where the sheeted zone is almost 5 km wide. We have found no direct evidence that these complexes are remnants of the roof of the pluton, but in the Shelburne pluton, which exhibits a similar sheeted complex on the east side, roof pendants occur throughout the pluton (Rogers, 1988), demonstrating that the present level of exposure is close to the original roof. Rogers (1988) reported two occurrences of beryl from the Shelburne pluton, one from Shelburne harbour, the other from a roadcut on Highway 103. We have not examined the former occurrence. Samples from the latter occurrence, although they closely resemble beryl in form and colour, were determined to be apatite by X-ray powder diffraction identification.

DISCUSSION

Enrichment of lithophile elements in pegmatites spatially associated with granitoid plutons, locally with the formation of an aureole of rare-element-rich pegmatites, is a well known phenomenon which has generated a large amount of literature (for example Martin and Cerny, 1992; Cerny, 1991, and references therein). Commonly the pluton is peraluminous like the Port Mouton (compare Shearer et al., 1992; Breaks and Moore, 1992). Despite the spatial relations between pegmatites and granite pluton, important questions about the source and composition of the fluids transporting the rare metals to the pegmatites and the mechanism of deposition remain unsolved. Some authours suggest the pegmatites and their contained metals were derived entirely by igneous differentiation of a granitoid parent, and that their emplacement is synmagmatic (as opposed to hydrothermal). In order to make such a model quantitatively fit field observations Shearer et al. (1992) were forced to assume multiple episodes of melting involving slightly differing protoliths and a particular composition (F-rich) for the mineralizing fluid. Other authors assume the host pluton derived from a sedimentary protolith by anatexis, extracting B and rare metals in the process. After igneous differentiation, the exotic components were delivered mainly via hydrothermal fluids (Breaks and Moore, 1992). Both of these models have drawbacks. The pure igneous differentiation model ignores the source of the rare metals, and assumes that the abundant evidence of a free vapour phase (quartz cores, aplite rims) is irrelevant. The anatectic model ignores the source of the heat driving the process, and has no obvious explanation for the rarity of rare-earth-enriched pegmatites associated with S-type granites. Because both models rely on igneous differentiation to enrich the magma in fluids, they both encounter the well known difficulties in bringing water-saturated magma to relatively shallow depths (about 10-11 km at Port Mouton, Hope et al., 1988).

The pegmatites of the Port Mouton pluton mineralogically and in P-T environment fall between the muscovite and rare-element classes of pegmatites in the classification of Cerny (1991). The Port Mouton region is a favourable site to examine the genesis of these pegmatites because of the suite of associated plutons, and the unusually clear record of events in the surroundings. The Barrington Passage pluton ranges from quartz diorite to granodiorite and contains virtually no pegmatite. Although it is mildly peraluminous, de Albequerque (1977) concluded that it could have been derived from the mantle with only slight crustal contamination. There is no evidence of a volatile phase. The Shelburne pluton consists

mainly of a biotite-dominant phase virtually identical to parts of the Barrington Passage, but it also contains a pegmatite component with quartz cores and abundant aplite suggesting that a volatile phase was present. The Port Mouton pluton contains a significant, but subordinate, biotite-dominant component similar to parts of the Barrington Passage, a major muscovite granite phase, and voluminous pegmatites. The differences in the three plutons cannot be due to differing levels of the exposed plutons, since the surrounding metamorphic aureoles give similar P-T conditions for all three (Hope et al., 1988), neither does it seem likely to be due entirely to differing differentiation histories since all three exhibit a broad range of compositions. We deduce that extra components and/or differing histories of crystallization produced pegmatites in the Shelburne and Port Mouton plutons but not in the Barrington Passage. We hope to identify and document the source of pegmatite-producing magma or fluid phase, and to constrain physical conditions favourable for the emplacement of rare-metal-bearing pegmatites by means of appropriate chemical and isotopic techniques.

The Port Mouton pluton has generally been described as posttectonic (Douma, 1988), however abundant evidence of tectonic activity during emplacement occurs in the form of cataclastic foliation. This foliation, and the accompanying emplacement and metamorphism, clearly post-date the early-Acadian folding of the Meguma Group (Keppie, 1985). The deformation and metamorphism are thus relatively young. Douma (1988) collected various Ar/Ar data suggesting ages of metamorphism as young as 310-330 Ma, but concluded that many of these ages have been reset. However, there seems to be no doubt that Port Mouton represents a major period of plutonism, metamorphism, and deformation younger than the major peraluminous plutons to the north.

ACKNOWLEDGMENTS

We are indebted to Barry Clarke of Dalhousie University who generously shared with us both his knowledge of the plutons and useful references. Careful critical reading by W.D. Sinclair has substantially improved the manuscript.

REFERENCES

Breaks, F.W. and Moore, J.M.
1992: The Ghost Lake batholith, Superior Province of northwestern Ontario: a fertile S-type peraluminous granite – rare element pegmatite system; Canadian Mineralogist, v. 30, p. 835-876.

Cerny, P.
1991: Rare-element granitic pegmatites Part 1; Anatomy and internal evolution of pegmatite deposits; Geoscience Canada, v. 18, p. 49-67.

de Albuquerque, C.A.R.
1977: Geochemistry of the tonalitic and granitic rocks of the Nova Scotia southern plutons; Geochimica et Cosmochimica Acta, v. 41, p. 1-13.

Douma, S.L.
1988: The Mineralogy, Petrology and Geochemistry of the port Mouton Pluton, Nova Scotia, Canada; M.S. thesis, Dalhousie University, Halifax, Nova Scotia, 324 p.

Halliday, A.N., Stephens, W.E., and Harmon, R.S.
1981: Isotopic and chemical constraints on the development of peraluminous Caledonian and Acadian granites; Canadian Mineralogist, v. 19, p. 205-216.

Hope, T.L., Douma, S.L., and Raeside, R.P.
1988: Geology of the Port Mouton – Lockeport area, southwestern Nova Scotia; Geological Survey of Canada, Open File 1768, 80 p.

Keppie, J.D.
1985: The Appalachian collage; in The Caledonide Orogen: Scandanavia and related areas (ed.) D.G. Gee and B.A. Sturt; John Wiley, New York, p. 1217-1226.

Kontak, D.J. and Chatterjee, A.K.
1992: The East Kemptville tin deposit, Yarmouth County, Nova Scotia: a Pb isotope study of the leucogranite and mineralised greisens – evidence for a 366 Ma metallogenic event; Canadian Journal of Earth Sciences, v. 29, p. 1180-1936.

Martin, R.F. and Cerny, P. (ed.)
1992: Grantic Pegmatites; Canadian Mineralogist, v. 30, pt. 3, p. 497-954.

O'Brien, B.H.
1986: Preliminary report on the geology of the Mahone Bay area, Nova Scotia; Geological Survey of Canada, Paper 85-1A, p. 789-794.

Rogers, H.D.
1988: Field relations, petrography and geochemistry of granitoid plutons in the Shelburne area, southern Nova Scotia; Geological Survey of Canada, Open File 1835, 128 p.

Shearer, C.K., Papike, J.J., and Jolliff, B.L.
1992: Petrogenetic links among granites and pegmatites in the Harney Peak rare-element granite-pegmatite system, Black Hills, South Dakota; Canadian Mineralogist, v. 30, p. 785-810.

Williams, H.
1979: Appalachian Orogen in Canada; Canadian Journal of Earth Sciences, v. 16, p. 792-807.

Geological Survey of Canada Project 730044

Lithology and preliminary paleoenvironmental interpretation of the Macumber and Pembroke formations (Windsor Group, Early Carboniferous), Nova Scotia

Denis Lavoie
Quebec Geoscience Centre, Sainte-Foy

Lavoie, D., 1994: Lithology and preliminary paleoenvironmental interpretation of the Macumber and Pembroke formations (Windsor Group, Early Carboniferous), Nova Scotia; in Current Research 1994-D; Geological Survey of Canada, p. 79-88.

Abstract: The Viséan Macumber and Westphalian or younger Pembroke formations occur along the basal Windsor Group. The Macumber consists of a lower interval of lime mudstones overlain by graded and laminated packstones and wackestones. The lime mudstones were deposited below storm wave base, whereas the coarser grained carbonates indicate rapid supply in a low energy setting. The overlying Pembroke shows a penetrative planar fabric associated with structural and recrystallization features supporting its mylonite interpretation. The Pembroke Formation is typified by massive, clast-supported and unsorted breccias. Two types of breccia are defined: 1) a lower breccia is interlayered with the mylonite and contains mylonite fragments, indicating a tectonic origin for the breccia; 2) an upper breccia unconformably overlies the first one with fragments of the lower breccia, reddish siliciclastic infillings and gravitational cements suggesting a late solution collapse karstic origin for this breccia.

Résumé : Les formations de Macumber (Viséen) et Pembroke (Westphalien ou plus jeune) sont à la base du Groupe de Windsor. La Formation de Macumber montre à sa base, des lime mudstones surmontés de packstones et wackestones granoclassés et laminés. Les mudstones se sont déposés sous la zone des vagues de tempêtes; les carbonates grossiers représentent un apport rapide dans un environnement calme. La Formation de Pembroke sus-jacente montre une fabrique planaire pénétrative associée à divers phénomènes structuraux et de recristallisation appuyant son interprétation de mylonite. Le Formation de Pembroke est constituée de brèches massives à support de fragments non triés. Deux types de brèches sont définis : 1) une brèche inférieure est interstratifiée avec la mylonite et contient des fragments de mylonite, indiquant une origine tectonique pour la brèche; 2) une brèche supérieure surmonte en discordance la première avec des fragments de celle-ci; des cavités remplies de silicoclastites rouges et des ciments gravitaires suggèrent un effondrement karstique tardif.

INTRODUCTION

The Viséan Macumber (Weeks, 1948) and the locally overlying Pembroke (Weeks, 1948) formations of the Windsor Group, with the laterally equivalent Gays River Formation, represent the first major carbonate deposits in the post-Acadian successor Magdalen Basin (part of the eastern Canada Maritimes Basin) of Nova Scotia. These units constitute the basal part of the first transgressive-regressive cycle of the Windsor Group (Giles, 1981). The reconnaissance of sedimentary paleoenvironments for the basal Windsor carbonates is critical for the reconstruction of initial marine infilling of the basin; moreover, the presence of base metal occurrences (Jubilee Zn-Pb deposit; Hein et al., 1993) further adds to the interest in studying these units.

Sedimentological and economic investigations of the basal Windsor carbonates started in the early fifties (Stacey, 1953; Sage, 1954; Schenk, 1967; Kirkham, 1978; Giles et al., 1979; Giles; 1981; Geldsetzer, 1977, 1978; among others). Over the years, however, major divergences for the proposed paleoenvironmental significance of basal Windsor carbonates arose. For one, the Macumber Formation is typified by a sub-centimetric planar fabric developed in limestones. The fabric has been interpreted as algal/microbial laminites (Schenk, 1967; Giles, 1981, among others). The environmental interpretation of these laminites is controversial; they were regarded either as an intertidal strandline deposit (Schenk, 1967), or a deep water (below wave base) deposit following a rapid and major flooding of the basin (Giles, 1981; Hein et al., 1993), or alternatively as a lacustrine deposit (Schenk et al., 1992). Similarly, the origin of the overlying and/or laterally equivalent Pembroke Formation or Breccia, was also the subject of much controversy (see Hein et al. (1993) for a recent review). The Pembroke has been interpreted either as a collapse breccia of karstic (Clifton, 1967; Smith and Collins, 1979) or evaporite solution (Smith and Collins, 1979) origin, or as a coarse grained storm deposit (Schenk, 1969). Moreover, the term Pembroke is also used to designate, in drill cores, a non-brecciated massive unit overlying the typically laminated material of the Macumber Formation (D. Sangster, pers. comm., 1993). The lack of a rigorous lithostratigraphic framework for the Pembroke coupled with the divergent interpretations for its origin has resulted in confusing models for this part of the basal Windsor carbonates.

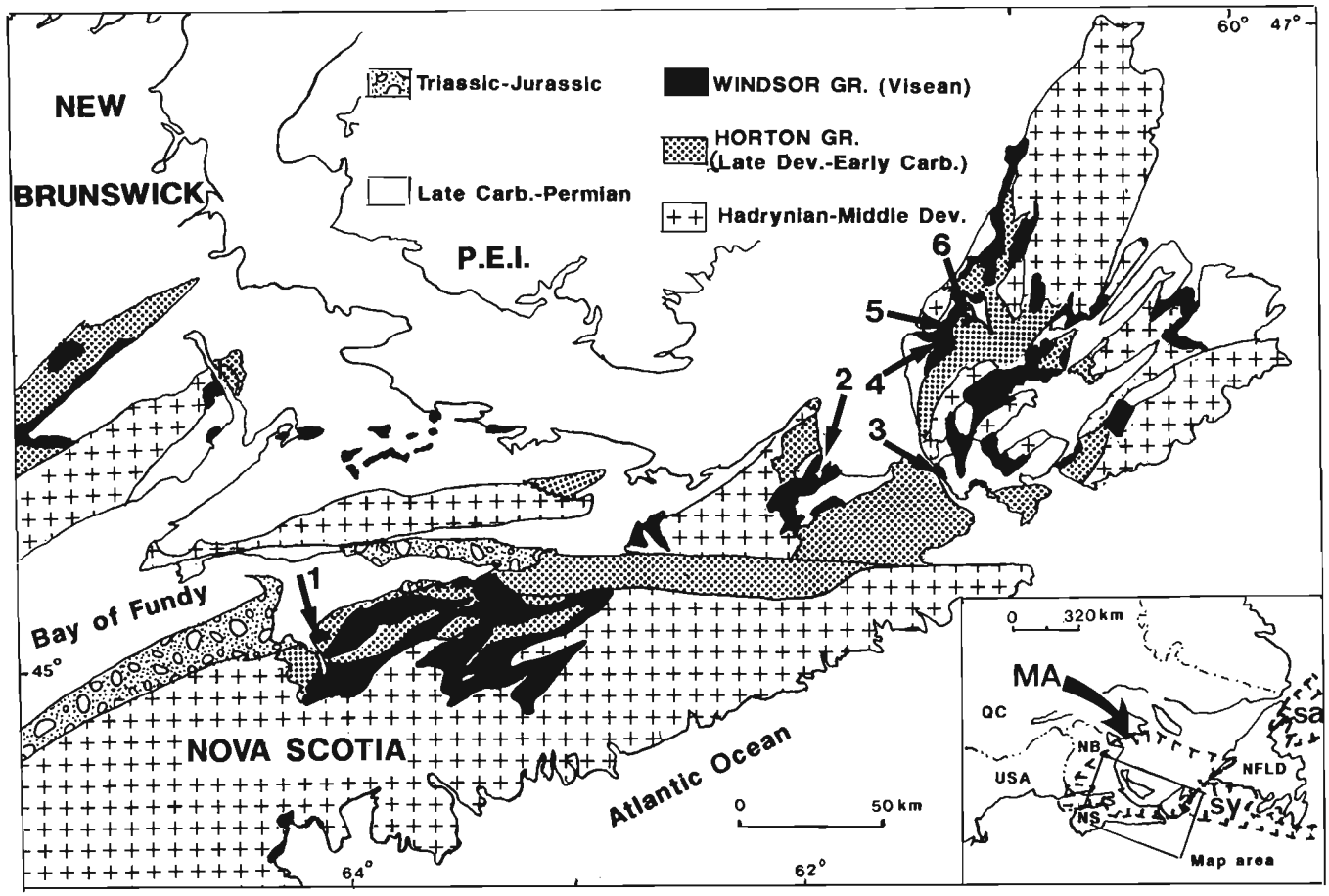

Figure 1. Simplified geological and location map of studied sections in Nova Scotia. Sections are: (1) Cheverie, (2) Crystal Cliff, (3) Port Hasting, (4) Southwest Mabou River, (5) Miramichi Brook, and (6) quarry west of Ainslie Lake. The inset locates the Magdalen Basin (MA), sa is for Saint-Anthony basin and sy is for Sydney Basin. Modified from Boehner et al. (1989).

Reconnaissance work during the 1992 field season showed that the typical planar fabric of the Macumber Formation is rather ascribable to intense mylonitization of limestones rather than resulting from microbial-controlled sedimentation (G. Lynch, pers. comm., 1992; Lynch and Giles, 1993). This new hypothesis for the origin of the planar fabric, if proven right, weakens all the previous paleoenvironmental interpretations for the Macumber, which for the most part have suggested a microbial origin for the planar fabric. Detailed measurements and descriptions of six of the most complete sections of the Macumber – Pembroke succession were done during the 1993 field season. This report presents the internal lithostratigraphy and preliminary paleoenvironmental interpretations for the Macumber and Pembroke formations.

GEOLOGICAL SETTING

The Lower Carboniferous Windsor Group outcrops in many structural sub-basins forming part of the Magdalen Basin (Fig. 1). The Magdalen successor Basin was initiated by the extensional collapse of the Acadian orogen in Late Devonian time (Lynch and Giles, 1993). A thick Hadrynian-Middle Devonian succession constitutes the basement of the successor basin. The Windsor Group (up to 6000 m; Howie and Barss, 1975) overlies either conformably to paraconformably the Upper Devonian – lowermost Carboniferous Horton Group or unconformably the Cambrian-Ordovician Meguma Group (Fig. 2). The Windsor Group is in turn conformably to unconformably overlain by a thick succession of Carboniferous to Jurassic siliciclastics (Fig. 2). The Windsor Group is made up of five transgressive – regressive cycles (Fig. 2) and contains almost exclusively the only marine record in the Magdalen Basin (Giles, 1981). However, its stratigraphy is strongly dominated by siliciclastic sediments and evaporite deposits; carbonates are only a minor part of the succession (Giles, 1981).

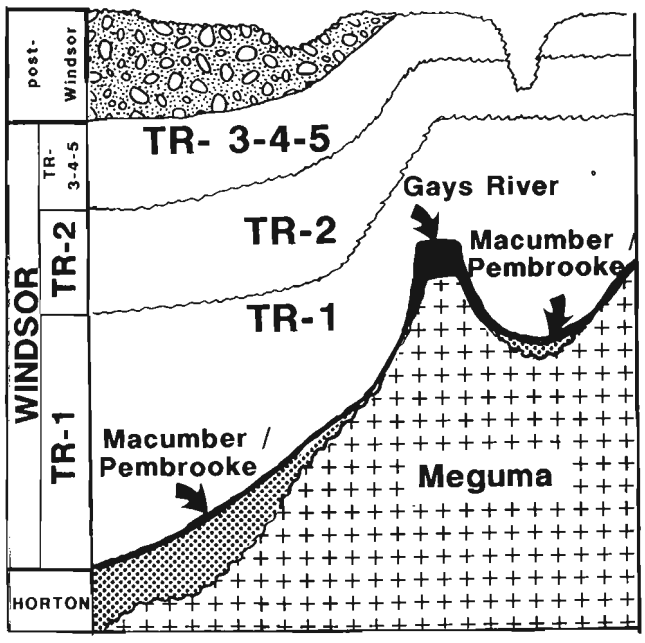

Figure 2. Major transgressive-regressive cycles in the Windsor Group and stratigraphic position of the Macumber-Pembroke succession. Modified from Giles (1981).

The Macumber Formation occurs basin-wide. It overlies the Horton Group, a continental to very shallow marine siliciclastic unit deposited in post-orogenic distensive fault-bounded basins (Hamblin and Rust, 1989). On the other hand, the laterally equivalent Gays River reefoid mounds unconformably overlie the metawackes of the Meguma Group. The described sections of the Macumber – Pembroke succession are in the Cheverie (section 1) and Crystal Cliff (section 2) areas on the mainland part of Nova Scotia, and in the Port Hasting (section 3) and Mabou (sections 4 to 6) areas on Cape Breton Island (Fig. 1, 3).

THE MACUMBER AND PEMBROKE FORMATIONS

The exposed Macumber – Pembroke succession ranges from 5.1 to 16.2 m in thickness (Fig. 3). If one agrees (as is the current usage) to assign breccias to the Pembroke Formation, then this portion of the basal Windsor is made up of interlayered Macumber and Pembroke formations on mainland Nova Scotia and of the Macumber Formation on Cape Breton Island (Fig. 3).

The underlying Horton Group (Fig. 4A, B) consists of a heterogeneous assemblage of siltstones and sandstones with abundant sedimentary structures (parallel and cross laminations, mudcracks, metre- to decametre-sized channels). Locally, an unsorted, clast-supported and heterolitic conglomerate is found underlying the Macumber (Fig. 4B). All these lithologies were interpreted to represent a dominant continental environment (Hamblin and Rust, 1989) with a minor marine component (clam-bearing sandstone at Cheverie; R. Moore, pers. comm., 1993).

Macumber lithology

For every measured section, the Macumber Formation consists of a lower 2 to 3 m thick succession of various, non platy limestones overlain by platy lithologies (Fig. 3). It is only for the lower succession that primary sedimentary structures can be recognized; the upper part of the Macumber is intensely recrystallized.

Lime mudstone

The lime mudstone lithofacies occurs invariably at the bottom of the described sections of the Macumber Formation (Fig. 3). It consists of 10 to 30 cm-thick beds (Fig. 5A) that show very fine argillaceous parallel laminations. Gastropods, sometimes coated by centimetre-thick algal-like material, are occasionally found. The lime mudstone is dark brown and some centimetre-sized pyrite nodules are, for some sections, found aligned parallel to bedding planes (Fig. 5A).

This lithofacies makes up less than 1 m of the lower part of the "pristine" Macumber. The lack of 1) wave-induced structures, 2) abundant open marine fauna and 3) bioturbation coupled with the dark colour of the lithofacies suggest an anoxic below fairweather wave base and storm wave base setting.

Wackestone and packstone

This lithofacies overlies the lime mudstone lithofacies. It consists of 15 to 25 cm-thick horizons commonly made up of alternating cm-sized couplets of normal- to inverse-graded micrite intraclasts, peloids and oolite-like material (Fig. 5B). Locally, these couplets form cross-laminated intervals but more commonly are in parallel-laminated successions (Fig. 5B).

The micrite intraclasts consist of millimetre- to rare centimetre-sized, rounded to sub-angular particles, which are associated with small micrite peloids in clast- to matrix-supported sediment. The matrix (30-65%) is made up of lime mudstone. Small oolite-like allochems are sometimes found in the lithofacies, however, their exact nature as well as their preservation state are currently unknown. The lithofacies conspicuously lacks any macrofauna and is devoid of bioturbation. The couplets are commonly capped by very thin calcareous shale laminae (Fig. 5B).

The wackestone-packstone lithofacies constitutes the uppermost 1 to 2 m-thick succession of the "pristine" Macumber. The sedimentary structures (normal and inverse grading, parallel and cross laminations), the preservation of lime and siliciclastic muds in otherwise coarse grained (sand-sized) sediment together associated with the lack of marine fauna, bioturbation, reworking of sedimentary structures and of convincing algal/calcimicrobe structures, indicate deep water (below storm wave base) resedimentation of carbonates.

The typical platy limestone of the Macumber

The platy lithofacies of the Macumber is found overlying the wackestone-packstone lithofacies (Fig. 3). This easily recognizable rock type has been described over the years as the

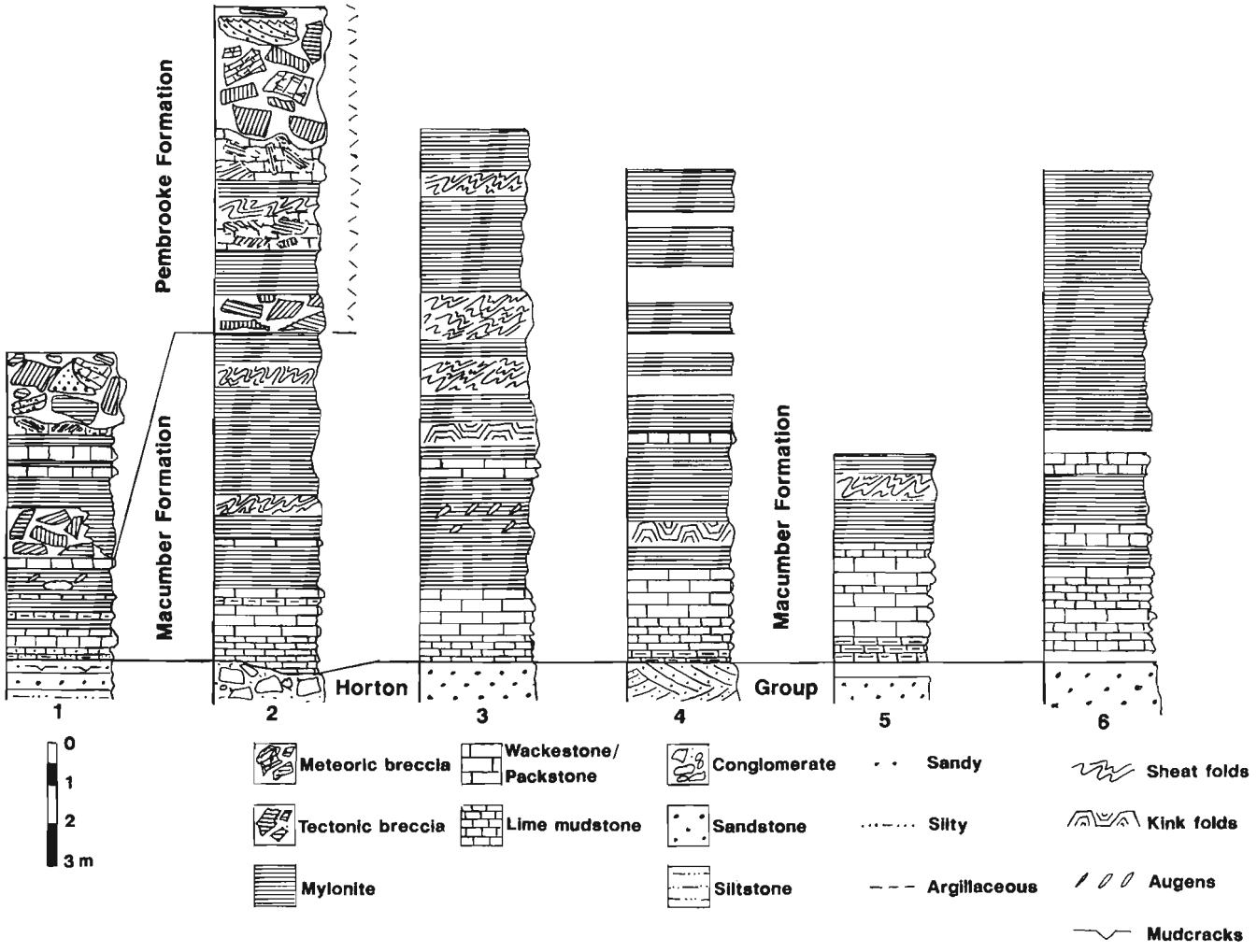

Figure 3. Lithostratigraphy of the Macumber and Pembroke formations. Location of sections in Figure 1.

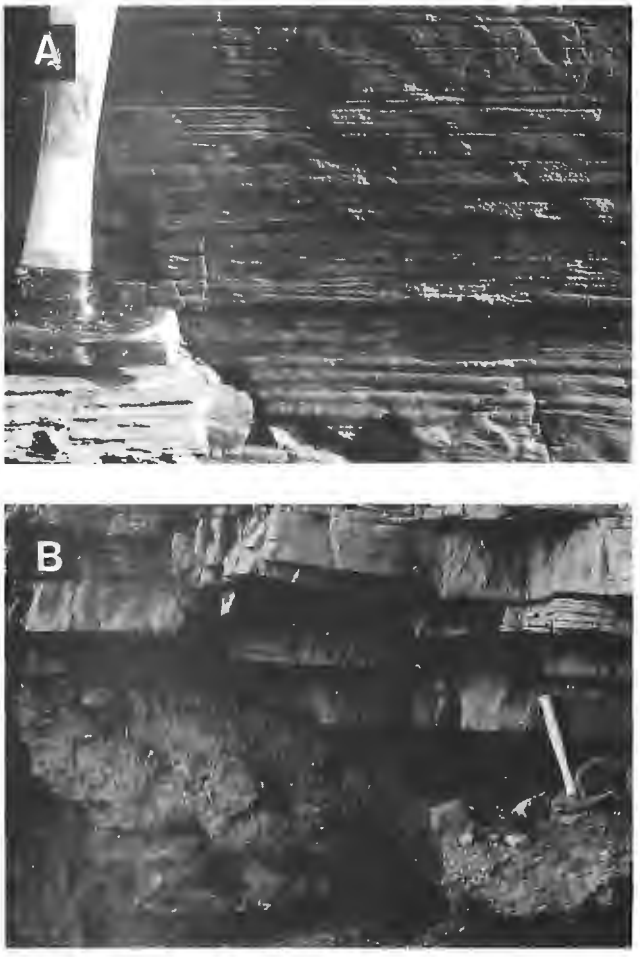

Figure 4. Horton Group. A) Parallel laminated siltstone, the lithofacies is mudcraked and represents intertidal muds. Section 1. B) Heterolitic, unsorted conglomerate of the Horton Group paraconformably overlain by plane-bedded lime mudstone of the Macumber Formation. Section 2.

typical Macumber lithology and constitutes more than 80% of the Macumber studied here. As stated in the introduction, the algal-microbial origin for the lithofacies is strongly entrenched in the Windsor Group literature (see above); however, the paleoenvironmental setting of the deposit is far less clear.

The platy limestone lithofacies of the Macumber (the "laminites" of previous workers) gradationally overlies the wackestone-packstone lithofacies. Preserved intraclasts and peloids in a mixed micrite-microspar matrix are found in the lowermost 5 to 20 cm interval of the platy limestone succession. Immediately overlying this thin interval, the lithofacies consists of alternating couplets of millimetre- to centimetre-thick microspar-spar carbonates and millimetre-sized siliciclastic laminae (Fig. 6A). The planar fabric is very regular and sharp, it does not show the typical algal-microbial crinkly aspect. Moreover, it is so penetrative that in most outcrops, this part of the Macumber weathers and breaks into millimetre-sized paper-like sheets. This lithology makes up the bulk of the Macumber, it is locally associated with peculiar features that are conspicuously absent in the lower "pristine" Macumber. These are: centimetre- to decimetre-wide highly recrystallized ovoid areas laterally continuous with the platy facies (Fig. 6B) and centimetre-sized elongated and rotated carbonate nodules or boudins (Fig. 6C). Moreover, small-scale faulting and folding are nicely developed along the platy lithofacies (Fig. 6A); kink folds ("stromatolites" of some previous workers) are developed in the lower part of the platy interval (Fig. 6D) whereas more complex multi-phase folds are typical of the upper part of the platy facies (Fig. 6E).

As a whole, the platy lithofacies of the upper part of the Macumber Formation lacks unequivocal field evidence for an algal-microbial origin, moreover, petrographic examination of few thin sections are also inconclusive in that aspect. The recrystallization, development of the intense platy fabric and the facies-restricted faulting and folding are seen as strong arguments for a tectonic origin for the platy facies of the Macumber. The tectonic mylonite and detachment fault

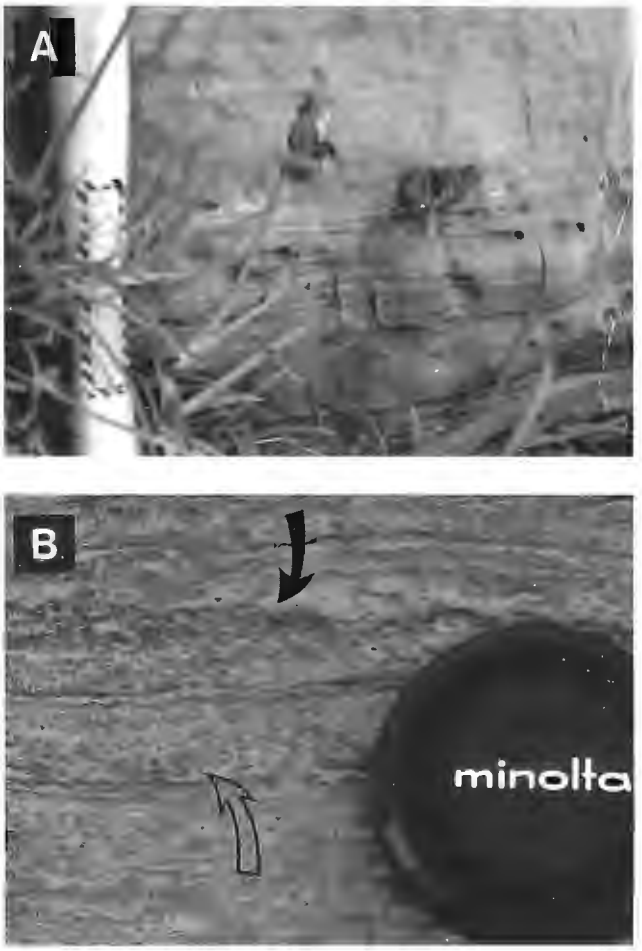

Figure 5. Macumber Formation. A) Thick-bedded lime mudstone with fine argillaceous parallel laminations. Note pyrite nodules aligned to bedding planes. Section 5. B) Cross-section view of centimetre-thick horizons of intraclastic-peloidal packstone and wackestone. Normal-graded horizon (open arrow) is overlain by inverse-graded bed (black arrow). Individual horizons are capped by millimetre-thick mudstone laminae. Lens cap is 7 cm. Section 5.

interpretation for the upper part of the Macumber Formation (Lynch and Giles, 1993) seems, from field and preliminary petrographic examination, the most coherent explanation for the observed lithology.

Pembroke lithology

From accepted but informal descriptions, the Pembroke is made up of breccia, and may include Macumber-like platy facies. Its upper limit coincides with the first evaporite deposits of the basal Windsor carbonates. In field exposures of the Magdalen Basin, the Pembroke interval is dominated by breccias with irregularly embedded Macumber-like platy lithologies (Fig. 3), whereas in drill cores, it commonly consists of a massive interval devoid of any bedding signs (D. Sangster, pers. comm., 1993).

The Pembroke Formation (*sensu* the first non-platy lithology overlying the Macumber) is described from two sections on mainland Nova Scotia (Fig. 1, 3). Two rock types were recognized in the interval assigned to the Pembroke Formation. The

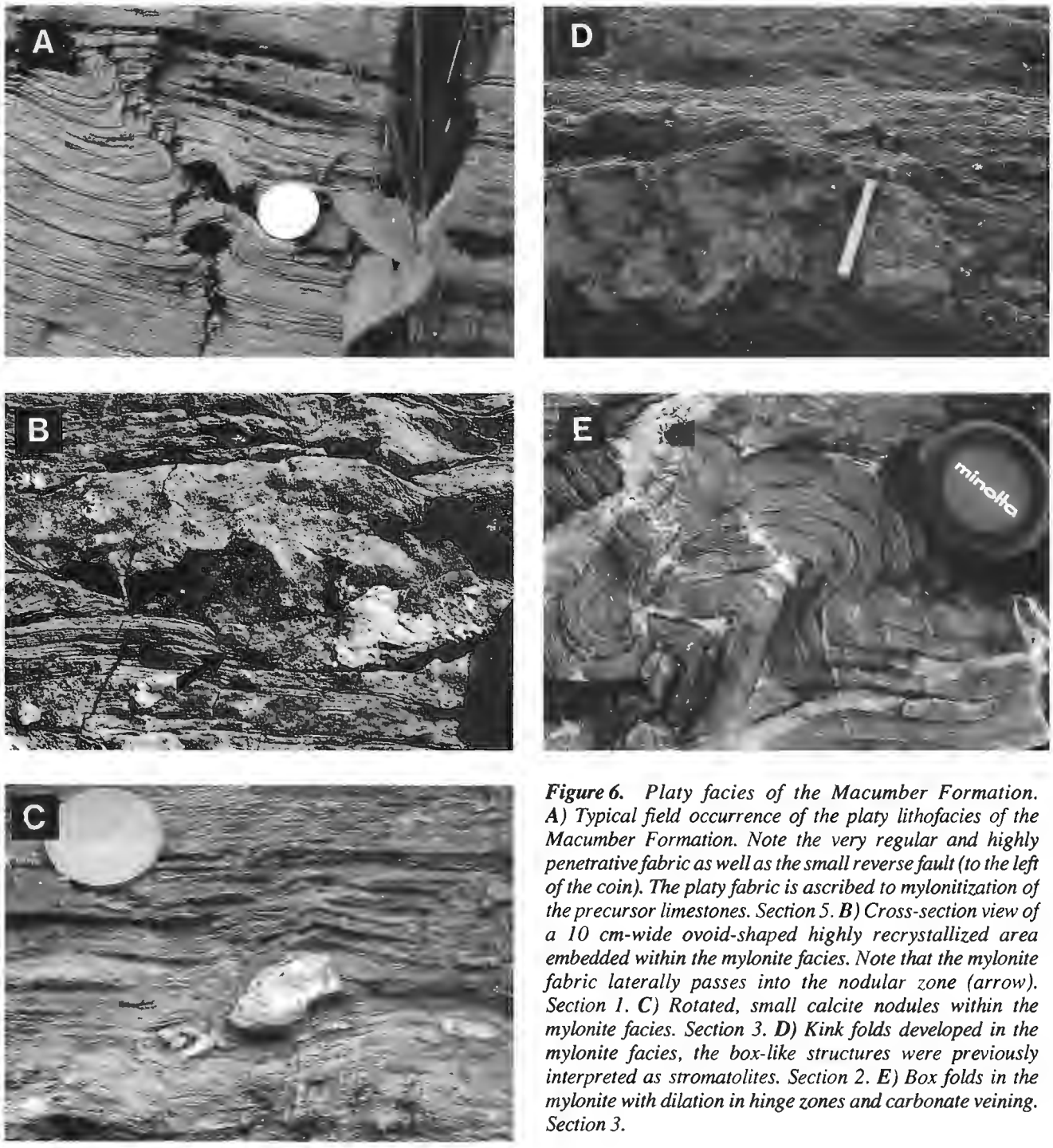

Figure 6. *Platy facies of the Macumber Formation.* ***A)*** *Typical field occurrence of the platy lithofacies of the Macumber Formation. Note the very regular and highly penetrative fabric as well as the small reverse fault (to the left of the coin). The platy fabric is ascribed to mylonitization of the precursor limestones. Section 5.* ***B)*** *Cross-section view of a 10 cm-wide ovoid-shaped highly recrystallized area embedded within the mylonite facies. Note that the mylonite fabric laterally passes into the nodular zone (arrow). Section 1.* ***C)*** *Rotated, small calcite nodules within the mylonite facies. Section 3.* ***D)*** *Kink folds developed in the mylonite facies, the box-like structures were previously interpreted as stromatolites. Section 2.* ***E)*** *Box folds in the mylonite with dilation in hinge zones and carbonate veining. Section 3.*

volumetrically minor one consists of a platy limestone lithology similar in its megascopic characteristics, to the typical Macumber platy lithology. However, the recrystallization of the lithology is commonly more pronounced and the resulting fabric is more massive, consisting of centimetre-sized, strongly indurated, plane-layered limestones (Fig. 7A). The volumetrically dominant lithology consists of breccias of at least two origins.

Tectonic breccia

The first type of breccia occurs sharply over the typical platy lithofacies of the Macumber Formation (Fig. 7A). For both measured sections, this breccia type is interbedded with metre-sized intervals of mylonitic limestones (Fig. 3, 7A).

Bedding is undiscernible at the outcrop scale and the breccia encompasses metre-thick intervals (Fig. 7A). The breccia is clast-supported and consists of millimetre- to decimetre-sized angular and unsorted fragments (Fig. 7A-D). The large-sized clasts are made up of mylonite fragments (Fig. 7D), whereas the matrix consists of finely crushed fragments of limestones (Fig. 7B). Interestingly, this breccia shows evidence for strong annealing as revealed by highly recrystallized and irregularly shaped intervals where individual clasts and matrix are lost in massive limestones (Fig. 7C, D).

The close association of this first breccia with the carbonate mylonite, its homogeneous composition, the lack of internal sedimentary structures or outcrop-scale granulometric trends and the strong annealing event suggest that this breccia is not a sedimentary deposit or related to karsting. It is interpreted as a tectonic breccia related to the mylonitization of the limestones at shallower structural settings or during a relatively higher strain rate (G. Lynch, pers. comm., 1992). Precise timing for the formation of the

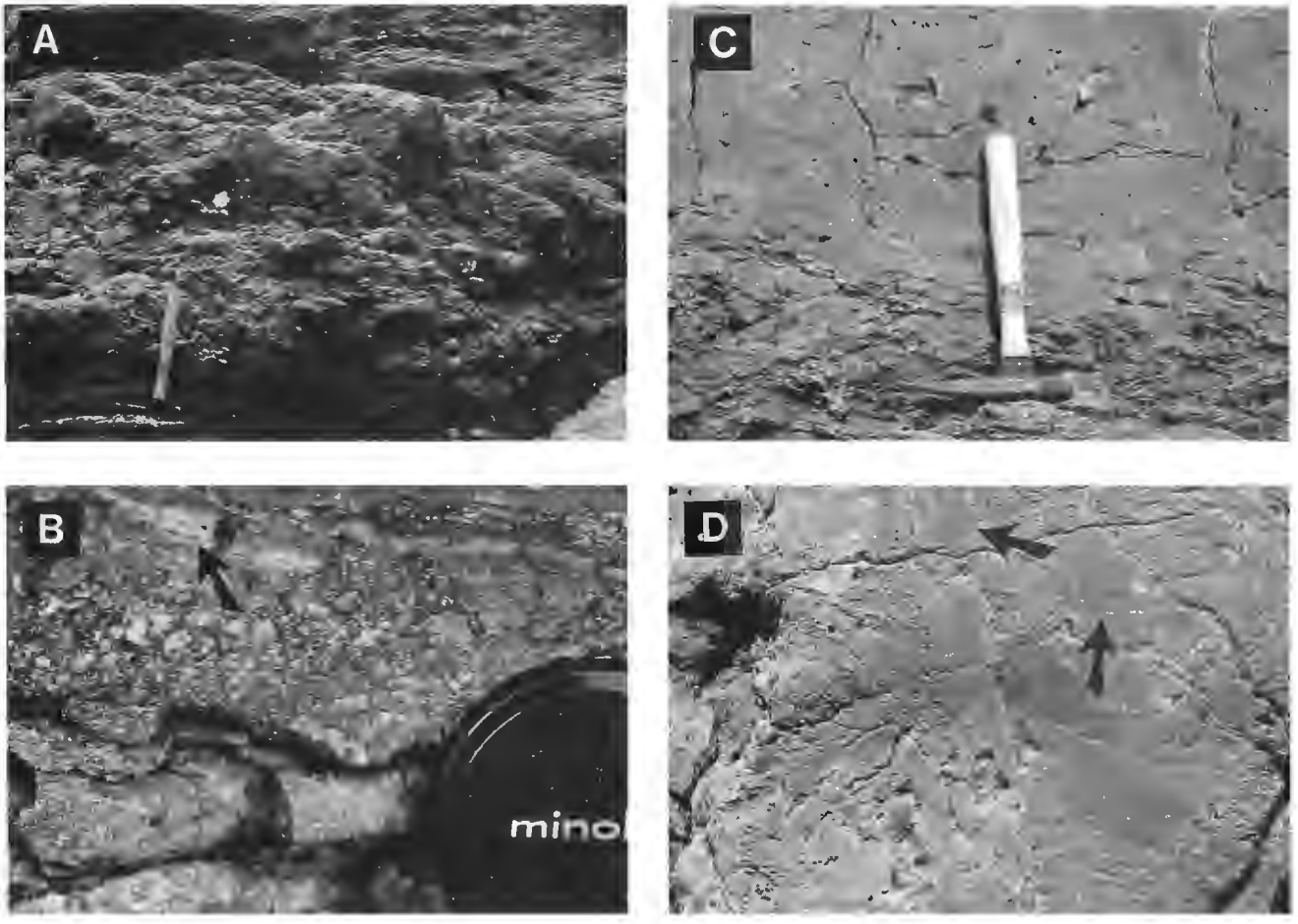

Figure 7. *Tectonic breccia of the Pembroke Formation.* ***A)*** *Massive, clast-supported and unsorted breccia interval made up of centimetre- to metre-sized mylonite fragments. This interval is overlain by non-brecciated, highly indurated mylonites (arrow) in turn passing into an other brecciated interval similar to the lower one. Section 2.* ***B)*** *Close-up view of the breccia matrix consisting of fine-crushed mylonite fragments (arrow). Section 2.* ***C)*** *Cross-section view of a massive interval within the tectonic breccia. Section 1.* ***D)*** *Close-up view of C) showing the annealing event almost completely masking the presence of mylonite fragments (arrows) in the resulting coarse grained sparry rock. Width of photograph is 20 cm. Section 1.*

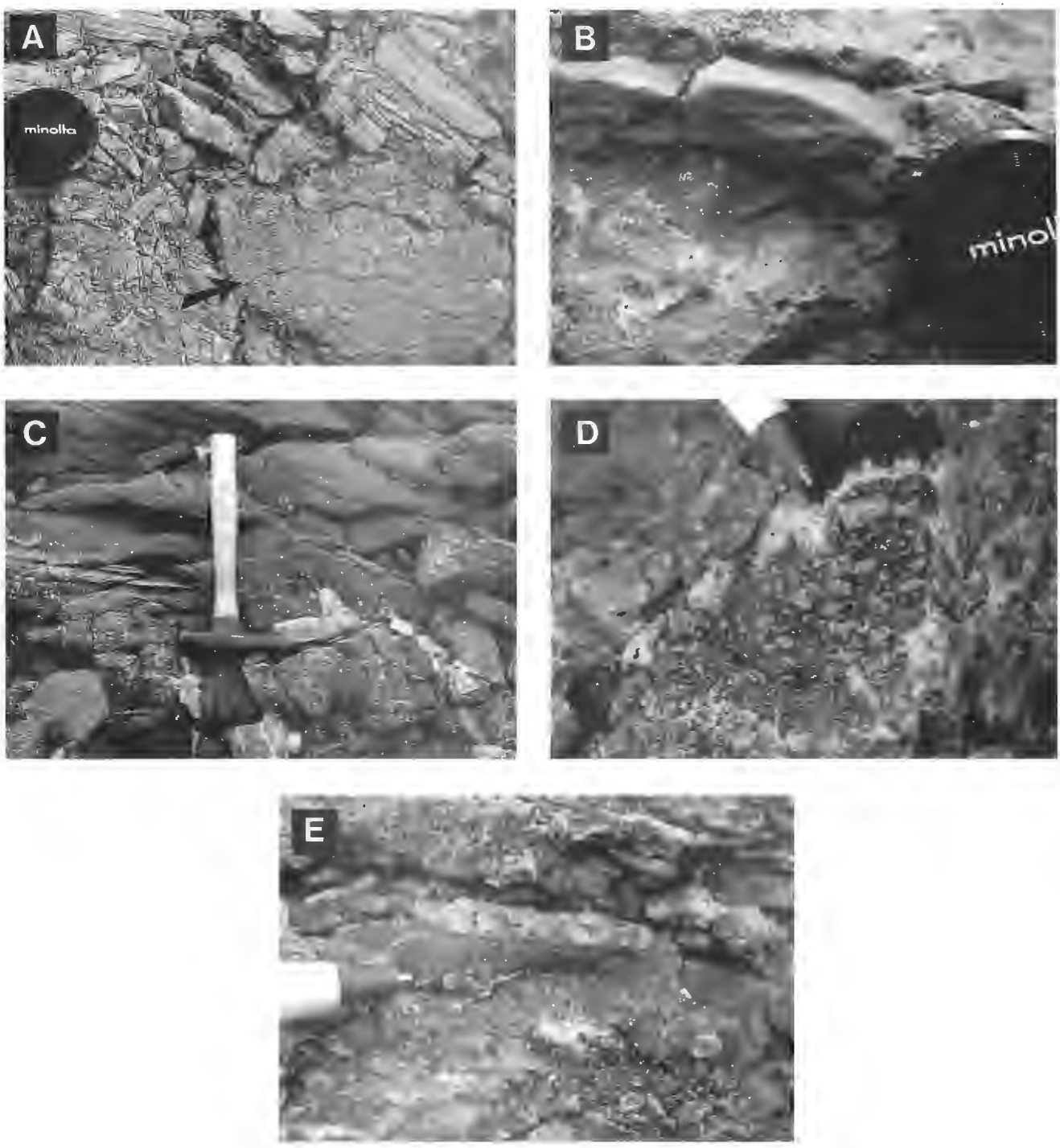

Figure 8. *Meteoric or karstic breccia of the Pembroke Formation.* ***A****) Cross-section view of the massive, clast- supported and unsorted breccia at the top of the Pembroke Formation. Note the angular mylonite fragments as well as angular tectonic breccia fragments (arrows). Section 2.* ***B****) Close-up view of cross-laminated, red siltstone filling a solution cavity in the breccia. Section 1.* ***C****) Cross-section view of part of a metre-sized interval of reddish graded and cross-stratified sandstone filling a cavity. Note the abrupt disappearance of calcite-filled fractures at the contact with the sandstone. Creek outcrop near Walton.* ***D****) Small cavity with isopachous gravitational calcite cement crust developed at the roof of the cavity. Fine- to coarse-grained limestones fragments fill the remaining pore space. Section 2.* ***E****) Calcite cements precipitated over geopetal and graded red siltstones. Section 2.*

breccia is currently unknown, however, regional tectonostratigraphic considerations suggest a Westphalian age (G. Lynch, pers. comm. 1993).

Meteoric breccia

A second type of breccia overlies the first one, the contact between the two is subtle and irregular at the outcrop scale (Fig. 3); it can only be ascertained by a close look at the nature of the matrix and from lithological nature of the clasts.

Bedding in the upper breccia is also undiscernible at the outcrop scale (Fig. 8A). The breccia is clast-supported and composed of centimetre- to metre-sized, angular fragments (Fig. 8A). Two type of clasts are recognized; 1) mylonite and 2) tectonic breccia (Fig. 8A). Clasts are chaotically piled up with no compositional or granulometric sorting. The usual matrix of the breccia consists of millimetre-sized limestone fragments, at no places is there any annealing visible. Moreover, centimetre- to metre-sized pockets of cross-stratified and locally graded, reddish calcareous siltstones and fine-grained sandstones (Fig. 8B, C) are found in the breccia. Isopachous calcite cement crusts sometimes line cavity walls, they either precede or postdate internal sediments (Fig. 8D, E). These locally gravitational cement crusts (Fig. 8D), are associated with either the siliciclastic reddish infill (Fig. 8E) or the usual fine grained brecciated matrix (Fig. 8D).

The presence of tectonic breccia fragments suggests a different and most likely late origin for the second breccia type. The abundant boulder sized fragments are hardly compatible with a storm deposit origin for the lithofacies. On the other hand, no significant evaporite intervals were seen within the Macumber-Pembroke interval studied. Therefore, the collapse breccia of evaporite solution origin seems unlikely, at least for the described sections. The most likely origin for the upper Pembroke breccia for the Antigonish and Cheverie sections is a collapse breccia of karstic origin. This scenario is based on the mixing of mylonite and tectonic breccia fragments, the pockets of cross-laminated and graded reddish siliciclastic sediments of interpreted continental origin and the gravitational calcite cement crusts likely of meteoric vadose origin. The age of this subaerial exposure is likely Westphalian or younger.

The collapse karstic interpretation for the Pembroke Breccia is reported in the literature (Clifton, 1967; Geldsetzer, 1977), however, this interpretation was put forward for the entire brecciated interval of this unit. Our study shows that karstic collapse of the basal Windsor carbonates indeed occurred, however, this event postdated a first brecciation event of relatively deeper tectonic origin.

CONCLUSIONS

The paleoenvironmental significance of the Macumber Formation has been, over the years, the subject of controversy. It has been interpreted as microbial-controlled biosedimentation either in lacustrine or shallow to deep marine settings. Recent field surveys for that part of the basal Windsor carbonates, however, suggest that the typical planar fabric of the Macumber (the "laminites" and "stromatolites" of previous workers) is, as suggested by Lynch and Giles (1993), best interpreted as a tectonic mylonite and detachment fault. The lowermost 2 m of the Macumber Formation were not overprinted by the tectonic fabric; lithofacies, faunal and sedimentary structures suggest a below storm wave base and likely anoxic setting for the onset of Carboniferous carbonate sedimentation in Magdalen Basin.

The Pembroke Formation is also enigmatic in its precise lithostratigraphic framework and paleoenvironmental significance. The Pembroke Formation, as currently understood (the first non laminated interval overlying the Macumber platy facies), is interbedded and laterally equivalent with the Macumber mylonite. A collapse karstic origin for the Pembroke Formation is documented for the upper part of the two studied sections of the Pembroke. However, a significant part of the Pembroke breccia is not related to subaerial exposure; the lower part of the breccia is a tectonic breccia formed in relatively deep structural settings. Moreover, the strong annealing observed in field outcrops could well account for the lack of breccias over the Macumber Formation in drill cores. This last hypothesis, however, will have to be supported by comparative petrographic examination of representative samples.

Together, the Macumber mylonite and Pembroke breccia are used to define the position of the Ainslie Detachment in Magdalen Basin (Lynch and Giles, 1993). This report supports the tectonic scenario for the platy facies of the Macumber and for part of the brecciated facies of the Pembroke. However, the use of the Pembroke breccia to ascertain structural settings should be taken with great care as a significant part of that breccia is related to late subaerial exposure (Westphalian or younger).

ACKNOWLEDGMENTS

Discussions with R. Boehner, R. Moore, D. Sangster and D. Kontak were much appreciated during a 1993 field trip. In particular, the vast experience of P. Giles helped a lot for the sometimes fairly local lithostratigraphy of the Windsor Group as well as for showing the locally "tough to get" best sections of the Windsor in Nova Scotia. Finally, G. Lynch was instrumental in the tectonic interpretation of the Macumber Formation, his critical reading of that manuscript is also much appreciated.

REFERENCES

Boehner, R.C., Giles, P.S., Murray, D.A., and Ryan, R.J.
1989: Carbonate buildups of the Gays River Formation, Lower Carboniferous Windsor Group, Nova Scotia; in Reefs, Canada and adjacent areas, (ed.) H.H.J. Geldsetzer, N.P. James and G.E. Tebbut; Canadian Society of Petroleum Geologists, Memoir 13, p. 609-621.

Clifton, H.E.
1967: Solution-collapse and cavity filling in the Windsor Group, Nova-Scotia, Canada; Bulletin of the Geological Society of America, v. 78, p. 819-832.

Geldsetzer, H.H.J.
1977: The Windsor Group of Cape Breton Island, Nova Scotia; in Report of Activities, Part A; Geological Survey of Canada, Paper 77-1A, p. 425-428.
1978: The Windsor Group in Atlantic Canada – an update; in Current Research, Part C; Geological Survey of Canada, Paper 78-1C, p. 43-48.

Giles, P.S.
1981: Major transgressive-regressive cycles in Middle to Late Visean rocks of Nova Scotia; Nova Scotia Department of Mines and Energy, Paper 81-2.

Giles, P.S., Boehner, R.C., and Ryan, R.J.
1979: Carbonate banks of the Gays River Formation in central Nova Scotia; Nova Scotia Department of Mines and Energy, Paper 78-7.

Hamblin, A.P. and Rust, B.R.
1989: Tectono-sedimentary analysis of alternate-polarity half-graben basin-fill successions: Late Devonian-Early Devonian Carboniferous Horton Group, Cape Breton Island, Nova Scotia; Basin Research, v. 2, p. 239-255.

Hein, F.J., Graves, M.C., and Ruffman, A.
1993: The Jubilee Zn-Pb deposit, Nova Scotia: the role of synsedimentary faults; in Mineral Deposit Studies in Nova Scotia, Volume 2, (ed.) A.L. Sangster; Geological Survey of Canada, Paper 91-9, p. 49-69.

Howie, R.D. and Barss, M.S.
1975: Upper Paleozoic rocks of the Atlantic provinces, Gulf of St. Lawrence, and adjacent continental shelf; in Offshore Geology of Eastern Canada, Volume 2; Geological Survey of Canada, Paper 74-30, p. 35-50.

Kirkham, R.V.
1978: Base metal and uranium distribution along the Windsor-Horton contact central Cape Breton Island, Nova Scotia; in Current Research, Part B; Geological Survey of Canada, Paper 78-1B, p. 121-135.

Lynch, G. and Giles, P.S.
1993: Extensional tectonics and evolution of the Upper Devonian-Carboniferous Maritimes Basin, Nova Scotia; Geological Association of Canada – Mineralogical Association of Canada, 1993 joint annual meeting, Edmonton, Program with abstracts, p. A-62.

Sage, N.M.
1954: The stratigraphy of the Windsor Group in the Antigonish quadrangles and Mahone Bay-St. Margarets Bay area, Nova Scotia; Nova Scotia Department of Mines, Memoir 3.

Schenk, P.E.
1967: The Macumber Formation of the Maritimes Provinces – a Mississippian analogue to Recent strand-line carbonates of the Persian Gulf; Journal of Sedimentary Petrology, v. 37, p. 365-376.
1969: Carbonate-sulfate-redbed facies and cyclic sedimentation of the Windsorian stage (Middle Carboniferous), Maritimes Provinces; Canadian Journal of Earth Sciences, v. 6, p. 1037-1066.

Schenk, P.E., von Bitter, P.H., and Matsumoto, R.
1992: A lacustrine origin for the Basal Windsor/Codroy Groups (Carboniferous) of Atlantic Canada – Introducing Loch Macumber!; Geological Association of Canada – Mineralogical Association of Canada, 1992 joint annual meeting, Wolfville, Program with abstracts, p. A-99.

Smith, L. and Collins, J.A.
1979: Unconformities, sedimentary copper mineralization, and thrust faulting in the Horton and Windsor groups, Cape Breton Island and central Nova Scotia; Neuvième Congrès International de stratigraphie et de Géologie du Carbonifère, Washington and Champaign-Urbana, v. 3, Southern Illinois University Press, p. 105-116.

Stacey, M.C.
1953: Stratigraphy and paleontology of the Windsor Group (Upper Mississippian) in parts of Cape Breton Island, Nova Scotia; Nova Scotia Department of Mines, Memoir 2.

Weeks, L.J.
1948: Londonderry and Bass River map-areas, Colchester and Hants Counties, Nova Scotia; Geological Survey of Canada, Memoir 245.

Geological Survey of Canada Project 920001

Stratigraphic omission across the Ainslie Detachment in east-central Nova Scotia[1]

Peter S. Giles and G. Lynch[2]
Atlantic Geoscience Centre, Dartmouth

Giles, P.S., and Lynch, G., 1994: Stratigraphic omission across the Ainslie Detachment in east-central Nova Scotia; in Current Research 1994-D; Geological Survey of Canada, p. 89-94.

Abstract: In parts of central and eastern Nova Scotia, the mapped distribution of the Viséan-Namurian Mabou Group suggests that it lies disconformably or unconformably on the Middle Viséan Macumber Formation (basal Windsor Group). Up to 1500 m of Windsor strata would be locally truncated by this unconformity, which is nowhere exposed at surface. Alternatively, we have previously proposed that major stratigraphic omission of this type, in concert with widespread indications of significant strain in the upper parts of the Macumber Formation, provides strong evidence for a regional detachment surface at or near the top of the Macumber. Near the Strait of Canso, calcareous mylonites occur in a 12 m thick interval between gently dipping Mabou shales and Macumber limestone. This bedding-parallel tectonite indicates that these rock units have been structurally superimposed with coincident stratigraphic omission, providing strong support for our detachment model.

Résumé : La répartition sur carte du Groupe de Mabou du Viséen-Namurien dans certaines parties du centre et de l'est de la Nouvelle-Écosse indique que le Groupe repose en disconformité ou en discordance sur la Formation de Macumber (base du Groupe de Windsor) du Viséen moyen. Jusqu'à 1 500 m de strates du Groupe de Windsor seraient par endroits disparus au-dessus de cette discordance qui n'est nulle part exposée en surface. Par ailleurs, nous avons déjà proposé qu'une absence de strates de ce type d'une telle importance, ajoutée à de nombreuses indications de forte déformation dans les parties supérieures de la Formation de Macumber, constitue une preuve solide de la présence d'une surface de décollement régionale au sommet de la Formation de Macumber ou à proximité. Près du détroit de Canso, il y a des mylonites calcareuses dans un intervalle de 12 m d'épaisseur entre les shales faiblement inclinés de Mabou et le calcaire de Macumber. Cette tectonite parallèle à la stratification indique que ces unités lithologiques ont été superposées structuralement et qu'en conséquence un intervalle stratigraphique a été supprimé, ce qui corrobore notre modèle de décollement.

[1] Contribution to Canada-Nova Scotia Cooperation Agreement on Mineral Development (1992-1995), a subsidiary agreement under the Canada-Nova Scotia Economic and Regional Development Agreement.
[2] Quebec Geoscience Centre, Sainte-Foy

INTRODUCTION

The recognition of major bedding-parallel detachment faults is often hampered by apparent stratigraphic regularity. If such a fault follows a so-called "flat", it may reside totally within one stratigraphic unit over large distances and may be expressed mainly by its strain signatures. No obvious omission of strata may be detected. On the other hand, where such a fault ramps, significant omission of strata will result, and large gaps in the stratigraphic record will accompany the strain features typical of the fault zone. Translation on these large faults, regionally sub-parallel to bedding, results in juxtaposition of parallel beds of quite distinct age across significant stratigraphic gaps.

In central and eastern Nova Scotia, fine grained sandstones, siltstones and shales of the lowermost Mabou Group are transitional and conformable with uppermost Windsor beds (Belt, 1965, p.791). In the same area, basal Mabou strata locally seem to lie unconformably on lowermost Windsor limestone (Norman, 1935; Kelley, 1967). Exposures of this supposed unconformity are not known, a factor commonly attributed to the recessive character of the shaley Mabou Group. Commonly, both conformable and unconformable relationships are implied by map patterns within one small structural basin. As much as 1500 m of Windsor strata are apparently truncated by this unconformity.

Belt (1965) noted that where the basal Mabou Group rested on the so-called "Ribbon limestone" at the base of the Windsor, that severe deformation and slivers of evaporites characterized the contact zone, clearly implying these contacts to be tectonic. This paper highlights a key locality, 6 km northwest of the Canso Causeway in the Aulds Cove area of eastern Nova Scotia (Fig. 1), where the supposed unconformity between the Mabou Group and the basal Windsor Macumber Formation is clearly a fault. We believe this fault to be the local expression of a regional detachment fault which we term the Ainslie Detachment (Lynch and Giles, 1993).

THE AULDS COVE SECTION

Carboniferous strata assigned to the Horton, Windsor and Mabou groups outcrop on the western side of the Strait of Canso, between the Canso Causeway and St. Georges Bay northwest of the village of Aulds Cove. Overlying mainly granitoid rocks of the pre-Carboniferous crystalline basement, the Horton comprises mostly fluviatile rocks, dominated by conglomeratic facies in the lower parts and becoming finer grained with shales and grey-green micaceous sandstones towards the top (northwesterly along the shore). Several rather large concealed intervals occur within the Horton succession, and the total thickness cannot be reliably determined at this locality. The youngest Horton Group strata in Nova Scotia fall within TN3 in the European classification (Utting et al., 1989). We presume that the succession at Aulds Cove is not younger than TN3 (Late Tournaisian).

The Windsor Group is represented by a single formation, the Macumber, characterized by laminated peloidal limestone, grey and greenish grey in colour. The thickness of the Macumber at this locality is estimated at 12-15 m. The Macumber is separated from underlying Horton Group sandstone by less than 1 m of concealed interval (true thickness). Beds of the Macumber limestone are essentially concordant with underlying Horton Group sandstones. A hiatus representing the Early Viséan appears to everywhere separate the Macumber from the underlying Horton Group (Utting et al., 1989).

The Mabou Group in the Aulds Cove section is dominated in its lower parts by grey shales and siltstones of the Hastings Formation of Belt (1965). Buff and grey banding at a scale of centimetres is common in parts of the formation which totals approximately 550 m in thickness. The buff-weathering bands are carbonate-rich and are typical regionally of the lower parts of the Mabou Group. Associated strata include several thin (<5 cm) stromatolitic limestones. Sedimentary structures include ripple marks (uncommon) and desiccation cracks. Small-scale cross-lamination is common. The Hastings Formation in the Aulds Cove section has not been dated palynologically. A correlative section 7.3 km to the west at Cape Jack (Fig. 1), similarly compressed with lower Mabou Group resting on Macumber Formation, contains *Schulzospora* sp (Barss, 1979). Utting (1987) considered *Schulzospora* to be a guide to his *Grandispora spinosa – Ibrahimispores magnificus* (SM) miospore zone, which he considered to be late Viséan in age.

At the top of the grey Hastings Formation, red, fine grained sandstones and red shales of the Pomquet Formation of Belt (1965) are in conformable and transitional contact. Sandstone is subordinate to red shale. The fine grained overall nature of the Pomquet is typical of the Mabou Group.

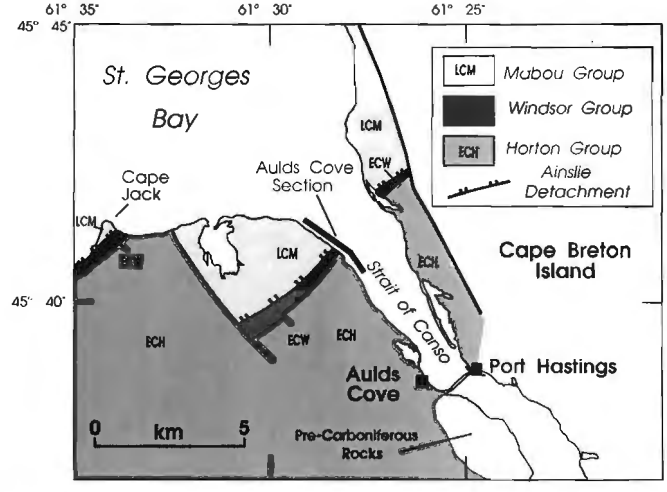

Figure 1. Geological map of the Strait of Canso area, showing the location of the Aulds Cove section (geology after Ferguson and Weeks, 1950, and Benson , 1970).

Rocks of the Pomquet Formation, in addition to their predominantly red colour, are typified by ubiquitous ripple marks. These are most commonly seen as climbing ripples in fine grained sandstone, but also as linear varieties in siltstone and silty shale. Interference patterns are common.

Small-scale tectonic deformation features are ubiquitous in both the Macumber and Hastings formations in the Aulds Cove section. In the Macumber Formation, fold axes trending 030°-047° and plunging 6°-13° predominate (Fig. 2A). Folds in this orientation are typically disharmonic box folds, and are characteristically tight in synclines and more open in anticlines. Other small folds related to westerly trending fractures (see below) trend at 276° and plunge at approximately 20°.

Folds in the Hastings Formation consistently trend between 301°-336° and plunge gently at 12°-22°. Fold axes plunge northeasterly, and almost all of the folds are s-shaped in section (Fig. 2C). In some instances, folds are more complex, with opposing vergences and box-fold geometries (Fig. 2B). These folds appear to accommodate space problems in the inner hinge zone of larger enveloping folds. Overall, folds in the Hastings Formation at the Auld Cove section bear remarkable similarity to fold styles exhibited regionally in the Macumber Formation.

Steep north-dipping faults cut both the Horton and Windsor groups in their contact zone. Offsets on these steep faults are demonstrably small, generally <15 cm, exceptionally reaching a few metres. They typically pass along their length into small flexures (Fig. 3A). Slickensides demonstrate primarily dip-slip movement on the fractures, and axial planes of contiguous flexures dip consistently to the north. Fold geometry in the flexures suggests that the steep faults are actually high-angle reverse faults with relative movement from north to south.

Near the northerly limits of exposed Hastings Formation, a pair of low-angle faults cut the Hastings. Small folds in the immediate hanging wall of the upper of these shears trend 028° and plunge at 22°. Their axial planes dip easterly at moderate angles, with asymmetry suggesting tops to the west sense of shear. The fault geometry suggests that the faults are thrusts.

Bedding-parallel fibrous calcite veins occur sporadically throughout the Hastings Formation and are folded with the bedding; fibre orientation in the veins is sub-perpendicular to bedding. Steeply dipping tension-gash arrays filled with coarsely crystalline calcite are more typical of the Macumber Formation. Thin calcite veins, steeply dipping and oriented northwesterly, cut both the Horton and Windsor groups, but are far less common in the Mabou Group.

Overall, the section dips consistently north-northwesterly at between 20° and 25°, through nearly 3 km of shoreline exposure crossing the Horton-Windsor-Mabou contact intervals. With the notable exception of rocks exposed in the Windsor-Mabou contact zone, which are described below, the section appears only moderately affected by regional deformation.

THE WINDSOR-MABOU CONTACT ZONE

A 12 m thick bedding-parallel shear zone separates typical Macumber limestone from typical Mabou shales. This shear zone along the Windsor-Mabou contact is represented by intermittent exposures of limestone over almost 50 m of beach and wave-cut bank. In the bank, the rock is buff to reddish buff, friable as if deeply weathered, contains 1-3 cm fragments of dark greenish-grey laminated limestone apparently derived from the underlying Macumber Formation. In the beach, the rock is better indurated and is in part swept bare low in the intertidal zone. It is in these exposures that the tectonic signatures imprinted on this rock are most evident.

Foliation is the most conspicuous macroscopic feature of this buff to pinkish-buff limestone. The foliation is defined by fine grained recrystallized carbonate layers, more coarsely crystalline white calcite layers, and surfaces marked by higher relative concentrations of mica (secondary) and quartz silt. Shear attenuation of fold limbs is typical. Recumbent mesoscopic folds with sub-horizontal axial planes and sheath folds at both microscopic and mesoscopic scales (Fig. 3B) are present. Foliated blocks of dark grey Macumber-like limestone are dispersed within the laminated host. The buff limestone lacks the calcite veining so typical of the Macumber, and does not exhibit the systematic macroscopic fold patterns of either the Macumber or the overlying Mabou Group at the Aulds Cove section.

In hand specimen, low-angle shear bands cut the lamination. Offset calcite veinlets demonstrate normal or dip-slip movement on these small shears. Asymmetric intrafolial folds show consistent down-to-the-southwest shear. These small-scale structures mimic fold style and fault geometry observed at outcrop scale near the top of the Macumber Formation throughout western Cape Breton Island.

Microscopically, this limestone is clearly foliated, not bedded. "Laminae" truncate small-scale folds and attenuate fold limbs. Irregular masses of white calcite are common, stretched along the foliation. Mineralogically, the tectonite comprises calcite with minor associated silt-sized quartz and occasional biotite and white-mica grains. The rock is finely porous, so much so that it may fail to react to a field acid test when wet, yet gives a strong reaction when dried.

DISCUSSION

The strain features, which characterize the foliated limestone marking the Windsor-Mabou contact zone at Aulds Cove, identify this rock as a tectonite (perhaps best termed a calc-mylonite), the maximum thickness of which approaches 12 m. The protolith is unknown, but is most probably Macumber Formation limestone. The "mylonite" is compelling evidence for a fault at this location in the stratigraphic column, and clearly refutes the unconformity model postulated by earlier mappers – anhydrite above and thinly bedded limestone below.

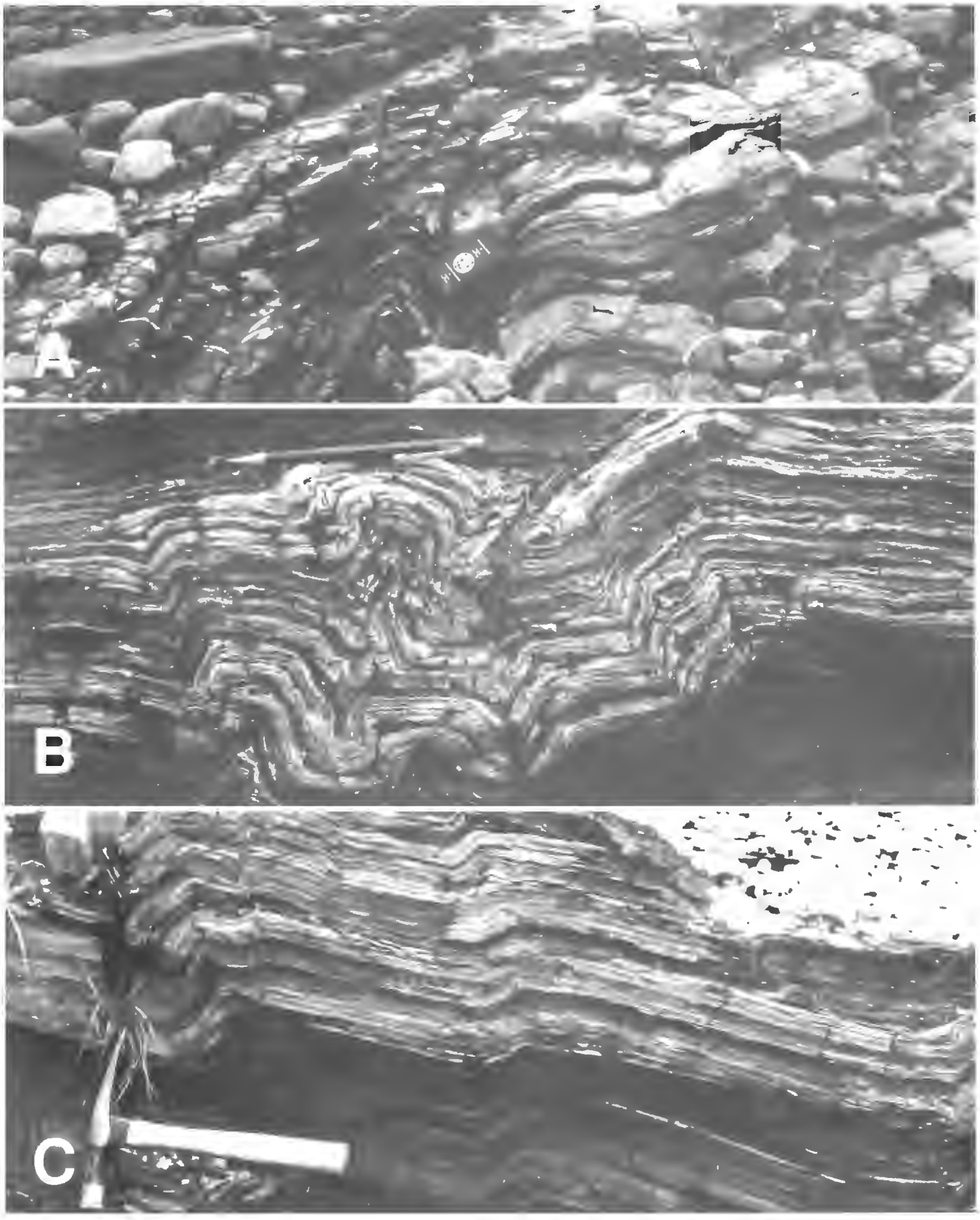

Figure 2. *Structural features of the Macumber and Hastings Formations;* ***A)*** *northerly trending folds in the Macumber Formation; note steep calcite veins cutting the fold limbs:* ***B)*** *box folds, Hastings Formation; note that the shear sense can be compared with that in C; pencil indicates scale:* ***C)*** *southwesterly verging kink folds in the Hastings Formation.*

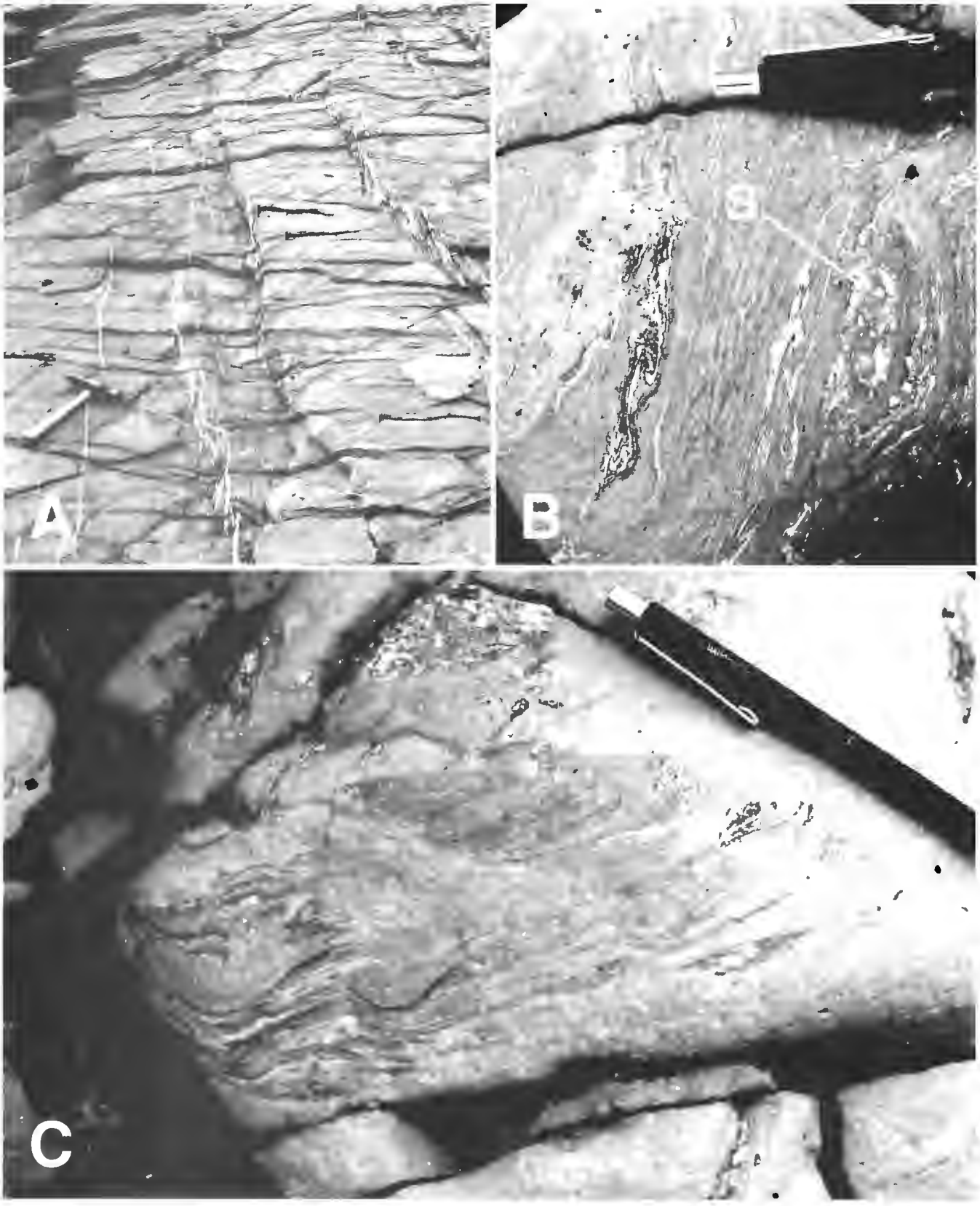

Figure 3. ***A****) westerly trending fractures passing into flexures, Macumber Formation bedding surface at Aulds Cove. B and C: Calc-mylonite separating the Hastings and Macumber Formations at Aulds Cove, Strait of Canso:* ***B****) convolute foliation and sheath folds (S) in the calc-mylonite:* ***C****) "gneissic" foliation in the Aulds Cove calc-mylonite.*

On a regional basis, the Macumber passes upwards in normal stratigraphic succession into 150-400 m of relatively pure anhydrite. The top of the Macumber is therefore normally a horizon of marked lithological discontinuity. The focus of significant strain at this level during regional tectonism is therefore predictable, and rationalizes the failure of the supposed "unconformity" to cut through the Macumber Formation to juxtapose Mabou Group on Horton Group strata. Erosion at the top of the Macumber Formation should indeed allow the latter relationship which has never been documented.

The orientation of the tectonic fabric and gently dipping axial planes of folds within the mylonite argue for a 'flat' fault sub-parallel to confining strata. This mylonite coincides with a gap in Viséan stratigraphy which includes almost the entire thickness of the Windsor Group which, in the Strait of Canso area, approaches 1500 m in thickness. Stratigraphic omission of this sort and scale, observed on a regional basis and contrasted with stratigraphic repetition predicted by thrust models, provides fundamental support for the interpretation of this fault surface as a gently dipping detachment (Lynch and Giles, 1993) developed in an extensional regime.

On a regional basis, similar strain features have been noted at the top of the Macumber Formation throughout much of eastern Nova Scotia and most of western Cape Breton Island. We have mapped the top of the Macumber Formation in western Cape Breton as the trace of a major extensional fault which we term the Ainslie Detachment (Lynch and Giles, 1993). The immediate hanging wall of the detachment may contain rocks ranging in stratigraphic position from lower Windsor to uppermost Windsor and Mabou Group. In some instances, reconstruction of detachment geometry suggests that associated fault splays may be responsible in part for the present distribution of rock units above the basal (Ainslie) detachment. In areas where stratigraphic gaps can clearly be documented in conjunction with significant deformation or strain, we believe that the detachment model best accounts for rapid and acute changes in the thickness of the basin fill.

CONCLUSIONS

A 12 m thick calc-mylonite marks the position of a major bedding-parallel fault which separates the basal Windsor from the Mabou Group at Aulds Cove. The omission of an estimated 1500 m of strata representing almost the entire Windsor Group across this fault provides strong evidence for an extensional fault model. Similar stratigraphic gaps and strain features at the same stratigraphic level regionally, are attributed to a major extensional fault (or fault system) which we term the Ainslie Detachment.

ACKNOWLEDGMENTS

D.J.W. Piper critically reviewed the manuscript and made suggestions for improvement, for which we are grateful. We also thank P.W. Durling and G. Grant for assistance in preparation of the illustrations.

REFERENCES

Barss, S.M.
1979: Palynological analysis of samples submitted for age determinations by P. Giles, Nova Scotia Department of Mines; Atlantic Geoscience Centre, Eastern Petroleum Geology Subdivision, Internal Report No. EPGS-PAL 83-79-MSB.

Belt, E.S.
1965: Stratigraphy and paleogeography of Mabou Group and related middle Carboniferous facies, Nova Scotia, Canada; Geological Society of America Bulletin, v. 76, p. 777-802

Benson, D.G.
1970: Geology Antigonish (east half), Nova Scotia; Geological Survey of Canada Preliminary Series, Map 2-1970, scale 1:50 000

Ferguson, S.A. and Weeks, L.J.
1950: Mulgrave map-area, Nova Scotia; Geological Survey of Canada, Map 995A; scale 1:63 360

Kelley, D.G.
1967: Baddeck and Wycocomagh map-areas; Geological Survey of Canada, Memoir 351; scale 1:63 360

Lynch, G. and Giles. P.S.
1993: Detachment Faulting in the Maritimes Basin (Upper Devonian-Carboniferous), Nova Scotia, Canada; Abstract; late orogenic extension in mountain belts; Montpellier. France, March 1993.

Norman, G.W.R.
1935: Lake Ainslie map-area, Nova Scotia; Geological Survey of Canada, Memoir 177, scale 1:63 360

Utting, J.
1987: Palynology of the Lower Carboniferous Windsor Group and Windsor-Canso boundary beds of Nova Scotia, and their equivalents in Quebec, New Brunswick and Newfoundland; Geological Survey of Canada, Bulletin 374

Utting, J., Keppie, J.D., and Giles, P.S.
1989: Palynology and stratigraphy of the Lower Carboniferous Horton Group, Nova Scotia; in Contributions to Canadian Paleontology; Geological Survey of Canada, Bulletin 396, p. 117-143

Geological Survey of Canada Project 920062

Geology of the eastern St. Mary's Basin, central mainland Nova Scotia[1]

J. Brendan Murphy[2], Timothy R. Stokes[2], Cashel Meagher[2], and Sarah-Jane Mosher[2]

Continental Geoscience Division

Murphy, J.B., Stokes, T.R., Meagher, C., and Mosher, S-J., 1994: Geology of the eastern St. Mary's Basin, central mainland Nova Scotia; in Current Research 1994-D; Geological Survey of Canada, p. 95-102.

Abstract: The eastern St. Mary's Basin, Nova Scotia, contains a Late Paleozoic intra-continental basin-fill that occupies the boundary between the Meguma and Avalon Composite terranes. These sedimentary rocks are traditionally assigned to the Horton Group. In general, the sequence faces southeast, coarsens upward, and thickens toward the basin's southeastern margin. Clasts were predominantly derived from the Meguma Terrane, and a sedimentological linkage with the Avalon Composite Terrane cannot be demonstrated. The sequence unconformably overlies units of the Meguma Terrane and is probably underlain by Meguma basement.

A strong tectonic influence on sedimentation is apparent along the southern flank of the basin with deposition of coarse conglomerates accompanying basin subsidence along northerly dipping listric normal faults. In contrast, the present northern margin (Chedabucto Fault) does not constitute the original basement margin, implying that an unknown portion of the basin and its Meguma basement lying north of this fault may have been tectonically removed.

Résumé : La partie est du bassin de St. Mary's en Nouvelle-Écosse contient des sédiments de remplissage de bassin intracontinental, datés du Paléozoïque tardif, qui occupent la limite entre le terrane de Meguma et le terrane composite d'Avalon. Ces roches sédimentaires ont été traditionnellement attribuées au Groupe de Horton. En général, la séquence est orientée face au sud-est, est négative, et s'épaissit vers la marge sud-est du bassin. Les clastes provenaient surtout du terrane de Meguma, et l'on ne peut prouver l'existence d'un lien sédimentologique avec le terrane composite d'Avalon. La séquence surmonte en discordance des unités du terrane de Meguma, et elle est probablement sus-jacente au socle de Meguma.

Une forte influence tectonique sur la sédimentation est apparente sur le flanc sud du bassin, le dépôt de conglomérats grossiers ayant accompagné la subsidence du bassin le long de failles listriques normales de pendage nord. Par contre, la marge nord actuelle (faille de Chedabucto) ne constitue pas la marge initiale du socle; donc une portion inconnue du bassin et de son socle de Meguma, située au nord de cette faille, a peut-être été enlevée par des processus tectoniques.

[1] Contribution to Canada-Nova Scotia Cooperation Agreement on Mineral Development (1992-1995), a subsidiary agreement under the Canada-Nova Scotia Economic and Regional Development Agreement.

[2] Department of Geology, St. Francis Xavier University, Antigonish, Nova Scotia B2G 1CO

INTRODUCTION

The St. Mary's Basin of central mainland Nova Scotia lies on the southern flank of the Late Paleozoic Maritimes Basin (Fig. 1). This larger basin comprises several intra-continental depocentres that are generally thought to have developed either during waning stages of the Acadian orogeny (e.g., Keppie, 1982) or as post-Acadian successor basins (e.g., Williams, 1978). The St. Mary's Basin averages 15 km in width and extends for about 130 km, from Chedabucto Bay in the east to the Bay of Fundy in the west. Basin-fill sediments have been traditionally assigned to the Late Devonian- Early Carboniferous Horton Group, and occupy the boundary between two terranes: the Avalon Composite Terrane of northern mainland Nova Scotia dominated by Late Precambrian volcanic and sedimentary rocks, and the Meguma Terrane of the southern mainland dominated by Cambrian and Ordovician metasedimentary rocks intruded by Devonian granitoid plutons.

PURPOSE AND OBJECTIVES

The study of the St. Mary's Basin forms part of the 1993-96 Canada-Nova Scotia Mineral Development Agreement and involves geological mapping and data collection of the area bounded by longitudes 61°30′W and 63°10′W and by latitudes 45°24′N and 45°15′N. The main objectives of the three-year project are to: (i) describe and map the bedrock geology of the St. Mary's sedimentary basin at a scale suitable for publication at 1:50 000, (ii) determine the geological history of the area, (iii) assess the link between the geology and known mineral occurrences in order to identify criteria that may aid mineral exploration, and (iv) investigate the relationship of the basin to the adjoining Avalon Composite and Meguma Terranes.

The relationship between the development and deformation of the basin is of first order importance for resolving the geological evolution of the area. Geophysical and geochemical anomalies suggest a more complicated geology than that indicated by the available geological maps, including the presence of igneous complexes which may yield information on the basin's tectonic setting.

PREVIOUS WORK

Successive Mineral Development Agreements have focused on the geology and the mineral potential of the rocks of the Meguma and Avalon terranes. However, the St. Mary's Basin has not been studied in detail since the 1960s. Fletcher and Faribault (1887) prepared the first geological maps of the area as part of a regional survey of northeastern mainland Nova Scotia. Schiller (1961, 1963) mapped the easternmost portion of the basin (parts of map sheets 11F/05 and 11F/04) at a scale of 1:63 360, as part of a study of the geology of Guysborough County. Benson (1967, 1974) mapped the majority of the basin (parts of map sheets 11E/07 and 11E/08) at scales of 1:63 360 and 1:50 000. He assigned all basin-fill sediments to the Horton Group which he considered to be Lower Carboniferous (Tournaisean) in age on the basis of paleontological evidence. He further divided the group into the Craignish, Strathlorne, and Ainslie formations on the basis of lithological and stratigraphic similarities with the type areas of these formations in Cape Breton Island as

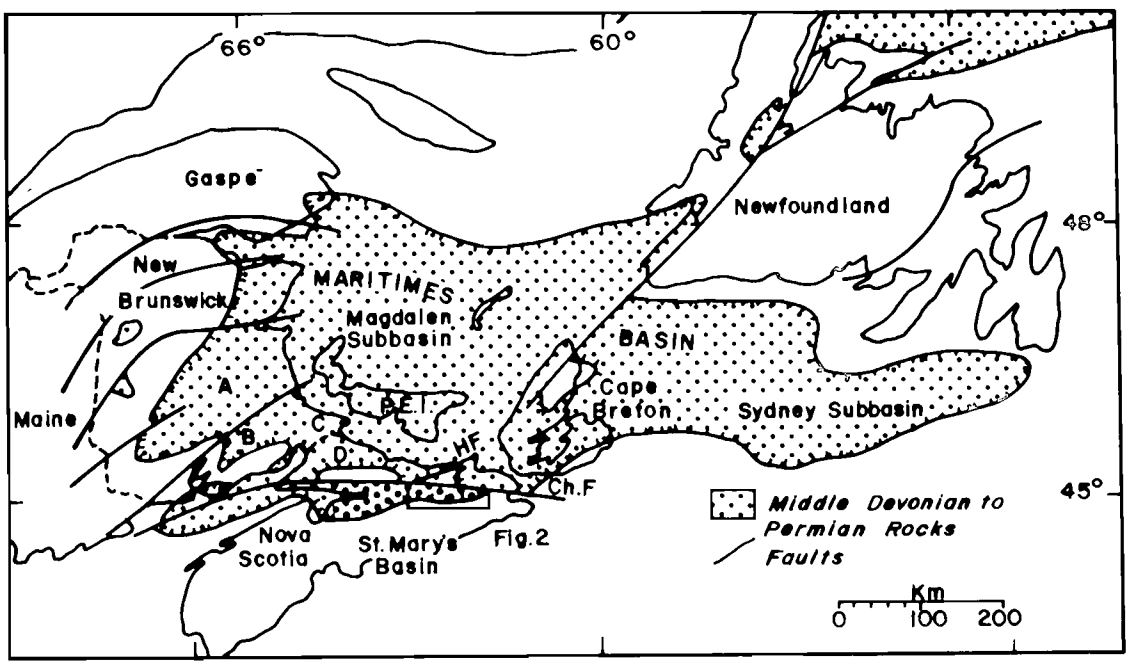

Figure 1. Location of St. Mary's Basin within the Maritimes Basin (Williams, 1978) of the Canadian Appalachians. HF-Hollow Fault, Ch.F-Chedabucto Fault. Diagram modified after Martel (1987).

described by Murray (1960) and Kelley (1967). According to Benson (1974), the St. Mary's Basin developed as a post-depositional graben as a result of left-lateral strike-slip and minor dip-slip on the Chedabucto Fault. Hill (1991) mapped the easternmost portion of the basin as part of a study which focused on the evolution of peraluminous granitoid rocks in the eastern Meguma Terrane. He assigned the rocks within this portion of the basin to the Gunns Brook Formation which he interpreted to be broadly correlative with part of the Horton Group.

TERMINOLOGY

The study area has generally been referred to as the St. Mary's Graben despite the fact that previous workers (e.g., Benson, 1974) interpreted the presence of a graben structure only in a restricted portion of the eastern basin separating the (Avalonian) Antigonish Highlands from the Meguma Terrane. Use of the genetic term "graben" has also been misleading since it is usually unclear whether the term is being used in reference to Late Paleozoic deposition in a fault-controlled basin, or to an extension of the Mesozoic Bay of Fundy rift system in which the Late Paleozoic sediments were preserved in a down-faulted block. We therefore prefer a nongenetic term and will refer to the study area as the St. Mary's Basin.

At present, we are uncertain whether the stratigraphic correlations made by Benson (1967, 1974) with the Horton Group in Cape Breton Island are appropriate. As outlined below, the study area is dominated by clastic rocks derived locally from the Meguma Terrane such that correlations with Cape Breton Island may give a misleading impression of stratigraphic and tectonic simplicity in units mapped as Horton Group. We are also reluctant to make correlations with the Horton Group type area until the results of palynological studies become available and we obtain better control on the depositional age of the basin-fill. At present, we prefer not to use formation names but, rather, number the units 1 to 5 in stratigraphic order.

CURRENT WORK

During the summer of 1993, the eastern St. Mary's basin was mapped between latitudes 45°24′N and 45°15′N and longitudes 61°30′W and 62°17′W (Fig. 2), and sampled for paleontological, petrographic, and geochemical studies and for radiometric dating. Palynological samples are currently being examined by Drs. Graham Dolby and John Utting of I.S.P.G., Calgary.

Five mappable units have been defined. On a regional scale, the sequence faces from northwest to southeast. However, the intensity of deformation varies markedly throughout the area and local facing reversals may occur near the hinges of folds. Relatively intense deformation affects the northern flank of the basin, with the production of small-scale isoclinal folds and locally developed mylonitic fabrics. In central portions of the basin, the rocks are deformed into broad folds with steep axial planes and subhorizontal fold axes. Along the southern flank of the basin, the rocks are only moderately tilted.

STRATIGRAPHY

The basin-fill is here divided into five mappable units (Fig. 2; Table 1). Contacts between these units are conformable and gradational with interlayering of the characteristic lithologies of adjacent units. This, together with the paleontological data of Benson (1974), suggests that the units are broadly coeval, and may be related by facies variations.

Unit 1 occurs only in the northwestern part of the map area where it consists of interbedded grey to dark grey fissile shale, siltstone, and sandstone. Individual beds range in thickness from about 2 mm to 5 mm. Bedding is generally convoluted and discontinuous and may be locally transposed into cleavage planes. Mylonitic fabrics are also developed locally. Contacts with adjacent units are not exposed in the map area, and its thickness is unknown. However, reconnaissance mapping in the western portion of the basin shows that it may be at least 1000 m in thickness and that it conformably underlies unit 2. It therefore represents the stratigraphically lowest unit of the map area. This interpretation contrasts with that of Benson (1974) who assigned the rocks of this unit to the Strathlorne Formation which he considered to overlie rocks of the central basin and to be stratigraphically equivalent to rocks of the southern basin.

Unit 2 is subdivided into units 2a and 2b. Unit 2a varies in thickness from 500 m in the east to 1000 m in the west and outcrops along a broad, regional, northeast-trending anticlinal axis. It is best exposed in the central basin along logging roads adjacent to Highway 348 (Fig. 2) and at the northern margin of the basin on East River St. Mary's. Unit 2a consists of subarkose to quartz arenite, interlayered with minor shale and siltstone. The subarkose and quartz arenite are grey to buff, indurated, medium- to coarse-grained, and moderately sorted with subangular to subrounded grains (Fig. 3). Feldspars are generally intensely weathered to kaolin. Beds range from about 2 to 10 m in thickness and contain variably defined but relatively continuous centimetre-scale laminations. Ripple marks and trough crossbedding are most visible on weathered surfaces. Coarser grained sediments commonly contain steeply dipping en echelon quartz veins that strike northwest to north-northwest (Fig. 3) Contacts between coarse-and fine-grained beds are generally sharp but occasionally gradational. Siltstone and shale beds are fissile, and predominantly dark grey. Organic debris occurs locally and the beds range up to 2 m in thickness and contain 2 mm to 5 mm thick laminations. These finer grained beds weather recessively and, in road sections, are poorly exposed in comparison to the very resistant coarser sediments.

In the eastern St. Mary's Basin, unit 2a is laterally continuous with unit 2b. They are interpreted as facies equivalents because they are both conformably overlain by unit 3. Unit 2b is at least 500 m thick and is distinguished from unit 2a by the lack of indurated subarkose and quartz arenite. Unit 2b is dominated by grey to green, interbedded, medium grained, well-sorted sandstone and fine grained siltstone and shale. The sandstone occurs in beds up to 2 m in thickness and is characterized by well-developed planar

crossbedding. The siltstones and shales are very similar to those of unit 2a. Unit 2b is well exposed on river sections in the vicinity of Highway 7, west of Lochiel Lake (Fig. 2).

Unit 3 consists predominantly of green sandstone with (minor) interlayered moderately sorted conglomerate, siltstone, and shale (Fig. 4, 5). The unit is well exposed on river sections in the vicinity of Caledonia (Fig. 2) and thickens markedly from west to east where it may attain a thickness of 1000 m. The green sandstones vary markedly but range in thickness from 0.5 m to 2 m and are fine- to coarse-grained with a gritty appearance. Trough crossbeds of up to 1 m in width and ripple marks are characteristic and, at one locality, a 1 m thick, grey massive limestone bed is interlayered with the sandstone. The sandstone and conglomerate are characterized by a variety of clasts typical of the Meguma Terrane lithologies including pelitic schist, metagreywacke, slate, micaceous granite, vein quartz, and muscovite (Fig. 6). Other lithologies include carbonaceous shale, siltstone, sandstone, carbonate, and organic debris which may be locally derived from within the basin.

Table 1. Stratigraphy and description of mappable units in the eastern St. Mary's Basin.

LEGEND OF LITHOLOGIES	
QUATERNARY	
Pleistocene and Recent	
5	Sand and gravel
LATE DEVONIAN - EARLY CARBONIFEROUS	
Horton Group	
4	Green to grey boulder to pebble conglomerate, interlayered with lithic arenite
3	Green to grey lithic arenite, minor pebble conglomerate, siltstone, and shale
2	2a Light to medium grey, medium- to coarse-grained quartz arenite and subarkose with interlayered grey to dark grey siltstone and shale
	2b Grey to green, lithic to arkosic sandstone and shale
1	Medium- to fine-grained, grey to dark grey siltstone and shale, locally mylonitic

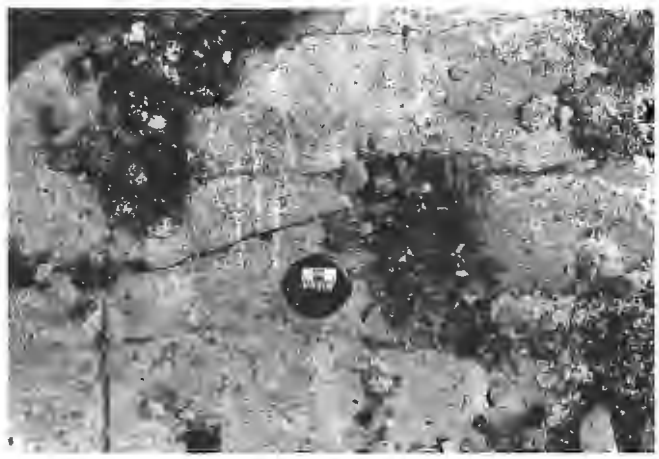

Figure 3. Indurated subarkose of unit 2a. Bedding strikes northeast, parallel to scale. Dilational quartz veins perpendicular to bedding are consistent with dextral shear.

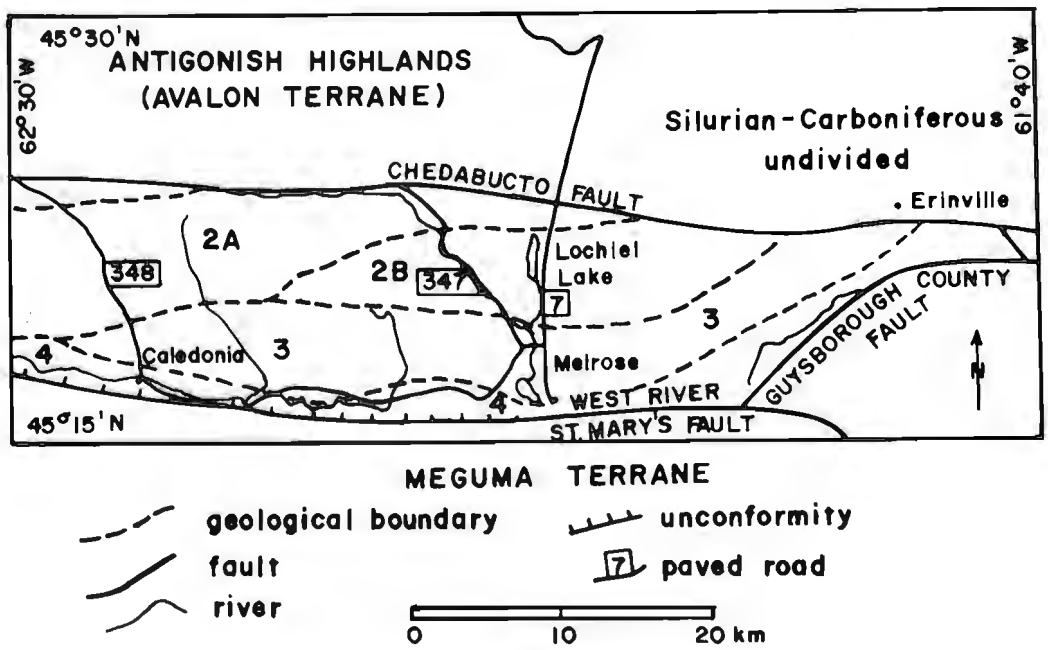

Figure 2. Summary of the geology of eastern St. Mary's Basin. See Table 1 for unit descriptions.

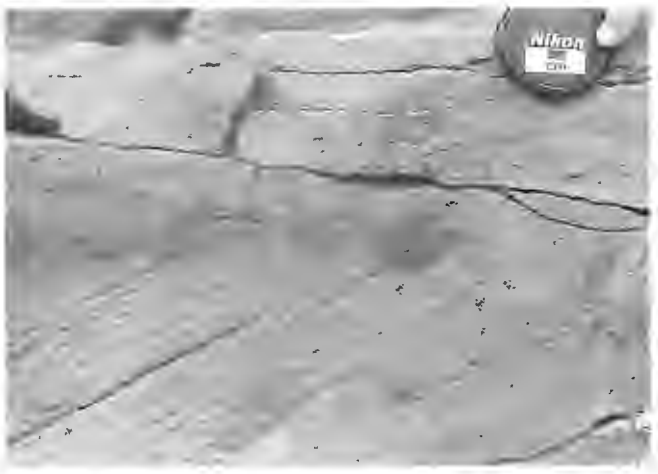

Figure 4. *Medium grained, moderately sorted sandstone of unit 3 displaying crossbedding.*

Figure 5. *Sandstones and moderately sorted conglomerates of unit 3a (upper left) offset by a steep southward dipping fault. Slickensides on fault surface support down to the south, normal movement.*

The contact of unit 3 with unit 2a is gradational over 500 m and, on the map, is positioned where indurated subarkose and quartz arenite become less abundant than green sandstone. The contact of unit 3 with unit 4 to the south is conformable and gradational, and is placed where poorly sorted conglomerates characteristic of unit 4 become more dominant than the sandstones of unit 3.

Unit 4 comprises very poorly sorted cobble to boulder conglomerates and interlayered sandstones (Fig. 7). Clast sizes generally range from less than 1 cm to 1 m. The unit extends along most of the southern margin of the map area (Fig. 2) and is well exposed along the banks of the West St. Mary's River, and along road and river sections in the Salmon Lake River area near the basin's southeastern margin (see Hill, 1991). The unit thickens markedly eastwards, ranging in thickness from about 100 m to 600 m. In the eastern portion

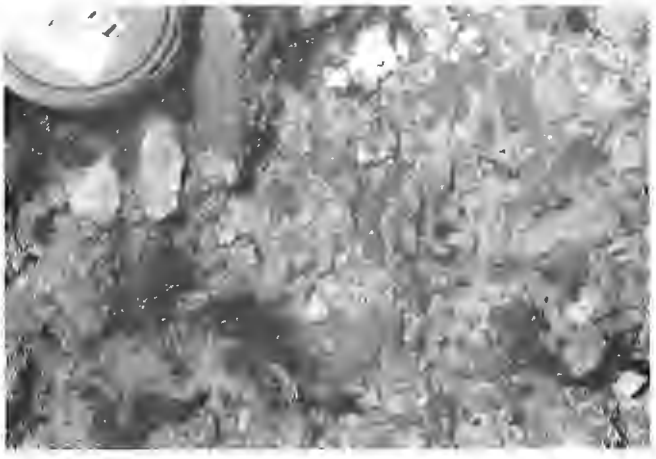

Figure 6. *Clasts in unit 3a conglomerates dominated by Meguma Terrane lithologies including greywacke (below lens cap), granite (top, centre), and pelitic schist (centre).*

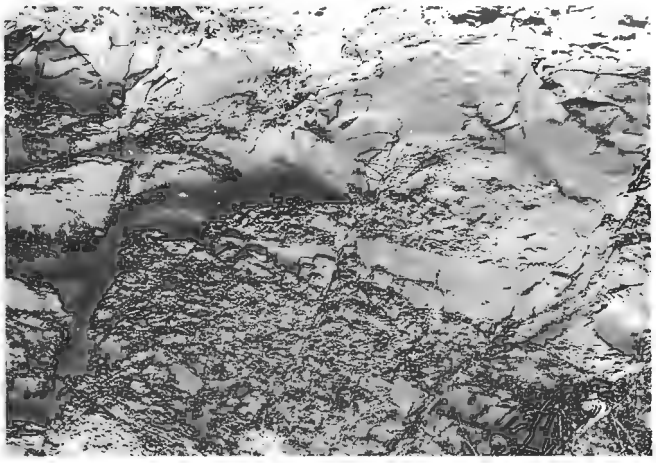

Figure 7. *Intertonguing between coarse cobble conglomerates and sandstones of unit 4. Steep, north-dipping fractures have limited normal offsets. Decrease in offset on individual fractures up stratigraphy suggests they may be broadly syndepositional.*

of the map area, the unit is in fault contact with rocks of the Meguma Terrane to the south, (along the West River St. Mary's and Guysborough faults, Fig. 2). However, in central and western portions of the area, the unit oversteps the West River St. Mary's Fault and rests with local angular unconformity on rocks of the Meguma Terrane (Fig. 2). The conglomerates locally vary in style from poorly sorted and matrix-supported to moderately sorted and clast-supported (Fig. 8). Normal and reverse graded bedding are common and clasts are typical of the Meguma Terrane (Fig. 9). The occurrence of these rocks along the southern margin of the St. Mary's Basin, and the obvious local derivation of the clasts, suggest that the these units are fanglomerates derived from Meguma basement. The sandstones are intertongued with the fanglomerates (Fig. 7) and are indistinguishable from those in unit 3.

Imbrication within the fanglomerate of unit 4 suggests a northward paleoflow direction. Hence, unit 3 may be a facies equivalent of unit 4. The upper contact of unit 4 is not exposed in the map area.

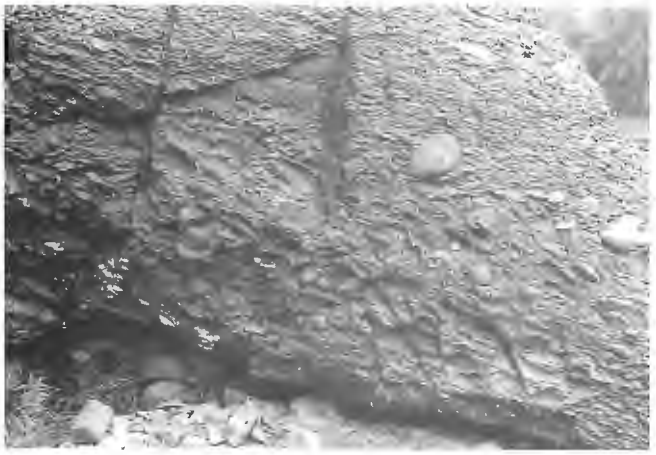

Figure 8. *Poorly sorted cobble conglomerate of unit 4. Clast lithologies are typical of the Meguma Terrane.*

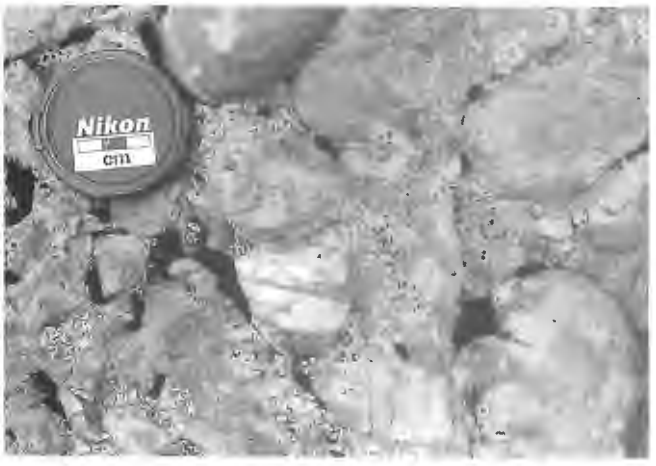

Figure 9. *Vein quartz clasts (centre) in coarse conglomerates of unit 4.*

ENVIRONMENT OF DEPOSITION

A detailed analysis of the depositional environments within the St. Mary's Basin awaits a comprehensive study of the sedimentology of each unit. However, the overall character of the clastic sedimentary rocks and the abundance of continental organic debris are consistent with the fluviatile to lacustrine environment characteristic of the Horton Group in mainland Nova Scotia. In general, the stratigraphy faces southeast, coarsens upwards, and thickens towards the southeastern margin of the basin. A strong tectonic influence on sedimentation along the southern flank of the basin is apparent in the poorly sorted conglomerates of unit 4, and the finer grained sandstones and conglomerates of unit 3. These units are interpreted to be locally derived from the adjacent Meguma Terrane to the south, and are considered to represent a northward-fining sequence associated with syndepositional tectonic instability along the southern basin margin. The two units likely represent facies variations within debris flow dominated fan deltas and may record the unroofing history of Meguma Terrane in their component clasts. The gentle dip of these units towards the fault is consistent with syndepositional subsidence along a northward dipping listric fault with a normal component of slip.

The finer grained, better sorted clastic rocks of units 2a and 2b may represent fluvial dominated fans associated with braided stream deposition and fine grained overbank facies. Clast lithologies are typical of the Meguma Terrane, but preliminary paleocurrent data and the improved sorting relative to units 3 and 4 suggest longitudinal flow along the axis of the basin. The predominance of quartz and feldspar clasts in unit 2a suggests a granitic source, although some of the coarse quartz clasts may represent vein material.

A preliminary evaluation of the environment of deposition of unit 1 awaits detailed analysis of exposures to the west of the map area. However, the character of these sediments, and those of unit 2a and 2b, do not vary with proximity to the Chedabucto Fault. Furthermore, the absence of clasts of Avalonian affinities implies that the proximity of the eastern St. Mary's Basin to the Avalon Terrane remains to be demonstrated and points out the need for definitive paleocurrent data. The above arguments indicate that the Chedabucto Fault does not constitute the original basin margin, and an unknown portion of the original basin has been tectonically removed. Consequently, there is no reason to suppose that rocks of the Meguma Terrane cannot be found north of the Chedabucto Fault.

STRUCTURE

The intensity of deformation varies markedly from south to north across the study area. Near the southern margin, rocks of units 3 and 4 dip gently or moderately to the south and are virtually undeformed. Although sedimentological and stratigraphic arguments indicate deposition adjacent to active faults, the lack of internal deformation suggests that the fanglomerates may drape underlying faults. Where rocks of the Meguma Terrane are exposed along the boundary, they display strong textural evidence of dextral shear (Fig. 10, 11).

Granites, typical of ca. 365 Ma Meguma Terrane granitoid rocks, have subhorizontal stretching lineations and well developed S-C fabrics indicative of dextral strike slip along the bounding faults. Ductile shear may either predate deposition of the Horton Group or be indicative of the tectonic activity that resulted in the formation of the St. Mary's Basin. The age of the shear zone is currently being determined by $^{40}Ar/^{39}Ar$ dating of muscovite.

At some southern localities in units 3 and 4, stratigraphic markers show north-side-down displacement along northerly dipping normal faults. Parallel fractures are dilational, filled with quartz, and cut across pebbles in the fanglomerates (Fig. 5, 12). These features are consistent with north-south extension. The age of this faulting is uncertain; it may be as young as the Early Mesozoic rifting associated with the emplacement of the North Mountain Basalt.

Figure 10. *S-C fabrics in granitoid rocks of the Meguma Terrane adjacent to the southern flank of the St. Mary's Basin. S-C relationships and subhorizontal stretching lineations (see Fig. 11) indicate dextral shear. Horton Group lithologies adjacent to this outcrop are undeformed and the contact is interpreted as an unconformity.*

Figure 11. *Subhorizontal stretching lineations in granitoid rocks of the Meguma Terrane. S-C relationships (see Fig. 10) indicate dextral shear.*

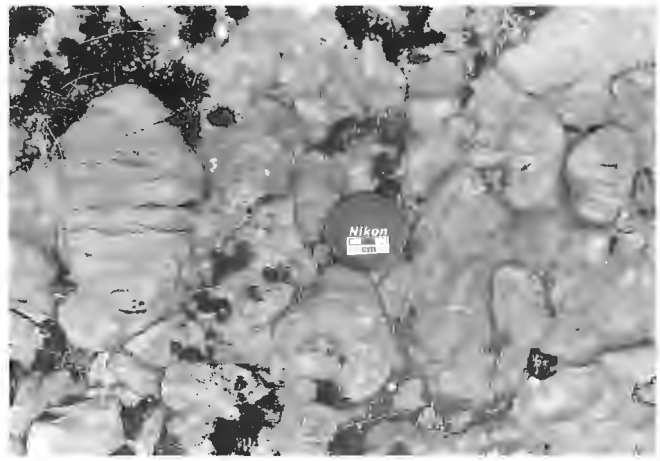

Figure 12. *Pebbles in conglomerates of unit 4 deformed by steep dilational fractures that parallel the basin margin. Fractures are commonly filled with quartz fibres growing perpendicularly to the fracture walls.*

The central portion of the St. Mary's Basin is dominated by upright, open to close, shallowly east-northeast- to northeast-plunging folds. The dominant structure is a broad anticline that exposes unit 2a in its core and can be traced, discontinuously, for about 15 km with a wavelength of about 4 km. Cleavage is very poorly developed, but, where present, is steeply dipping and axial planar. Quartz-filled, en echelon tension gashes are common in the subarkoses and quartz arenites of unit 2a (Fig. 3). They are predominantly steeply dipping and strike north-northwest. The orientation of the folds and tension gashes are consistent with dextral shear on the bounding faults.

The structural evolution of the northern part of the map area is dominated by the effects of the Chedabucto Fault. Along the entire length of this fault, beds steepen markedly and are rotated clockwise, consistent with dextral shear. This movement locally imparts a mylonitic fabric on the lithologies of unit 1. However, shear fabrics are not as recognizable in the more competent siliceous sediments of unit 2a and 2b.

ECONOMIC POTENTIAL

Although numerous mineral occurrences have been documented within the St. Mary's Basin, particularly adjacent to major faults, it is difficult to evaluate the mineral potential of the area without a better understanding of its geological evolution. Such an understanding also bears directly on Avalon-Meguma relationships and may offer new perspectives on the geological evolution and general mineral potential of these terranes.

The abundance of vein quartz detritus in clastic sedimentary rocks derived from erosion of the Meguma Terrane (Fig. 8), indicates a potential for paleoplacer deposits. Gold occurrences in the coarse conglomerates of unit 4 have been reported in the eastern part of the basin (see Hill, 1991) and may represent such paleoplacers. However, delineation of further potential deposits awaits detailed sedimentological studies.

Utting and Hamblin (1991), in a study of the thermal maturity of the Horton Group concluded that the rocks of the St. Mary's Basin had characteristics intermediate between the oil and gas windows.

SUMMARY AND DISCUSSION

Mapping in the eastern St. Mary's Basin has revealed previously unrecognized systematic regional variations in stratigraphy, sedimentology, and structural geology. The basin-fill sequence is dominated by intra-continental fluviatile and lacustrine clastic sedimentary rocks that coarsen upwards and face towards the southeastern flank of the basin. The Meguma Terrane provided the sediment source. Deposition along the southern basin margin may be related to alluvial fan debris flows, whereas longitudinal transport may be more important in central portions of the basin. There is no definitive evidence of a clastic contribution from the Avalon Terrane. Since the basin-fill oversteps the West St. Mary's Fault, the St. Mary's Basin is probably underlain by predominantly Meguma Terrane basement. The presence of coarse cobble conglomerates along the southern flank of the basin indicates that this margin was tectonically active during deposition. The conglomerates thicken markedly eastwards along the margin, suggesting that the main sediment source lay to the southeast. Dextral shear kinematic indicators in ca. 365 Ma granitoid rocks along this margin may record the style of Late Devonian tectonic activity associated with basin development. The gently southward dipping attitude of units along the basin's southern flank is consistent with syndepositional motion on northerly dipping listric faults.

The character of the sedimentary rocks does not vary with proximity to the northern margin of the basin, suggesting that predominantly dextral motion along the Chedabucto Fault has removed a portion of the basin. Meguma Terrane rocks underlie the present eastern St. Mary's Basin, and furthermore, may be found north of the Chedabucto Fault. The original relationship of the eastern St. Mary's Basin to the Avalon Composite Terrane remains to be demonstrated. Rocks traditionally assigned to the Horton Group in the Avalon Composite Terrane of northern Nova Scotia (e.g., Boehner and Giles, 1982, 1993) and Cape Breton Island (e.g., Hamblin and Rust, 1989) generally contain locally derived clasts. At present, suggestions that the Horton Group constitutes a simple overstep sequence across terrane boundaries cannot be substantiated in the eastern St. Mary's Basin and may mask complex Late Paleozoic tectonic events. The intensity of deformation within the St. Mary's Basin increases northwards and is consistent with dextral motion along the Chedabucto Fault. The age of this deformation is presently unclear.

ACKNOWLEDGMENTS

We thank Fred Chandler for organizational support; Fred Chandler, Quentin Gall, John Waldron, Bob Ryan, Tony Hamblin, Peter Giles, Duncan Keppie, Damian Nance, Wes Gibbons, and Sandra Barr for discussions; and Peter Giles and Damian Nance for reviewing the manuscript.

REFERENCES

Benson, D.G.
1967: Geology of the Hopewell map area, Nova Scotia; Geological Survey of Canada, Memoir 343, 58 p.
1974: Geology of the Antigonish Highlands, Nova Scotia; Geological Survey of Canada, Memoir 376, 92 p.

Boehner, R.C. and Giles, P.S.
1982: Geological map of the Antigonish Basin, Nova Scotia; Nova Scotia Department of Mines and Energy Map 82-2, scale 1:50 000.
1993: Geology of the Antigonish Basin, Antigonish County, Nova Scotia; Nova Scotia Department of Natural Resources, Mines and Energy Branches, Memoir 8, 109 p.

Fletcher, H. and Faribault, E.R.
1887: Geological surveys and explorations in the counties of Guysborough, Antigonish, Pictou, Colchester and Halifax, Nova Scotia from 1882-1886; Geological Survey of Canada, Annual Report, v. II, 1886, pt. P, p. 5-128.

Hamblin, A.P. and Rust, B.R.
1989: Tectono-sedimentary analysis of alternate polarity half-graben basin-fill successions: Late Devonian-Early Carboniferous Horton Group, Cape Breton Island, Nova Scotia; Basin Research, v. 2, p. 239-255.

Hill, J.D.
1991: Petrology, tectonic setting and economic potential of Devonian peraluminous granitoid plutons in the Canso and Forest Hill areas, eastern Meguma Terrane, Nova Scotia; Geological Survey of Canada, Bulletin 383, 96 p.

Kelley, D.G.
1967: Some aspects of Carboniferous stratigraphy and depositional history in the Atlantic Provinces; in Collected Papers on Geology of the Atlantic Region, (ed.) E.R.W. Neale and H. Williams; Geological Association of Canada, Special Paper No. 4, p. 213-228.

Keppie, J.D.
1982: Tectonic map of Nova Scotia; Nova Scotia Department of Mines and Energy Map, scale 1:500 000.

Martel, A.T.
1987: Seismic stratigraphy and hydrocarbon potential of the strike-slip Sackville sub-basin, New Brunswick; in Sedimentary Basins and Basin Forming Mechanisms, (ed.) C. Beaumont and A.J. Tankard; Canadian Society of Petroleum Geologists, Memoir 12, p. 319-334.

Murray, B.C.
1960: Stratigraphy of the Horton Group in parts of Nova Scotia; Nova Scotia Research Foundation Publication.

Schiller, E.A.
1961: Guysborough, Nova Scotia; Geological Survey of Canada, Map 27-1961.
1963: Mineralogy and geology of the Guysborough area, Nova Scotia, Canada; Ph.D. thesis, University of Utah, 162 p.

Utting, J. and Hamblin, A.P.
1991: Thermal maturity of the Lower Carboniferous Horton Group, Nova Scotia; International Journal of Coal Geology, v. 19, p. 439-456.

Williams, H.
1978: Tectonic lithofacies map of the Appalachians; Memorial University Map 1, Department of Geology, Memorial University of Newfoundland, St. John's, Newfoundland, scale 1:1 000 000.

Geological Survey of Canada Project 760027

Earliest Carboniferous plutonism, western Cobequid Highlands, Nova Scotia[1]

Georgia Pe-Piper[2] and I. Koukouvelas[2]
Atlantic Geoscience Centre

Pe-Piper, G. and Koukouvelas, I., 1994: Earliest Carboniferous plutonism, western Cobequid Highlands, Nova Scotia; in Current Research 1994-D; Geological Survey of Canada, p. 103-107.

Abstract: Earliest Carboniferous plutons of the western Cobequid Highlands (Cape Chignecto-Apple River, Hanna Farm, West Moose River, and North River) consist primarily of granite, with minor diorite phases, particularly in the Cape Chignecto pluton. Diorite is spatially associated with two major fault systems, the Cobequid and Kirkhill faults. Mylonitic zones and asymmetric folds provide evidence of almost synchronous towards the north and towards the south ductile motion in the plutons, interpreted to be related to the process of emplacement.

Résumé : Les plutons du Carbonifère initial dans l'ouest des hautes terres de Cobequid (Cape Chignecto-Apple River, Hanna Farm, West Moose River et North River) sont principalement composés de granite et renferment quelques phases mineures de diorite, en particulier dans le pluton de Cape Chignecto. La diorite est associée dans l'espace à deux grands systèmes de failles, celles de Cobequid et de Kirkhill. Dans les plutons, des zones mylonitiques et des plis asymétriques révèlent l'existence de mouvements ductiles dirigés à la fois vers le nord et vers le sud, qui sont presque contemporains l'un de l'autre et qui seraient liés aux processus de mise en place des intrusions.

[1] Contribution to Canada-Nova Scotia Cooperation Agreement on Mineral Development (1992-1995), a subsidiary agreement under the Canada-Nova Scotia Economic and Regional Development Agreement.
[2] Department of Geology, Saint Mary's University, Halifax, Nova Scotia B3H 3C1

INTRODUCTION

Geological setting

The Cobequid Highlands consist principally of late Proterozoic Avalonian igneous and low grade metasedimentary rocks, minor ?Ordovician, Silurian, and early Devonian sedimentary rocks, late Devonian and early Carboniferous volcanic rocks (Fountain Lake Group), and earliest Carboniferous diorite and granite plutons (Donohoe and Wallace, 1982, 1985). The Cobequid Fault is a 500 m wide fault zone marking the southernmost extent of crystalline rocks, but in most places it separates the upper Namurian Parrsboro Formation to the south from deformed early Carboniferous sediments (Londonderry and Greville River formations). Several subparallel major faults 1-5 km north of the Cobequid Fault (Londonderry, Kirkhill, and Rockland Brook faults) were mapped by Donohoe and Wallace (1982).

The plutons of the western Cobequid Highlands, using the nomenclature of Donohoe and Wallace (1982), are (from west to east) (Fig. 1):

- The Cape Chignecto pluton, bounded to the south by the Cobequid Fault in the west and the Kirkhill Fault in the east. The New Yarmouth and Fire Tower plutons of Donohoe and Wallace (1982) are phases of the Cape Chignecto pluton and the Apple River pluton is interpreted as an inlier of the same plutonic body (Waldron et al., 1989).
- The Hanna Farm pluton (Pe-Piper and Turner, 1988), located largely north of the Kirkhill Fault. Nearby plutonic rocks termed the Davidson Brook pluton by Donohoe and Wallace (1982) may be related.
- The West Moose River pluton, located immediately north of the Cobequid Fault (Pe-Piper et al., 1991).
- The North River pluton (Pe-Piper, 1991), located several kilometres north of the Cobequid Fault, is bounded on its southern side by an un-named fault and on its northern side by a possible continuation of the Kirkhill Fault.

Most of the diorite-gabbro and smaller granite plutons of the Cobequid Highlands appear to be of earliest Carboniferous age. Two plutons (Cape Chignecto, Pleasant Hills) have yielded U/Pb zircon dates of 360 Ma (R. Doig, pers. comm., 1992), corresponding to the Devonian-Carboniferous boundary. The Rb/Sr isochrons on the major plutons are of early Carboniferous age (Donohoe et al., 1986; Pe-Piper et al., 1989), but are suspect because of the extensive hydrothermal alteration. The Wyvern diorite has yielded a K/Ar hornblende date of 357 Ma. The Cape Chignecto Pluton shows northwest-vergent thrusting and the development of ductile fabrics that have been dated at 329 ± 11 Ma (K/Ar on biotite) (Namurian) by Waldron et al. (1989) and are cut by undeformed dykes.

Purpose

Mapping and field investigations in the summer of 1993 included: a) mapping of the extent of the various plutonic phases, and b) study of the character of early ductile deformation in the plutons.

DISTRIBUTION OF PLUTONIC PHASES

The plutons of the western Cobequid Highlands consist primarily of granite, with minor diorite (Fig. 1). Diorite is spatially associated with major fault systems, namely the Cobequid and Kirkhill faults and the fault splay along the southern margin of the North River pluton. In the Hanna Farm, West Moose River, and North River plutons, at least some of the diorite-gabbro

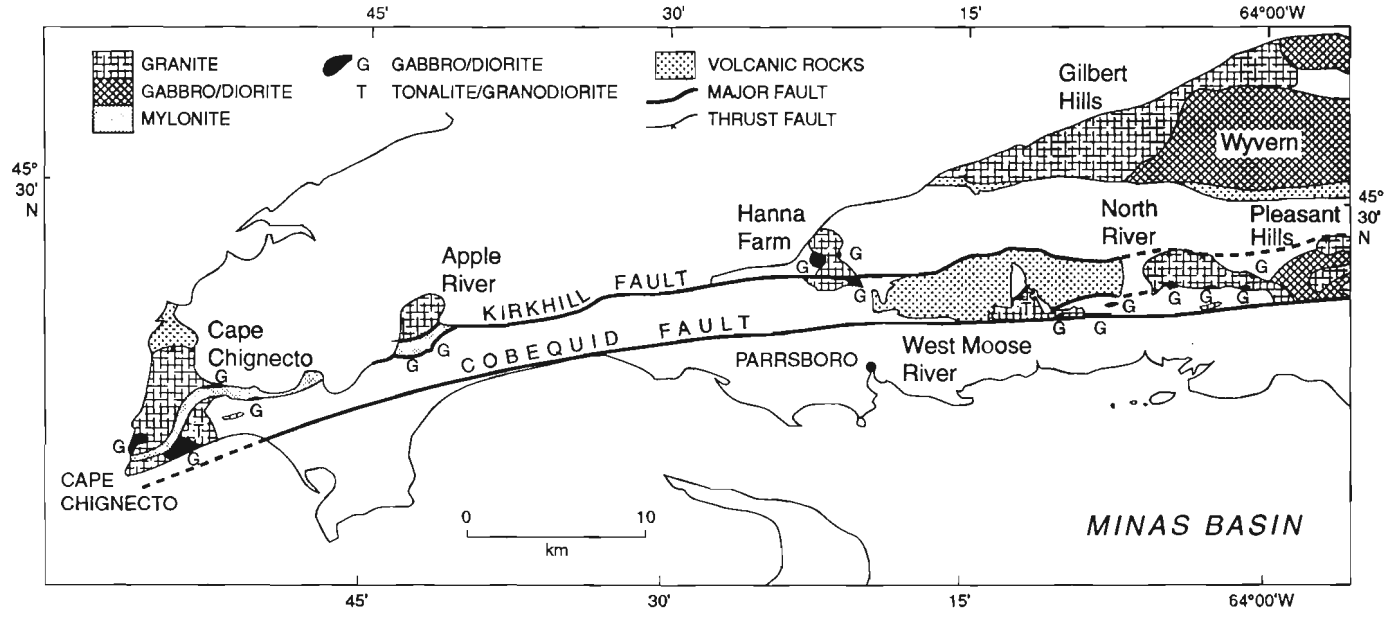

Figure 1. Map showing earliest Carboniferous plutons of the western Cobequid Highlands and the principal plutonic phases present.

appears to predate the granite, with granite being intruded near the contact of the gabbro with country rock. In the Cape Chignecto and North River plutons, some gabbro-diorite has intruded and hybridized earlier granite.

Plutons south of the Kirkhill Fault (southern Cape Chignecto, West Moose River) include granodiorites and porphyries (Fig. 1). Similar rocks are also found in the Pleasant Hills pluton, which also lies south of the projected eastward trend of the Kirkhill Fault. The northern plutons (northern Cape Chignecto, Apple River, Hanna Farm, and North River) all consist almost exclusively of granite, in places cut by diabase dykes.

EARLY DUCTILE DEFORMATION IN THE PLUTONS

Evidence of early ductile deformation within the plutons is widespread in river sections, however, relationships are most clearly seen in the Cape Chignecto pluton north of the mouth of Baldrock Brook. Here, diorite has intruded granite (indicated by diorite sheets injecting more extensive granite and chilled margins to some diorite). Some granite has been partially melted and assimilated by the dioritic magma to yield granodiorite, which locally cuts the diorite as veins.

Ductile deformation of the granite-diorite contacts and of partially digested granitic bodies has resulted in asymmetric folds and flame structures (Fig. 2), most of which show top-to-north sense of shear, although about 30% of the structures show top-to-south asymmetry. Sense of shear is also indicated by imbrication of feldspar phenocrysts (Fig. 2D) and of diorite xenoliths in granodiorite. The orientation of large undeformed feldspar phenocrysts in some ptygmatically folded granodiorite veins (Fig. 2B) suggests that at least some of the deformation is synmagmatic.

Postcrystallization deformation in this area includes local development of a strong mylonitic fabric with a corresponding mineral lineation. Some kinematic indicators show top-to-north deformation (as noted by Waldron et al., 1989), but

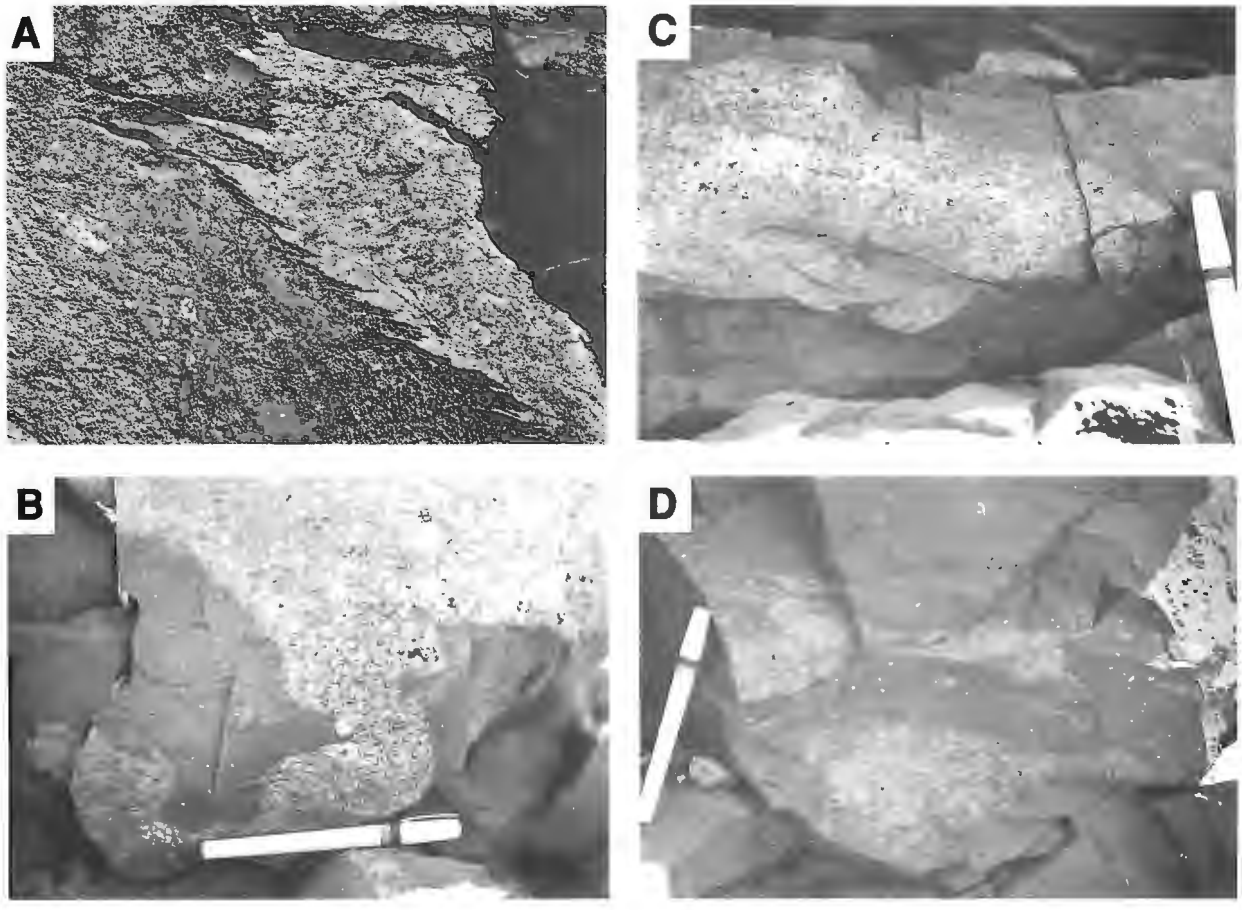

Figure 2. *Photographs showing early ductile deformational structures with motion principally top to north. Coast north of Baldrock Brook.* ***A.*** *Flame structures between granite (right) and diorite (left) suggesting top to left (north) motion. Diorite close to the contact is finer grained (chilled).* ***B.*** *Folded granodiorite vein cutting diorite with a synmagmatic foliation in feldspar phenocrysts (parallel to pen).* ***C.*** *Vein of partially digested granite in diorite, with diorite flames suggesting top to left (north) shear.* ***D.*** *Streaked out veins of partly digested granite in diorite. "Wings" of granite suggest top to left (north) motion, also indicated by imbricated feldspar phenocrysts (arrow).*

others show top-to-south movement (Fig. 3A). Minor aplite and pegmatite sheets cut the deformed granite. Deformed epidote veins that cut all the igneous phases also show top-to-south sense of shear from asymmetric ptygmatic folds (Fig. 3B). More brittle structures with a similar southward sense of motion include large north-dipping thrust zones with C-S structures.

An intense zone of mylonitic deformation cuts the eastern part of the Cape Chignecto pluton immediately north of the Kirkhill Fault and continues across the southwestern part of the pluton (Fig. 1). This zone continues along the southern margin of the Apple River pluton, which Waldron et al. (1989) regarded as part of the Cape Chignecto pluton. A second zone of intense mylonitic and brittle deformation extends along the south coast of the peninsula immediately north of the Cobequid Fault. Tectonic slices of deformed granite and diorite are intercalated with Horton Group sediments immediately south of the Kirkhill Fault (Fig. 1). A similar relationship is seen south of the Kirkhill Fault at the Hanna Farm pluton, which otherwise shows little deformation.

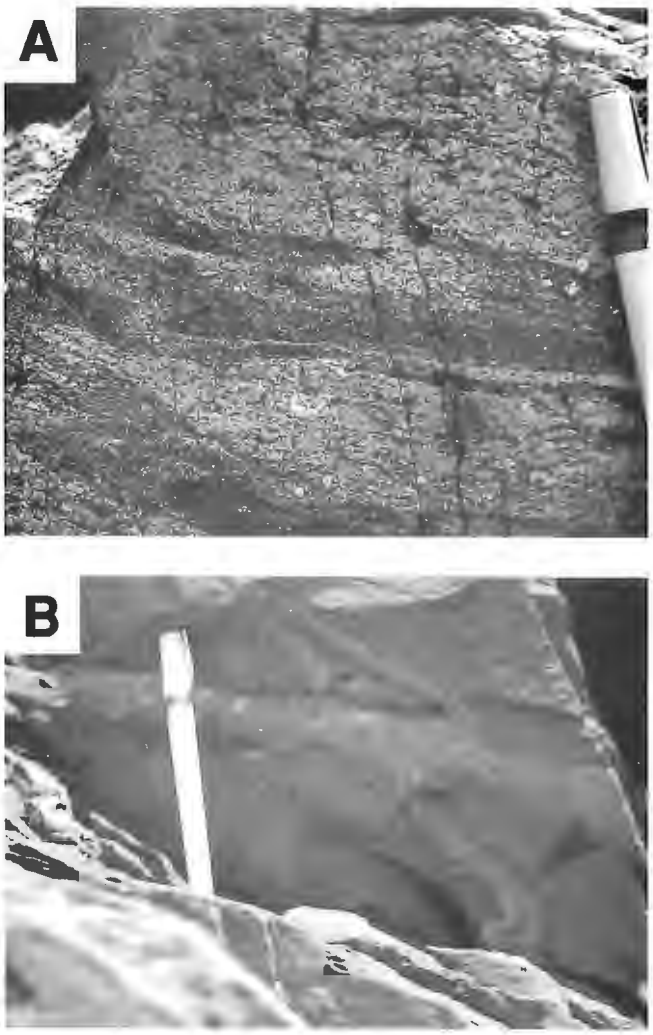

Figure 3. *Photographs showing later ductile deformational structures with motion principally top to south. Coast north of Baldrock Brook.* ***A.*** *Z-folds in mylonitic granite suggesting top to right (south) motion.* ***B.*** *Epidote veins (arrow) cutting diorite and thin granite vein, with asymmetric folding suggesting top to right (south) motion.*

In general, the West Moose River and North River plutons are substantially less deformed than the Cape Chignecto pluton. At the northern margin of the North River pluton, asymmetrically folded microdykes, sigmoidal foliation planes, and tension gashes all indicate north-directed thrusting in the country rock up to 500 m north of the contact. In the West Moose River and North River plutons, small granitic dykes oblique to the northern contact show sinistral offset in horizontal exposures and northwest-directed thrusting in vertical section.

Movement to the south in the southern part of the West Moose River and North River plutons is recognized from deformation of quartz veins and mafic dykes, and ptygmatic folding of epidote veins. In the West Moose River pluton, deformation of the granite near the Cobequid Fault is mylonitic. This deformation is accompanied by evidence of dextral shear. Large scale flat-lying faults with top to the south displacement are seen in the North River and West Moose River plutons, similar to those seen in the Cape Chignecto pluton. Bodies of Jeffers Group country rock mapped as roof pendants by Pe-Piper et al. (1991) show top-to-south ductile deformation structures and are cut by unusual white granite veins, which may indicate that they are the remnants of an upper thrust sheet.

DISCUSSION

Mode of emplacement of the plutons

Several lines of evidence suggest that the Cobequid fault zone was probably the main path for magma ascent at depth. It is larger than any of the other east-west faults in terms of its present offset and width of the deformation zone. Both outcrop studies and aeromagnetic data (Piper et al., in press) indicate that mafic magma emplacement in the western Cobequid Highlands was concentrated along the Cobequid Fault zone and the Kirkhill Fault a few kilometres to the north.

The 500 m wide strain aureole in country rock north of the main contact of the plutons (particularly clear in the North River and West Moose River plutons) suggests that magma emplacement was forceful. Emplacement probably took place on southwest-dipping thrust planes, evidence for which is seen in country rock and in continued motion in the plutons. The largest thrust faults may now be represented by some of the major east-west faults, such as the Kirkhill Fault and the fault at the southern margin of the North River pluton. Magma emplacement along the thrusts would result in expansion of the hanging wall and the production of a staircase-like geometry for the plutons, with several kilometres of relief (Fig. 4).

The occurrence of sediments with granite clast conglomerates intruded by granitic veins at the northern edge of the Pleasant Hills pluton (Piper, 1994) suggests that magma emplacement moved progressively northward, eventually invading sediments deposited on the northern margin of the emplaced granites. After voluminous magma supply ceased,

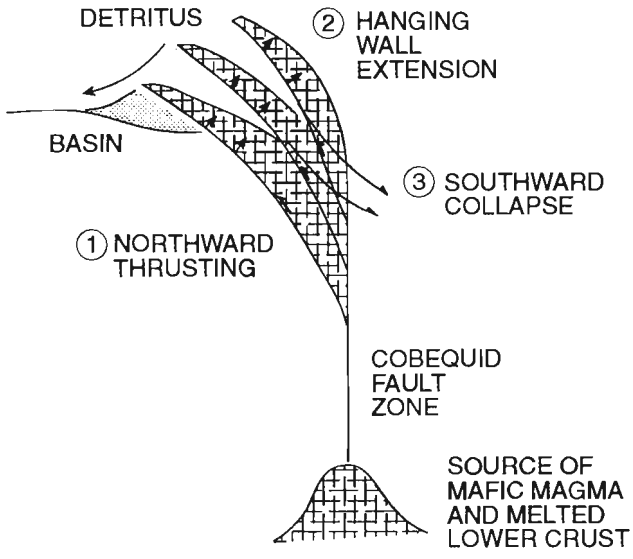

Figure 4. Cartoon showing emplacement processes of the granitic plutons and their relationship to marginal basins.

the emplaced magma would have progressively solidified. The south-directed structures seen in the southern parts of the plutons are inferred to result from the passive southward collapse of the dome-like structure produced during magma emplacement. Deepest structural levels are now exposed north of the Kirkhill Fault.

REGIONAL CORRELATIONS

It might be expected that the transition from the phase of forceful emplacement to southward collapse of the plutons would correspond to the tectonic events in the surrounding basins. Waldron et al. (1989) correlated the northward thrusting with the increased supply of coarse sediment in the Namurian and the mid-Namurian unconformity between the West Bay and Parrsboro formations; however, this correlation is based principally on one K/Ar date of 329 ± 11 Ma on deformed biotite. The presence of granitic clasts in Horton Group sediments (Piper, 1994) indicates that significant uplift may have taken place earlier. The presence of undeformed pegmatite cutting deformed Cape Chignecto granite suggests that deformation was largely complete before complete cooling and crystallization of the granitic magma. Thus the end of northward-directed thrusting may correspond to the widespread unconformity between the Horton and Windsor groups.

CONCLUSIONS

Earliest Carboniferous plutons of the western Cobequid Highlands consist primarily of granite, with minor diorite. Locally, granite has been emplaced along contacts between diorite and country rock. Diorite is spatially associated with major fault systems, namely the Cobequid, Kirkhill, and Rockland Brook faults. Plutons south of the Kirkhill Fault (southern Cape Chignecto, West Moose River, Pleasant Hills plutons) also include granodiorites and porphyries. All the plutons show evidence of ductile deformation. Mylonitic zones and asymmetric folds provide evidence of displacement to the north in the northern parts of all the plutons. Displacement to the south, both ductile and ductile-brittle, is seen in the southern parts of several plutons.

The Cobequid fault zone was probably the main path for magma ascent at depth and upper crustal magma emplacement was forceful. Emplacement took place along pre-existing zones of weakness: on southwest-dipping thrust planes now represented by some of the major east-west faults of the Cobequid Highlands. Magma emplacement along the thrusts resulted in expansion of the hanging wall and the production of a staircase-like geometry for the plutons, with several kilometres of relief. After voluminous magma supply ceased, the emplaced magma progressively solidified. During this time, the resulting dome-like structure passively collapsed southward, producing the south-directed structures seen in the southern parts of the plutons.

REFERENCES

Donohoe, H.V. and Wallace, P.I.
1982: Geological map of the Cobequid Highlands, Nova Scotia; Nova Scotia Department of Mines and Energy, scale 1:50 000.

Donohoe, H.V. Jr. and Wallace, P.I.
1985: Repeated orogeny, faulting and stratigraphy of the Cobequid Highlands, Avalon Terrane of northern Nova Scotia; Geological Association of Canada-Mineralogical Association of Canada Joint Annual Meeting, Guidebook 3, Fredericton, New Brunswick, 77 p.

Donohoe, H.V., Jr., Halliday, A.N., and Keppie, J.D.
1986: Two Rb-Sr whole rock isochrons from plutons in the Cobequid Highlands, Nova Scotia, Canada; Maritime Sediments and Atlantic Geology, v. 22, p. 148-154.

Pe-Piper, G.
1991: Granite and associated mafic phases, North River pluton, Cobequid Highlands; Atlantic Geology, v. 27, p. 15-28.

Pe-Piper, G. and Turner, D.S.
1988: The Hanna Farm pluton. Cobequid Highlands: petrology and significance for motion on the Kirkhill fault; Maritime Sediments and Atlantic Geology, v. 24, p. 171-183.

Pe-Piper, G., Cormier, R.F., and Piper, D.J.W.
1989: The age and significance of Carboniferous plutons of the western Cobequid Hills, Nova Scotia; Canadian Journal of Earth Sciences, v. 26, p. 1297-1307.

Pe-Piper, G., Piper, D.J.W., and Clerk, S.B.
1991: Petrogenesis of an A-type granite pluton and associated mafic phases, Cobequid Highlands, Nova Scotia; Canadian Journal of Earth Sciences, v. 28, p. 1058-1072.

Piper, D.J.W.
1994: Late Devonian - earliest Carboniferous basin formation and relationship to plutonism, Cobequid Highlands, Nova Scotia; in Current Research 1994-D, Geological Survey of Canada.

Piper, D.J.W., Pe-Piper, G., and Loncarevic, B.D.
in press: Devonian-Carboniferous deformation and igneous intrusion in the Cobequid Highlands; Atlantic Geology.

Waldron, J.G.F., Piper, D.J.W., and Pe-Piper, G.
1989: Deformation of the Cape Chignecto Pluton, Cobequid Highlands, Nova Scotia: thrusting at the Meguma-Avalon boundary; Atlantic Geology, v. 25, p. 51-62.

Geological Survey of Canada Project 920062

Late Devonian-earliest Carboniferous basin formation and relationship to plutonism, Cobequid Highlands, Nova Scotia[1]

David J.W. Piper
Atlantic Geoscience Centre, Dartmouth

Piper, D.J.W., 1994: Late Devonian-earliest Carboniferous basin foramtion and relationship to plutonism, Cobequid Highlands, Nova Scotia; in Current Research 1994-D; Geological Survey of Canada, p. 109-112.

Abstract: Upper Devonian-lower Carboniferous basin sediments in the Cobequid Highlands with Horton Group affinities have been re-examined. The Rapid Brook and Greville River Formations are respectively proximal and distal facies of a single alluvial fan-fluviatile-lacustrine unit. Similar facies occur south of the North River Pluton, north of the Pleasant Hills pluton, and in the Tournaisian Nuttby Formation. Oldest conglomerates contain clasts of undeformed granite, higher conglomerates contain rhyolites and foliated granites, and locally the conglomerates are intruded by granite veins.

Reconnaisance work on the Fountain Lake Group of the eastern Cobequid Highlands shows that the Diamond Brook Formation underlies (rather than overlies) the Byers Brook Formation and was tilted to near vertical before intrusion of the earliest Carboniferous plutons. This sequence records major late Devonian basin subsidence. Early Carboniferous basins developed in response to thrust and collapse structures associated with forceful intrusion of granites along the Cobequid Fault zone.

Résumé : Les sédiments de bassin du Dévonien supérieur au Carbonifère inférieur dans les hautes terres de Cobequid, qui présentent des affinités avec le Groupe de Horton, ont été réexaminés. Les formations de Rapid Brook et de Greville River sont respectivement les faciès proximal et distal d'une même unité comportant des sédiments de cône alluvial, des sédiments fluviatiles et des sédiments lacustres. Des faciès semblables sont présents au sud du pluton de North River, au nord du pluton de Pleasant Hills et dans la Formation de Nuttby du Tournaisien. Les conglomérats les plus anciens renferment des clastes de granite non déformé, les conglomérats plus hauts dans la séquence renferment des rhyolites et des granites foliés, et les conglomérats sont pénétrés, par endroits, par des veines de granite.

Le travail de reconnaissance effectué dans le Groupe de Fountain Lake, dans l'est des hautes terres de Cobequid, révèle que la Formation de Diamond Brook est sous-jacente, plutôt que sus-jacente, à la Formation de Byers Brook et a été basculée presque à la verticale avant l'intrusion des plutons les plus anciens du Carbonifère. Cette séquence témoigne d'une importante subsidence du bassin au Dévonien tardif. L'évolution des bassins du Carbonifère précoce a été influencée par des phénomènes de charriage et d'effondrement associés à l'intrusion forcée de granites le long de la zone de failles de Cobequid.

[1] Contribution to Canada-Nova Scotia Cooperation Agreement on Mineral Development (1992-1995), a subsidiary agreement under the Canada-Nova Scotia Economic and Regional Development Agreement.

INTRODUCTION

General setting

The Cobequid Highlands (Donohoe and Wallace, 1982, 1985) consist principally of late Proterozoic Avalonian igneous and low grade metasedimentary rocks, minor (?)Ordovician, Silurian, and early Devonian sedimentary rocks, late Devonian and early Carboniferous volcanic rocks (Fountain Lake Group), and earliest Carboniferous diorite and granite plutons (Fig. 1). Late Devonian and Carboniferous sedimentary rocks outcrop around the periphery of the highlands and are locally deformed. The Cobequid Fault is a 500 m wide fault zone marking the southernmost extent of crystalline rocks, but in most places it separates the upper Namurian Parrsboro Formation to the south from deformed early Carboniferous sediments (Londonderry and Greville River formations).

Devono-Carboniferous igneous rocks

The Fountain Lake Group in the eastern Cobequid Highlands (Byers Brook and Diamond Brook formations) consists of felsic volcanics and basalt flows locally interbedded with sedimentary rocks. The Diamond Brook Formation (principally basalts) contains Emsian-Eifelian and Tournaisian spores (Donohoe and Wallace, 1982). Felsic volcanic rocks have yielded a Rb/Sr isochron of ~387 Ma (Pe-Piper et al., 1989). The widespread diorite/gabbro and smaller granite plutons of the Cobequid Highlands appear to be of earliest Carboniferous age. Two plutons have yielded U/Pb zircon dates of 360 Ma (R. Doig, pers. comm., 1991), corresponding to the Devonian-Carboniferous boundary. The Fountain Lake Group volcanic rocks of the western Cobequid Highlands appear broadly synchronous with intrusion of the plutons. The Cape Chignecto Pluton shows northwest-vergent thrusting and the development of ductile fabrics which were tentatively dated at 329 ± 11 Ma (K/Ar on biotite; Namurian; Waldron et al., 1989). Probably coeval brittle thrusts in the Fountain Lake Group are cut by later dykes.

Recent work (Pe-Piper and Koukouvelas, 1994) has shown that all the plutons in the western Cobequid Highlands show evidence of ductile deformation. Mylonitic zones and asymmetric folds provide evidence of displacement to the north in the northern parts of each pluton. Displacement to the south, both ductile and ductile-brittle, is seen in the southern parts of several plutons. They interpreted these structures as due to forceful intrusion of magma along southwest-dipping thrust planes, producing magmatic expansion of the hanging wall and a staircase-like geometry for the plutons, followed by passive collapse southward.

Previous work on Middle Devonian-Lower Carboniferous sedimentary rocks

Donohoe and Wallace (1982, 1985) identified several Middle Devonian-Lower Carboniferous clastic sediment sequences. In the central Cobequid Highlands, the Murphy Brook Formation disconformably overlies the Silurian Wilson Brook Formation and comprises black siltstones interbedded with polymictic and rhyolite-clast conglomerate. Plant fossils are of late Emsian to early Eifelian age (A. Kasper, in Donohoe and Wallace, 1985). In the east, sediments interbedded with volcanic rocks of the Diamond Brook Formation contain Emsian-Eifelian and Tournaisian spores (Donohoe and Wallace, 1982). Martel et al. (1993) have re-interpreted the younger spores as Famennian. The Fountain Lake Group is unconformably overlain by the unfossiliferous Falls Formation, comprising red-brown polymictic alluvial fan conglomerate and wacke (Fralick, 1980). In the south-central highlands, the Nuttby Formation (with Tournaisian spores) comprises red and grey siltstones, wackes, and polymictic conglomerate. In the western highlands, the Rapid Brook Formation comprises principally conglomerate and wacke; the Greville River Formation comprises siltstones and wackes, and contains plant fossils of uncertain age. Although Donohoe and Wallace (1985) suggest that the Rapid Brook formation unconformably overlies Fountain Lake Group to the north, Waldron et al. (1989) showed that the rocks immediately north of the Rapid Brook Formation are in fact mylonitized granites. The youngest deformed rock unit in the

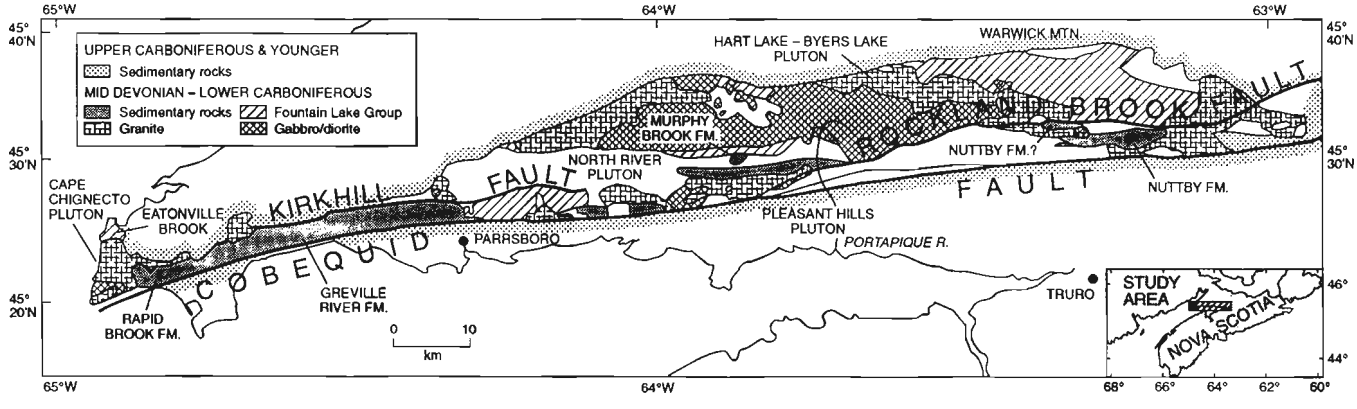

Figure 1. Location map showing mid-Devonian-Lower Carboniferous basin sediments of the Cobequid Highlands, and associated Fountain Lake Group volcanic rocks and plutons. Base map modified from Donohoe and Wallace (1982).

Cobequid Highlands is the Londonderry Formation with late Visean to early Namurian spores. The West Bay formation is lithologically and palynologically correlative, and is overlain unconformably by the late Namurian Parrsboro Formation (Donohoe and Wallace, 1985).

Donohoe and Wallace (1982) mapped several rock units of uncertain age that have been re-examined because of their possible similarity to the Nuttby, Greville River, and Rapid Brook formations. These include: (1) an unfossiliferous unnamed "Silurian" section (11B of Donohoe and Wallace, 1985) south of the North River pluton, including siltstone, wacke, and granite-clast conglomerate; (2) granite-clast polymictic conglomerate assigned to the Silurian Wilson Brook Formation north of the Pleasant Hills pluton; and (3) an area originally mapped as Nuttby Formation, but assigned an older age based on an intrusive contact with granite identified as the Neoproterozoic Debert Pluton (unit 5A of Donohoe and Wallace, 1985).

RAPID BROOK-GREVILLE RIVER FORMATIONS

South of the granitic plutons of the western Cobequid Highlands (Cape Chignecto, Apple River, and Hanna Farm plutons), the Rapid Brook and Greville River formations are respectively proximal and distal facies of the same alluvial fan-fluviatile-lacustrine unit. Facies present include moderately sorted conglomerate; thick bedded, medium quartz wacke (locally channelled and crossbedded), medium bedded, grey, fine sandstone and coarse siltstone; dark argillite with siltstone laminae and rare fine sandstone; and purplish siltstone. Many of these facies are common elsewhere within the Horton Group, for example within the type area (Martel, 1990) and in the Strathlorne Formation of Cape Breton Island (Hamblin, 1992). Oldest conglomerates of the Rapid Brook facies contain clasts of undeformed granite and diorite; higher conglomerates contain clasts of rhyolite, vein quartz and foliated granite. These sedimentary rocks lie between the Kirkhill and Cobequid faults and are tightly folded and cleaved. Outcrop is intermittent in most brook sections, so that true stratigraphic thickness is difficult to determine. Tectonic intercalations of granite occur locally. Contacts with the plutonic rocks everywhere appear to be faulted.

Small outcrops also occur north of the Cape Chignecto pluton, in Eatonville Brook, where polymictic conglomerates equated with the Falls Formation (Salas, 1985) unconformably overlie both Fountain Lake rhyolite and deformed siltstone and wacke of the Greville River Formation.

ROCKS SOUTH OF THE NORTH RIVER PLUTON

South of the North River pluton, sedimentary rocks similar to the Greville River and Rapid Brook formations are exposed in the East, Bass, and Harrington rivers and on Lynn road. As south of the Cape Chignecto pluton, the sequence is folded and outcrop discontinuous. Lithologies include quartz wacke, greenish and purplish siltstone and fine wacke, dark argillite, and rare granule conglomerates with clasts principally of vein quartz and rhyolite. Two samples of dark argillite submitted for palynology were barren. Donohoe and Wallace (1982) recorded granite clast conglomerate. The structural setting of this unit is similar to that of the Rapid Brook-Greville River formations near the Cape Chignecto pluton, lying between the Cobequid and Kirkhill faults immediately south of a granitoid pluton and including tectonic intercalations of granite. The sequence is therefore regarded as correlative with the type Greville River and Rapid Brook formations, rather than being "undivided Silurian-Devonian" as mapped by Donohoe and Wallace (1982, 1985). In the lower Harrington River, this unit is intruded by a sill of microgranite.

NORTHERN MARGIN OF THE PLEASANT HILLS PLUTON

At the northern margin of the Pleasant Hills pluton, purplish and green siltstones, sandstones, and conglomerates outcrop in the Economy River. Large rounded pebbles of granite occur in some conglomerates and pebbly sandstones. Other conglomerates contain principally subangular rhyolite clasts. Granule conglomerates consist principally of rhyolitic detritus and vein quartz. Thin sections show that granite clasts are similar to some lithologies in the Pleasant Hills pluton and do not resemble the South Mountain batholith of southern Nova Scotia.

Hornfels and granitic veins show that this sedimentary unit is in igneous contact with a fine grained granitic phase of the Pleasant Hills pluton. Both the granite and the sediment unit show northward-directed thrusting. The presence of granite clasts and the crosscutting granite veins suggest that this unit is essentially synchonous with the Pleasant Hills pluton and therefore of earliest Carboniferous age. It is thus an age equivalent of the type Horton Group.

Northwards, the contact of this Horton unit with the Silurian Wilson Brook Formation can be readily mapped. The Wilson Brook Formation contains parallel and wavy laminated fine sandstones that weather distinctively, and fresh surfaces of siltstones show bioturbation. In contrast, the sandstones and siltstones in the Horton unit are massive. In the west branch of Economy River, the Horton unit appears to be thrust over the Wilson Brook Formation.

In the Portapique River, laminated sandstones and bioturbated siltstones of the Wilson Brook Formation can be mapped for about 60 m stratigraphically below the lowest (late Llandovery) fossil occurrence. Below this is approximately 100 m stratigraphic thickness of massive grey siltstones and sandstones. Southwards, these rocks pass into mylonites of the Rockland Brook fault zone, but a similar lithology is intruded by the Pleasant Hills pluton in the vicinity of Bass River. Although this lithology might be a fine grained unbioturbated facies of the Wilson Brook Formation, it more closely resembles parts of the Horton unit.

NUTTBY FORMATION

The Tournaisian Nuttby Formation of the eastern Cobequid Highlands consists of a range of lithologies similar to those in the Greville River and Rapid Brook formations: moderately sorted conglomerate with scoured bases to beds; cross-bedded medium quartz wacke; medium bedded, fine sandstone and siltstone; black argillite with silty laminae; and rare limestone. These sediments represent alluvial fan, fluvial, and lacustrine environments. The oldest conglomerates contain principally quartzite and mylonite clasts; higher conglomerates contain pebbles principally of rhyolite. The overall structure is broadly synclinal and shows a transition from proximal (conglomerates) to distal (black argillite) facies from south to north.

An area around the upper Chiganois River was originally mapped as Nuttby Formation by Donohoe and Wallace (1982), but later was assigned an older age based on an intrusive contact with granite identified as the Neoproterozoic Debert Pluton (unit 5A of Donohoe and Wallace, 1985). The lithologies in this area are like the type Nuttby Formation. We have found no intrusive contact with the nearby granite, the lithology of which is more like the typical Carboniferous granites of the region than the Neoproterozoic Debert pluton (G. Pe-Piper, pers. comm., 1993). We therefore concur with the original assignment of this area to the Nuttby Formation.

FOUNTAIN LAKE GROUP

Reconnaisance studies of the Fountain Lake Group suggest that many of the contacts mapped by Donohoe and Wallace (1982) and used as the basis of their chronology (Donohoe and Wallace, 1985) are tectonic. For example, it is not possible to demonstrate an unconformable relationship between the Fountain Lake Group and the Murphy Brook Formation north of Economy Lake; the regional setting makes a fault contact more likely. The mapped intrusive contact of the Folly Lake Pluton with the Fountain Lake Group in the upper Portapique River is a thrust fault.

Preliminary work on the Fountain Lake Group of the eastern Cobequid Highlands (between Warwick Mountain and the Hart Lake-Byers Lake pluton) suggests that the Diamond Brook Formation underlies (not overlies, as previous mapped) the Byers Brook Formation. Way-up indicators include basaltic flows and scours in siltstones and are consistently to the south. A tectonic contact between the two formations cannot be excluded. Both formations were folded or tilted to near vertical before intrusion of the earliest Carboniferous plutons. Many large gabbro dykes cut the Byers Brook Formation.

DISCUSSION AND CONCLUSIONS

The mid- to late Devonian volcanic pile of the eastern Cobequid Highlands comprises principally basalt in its lower part and principally rhyolite in its upper part. The strong subsidence and tilting of the eastern Fountain Lake Group is similar to that in deep basins imaged by seismic reflection profiles in the southern Magdalen Basin (Durling and Marillier, 1990). Pre-Horton sedimentation is also represented by the Middle Devonian Murphy Brook Formation.

Basin sediments containing granitic clasts, to the north and south of the granitic plutons along the Cobequid Fault zone in the western Cobequid Highlands, postdate pluton emplacement, which on the basis of available dates took place at about the Devonian-Carboniferous boundary. These sediments are thus probably time equivalents of the Horton Group and correlative with the Lower Carboniferous Nuttby Formation, as suggested by Donohoe and Wallace (1985). Their facies are similar to those found in the type Horton Group. The conglomerates were shed from adjacent highlands, which appear to have developed in response to uplift of the plutons as a result of forceful intrusion and northward thrusting from the Cobequid Fault zone and subsequent southward collapse (Pe-Piper and Koukouvelas, 1994).

REFERENCES

Donohoe, H.V. and Wallace, P.I.
1982: Geological map of the Cobequid Highlands, Nova Scotia; Nova Scotia Department of Mines and Energy, scale 1:50 000.

Donohoe, H.V. Jr. and Wallace, P.I.
1985: Repeated orogeny, faulting and stratigraphy of the Cobequid Highlands, Avalon Terrane of northern Nova Scotia; Geological Association of Canada - Mineralogical Association of Canada Joint Annual Meeting, Guidebook 3, Fredericton, New Brunswick, 77p.

Durling, P.W. and Marillier, F.J.Y.
1990: Structural trends and basement rock subdivisions in the western Gulf of St. Lawrence, Northern Appalachians; Atlantic Geology, v. 26, p. 79-95.

Fralick, P.W.
1980: Tectonic and sedimentological development of a late Paleozoic wrench basin: the eastern Cumberland Basin, Maritime Canada; M.Sc. thesis, Dalhousie University, Halifax, Nova Scotia.

Hamblin, A.P.
1992: Half-graben lacustrine sedimentary rocks of the lower Carboniferous Strathlorne Formation, Horton Group, Cape Breton Island, Nova Scotia, Canada; Sedimentology, v. 39, p. 263-284.

Martel, A.T.
1990: Stratigraphy, fluviolacustrine sedimentology and cyclicity of the late Devonian/early Carboniferous Horton Bluff Formation, Nova Scotia, Canada; Ph.D. thesis, Dalhousie University, Halifax, Nova Scotia, 297 p.

Martel, A.T., McGregor, D.C., and Utting, J.
1993: Stratigraphic significance of Upper Devonian and Lower Carboniferous miospores from the type area of the Horton Group, Nova Scotia; Canadian Journal of Earth Sciences, v. 30, p. 1091-1098.

Pe-Piper, G. and Koukouvelas, I.
1994: Earliest Carboniferous plutonism, western Cobequid Highlands, Nova Scotia; in Current Research 1994-D, Geological Survey of Canada.

Pe-Piper, G., Cormier, R.F., and Piper, D.J.W.
1989: The age and significance of Carboniferous plutons of the western Cobequid Hills, Nova Scotia; Canadian Journal of Earth Sciences, v. 26, p. 1297-1307.

Salas, C.J.
1985: Braided fluvial architecture with a rapidly subsiding basin: the Pennsylvanian Cumberland Group, southwest of Sand River, Nova Scotia; M.Sc. thesis, University of Ottawa, Ottawa, Ontario.

Waldron, J.G.F., Piper, D.J.W., and Pe-Piper, G.
1989: Deformation of the Cape Chignecto Pluton, Cobequid Highlands, Nova Scotia: thrusting at the Meguma-Avalon boundary; Atlantic Geology, v. 25, p. 51-62.

Geological Survey of Canada Project 920062

A progress report on the geology of the Stellarton Gap, Nova Scotia, including the Stellarton Coal Basin[1]

F.W. Chandler, Quentin Gall[2], Kevin Gillis[3], Rob Naylor[4], and John Waldron[5]

Continental Geoscience Division

Chandler, F.W., Gall, Q., Gillis, K., Naylor, R., and Waldron, J., 1994: A progress report on the geology of the Stellarton Gap, Nova Scotia, including the Stellarton Coal Basin; in Current Research 1994-D; Geological Survey of Canada, p. 113-122.

Abstract: The following stratigraphic revisions are suggested: the Falls and Claremont formations should be included in one formation; the Boss Point Formation is less, and the Middle River Formation more, widespread than previously thought; the Middle River should be combined with the New Glasgow Formation as one formation.

Calcrete, possible vertisols, and abundant plant remains indicate a tropical seasonal climate during the Westphalian. Major redox boundaries at the base of the Malagash, the top of the Boss Point, and particularly the base of the Boss Point formation are likely sites for base metal mineralization. Folds in Carboniferous rocks are probably related to dextral wrench faulting.

The 2600 m coal- and oil shale-bearing Westphalian Stellarton Formation, of the 120 km^2 Stellarton Basin comprises lacustrine delta sequences including delta plain, distributary channel, mouth bar, distal bar, and prodelta deposits. Coal and oil shale precursors accumulated when sediment supply became restricted.

Résumé : Les révisions stratigraphiques suivantes sont proposées : les formations de Falls et de Claremont devraient être regroupées en une seule; la Formation de Boss Point est moins étendue et la Formation de Middle River plus étendue qu'on ne le croyait; les formations de Middle River et de New Glasgow devraient être regroupées en une seule.

Des encroûtements calcaires, de possibles vertisols et des restes végétaux abondants, indiquent l'existence d'un climat tropical saisonnier pendant le Westphalien. Les grandes limites d'oxydo-réduction existant à la base de la Formation de Malagash, au sommet de la Formation de Boss Point et en particulier à la base de la Formation de Boss Point sont les sites probables de minéralisations en métaux communs. Les plis qui ont déformé les roches du Carbonifère sont probablement associés à des failles de coulissage à déplacement dextre.

La Formation de Stellarton, d'âge westphalien et de 2 600 m d'épaisseur, composée de shales houillers et pétrolifères, qui occupe les 120 km^2 du bassin de Stellarton, englobe des séquences de delta lacustre, notamment des dépôts de plaine deltaïque, de chenaux distributaires, de barre d'embouchure, de barre distale et de prodelta. Les shales houillers et pétrolifères se sont accumulés quand l'apport de sédiments s'est raréfié.

[1] Contribution to Canada-Nova Scotia Cooperation Agreement on Mineral Development (1992-1995), a subsidiary agreement under the Canada-Nova Scotia Economic and Regional Development Agreement.

[2] Department of Earth Sciences, Carleton University, Ottawa, Ontario K1S 5B6

[3] Nova Scotia Department of Natural Resources, 32 Bridge Avenue, Stellarton, Nova Scotia BOK 1SO

[4] Nova Scotia Department of Natural Resources, P.O Box 698, 1701 Hollis St., Halifax, Nova Scotia B3J 2T9

[5] Geology Department, St. Mary's University, Halifax, Nova Scotia B3H 3C3

INTRODUCTION

The Stellarton Gap lies between the pre-Carboniferous Cobequid (Donahoe and Wallace, 1982; Murphy et al., 1988) and Antigonish (Murphy et al., 1991) Highlands (Fig. 1). It is underlain by Carboniferous rocks and is crossed by a Westphalian (Yeo, 1985), east-northeast dextral wrench fault system, site of the important Stellarton Coal Basin (Gibling et al., 1991). Also present are the Windsor Group, host elsewhere of important Pb-Zn deposits, and the Westphalian Pictou Group, that hosts a number of Cu (Ryan et al., 1986) and Pb-Zn (Sangster and Vaillancourt, 1990) occurrences.

Mapping of the Stellarton Gap will complete coverage of the Carboniferous rocks between and to the north of the two highlands. Gillis, Naylor, and Waldron are responsible for discussion of rocks of the Stellarton Coal Basin and Chandler and Gall for surrounding rocks.

STRATA OUTSIDE THE STELLARTON BASIN

Structural geology

The structure of the map area (Fig. 1) is dominated by two major dextral faults (Cobequid and Hollow) and by en echelon, east-northeast plunging folds, the Scotsburn Anticline and

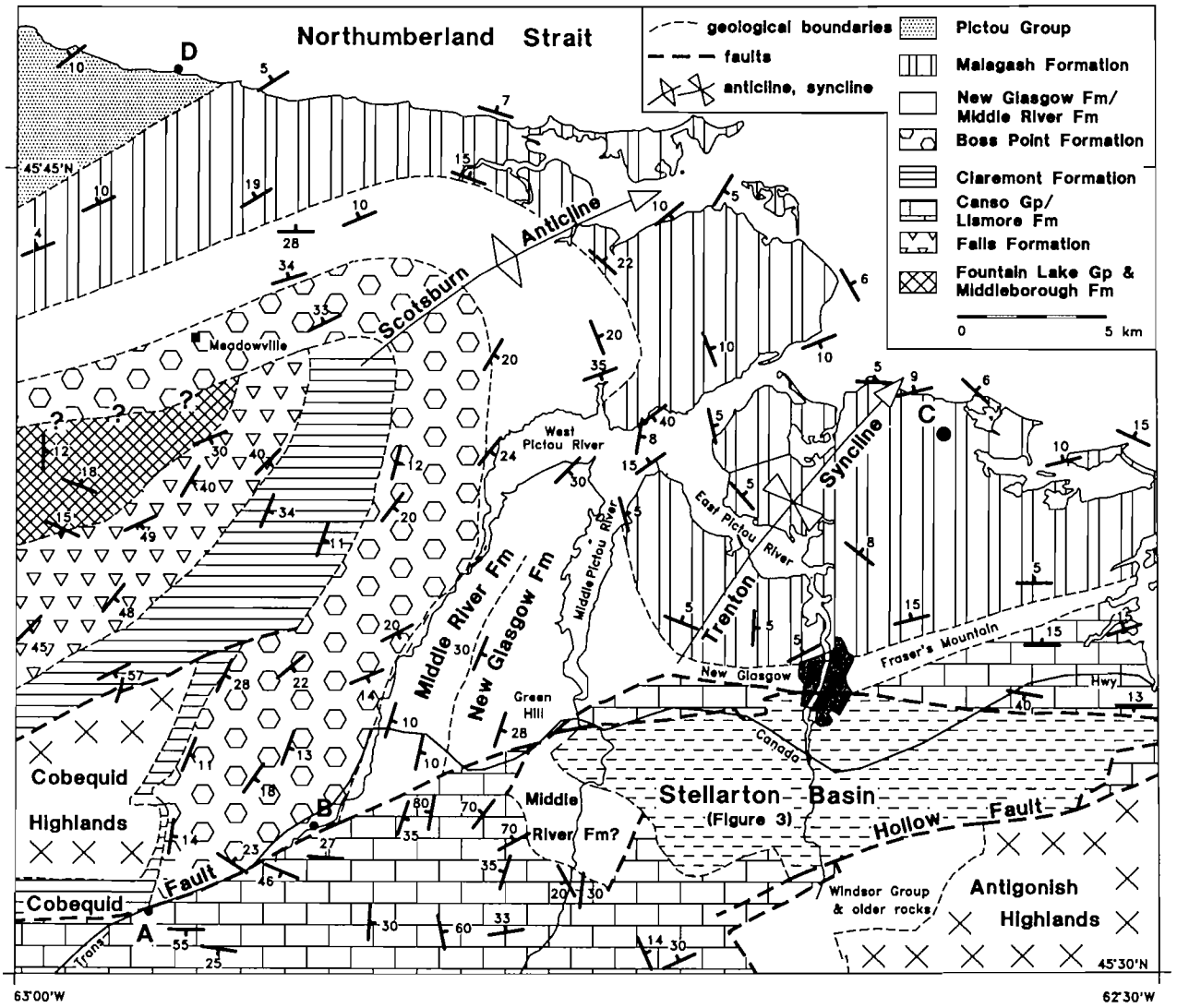

Figure 1. Geological sketch map of the Cumberland Gap, Nova Scotia, NTS 11E/10, 11E/15.

Trenton Syncline. Preliminary mapping suggests a similarly oriented anticline in the Lismore Formation on the northern margin of the Stellarton Basin. Orientation of these folds and possible swing of the Scotsburn fold axis toward east-west with time, suggest their formation is related to the dextral wrench zone (Wilcox et al., 1973).

Fountain Lake Group (Devono-Carboniferous) and (?)Middleborough Formation (Visean)

The affinity and distribution of rocks older than the Falls Formation (see below) in the core of the Scotsburn Anticline are uncertain. Gillis (1964) assigned them to the lower unit of the River John Group. Donahoe and Wallace (1982) divided this unit into a southern basaltic, and a northern sedimentary member of the Devono-Carboniferous Diamond Brook Formation. Ryan and Boehner (1990) reassigned the northern member to the upper Visean Middleborough Formation. They described it as mainly red and brown mudstone and siltstone overlain disconformably by the Claremont or Boss Point formations. In the map area these rocks are unusually deformed and primarily comprised of grey to greenish-grey sandstone with plant fragments, and subordinate interbedded grey micrite conglomerate and red siltstone-mudstone. These drab lithologies are reminiscent of the Boss Point Formation (see below), but could also belong to the Namurian Shepody Formation, that overlies the Middleborough (Ryan and Boehner, in press). Assignment of these drab beds to the overlapping Boss Point fits with our mapping, which suggests that the Boss Point Formation strikes into the Middleborough Formation as mapped by Ryan and Boehner (1990) immediately west of the map area, if the deformation is discounted. Unfortunately the Claremont Formation (see below), which separates the Shepody and Boss Point was not found on the north limb of the Scotsburn Anticline.

Falls Formation (Devono-Carboniferous)

A conglomerate on the south limb of the Scotsburn Anticline was termed the upper unit of the River John Group (Gillis, 1964) and the Falls Formation by Donahoe and Wallace (1982). The Falls Formation in the map area is comprised of interbedded red boulder to pebble orthoconglomerate, with lesser red and grey sandstone and minor mudstone and mafic volcanic flows. Conglomerate is locally size graded, size stratified, and imbricate. Clasts are subangular to angular, poorly sorted, and, in decreasing abundance, consist of: basalt, feldspar porphyry, polycrystalline quartz, red sandstone to siltstone, mafic phyllite, gabbro, and fossiliferous (brachiopod) limestone. A gloss resembling desert varnish, on many basalt clasts, as well as local calcite cement, may be evidence of arid climate. The angularity, large size, and poor sorting of the orthoconglomerate clasts, suggests that the environment of deposition was alluvial, with many clasts being derived from nearby volcanics.

Canso (Mabou) Group (Namurian A)

The Canso Group (Mabou Group, Ryan and Boehner, in press), nonmarine red and grey shale and sandstone (Bell, 1944), outcrops in the extreme southwest part of the area Donahoe and Wallace (1982). It is truncated against basement rocks of the Cobequid Highlands by the Cobequid Fault, and to the east (Yeo, 1987) unconformably underlies the (?)Middle River and Stellarton Formations. The weak metamorphism and fracture cleavage of these often steeply dipping rocks is in contrast with their absence from other Carboniferous rocks so far studied in the area. Eastward, the group contains significantly more, less metamorphosed, redbeds. In the map area the group consists of rusty weathering, strongly indurated, greywacke interbedded with cherty argillite or phyllite, interbedded on scales of several metres or less. In new exposure in an isoclinaly folded, steeply dipping, 400 m long section along the Trans-Canada Highway (location A, Fig. 1), rocks of the group are grey except for a 3 m interval of redbeds. Sand beds show a few crossbeds. Wave ripples with wavelengths as small as 1 cm and mud cracks in the argillites indicate emergence and very shallow water deposition at times.

Lismore Formation (Namurian A)

This unit underlies the New Glasgow Formation east of New Glasgow, is truncated to the south against the Stellarton Formation by the Cobequid Fault and extends about 25 km east of the map area where Benson (1974) included it in the Canso Group. It is significantly less deformed and metamorphosed than the Canso Group in the map area. Reasons could be: (a) effects of the faulting on the Canso Group, (b) possibility that the Canso Group of the map area belongs to the lacustrine facies of the Horton Group, which it resembles (pers. comm., R. Moore, 1992), and (c) that it might not be part of the Canso Group. In the map area the formation consists of fine- to medium-grained, generally green, uncommonly red, micaceous, fluvial sandstone with plant fragments. Overbank fines are drab or red with rare rootlets. Grey mudchip conglomerate at bases of sandstone units and limestone conglomerate units are also present.

Claremont Formation (Late Namurian-Early Westphalian A)

West of the map area, Ryan (1984, 1985) mapped an up to 700 m thick, reddish brown conglomerate, assigning it to the Millsville Formation of Bell (1926) as did Yeo (1987) in the Stellarton Gap. Gillis (1964) and Ryan et al. (1991), assigned it to the Claremont Formation. Ryan et al. (1992) interpreted it as an alluvial fan deposit, shed north from the Cobequid Highlands. As in the map area, this unit unconformably (Gillis, 1964, p. 38) overlies pre-Pennsylvanian strata north of the Cobequid Highlands immediately west of the map area

and is conformably overlain by the Boss Point Formation (Ryan and Boehner, in press). In the map area the formation was found only on the south limb of the Scotsburn anticline. It is mainly a red, crudely size stratified, cobble to pebble orthoconglomerate, with minor red interbedded sandstone. Sorting is poor, rounding is good, and imbrication was noted. Granitic clasts, noted by Gillis (1964) to dominate the unit, are abundant and probably come from underlying plutons in the Cobequid Highlands. Other clasts are green, red, and white quartzite and red sandstone, pebble conglomerate, and greenstone. The granite clasts distinguish the unit from the basalt clast-rich Falls Formation (Gillis, 1964; Yeo, 1987); however, to the west, Ryan (pers. comm., 1993) included rocks of the Falls Formation in the Claremont Formation, regarding the differences in clast lithology as due to differing source areas. Therefore, although the Falls and Claremont formations are clearly separable in the map area, there may well be a case for defining them as members of one formation.

Boss Point Formation (Westphalian A)

The Boss Point Formation (Ryan et al., 1991) was described from immediately west of the map area Ryan (1984) as 200-600 m of grey to brown, carbonaceous, quartz sandstone. In 1993 it was found to be less extensive in the Scotsburn Anticline (Fig. 1), than previously shown (Yeo, 1987). It strikes southwest into an area shown by Ryan and Boehner (in press) as underlain by the Middleborough Formation (see above). East of New Glasgow the formation appears absent.

In the Stellarton Gap it is composed of green and grey, medium- to fine-grained micaceous sandstone, rich in organic material, from diffuse black dust to coalified logs and tree roots. In larger exposures, overbank grey mudstone units several metres thick are visible. Lenses of carbonate, pyritized wood fragments (location B; Fig. 2), and grey mudchips occur among crossbedded sand beds, and grey and rarely red mud pebbles occur at sand bed bases. Redbeds are present in the formation up to 4 km north of the Cobequid Fault, where they resemble the Middle River Formation.

Figure 2. *Pyritized wood fragment (black) in sandstone of the Boss point Formation, Location B, Figure 1, pyrite nodules arrowed. GSC 1993-248*

Middle River Formation (Westphalian B)

Along the West River of Pictou, this red unit consists of micaceous sandstone interbedded with siltstone and blocky mudstone, in some cases in upward-fining cycles. Minor pebble to cobble conglomerate consists of fine grained sandstone of various colours and rare quartzite, reminiscent of the New Glasgow Formation (below). Red mud chip conglomerate occurs at sand bed bases. Sedimentary structures include crossbeds, abundant current lineations, current and wave ripples, mud cracks, and possible wrinkle marks (Teichert, 1970). Mudstone units contain bleached root and stem traces, and rare plant fragments.

Immediately west of this map area, Ryan (1985) mapped the Pictou grey beds (Malagash Formation of this report) to directly overlie the Boss Point, but Yeo (1987) showed the Middle River Formation as absent on the north limb of the Scotsburn Anticline. The unit is present on the northern limb of the anticline as far west as longitude 62°56.5'W. Southeast of the anticline, Yeo (1987), correlated two units, one on each side of the Cobequid Fault, as Middle River. His map (1987) showed the Middle River Formation underlying the New Glasgow conglomerate, though he reported it to overlie the New Glasgow (Yeo, 1985). Fralick and Schenk (1981, p. 92) however, seemingly addressing only the latter of Yeo's (1987) outcrop areas reported the Middle River to overlie the New Glasgow. Further, their description of the Middle River west of the Stellarton Basin does not apply well to the Middle River north of the Cobequid Fault. Therefore it is quite possible that Yeo's (1987) two areas of Middle River are not correlative.

New Glasgow Formation (Westphalian B)

The New Glasgow Formation forms the prominent, north-sloping Green Hill and east-sloping Fraser's Mountain. It consists of red, poorly sorted boulder to pebble conglomerate interbedded with red sandstone and mudstone. Rare megaclast imbrication indicates northward transport. Clasts are moderately well rounded and dominantly composed of red and drab fine grained sandstone, in contrast to other conglomerates in the area, which contain appreciable amounts of igneous material. Conglomerate units are internally, subtly size stratified and contain sandstone beds. Paraconglomerate and thick crossbedded sandstone units are absent. White calcite with geopetal fabric commonly cements the conglomerate and calcrete nodules characterize interbedded fine clastics. This carbonate indicates aridity. Decrease in abundance of the calcrete up through the unit may indicate an increasing rate of sedimentation.

Both abundance of conglomerate relative to sandstone beds and size of megaclasts demonstrate upward coarsening. From a maximum of about 60 cm, clast size decreases north. Formational thickness is difficult to assess, because the unit grades downward into the Middle River Formation. Thus it could be combined with the Middle River Formation in one upward-coarsening redbed formation, with the latter extending as a distal facies, west along the north limb of the Scotsburn Anticline.

A Westphalian late A-B, (Yeo and Gao, 1987) 0-600 m thick red polymict alluvial fan conglomerate (Cumberland coarse facies) overlies the Boss Point Formation, 20 km west of the map area and contains clasts of Carboniferous sandstone, (Ryan, 1984, 1985). This unit, the Polly Brook Formation of Ryan et al. (1991) may be a tectonic equivalent of the New Glasgow Formation.

Malagash Formation (Westphalian C-D)

West of the map area Ryan (1984) divided the Pictou Group into the Pictou greybeds, and the overlying Pictou redbeds of Westphalian C-D age. Yeo (1987) named the Pictou grey beds the Merigomish formation in this map area. Ryan et al. (1991) removed the grey beds from the group, naming them the Malagash Formation. The unit underlies much of the northeast part of the map area, and is at least 422 m thick in drill core (NSDMR stratigraphic drill core, P 58). It contains two major lithologies; (a) crossbedded grey-green, feldspathic, fluvial channel sandstone stacked in sequences of up to 60 m, with muscovite, disseminated black plant debris, and quartz and pink feldspar pebbles up to 2 cm in size, especially at crossbed bases; and (b) red, rarely mottled or grey, friable mudstone with interlayered rippled pink siltstone beds, bleached root traces, and white calcrete nodules. Minor facies associated with the channel sands include sparsely pyritic plant remains, with logs up to 5 m long; limestone pebble conglomerate – presumably reworked floodplain calcrete; red and rarely grey mud pebble conglomerate; and coal beds up to several centimetres thick. Within the mudstones, soil horizons of mottled, slickensided friable mudstone may be vertisols and black laminated argillite units may be lake deposits. The Malagash sandstone differs from the similar Boss Point in abundance of coarse, feldspathic sandstone, presence of quartz and feldspar pebbles, and generally red, overbank mudstones.

Pictou Group (Westphalian D-early Permian)

Of the three fluvial redbed formations of the group west of the map area (Ryan, 1984), only the lowest, the Balfron Formation is present, in the extreme northwest. Ryan (1985) Interpreted it as deposited in an environment like that of the Malagash Formation, with low sinuosity (possibly anastomosing) streams yielding channel sands with basal lag conglomerates. Fines, including swamp limestones, were deposited on floodplains.

In the map area the Balfron Formation consists of fine grained to gravelly, crossbedded, dominantly red sandstone units with, in some cases, calcite-cemented, basal red or green mudchip, quartz and pink feldspar pebbles conglomerate. It may contain moderate amounts of hematized or unoxidized plant trash. Red to mottled siltstone caps fining upward sandstone sequences.

Paleocurrents

Paleocurrents for correlative units west of the map area (Ryan et al., 1987) and in an inclusive regional study (Gibling et al., 1991) show broadly northward currents agreeing with reconnaissance measurements taken in 1993 in the map area.

Base metal potential

Copper

Copper mineralization in the late Carboniferous sedimentary rocks of northern Nova Scotia is commonest in the Pictou Group (Ryan et al., 1986). Redbed copper occurrences are concentrated in locally pyritized, carbonaceous fluvial channel lags and Kupferschiefer type occurs in grey shale (Ryan, 1985, 1991). At Canfield Creek (Ryan et al., 1986) Chandler found mineralization to occur in grey sandstones directly beneath reduced, overbank swamp (G. Dolby, pers. comm., 1987) deposits in an otherwise red barren sequence.

Redbed formations in the map area, suitable as aquifers for cupriferous solutions are the Falls, Claremont, Middle River-New Glasgow and Balfron. As yet the degree of diagenetic reddening in these formations, important in a copper source (Walker, 1986) is not assessed. The Boss Point and Malagash Formations, containing abundant woody material and pyrite, are potential mineralization sites, but significant red sandstone aquifers are absent from them, though some finer sands in the Malagash are red. Therefore likely sites for copper mineralization are the major redox boundaries at the upper and lower boundary of the Boss Point Formation and the lower boundary of the Malagash Formation (Rose, 1986). It is significant that the Dorchester Copper deposit (McLeod and Ruitenberg, 1978) and other copper occurrences at present being investigated in New Brunswick (M. McLeod, pers. comm., 1993) occur in grey fluvial channel sands at the base of the Boss Point. Of interest is Fletcher's (1903) definition of a copper zone north of the Scotsburn Anticline that coincides closely with the Middle River-New Glasgow Formation. The one new example of copper mineralization found in 1993, of chalcopyrite and malachite fringing coal fragments (Fig. 2) is in grey sandstone at the base of the Balfron Formation (location D, Fig. 1). Of five other Cu showings in the map area north of the Cobequid Fault (Ryan, 1991; Yeo, 1987), three are close to red-drab formational boundaries.

Another Cu metallotect is the Cobequid Fault which at Salt Springs brings chloride solutions, a major Cu solvent (Rose, 1986) into the vicinity of, for example, the Boss Point-Middle River formation boundary. This factor may have operated in the formation of the Canfield Deposit, west of the map area (see Ryan et al., 1986), which lies on the flank of a salt dome.

Lead and zinc

In winter 1992-93 Rio Algom Exploration Inc. measured >10 000 ppm Pb over 0.45 m (atomic absorbtion spectroscopy), >10 000 ppm Zn over 0.5 m (inductively coupled plasma, optical emission) and >10 000 ppm Pb and Zn over 0.34 m from drill core M1 in the Boss Point Formation at Meadowville (Fig. 1). Sangster and Vaillancourt (1990) concluded Pb mineralization at Yava is richest in the grey, quartz, kaolinite, plant debris rich, Westphalian A, Silver Mine Formation, where it overlies channels in felsic basement. Close lithological similarity between the Boss Point and the Silver Mine Formation, were noted by the first writer and by D. Sangster (pers. comm., 1993). A point of difference is that although basement to the Boss Point occurrence includes the granite-rich Claremont Formation similar to the Uist Formation at Yava, it lacks gypsum-rich units and a subjacent major unconformity on felsic igneous rocks.

STRATA WITHIN THE STELLARTON BASIN

Introduction

The 6 km x 20 km. Stellarton Basin (Fig. 1, 3) has been the subject of geological research for over 145 years. Early workers (e.g., Bell, 1940) recognized it as fault bounded and containing approximately 2600 m of coal-bearing Westphalian strata which he designated the Stellarton Formation. Hacquebard and Donaldson (1969) were the first to clearly suggest that the basin was an isolated sub-basin and not a structural remnant of a much larger coal basin. Subsequently Yeo and Gao (1987) and Naylor et al. (1989; 1992) agreed that the basin was a late Westphalian B to early D depocentre/sub-basin of the much larger Maritimes Basin. The main purpose of our research is to refine stratigraphic, depositional, and structural models of the Stellarton Formation to aid future coal exploration and mine planning within it.

Structural geology

The Stellarton Basin, located at a releasing bend in the Cobequid-Hollow fault system (Fig.1), approximates a classic pull-apart structure formed under dextral progressive simple shear (Yeo and Gao, 1987). However faults within the basin show a variety of orientations and some are curved. Movements on curved faults would have led to additional syn- or postdepositional folding of the Stellarton Formation. The complexity of the fold pattern is therefore interpreted to be partly due to fault-bend folding, in addition to homogenous distortion of the entire basin.

Stratigraphy and depositional environments

Bell (1940) proposed a six Member division of the Stellarton Formation (Fig. 3). The redbed dominated Skinner Brook and Plymouth members are best developed near the basin margins and interfinger toward the basin centre with the grey coal-bearing strata of the Westville and Albion members. The Coal Brook and Thorburn members contain a total of 42 oil shale beds interbedded with coal, grey mudrock, and sandstone.

The Stellarton Formation consists of lacustrine, swamp, and alluvial fan deposits exhibiting rapid lateral facies changes (Naylor et al., 1989). Despite the complex lithostratigraphy, correlation of coal seams and oil shales has provided a detailed stratigraphic framework for depositional modelling (Naylor et al., 1989). Currently we are studying two stratigraphic intervals: the Foord to Cage seam interval of the Albion Member, and oil shale 35 to 36 of the Coal Brook Member (Fig. 3 and 4). Figure 4 illustrates examples of the typical stratigraphy and sedimentology of each of the study intervals.

The Foord to Cage seam interval can show marked lateral thickness changes with a decrease in thickness usually accompanied by an overall fining (Fig. 4A). Immediately below the Foord seam the interval consists of impure coals and carbonaceous to coaly mudrock interbedded with mudrock and fine grained sandstone (Fig. 4A, B). Development of roots and immature paleosols with siderite nodules (Fig. 4B) have extensively disrupted bedding of the mudrock and fine grained sandstone. Underlying this unit is an oil shale-dominated interval that locally contains some sandstone and mudrock interbeds (Fig. 4A). The oil shale is black, may exhibit faint colour banding and locally contains ostracode, bivalve, fish, insect wing, and plant fossils (Fig. 4A). Between the oil shale unit and the top of the Cage seam the dominant lithologies are rhythmically layered claystone with varve-like laminae and lenticular to ripple-bedded siltstone and fine grained sandstone (Fig. 4A, C). Plant fragments, siderite bands, and rare possible desiccation cracks occur in the rhythmically layered mudrock. The rippled sandstone contains occasional bivalve escape burrows (Fig. 4C).

The interval between oil shale 35 and 36 of the Coal Brook Member also exhibits significant lateral thickness changes (Fig. 4D). The thickest intervals (e.g., drill hole 0395 Fig. 4D) consist largely of fine- to medium-grained planar bedded and rippled sandstone. When planar bedded sandstone is dominant, parting lineations, tool marks, erosional contacts, intraformational clasts, and transported fossil trees are common (Fig. 4E.). When rippled and planar bedded sandstone are about equally abundant they commonly form 10 cm to 50 cm fining-upward sequences capped by thin (<2 cm) claystone drapes (Fig. 4F). The rippled sandstone contains occasional bivalve escape burrows and numerous laminae of finely macerated organic matter. The interbedded planar bedded and rippled sandstone pass laterally and vertically into rippled sandstone interbedded with siltstone with lenticular laminae (Fig. 4D). These intervals consist of 5 to 30 cm thick sequences capped by thin claystone drapes (Fig. 4G). The rippled sandstone and siltstone with lenticular laminae pass laterally and vertically into mudrocks with varve-like laminae (Fig. 4D). Sedimentary structures in the strata between oil shales 35 and 36 are excellently preserved and bioturbation by roots was noted only immediately beneath oil shale 35 in drill hole 0395 (Fig. 4B).

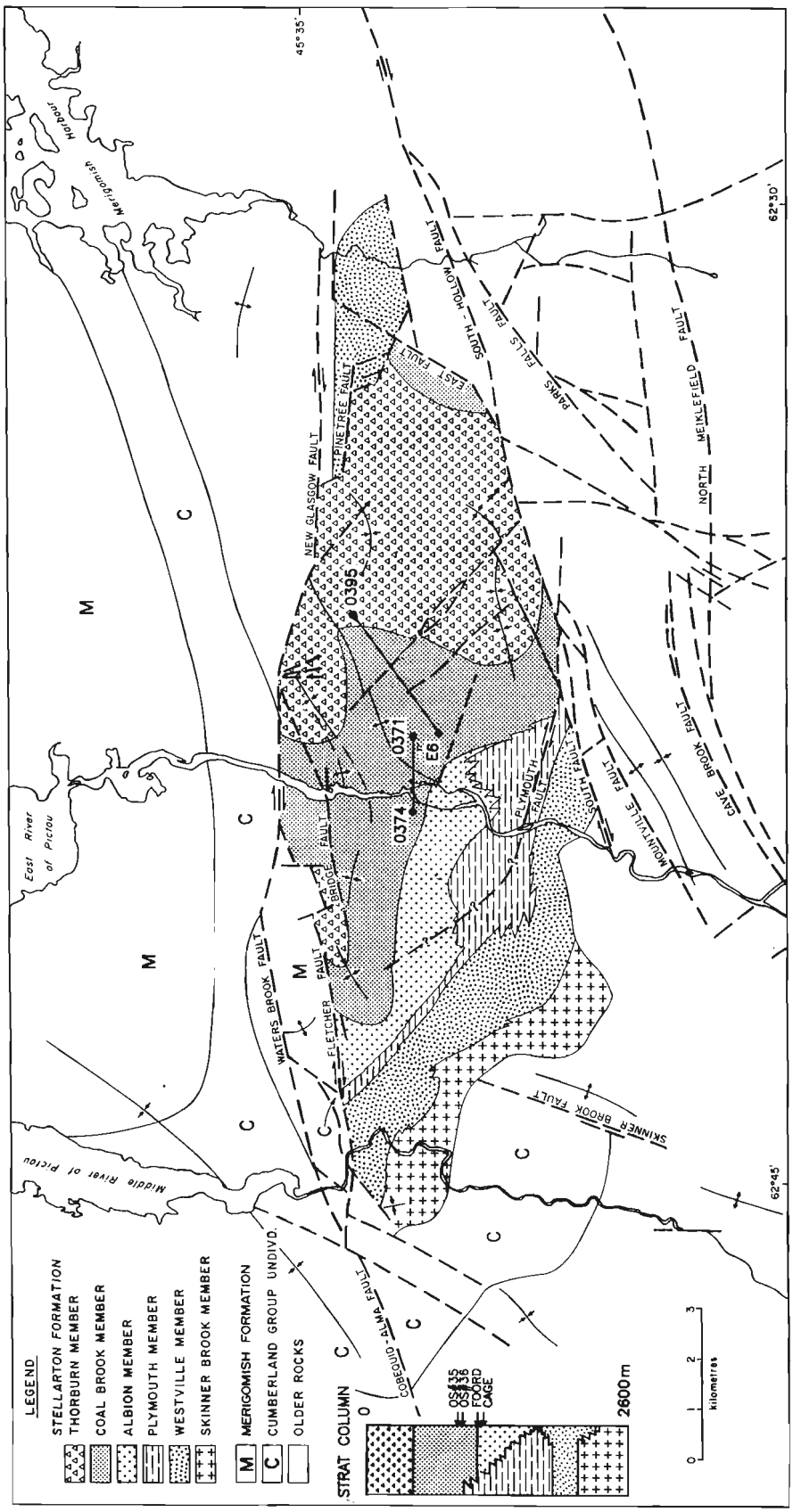

Figure 3. *Geological map and stratigraphic column of the Stellarton Basin showing member subdivisions, location of the Foord and Cage seams, oil shales 35 and 36 and the cross-sections illustrated by Figure 4.*

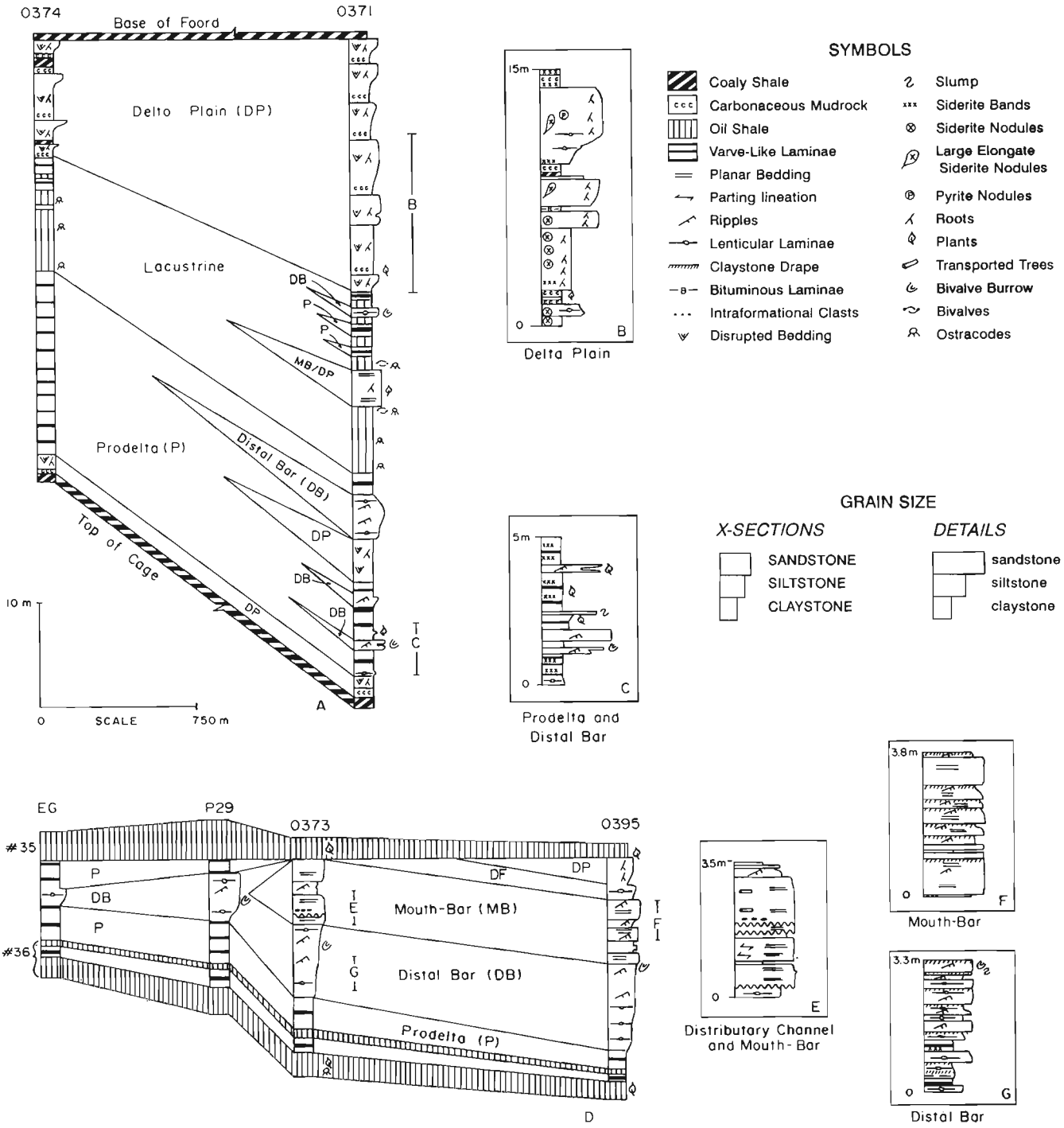

Figure 4. *Cross-sections and detailed graphic logs of the Foord to Gage seam and oilshale 35 to 36 intervals, illustrating the typical stratigraphy, sedimentology, and deposit types of the Albion Member (Fig. 4A-C) and the Coal Brook Member (Fig. 4D-G).*

Coal, carbonaceous mudrock, rooted siliciclastics, and paleosols are unique to the Albion study interval. Thick, laterally extensive coals such as the Ford (maximum 13.4 m) and Cage appear to have formed from mires covering much of the basin floor. Thin impure coals and coaly mudstones probably originated as localized mires and poorly drained swamps on lacustrine delta plains. The siliciclastics with extensively disrupted bedding, paleosols, and roots are interpreted to be abandoned lacustrine delta plain deposits.

The Albion and Coal Brook study intervals both contain sandstone with rippled and planar bedding, siltstone with lenticular laminae, and rhythmically layered claystone with varve-like laminae. The rarity of desiccation features, paleosols, and fossil roots, coupled with the varve-like bedding of the mudrocks suggests that these are subaqueous deposits of lacustrine deltas that partly infilled perennial lakes. Planar bedded sandstones are interpreted as mouth-bar and subaqueous distributary channel deposits (Figs. 4E, F). Siltstone with lenticular laminae and rippled sandstone are interpreted as distal bar deposits (Fig. 4G). Claystones with varve-like laminae are likely the most distal (prodelta) lacustrine delta deposits.

The oil shales of both study intervals are very similar except that the Albion oil shales seem to contain less organic material. The fine grain size of these oil shales suggests that they formed in lakes with a very restricted sediment supply. Strongly reducing conditions in lake bottom sediments would have allowed preservation of plant material, ostracodes, bivalves, and insect wings. Oxygenated waters would have been required to allow colonization of the lakes by bivalves and ostracodes.

ACKNOWLEDGMENTS

Tom Connors and Shirley Ross of the Stellarton Office, and Jim Langille and Bill Palmer of the core library of the Nova Scotia Department of Natural Resources provided very helpful logistical support. Bob Boehner of NSDNR and Brendan Murphy of St. Francis Xavier University gave valuable geological and logistical advice. Finally, in sharing with us his extensive experience in late Carboniferous rocks, Bob Ryans (NSDNR) greatly increased the depth of our perception.

REFERENCES

Bell, W.A.
1926: Carboniferous Formations of the Northumberland Strait, Nova Scotia; Geological Survey of Canada, Summary Report, 1924, Part C, p. 142-180.
1940: The Pictou Coalfield Nova Scotia; Geological Survey of Canada, Memoir 225, 160 p.
1944: Carboniferous rocks and fossil floras of northern Nova Scotia; in Canada Department of Mines and Resources, Mines and Geology Branch, Bureau of Geology and Topography, Geological Survey of Canada, Memoir 238, p. 1-54.

Benson, D.G.
1974: Geology of the Antigonish Highlands, Nova Scotia; Geological Survey of Canada, Memoir 376, 92 p.

Donahoe, H.V. and Wallace, P.I.
1982: Geological Map of the Cobequid Highlands, Colchester, Cumberland and Pictou Counties, Nova Scotia; Nova Scotia Department of Mines and Energy, Map 82-9, scale 1:50 000.

Fletcher, H.
1903: Pictou County, Nova Scotia; Geological Survey of Canada, Sheet No. 46, Part P, Annual report, V. V, Part II, 1890-1991, scale 1 inch to 1 mile.

Fralick, P.W. and Schenk, P.E.
1981: Molasse deposition and basin evolution in a wrench tectonic setting: the late Paleozoic, Eastern Cumberland Basin, Maritime Canada; in Sedimentology and tectonics in alluvial basins, (ed.) A.D. Miall; Geological Association of Canada, Special Paper 23, p. 77-97.

Gibling, M.R., Calder, J.H., Ryan, R., van de Poll, H.W., and Yeo, G.M.
1991: Late Carboniferous and Early Permian drainage patterns in Atlantic Canada; Canadian Journal of Earth Sciences, v. 29, p. 338-352.

Gillis, J.W.
1964: Geology of Northwestern Pictou County, Nova Scotia, Canada; Ph.D. thesis Pennsylvania State University, 130 p.

Hacquebard, P.A. and Donaldson, J.R.
1969: Carboniferous coal deposition associated with floodplain and limnic environments in Nova Scotia; Geological Society of America, Special Paper 114, p. 143-190.

McLeod, M.J. and Ruitenberg, A.A.
1978: Geology and mineral deposits of the Dorchester area, map area W-22, W-23 (21H/15E, 21H/16W); New Brunswick Department of Mineral Resources, Mineral Resources Branch, Map Report 78-4, 27 p.

Murphy, J.B., Keppie, J.D., and Hynes, A.J.
1991: The Geology of the Antigonish Highlands, Nova Scotia; Geological Survey of Canada, Paper 89-10, 115 p.

Murphy, J.B., Pe-Piper, G., Nance, D., Turner, D., and Piper, D.J.W.
1988: Preliminary Geological Map of the Eastern Cobequid Highlands; Geological Survey of Canada, Open File 1788, 2 maps, scale 1:50 000.

Naylor, R.D., Kalkreuth, W., Smith, W.D., and Yeo, G.M.
1989: Stratigraphy, sedimentology and depositional environments of the coal-bearing Stellarton Formation, Nova Scotia; in Contributions to Canadian Coal Geoscience, Geological Survey of Canada, Paper 89-8, p. 2-13.

Naylor, R.D., Calder, J.H., Ryan, R.J., and Martel, T.A.
1992: Controls on formation of upper Carboniferous coals in the intermontane Stellarton and Cumberland Basins of Atlantic Canada; in Proceedings of the Canadian Coal and Coalbed Methane Geoscience Forum Parksville, British Columbia, p. 365-397.

Rose, A.W.
1986: Mobility of copper and other heavy metals in sedimentary environments; in Sediment-hosted Stratiform Copper Deposits, (ed.) R.W. Boyle, A.C. Brown, C.W. Jefferson, E.C. Jowett, and R.V. Kirkham, Geological Association of Canada, Special Paper 36, p. 97-110.

Ryan, R.J.
1984: Upper Carboniferous strata of the east half of the Tatamagouche syncline, Cumberland Basin, Nova Scotia; in Current Research, Part A; Geological Survey of Canada, Paper 84-1A, p. 473-476.
1985: Upper Carboniferous strata of the Tatamagouche syncline, Cumberland Basin, Nova Scotia; in Current Research, Part A; Geological Survey of Canada, Paper 85-1A, p. 481-490.
1991: Selected mineral occurrences of the Cumberland and Stellarton Basins and their metallogenic implications; Nova Scotia Department of Mineral Resources, Open File Report 91-016, 197 p.

Ryan, R.J. and Boehner, R.C.
1990: Cumberland Basin geological map, Tatamagouche and Malagash, Cumberland, Colchester and Pictou Counties; Nova Scotia Department of Natural Resources, Map 90-14, scale 1:50 000.

Ryan, R.J., Boehner, R.C., and Calder, J.H.
1991: Lithostratigraphic Revisions of the upper Carboniferous to lower Permian strata in the Cumberland Basin, Nova Scotia and the regional implications for the Maritimes Basin in Atlantic Canada; Bulletin of Canadian Petroleum Geology, v. 39, p. 289-314.
in press: Geology of the Cumberland Basin, Colchester and Pictou Counties, Nova Scotia; Nova Scotia Department of Mines and Energy, Memoir 8.

Ryan, R.J., Boehner, R.C., Stea, R.R., and Rogers, P.J.
1986: Geology, geochemistry and exploration applications for the Permo-Carboniferous redbed copper deposits of the Cumberland Basin, Nova Scotia, Canada; in Sediment-hosted Stratiform Copper Deposits, (ed.) R.W. Boyle, A.C. Brown, C.W. Jefferson, E.C. Jowett, and R.V. Kirkham; Geological Association of Canada, Special Paper 36, p. 245-256.

Ryan, R.J., Calder, J.H., and Boehner, R.C.
1987: Pennsylvanian sediment dispersal trends in the Cumberland Basin of northern Nova Scotia; Nova Scotia Department of Mines and Energy, Report 88-1, p. 165-169.

Ryan, R.J., Grist, A.M., and Zentilli, M.
1992: The Paleozoic maritimes basin of eastern Canada: metallogenetic implications of a fission track study; Mineralogical Association of Canada, Short Course handbook on low temperature thermochronology, (ed.) M. Zentilli and P.H. Reynolds; p. 141-155.

Sangster, D.F. and Vaillancourt, P.D.
1990: Geology of the Yava sandstone-lead deposit, Cape Breton Island, Nova Scotia, Canada; in Mineral deposit Studies in Nova Scotia, Volume 1, (ed.) A.L. Sangster; Geological Survey of Canada, Paper 90-8, p. 203-244.

Teichert, C.
1970: Runzelmarken (wrinkle marks); Journal of Sedimentary Petrology, v. 40, p. 1056-1057.

Walker, T.R.
1986: Application of diagenetic alterations in redbeds to the origin of copper in stratiform copper deposits; in Sediment-hosted Stratiform Copper Deposits; (ed.) R.W. Boyle, A.C. Brown, C.W. Jefferson, E.C. Jowett, and R.V. Kirkham; Geological Association of Canada, Special Paper 36, p. 83-96.

Wilcox, R.E., Harding, T.P., and Seely, D.R.
1973: Basic Wench Tectonics; American Association of Petroleum Geologists, Bulletin, v. 57, p. 74-96.

Yeo, G.M.
1985: Upper Carboniferous sedimentation in northern Nova Scotia and the origin of the Stellarton Basin; in Geological Survey of Canada, Paper 85-1B, p. 511-518.
1987: Geological Map of the New Glasgow-Tony River area (NTS 1E/10 and 11E15): Geological Survey of Canada, Open File 1656, scale 1:50 000.

Yeo, G.M. and Gao, R.
1987: Stellarton Graben: a late Carboniferous pull apart basin in northern Nova Scotia; in Basins and basin forming mechanisms; (ed.) C. Beaumont and T. Tankard; Canadian Society of Petroleum Geologists, Memoir 2, p. 299-309.

Geological Survey of Canada Project 760027

Petrology and geochemistry of altered volcanic and sedimentary rocks associated with the FAB stringer sulphide zone, Bathurst, New Brunswick[1]

David R. Lentz[2] and Wayne D. Goodfellow
Mineral Resources Division

Lentz, D.R. and Goodfellow, W.D., 1994: Petrology and geochemistry of altered volcanic and sedimentary rocks associated with the FAB stringer sulphide zone, Bathurst, New Brunswick; in Current Research 1994-D; Geological Survey of Canada, p. 123-133.

Abstract: The FAB zone is a laterally extensive zone of transposed stringer vein and disseminated sulphide mineralization that crosscuts the Nepisiguit Falls Formation and the underlying Patrick Brook Formation. These siliceous chlorite-sulphide veins are pyrrhotite-rich with lesser amounts of pyrite, sphalerite, and chalcopyrite with grades of 0.2 to 0.5% Cu and 0.2 to 1.0% Zn. Five core intervals from two drill holes (229-1 and 229-2) were analyzed for chemostratigraphic and alteration studies. The Patrick Brook, Nepisiguit Falls and Flat Landing Brook formations are distinguished on the basis of their TiO_2, Zr, Y, Yb, Sc, Cr, and V contents. Sulphide veins occur with two alteration types in the Nepisiguit Falls and Patrick Brook formations: i) albite-Mg chlorite alteration with elevated Na, Ca, Mg, and CO_2 contents relative to least-altered parent rocks; and ii) vent-proximal Fe chlorite-quartz alteration with high Fe, S, Co, Cu, and Zn contents relative to least-altered parent rock. The latter type is texturally and mineralogically similar to stringer sulphide mineralization underlying the Brunswick No. 12 deposit.

Résumé : La zone FAB est une zone de grande étendue latérale composée d'une minéralisation transposée de sulfures filoniens et disséminés qui recoupe la Formation de Nepisiguit Falls et la Formation de Patrick Brook sous-jacente. Ces filons siliceux à sulfures et chlorite sont riches en pyrrhotine et continnent des quantités moindres de pyrite, de sphalérite et de chalcopyrite avec des teneurs en Cu de 0,2 à 0,5 % et en Zn de 0,2 à 1,0 %. Cinq intervalles carottés provenant de deux trous (229-1 et 229-2) ont été analysés afin de déterminer le stratigraphie chimique et d'étudier l'altération. Les formations de Patrick Brook, de Nepisiguit Falls et de Flat Landing Brook se distinguent par leurs teneurs en TiO_2, Zr, Y, Yb, Sc, Cr et V. Les filons sulfurés sont accompagnés de deux types d'altération dans les formations de Nepisiguit Falls et de Patrick Brook : i) une altération d'albite-chlorite magnésienne à fortes teneurs en Na, Ca, Mg et CO_2 par rapport aux roches mères moins altérées; et ii) une altération de chlorite ferrifère-quartz à proximité de la zone de griffon à teneurs élevées en Fe, S, Co, Cu et Zn par rapport aux roches mères moins altérées. Ce deuxième type est, par sa texture et sa minéralogie, semblable à la minéralisation en filonnets sulfurés située sous le gisement Brunswick n° 12.

[1] Contribution to Canada-New Brunswick Cooperation Agreement on Mineral Development (1990-1995), a subsidiary agreement under the Canada-New Brunswick Economic and Regional Development Agreement.
[2] Geological Survey of Canada, P.O. Box 50, Bathurst, New Brunswick E2A 3Z1

INTRODUCTION

The FAB zone, the most significant known base-metal occurrence between the Brunswick No. 6 and 12 deposits (Fig. 1), consists of a large pyrrhotite-pyrite-rich stringer zone with associated intense chloritic and sericitic alteration. The mineralization transgresses the contact between crystal tuffite of the Nepisiguit Falls Formation and shale of the Patrick Brook Formation. These formations comprise the stratigraphic footwall to the Brunswick horizon located about 500 m to the west (Fig. 2 and 3).

Named after Fred A. Boylen, the zone was first staked by FAB Metal Mines Limited and was drilled extensively during the early 1950s. The FAB zone consists of chalcopyrite-pyrrhotite-pyrite mineralization that crosscuts graphitic shale and quartz wacke of the Patrick Brook Formation and crystal-rich volcaniclastic rocks of the Nepisiguit Falls Formation, but does not extend into the overlying Flat Landing Brook Formation. The lithostratigraphy, structure, and alteration mineralogy have been described by Lentz and Goodfellow (1993a). Of the 229- and 218-series diamond-drill holes (DDH) used in the geological compilation, DDH 229-1 and 229-2 transect a portion of the sulphide stringer zone and best illustrate the hydrothermal alteration associated with the FAB zone (Fig. 2 and 3). In order to determine the geochemical characteristics of the Flat Landing Brook, Nepisiguit Falls, and Patrick Brook formations, to quantify chemical changes related to hydrothermal alteration, and to compare mineralogical and geochemical effects of alteration at FAB with those documented for the Brunswick No. 12 deposit, a total of 24 samples were taken from DDH 229-1 and 229-2. These include 9 from the Patrick Brook Formation, 11 from the Nepisiguit Falls Formation, and 4 from the Flat Landing Brook Formation in five core segments (A-E). This work is part of a New Brunswick-Canada Agreement on Mineral Development project to map and mineralogically and geochemically characterize hydrothermal alteration associated with massive sulphide deposits of the Brunswick Belt.

STRATIGRAPHY

The rocks in the FAB area have been described in the context of the tectonostratigraphic framework of the Bathurst Camp (van Staal and Fyffe, 1991; Rice and van Staal, 1992) and the nearby Brunswick No. 12 massive sulphide deposit (Luff et al., 1992; Fig. 1). Protolith names are used even though the rocks have, in many cases, been intensely deformed and metamorphosed to upper greenschist grade.

In the vicinity of the FAB zone, the least-altered rocks of the Patrick Brook Formation consist of grey to black, thin- to thick-layered light shale (slate) and quartz wacke (cf., Rice and van Staal, 1992; see Fig. 5a below). These rocks are texturally and mineralogically similar and stratigraphically

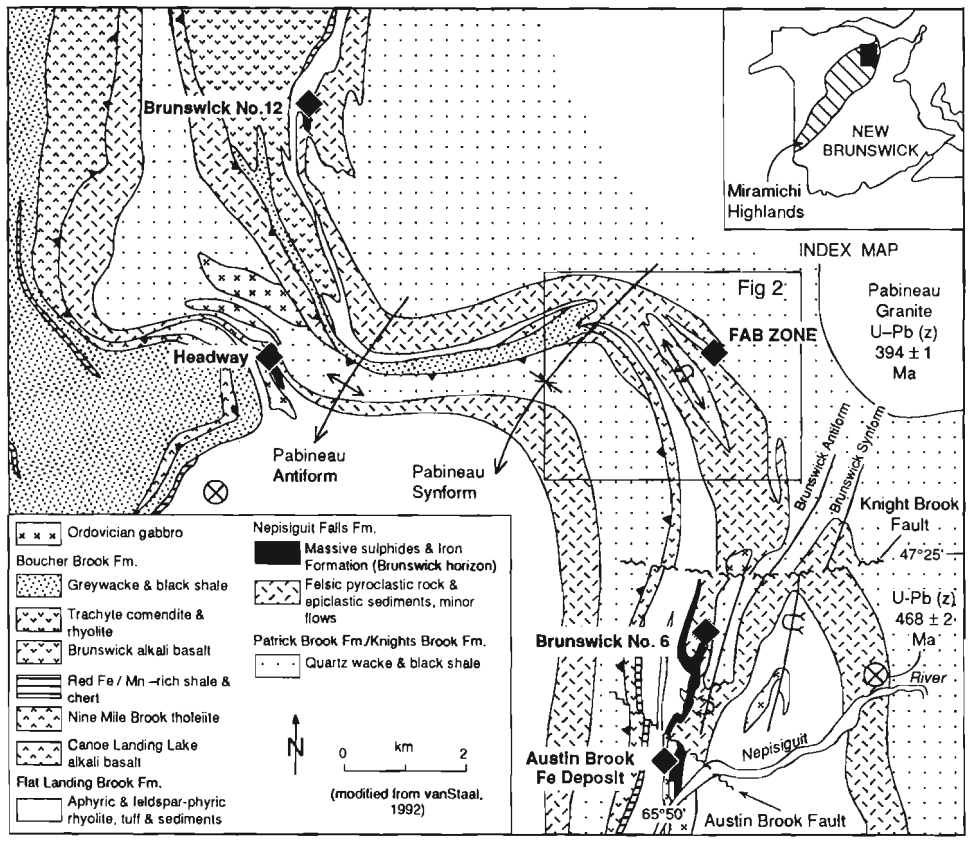

Figure 1. *Geology of the Brunswick No. 6 and 12 deposits and adjacent areas (modified after van Staal, 1992) with the location of the FAB area (Fig. 2).*

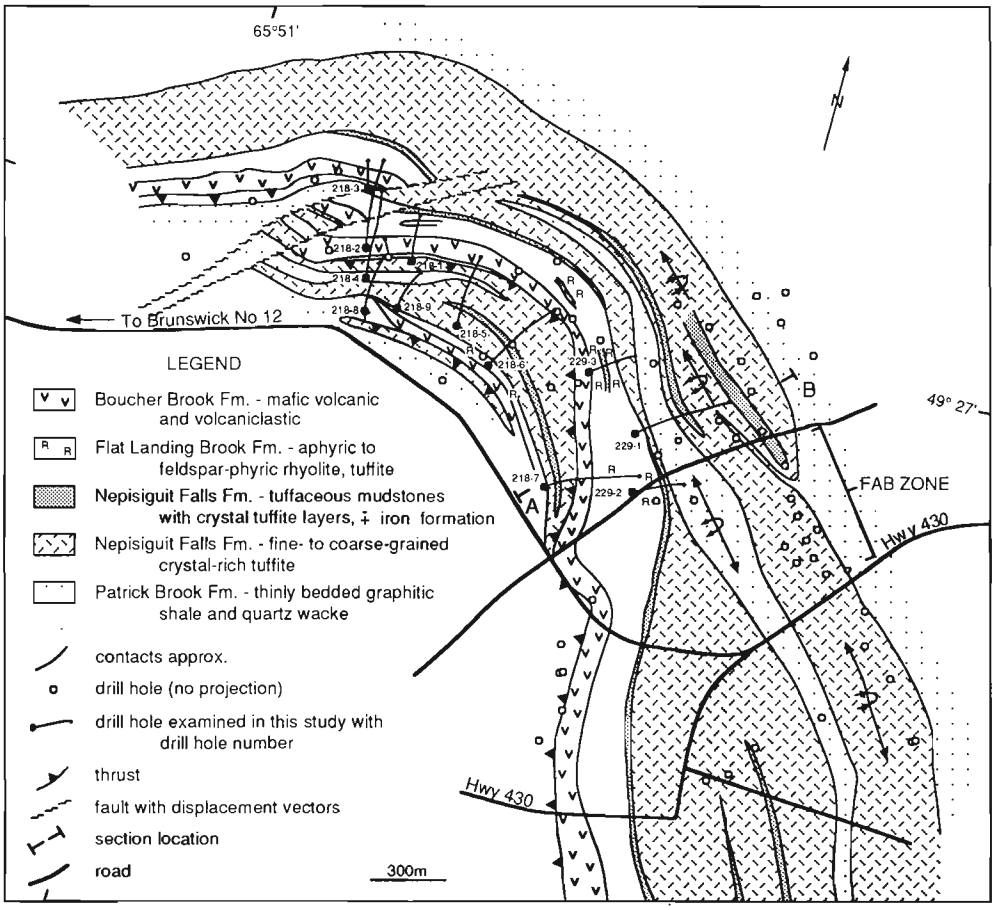

Figure 2. *Geological compilation of the FAB area showing drill holes DDH 229 and 218 examined in this study. A-B profile is illustrated in Figure 3 (modified from Brunswick Mining and Smelting Corporation Limited map).*

equivalent to the older metasedimentary rocks (OM) at the Brunswick No. 12 deposit (cf., Luff et al., 1992). Rare vitreous volcanic quartz phenoclasts are present. Graphite and minor pyrite (<1 vol.%) are common in the least-altered areas. Grey-green, fine- to medium-grained, massive diorite-gabbro dykes, up to 40 m in apparent thickness, occur near the contact between the Patrick Brook and Nepisiguit Falls formations. The general absence of sulphide veins and alteration in these dykes near and within the FAB zone indicates that they postdate the main mineralizing episode (Lentz and Goodfellow, 1993a).

In the FAB area, volcaniclastic rocks of the Nepisiguit Falls Formation exhibit grading, heterogeneous crystal size and distribution, and are interlayered with homogeneous, fine grained sedimentary rocks, probably tuffaceous in origin. These features are consistent with subaqueous reworking of pyroclastic rocks similar to those at the Nepisiguit Falls-type locality (cf., van Staal et al., 1992). Weakly altered Nepisiguit Falls rocks are present in the FAB area, but they are rare near the FAB mineralized zone. The rocks are beige or buff to light green and contain numerous fine- to coarse-grained, vitreous quartz and feldspar phenoclasts. These altered volcaniclastic

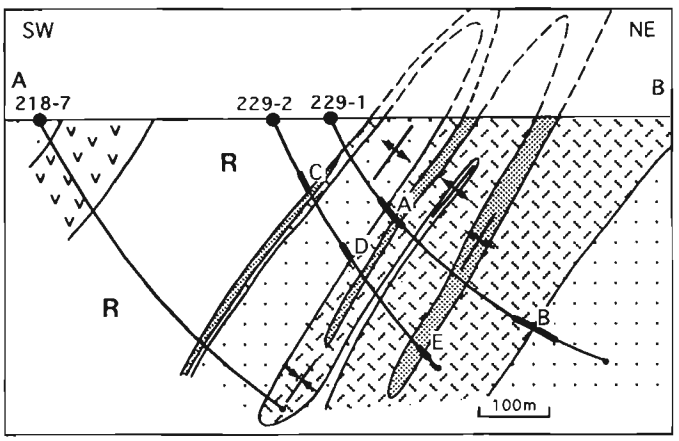

Figure 3. *Geological section through the FAB occurrence showing the structural repetition of stratigraphic units. The Brunswick horizon occurs at the contact between the Flat Landing Brook and Nepisiguit Falls formations. Letters A to E represent sampled segments (Fig. 7a, b). See Figure 2 for legend and symbols.*

and sedimentary rocks generally have a better developed fabric than weakly altered volcaniclastic rocks of the Nepisiguit Falls Formation. The Flat Landing Brook Formation comprises aphyric to feldspar-phyric rhyolite, flow-top breccias and hyaloclastites (McCutcheon, 1992), and possibly reworked crystal tuffites from the stratigraphically underlying Nepisiguit Falls Formation.

Mafic volcanic flows, hyaloclastites, and interbedded reddish, greenish to dark grey, and black shale and chert of the Boucher Brook Formation overlie the felsic volcanic rocks of the Flat Landing Brook Formation. The mafic volcanic rocks are mineralogically and texturally heterogenous and correlative with alkali basalt that overlies the Brunswick No. 12 deposit. The sedimentary rocks may be recognized by their medium to dark green chlorite and lime green epidote, the latter of which is generally absent in the felsic volcaniclastic rocks.

STRATIGRAPHIC AND STRUCTURAL INTERPRETATION

The rocks the FAB area have been subdivided into eastern and western domains that are separated by a zone of high strain located near the top of the Brunswick alkali basalt (Boucher Brook Formation; Fig. 1 and 2). This zone is interpreted to be a thrust fault (van Staal, 1992). The rocks have been folded by several tight to isoclinal F_1 and F_2 folds (S_1S_2 composite fabric) that can explain the stratigraphic repetition of units (Fig. 2 and 3). In the FAB zone, the stringer-sulphide veins crosscut or transgress the contact between the Nepisiguit Falls and Patrick Brook formations, similar to syngenetic/epigenetic stringer-sulphide veins at the Brunswick No. 12 deposit, indicating stratigraphic continuity between these formations. The most highly mineralized sedimentary rocks, which are similar to the mineralized footwall sedimentary rocks at the Brunswick No. 6 and 12 deposits, form a structural keel within the crystal-rich tuffites at the structural base of the Nepisiguit Falls sequence (Fig. 3). Open to tight refolding of the composite S_1 and S_2 fabric is attributed to the steeply south-plunging Pabineau synform (F_5) north of the FAB occurrence (Fig. 1 and 2). There are several major northeast-trending faults (Fig. 2) that are recognized by brecciated zones containing milky white bull quartz veins and altered cataclastic zones (Lentz and Goodfellow, 1993a).

Despite the structural complexities, a stratigraphic feature that is readily apparent is the westward thinning of the volcaniclastic and related sedimentary rocks of the Nepisiguit Falls Formation (Fig. 2 and 3). Stratigraphic thinning of these sedimentary rocks has been observed in the eastern structural domain, where the chlorite-siderite iron-formation (Brunswick exhalative horizon) overlies a thin bed of footwall sedimentary rocks. In this area, a less than 1 m thick chert-chlorite iron-formation, noted in DDH 229-2, is directly overlain by rhyolite of the Flat Landing Brook Formation that dips uniformly westward. The footwall sedimentary rocks and crystal tuffites are variable in thickness and degree of alteration beneath the iron-formation to the north and south along this fold limb, although alteration intensity is less than that around the FAB zone.

The abundance of veins and the attendant intensity of alteration decrease north and south of the FAB zone, although minor sulphide mineralization occurs along the contact between the Nepisiguit Falls and Patrick Brook formations. Stringer-sulphide mineralization, similar to the FAB zone, is also present for several kilometres to the south between the FAB zone and the Brunswick No. 6 deposit. The intensity of alteration within the crystal tuffites generally decreases toward the west, coincident with the thinning of the Nepisiguit Falls Formation, although a thin package of altered and veined footwall sedimentary rocks (Nepisiguit Falls Formation) was intersected (DDH 229-2) on the eastern limb of the large F_2 anticline that is cored by rocks of the Patrick Brook Formation. Significant exhalative sulphide mineralization has not been found along the Brunswick horizon in this area.

STRINGER-SULPHIDE MINERALIZATION AND ALTERATION MINERALOGY

In many areas within the FAB zone, dark grey to black graphitic shale and quartz wacke of the Patrick Brook Formation have been so intensely altered, particularly near zones of stringer-sulphide veins, that they resemble fine grained, light grey-green sericitized tuff, silicified tuff, and chert (Fig. 4). In addition to the sulphide veining and bleaching (destruction of organic matter), chloritization, sericitization, and silicification are recognized in moderately to intensely altered rocks. Even in the weakly to moderately altered rocks, textural mottling has partly to entirely obliterated bedding features. Intense sulphide veining and chloritization have destroyed all primary textures in some areas. Altered rocks of the Patrick Brook Formation have been misidentified as fine-grained, tuffaceous sedimentary rocks in the past; however, they may be distinguished from the tuffites by their thin-bedded character and association with quartz wacke. Siliceous sulphide veins (1 to 5 vol.%) also cut unaltered graphitic shales of the Patrick Brook Formation. These features are similar to those described for graphitic shales near the core of the Brunswick No. 12 hydrothermal discharge conduit (cf., Lentz and Goodfellow, 1993b, c).

The crystal-rich tuffites and sedimentary rocks of the Nepisiguit Falls Formation exhibit various degrees of chloritic, sericitic, and silicic alteration both within and adjacent to zones of sulphide veining. Alteration imparts a mottled appearance due to replacement of primary textural features by alteration assemblages. This includes feldspar-destructive alteration that when metamorphosed and tectonically deformed has generated quartz-augen schists (Lentz and Goodfellow, in press; Fig. 5a). Some of the sulphide veins have a bedded appearance that superficially resembles exhalative sulphides (Fig. 5b). Fe-rich hydrothermal chlorite is commonly associated with pyrite porphyroblasts in a chloritic and siliceous pyrrhotite vein groundmass (Fig. 5c). In some areas, quartz-sulphide veins occur in weakly to moderately altered,

quartz-feldspar crystal-rich tuffite indicating that sulphide mineralization is also outside areas of intense hydrothermal alteration.

Rhyolites of the Flat Landing Brook Formation that stratigraphically overlie the siderite-chlorite iron-formation are weakly veined and altered up to 30 m above the contact. The rhyolite is bleached and brecciated in situ (pseudopyroclastic texture), contains minor sulphide veins, and is altered to sericite and chlorite, which generally increase in abundance toward the contact with the iron-formation. This alteration may be related to the mineralizing event or may be a product of localized hydrothermal alteration, which accompanied rhyolite emplacement and brecciation.

Sulphide veins are associated with different types and intensities of hydrothermal alteration. Felsic volcanic rocks cut by minor pyrite-quartz veins are altered to Mg-rich chlorite (brownish-green birefringence) that coexists with phenoclastic and secondary chessboard albite and carbonate (Fig. 6a). The presence of albite, low sulphide- and high Mg-contents are consistent with a distal hydrothermal facies around a seafloor vent complex. The more common pyrrhotite-rich sulphide veins have variable proportions of fine- to coarse-grained sericite, Fe-chlorite (berlin blue birefringence), and quartz intergrown with pyrrhotite, pyrite (Fig. 6b), and lesser sphalerite, chalcopyrite, arsenopyrite, and minerals tentatively identified as tetrahedrite and bismuthinite. The vein selvages may be sharp, although in areas of intense stringer-sulphide mineralization, they are diffuse. Chlorite is relatively uniform in composition beyond the vein, based on consistency of berlin blue birefringence, indicating that Fe chloritization is pervasive and may precede vein formation. Some of the quartz-rich veins have behaved more competently than the mica-rich veins and micaceous phyllites during ductile deformation and metamorphism (Fig. 6c). Euhedral, coarse grained pyrite and complex sulphide intergrowths occur in the least-deformed quartz-rich veins (Fig. 6c, d). The skeletal pyrite-arsenopyrite intergrowth in the FAB occurrence is identical to that described in the stringer zone at the Brunswick No. 12 deposit (Lentz and Goodfellow, 1993b). Mylonitization and subgrain replacement of coarse grained quartz in siliceous sulphide veins is evident within discrete deformation bands. Coarse grained pyrite that occurs in recrystallized pyrrhotite displaying 120° grain boundaries are probably porphyroblasts, whereas cataclastic deformation of some pyrites has produced angular and subrounded pyrite aggregates.

GEOCHEMISTRY

Element-abundance profiles along drill holes from the 5 core segments sampled were plotted to illustrate the control of lithology and alteration on the major- and trace-element geochemistry (Fig. 7a, b). These data are supplemented by chemical

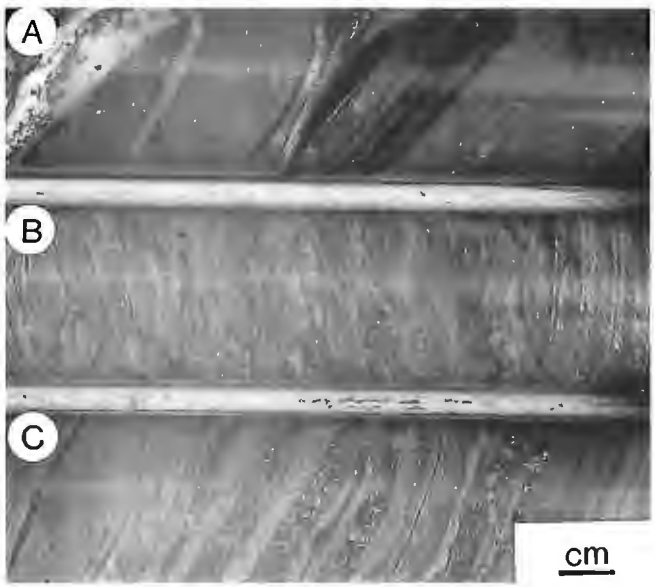

Figure 4. Photographs of drill core showing sulphide veining and hydrothermal alteration in rocks of the Patrick Brook Formation. A) thin-bedded graphitic shale-quartz wacke (Sample LPA-299; DDH 229-2-219.8 m); B) Thin-layered, chloritic and sericitic phyllite with a few layer-parallel, pyrrhotite veinlets (Sample LPA-300; DDH 229-2-224.6 m); C) massive sericitic quartz wacke with layer-parallel, quartz-pyrrhotite-pyrite veins with coarse grained pyrite porphyroblasts; Sample LPA-298; DDH 229-2-230.7 m).

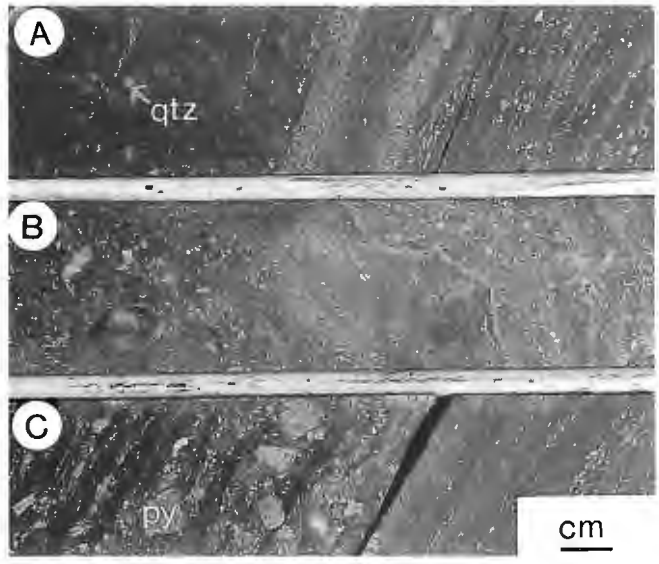

Figure 5. Photographs of drill core showing sulphide veins cutting Fe-rich chloritic sedimentary rocks and related quartz-augen schist of the Nepisiguit Falls Formation. A) Intensely altered chloritic sedimentary rock with numerous layer-parallel pyrite-pyrrhotite veinlets (Sample LPA-303; DDH 229-2-434.0 m); B) semi-massive chalcopyrite-pyrite-pyrrhotite veins cutting siliceous and chloritic sedimentary rock (Sample LPA-304; DDH 229-2-435.9 m); C) layer-parallel pyrrhotite-pyrite veins cutting chloritic and siliceous sedimentary rock with cataclastic pyrite porphyroblasts (Sample LPA-305; DDH 229-2-438.3 m).

analyses of weakly altered rocks from the Nepisiguit Falls Formation intersected in DDHs 229-3, 218-3, and 218-4 (Table 1).

One of the major impediments to determining the stratigraphy, unravelling the structure, and identifying favorable targets for massive sulphide exploration is discriminating between sedimentary rocks of the Patrick Brook, Nepisiguit Falls, and Flat Landing Brook formations. Rocks of the Patrick Brook Formation were sampled in three core segments (A, B, D), which coincide with a transition from weak to moderate alteration. Large compositional variations are controlled dominantly by the relative proportion of shale versus quartz wacke in the core segments spanning the Patrick Brook Formation. The quartz wacke ($SiO_2 \geq 85$ wt.%) is low in TiO_2, Al_2O_3, FeO, MgO, K_2O, and compatible trace-element contents (Fig. 8A-D), but high in Zr content compared to

Figure 7. Geological and geochemical profiles of A) DDH 229-1 and B) DDH 229-2. Symbols are: alteration (column A) = cross hatching; BH = Brunswick horizon; column B = percentage of disseminated and vein sulphides; ▲ – Flat Landing Brook Formation; ● – Nepisiguit Falls Formation; ▼ – Patrick Brook Formation. Core segments sampled in this study labelled A to E, consecutively. (See also Fig. 2, 3)

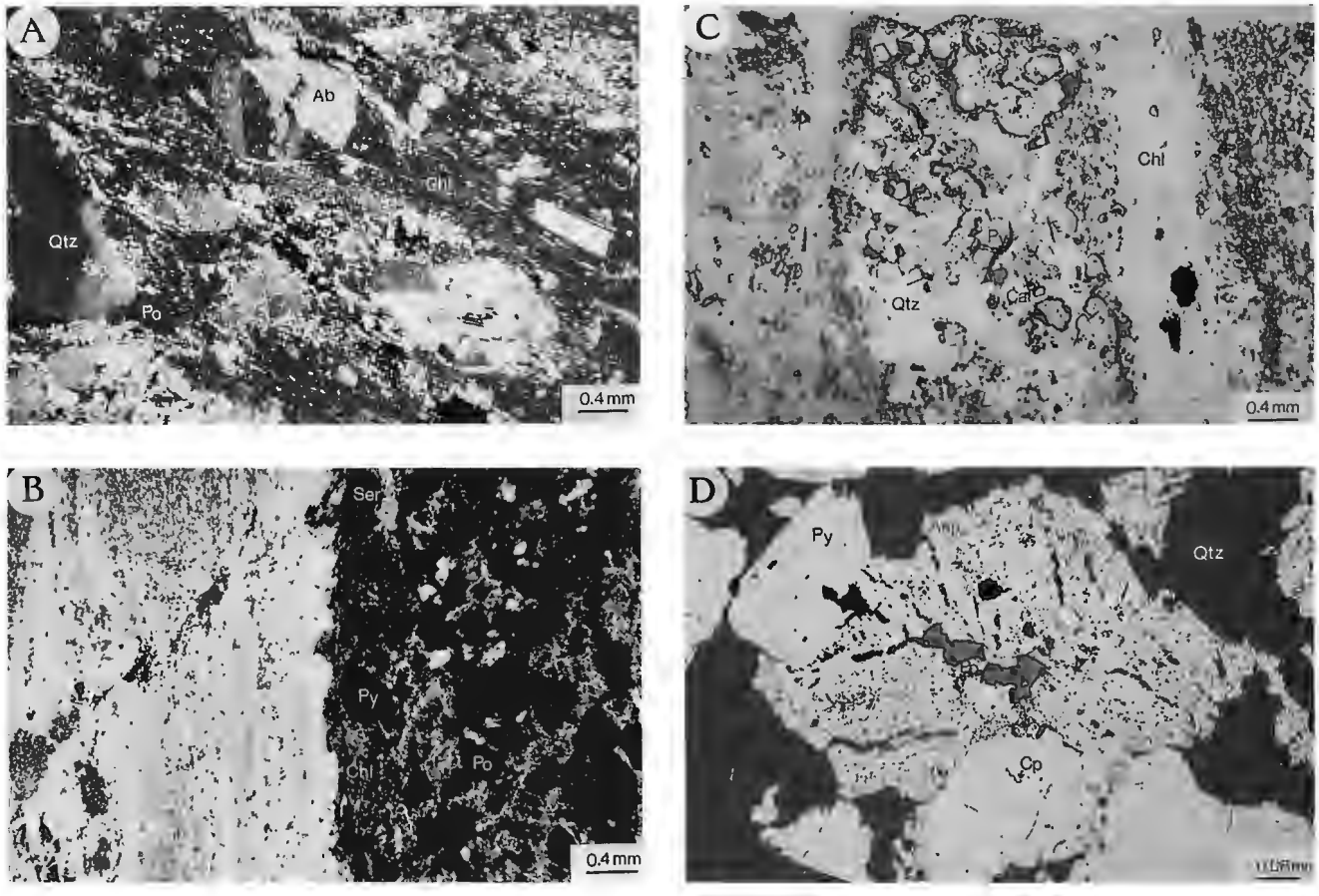

Figure 6. Photomicrographs showing mineralogy and textures of sulphide-rich veins. A) Moderately altered, medium grained, quartz-feldspar, crystal-rich tuffite cut by quartz-pyrite-chalcopyrite veins containing a Mg-rich chlorite-albite-silica matrix. Albite occurs as phenoclasts and as chessboard albite (LPA-288; DDH 229-1-413.0 m) (cross-polarized light). B) Margin of layer-parallel, quartz-sulphide-Fe chlorite vein cutting a foliated fine grained schist (Patrick Brook Formation) (LPA-290; DDH 229-1-416.7 m) (cross-polarized light). C) Coarse grained, pyrite-chalcopyrite-bearing quartz zone hosted by foliated chlorite with cataclastically deformed granular quartz and pyrite (LPA-288; DDH 229-1-413.0 m) (plane-polarized transmitted and reflected light). D) Complex intergrowth of arsenopyrite, pyrite, pyrrhotite, sphalerite, and minor chalcopyrite hosted by coarse grained quartz and pyrite (LPA-290; DDH 229-1-416.7 m) (plane-polarized reflected light).

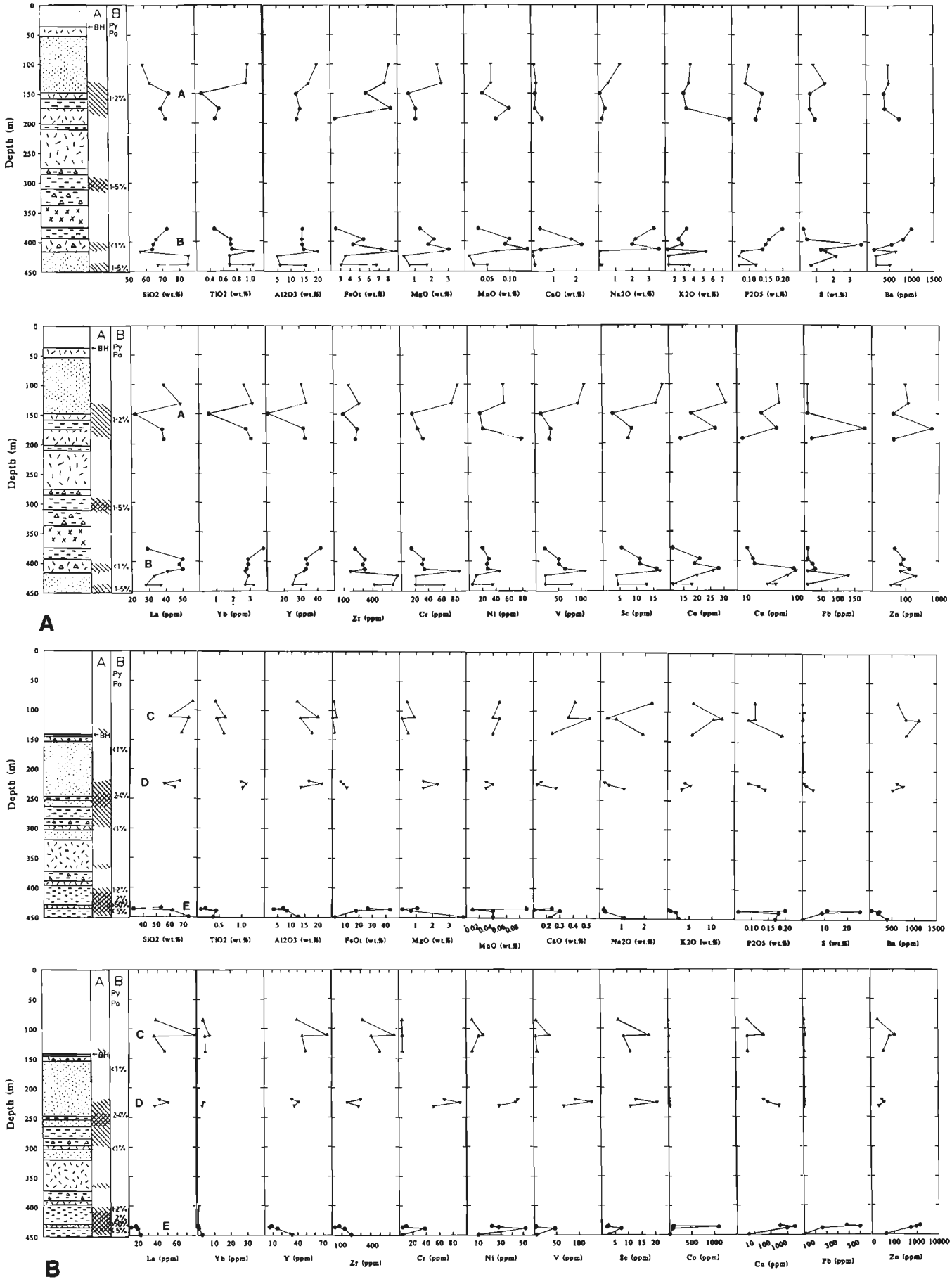
Depth (m)
A
B
Py
Po
BH
A
B
C
D
E
SiO2 (wt.%)
TiO2 (wt.%)
Al2O3 (wt.%)
FeOt (wt.%)
MgO (wt.%)
MnO (wt.%)
CaO (wt.%)
Na2O (wt.%)
K2O (wt.%)
P2O5 (wt.%)
S (wt.%)
Ba (ppm)
La (ppm)
Yb (ppm)
Y (ppm)
Zr (ppm)
Cr (ppm)
Ni (ppm)
V (ppm)
Sc (ppm)
Co (ppm)
Cu (ppm)
Pb (ppm)
Zn (ppm)

A

B

shale. Some of the immobile-element variations in rocks of the Nepisiguit Falls Formation are a result of mass addition of hydrothermal components, particularly in segment E (Fig. 7b). The Patrick Brook Formation rocks should only display mass increases of up to 10% due to the relatively weak alteration and less than 5 vol.% veins present. The composition of the Patrick Brook Formation is similar to the average Cambro-Ordovician shale-quartzite (cf., Lentz and Goodfellow, 1993c).

Titanium oxide and compatible trace elements because no modifier are higher in the Patrick Brook Formation than the Nepisiguit Falls Formation, indicating that the provenance of the epiclastic Patrick Brook Formation is different from that of the volcaniclastic rocks of the Nepisiguit Falls Formation. The weakly to moderately altered Nepisiguit Falls volcaniclastic rocks are composition very similar to the weakly to moderately altered volcaniclastic rocks (quartz-augen schist) from the Brunswick No. 6 deposit (Lentz and Goodfellow,

Table 1. Mean chemical composition of sedimentary and volcanic rocks from the FAB area, Bathurst, New Brunswick.

Fm	PB		FLB		NF		Altered NF	
n	9	1s	4	1s	14	1s	5	1s
SiO_2 wt.%	66.8	11.2	69.3	7.5	68.7	3.9	55.2	13.3
TiO_2	0.94	0.15	0.51	0.11	0.61	0.17	0.43	0.29
Al_2O_3	14.90	5.91	15.60	3.61	13.89	1.16	9.55	4.82
FeO_T	7.08	2.52	1.62	1.30	4.58	1.66	19.89	15.79
MgO	1.74	0.84	0.50	0.30	2.22	1.02	1.36	1.11
MnO	0.04	0.02	0.05	0.01	0.07	0.03	0.07	0.05
CaO	0.15	0.06	0.38	0.12	0.89	0.99	0.66	0.89
Na_2O	0.44	0.46	1.30	0.95	1.18	1.13	1.24	1.53
K_2O	3.42	1.38	8.40	3.34	3.65	1.39	1.42	0.98
P_2O_5	0.10	0.02	0.13	0.04	0.14	0.03	0.15	0.05
H_2O	3.0	1.5	1.2	0.9	2.62	0.75	nd	nd
CO_2	0.1	0.1	0.2	0.1	0.7	1.2	0.3	0.6
S	1.66	1.31	0.08	0.16	0.37	0.31	10.1	9.6
Ba ppm	493	184	843	191	530	220	234	188
Rb	137	74	176	84	143	29	nd	nd
Sr	26	19	56	5	38	31	25	21
Zr	337	189	470	141	250	70	171	131
Y	32	5	52	16	31	7	19	13
Nb	20	5	11	5	16	5	nd	nd
La	39.7	7.2	50.0	19.9	37.6	10.1	29.2	18.3
Yb	3.02	0.33	5.2	1.7	2.78	0.71	1.42	1.32
Cu	84	105	15	20	15	9	813	1114
Pb	23	40	13	5	26	45	219	213
Zn	76	57	61	44	99	145	624	565
Ni	36	18	9	5	28	17	31	12
Cr	63	27	5	0	29	15	24	15
V	81	38	14	14	44	24	34	29
Sc	13.0	5.8	11	5.0	9.1	3.9	7.8	5.9

NOTES: FeO_T denotes total Fe reported as FeO; Formation Names; FLB = Flat Landing Brook, PB = Patrick Brook. Analyses from DDH 229-1 and 2. NF = weakly altered rocks from the Nepisiguit Falls Formation in DDH's 229-1, 229-2, 229-3, 218-3, and 218-4; NF Altered = intensely altered rocks in DDH's 229-1 and 229-2; nd = not determined. The analyses were done at the Geochemical Laboratories of the Geological Survey of Canada. Major elements and Ba, Nb, Rb, Sr, and Zr were determined by fused disk X-ray fluorescence spectroscopy; the remaining trace elements were analysed by Inductively Coupled Plasma - Emission Spectroscopy (ICP-ES). S, CO_2, and H_2O were determined by wet chemical methods. 1s - 1 standard deviation.

1992a). Feldspars are locally preserved in segments B and E. Compared to the Flat Landing Brook Formation, the Nepisiguit Falls rocks have slightly lower Zr, Y, and Yb contents (Fig. 8E-H), although the Flat Landing Brook rocks are chemically quite variable, possibly due to alteration. These results are consistent with the higher high-field-strength-element content of the Flat Landing Brook Formation than the Nepisiguit Falls Formation (Lentz and Goodfellow, 1992b).

Average element abundances for weakly altered felsic volcanic rocks of the Nepisiguit Falls Formation are presented in Table 1. The weakly altered rocks of the Nepisiguit Falls Formation include those that are least altered and those that are affected by keratophyric alteration (seawater Mg-Na metasomatism), whereas the altered Nepisiguit Falls Formation rocks are chloritized and cut by sulphide veins. The Al_2O_3 and most other immobile elements (TiO_2, Zr, Y, Yb) show an apparent decrease of approximately 30% due mostly to a volume gain that resulted from the precipitation of sulphides in open fractures, similar to the sulphide veins underlying the Brunswick No. 12 massive sulphide deposit (Lentz and Goodfellow, 1993c).

Some of the Nepisiguit Falls volcaniclastic rocks in segment B have relict alkali feldspar and albite phenoclasts, secondary chessboard albite and moderately high contents of CaO, MgO, MnO, and CO_2 due to keratophyric seawater alteration. The presence of Cu-Zn-bearing pyrrhotite veins, however, suggests that the rocks were altered by a combination of locally entrained heated seawater and discharge-related ore-forming fluids.

Nepisiguit Falls rocks within the zone of intense stringer-sulphide veining coincide with sericitization and intense chloritization (Fig. 9). Toward the stringer-sulphide zone, which is interpreted to be the core of the hydrothermal fluid upflow zone, the proportion of muscovite decreases and the chlorite content increases and becomes progressively more Fe-rich (berlin blue birefringence). These features are similar to the mineralogical and mineral chemistry changes from the margins to the core of the of the feeder-conduit underlying the Brunswick No. 12 deposit. The most altered and stringer-sulphide-rich segment (E) (396.8-440.4 m grading 0.09% Pb, 0.14% Zn, 0.09% Cu, and 2.7 g/t Ag) is hosted in sedimentary rocks of the Nepisiguit Falls Formation. These sedimentary rocks are correlative with similar rocks cut by sulphide veins in DDH 229-1 (284.4-305.4 m grading 0.01% Pb, 0.22% Zn, 0.08% Cu, and 1.4 g/t Ag). Segment A is correlative with segment D (down dip), which is slightly more altered. The sulphide-rich samples in segment E are compositionally very similar to stringer-sulphide mineralization at Brunswick No. 12 (Goodfellow, 1975; Lentz and Goodfellow, 1993c), which contains high base-metal and Co contents and high Cu/Zn ratios.

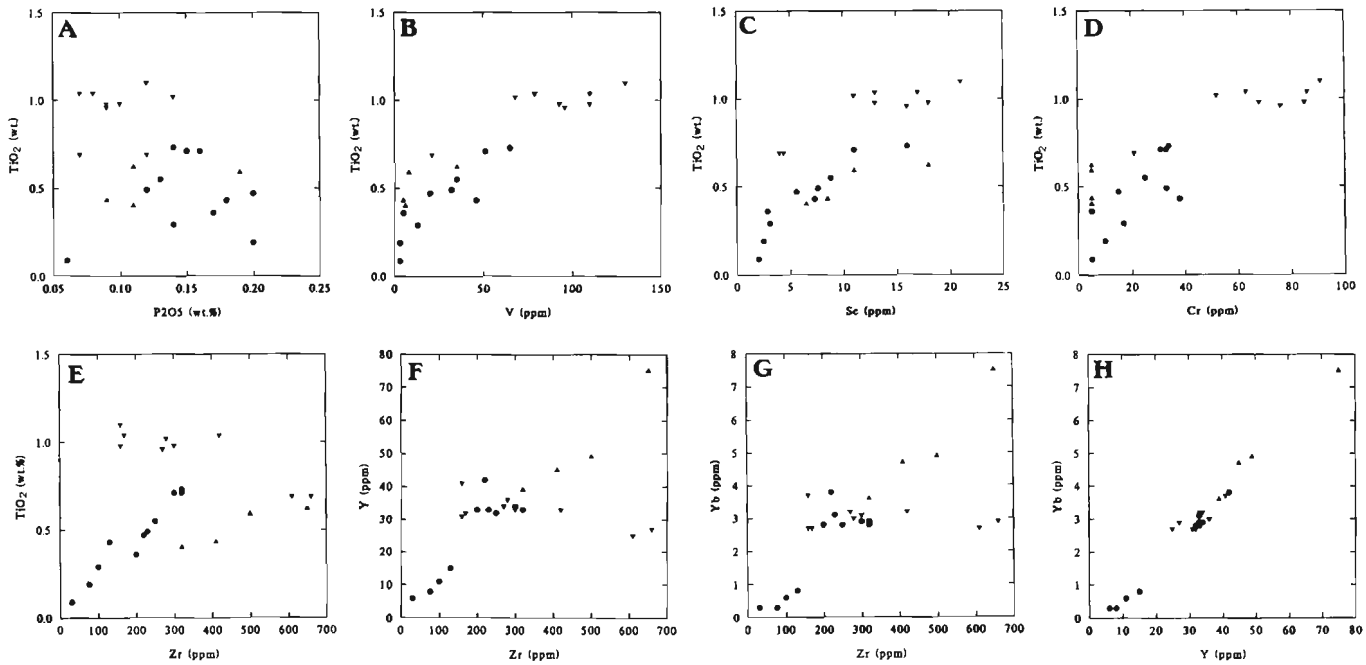

Figure 8. Chemical variation diagrams illustrating the compositional differences between the Flat Landing Brook, Nepisiguit Falls, and Patrick Brook formations: A) TiO_2 versus P_2O_5,; B) TiO_2 versus V; C) TiO_2 versus Sc; D) TiO_2 versus Cr; E) TiO_2 versus Zr; F) Y versus Zr; G) Yb versus Zr; H) Yb versus Y Symbols: ▲ = Flat Landing Brook Formation; ● = Nepisiguit Falls Formation; ▼ = Patrick Brook Formation.

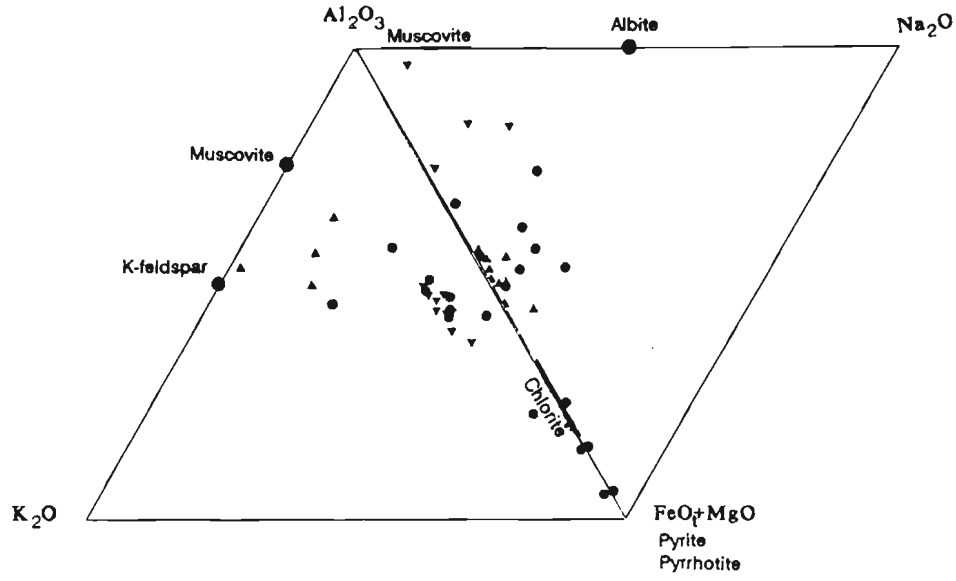

Figure 9. *Al_2O_3-K_2O-FeOt+MgO (AFK) and Al_2O_3-Na_2O-FeOt+MgO (ANF) molecular proportion diagrams illustrating the approximate relative proportions of albite, K-feldspar, muscovite, chlorite, pyrite, and pyrrhotite. Symbols: ▲ = Flat Landing Brook Formation; ● = Nepisiguit Falls Formation; ▼ = Patrick Brook Formation.*

DISCUSSION

The stringer-sulphide and associated alteration zone in the FAB occurrence is similar to the conduit sulphides and related hydrothermal alteration that underlie the Brunswick No. 6 and 12 deposits (Goodfellow, 1975; Juras, 1981; Nelson, 1983; Lentz and Goodfellow, 1992b; Luff et al., 1993). The bleaching of carbonaceous shale of the Patrick Brook Formation by hydrothermal fluids has partly or entirely destroyed organic carbon, probably by the hydrolysis of carbon to CH_4 and the oxidation of carbon to CO_2.

Carbonate alteration in the Nepisiguit Falls rocks does not correspond with the intensity of stringer-sulphide veining and associated silicate alteration. Rather, it is irregular in weak to moderately altered rocks of the Nepisiguit Falls Formation (e.g., segment B up to 1.4% CO_2) and is either related to retrograde $CaCO_3$ precipitation during keratophyric alteration or the interaction between Ca-bearing seawater and hydrothermally generated methanogenic CO_2. Alternatively, diagenetic carbonates may form by bacterial oxidation of CH_4 to CO_2 mixing with seawater under lower temperature conditions at the margins of the vent complex, similar to Middle Valley, northern Juan de Fuca Ridge (Goodfellow et al., in press).

The mixing of outflowing hydrothermal fluids with cold, entrained seawater may have promoted the precipitation of sulphides at the FAB occurrence. The addition of Mg (Mg chloritization) and Na (albitization) to rocks on the margins of the fluid discharge conduit is evidence for significant seawater entrainment into the hydrothermal system. The mixing of outflowing hydrothermal fluid with downwelling seawater, near the margins of a fluid upflow zone, has been documented for an active vent site in Middle Valley, Juan de Fuca Ridge (Goodfellow et al., in press).

The occurrence of transposed sulphide veins and disseminations that transgress the Patrick Brook and overlying Nepisiguit Falls formations, their high pyrrhotite-chalcopyrite contents relative to sphalerite and galena, and their association with attendant intense chloritic and minor siliceous alteration with chemical similarities to the stringer zone Brunswick No. 12 is convincing evidence for a hydrothermal stockwork feeder zone analogous to that associated with proximal seafloor massive sulphide deposits (Goodfellow, 1975; Jambor, 1979; Luff et al., 1992; Lentz and Goodfellow, 1993c). As yet, no exalative sulphides (Brunswick horizon) have been found within the very tightly infolded footwall sedimentary rocks of the Nepisiguit Falls Formation near the base of the folded volcaniclastic sequence. The stockwork alteration features, style of sulphide veining, and sulphide mineralogy are similar to epigenetic mineralization at hydrothermally active, sedimented rifts (Zierenberg and Shanks, 1983; Davis et al., 1987; Goodfellow and Franklin, in press). The extent of sulphide-stringer mineralization at the FAB occurrence, its similarity to the Brunswick No. 12 sulphide-stringer zone, and its stratigraphic position just below the Brunswick horizon indicates that the FAB vent complex probably generated a large seafloor sulphide deposit comparable to the Brunswick No. 12 deposit. This sulphide deposit has either been destroyed by erosion or remains to be discovered.

ACKNOWLEDGMENTS

We thank the staff of Brunswick Mining and Smelting Limited for their encouragement with this study and continuing studies in the area. The manuscript benefitted from a reviews by Alain Caron (NBDNRE), John Langton (NBDNRE), Steve McCutcheon (NBDNRE), and Jan Peter (GSC). This project is funded by the Canada-New Brunswick Cooperation Agreement on Mineral Development (MDA2).

REFERENCES

Davis, E.E., Goodfellow, W.D., Bornhold, B.D., Adsead, J., Blaise, B., Villinger, V., and Le Cheminant, G.
1987: Massive sulfides in a sedimented rift valley, northern Juan de Fuca Ridge; Earth and Planetary Science Letters, v. 82, p. 49-61.

Goodfellow, W.D.
1975: Rock geochemical exploration and ore genesis at Brunswick No. 12 deposit; Ph.D. thesis, University of New Brunswick, Fredericton, New Brunswick.

Goodfellow, W.D. and Franklin, J.M.
in press: Geology, mineralogy and geochemistry of massive sulfides in shallow cores, Middle Valley, Northern Juan de Fuca Ridge; Economic Geology.

Goodfellow, W.D., Grapes, K., Cameron, B., and Franklin, J.M.
in press: Hydrothermal alteration associated with massive sulphide deposits, Middle Valley, Northern Juan de Fuca Ridge; Canadian Mineralogist, v. 31.

Jambor, J.L.
1979: Mineralogical evolution of proximal distal features in New Brunswick massive-sulphide deposits; Canadian Mineralogist, v. 17, p. 79-87.

Juras, S.J.
1981: Alteration and sulphide mineralization in footwall felsic and sedimentary rocks, Brunswick No. 12 deposit, Bathurst, New Brunswick, Canada; M.Sc. thesis, University of New Brunswick, Fredericton, New Brunswick.

Lentz, D.R. and Goodfellow, W.D.
1992a: Re-evaluation of the petrology and depositional environment of felsic volcanic and related rocks in the vicinity of the Brunswick No. 12 massive sulphide deposit, Bathurst Mining Camp, New Brunswick; in Current Research, Part E; Geological Survey of Canada, Paper 92-1E, p. 333-342.

1992b: Re-evaluation of the petrochemistry of felsic volcanic and volcaniclastic rocks near the Brunswick No. 6 and 12 massive sulphide deposits, Bathurst Mining Camp, New Brunswick; in Current Research, Part E; Geological Survey of Canada, Paper 92-1E, p. 343-350.

1993a: Stringer sulphide mineralization and alteration around the FAB base-metal occurrence, Bathurst Mining Camp, New Brunswick; in Current Research, (comp., ed.) S.A. Abbott; New Brunswick Department of Natural Resources and Energy, Minerals and Energy Division, Geoscience Report 93-1, p. 91-103.

Lentz, D.R. and Goodfellow, W.D. (cont.)
1993b: Mineralogy and petrology of the stringer sulphide zone in the Discovery Hole at the Brunswick No. 12 massive sulphide deposit, Bathurst, New Brunswick; in Current Research, Part E; Geological Survey of Canada Paper 93-1E, p. 249-258.

1993c: Geochemistry of the stringer sulphide zone from the Discovery Hole at the Brunswick No. 12 massive sulphide deposit, Bathurst, New Brunswick; in Current Research, Part E; Geological Survey of Canada, Paper 93-1E, p. 259-269.

in press: Petrology and mass-balance constraints on the origin of quartz-augen schist associated with the Brunswick massive-sulfide deposits, Bathurst, New Brunswick; Canadian Mineralogist, v. 31.

Luff, W., Goodfellow, W.D., and Juras, S.
1992: Evidence for a feeder pipe and associated alteration at the Brunswick No. 12 massive sulphide deposit; Exploration and Mining Geology, v. 1, p. 167-185.

Luff, W.M., Lentz, D.R., and van Staal, C.R.
1993: The Brunswick No. 12 and No. 6 Mines, Bathurst Camp, northern New Brunswick; in Guidebook to the Metallogeny of the Bathurst Camp, (ed.) S.R. McCutcheon and D.R. Lentz, Trip 4, Bathurst '93 Third Annual CIM Geological Field Conference, p. 75-105.

McCutcheon, S.R.
1992: Base-metal deposits of the Bathurst-Newcastle district: characteristics and depositional models; Exploration and Mining Geology, v. 1, p. 105-119.

Nelson, G.A.
1983: Alteration of footwall rocks at Brunswick No. 6 and Austin Brook deposits, Bathurst, New Brunswick, Canada; M.Sc. thesis, University of New Brunswick, Fredericton, New Brunswick.

Rice, R.J. and van Staal, C.R.
1992: Sedimentological Studies in the Ordovician Miramichi, Tetagouche, and Fournier groups in the Bathurst camp and the Belledune-Elmtree Inlier, northern New Brunswick; in Current Research, Part D; Geological Survey of Canada, Paper 92-1D, p. 257-264.

van Staal, C.R.
1992: Geology and structure of the Brunswick Mines area (21-P5 e, f); New Brunswick Department of Natural Resources and Energy, Mineral Resources Open File Map 91-40f.

van Staal, C.R. and Fyffe, L.R.
1991: Dunnage and Gander Zones, New Brunswick: Canadian Appalachian Region; New Brunswick Department of Natural Resources and Energy, Mineral Resources, Geoscience Report 91-2, 39 p.

van Staal, C.R., Fyffe, L., Langton, J.P., and McCutcheon, S.R.
1992: The Ordovician Tetagouche Group, Bathurst Camp, northern New Brunswick, Canada: History, tectonic setting, and distribution of massive sulphide deposits; Exploration and Mining Geology, v. 1, p. 93-103.

Zierenberg, R.A. and Shanks, W.C., III
1983: Mineralogy and geochemistry of epigenetic features in metalliferous sediment, Atlantis II Deep, Red Sea; Economic Geology, v. 78, p. 57-72.

Geological Survey of Canada Project 790033

A gamma-ray spectrometric study of the footwall felsic volcanic and sedimentary rocks around Brunswick No. 6 massive sulphide deposit, northern New Brunswick[1]

David R. Lentz[2]
Mineral Resources Division

Lentz, D.R., 1994: A gamma-ray spectrometric study of the footwall felsic volcanic and sedimentary rocks around Brunswick No. 6 massive sulphide deposit, northern New Brunswick; in Current Research 1994-D; Geological Survey of Canada, p. 135-141.

Abstract: Hydrothermal alteration in the footwall to the Brunswick deposits is manifested by feldspar-destructive alteration coincident with modal increases in chlorite at the expense of sericite. This phenomenon results in K depletion halos in the footwall to these deposits. In situ gamma-ray spectrometric measurements of the footwall rock outcrops around the Brunswick No. 6 deposit show that the exposed upper sequence of altered volcaniclastic rocks (quartz-augen schist + footwall sedimentary rocks) have lower K contents (average 2.0 ± 0.3 wt.%) than the lower sequence of less-altered pyroclastic rocks (3.5 ± 0.3 wt.%). eU is variable throughout but less abundant in altered rocks. eTh is variable in the upper volcaniclastic package due to sedimentary reworking or mass changes occurring during alteration. K/eTh ratios enhance the alteration trends by focusing on the relative change. Inexpensive rapid in situ gamma-ray spectrometric analyses are useful in alteration and possibly chemostratigraphic analysis in the Bathurst Camp.

Résumé : L'altération hydrothermale dans l'éponte inférieure des gisements Brunswick se manifeste par la disparition des feldspaths et par une augmentation concomitante de l'abondance modale de la chlorite aux dépens de la séricite. Ce phénomène se traduit dans l'éponte inférieure de ces gisements par des halos d'appauvrissement en K. Des mesures spectrométriques in situ du rayonnement gamma sur les affleurements de l'éponte inférieure autour du gisement Brunswick n° 6 indiquent que la séquence supérieure affleurante de roches volcanoclastiques altérées (schiste oeillé à quartz et roches sédimentaires de l'éponte inférieure) ont des teneurs en K plus faibles (moyenne de 2,0 ± 0,3 % en poids) que la séquence inférieure de roches pyroclastiques moins altérées (3,5 ± 0,3 % en poids). La valeur eU varie, mais elle est moins élevée dans les roches altérées. La valeur eTh est variable dans l'ensemble volcanoclastique supérieur à cause d'un remaniement sédimentaire ou de changements de masse survenus au cours de l'altération. Les valeurs du rapport K/eTh accentuent les axes d'altération en soulignant les changements relatifs. Les analyses spectrométriques in situ du rayonnement gamma, rapides et peu coûteuses, sont apparues utiles pour analyser l'altération et la stratigrahie chimique dans le camp minier de Bathurst.

[1] Contribution to Canada-New Brunswick Cooperation Agreement on Mineral Development (1990-1995), a subsidiary agreement under the Canada-New Brunswick Economic and Regional Development Agreement.
[2] Geological Survey of Canada, P.O. Box 50, Bathurst, New Brunswick E2A 3Z1

INTRODUCTION

It is well known that feldspar-destructive alteration occurs in the footwall of many massive sulphide deposits, including those in the Bathurst mining camp (Jambor, 1979). The footwall to the massive sulphides and Algoma-type iron-formation of the "Brunswick horizon" were, for the most part, originally crystal-rich tufflavas with quartz and alkali feldspar phenoclasts and/or possibly porphyritic intrusions that were deformed and metamorphosed into quartz-feldspar-augen schists (Lentz and Goodfellow 1992a, in press; Fig. 1). Feldspar hydrolysis has been described within the footwall hydrothermal vent complex at both Brunswick No. 6 and 12 deposits (Pearce, 1963; Goodfellow, 1975; Juras, 1981; Nelson, 1983; Luff et al., 1992; Lentz and Goodfellow, 1992a, b, in press). In general, K_2O and Na_2O content decreases with initial hydrolysis of feldspar and decreases further with increasing alteration intensity because secondary K mica is replaced by Mg-Fe chlorite (Luff et al., 1992; Lentz and Goodfellow, in press). The K_2O content of the footwall volcaniclastic rocks is one reliable measure of the alteration intensity, therefore, in situ gamma-ray spectrometric analyses

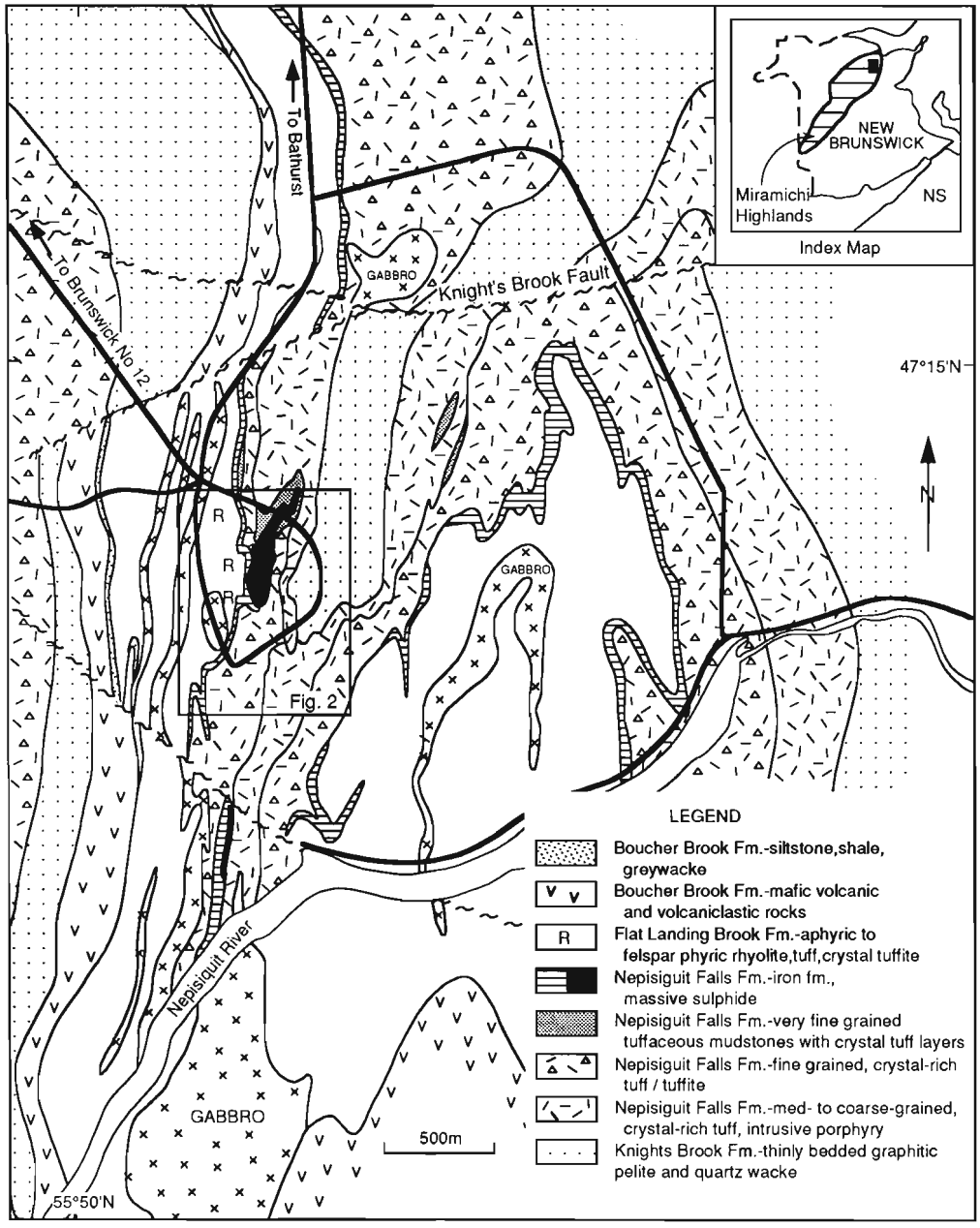

Figure 1. Regional geology around the Brunswick No. 6 and Austin Brook Iron Mines. Outlined is the geology of the Brunswick No. 6 massive sulphide deposit (modified after Luff et al., 1993).

should be a rapid analytical tool for identifying alteration intensity within a given felsic volcanic sequence. This work represents part of a New Brunswick-Canada Agreement on Mineral Development project to map and mineralogically and geochemically characterize hydrothermal alteration associated with massive sulphide deposits of the Brunswick Belt.

ANALYTICAL METHODS

Gamma-ray spectrometric measurements were made on outcrop surfaces with a four-channel, portable gamma-ray spectrometer (McPhar Spectra 44) equipped with a 7.5 x 7.5 cm thallium-activated, sodium iodide (NaI) crystal. The conversion factors for calculating element abundances were obtained by calibrating the spectrometer on the portable calibration pads located at the Canada Centre for Remote Sensing aircraft hanger at Uplands Airport, Ottawa, Ontario. In the field, the instrument was calibrated twice daily with a ^{137}Cs source to correct for drift. The integrated counting time was 2 minutes. The abundances of K, eU, and eTh were determined from the intensities of ^{40}K (1.46 MeV), ^{214}Bi (1.76 MeV), and ^{208}Tl (2.61 MeV) respectively. Uranium and thorium are expressed as equivalent units (eU ppm and eTh ppm). The abundance of U and Th are proportional to the abundances of the daughter elements if parent-daughter equilibrium was maintained (Killeen and Cameron, 1977). Precision was determined based on numerous replicate analyses; less than 0.2% for K and less than 1 ppm for both eU and eTh. Accuracy was determined by comparison with whole-rock chemical sample sites of McCutcheon (1990) and is discussed further in the text.

FIELD AND PETROLOGIC RELATIONSHIPS

The Brunswick No. 12 and 6 massive sulphide deposits are situated 10 km apart and 27 km southwest of Bathurst, New Brunswick (Fig. 1). The Austin Brook Iron Mine is approximately 1 km south of the Brunswick No. 6 deposit (Fig. 1). The massive sulphide deposits and associated iron-formation known as the "Brunswick horizon", occur near the upper part of the Nepisiguit Falls Formation of the Tetagouche Group (van Staal et al., 1992; Luff et al., 1993; Fig. 2). As all rocks within the Bathurst Camp are metamorphosed, premetamorphic rock names are used, although the well known metamorphic abbreviations are included in places.

The Knight's Brook Formation or older metasedimentary rocks (OM) in mine terminology is composed of quartz wackes and siltstones with minor intercalated graphitic schists (Fig. 2). The contact with the overlying Nepisiguit Falls Formation is commonly tectonized but appears to be conformable.

In general, the Nepisiguit Falls Formation consists of two recognizable stratigraphic units; 1) a lower unit of unaltered homogeneous quartz-feldspar crystal-rich tufflava and an upper unit of mixed quartz-feldspar crystal-rich volcaniclastic and fine grained tuffaceous sedimentary rocks (footwall sedimentary rocks; Fig. 2). In general, quartz and feldspar are coarse grained (3-10 mm) and constitute 20 to 40 vol.% of the rock hosted within a cryptocrystalline groundmass. The homogeneous crystal tuff is considered to be tufflava (Langton and McCutcheon, 1993) rather than porphyry because of the consistent stratigraphic relationship with the volcaniclastic unit. The granular crystal-rich tuff/tuffite overlies the massive type and contains a high percentage of rounded crystals, i.e., tuffite, but locally magmatically broken crystal-shards and possibly relict pumice fragments (Nelson, 1983) are preserved. Quartz and feldspar occur as phenocrysts and phenoclasts in both the tufflava and volcaniclastic facies, respectively, of the Nepisiguit Falls rocks elsewhere along the Brunswick Belt, but are termed quartz-feldspar-augen schists (Fig. 3a) when deformed and metamorphosed. The altered equivalents of these two units in the Nepisiguit Falls Formation are devoid of feldspar and only contain relict quartz, therefore are termed quartz-augen schists (Fig. 3b) when deformed and metamorphosed. At the Brunswick No. 6 deposit,

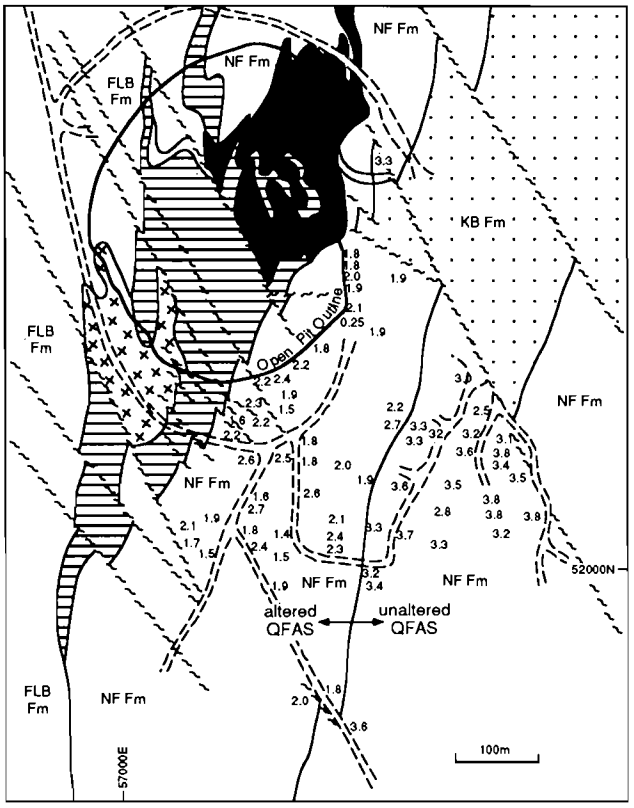

Figure 2. Detailed geology of the Brunswick No. 6 massive sulphide deposit (after Boyle and Davies, 1964) with present pit outline with K wt.% values located on outcrops in the stratigraphic and structural footwall (see Fig. 1 for location). Patterns: dotted – Knight's Brook Formation quartz wackes and grey shales (schist), lined – iron-formation, black – massive sulphides, FLB Fm – hanging-wall rhyolite and rhyolite breccias of the Flat Landing Brook Formation, NF Fm – footwall felsic crystal-rich tufflavas and volcaniclastic rocks and fine grained tuffaceous sedimentary rocks of the Nepisiguit Falls Formation (QFAS, QAS, and FW), x – Ordovician gabbros.

the altered crystal-rich volcaniclastic and sedimentary unit are juxtaposed against the least-altered crystal-rich tufflava, which has been described as a shear zone by Pearce (1963); however, the contact between the two units of the Nepisiguit Falls Formation is not well exposed around the mine. In the authors opinion, the contact is sheared parallel to the S_1S_2 composite foliation, which could explain the sharp contrast in alteration between the two lithologies.

The quartz-augen schist is a fine- to medium-grained rock with approximately 20 to 30 vol.% quartz crystals and mica-quartz pseudomorphs having an average grain size between 2 and 5 mm. Fine grained, chlorite-sericite-rich footwall sedimentary rocks with minor medium- to fine-grained crystal tuffite lenses (quartz-augen schist) occur in the immediate footwall to the deposit. The footwall sedimentary rocks are probably resedimented tuff derived from the crystal tuffs to which they are lateral equivalents. McCutcheon (1990, 1992) proposed an epiclastic origin for the quartz-augen schist at Brunswick No. 12, based on the absence of feldspar due to weathering, the sphericity of quartz, and the high proportion of quartz to matrix. However, the absence of feldspar is best explained as an alteration phenomenon because least-altered crystal-rich tufflavas (quartz-feldspar-augen schist) are altered to a quartz-sericite-chlorite rock in the hydrothermal alteration zone beneath the Brunswick No. 12 deposit (Goodfellow, 1975; Juras, 1981; Luff et al., 1992; Lentz and Goodfellow, 1992a) that is supported by pseudomorphic replacement of alkali feldspar by mica and quartz both here and at Brunswick No. 12 (Lentz and Goodfellow, in press). These altered rocks were deformed into quartz-augen schist. Alkali feldspar phenoclasts and groundmass constituents would have been more easily altered in the permeable volcaniclastic rocks compared to the welded tufflavas.

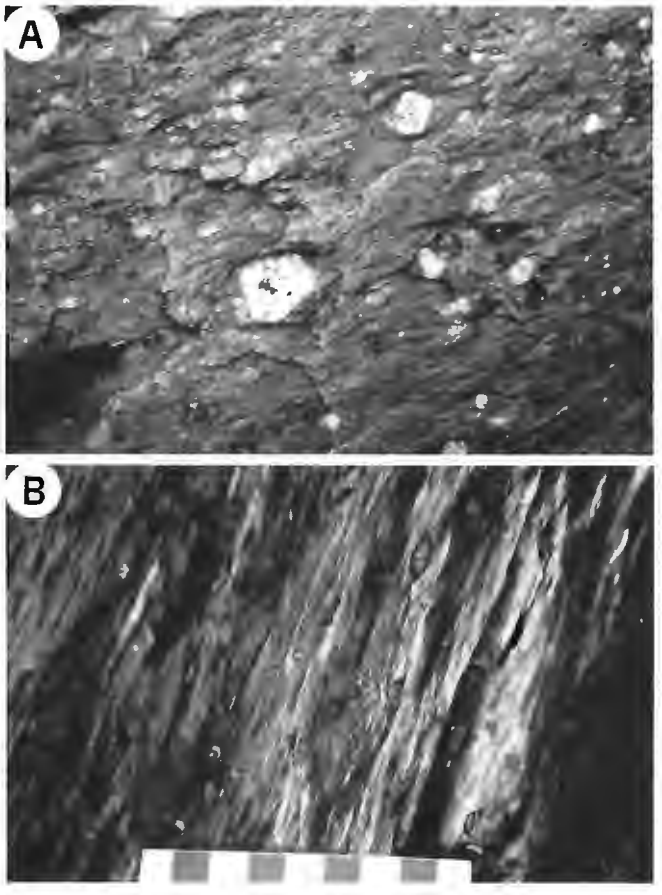

Figure 3. *A) Quartz-feldspar-augen schist (QFAS), which represents least-altered crystal-rich tufflava in the footwall with angular to euhedral, pristine quartz and microperthitic alkali feldspars. B) Quartz-augen schist (QAS) in altered crystal-rich tuffite with tectonically(?) rounded quartz augen of both volcanic (vitreous) and metasomatic (milky) origin. Feldspar are replaced by mica-quartz-rich assemblage.*

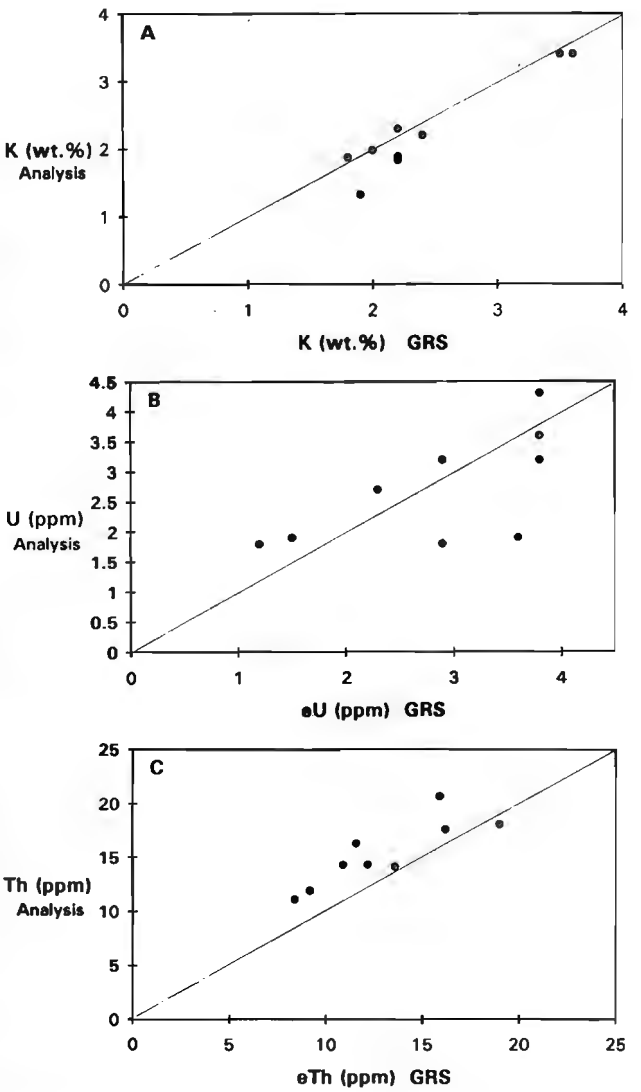

Figure 4. *Correlation of several in situ gamma-ray spectrometric (GRS) measurements with geochemical analyses of McCutcheon (1990) from the Brunswick No. 6 deposit. A) K (wt.%) analysis (chemical) versus K (wt.%) GRS measurement, B) U (ppm) analysis (chemical) versus eU (ppm) GRS measurement, C) Th (ppm) analysis (chemical) versus eTh (ppm) GRS.*

HYDROTHERMAL ALTERATION

At Brunswick No. 6, footwall alteration was first described in detail by Pearce (1963) and later by Nelson (1983). Based on modal and chemical analysis, Pearce (1963) showed that alkali feldspar and groundmass were replaced by quartz, muscovite, and chlorite in the vicinity of the deposit. He showed that K_2O decreases at the expense of Fe and Mg in the volcaniclastic rocks. He also noted that the alteration was probably not isovolumetric based on the variable Al_2O_3 contents. Using an isocon diagram, Lentz and Goodfellow (in press) illustrated these same geochemical characteristics in the footwall to the Brunswick No. 6 deposit. At Brunswick No. 12, K_2O decreases towards the core of the hydrothermal discharge system (Luff et al., 1992; Lentz and Goodfellow, in press). Therefore, documentation of K content should be a useful lithogeochemical exploration tool. In situ gamma-ray spectrometric analysis for K is a rapid chemical technique for determining the degree of alteration.

GAMMA-RAY SPECTROMETRY

Although gamma-ray spectrometry is a widely accepted method of rapid geochemical analysis for K, U, and Th, several of the in situ gamma-ray spectrometric measurements were correlated with previous geochemical sample sites (McCutcheon, 1990) in order to test the reliability of the method. Figure 4 illustrates the good correlation between the K, U, and Th geochemical analyses and the in situ gamma-ray spectrometric analyses supporting the reliability of the method. This is remarkable considering that the precise spot on the outcrop of the previous sample from McCutcheon (1990) could not be reliably determined.

The radiometric measurements were made on relatively flat surfaces to the southeast of the pit where numerous outcrops exist. There is little or no outcrop elsewhere around the deposit except along the pit perimeter, which is not accessible. Sixty-five outcrop gamma-ray spectrometric measurements were taken, as well as an additional ten measurements along a profile in the liming trench that transects chlorite-sericite-rich sedimentary rocks in the immediate footwall at the northeast end of the deposit. These two sets of data will be examined separately, the purpose of which will become apparent later.

Table 1. Average gamma-ray spectrometric (GRS) analyses from the Brunswick No. 6 deposit

		K wt.%		eU ppm		eTh ppm	
	n	x	1s	x	1s	x	1s
QAS-FW	42	2.0	0.3	2.6	0.7	14.9	3.1
Q(F)AS	8	3.1	0.3	3.2	0.5	12.5	1.3
QFAS	15	3.5	0.3	3.6	0.7	12.7	1.4

NOTES: QAS - quartz-augen schist (altered volcaniclastic), FW - footwall sedimentary rocks, Q(F)AS - quartz-(feldspar)-augen schist (weakly altered tufflava), and QFAS - quartz-feldspar-augen schist (least-altered tufflava). "e" - equivalent units assuming equilibrium between measured radiogenic daugther and parent. x = mean, 1s = 1 standard deviation.

The sample sites were subdivided into altered volcaniclastic rocks (quartz-augen schist + footwall sedimentary rocks) if feldspar was absent; weakly altered crystal tufflava (quartz-(feldspar)-augen schist) if remnant feldspar remained; and least-altered crystal tufflava (quartz-feldspar-augen schist) if feldspars and matrix looked pristine (unaltered). Table 1 summarizes the average analyses from the three subdivisions. The quartz-augen schist is low in K (2.0 wt.%) relative to both the quartz-(feldspar)-augen schist (3.1 wt.%) and quartz-feldspar-augen schist (3.5 wt.%). The distribution of K contents in the footwall quartz-augen schist and the quartz-feldspar-augen schist is somewhat erratic and does not show a progressive decrease into the deposit possibly because this portion of the deposit is on the margin of the hydrothermal feeder system and does not transect the core and stringer zone. Another important consideration is effect of metamorphic alteration associated with intense S_1S_2 fabric development (van Staal and Williams, 1984) that may be responsible for some of the K variation in both quartz-feldspar-augen schist and quartz-augen schist. Lentz and Goodfellow (1992b) found that the quartz-augen schist and quartz-feldspar-augen schist at Brunswick No. 6 had K contents of 1.91 ± 0.25 and 3.41 ± 0.12 wt.%, respectively, similar to this study (Table 1). The eTh contents are similar to those summarized in Lentz and Goodfellow (1992b) but variable in the quartz-augen schist unit. They also found that Th seemed to behave as an immobile element based on correlations with other relatively immobile components. The higher variance in eTh contents may reflect: 1) large variations in crystal-matrix ratio, 2) two different source areas for volcaniclastic constituents, or 3) small volume changes (<20%) resulting from alteration. Interestingly, many of the fine grained footwall sedimentary rocks commonly have lower eTh than the quartz-augen schist; therefore, variations in crystal-matrix ratios are probably not responsible for all the eTh variation. The positive correlation between K and eTh abundance (Fig. 5) lends support to the alteration hypothesis, but this remains to be proven.

The trench profile is located immediately north of the entrance ramp located on the east-northeast side of the open pit (Fig. 2). This is the southern extension of altered footwall sedimentary rocks that thickens to the north around the folded massive sulphide lens. The main alteration zone occurs at the north end of the deposit. This profile was measured in a relatively narrow trench 3 m wide and 2 m deep with outcrop exposed along the face. Measurements were taken along the face of the trench approximately every 5 m. Unfortunately, the gamma-ray spectrometric measurements are evidently anomalous in K and eTh, possibly reflecting the non-ideal measurement conditions with high background (Fig. 6). However, the relative variation in K, eU, and eTh are important as absolute numbers so these were profiled to illustrate the decrease in K, eU, and eTh from the intensely sericitic to chloritic footwall sedimentary rocks located directly beneath a massive pyritic lens (Fig. 6). If considered immobile, the decrease in Th in the chloritic footwall immediately beneath the deposit is consistent with 30 to 60% mass-volume gain.

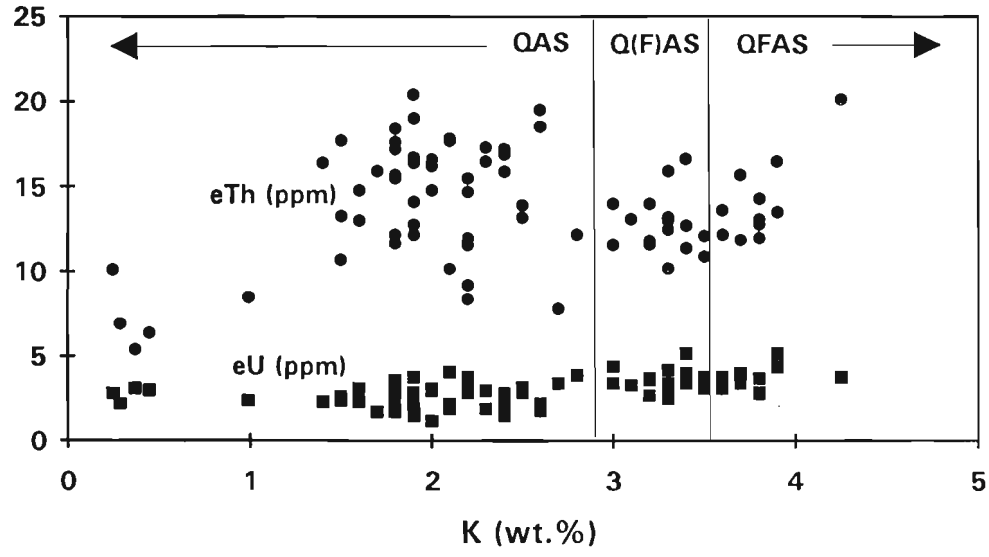

Figure 5. *Covariation between gamma-ray spectrometric K and eU and eTh for footwall rocks around the Brunswick No. 6 deposit.*

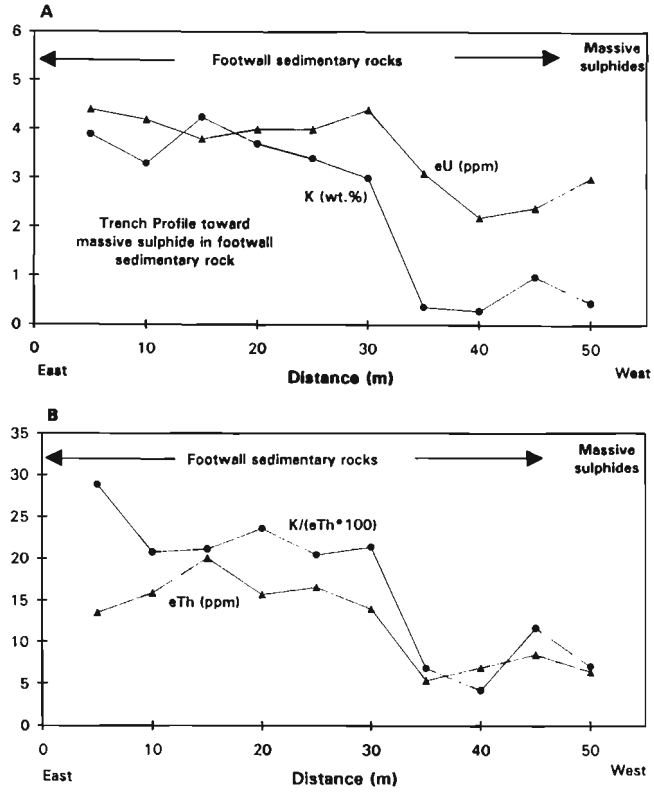

Figure 6. *Gamma-ray spectrometric (GRS) geochemical profile at approximately 5 m intervals from footwall sedimentary rocks toward the pyritic massive sulphide lens at the northeast end of the open pit. The liming trench is located immediately north of the entrance ramp to the open pit. **A)** K (wt.%) and eU (ppm) versus distance along the profile, **B)** eTh (ppm) and K/(eTh*100) versus distance along the profile. The massive pyritic lens occurs at approximately 52 m.*

DISCUSSION

Although the contact between the lower coarse grained, crystal-rich tufflavas and upper coarse grained, crystal-rich volcaniclastic/sedimentary rocks may be faulted or stratigraphic, the upper unit probably represents a submarine cold debris flow. Therefore, unless these rocks were subareally weathered, for which there is no evidence, the upper volcaniclastic unit should have contained phenoclastic alkali feldspar as is evident north of the Knight's Brook fault (Fig. 1). The ubiquitous absence of alkali feldspar around the Brunswick No. 6 sulphide and Austin Brook Fe deposits suggests that the hydrothermal system was large and possibly poorly focused in comparison to the Brunswick No. 12 deposit.

Leaching of K during hydrolysis of alkali feldspar and groundmass constituents in the footwall pyroclastic and volcaniclastic rocks is a well established phenomena beneath most felsic volcanic-hosted, proximal massive sulphide deposits including those of the Bathurst mining camp. Therefore, in situ gamma-ray spectrometric analyses for K, eU, and eTh can help delineate the alteration halo around proximally situated massive sulphide deposits. K/eTh ratios can enhance the data because Th, which should behave as an immobile element, acts as a mass-balance correction for the K data and may also help to define units within the stratigraphy. This rapid and inexpensive analytical technique could be used in assessing outcrops and trenches. Continuous down-hole gamma-ray spectrometric logging could also be useful in alteration and chemostratigraphic analysis.

ACKNOWLEDGMENTS

I would like to thank the staff of Brunswick Mining and Smelting Limited for their co-operation and encouragement with alteration studies in the area. Extensive discussions with

Steve McCutcheon, Rob Shives, and Cees van Staal were greatly appreciated. The manuscript benefitted from reviews by Brian Charbonneau, Ken Ford, Wayne Goodfellow, Steve McCutcheon, and Dave Sinclair. This project is funded by the Canada-New Brunswick Cooperation Agreement on Mineral Development (MDA2).

REFERENCES

Boyle, R.W. and Davies, J.L.
1964: Geology of the Austin Brook and Brunswick No. 6 sulphide deposits, Gloucester County, New Brunswick; Geological Survey of Canada, Paper 63-64, 23 p.

Goodfellow, W.D.
1975: Major and minor element halos in volcanic rocks at Brunswick no. 12 sulphide deposit, N.B., Canada; in Geochemical Exploration 1974, (ed.) I.L. Elliot and W.K. Fletcher; Elsevier, Amsterdam, p. 279-295.

Jambor, J.L.
1979: Mineralogical evolution of proximal-distal features in New Brunswick massive sulphide deposits; Canadian Mineralogist, v. 17, p. 79-87.

Juras, S.J.
1981: Alteration and sulphide mineralization in footwall felsic and sedimentary rocks, Brunswick No. 12 deposit, Bathurst, New Brunswick, Canada; M.Sc. thesis, University of New Brunswick, Fredericton, New Brunswick.

Killeen, P.G. and Cameron, G.W.
1977: Computation of in situ potassium, uranium, and thorium concentrations from portable gamma-ray spectrometer data; in Report of Activities, Part A; Geological Survey of Canada, Paper 77-1A, p. 91-92.

Langton, J.P. and McCutcheon, S.R.
1993: Brunswick Project, New Brunswick; in Current Research, (comp. ed.) S.A. Abbott; New Brunswick Department of Natural Resources and Energy, Minerals Resources, Information Circular 93-1, p. 31-51.

Lentz, D.R. and Goodfellow, W.D.
1992a: Re-evaluation of the petrology and depositional environment of felsic volcanic and related rocks in the vicinity of the Brunswick No. 12 massive sulphide deposit, Bathurst Mining Camp, New Brunswick; in Current Research, Part E; Geological Survey of Canada, Paper 92-1E, p. 333-342.

1992b: Re-evaluation of the petrochemistry of felsic volcanic and volcaniclastic rocks near the Brunswick No. 6 and 12 massive sulphide deposits, Bathurst Mining Camp, New Brunswick; in Current Research, Part E; Geological Survey of Canada, Paper 92-1E, p. 343-350.

in press: Petrology and mass-balance constraints on the origin of quartz-augen schist associated with the Brunswick massive sulfide deposits, Bathurst, New Brunswick; Canadian Mineralogist, v. 31, pt. 4.

Luff, W., Goodfellow, W.D., and Juras, S.
1992: Evidence for a feeder pipe and associated alteration at the Brunswick No. 12 massive sulphide deposit; Exploration and Mining Geology, v. 1, p. 167-185.

Luff, W.M., Lentz, D.R. and van Staal, C.R.
1993: The Brunswick No. 12 and No. 6 Mines, Bathurst Camp, northern New Brunswick; in Guidebook to the Metallogeny of the Bathurst Camp, (ed.) S.R. McCutcheon and D.R. Lentz; Trip 4, Bathurst'93 Third Annual CIM Geological Field Conference, p. 75-105.

McCutcheon, S.R.
1990: Base-metal deposits of the Bathurst-Newcastle district; in Field guide to massive sulphide deposits in northern New Brunswick, (ed.) L.R. Fyffe; Base-metal Symposium 1990, Minerals and Energy Division, Department of Natural Resources and Energy, New Brunswick, p. 42-71.

1992: Base-metal deposits of the Bathurst-Newcastle district: characteristics and depositional models; Exploration and Mining Geology, v. 1, p. 105-119.

Nelson, G.A.
1983: Alteration of footwall rocks at Brunswick No. 6 and Austin Brook deposits, Bathurst, New Brunswick, Canada; M.Sc. thesis, University of New Brunswick, Fredericton, New Brunswick.

Pearce, T.H.
1963: The petrochemistry and petrology of the quartz-feldspar porphyry, Bathurst, New Brunswick; M.Sc. thesis, University of Western Ontario, London, Ontario.

van Staal, C.R. and Williams, P.F.
1984: Structure, origin and concentration of the Brunswick 12 and 6 orebodies; Economic Geology, v. 79, p. 1669-1692.

van Staal, C.R., Fyffe, L.R., Langton, J.P., and McCutcheon, S.R.
1992: The Ordovician Tetagouche Group, Bathurst Camp, northern New Brunswick, Canada: History, Tectonic Setting, and distribution of massive-sulphide deposits; Exploration and Mining Geology, v. 1, p. 93-103.

Geological Survey of Canada Project 790033

Maquereau Group lavas, southern Gaspésie, Quebec Appalachians

Jean H. Bédard and Caroline Wilson[1]
Quebec Geoscience Centre, Sainte-Foy

Bédard, J.H. and Wilson, C., 1994: Maquereau Group lavas, southern Gaspésie, Quebec Appalachians; in Current Research 1994-D; Geological Survey of Canada, p. 143-154.

Abstract: Most Maquereau Group lavas are tholeiitic basalts to ferro-andesites that exhibit an Fe-Ti-enrichment trend. Subordinate alkaline basalts are generally enriched in TiO_2, P_2O_5, Nb and light rare-earth elements. Most major and trace element paleotectonic discriminants do not favour an arc-related environment. An intra-continental rift, or an incipient spreading ridge environment are most consistent with the geochemical data and field relationships. Many Maquereau lavas contain pyrite+chalcopyrite and have high Cu-contents; they thus represent a plausible source rock for the Cu-sulphide veins in the area.

Résumé : Les laves du Groupe de Maquereau sont principalement des basaltes et des ferro-andésites tholéiitiques avec patron d'enrichissement en Fe-Ti. Les laves alcalines, plus rares, sont généralement enrichies en TiO_2, P_2O_5, Nb et terres rares légères. Les discriminants géochimiques paléotectoniques ne favorisent pas un environnement d'arc. Un environnement de rift continental, ou de ride océanique naissante sont compatibles avec les données géochimiques et les relations de terrain. Les laves du Groupe de Maquereau contiennent souvent de la pyrite et de la chalcopyrite, et ont des teneurs élevées en Cu; ce sont donc des roches sources plausibles pour les veines de sulfures de cuivre de la région.

[1] 258, rue Principale, Ste-Justine, Québec G0R 1Y0

GENERAL RELATIONS

The Maquereau Group of southern Gaspésie, Quebec (Fig. 1), comprises up to 10 km of pre-Early Ordovician lavas and clastic rocks, and is assigned to the Humber Zone of the Canadian Appalachians (Williams and St-Julien, 1982; DeBroucker, 1987). To the west, a mélange (Port-Daniel Complex) separates the Maquereau Group from the Ordovician age flysch deposits of the Mictaw Group. The Port Daniel Complex is composed of igneous and sedimentary blocks in a sedimentary matrix. Both the Port Daniel mélange and Mictaw Group belong to the Dunnage Zone (Williams and St-Julien, 1982). Maquereau Group rocks are unconformably overlain by Silurian rocks of the Chaleurs Group to the south (Logan, 1846), and are separated from Chaleurs Group rocks to the north by a major shear zone, which also contains slivers of Grenvillean age gneiss. These gneissic slivers were interpreted to signify that the Maquereau lavas were deposited upon continental crust (DeBroucker, 1987). The Maquereau Group has been affected by up to five phases of ductile deformation (Ringele, 1982), is dissected by several important reverse faults (Caron, 1984; DeBroucker, 1987), and has been metamorphosed to greenschist grade, in contrast to the prehnite-pumpelleite grade of surrounding Silurian and carboniferous rocks. On the basis of sedimentological similarities, the Maquereau Group has been correlated (St-Julien and Hubert, 1975; DeBroucker, 1987; Cousineau, 1990) with Iapetus rift margin rocks of the Shickshock and Caldwell groups. This paper characterizes the lavas of the Maquereau Group with regard to their petrological, geochemical, and tectonic affinity.

The generally poor outcrop, penetrative deformation, and metamorphism of these rocks commonly obscure contact relations between lavas and sediments. Most metabasalt layers are probably extrusive, and in places pillows are recognizable, though DeBroucker (1987) also reports intrusive contacts between mafic dykes or sills and host sediments and lavas. The most common sedimentary rocks are quartzofeldspathic sandstones derived from Grenvillean sources, with subordinate conglomerates and metapelites (DeBroucker, 1987). The metasediments also contain clasts of mafic volcanic rocks, which imply local recycling of Maquereau lavas (DeBroucker, 1987).

PETROGRAPHY, MINERALOGY, AND ALTERATION

Most Maquereau Group lavas are phenocryst-poor, very fine-grained, microdiabasic rocks. Phenocrysts generally represent only a small proportion (<15%) of the rock. Pseudomorphs after plagioclase, pyroxene, and/or olivine phenocrysts were recognized. Magnetite-ilmenite microphenocrysts are common. Descriptions of the new samples are in the appendix. Pillow lavas MAQ54 and 125, and JB83-45 and 46 (in Bédard, 1986) contain 5-10% mafic phenocrysts in a groundmass that appears to have a microspinifex texture. One "volcanic" band (MAQ122) is composed of medium- to coarse-grained ferro-gabbroic rocks and may represent a slowly-cooled sill. Some "meta-volcanic" samples (MAQ127) contain abundant quartz and feldspar grains and could represent sandy siltstones with a large volcanogenic fraction, or tuffaceous deposits of a hybrid eruption. The latter are plotted separately on the variation diagrams (filled triangles on Figures 2 to 7), but seem to lie along the main tholeiitic trend.

Greenschist facies metamorphism and deformation has almost completely destroyed the original textures and mineralogy of these rocks. Relict clinopyroxene was analyzed on a Cameca Camebax in Ottawa. Details of the analytical procedure will be presented elsewhere. Many probe analyses gave low totals, suggesting incipient hydration. All analyzed clinopyroxenes are augites with Mg/Mg+Fe between 0.62 and 0.78. The Ca-depletion trend is shallower than that of the Skaergaard intrusion, and resembles the magnesian end of the Palisades sill trend (Walker et al., 1973). Samples MAQ122A and B of the alkaline suite were analyzed, but their pyroxenes do not differ significantly from those in the tholeiitic rocks (e.g. Fig. 8). Tholeiitic sample MAQ116A does, however, contain clinopyroxenes with Ti and Al contents higher than those of the other rocks. Plagioclase is completely replaced by assemblages of albite (Ab_{92-99} one analysis at Ab_{85}), epidote, quartz, and hematite. Mafic minerals are replaced by chlorite, titanite, iddingsite, pumpelleite(?) talc, hematite, magnetite, and goethite(?) There are abundant pre- and postkinematic veins filled with combinations of epidote>calcite>quartz>chlorite>pyrite>chalcopyrite>hematite>magnetite>zoisite(?)>talc or actinolite(?). Silicification is observed locally (e.g., sample MAQ123, plotted as a star on the figures). Sulphides are almost ubiquitous, generally as disseminations and clots up to 1.5 cm in length, locally in veins. Sulphide clots form elongated, lineation-parallel ovoids; and incipiently brecciated pyrite cubes are commonly rimmed by chalcopyrite and a third, purplish-coloured sulphide containing Cu and Fe (qualitative analysis).

GEOCHEMISTRY

Major and trace elements were analyzed by X-ray Fluorescence on fused glass and pressed powder pellets, and by INAA at the INRS labs in Quebec and at Université de Montréal. Because of the intense veining and metamorphism, CaO, MgO, SiO_2, Na_2O, K_2O are only partly reliable indicators of the original lava chemistry. Other elements are less easily remobilized (see Jenner and Swinden, 1993 p. 438). Chromium and nickel decrease together, while Zr, Y, Fe_2O_3, TiO_2, and P_2O_5 increase with decreasing MgO (Fig. 2 and 4). The data allow subdivison of Maquereau Group lavas into three groups: alkaline, tholeiitic, and ferro-andesitic. The ferro-andesite has low MgO, high SiO_2, and Fe_2O_3. Alkaline rocks generally have Na_2O>3.5 wt.%, and tend to be enriched in some or all of the following elements: Nb, Y, Zr, TiO_2, and P_2O_5, in comparison to the tholeiitic group. Alkaline lavas have light rare-earth element enriched profiles while tholeiites range from LREE-depleted to enriched (Fig. 3). The tholeiitic group may require further subdivision. Tholeiitic and alkaline lavas tend to have distinct Nb/Y and Zr/Y ratios (Fig. 3). Tholeiitic lavas show an FeO-enrichment trend similar the Skaergaard intrusion, but at lower TiO_2, and higher

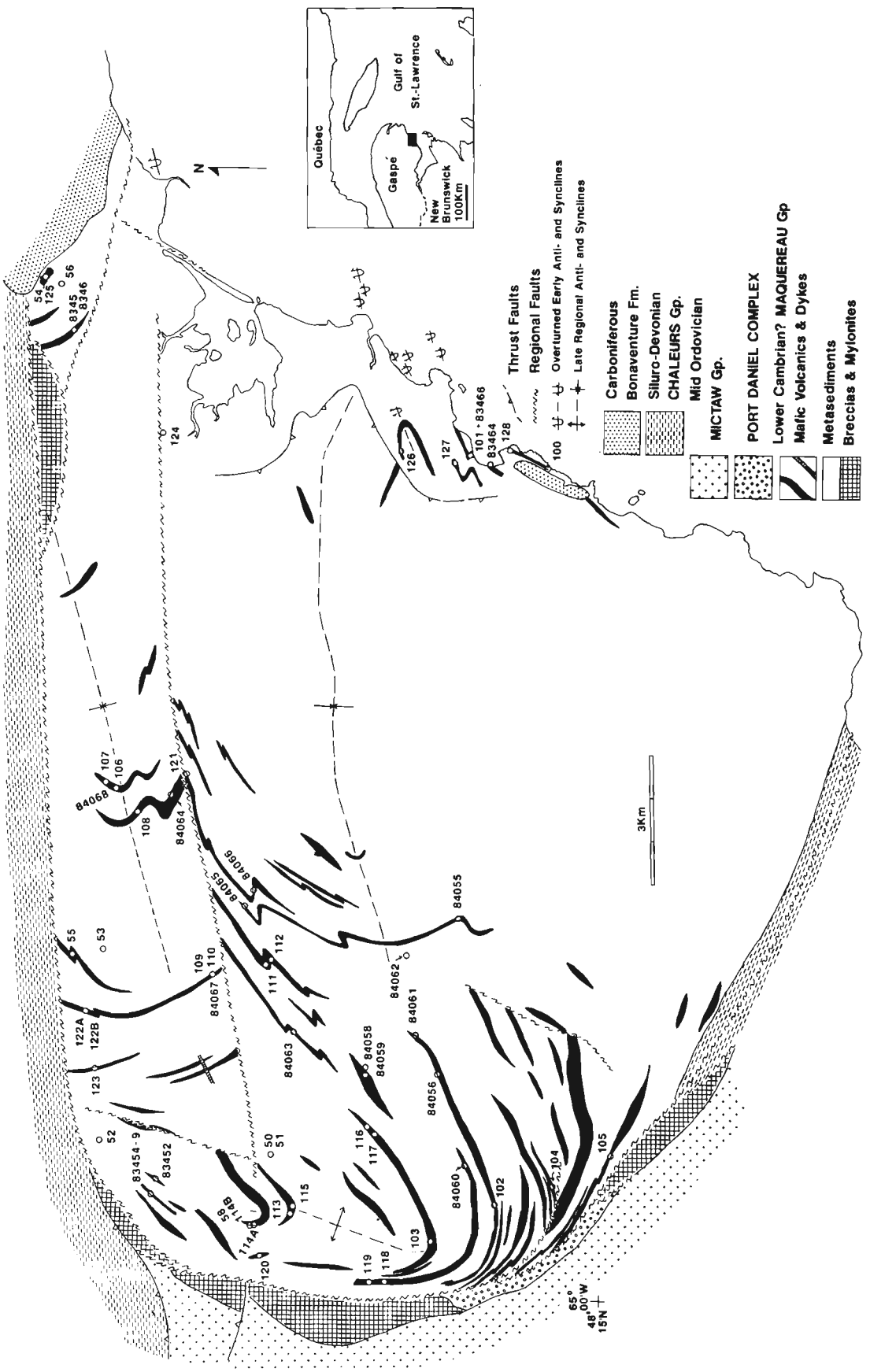

Figure 1. *Map of the Maquereau Inlier, adapted from Caron (1984) and DeBroucker (1987). Samples without prefixes are from the 92-93 field seasons.*

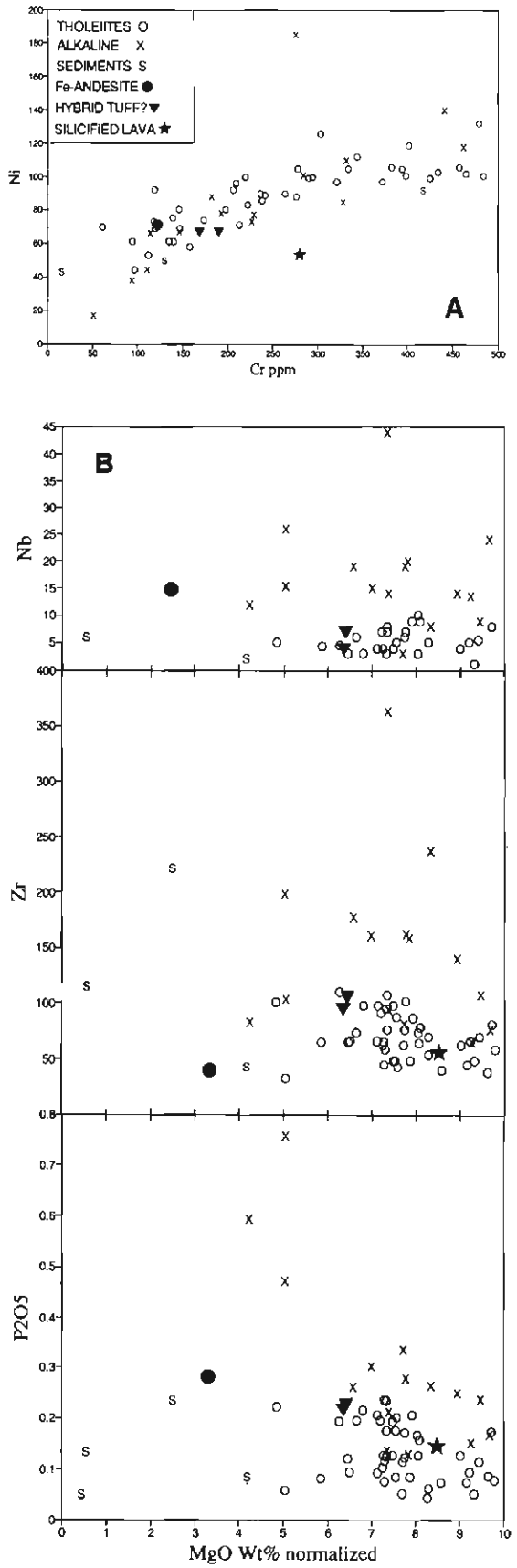

Figure 2. A) Ni vs. Cr, B) MgO vs. Nb; MgO vs. Zr; and MgO vs. P_2O_5.

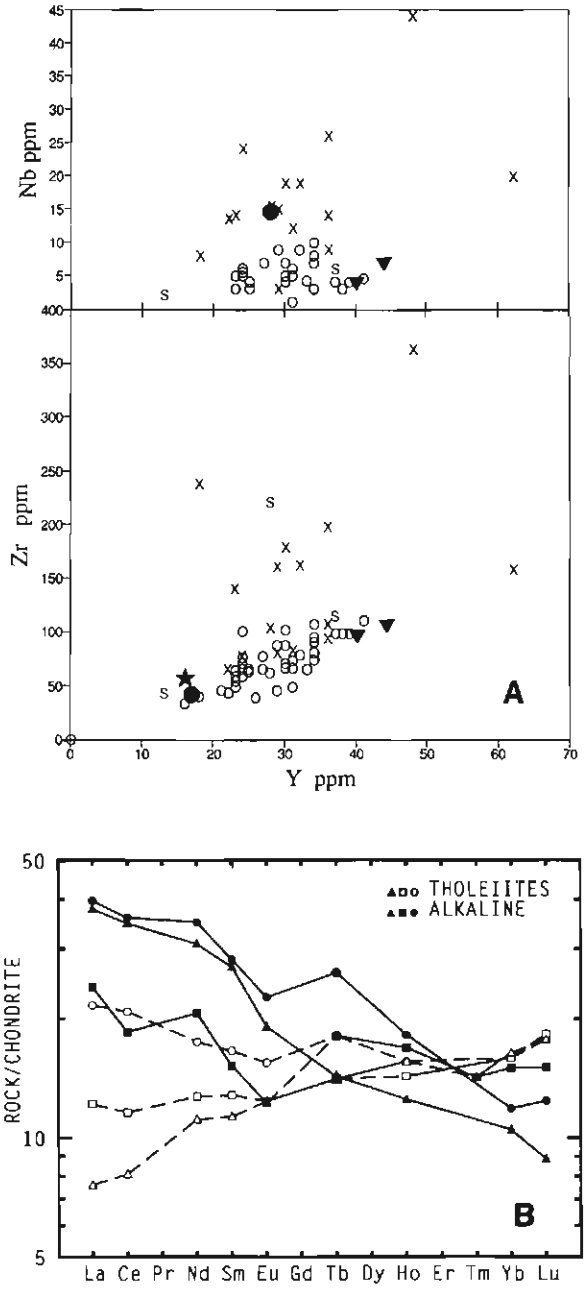

Figure 3. A) Whole rock analyses of Maquereau Group rocks. Zr vs. Y and Nb vs. Y, B) Chondrite-normalized rare-earth diagram. See Figure 2 for explanation of symbols.

SiO_2 contents (Fig. 4). Maquereau Group lavas are Cu-rich (mostly 60-140 ppm) and provide a possible source of copper for the vein-type Cu-sulphide deposits in the area.

TECTONIC ENVIRONMENT

The FeO-TiO_2 enrichment trend shown by Maquereau lavas implies a tholeiitic affinity (Fig. 4 and 5). While tholeiitic lavas do occur in arc environments, associations of tholeiitic and alkaline lavas and ferro-andesites are most common in continental flood basalt or rifted margin environments. Most of the trace element discriminants (Fig. 6) classify rocks of the alkaline suite as "within-plate" or "alkaline", and rocks of the tholeiitic suite as ocean floor basalt (OFB). The V versus Ti plot of Shervais (1982) (Fig. 7) suggests an arc affinity for many of the tholeiites. This may be due to remobilization of V during hematization of magnetite micro-phenocrysts(?).

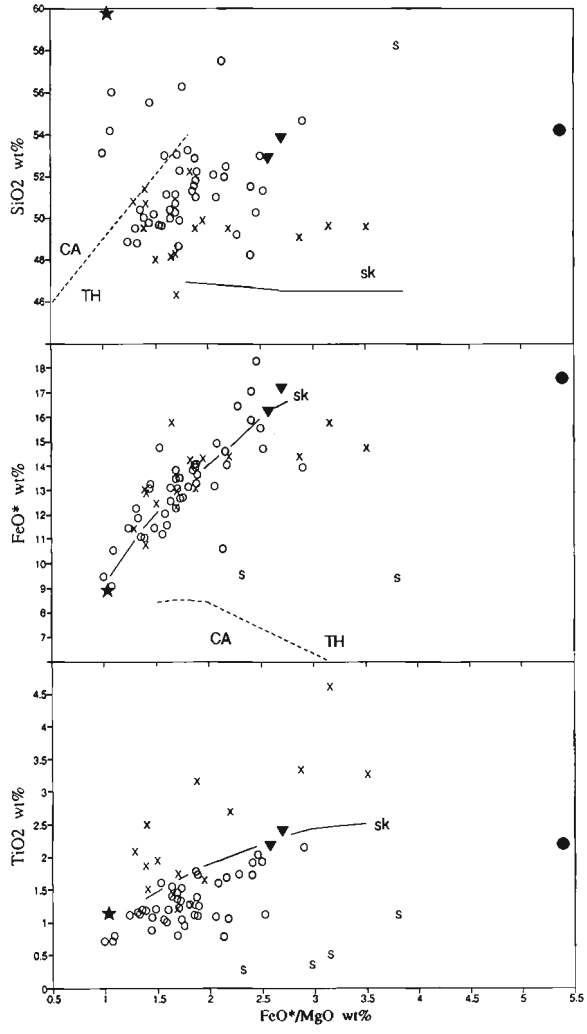

Figure 4. Whole rock analyses of Maquereau Group rocks. TiO_2, FeO, and SiO_2 vs. FeO*/MgO discriminant diagrams of Miyashiro (1973). sk = Skaergaard, TH = tholeiitic, CA =calc-alkaline. See Figure 2 for explanation of symbols.*

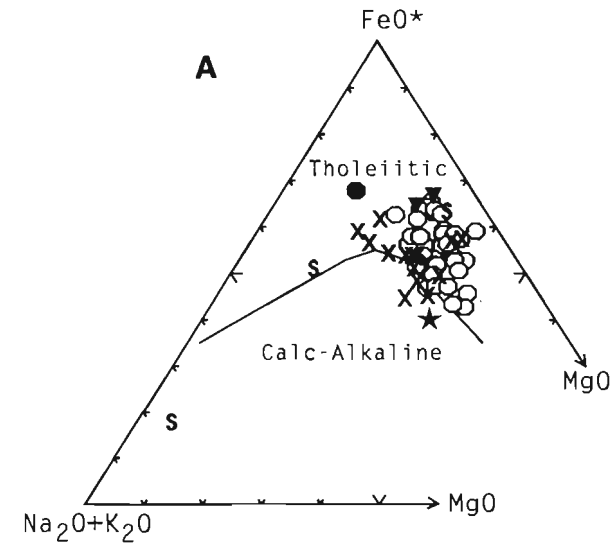

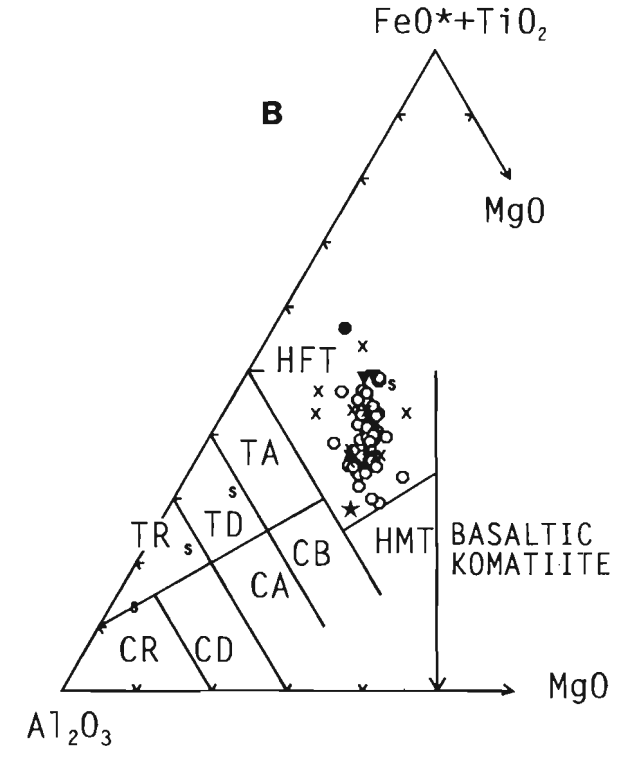

Figure 5. A) Na_2O+K_2O-FeO-MgO diagram of Irvine and Baragar (1971), B) cationic Al_2O_3-FeO*+TiO_2-MgO diagram of Jensen (1976), HMT and HFT are high-Mg and high-Fe tholeiites, respectively; CB, CA, CD, CR are calc-alkaline basalt, andesite, dacite and rhyolite, respectively; TA, TD, and TR are Tholeiitic andesite, dacite, and rhyolite, respectively.*

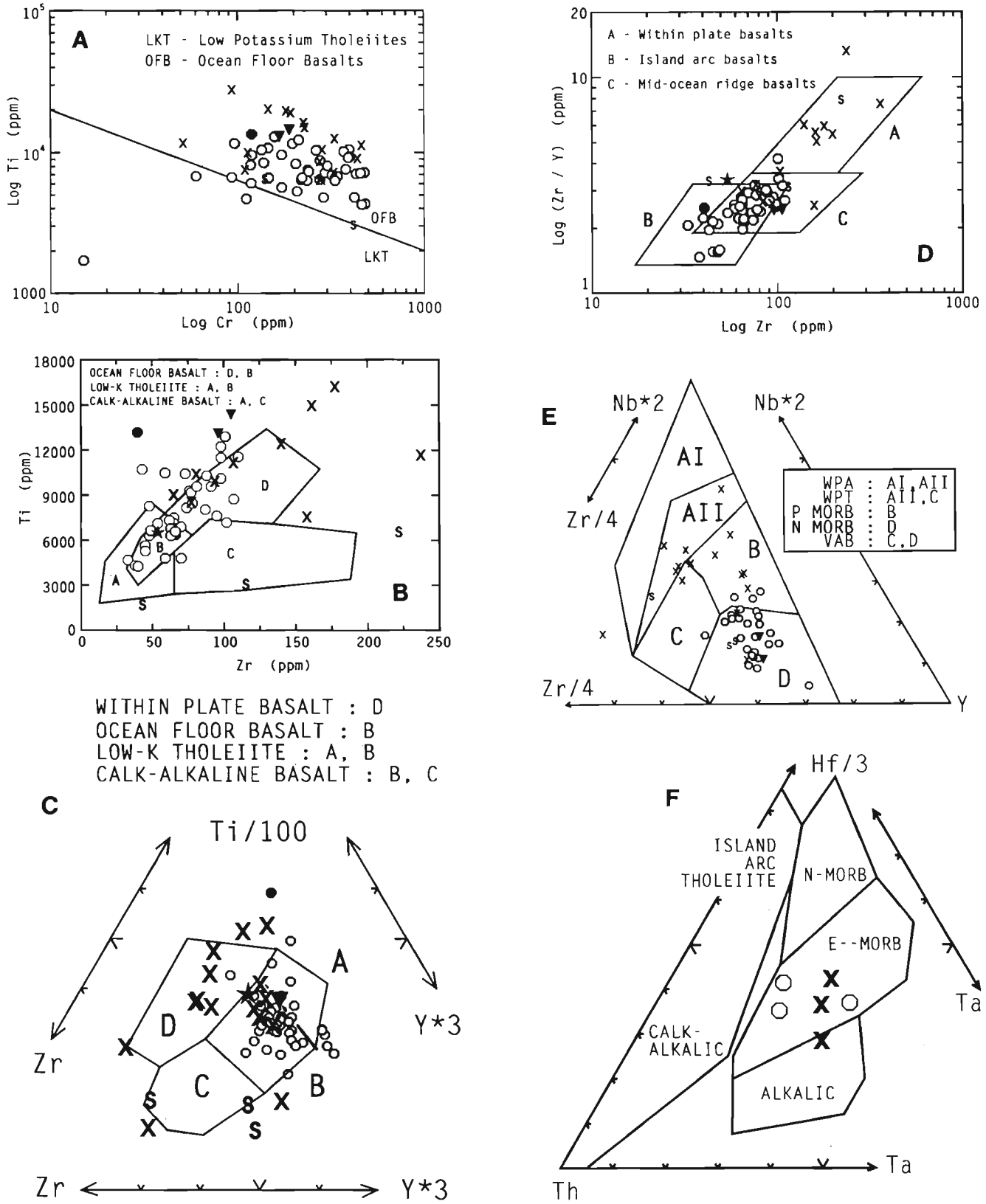

Figure 6. *A) Whole rock analysis of Maquereau Group rocks. Log Ti vs. Log Cr (Pearce, 1975), B) Log Ti vs. Log Zr, and C) Zr-Ti 100-Y*3 (Pearce and Cann, 1973), D) Log Zr/Y vs. Log Zr (Pearce and Norry, 1979), E) Zr/4-Nb*2-Y (Meschede, 1986), WPA and WPT are within plate alkaline and within plate tholeiitic, P MORB and N MORB are plume MORB and normal MORB, VAB is volcanic arc basalt, F) Th-Hf/3-Ta (Wood, 1980). See Figure 2 for explanation of symbols.*

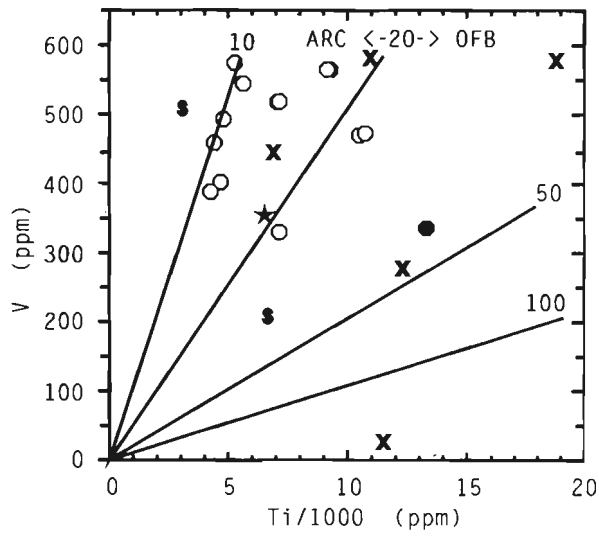

Figure 7. Whole rock analyses of Maquereau Group rocks. V vs. Ti/1000 classification diagram of Shervais (1982).

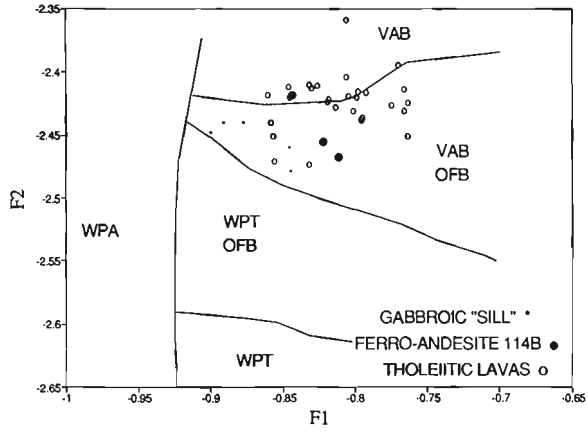

Figure 8. F1-F2 discriminant of Nisbet and Pearce (1977) for clinopyroxenes from Maquereau Group rocks. See Figure 2 for explanation of symbols.

Clinopyroxene data straddle the volcanic arc basalt/ocean-floor basalt fields on the clinopyroxene F1-F2 discriminant diagram of Nisbet and Pearce (1977) (Fig. 8). This result is problematical, since the pyroxene chemistry may have been affected by rapid cooling and nonequilibrium partitioning of elements into the pyroxene structure.

CONCLUSIONS

Maquereau Group lavas are dominantly subalkaline tholeiitic basalts, with subordinate alkaline basalts and ferro-andesites. The tholeiites exhibit a classic Fe-Ti-enrichment trend. The alkaline lavas are enriched in TiO_2, P_2O_5, and Nb. Trace and major element discriminants imply an N-MORB-like chemistry for the most depleted tholeiites, while the least depleted tholeiites resemble E-MORB or continental flood basalts. The geochemical data and geological associations suggest that the Maquereau Group is not of arc affinity, but represents a transition from rifted continental margin to seafloor-spreading environments.

ACKNOWLEDGMENTS

Fieldwork in 1983 and 1984, and analyses by C. Wilson, were financed by the Ministère de l'Énergie et des Ressources du Québec, and by N.S.E.R.C. grants to J. Ludden (Université de Montréal). Samples 100-128 were collected by G. Camiré, who also provided comments. K. Oravec helped to collect samples 50-58. M. Malo reviewed the manuscript and provided many useful suggestions. Rocks were analyzed by J.-P. Ricqbourg, J. Ludden, M. Greendale, A. Hébert, and G. Gauthier. Y. Houde assisted with drafting. Some figures were produced with NEWPET by Daryl Keen (Memorial Univeristy of Newfoundland). This is MERQ contribution number 93-5110-24.

REFERENCES

Bédard, J.H.,
1986: Les suites magmatiques Paléozoïques de la Gaspésie; Ministère de L'Énergie et des Ressources du Québec, ET84-09, 111 p.

Caron, A.
1984: Géologie de la région de Chandler, Gaspésie; Ministère de L'Énergie et des Ressources du Québec, DP86-07.

Cousineau, P.
1990: Le Groupe de Caldwell et le domaine océanique entre Saint-Joseph-de-Beauce et Sainte-Sabine; Ministère de L'Énergie et des Ressources du Québec, MM87-02, 165 p.

DeBroucker, G.
1987: Stratigraphie, pétrographie et structure de la boutonnière de Maquereau-Mictaw (Région de Port Daniel, Gaspésie); Ministère de L'Énergie et des Ressources du Québec, MM86-03, 160 p.

Irvine, T.N. and Baragar, W.R.A.
1971: A guide to the chemical classification of the common volcanic rocks; Canadian Journal of Earth Sciences, v. 8, p. 523-548.

Jenner G.A. and Swinden, H.S.
1993: The Pipestone Pond Complex, central Newfoundland: complex magmatism in an eastern Dunnage Zone ophiolite; Canadian Journal of Earth Sciences, v. 30, p. 434-448.

Jensen, L.S.
1976: A new cation plot for classifying subalkalic volcanic rocks; Ontario Department of Mines, Miscellaneous Paper N. 66.

Logan, W.E.
1846: Progress Report for 1844; Geological Survey of Canada

Meschede, M.
1986: A method of discriminating between different types of mid-ocean ridge basalts and continental tholeiites with the Nb-Zr-Y diagram; Chemical Geology, v. 56, p. 207-218.

Miyashiro, A.
1973: The Troodos ophiolitic complex was probably formed in an island arc; Earth and Planetary Science Letters, v. 19, p. 218-224.

Nisbet, E.G. and Pearce, J.A.
1977: Clinopyroxene composition in Mafic Lavas from different tectonic settings; Contributions to Mineralogy and Petrology, v. 63, p. 149-160.

Pearce, J.A.
1975: Basalt geochemistry used to investigate past tectonic environments on Cyprus; Tectonophysics, v. 25, p. 41-67.

Pearce, J.A. and Cann, J.R.
1973: Tectonic setting of basic volcanic rocks determined using trace element analyses; Earth and Planetary Science Letters, v. 19, p. 290-300.

Pearce, J.A. and Norry, M.J.
1979: Petrogenetic implications of Ti, Zr, Y, and Nb variations in volcanic rocks; Contributions to Mineralogy and Petrology, v. 69, p. 33-47.

Ringele, H.
1982: La déformation taconienne en Gaspésie du Sud: Le Groupe de Maquereau et son encaissant; M.Sc. thesis, Université de Montréal, 68 p.

Shervais, J.W.
1982: Ti-V plots and the petrogenesis of modern and ophiolitic lavas; Earth and Planetary Science Letters, v. 59, p. 101-118.

St.-Julien, P. and Hubert, C.
1975: Evolution of the Taconic Orogen in the Québec Appalachians: American Journal of Science, v. 275A, p. 337-362.

Walker, K.R., Ware, N.G., and Lovering, J.F.
1973: Compositional variations in the pyroxenes of the differentiated palisades sill, New Jersey; Geological Society of America Bulletin, v. 84 p. 89-110.

Williams, H. and St-Julien, P.
1982: The Baie-Verte-Brompton Line: Early Paleozoic continent ocean interface in the Canadian Appalachians; in Major structural zones and faults of the northern Appalachians, (ed.) P. St-Julien and J.Béland; Geological Association of Canada, Special Paper No. 24, p. 177-208.

Wood, D.A.
1980: The application of a Th-Hf-Ta diagram to problems of tectono-magmatic classification, and to establishing the nature of crustal contamination of basaltic lavas of the British Tertiary volcanic province; Earth and Planetary Science Letters, v. 50, p. 11-30.

Geological Survey of Canada Project 920001

APPENDIX

Sample descriptions

ep = epidote, cc = calcite, qz = quartz; hem = hematite; mt = magnetite; chl = chlorite; ilm = ilmenite; sp = titanite; lx = leucoxene; py = pyrite; cpy = chalcopyrite; ab = albite; plag = plagioclase; cpx = clinopyroxene; AIC = Anomalous Interference Colours; GC = geochemistry fraction; f/g = fine grained; m/g = medium grained c/g = coarse-grained

MAQ50 Grey-green slate.

MAQ51 Pink-green sandstone. Angular feldspar (partially sericitized), lesser quartz grains (5:1 ratio, av. 0.5 mm, max. 2 mm), also mafic and opaque grains ~5%, rare f/g shale or volcanic clasts, and lithic clasts of plag+qz. Groundmass ~15% rich in chl+cc.

MAQ52 Pink-green sandstone. Porous white veinlets.

MAQ53 Grey-green slate with rusty-red interlayers.

MAQ54 Green pillow lavas. Pale green matrix, ~5% mafic phenocrysts (<1 mm); GC sample has ~5% ep-rich veins cutting hem+qz veins (<1 cm).

MAQ55 f/g diabasic basalt. Contains rare plag phenocrysts (<2 mm), and prismatic glomerocrysts (cpx(?) or plag(?)) replaced by ep+chl+qz+ab?, with cc in tensional fractures. Groundmass dominated by turbid plag laths, and interstitial chl+ep+ab(?)+opaques. Rare ophitic cpx relics. Sulphides form small oikocrysts. GC fraction has a few rust-red veins and some ep veins.

MAQ56 f/g-m/g dark green qz-rich sandstone; qz grains (1-3 mm) are rounded to angular, many strained; plag is less abundant and smaller. Also 1-2% small opaque grains. Interstices contain sericite and carbonate. The GC fraction has a few cc+qz veins in it.

MAQ58 Feldspar-phyric metalava. Groundmass has very f/g altered plag microlites with chl+ep+oxide? Rare (1-3%) plag phenocrysts ~2 mm, and glomerocrysts. Also 2-5% white xenoliths(?) or boudinged veins, or deformed amygdales (<3 cm), that contain qz with a mortar texture, with many strained grains. The larger feldspar grains looks like perthite or antiperthite; cc fills the interstices. The GC sample contains some of this felsic material, also some of the veins. Pods of chl (purple-blue AIC) are either amygdales or boudinaged veins. They are cut by qz and qz+cc veins, some with chl fills. Also see turbid bands rich in organic(?) material.

MAQ100 Massive f/g, weakly foliated metabasalt. Penetrative schistosity 027,48. Mineral lineation 24,085. Groundmass dominated by chl+cc+mt+ep(?); chl has grey AIC; mt (~10%) as fine euhedral grains, commonly fragmented (brecciated schlieren) or hollow. Outcrop has numerous veins of qz+cc+mt (262,85 & 000,55) with rare ep at vein margins. A few veinlets included in GC.

MAQ101 Massive f/g metabasalt. Schistocity 324,35. Rock dominated by chl (~50%). Plagioclase pseudomorphs are rare and generally epidotized. Oxides (~8%, av. ~ 0.5 mm) occur as lamellar to skeletal ilm/mt intergrowths/exsolutions; py as rare f/g aggregates. Numerous qz+cc veins. GC contains a few chl+ep+qz and qz+cc veins. Veins contain ep that appears brecciated, and is enveloped by chl with purple AIC; qz looks late, locally, filling shear zones. Other veins are composed of f/g cc associated with qz.

MAQ101V Same as MAQ101 but with 15% folded qz+chl+ep veins in GC.

MAQ102 Massive microdiabase. Very f/g chl+ep+sp(?)+talc(?) rock. Relic lath texture, laths of plagioclase replaced by turbid ep. Amorphous groundmass may also contain sp or lx, and perhaps talc? Fine grained, spongy-textured oxides (<3%) look like mix of mt and hem. Rare cubes of py are embayed by grey oxide. GC is rich in small ep veins (8%). Veins may be 100% ep, or be composed of qz>cc. Veins are commonly disaggregated.

MAQ103 Massive speckly-textured, microdiabase. Rock dominated by ep+qz+chl+fibrous talc or actinolite+mt/hem+sp(?); mt is euhedral. Rare f/g plag lath pseudomorphs. Honey-coloured prisms may be after cpx. Early anastomozing/discontinous veinlets (type 1) are composed of wall-perpendicular, needle-like fibres of actinolite(?) or talc(?) or chl(?). Others have random splays of these fibrous minerals in qz. These early fibre veins are cut by veins dominated by strained and sutured qz grains±cc±fibrous-platy hem (type 2). The walls of type 2 veins may have discontinuous rinds of type 1 fibrous talc(?) or chl(?) along their borders. Type 3 veins are thin and laterally discontinuous. They are composed of ep± iddingsite, and locally, are embedded in qz veins. Pyrite framboids are present in the GC fraction, but the larger veins were removed.

MAQ104 Foliated (112,78) microdiabase. Ovoid microdiabasic lenses have plag micro-laths (replaced by qz) and cpx prisms (replaced by cc). Minor euhedral mt+ilm intergrowths, some with chl overgrowths also occur. The diabasic lenses are separated by a schistose chl+qz+mt/ilm+minor cc+hem rock. The foliation is cut by veins of wall-crystallized prismatic ep, with cc±qz vein-infills. GC fraction contains 10-15% of these ep veins, folded and boudinaged. Qz fills fractures that are perpendicular to extension. This vein set is locally porous.

MAQ105 F/g to m/g, clotty-textured basaltic schist. Lenses and balls of prismatic ep and microcrystalline qz are boudinaged; cc is mechanically recrystallized and locally abundant. The matrix is dominated by chl+ep+sp(?). Chl commonly forms sprays, while the ep+sp occurs as clots. The groundmass is commonly very red, implying the presence of abundant hem. Py also is boudinaged, and contains numerous silicate inclusions. Py is also commonly replaced by grey Fe-oxides. There are numerous foliation-parallel and perpendicular veins of qz+ep+hem.

MAQ106 Speckly-textured microdiabase. Oxide phenocrysts (0.5-1 mm 5-10%) are intergrowths of mt and ilm(?) or rutile(?), and form local concentrations. There are large ovoid framboids of py+cpy. Most of rock is composed of cpx+plag (30/30) with ~30% interstitial qz and albite and abundant chl. Plag is almost completely sericitized, with rare, clear ab patches. Cpx is acicular, pale brown, with darker rims and longitudinal twins. Several small ep+qz veins are present in GC.

MAQ107 Same outcrop as 106. F/g to aphyric metabasalt. 10% 0.5 mm hem pseudomorphs after plag(?). Most of rock is dark and turbid mass of (?)chl+ep+cc(?) with minor disseminated cubes of brown-grey mt or ilm, and very f/g anhedral hem. Veins are sheared cc>qz>chl±minor hem, a few of which are included in GC.

MAQ108 Pale green metabasalt. Dominated by f/g mass of cc>qz>ep>talc(?)+sp or lx(?) and <5% f/g disseminated py cubes. The rock contains 10-15%, 1-3 mm, plag phenocryst and glomerophenocryst pseudomorphs, all partly replaced by ep.

MAQ109A Dark green massive metabasalt sampled several metres from contact with sediments. Very f/g microdiabasic texture. Plagioclase microlites replaced by ab+ep; cpx by chl. Subeuhedral (~10%) oxides are either mt or ilm. A second oxide phase is more anhedral, whiter, and may be hem. Mt or ilm are commonly partly altered to sp or lx. Minor qz and cc in groundmass. GC contains 2-4% qz+ep veinlets. In thin section the veins are filled with dark and turbid material.

MAQ109B Green, f/g metabasalt sampled several metres from contact with sediments. Plag microlaths typically replaced by cc, minor ep and sphene(?) Local speckles of hem. One large patch of py cubes rimmed by mt. Locally, plag forms wormy intergrowth with chl characterized by purple AIC. Minor chl±qz veins included in GC.

MAQ109C Sandstone near contact with volcanics. Grains are angular, and appear sorted (av. ~ 0.3 mm). Qz/feldspar ~1. Qz shows undulatory extinction, plag has folded and sheared twins. About 15-20% interstitial very f/g qz and minor chl(?) and unidentified turbid material; rare zircon and muscovite grains also present. Numerous qz (15%) and ep (10%) veins. At periphery of one vein, an unusual vermicular intergrowth of chl(?) and qz was observed.

MAQ110 Same band as 109. Grey foliated, flaser-textured metabasalt. Schistose chl+cc+ qz or plag+oxide+lx(?) Oxides (~5%) are very f/g, anhedral mt or hem. Plag pseudomorphs are well preserved. Chl has pale brown AIC and locally forms veins. 2-3% veins in GC.

MAQ111 Dark massive microdiabase. Cut by ep veins (not included in GC). 50/50 cpx/plag. Cpx forms small, very pale brown prisms, with augite twins, partly altered. Plag generally very altered, but many grains have relic plag. Groundmass is less clearly granophyric than 106 and seems finer grained. Oxides, mt+ilm? ~5-8%. Chl has blue-green AIC; A large, 5 mm sulphide patch in analyzed fraction; in thin section ~80% py, 20% cpy.

MAQ112B Same layer as 111. Fresh Fe-rich microgabbro. Cpx very clean, with brown turbid rims. Plag forms chain-like grains. Oxides (~10%) as large composite ilm+mt grains. Sulphides as fine disseminated py, and as large individual composite grains composed of py+cpy+a reddish phase (bornite?)+2 different grey-blue phases are also present (chalcocite(?) tetrahedrite(?)). Rare qz veins with porosity (included in GC).

MAQ113A Foliated lensoid partially hæmatized metabasalt. Outcrop has rusty surface with traces of py and a few cc veins. Rock is composed of schistose and carbonated domains. Schistose domain composed of foliated chl+plag+opaques(lx?). Carbonated domain composed of very f/g cherty-looking stuff with pink tinge and 5-10% f/g mt+ilm(?). There are also dismembered cc+qz veins.

MAQ113B Dark grey, f/g, unfoliated, microdiabasic metabasalt sampled near 113A. Mostly composed of alb+chl+lx(or ep?). Very rare equant grains of mt+ilm(?), most oxides are very f/g speckly hem? in groudmass. Pools of cc are associated with turbid black-red veins of hem+organic matter and goethite; ~20% clasts of chert (metasomatic?).

MAQ114A Very f/g dark grey, strongly foliated metabasalt. Dominant crenulated fabric is outlined by chl+ep(turbid)+qz(?)+cc(?)+mt(?). Chl is either grey-green or purple (AIC). Cc commonly forms boudins. Oxides are mostly grey mt(?), some more fibrous and brighter (hem?); minor py, commonly with mt rims. Subordinate cpy, rarely with mt rims. Layer-parallel epidote and qz veins are refolded into schistosity. All disrupted by crenulation. Crenulation surface filled by qz+cc+turbid black material.

MAQ114B Dark grey f/g microdiabasic metabasalt. Same place as 114A but less altered and deformed. Cpx locally as fresh prisms. Plag forms acicular laths and elongated wedges. Oxides are mt+ilm (~10%). Groundmass chl is blue-green; some may be pumpelleite. Medium grained (1-3 mm) ovoid clots of py+minor cpy (1-3%). Pale green veins ~3% in GC. Also veins with cc+black turbid material.

MAQ115 Same volcanic band as 114. Fine grained, amygdaloidal, foliated (253,33) greenschist with rusty surface and disseminated sulphides. Mostly composed of microdiabase. Plag as short stubby microlites. Chl forms lensoid layers and is commonly associated with qz. There are 20-30% amygdules or boudins of qz>hem>goethite. Boudins composed either of qz (multigranular) or cc, locally both. Boudins are often coated with f/g reddish hem or goethite. Veins of cc and cc+hem±amorphous f/g goethite are slightly folded in thin section, but in hand specimen there are numerous foliation-parallel goethite veinlets. Locally large cubes of py have cpy rims, in turn surrounded by grey dark low-reflectance opaque oxide(?) and then by amorphous goethite.

MAQ116A Massive microdiabase. Plag laths altered to turbid mass of ep+ab(?) Cpx prisms mostly fresh, colourless. Pools of interstitial micro-crystalline qz and small sp pseudomorphs after oxides. 2-3 large sulphide grains, rest occur as very f/g disseminations. Py/cpy = 5/1. 2 Vein types: 1) very thin veins cutting schistosity composed of pale brown fibres with parallel extinction and blue-tinged interference colours, grown perpendicular to vein walls (talc?) and separated by pools of colourless prehnite(?) with grey interference colour. These veins form en-echelon arrays, offset by shear veins (type 2) that contain fibrous ep+chl (radial clusters with purple and green AIC)+cc+oxides (including hem). The larger veins were not included in GC.

MAQ116B Finer grained than 116A and more altered, no fresh cpx. Large ovoid boudinaged pseudomorphs after plag(?) phenocrysts (10%, 1-3 mm) consist of pink-red amorphous near-isotropic material (hydrogarnet?). Boudin infilled by extension-parallel fibres of cc. Interfibres of chl+hem appear towards sides of these cc fibre-bundles. Cc fibre bundles also contain cubes of mt and py and fibrous clots of hem. Py contains small purplish bleb. Hand specimen also marked by 5-10% small, chl+hem pseudomorphs after (?)cpx or olivine(?) flattened in foliation plane.

MAQ117A Same volcanic band as 116. 117A is an altered facies of 117B. Much more turbid. Contains large discordant veins (2 mm wide) of qz+cc as vein-perpendicular fibres. The coarse cc+qz fibres are decorated by plumose chl(?) or talc(?).

MAQ117B Massive f/g metabasalt. Cpx is f/g and commonly fresh. Plag laths are replaced by turbid ep(?). Rare (<1%) disseminated py+cpy. Groundmass mostly composed of qz+chl+cc. Rare <5% veins of chl, goethite, and pale green zoisite(?).

MAQ118A Massive flow or dyke of microdiabase, weakly foliated. Plag (<0.5 mm) as turbid laths. Cpx often clean. Groundmass composed of chl+qz+ep (turbid and f/g) or lx. Qz may coat plag and cpx grains. Ovoids of sulphide in GC, flattened along foliation plane and stretched parallel to lineation. Early, discontinuous veinlets of chl(grey-blue AIC)+qz+turbid red hem. Rare, slightly more coherent veins of ep+qz+chl (blue AIC).

MAQ118B Microdiabase, less foliated and hematized than A.

MAQ119 Weakly foliated, speckly microdiabase. Groundmass dominated (~75%) by turbid ep-rich material, pseudomorphous after plag(?) rest is cc+qz+chl (blue AIC), minor mt and rare py. Some pools of chl have red AIC. Py generally ragged-looking and may have mt rims. Early veins are boudinaged qz+ep. One large ep vein in hand specimen (trimmed from GC). Also see veins with qz+py+purplish sulphide. Late-kinematic veins of very weakly deformed cc+qz.

MAQ120 Foliated and crenulated microdiabase. Mostly looks like 119, except chl(?) looks deformed, has fibrous habit and 1st order blue IC, may actually be talc. Very f/g disseminated py, a few larger euhedral mt grains. Rare chl microveins.

MAQ121A Fractured and partly altered micro-ophitic gabbro. Fresh cpx forms oikocrystic or ophitic grains. Much cpx is altered to chl (bright red-purple-blue AIC). Plag laths all replaced by turbid ep+ab-rich material. Groundmass dominated by chl+cc+oxides. Most oxides are altered mt+ilm, replaced by f/g spongy aggregate of hem+goeth(?) One sulphide clot dominated by py+minor reddish sulphide (~112B) and a cream-coloured sulphide (pyrrhotite?) 1 small pale green vein (trimmed from GC).

MAQ121B Similar micro-gabbro; fewer veins, no py. One small veinlet of cc+red amorphous hem(?)+goeth(?).

MAQ122A Fractured m/g oxide-gabbro (2-5 mm laths). 30-40% subhedral plag, locally euhedral cumulus with included needles of apatite; replaced by ab+ep, rare sprays of chl. Some laths are deformed. 25-30% sub-ophitic, clear pale brown cpx. ~15% oxides, as blades or latticework after partially replaced, exsolved mt+ilm. Some grains have finer exsolutions. ~20% groundmass chl+ep, very f/g, green AIC. Fractures coated with hem+goeth.

MAQ122B Finer grained facies, ~10% 1 mm pseudomorphs after ol(?) phenocrysts. More porphyritic than A, with ovoid cpx and euhedral plag in a partly altered, quartzofeldspathic, felsite-textured groundmass. Oxides fresher, some composite mt+ilm. Ilm looks homogeneous, mt as coarsely-exsolved blades. Minor ep and goethite veins.

MAQ123 Massive f/g to aphyric. Either strongly silicified or a sandy siltstone. ~15% qz, rounded to angular. ~10% square chloritized grains (altered cpx?). Rare white mica. A few zircon or sp grains? Most of matrix is amorphous very f/g talc(?)+chl(?)+qz(?). A 10 mm wide band of hydrothermalized material in centre is rich (15%) in sulphide and is bounded by goethite-rich haloes. Sulphides are framboidal clusters of smaller grains. Mostly py, some late cpy. Rare chl(?) veins.

MAQ124 Pebbly sandstone. Quartz dominant, plag rare. Grains are anhedral to angular. Largest grains ~2 mm, av. 0.5-0.8 mm. Groundmass is turbid, quartz-rich material. Rare muscovite and zircon grains. Has dark laminae (organics?) and numerous qz veins.

MAQ125A Pillowed metavolcanic. Mostly aphyric turbid devitrified glass as polygonal domains separated by blades of ol or plag pseudomorphs (micro-spinifex texture). 2-3% ovoids, ~1 mm, ol or cpx replaced by chl. Dominant vein type is ep+qz+sulphide. Cubes of py+cpy associated with a brown-purple sulphide, py+cpy also present disseminated in groundmass. Early veins are cut and offset by cc+qz veins that may have discontinuous rinds of fibrous (vein-perpendicular) talc(?) at their margins. A third vein set cuts all above, and is composed of same fibrous material. Veins are ~5% of GC.

MAQ125B Metabasalt, similar to 125A but a bit coarser. Faint microdiabasic texture, with plag microlites and fine interstitial cpx. Rare 0.5 mm sized plag (pseudomorphed, but twins visible), and chl+ep pseudomorphs after ol(?) (5%) phenocrysts. Groundmass also contains minor disseminated mt, cpy, and a purple sulphide. Common (5-10%) veins of ep>qz>hem>chl veins in hand specimen. In thin section see cc+qz+talc(?)+mt or hem veins.

MAQ126 Plagioclase-phyric metabasalt, massive. 2-3%, 4 mm plag grains and clots. Microdiabasic groundmass, looks silicified(?) 10% qz+cc(?) veins, white and pink, associated with porosity. 2-3 cm amydules filled with chl(?) (trimmed off from GC).

MAQ127A Massive f/g speckly greenstone. Abundant chl+turbid hem(?)+ clear plag or qz. Abundant ovoid to angular-equant qz grains, suggesting this may be a siltstone?. ~15% opaques (lx? and hem?). Very carbonatized. Veins of cc+qz, common very thin chl veins.

MAQ127B Sampled 3-4 m above A. Matrix dominated by cc+chl+qz. Chl (purple AIC) commonly forms foliation-parallel laminae. Qz commonly looks like ovoid/angular grains of sand (sandstone?) 5-10% f/g mt. 2 generations of veins cc>qz. 15% qz veins in analyzed fraction.

MAQ128 Probable dyke 2-3 m wide. Hem-qz breccia. Groundmass very carbonated f/g, with lots of chl and f/g oxides. Cc+qz veins folded, and cut by fibrous cc vein.

Stress relief and incidental geological observations in and around Ottawa, Ontario

John Adams and Clark Fenton
Geophysics Division

Adams, J. and Fenton, C., 1994: Stress relief and incidental geological observations in and around Ottawa, Ontario; in Current Research 1994-D; Geological Survey of Canada, p. 155-160.

Abstract: Stress relief, in the form of small horizontal movements in Paleozoic strata, has been observed in three excavations in the Ottawa region. Movement is revealed by the offset of closely-spaced borehole half-barrels in the excavation walls. Three other excavations show no evidence for stress relief. When present, such strain relaxation features provide important evidence on the orientation and magnitude of the local (shallow) stress field. In addition to these minor horizontal movements, further evidence of post-Ordovician strike-slip faulting in the Ottawa region is described.

Résumé : Un relâchement de contraintes, sous la forme de petits mouvements horizontaux dans des couches paléozoïques, a été observé dans trois excavations de la région d'Ottawa. Le déplacement est indiqué par le décalage de demi-corps cylindriques (traces de carottes) peu espacés dans les parois d'excavation. Trois autres excavations ne présentent aucun indice de relâchement de contraintes. Lorsqu'ils sont présents, ces indices de relâchement de contraintes donnent des indications importantes sur l'orientation et l'amplitude du champ des contraintes local (peu profond). En plus de ces déplacements horizontaux mineurs, sont décrits les indices de décrochements postordoviciens dans la région d'Ottawa.

INTRODUCTION

Stress relief phenomena following excavation in bedrock (reflecting the release of strain energy stored elastically in the rock) have engineering implications as well as providing important evidence on the local stress field. Stress relief can cause vertical bedrock heave ('quarry-floor buckles' or pop-ups) in excavation floors, lateral displacements on excavation walls (including 'offset boreholes'), and squeeze problems in tunnels. Previous examples from engineering excavations in southern Ontario include the Dufferin Quarry, Milton (Lo, 1978) and the McFarland Quarry, Ottawa (Adams, 1982), the Scotia Plaza excavation in Toronto (Trow and Lo, 1989), and the Thorold tunnel on the Niagara Peninsula (Bowen et al., 1976).

For aesthetic, economic, and stability reasons, many rock faces are 'pre-split' during excavation; this involves drilling closely-spaced boreholes for small explosive charges along the intended edge of the excavation and their controlled sequential detonation. A pre-split face is usually vertical and planar, and is traversed vertically by semi-circular borehole walls, sometimes called 'half-barrels' (e.g., Fig. 1). In competent rock, the half-barrels are well preserved, and the presence or absence of lateral displacements on the face can be determined to within a few millimetres. Offset boreholes have previously been documented (and sometimes misinterpreted) by Schäfer (1979), Block et al. (1979), and Bell (1985). Though some have attributed all the deformation to blast heave or to the effect of drilling through voids (Zhongyou, 1986), common features confirming the endogenic origin of the displacements are: systematic offset of half-barrels; displacements of competent unfractured beds on incompetent weak layers; up-dip motion, indicating movement against gravity; and movement oblique to the excavation wall, indicating more than a passive sagging of the strata into the excavation.

Figure 1. *Offset boreholes in gneiss just west of Baskatong Reservoir. Photograph taken in August 1980.*

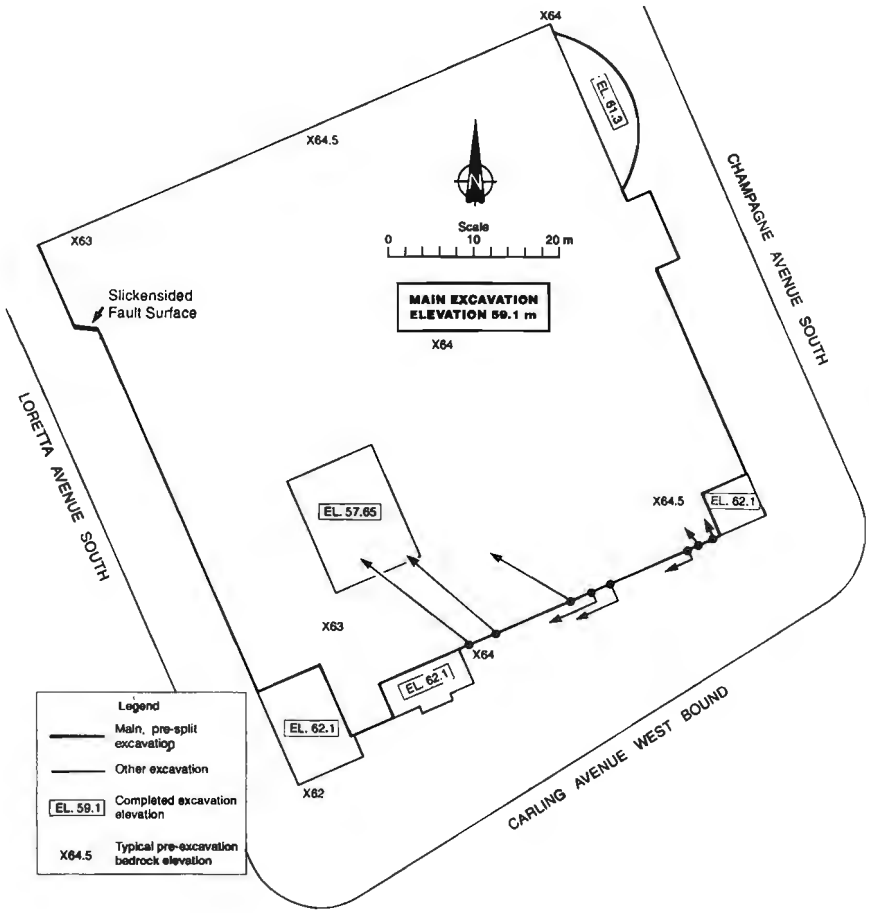

Figure 2.

Map of 1993 excavation on Carling Avenue, showing the pre-excavation elevations, the completed excavation floor (all elevations are in metres relative to sea level), and vector displacements of the offset boreholes on the pre-split face (arrows, longest arrow represents 20 mm displacement; see Table 1 for values). Note that the position of each station along the face is estimated, not surveyed, and that for the three boreholes for which inward displacement was not determined, the along-face component is drafted below the line for clarity.

We report here some recent occurrences of stress relief in the Ottawa region, as well as some unaffected excavations. All but one of the excavations are cut into the middle Ordovician limestone that forms the bedrock surface under much of Ottawa. In addition, we report on some incidental observations that bear on post-Ordovician fault movements in the Ottawa area. Because of the urban location of most of the localities we suggest that geologists intending to visit any of these localities use a street map of the National Capital Region.

EXCAVATIONS SHOWING STRESS RELIEF PHENOMENA

Baskatong, Quebec

A few kilometres west of the Baskatong Reservoir, 150 km north of Ottawa, a pre-split face shows boreholes offset by up-dip movement (Fig. 1). The 6 m high, north-northwest-trending face is blasted in gneiss on the northeast side of Highway 117. Displacement occurred on two weathered mafic layers dipping 11° to the northwest, with movement of 70 mm on the lower and about 25 mm on the upper. There is almost no movement into the excavation, suggesting that the movement direction towards 155° is a good indication of the local stress orientation.

Hull, Quebec

A semicircular trench excavated 4-5 m into limestone in Hull, for the Boulevard St. Laurent exit ramp from Highway 550 westbound, has well developed offset boreholes on three shaley horizons. The predominant transport direction is 065°, consistent with the regional stress direction (e.g., Adams, 1987; Adams and Bell, 1991). As we understand this exposure is the subject of a M.Sc. thesis, we do not describe it further.

Carling Avenue, Ottawa, Ontario

In April 1993, we examined the excavation for a two-storey underground parking garage at the site of the Dow's Lake Court building of the Canadian Medical Protective Association, on the north side of Carling Avenue between Champagne Avenue South and Loretta Avenue South. A pre-excavation survey indicated a nearly-flat bedrock surface, and the excavation, blasted into limestone to a depth of about 5 m over a 3600 m^2 area, was complete at the time of our visit (Fig. 2). The north-northwest side was rough-blasted in anticipation of a future extension, but the other three sides used controlled pre-splitting and had excellent faces with clean half-barrels. No offsets were seen on the two faces perpendicular to Carling Avenue, but the Carling face showed oblique offset of the boreholes (Fig. 3). On this face, the limestone beds dip 5° to the east, and the offsets represent not only movement into the excavation (as might be expected by passive relaxation) but also movement up-dip (Fig. 4). Movement occurred on two shaley horizons, with the small movements on the upper shale layer near the southeast corner being transferred to movements on the lower shale by a vertical zone of fractured rock. The fracture zone occurred on one of three prominent and several minor planes cutting the excavation edge obliquely; locally they had caused failure of the neatly-blasted rock face (see Fig. 4).

The movement of the upper rock is most simply described as the component along the excavation (towards west-southwest) and the component of inward motion (Table 1); we treat the movements as if they occurred on a single detachment horizon. Inward motion increases up-dip from the southeast corner of the excavation, while west-southwest motion is less regular. The large motions near the southwest corner are towards 311° (Fig. 2). We interpret the inward movements to represent strain relief of the rock due to the removal of the confining stress previously provided by the excavated rock. The west-southwest movements are likely to be consequent, in that once the inward movement had begun, the rock could

Figure 3. *Typical offset borehole showing oblique movement of upper rock (inward and to the right) on the lower shaley horizon. GSC 1993-255B*

Figure 4. *View (from the northwest) of Carling Avenue excavation, showing the pre-split face, shaley layers accommodating movement (arrows), and local failures caused by fracture planes oblique to the face. GSC 1993-255A*

Table 1. Displacements of boreholes along Carling excavation (see Fig. 2)

Station	Inward (mm)	to WSW (mm)
East end G	3	0
H	3	2
I	-	6
E	-	8
D	-	8
C	10	10
B	15	8
West end A	18	9

Notes: movements in millimetres
- not determined

also move up dip along the excavation, and because the strata dip, the shaley horizons daylight near the southwest corner of the excavation and the limestone beds are not pinned there as they would have been had the strata been horizontal.

For a beam, pinned at one end and allowed to relax from a previously-imposed stress, the incremental displacements should progressively increase away from the pin. A 9 mm lengthening over the width of the excavation (taken to be 40 m to account for the daylighting of the strata) and a Young's Modulus of 50 GPa gives a relieved stress of about 10 MPa, which though high, is within the scatter of stress magnitudes measured by overcoring at 5-10 m depths (e.g., Adams and Bell, 1991, Fig. 8). The only Ottawa stress measurement we are aware of was 2.3 MPa determined in limestone at or near the surface by Coates and Grant (1966), though Adams (1982) estimated 30 MPa for northeast- and 10 MPa for northwest-directed stresses from a crude analysis of quarry-floor buckles in the McFarland Quarry. Although the computed stresses are very high, the amount of inward movement (20 mm) is small and any future movements should be accommodated by the granular backfill that has been placed between the building foundation and the bedrock face.

The inward movements, which do increase progressively away from the southeast 'pin', are up to twice as large as the lateral west-southwest movements. Since there is no reason to presume that the pre-excavation stresses changed so rapidly, we interpret the increase in displacement to an increasing width of rock that became detached. In our view, therefore, a roughly triangular body of rock, extending from one corner at the southeast pin, along the excavation to where the strata daylighted, and thence south-southeast for some 50-100 m may have moved on the shale layers. Slip on these surfaces would have been zero to extremely slight near the southeast pin and increased to about 20 mm towards the southwest corner of the excavation. In the 311° direction, the ground would have lengthened, perhaps enough to be detectable by surveying, as found in building basements adjacent to the Scotia Plaza excavation in Toronto (Trow and Lo, 1989).

We saw no inward movement on either of the sides perpendicular to Carling Avenue. While movement might have occurred at the excavation floor, where it is difficult to find, we are inclined to think none occurred. This is surprising, because these two sides are normal to the regional maximum horizontal stress direction (typically east-northeast, Adams, 1982; Adams and Bell, 1991), so that larger displacements than on the Carling Avenue face would be expected. However, just 100 m east of the excavation, a 5 m deep trench was cut several decades ago into the limestone to carry the Canadian Pacific Railway line through the neighbourhood (parallel to Champagne Avenue South) and under Dow's Lake. Safety considerations have prevented us from examining the trench walls for offsets, but we feel that its excavation must have relieved rock stress in the vicinity, certainly for tens of metres and perhaps far enough to affect the Carling excavation. The distance affected will depend on the friction of the shale layers and the dip of the limestone strata. However, such prior stress relief would explain the lack of inward movement on the excavation walls parallel to the trench.

EXCAVATIONS NOT SHOWING STRESS RELIEF PHENOMENA

Nepean, Ontario

The southwest leg of the Ottawa-Carleton bus transitway, just north of where it passes under Highway 417, is cut 3-4 m into limestone, and trends northwest. Despite the excellent exposure and good quality of the half-barrels, no offset is visible.

Highway 17, Orleans, Ontario

Excavation for the Highway 17 underpass at Champlain Street in Orleans (by the Place d'Orleans Shopping Centre) has removed 1-2 m of till and postglacial sediments and excavated 2-4 m into the underlying limestone. Closely-spaced drill holes along the margins have encouraged a clean, pre-split face, and at the time of writing about two-thirds of the excavation is complete. While the completed walls are in good condition, no offsets of the boreholes have been found (as of October 10, 1993). This excavation trends 062°, roughly parallel to the expected maximum horizontal stress direction. Of incidental interest in this exposure is a suite of veins striking 120-125° and dipping vertically to 80° to the southwest. These veins contain calcite (finely crystalline to coarsely crystalline) and sulphides (dominantly pyrite and marcasite, but also chalcopyrite; galena is present elsewhere in the Ottawa Valley) that are banded in a manner suggesting multiple episodes of deposition.

Tenth Line, Orleans, Ontario

A deep north-northwest-trending excavation on Tenth Line Road, just south of St. Joseph Boulevard, extends through 10-15 m of postglacial clay and 4-5 m into the bedrock. Here the blasting was less controlled than required to produce a pre-split face, but the few remaining half-barrels are not offset.

CONCLUSIONS REGARDING STRESS RELIEF PHENOMENA

As can be seen from the above, not all excavations into the limestone show stress relief effects. In some cases a lack of movement may be due to prior stress relief (e.g., Carling Avenue), while others show no evidence for being destressed (either by prior excavation or local erosion). Our poor understanding of the shallow stress field, the physical properties of the bedded limestones and shales that promote or prevent movement, and the effect of transient hydrostatic or gas pressures that may act during or after blasting, limits our ability to explain why stress relief is seen in some but not other excavations. Where present, the stress relief phenomena do provide important and inexpensive indications of the shallow stress field, though our use of that data as an indication of regional stresses must be tempered by our lack of understanding of the local situation.

EVIDENCE FOR STRIKE-SLIP MOTIONS ON OTTAWA FAULTS

Faults that offset the Ordovician strata in the Ottawa area are commonly described as normal faults, some of which are related to the formation of the Ottawa-Bonnechere Graben (Kay, 1942). Indeed, where stratal offsets are seen in quarries, normal separations are the most often seen. To our knowledge only Saull and Williams (1974) and Norris (1967) have published evidence for horizontal motions on these faults.

Saull and Williams (1974) describe low-angle slickensides on normal fault surfaces from three locations in the Ottawa Valley. At one, exposed on the Ottawa River Parkway, about 100 m west of Slidell Street, and 2.8 km west of Parliament Hill, low-angle slickensides overprint down-dip slickensides on a splay of the Gloucester fault. Total vertical offset across this fault is about 500 m, though across the individual splay faults it is 100 m or less. The low-angle slickensides are still clearly visible (Fig. 5). In addition, calcite lenses on the plane of the fault show nearly orthogonal sets of slickensides on opposite surfaces, indicating periods of normal and strike-slip motion.

Norris (1967), described a fold still partly exposed on Highway 417, observing slickensides raking 17° on near-vertical faults, with steps indicating left-lateral motion. On an outcrop half a mile to the northeast (about at Bayswater Avenue) he found "similar northwest-trending, slickensided, near-vertical fractures on bedrock limestone. Striae and steps on three of them indicate left-lateral motion, and on two others, right lateral" (p. 312). Both these exposures are in splays of the Gloucester fault, the latter on the same splay observed by Saull and Williams (1974) on the Parkway.

In the Carling Avenue excavation we observed a 6 m wide by 3 m high, calcite-coated fault surface, striking 095° and dipping to the north, covered with horizontal slickensides (Fig. 6). The Paleozoic map of Ottawa (Williams et al., 1984) places an extension of the Ottawa River Parkway fault strand within one block of the Carling Avenue excavation, and its proximity supported by the abnormally steep (in a regional sense) dips in the excavation. Thus, there is now evidence at three localities that the most recent faulting episode on or near this splay of the Gloucester fault has been strike-slip motion.

It is important to note and document any evidence for strike-slip faulting in the Ottawa region of the St. Lawrence Platform. This is particularly so in the light of the suggestion made by Shaw (1993). Shaw, in a provocative paper that challenges the conventional wisdom, suggests that the post-Middle Ordovician faults along the St. Lawrence River in the

Figure 5. *Low-angle slickensides, raking about 10° to the northwest, in a splay of the Gloucester fault on the Ottawa River Parkway. Slickensides are developed on a fault breccia, with individual clasts being striated.*

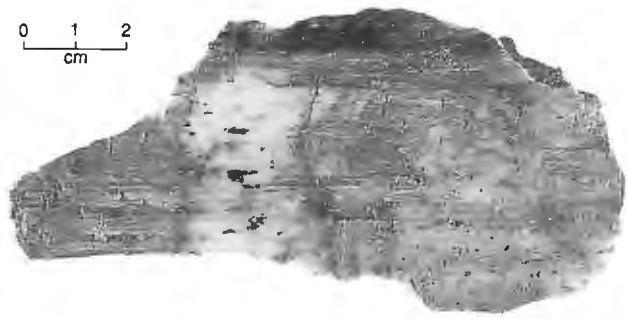

Figure 6. *Hand specimen of calcite lens from the fault plane in the Carling Avenue excavation, showing the strong development of horizontal slickensides. GSC 1993-262*

Quebec lowlands are strike-slip and not normal faults as originally described. That is, the observed stratigraphic offsets across the faults are the result of several tens of kilometres of horizontal displacement rather than less than a kilometre of normal slip. Shaw attributed the strike-slip displacements he documented to the approach of the Middle to Late Ordovician Taconic front. The age of faulting in the Ottawa area is still unknown, but even if the chief offsets on the Ottawa faults are normal and occurred in post-Ordovician or post-Silurian times, the evidence suggests a subsequent period of strike-slip motion. In the regional setting, evidence for low-angle slickensides in Monteregian volcanic intrusives near Montreal (Saull and Williams, 1974) and on a Jurassic dyke near Picton, Ontario (McFall, 1990) suggest at least some of the strike-slip motion may have occurred in or after the Cretaceous, and so the Ottawa observations shed some light on some of the youngest tectonic activity in the area.

'HAMMERING' ON CALCITE-FILLED JOINTS

Euhedral calcite crystals (dogspar) are common in the middle of calcite veins in Ottawa area limestones. However, in the Highway 17 underpass in Orleans, and in the Francon Quarry on Bearbrook Road, 4 km to the west, it is evident that while the vein-centre calcite originally had euhedral terminations, the vein-centre surface now appears to have been 'hammered'. The appearance is as if one had gently tapped a surface of euhedral calcite crystals with a large hammer to crush the highest crystals. These surfaces are not sheared, and do not have the slickensides seen on some calcite-coated surfaces, leading us to suggest that the in-plane displacement on the surface is negligible. Others may have a better explanation for this effect, but we suggest it is due to grinding of the joint surfaces against each other, during repetitive and reversing, low-displacement normal-to-plane movements as the imposed crustal stresses have changed. This may reflect stress changes during several deglacial/glacial cycles, cyclic changes in tectonic stresses over hundreds of millions of years, or, more speculatively, near-surface changes due to annual temperature changes.

CONCLUSIONS

Stress relief phenomena, of the type we describe here, are important for understanding the local stress field and making sensible engineering decisions during design and excavation. Often their importance is not recognized, and their occurrence goes unnoted. There is at the moment no GSC, provincial, or municipal geologist assigned to examine bedrock excavations in the Ottawa metropolitan area, and so valuable strain relief, stratigraphic, and structural information uncovered in these transitory excavations often passes unrecorded and unreported. In the Ottawa area, such observations would also improve understanding of the Ottawa-Bonnechere graben faults. These faults and their seismotectonic significance are important because they have been widely implicated as the locus of earthquakes in the Ottawa Valley.

ACKNOWLEDGMENTS

We thank Steve Kisilenko and Charlie Muir of Concordia Project Management for allowing access to the Carling Avenue excavation and for providing the excavation drawings, and the management of the Francon Quarry for permitting access. Joe Wallach called our attention to the Hull offset boreholes. We thank B. Sanford and J. Drysdale for helpful reviews.

REFERENCES

Adams, J.
1982: Stress-relief buckles in the McFarland quarry, Ottawa; Canadian Journal of Earth Sciences, v. 19, p. 1883-1887.
1987: Canadian crustal stress data – a compilation to 1987; Geological Survey of Canada, Open File 1622, 130 p.

Adams, J. and Bell, J.S.
1991: Crustal stresses in Canada; in Neotectonics of North America, (ed.) D.B. Slemmons, E.R. Engdahl, M.D. Zoback, and D.D. Blackwell; Decade Map Volume 1, Geological Society of America, Boulder, Colorado, p. 367-386.

Bell, J.S.
1985: Offset boreholes in the Rocky Mountains of Alberta, Canada; Geology, v. 13, p. 734-737.

Block, J.W., Clement, R.C., Lew, L.R., and de Boer, J.
1979: Recent thrust faulting in southeastern Connecticut; Geology, v. 7, p. 79-82.

Bowen, C.F.P., Hewson, F.I., MacDonald, D.H., and Tanner, R.G.
1976: Rock squeeze at Thorold tunnel; Canadian Geotechnical Journal, v. 13, p. 111-126.

Coates, D.F. and Grant, F.
1966: Stress Measurements at Elliot Lake; Canadian Mining and Metallurgical Bulletin, v. 59, p. 603-613.

Kay, G.M.
1942: Ottawa-Bonnechere graben and Lake Ontario homocline; Geological Society of America Bulletin, v. 53, p. 585-646.

Lo, K.Y.
1978: Regional distribution of in situ horizontal stresses in rocks in southern Ontario; Canadian Geotechnical Journal, v. 15, p. 371-381.

McFall, G.H.
1990: Faulting of a Middle Jurassic, ultramafic dyke in the Picton Quarry, Picton, southern Ontario; Canadian Journal of Earth Sciences, v. 27, p. 1536-1540.

Norris, D.K.
1967: Structural analysis of the Queensway folds, Ottawa, Canada; Canadian Journal of Earth Sciences, v. 4, p. 299-321.

Saull, V.A. and Williams, D.A.
1974: Evidence for recent deformation in the Montreal area; Canadian Journal of Earth Sciences, v. 11, p. 1621-1624.

Schäfer, K.
1979: Recent thrusting in the Appalachians; Nature, v. 280, p. 223-226.

Shaw, B.R.
1993: Strike-slip interpretation of basin-bounding faults of the St. Lawrence lowlands basin in the Quebec City area, Canada; American Association of Petroleum Geologists Bulletin, v. 77, p. 743-760.

Trow, W.A. and Lo, K.Y.
1989: Horizontal displacements induced by rock excavation: Scotia Plaza, Toronto, Ontario; Canadian Geotechnical Journal, v. 26, p. 114-121.

Williams, D.A., Rae, A.M., and Wolf, R.R.
1984: Paleozoic geology of the Ottawa area, southern Ontario; Ontario Geological Survey, Map P.2716, Geological Series, Preliminary Map scale 1:50 000.

Zhongyou, L.
1986: Comment on "Offset boreholes in the Rocky Mountains of Alberta, Canada; Geology, v. 14, p. 542-543.

Geological Survey of Canada Project 860047

National gravity survey program of the Geological Survey of Canada, 1993-94

D.B. Hearty and R.A. Gibb
Geophysics Division

Hearty, D.B. and Gibb, R.A., 1994: National gravity survey program of the Geological Survey of Canada, 1993-94; in Current Research 1994-D; Geological Survey of Canada, p. 161-163.

Abstract: Three gravity surveys were completed under the national gravity survey program in 1993; two were reconnaissance surveys located in the southern Yukon Territory and northwestern British Columbia, and in Coronation Gulf in the Arctic, and one was a detail gravity survey on two ice caps on Baffin Island. Approximately 1800 new gravity stations were added to the National Gravity Database and two Open File gravity maps were produced as a result of these surveys. An international co-operative project to compile and adjust the national gravity networks for Brazil and Uruguay was completed with funding support from the Pan American Institute for Geography and History (PAIGH).

Résumé : En 1993, trois levés gravimétriques ont été réalisés dans le cadre du programme national de levés gravimétriques; deux étaient des levés de reconnaissance dans le sud du Yukon et dans le nord-ouest de la Colombie-Britannique ainsi que dans le golfe de Coronation dans l'Arctique, et un était un levé gravimétrique détaillé sur deux calottes glaciaires de l'île de Baffin. Environ 1 800 nouvelles stations gravimétriques ont été ajoutées à la base de données gravimétriques nationale et deux cartes gravimétriques publiées dans les Dossiers publics ont été produites à la suite de ces levés. Un projet de collaboration internationale pour compiler et corriger les réseaux gravimétriques nationaux du Brésil et de l'Uruguay a été complété grâce au financement de l'Institut panaméricain de géographie et d'histoire.

INTRODUCTION

In 1993-94, the national gravity mapping program comprised two reconnaissance surveys and a local survey over two ice caps. The regional gravity surveys fill major voids in the gravity coverage in the western Cordillera and in the Arctic channels and represent significant progress towards the completion of reconnaissance mapping of Canada's landmass and adjacent offshore areas. The local ice cap survey was part of a joint research project with the Glaciology Section, Terrain Sciences Division to monitor elevation changes on polar ice caps.

Details of these surveys and highlights from the gravity standards program and gravity map production are given below.

CANADIAN CORDILLERA

In a major international cost-sharing effort, Geophysics Division (GSC), Pacific Geoscience Centre (GSC), Geodetic Survey Division (SMRSS), Mapping and Charting Establishment (DND), and the U.S. Defense Mapping Agency (DMA), have completed the reconnaissance gravity survey of the southwest part of the Yukon and western British Columbia as far south as Terrace. Approximately 1550 gravity observations with a spacing of 10-12 km, covering 15 1:250 000 map sheets, were collected in this final year of a three year survey program. This year's survey brings the total number of observations, since 1991 when the survey commenced, to 5166. This survey marks a major benchmark in the National Gravity Mapping Program; the area covered encompasses 450 000 km^2 of the Yukon, the Northwest Territories and British Columbia. The cost of this $4M project was shared by the GSC and the U.S. Defense Mapping Agency in the ratio 1:3 with essential program management in the field and personnel support from DND. The data collected will augment the National Gravity Database, will guide future, more detailed surveys, and will contribute (i) to resource potential and structural investigations by industry clients, provincial and territorial agencies, and the GSC, (ii) to a better definition of the geoid for the land surveying industry, and (iii) to the North American Defence Plan.

ARCTIC CHANNELS

During March and April 1993, a gravity and bathymetry survey was completed on the ice surface in Coronation Gulf between Coppermine and Richardson Island. The survey, part of the National Gravity Mapping Program, was carried out by the Geophysics Division in co-operation with the Canadian Hydrographic Service and Polar Continental Shelf Project. The survey output was 435 gravity stations with corresponding bathymetry established at a spacing of 6 km using portable GPS receivers (TANS Pathfinder model) in differential mode. The bathymetry survey was year one of a four year project to complete the reconnaissance bathymetry mapping for a major tanker route through the Arctic islands. The bathymetry data will be used to test a Through the Ice Bathymetry System (TIBS) recently developed for CHS to acquire detailed bathymetry in shallow water areas.

BAFFIN ISLAND ICE CAPS

In early May, the Geophysics Division in collaboration with the Glaciology Section of Terrain Sciences Division, Memorial University, PCSP and the Science Institute of the Northwest Territories established 24 gravity sites on the top of the Penny Ice Cap and 12 sites on the top of the Barnes Ice Cap. The gravity sites are collocated with automatic weather stations established by Memorial University and precise horizontal positions have been determined by differential GPS using Trimble Pathfinder receivers. The sites provide baseline measurements of gravity which can be repeated over the years to determine the growth or shrinkage of glaciers and ice caps as a measure of climatic change. Gravity ties were made between the ice caps and Iqaluit using four LaCoste and Romberg gravity meters. Two sites on the Penny Ice Cap were re-occupations of sites established in 1966 and revisited in 1992.

GRAVITY STANDARDS

The Canadian Gravity Standardization Net (CGSN) consists of some 2000 gravity reference sites which provide datum for all relative gravity surveys that comprise the National Gravity Mapping Program and for geophysical exploration industry surveys. Approximately 40 gravity control stations in southwestern Quebec and southeastern Ontario were inspected as part of the annual program to ensure the integrity of this network. Stations were categorized according to national standards, descriptions were compiled and corresponding databases were updated. Three LaCoste and Romberg gravity meters and one Scintrex gravity meter were calibrated over the Ottawa to Inuvik calibration line. This survey provided updated scale factors for all four meters and an evaluation of their performance over almost the entire gravity range for Canada.

GRAVITY DATABASE AND MAP PRODUCTION

The National Gravity Database contains more than 700 000 gravity data points corresponding to a variety of land, ice, and marine measurements for the Canadian landmass, lakes, and adjacent offshore seas. This year approximately 3120 new data points from regional or site specific surveys collected by the Geophysics Division and other agencies, were added to the digital holdings. These data, along with all previously collected data, are available through the Geophysical Data Centre in digital, gridded, profile, or map form. Nine Bouguer anomaly and four free air anomaly maps in the National Earth Science Series (NESS) were printed in June 1993 and are available for purchase through the GSC Publications Office. These colour thematic maps, published at 1:1 000 000 scale, bring the total number of available NESS maps to 69 (50 Bouguer anomaly and 19 free air anomaly) and represent almost complete coverage of the Canadian landmass and adjacent offshore to latitude 60°N. One Open File Bouguer gravity map was produced at a scale of 1:1 000 000 (GSC Open File 2733, Bouguer Gravity, Yukon and NWT).

INTERNATIONAL COOPERATION

Between July 12 and September 8, phase I of a three year international project to recompile and readjust the Latin American Gravity Standardization Net (LAGSN95) was completed at the Geophysics Division with funding support from the Pan American Institute of Geography and History (PAIGH). Participants in the project included Eng. Iris Pereira Escobar of the Observatorio Nacional do Brasil (ONB); Philip Salib, GSC; and Ken McConnell, chairman of the Geophysics Commission's LAGSN95 Working Group. During the two month visit by Dr. Escobar, 249 control stations and 4646 new measurements for the national networks for Brazil and Uruguay were compiled, processed, and added to the LAGSN database. In addition, international connections to Argentina and Paraguay and ten absolute measurements were incorporated in the adjustment. The processing resulted in adjusted gravity values on an absolute datum for the Brazil and Uruguay national gravity nets and identified outstanding requirements to complete LAGSN95 to a consistent standard.

Geological Survey of Canada Projects 930029, 930030, 930031, 930033

Aeromagnetic survey program of the Geological Survey of Canada, 1993-94

R. Dumont, P.E. Stone, F. Kiss, K. Anderson, D.J. Teskey, R.A. Gibb, and G. Palacky[1]
Geophysics Division

Dumont, R., Stone, P.E., Kiss, F., Anderson, K., Teskey, D.J., Gibb, R.A., and Palacky, G., 1994: Aeromagnetic survey program of the Geological Survey of Canada, 1993-94; in Current Research 1994-D; Geological Survey of Canada, p. 165-168.

Abstract: In 1993, high resolution aeromagnetic surveys totalling 147 000 line km were flown in British Columbia, Saskatchewan, and Manitoba. These surveys were partially funded under Mineral Development Agreement (MDA) programs, by GSC and by industry. Two detailed airborne electromagnetic-magnetic surveys totalling 20 000 line km were flown in the Chibougamau greenstone belt of Quebec and funded under the Special Assistance Program for the Mining Sector of the Chapais-Chibougamau Region (1992-1995). As part of a Canada-wide program, the aeromagnetic profile data set for Quebec has now been levelled to eliminate the effect of survey datum changes and survey boundaries and work has commenced on levelling profile data for the Northwest Territories. The third phase of a three year program to collect aeromagnetic data north and west of Axel Heiberg Island as part of the Polar Margin Aeromagnetic Program, was completed in 1993 by the Institute for Aerospace Research. Data are being processed for release in early 1994.

Résumé : En 1993, des levés aéromagnétiques haute résolution ont été réalisés sur 147 000 km linéaires en Colombie-Britannique, en Saskatchewan et au Manitoba. Ces levés ont en partie été financés, dans le cadre des ententes sur l'exploitation minérale, par la CGC et l'industrie. Deux levés électromagnétiques-magnétiques aéroportés sur 20 000 km linéaires dans la ceinture de roches vertes de Chibougamau au Québec ont été financés par le Programme de soutien du secteur minier de la région de Chapais-Chibougamau (1992-1995). Dans le cadre d'un programme pancanadien, les données de profils aéromagnétiques recueillies au Québec ont été nivelées pour éliminer l'effet des changements du niveau de référence et des limites des levés, et des travaux de nivellement des données de profils dans les Territoires du Nord-Ouest ont été entrepris. La troisième phase d'un programme de trois ans pour recueillir des données aéromagnétiques au nord et à l'ouest de l'île Axel Heiberg dans le cadre du Programme aéromagnétique de la marge polaire, a été terminée en 1993 par l'Institut de recherche aérospatiale. Les données actuellement traitées seront diffusées au début de 1994.

[1] Mineral Resources Division

INTRODUCTION

The aeromagnetic survey program of the Geological Survey of Canada continued in 1993-94 with activity in three continuing projects in Saskatchewan-Manitoba, southern Alberta and the Axel Heiberg area. New projects include a total field aeromagnetic survey in British Columbia and an airborne electromagnetic-magnetic survey in the Chapais-Chibougamau region of Quebec. Survey activity for 1993 is shown in Figure 1 and summarized in Table 1.

BRITISH COLUMBIA

Flying in three survey blocks in British Columbia, totalling 110 000 line km, was completed in 1993. Under a cost-sharing agreement with GSC, two oil company partners participated in the northwest and southeast survey blocks where the data are expected to contribute to the understanding of deep structure beneath the Cordillera. The aeromagnetic survey of the interior plateau block has been partially funded under the Canada-British Columbia Agreement on Mineral Development (1991-1995) and will support detailed geological mapping being carried out under that program and future mineral exploration.

SOUTHERN ALBERTA

Line contour maps and digital data (33 940 line km) for the Cypress Hills, total field aeromagnetic survey funded under the Canada-Alberta Agreement on Mineral Development (1992-1995), were released on open file in May 1993. Six residual total field, colour interval maps were released in July 1993.

SASKATCHEWAN AND MANITOBA

The third phase of a four year program to complete the regional aeromagnetic coverage of southern Saskatchewan and Manitoba was carried out in 1993. This year's program was funded by the GSC and Saskatchewan Energy and Mines in Saskatchewan (23 000 line km) and by the GSC and one industry partner in Manitoba (13 800 line km). Both portions of the survey were also partly funded by the Canada-Saskatchewan and Canada-Manitoba Partnership Agreements on Mineral Development (1990-1995). These surveys meet the dual objectives of mapping the Precambrian basement beneath the Phanerozoic cover and of providing a fundamental tool for kimberlite exploration. A suite of aeromagnetic maps donated to the GSC by PanCanadian Petroleum has been digitized and the derived map and digital data have been released. In addition, a detailed survey

Table 1. Aeromagnetic survey activity in 1993-94.

SURVEY	TYPE	LINE KM	LINE SPACING	ALTITUDE	YEAR OF PUBLICATION
British Columbia 1993-94	Aeromagnetic Total Field	3 600 4 800 82 700 19 100	1.6 km 1.6 km 0.8 km 0.8 km	1 370 m ASL 1 830 m ASL 305 m MTC 305 m MTC	1997 1997 1994 1995
Saskatchewan Phase III 1993-94 (Yorkton area)	Aeromagnetic Total Field	23 000	800 m	150 m MTC	1994
Saskatchewan PanCanadian Petroleum Survey 1965 (North Battleford)	Aeromagnetic Total Field (digitized data)	26 611	3 250 m	984 m ASL	1993
Saskatchewan Rio Algom Survey 1991 (Shellbrook)	Aeromagnetic Total Field	11 446	250 m	75 m MTC	1993
Manitoba Phase III 1993-94 (Riding Mountain)	Aeromagnetic Total Field	13 800	800 m	150 m MTC	1994
Quebec 1993 Lac Verneuil area	Aeromagnetic Frequency Domain EM	9 500	100 m	30 m MTC	1993
Quebec 1993-94 Lac des Vents area	Aeromagnetic Frequency Domain EM	10 500	100 m	30 m MTC	1994
Axel Heiberg 1993-94	Aeromagnetic Total Field	12 430	4 km	305 m MTC	1994

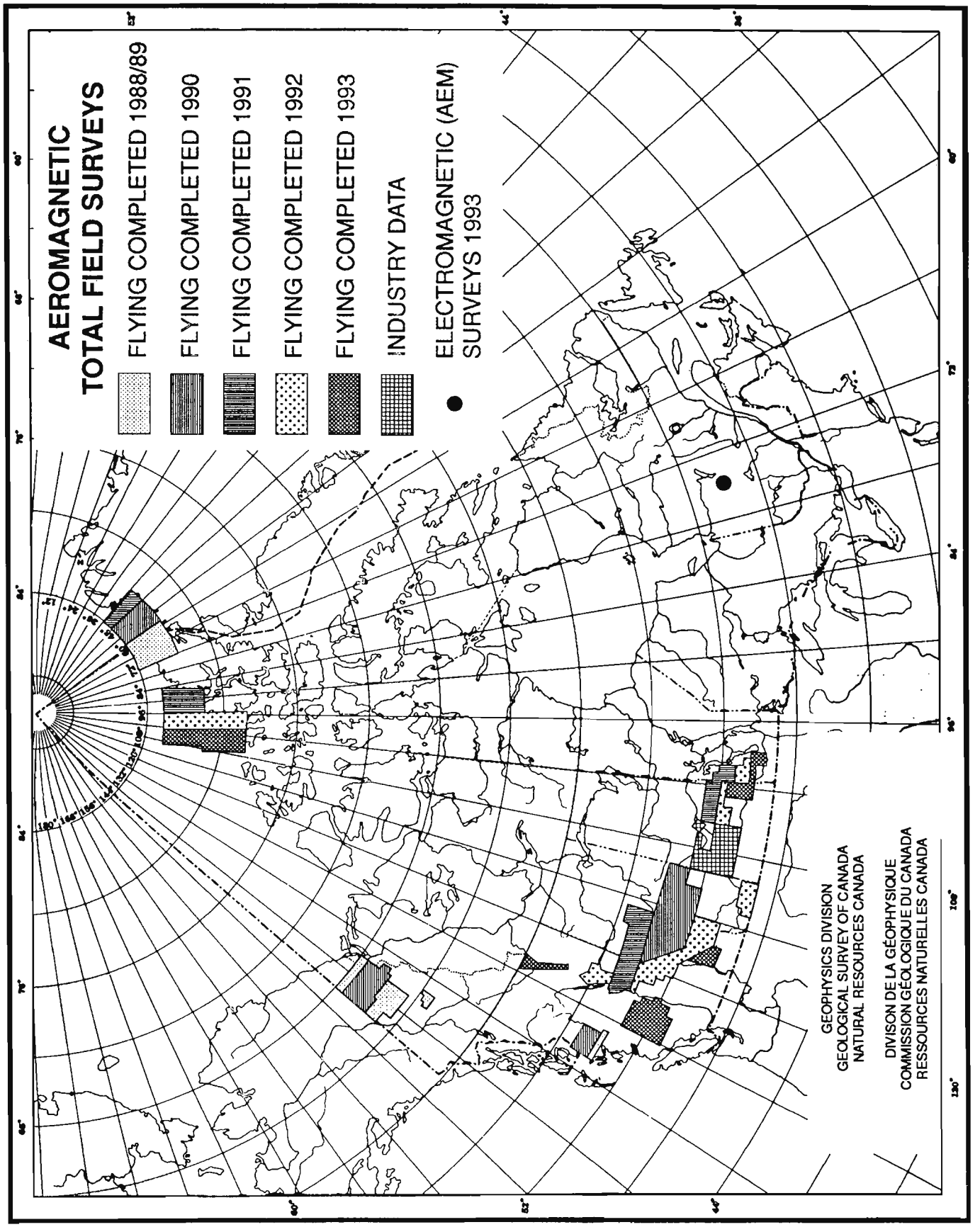

Figure 1. Aeromagnetic surveys in progress, 1993-94.

southwest of Prince Albert, acquired from Rio Algom Ltd. as part of the joint industry-government program, has been compiled and published.

AXEL HEIBERG

The GSC has compiled aeromagnetic data (12 430 line km) collected over the Arctic Ocean northwest of Axel Heiberg Island. The survey was flown in three phases (1991-1993) under the Polar Margin Aeromagnetic Program (PMAP) by the Institute for Aerospace Research (IAR). Digital data and the associated aeromagnetic maps will be released as an open file publication in 1994.

QUEBEC

A systematic multicoil, multifrequency, helicopter-borne electromagnetic and magnetic survey of a greenstone belt located in the Chapais-Chibougamau region was flown in early 1993. This survey is a three year program to be completed in 1995-96 under the Special Assistance Program for the Mining Sector of the Chapais-Chibougamau Region (1992-1995). The Ministère de l'énergie et des ressources du Quebec (MERQ) and the GSC are cooperating to provide new digital survey data and geophysical maps resulting from these jointly funded airborne electromagnetic-magnetic surveys which are designed to stimulate mineral exploration in the area.

Data resulting from the first phase of this program, a 9500 line km survey flown in the Lac Verneuil area, southwest of Chibougamau were published as an open file by MERQ in the fall of 1993. The second phase, a 10 500 line km survey in Lac des Vents area (to the south and adjacent to the Lac Verneuil area) is now in progress. The results from this survey will be released in the summer of 1994.

QUEBEC AND NORTHWEST TERRITORIES

The editing and levelling of the aeromagnetic profile data set for all of Canada has been undertaken by the GSC to achieve a homogeneous levelled data set free from survey boundary effects. With this process, seamless and finer magnetic grids can be generated more economically and more efficiently for government, industry and university clients. In 1993, the GSC, in co-operation with MERQ, processed and levelled the aeromagnetic data set for the entire province of Quebec. Levelling of the aeromagnetic data for the Northwest Territories was also initiated by the GSC.

Geological Survey of Canada Projects 850058, 910028, 910029, 920024, 930002

Determination of permeability-compaction relationship from interpretation of permeability-stress data for shales from eastern and northern Canada

T.J. Katsube and K. Coyner[1]
Mineral Resources Division

Katsube, T.J. and Coyner, K., 1994: Determination of permeability-compaction relationship from interpretation of permeability-stress data for shales from eastern and northern Canada; in Current Research 1994-D; Geological Survey of Canada, p. 169-177.

Abstract: Shale permeabilities as a function of stress (k-P_e) are being measured to obtain information on permeability change as subsiding muds transform into tight shales, resulting from increasing depth of burial. This is to provide information of high accuracy required for hydrocarbon charge models used in petroleum resource evaluation of Canadian east coast frontier basins.

Results suggest that the k-P_e relationship consists of a three exponential curve system, the first (smallest P_e values) representing restoration of widened pores resulting from stress release of rock samples brought to surface. The third (largest P_e values) represents reduction of pore sizes resulting from increasing effective stress (P_e). The second curve is proposed to represent compacting deposits in widened pores, resulting from overpressure development subsequent to compaction at higher stresses, implying that the third curve contains the information required for hydrocarbon charging models.

Résumé : Des mesures de la perméabilité des shales en fonction de la contrainte effective (k-P_e) sont actuellemnt effectuées afin de recueillir des renseignements sur le changement qui se produit dans la perméabilité au fur et à mesure que les boues en subsidence se transforment en shales peu perméables avec l'accroissement de la profondeur d'enfouissement. Cela permettra de recueillir des données très précises pour l'élaboration des modèles de remplissage des réservoirs utilisés pour évaluer les ressources pétrolières dans les bassins des régions pionnières sur la côte Est du Canada.

Les résultats portent à croire que le lien k-P_e consiste en un système à trois courbes exponentielles. La première courbe (les valeurs P_e les plus petites) représente le rétablissement de pores élargis par suite du relâchement de contraintes dans les échantillons de roches remontées à la surface. La troisième courbe (les valeurs P_e les plus grandes) représente la réduction de la dimension des pores par suite de l'augmentation de la contrainte effective (P_e). La deuxième courbe représenterait les dépôts en voie de compaction aux pores préalablement élargis, résultat du développement d'une surpression à la suite d'une compaction à des contraintes plus élevées; par conséquent, cette troisième courbe contiendrait l'information requise pour les modèles de remplissage des réservoirs d'hydrocarbures.

[1] Verde GeoScience, R.R.#1, Box 117, Tunbridge, Vermont U.S.A. 05077

INTRODUCTION

Petrophysical studies of shales are being carried out to provide information required for hydrocarbon charge models used in petroleum resource evaluation of the Canadian east coast frontier basins (Mudford and Best, 1989; Williamson, 1992; Williamson and Smyth, 1992; IRAS, 1992, 1993; Katsube and Williamson, 1994). The main objective of the study is to obtain reliable information on formation permeability change as subsiding muds are transformed into tight shales resulting from increasing depth of burial.

Information on lithological seal histories are essential when reconstructing formation pore pressures as they evolve in response to the sediment compaction disequilibrium processes (Mudford, 1988; Mudford and Best, 1989; Williamson, 1992; Williamson and Smyth, 1992). Excess pressure developments and their timing play an important role in hydrocarbon migration. Such information is obtained from the permeability history of the formation (Williamson, 1992; Williamson and Smyth, 1992). Currently for the Canadian east coast basins, the permeability history, i.e., the permeability-time curves, are derived indirectly from porosity-depth relationships (Williamson, 1992; Williamson and Smyth, 1992). The resulting permeabilities are verified by current day permeability values obtained from experimental measurements on shale samples from these formations.

It seems logical that permeability-time data be obtained from experimental measurements of permeability-stress, currently being performed on shales from eastern and northern Canada (Katsube et al., 1991; Coyner et al., 1993). Various experimental problems are being overcome to increase the accuracy with which extremely low permeabilities of shale and compacted mud are measured (Coyner et al., 1993). However, difficulties exist in the analysis and interpretation of the results. One question is whether the permeability-stress relationship follows an exponential or a power law (Mudford et al., 1991). Existing data (Coyner et al., 1993) indicate that permeability-stress curves may consist of a number of exponential curves, rather than a single curve. The purpose of this study is to find ways of extracting the necessary information from the complex curve system, in order to improve the accuracy and reliability of the data input to the hydrocarbon charge models. This paper presents permeability-stress data, shows the complexity of the relationship between the two parameters, and provides some explanations for those complexities.

Permeability generally decreases with increasing effective stress. Shi and Wang (1986) expressed the permeability (k) versus effective stress (P_e) relationship empirically by a power curve, using the experimental data by Morrow et al. (1984):

$$k = k_0 (P_e/P_0)^{-q} \quad (1)$$

where k_0 and P_0 are the permeability and pressure at atmospheric conditions, and q is an empirically determined coefficient. The same relationship for tight shales has been expressed by an exponential curve (Katsube et al., 1991):

$$k = k_0 \exp(-\alpha P_e) \quad (2)$$

where α is an empirically determined coefficient.

EXPERIMENTAL DATA

Experimental data for permeability-stress ($k\text{-}P_e$) of shales is available for 10 solid samples (numbers V-1 to V-10) and one unconsolidated sample (number V-SF-1) from the Venture Gas Field, Eastern Canada, and two solid samples (B-5 and B-9) from the Beaufort-Mackenzie Basin, northern Canada. The data for the 10 Venture solid samples including location and depth of sample are found in the literature (Katsube et al., 1991; Coyner et al., 1993). The permeability-stress data for the other three samples are listed in Tables 1 and 2. Information on the location and depth for the Beaufort-MacKenzie samples is in Katsube and Best (1992). The lithological and petrofacies classification for the solid samples can be found in Katsube and Williamson (in press) for the Venture samples, and in Katsube and Best (1992) for the Beaufort-Mackenzie samples. The permeability-stress data are listed in Table 3 for two granite samples which are used, in this study, for comparison purposes.

The solid specimens used for measurement are cylindrical discs with a diameter of 25.4 mm (1 inch) and thicknesses of 5-10 mm. First, cylindrical plugs with a diameter of 25.4 mm (4 inch) were cored in the vertical direction from 101.6 mm split core samples, as described in the literature (Katsube et al., 1990, 1991), and then cut into these discs. The unconsolidated specimen is a cylindrical plug with the same diameter and a thickness of 20-35 mm.

Sample permeabilities may be measured using either constant flow, constant head, or transient pulse decay (TPD) techniques. The first two techniques follow directly from the application of Darcy's Law using steady state conditions and are more appropriate for samples with permeabilities in the order of 10^{-15} m^2 (1 md) or greater. If permeabilities are lower, the flow rates are commonly too small for precise determination using typical laboratory apparatus for the first two techniques. Instead, the transient pulse decay technique, first introduced by Brace et al. (1968), has greater resolution for low permeability measurements. The transient pulse decay technique is used to measure the permeabilities of these shale samples. Further details on the measuring techniques and procedures used for these samples are described in

Table 1. Permeability (k) as a function of confining pressure (P) for an unconsolidated sea floor sample from offshore Nova Scotia.

Samples/ (Mes. No.)	Pressures (MPa)			Permeability (10^{-21} m^2)
	Confining	Pore	Effective	
V-SF-1	6.0	5	1.0	443
	7.0	5	2.0	325 ± 5
	8.0	5	3.0	223 ± 8
	9.0	5	4.0	157 ±22
	10.0	5	5.0	97 ± 8
	11.0	5	6.0	60 ± 1
	12.0	5	7.0	63
	13.0	5	8.0	62.5 ± 5
	14.0	5	9.0	61.5 ± 5
	15.0	5	10.0	57 ± 2

Coyner et al. (1993). Details of the measurement procedure used for the two granite samples are found in Annor (1986) and Coyner (1979).

SINGLE SEGMENT k-P_e CURVE INTERPRETATION

Sample permeability (k) generally decreases with increasing effective stress (P_e). Altough the data for many of the samples would be more appropriately interpreted as a two or three segment curve, as described later, the data for all of the samples have first been interpreted and analyzed as a single segment curve. The results obtained by deriving the values of the coefficients, k_0 and α, using the single exponential curve (equation 2) to fit the data are listed in Table 4. The number of data points (N) used for analysis are also listed in that table. Only the single exponential curve interpretation (equation 2) has been applied to samples with small numbers of data points (N), generally less than 4 or 5, such as V-2 and V-5. The reduced major axis, RMA (Davis, 1986; Katsube and Agterberg, 1990), is used to determine the coefficients when performing these regression analyses.

TWO SEGMENT k-P_e CURVE INTERPRETATION

A typical example of the permeability-stress (k-P_e) relationship is displayed in Figure 1a on a semi-log scale, for sample V-7. These data are interpreted to consist of two segments, expressed by exponential curves (equation 2)

$$\text{Curve \#1:}\quad k = k_{01}\exp(-\alpha_1 P_e), \tag{3}$$

$$\text{Curve \#2:}\quad k = k_{02}\exp(-\alpha_2 P_e). \tag{4}$$

These curves intersect at a point represented by transitional stress, P_{et}. Curve #1 and Curve #2 represent the ranges of smaller and larger values for P_e. The same data are repeated in Figure 1b, this time with the error bars included. The existence of the transitional stress (P_{et}) dividing the data into two sections is relatively clear, regardless of the large error bars. These data also show a relatively good fit with a power curve (equation 1), as displayed in Figure 1c, with a correlation factor of 0.98. However, in this study, the two-segment exponential curve interpretation is preferred.

Table 2. Permeability (k) as a function of confining pressure (P) for the Beaufort-MacKenzie Basin offshore Northwest Territories, Northern Canada.

Samples	Pressures (MPa)			Permeability (10^{-21} m^2)
	Confining	Pore	Effective	
B-5	20	10	10	46 ± 2
	25	10	15	22 ± 2
	30	10	20	24 ± 2
	40	10	30	16.2 ± 0.2
	45	10	35	13.8 ± 0.2
	50	10	40	12.6 ± 0.2
	60	10	50	8.2 ± 0.8
	70	10	60	7.8 ± 0.1
	80	10	70	6.8 ± 0.1
	90	10	80	6.4 ± 0.1
	100	10	90	5.9 ± 0.1
	110	10	100	5.0 ± 0.1
B-9	12.5	10	2.5	390
	15.0	10	5.0	409
	17.5	10	7.5	286
	20.0	10	10.0	265
	22.5	10	12.5	259
	25.0	10	15.0	238
	27.5	10	17.5	221
	30.0	10	20.0	203
	32.5	10	22.5	177
	35.0	10	25.0	158
	40.0	10	30.0	141
	45.0	10	35.0	129
	50.0	10	40.0	112
	60.0	10	50	82
	70.0	10	60	74
	80.0	10	70	58
	90.0	10	80	54
	100.0	10	90	47
	110.0	10	100	39

Table 3. Permeability (k) as a function of confining pressure (P_c) for a Lac du Bonnet granite (WN1-346: Annor, 1986) and a Chelmsford granite sample (CHM-1: Coyner, 1979).

Sample/ (Mes. No.)	Pressures (MPa)			Permeability (10^{-18} m^2)
	Confining	Pore	Effective	
WN1-346	4.14	3.45	1.38	3120
	4.83	2.24	1.90	1380
	6.90	3.14	3.76	560
	8.28	3.46	4.82	360
	11.72	3.46	8.26	280
	13.79	3.46	10.33	170
	17.24	3.46	13.78	80
	20.69	3.46	17.23	40
	24.13	3.46	20.67	30
CHM-1	4	2	2	4420
	8	4	4	3640
	12	6	6	3240
	16	8	8	2680
	20	10	10	2370
	24	12	12	1780
	28	14	14	1560
	32	16	16	1340
	36	18	18	1180
	39	21	18	814
	50	26	24	556
	51	25	26	430
	55	25	30	280
	60	25	35	208
	65	25	40	145
	70	25	45	101
	75	25	50	54
	100	25	75	24.5
	125	25	100	11.6
	150	25	125	3.48
	175	25	150	2.82
	200	25	175	0.979

The transitional point (P_{et}) for these two curves is represented by P_{e12}, and is derived by inserting it into equations (3) and (4) as follows:

$$k_{01}\exp(-\alpha_1 P_{e12}) = k_{02}\exp(-\alpha_2 P_{e12}),$$

therefore

$$P_{e12} = \ln(k_{01}/k_{02})/(\alpha_2 - \alpha_1). \quad (5)$$

The results of interpretations for 10 samples (W-346, CHM-1, V-1, V-3, V-6, V-7, V-8, V-9, B-5, and B-9) are listed in Table 4. When N is too small for curve fitting, such as the cases for sections of the data for 4 samples (V-1, V-6, V-8, and V-9), only ranges for the values of k_{01}, k_{02}, α_1, α_2 and P_{e12} are listed. The data for CHM-1 are displayed slightly differently from the other samples in Table 4, for reasons explained later.

The error range, ε, for P_{e12} (Table 4) is determined by using the normal regression lines, NRL (Katsube and Agterberg, 1990), of the two curves on a semi-log plot. First, transitional stress, $P_{e\varepsilon a}$, is determined from the normal regression lines with the smaller slope of the first curve and then with the larger slope of the second curve. Then, the transitional stress, $P_{e\varepsilon b}$, is determined from the normal regression lines with the larger slope of the first curve and that with the smaller slope of the second curve. The value of ε is determined by taking the larger of the two differences, $P_{e\varepsilon a}$-P_{e12} and P_{e12}-$P_{e\varepsilon b}$.

Now arises the question of the "cause of the transitional point". Annor (1986) observed the existence of a transitional point in the k-P_e curve (Fig. 2) when measuring granite samples (e.g., W-346), and suggested that it was related to the in situ effective stress. His original data were plotted on a

Table 4. Permeability characteristics of shale samples from the Venture Gas Field, Eastern Canada (V-Series), and the Beaufort-MacKenzie Basin, Northern Canada (B-Series), and granite samples (W- and CHM- Series).

Sample	N (N_1,N_2,N_3)	k_{01}	k_{02}	k_{03}	α_1	α_2	α_3	P_{e12}	P_{e23}
W-346	9	1950.			0.227				
	4,7	5754.	1023.		0.605	0.180		4.1±2*	
CHM-1	22	2399.			0.052				
	17,5	-	5370.	263.	-	0.093	0.032	-	49.3
V-1	4	6.6	<2.3		0.064	<.029		10-40	
	3,2	14.1			0.215				
V-2	3	140.			0.103				
V-3	13	831.	50.1		0.142	0.083		35.1±1	
	10,5	1410.			0.181				
V-4	5	56.2			0.080				
V-5	3	31.6			0.045				
V-6	18	1.6	1.3		0.132	0.101		<5.0	
	9,16	>1.6			>0.132				
V-7	14	16.2	4.6		0.074	0.045		24.3±4*	
	7,8	26.3			0.117				
V-8	5	61.7	38.		0.032	0.021		10-20	
	2,4	>62.			>0.032				
V-9	8	3.8	3.6		0.058	0.056		<15.	
	3,6	-			-				
V-10	5	15.1			0.081				
B-5	16	33.1			0.023				
	3,8,10	98.0	49.0	14.5	0.081	0.036	0.011	15.3	48.7
	3,8,6	98.0	49.0	17.4	0.081	0.036	0.013	15.4	44.3
B-9	19	371.			0.030				
	9,11	437.	269.		0.042	0.021		23.3	
	9,6,6	437.	347.	174.	0.042	0.029	0.015	18.5	48.8
	9,7,4	437.	275.	155.	0.042	0.023	0.014	24.6	63.0
Units		nd	nd	nd	MPa^{-1}	MPa^{-1}	MPa^{-1}	MPa	MPa

N (N_1,N_2,N_3) = Number of data points used for curve fitting (Number of points used for curves 1, 2 and 3).
k_{01}, k_{02}, k_{03} = Permeabilities at atmospheric pressures for curves 1, 2 and 3.
α_1, α_2, α_3 = Coefficients for curves 1, 2 and 3.
P_{e12}, P_{e23} = Transitional Stress between curves 1 and 2, and 2 and 3, respectively.
* = Values estimated directly from k-P_e plots.

linear scale. The idea of this relationship is consistent with the non-linear stress-strain or crack porosity concept (Walsh, 1965; Brace, 1965; Annor and Katsube, 1983; Katsube and Mareschal, 1993), which indicates that rock samples extracted from great depths will expand due to stress release, resulting in the widening of certain pores. This implies, that a rock sample under increasing pressure, at stresses below the in situ stress, will be in the situation of restoring the widened pores to their original condition. Similarly, at stresses above the in situ stress, the sample will be in a situation where the original pores are being reduced in size. These two different conditions would explain the reason for the existence of the point of transitional stress that would create the two separate curves.

The hydrostatic stress, P_h, lithostatic stress, P_l, and hydrostatic effective stress, P_{eh}, were calculated for all of the samples at their in situ true depths, using the following equations:

$$P_x = \gamma_x gh, \tag{6}$$

$$P_{eh} = P_l - P_h, \tag{7}$$

where γ_x is the bulk density (in kg/m^3), g is the acceleration due to gravity (9.81 m/s^2) and h is the true depth (in m) at which the sample was taken. When γ_x is the bulk density of water, γ_w, then P_x in equation 6 is P_h. When γ_x is the bulk density of the rock, γ_r, then P_x is P_l. The results of these calculations are listed in Table 5a. The values of γ_w and γ_r used for the calculations of P_h, P_l and P_{eh} of these rock samples are listed in Table 5b.

While the value of P_{e12} for the granite sample (W-346) is similar to its value for P_{eh}, the values of P_{e12} for the tight shale samples are usually considerably smaller (Table 5a). This is inconsistent with the suggestion by Annor (1986). However,

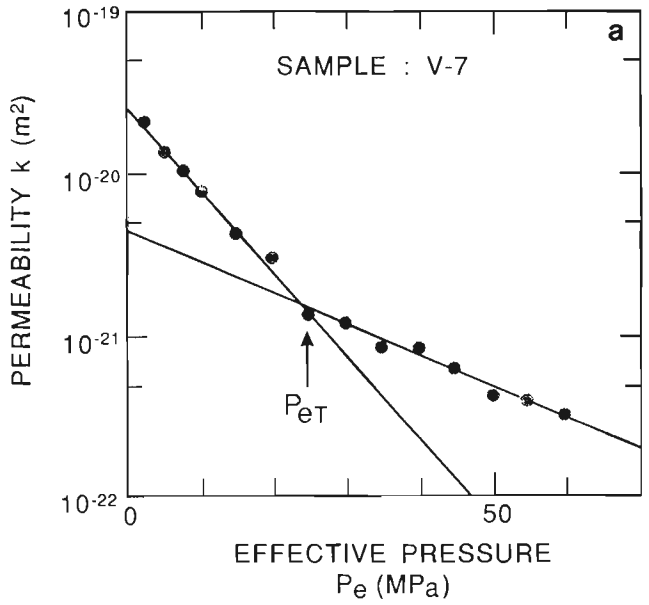

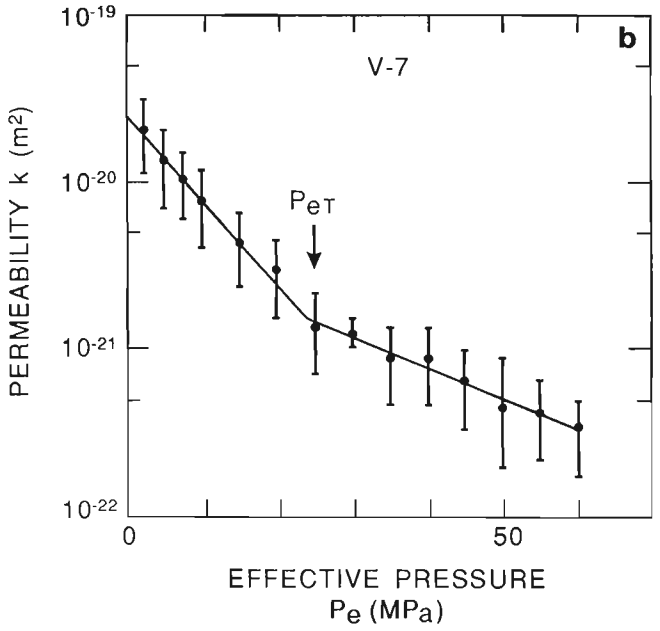

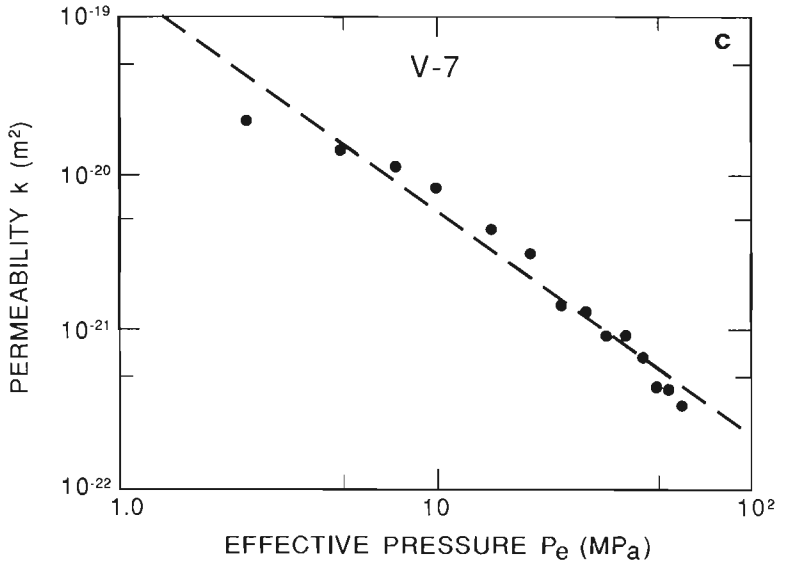

Figure 1.

*Typical example of the permeability-stress (k-P_e) relationship (shale sample V-7), **(a)** consisting of two exponential curves, **(b)** same exponential curves with error bars included (Best and Katsube, 1993), and **(c)** the same data displayed as a power curve.*

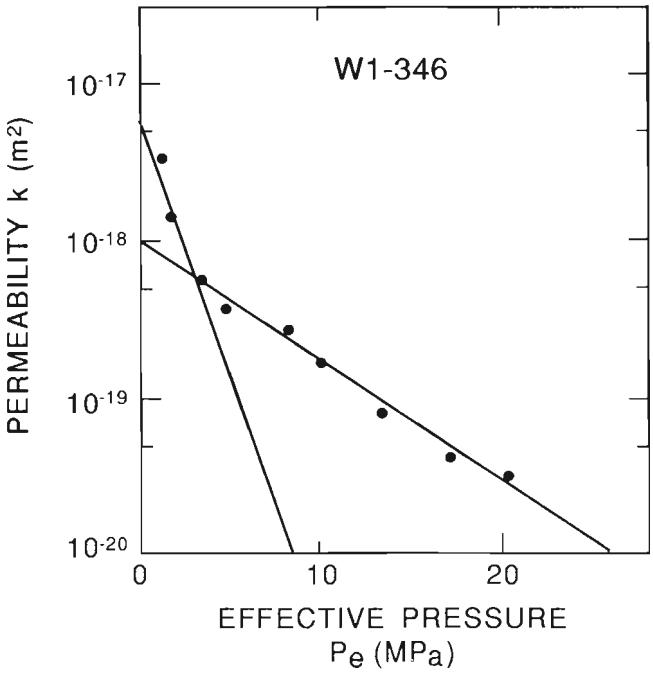

Figure 2. Permeability-stress (k-Pe) relationship (Annor, 1986) for a granite sample (W-346) consisting of two exponential curves.

it has been indicated that all of these shale samples are from overpressured zones (Katsube et al., 1991; Katsube and Best, 1992). Therefore, it is suggested that the in situ overpressure added to the hydrostatic pore pressure has reduced the effective stress on the shales, thus causing P_{e12} values to be smaller than the P_{eh} values. Results of further studies on the overpressure effects can be found elsewhere (Best and Katsube, 1993).

THREE SEGMENT k-P_e CURVE INTERPRETATION

Another typical example of the permeability-stress (k-P_e) relationship is displayed in Figure 3, for sample B-5. In this case, the curve comprises three exponential curves, with two transitional stresses, P_{e12} and P_{e23}. The third curve represents the range for the largest values of P_e, and is expressed by

$$\text{Curve \#3:} \quad k = k_{03}\exp(-\alpha_3 P_e), \tag{8}$$

P_{e23} representing the intersection between curves #2 and #3. The same method, used to determine P_{e12}, is used to determine P_{e23}. That is by replacing k_{01}, k_{02}, α_1 and α_2 in equation 5 with k_{02}, k_{03}, α_2 and α_3 (Fig. 4):

$$P_{e23} = \ln(k_{02}/k_{03}) / (\alpha_3 - \alpha_2). \tag{9}$$

Table 5a. Pressure regime for the shale and granite samples.

Sample	h	N	P_{em}	P_h	P_l	P_{eh}	P_{e12}	P_{e23}
W-346	0.35	9	1.4-20.7	3.4	9.0	5.6	4.1±2	
CHM-1	0	22	2-175	0	0	0	-	49.3
V-1	4.70	4	2.5-40	51.2	111.4	60.2	10-40	
V-2	4.70	3	10-30	51.2	111.4	60.2		
V-3	4.92	13	2.8-60	53.6	116.6	63.0	34.±1	
V-4	4.96	5	5-40	54.0	117.0	63.0		
V-5	5.12	3	10-30	55.8	121.3	65.5		
V-6	5.13	18	3.5-20	55.8	121.3	65.5	<5.0	
V-7	5.27	14	2.5-60	57.4	124.9	67.5	24.±4	
V-8	5.27	5	10-60	57.4	124.9	67.5	10-20	
V-9	5.55	8	10-40	60.4	131.5	71.1		
V-10	5.57	5	2.5-60	60.7	132.0	71.3		
B-5	3.76	16	10-100	39.5	94.0	54.5	15.3-15.4	44.3-48.7
B-9	2.44	19	2.5-100	25.6	61.0	35.4	18.5-24.6	48.8-63.0
Units	km		MPa	MPa	MPa	MPa	MPa	MPa

h = True vertical depth
N = Number of data points
P_{em} = Effective stress used for measurement
P_h = Hydrostatic stress
P_l = Lithostatic stress
P_{eh} = Effective stress - hydrostatic: $P_{eh} = P_l - P_h$
P_{e12} = Transitional stress between curves 1 and 2
P_{e23} = Transitional stress between curves 2 and 3

The results of interpretation for the only two samples (B-5 and B-9) showing a second transitional point are listed in Table 4.

Although the data for these two samples have been interpreted to represent a three-segment curve, the accuracy of the interpretation must be taken into consideration, since the transitional points are not always very distinct. Therefore, results for different interpretations, such as for one, two and three segment cases are all listed in Table 4.

The reason for the existence of a second transitional point (P_{e23}) is not known at this time. However, it may be related to the effective stress (P_{eh}) without the overpressure, since the two values are similar (Table 5a). This is supported by the fact that the data for sample B-9 show somewhat similar results (Table 5a). The relationship between P_{23} and P_{eh} are shown in Figure 5 for four samples (W-346, CHM-1, B-5, and B-9). The value of P_{e23} is represented by P_{e12} for sample W-346, since this sample is not overpressured. The data for CHM-1 are interpreted to consist of three segments with the first segment missing, since the sample was taken from the

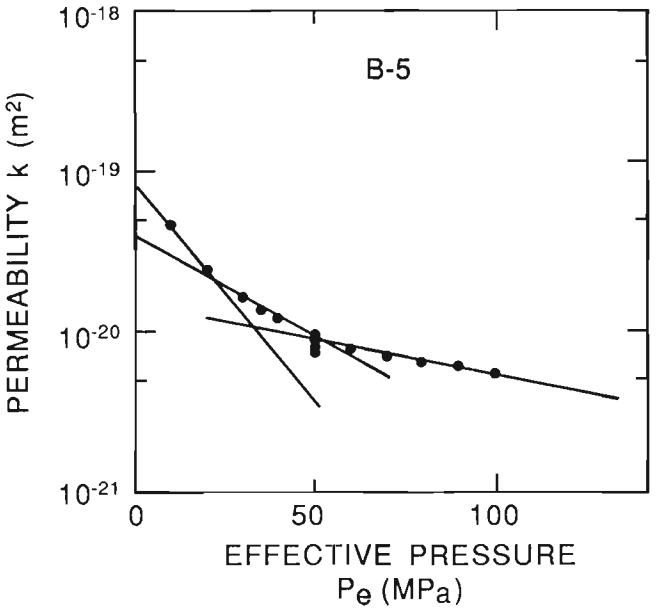

Figure 3. Typical example of the permeability-stress (k-P_e) relationship (shale sample B-5) consisting of three exponential curves.

Table 5b. Values used to calculate or represent hydrostatic (P_h) and lithostatic (P_l) stresses.

Rock Types	Series	γ_w	γ_r	P_h	P_l
Granites	W, CH	997	2630*	9.78	25.8
Shales	V	1110*	-	10.9	23.7*
Shales	B	1070**	-	10.5	25.0**
Units		kg/m³	kg/m³	MPa/km	MPa/km

W = Canadian Shield
CH = Chelmsford
V = Venture Gas Field, offshore Nova Scotia
B = Beaufort-Mackenzie basin
γ_w = Density values used for ground or sea water
γ_r = Bulk density of rocks
\+ = From Annor and Jackson (1987)
* = From Best and Katsube (1993)
** = From Issler (Pers. Comm., 1993)

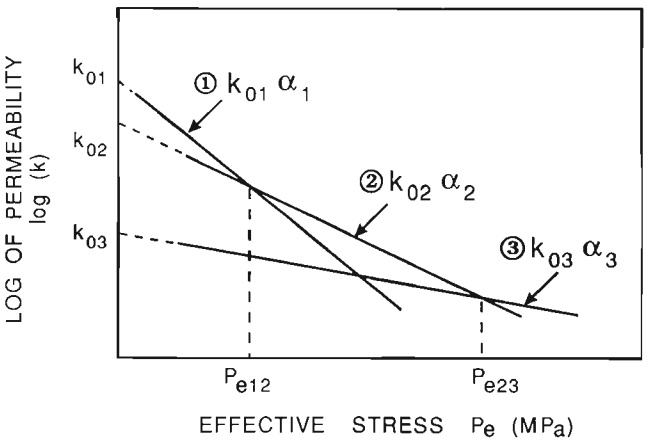

Figure 4. The relationship between the coefficients k_{01},k_{02}, k_{03}, α_1, α_2, α_3 and the transitional points P_{e12}, P_{e23} for the three exponential curves 1, 2 and 3.

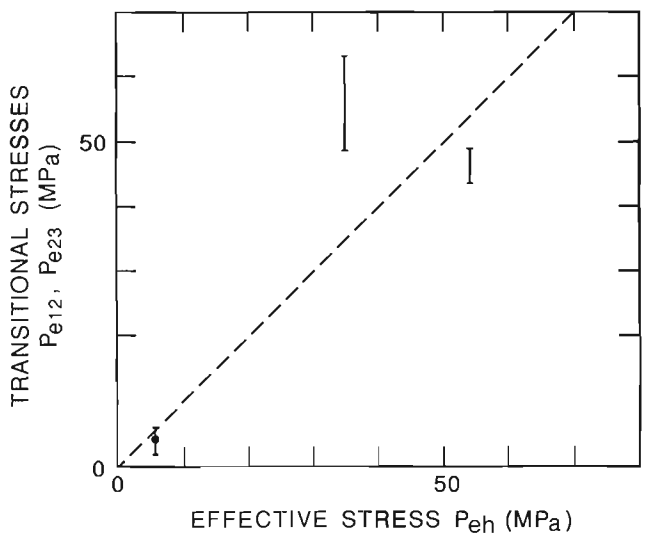

Figure 5. Relationship between the second transitional stress (P_{e23}) and the effective stress (P_{eh}) for four samples (W-346, CHM-1, B-5 and B-9). The value of P_{e23} is represented by P_{e12} for sample W-346, since the sample is not from an overpressured zone. The value of P_{e12} for Sample CHM-1, for which no value is listed in Tables 4 and 5a, is interpreted to be 0 since the sample is from the surface. The broken line represents $P_{e12} = P_{eh}$, or $P_{e23} = P_{eh}$.

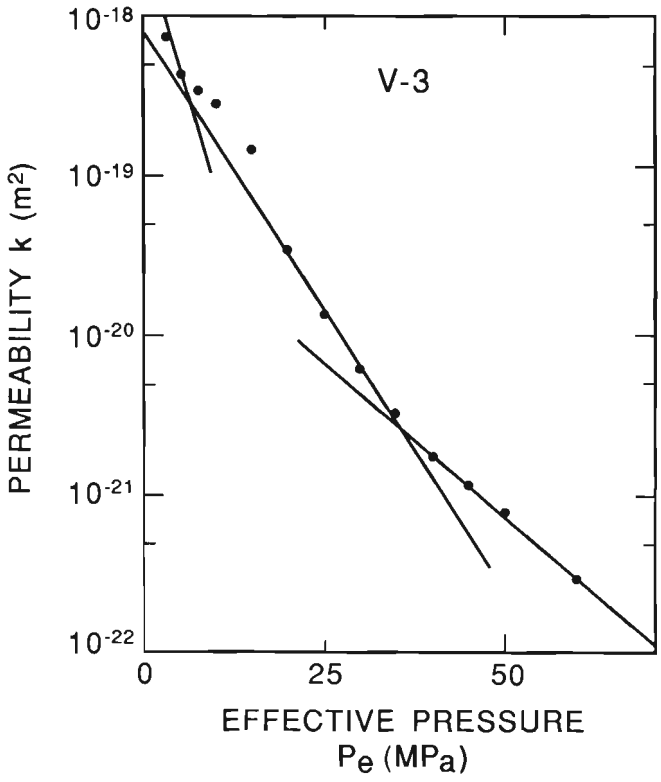

Figure 6. Permeability-stress (k-P_e) relationship for shale Sample V-3.

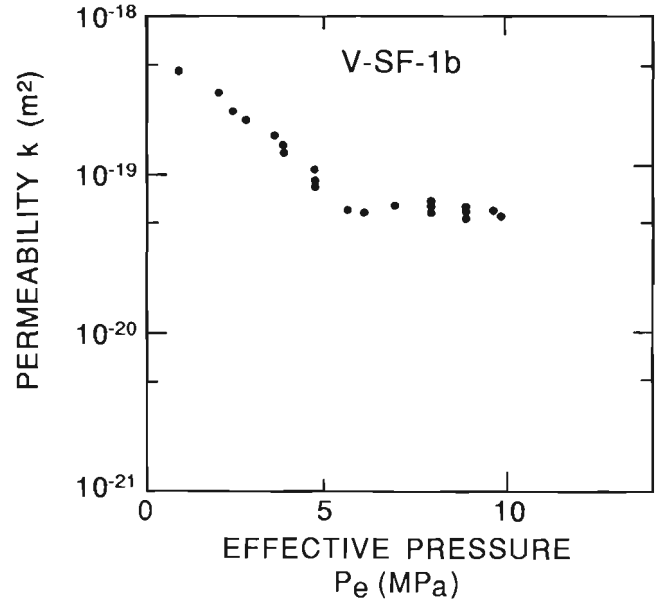

Figure 7. Permeability-stress (k-P_e) relationship for an unconsolidated mud sample (V-SF-1) from the ocean floor, offshore Nova Scotia.

surface. Therefore, transitional stress (P_{et}) of this sample is interpreted to be P_{e23} (Tables 4 and 5a) instead of P_{e12}, for this reason.

The permeability-stress (k-P_e) relationship for sample V-3 is displayed in Figure 6. Although these data have been interpreted to represent a two-segment curve (Table 4), there are indications that another curve might exist in the range for small values of P_e. This possibility may seem remote if considering Figure 6 in isolation. However, as shown in Figure 7 for an unconsolidated mud sample from the ocean floor, a transitional point does exist at a pressure (about 5 MPa) well below the P_{et} and P_{eh} values of these shales (Table 5a). The reason for the existence of this transitional point cannot be satisfied by previous explanations, since this sample has not undergone overburden stresses in the past, and is being compacted for the first time in this experiment. This transitional point is probably where the constituent clay, silt or sand grains are approaching a situation where they make contact.

DISCUSSION AND CONCLUSIONS

There is sufficient evidence, in these permeability-stress (k-P_e) data sets, to suggest that the k-P_e relationship consists of at least two exponential curves. The two granite and eight shale samples used in this study support this suggestion. The four shale samples that have been interpreted to consist only of a single exponential curve, do not have enough data points to support a multiple-curve system. Only two shale samples have shown evidence of a three curve system. However, these are the only two shale samples with data above an effective stress (P_e) of 60 MPa. One of the granite samples (CHM-1) has data up to 175 MPa, but has shown evidence of only two exponential curves. However, this is the only sample taken from near surface, suggesting that the two observed curves are actually the second and third curve segments of this data. The reason for this will be explained later. Therefore, it is proposed that the k-P_e relationship, seen in the experimental data obtained from laboratory measurements, consists of at least three exponential curves.

In this three-curve system, previous work (Walsh, 1965; Brace, 1965; Annor and Katsube, 1983; Katsube and Mareschal, 1993) provides sufficient reasons to believe that the first curve (smallest P_e values) represents the restoring of pores that were widened as a result of stress release. Samples taken at depth would expand when brought to the surface, because of stress release. The same work provides similar reasons to believe that the third curve (largest P_e values) represents the reduction of pore sizes as a result of increasing effective stress (P_e). However, new explanations are offered for the second curve observed in this study. In the case of the granites, it is proposed that it represents the compacting of deposits in pores that were widened as a result of the rock body being uplifted to the surface. In the case of the shales, it is proposed that the second curve represents also the compacting of deposits in widened pores, but in this case, it is widening which resulted from overpressure that developed subsequent to compaction at higher effective stresses. That is, the excess pore pressure that subsequently developed forced open the pores that were once closed as a result of compaction.

This study suggests that the k-P_e relationship contains historical information of the sample. While the first curve of the three-curve system represents a man-made event, the second and third contain significant geological and petrophysical information of the sample's history. The third curve would provide the necessary information to predict the pore pressure history, when reconstructing the hydrocarbon charging histories of a sedimentary basin. If uplifts and past overpressure events were to be considered, the second curve may also provide important information. However, this study indicates, that the main difficulty in the interpretation and analysis of the k-P_e data is in how to determine which section of the data represents the second or third curve (as defined in this paper).

ACKNOWLEDGMENTS

The authors are grateful to M. Williamson (AGC) and M. Best for their support, direction and advice provided to this study, and for making the arrangements to supply the unconsolidated sample (V-SF-1) and the Beaufort-Mackenzie Basin samples (B-5 and B-9). The authors sincerely thank L.D. Dyke (GSC, Ottawa) for critically reviewing this paper and for his encouraging comments.

REFERENCES

Annor, A.
1986: The effects of pressure and temperature on the permeability and porosity of selected crystalline rock samples; CANMET (Canada Centre for Mineral and Energy Technology) Report, M&ET/MRL 86-8, 290 p.

Annor, A. and Katsube, T.J.
1983: Nonlinear elastic characteristics of granite rock samples from Lac du Bonnet batholith; in Current Research, Part A; Geological Survey of Canada, Paper 83-1A, p. 411-416.

Best, M.E. and Katsube, T.J.
1993: Possible effect of overpressure on shale permeabilities; in Society of Exploration Geophysicists Expanded Abstracts with Biographies, 1993 Technical Program, 63rd Annual Meeting and International Exhibition, p. 1237-1240.

Brace, W.F.
1965: Some new measurements of linear compressibility of rocks; Journal of Geophysical Research, v. 70, p. 391-398.

Brace, W.F., Walsh, J.B., and Frangos, W.T.
1968: Permeability of granite under high pressure; Journal of Geophysical Research, v. 73, p. 2225-2236.

Coyner, K.
1993: New laboratory measurements of permeability and resistivity for crystalline rocks; Summary Ph.D. Thesis, Massachusetts Institute of Technology, U.S.A., p. 32.

Coyner, K., Katsube, T.J., Best, M.E., and Williamson, M.
1993: Gas and water permeability of tight shales from the Venture Gas Field offshore Nova Scotia; in Current Research, Part D; Geological Survey of Canada, Paper 93-1D, p. 129-136.

Davis, J.C.
1986: Statistics and data analysis in geology; John Wiley & Sons, p. 200-204.

IRAS
1992: Industry Research Associates Scheme; Hydrocarbon Charge Modelling Project, Newsletter, v. 3, December 1992.
1993: Industry Research Associates Scheme; Hydrocarbon Charge Modelling Project, Newsletter, v. 4, June 1993.

Katsube, T.J. and Agterberg, F.P.
1990: Use of statistical methods to extract significant information from scattered data in petrophysics; in Statistical Applications in the Earth Sciences, (ed.) F.P. Agterberg and G.F. Bonham-Carter; Geological Survey of Canada, Paper 89-9, p. 263-270.

Katsube, T.J. and Best, M.E.
1992: Pore structure of shales from the Beaufort-MacKenzie Basin, Northwest Territories; in Current Research, Part E; Geological Survey of Canada, Paper 92-1E, p. 157-162.

Katsube, T.J. and Mareschal, M.
1993: Petrophysical model of deep electrical conductors; Graphite lining as a source and its disconnection due to uplift; Journal of Geophysical Research, v. 98, B5, p. 8019-8030.

Katsube, T.J. and Williamson, M.A.
1994: Petrophysical studies of shales for hydrocarbon charge modelling and resource evaluation; in Current Research 1994-D; Geological Survey of Canada.
in press: Effect of diagenesis on shale nano-pore structure and implications for sealing capacity; presented at the Conference on Diagenesis, Overpressure and Reservoir Quality, Cambridge, U.K., 25-26 March 1993.

Katsube, T.J., Best, M.E., and Mudford, B.S.
1991: Petrophysical characteristics of shales from the Scotian shelf; Geophysics, v. 56, p. 1681-1689.

Katsube, T.J., Murphy, T.B., Best, M.E., and Mudford, B.S.
1990: Pore structure characteristics of low permeability shales from deep formations; in Proceedings of the 1990 Society of Core Analysts, 4th Annual Technical Conference, August, 1990, Dallas, Texas, SCA-9010, p. 1-21.

Morrow, C., Shi, L., and Byerlee, J.
1984: Permeability of fault gauge under confining pressure and shear stress; Journal of Geophysical Research, v. 89, p. 3193-3200.

Mudford, B.S.
1988: Modelling the occurrence of overpressures on the Scotian Shelf, offshore Eastern Canada; Journal of Geophysical Research, v. 93, p. 7845-7855.

Mudford, B.S. and Best, M.E.
1989: Venture Gas Field, offshore Nova Scotia; case study of over- pressuring in region of low sedimentation rate; American Association of Petroleum Geologists Bulletin, v. 73, p. 1383-1396.

Mudford, B.S., Gradstein, F.M., Katsube, T.J., and Best, M.E
1991: Modelling 1 D compaction - driven flow in sedimentary basins; a comparison of the Scotian Shelf, North Sea and Gulf Coast; in Petroleum Migration, (ed.) W.A. England and A.J. Fleet; Geological Society Special Publication, No 59, The Geological Society, London, p. 65-85.

Shi, Y. and Wang, C-y.
1986: Pore pressure generation in sedimentary basins; overloading versus aquathermal; Journal of Geophysical Research, v. 91, p. 2153-2162.

Walsh, J.B.
1965: The effect of cracks on the compressibility of rock; Journal of Geophysical Research, v. 70(2), p. 381-389.

Williamson, M.A.
1992: The subsidence, compaction, thermal and maturation history of the Egret Member source rock, Jeanne D'Arc Basin, offshore Newfoundland; Bulletin of Canadian Petroleum Geology, v. 40, no. 2, p. 136-150.

Williamson, M.A. and Smyth, C.
1992: Timing of gas and overpressure generation in the Sable Basin offshore Nova Scotia; Bulletin of Canadian Petroleum Geology, v. 40, no. 2, p. 151-169.

Geological Survey of Canada Project 870057

Shale petrophysics and basin charge modelling

T.J. Katsube, and M. Williamson[1]
Mineral Resources Division

Katsube, T.J. and Williamson, M., 1994: Shale petrophysics and basin charge modelling; in Current Research 1994-D; Geological Survey of Canada, p. 179-188.

Abstract: Hydrocarbon charge models developed for Canadian frontier basins involve reconstruction of basin sealing histories as partial control on petroleum migration and distribution. Accurate information on permeability mechanisms in muds during their transformation to shales are key to understanding seal development. Difficulties exist in obtaining the required information from permeability-stress measurements. Therefore, various petrophysical studies are underway for the resolution.

These studies target the Critical Depth of Burial, diagenetic processes, pore structure evolution and connectivity, effect of subsidence rates and geochemical balance as being concepts of importance.

Permeability and porosity decrease with burial depth is rapid as muds approach maximum compaction at the Critical Depth of burial (2.4-3.2 km), but subsequently level off. Shale pore throats are reduced to nano-pores (3 to 14 nm) at the Critical Depth of burial, resulting in extremely low permeabilities. Rapid subsidence, however, delays this process. Geochemical balance links evolution of geochemical and petrophysical processes.

Résumé : Afin d'établir des modèles du remplissage des réservoirs d'hydrocarbures dans les bassins des régions pionnières du Canada, il faut d'abord reconstituer l'évolution de l'étanchéité dans les bassins, qui a contrôlé en partie la migration et la répartition des hydrocarbures. Il est essentiel d'obtenir des renseignements précis sur les mécanismes de perméabilité dans les boues au cours de leur transformation en shales afin de comprendre le développement de couches étanches. La cueillette des renseignements requis à partir des mesures de perméabilité-contrainte présente certaines difficultés. Par conséquent, diverses études pétrophysiques sont en cours afin de résoudre ces problèmes.

Ces études portent sur des concepts importants, à savoir la profondeur critique d'enfouissement, les processus diagénétiques, l'évolution et la connexion des pores, les effets de la vitesse de subsidence et le bilan géochimique.

La réduction de la perméabilité et de la porosité en fonction de la profondeur d'enfouissement est rapide au fur et à mesure que les boues s'approchent de leur compaction maximale à la profondeur d'enfouissement critique (2,4-3,2 km); elle se stabilise par la suite. Les pores du shale deviennent plus petits, passant à des nanopores (entre 3 et 14 nm) à la profondeur critique d'enfouissement, ce qui produit des perméabilités extrêmement faibles. Toutefois, la subsidence rapide retarde le processus. Le bilan géochimique relie l'évolution des processus géochimiques et pétrophysiques.

[1] Atlantic Geoscience Centre, Dartmouth

INTRODUCTION

Petrophysical studies of shales are being carried out to provide information for hydrocarbon charge models being developed for Canadian east coast frontier basins (Williamson, 1992; Williamson and Smyth, 1992; IRAS, 1992, 1993). Quantitative understanding of geological uncertainty is essential when reconstructing the histories of deposition, burial, compaction, temperature, pressure, and hydrocarbon generation/expulsion during development of sedimentary basins. Reduction of uncertainties through ancillary sensitivity studies builds confidence in basin analysis models of use to the petroleum industry for resource evaluation and prospect ranking. Therefore, this modelling activity requires information of the highest quality on the change in petrophysical characteristics of muds as they are transformed into shale (which commonly form the basinal seals) with increasing depth of burial (Mudford, 1988; Mudford and Best, 1989; Williamson, 1992; Williamson and Smyth, 1992).

Although there is abundant petrophysical information for reservoir rocks, such as sandstones and carbonate rocks, there is an absence of similar information for shales (Mudford and Best, 1989). The main objective of this study is to fill this information gap. However, there exist numerous problems in the obtaining of reliable petrophysical data on shales, because their permeabilities are extremely low and their pore structure differs considerably (Katsube et al., 1990, 1991, 1992b) from that of reservoir rocks. These problems exist in measurement, analysis and data interpretation. The purpose of this paper is to provide a brief overview of the current state of knowledge on shale petrophysical properties, and to outline some of the studies (e.g., Katsube et al., 1990, 1991, 1992a,b; Katsube and Best, 1992; Katsube and Issler, in prep.; Katsube, 1992, 1993; Coyner et al., 1993; Loman et al., 1993) underway to obtain the required information. These studies have caused expertise to develop for acquiring petrophysical information for extremely low permeability and porosity rocks, and for synthesis of specialized data produced by various specialists.

HYDROCARBON CHARGE MODELLING AND RESOURCE EVALUATION

The modelling project

A major collaborative research effort, with participation from industry, universities and other government departments, termed the Hydrocarbon Charge Modelling Project (HCMP), is underway (IRAS, 1992, 1993; Williamson, 1992; Williamson and Smyth, 1992) to develop predictive models that can assess the geological risk and uncertainty associated with hydrocarbon resource evaluation. This project is co-ordinated by the Atlantic Geoscience Centre (AGC, Dartmouth, Nova Scotia) of the Geological Survey of Canada (GSC), and is developing and applying quantitative basin analysis-numerical simulation techniques to an extensive seismic and well data set from Canada's east coast offshore basins. Through an inter-disciplinary approach, the project aims to quantify the geological, physical and chemical dynamics that controlled the distribution of hydrocarbons. The project encompasses research activities ranging from molecular scale (e.g. source rock activation energies and rate of kerogen breakdown) to crustal scale processes (e.g. timing and influence of crustal geodynamics, basin creation and rifting-induced thermal perturbations). Translation of the results of these activities into a comprehensive, quantitative, practical set of information is intended to form a solid scientific base that will assist exploration and production professionals in their efforts to find and produce hydrocarbons offshore eastern Canada.

The Hydrocarbon Charge Modelling Project has access to industry seismic data (over 1 million line kilometres of seismic, much of it in digital form) together with a comprehensive link to geological, engineering and petrophysical data sets from over 300 offshore wells. The project also draws upon over four decades of petroleum geoscience research at the Atlantic Geoscience Centre that have produced comprehensive basinal syntheses and atlases (Keen and Williams, 1990). In addition, access to high quality, powerful UNIX based work stations and associated interpretive software (e.g. Landmark, BasinMod etc.) allows AGC to perform much of this research on a par with industry.

An emphasis of this research activity is the detailed evaluation and analytic examination of the numerous assumptions commonly used in developing basin models and charge assessments. This includes, for example, specific research activities that obtain kerogen kinetic parameters/activation energies specific to the source rocks encountered in basins of interest. Basic research is being performed on fluid transmissive histories of faults, and the sequence stratigraphic review of the Cenozoic wedge of sediments in the basins. The latter particularly seems to control some of the basin's later formation pore pressure histories. The results of this research, when combined with Canadian east coast case studies, allow us to significantly reduce the geological risk and uncertainty associated with our predictive models of resource distribution. As a result of this research, we are able not only to provide case history studies of Canadian frontier basins, but also generic research products for world-wide use. Therefore, broad and significant collaborative support from industry and other organizations exists and is encouraged.

One of the original examples of the targeted research initiatives by the AGC was the development, together with the GSC's Mineral Resources Division (MRD), of research activities to obtain basic information on petrophysical properties of basinal shale seals, particularly the evolution of these properties with compaction and diagenesis. This initiative was driven by the need for such information for use in pore pressure numerical simulation programs. This petrophysical research activity has now developed into activities on a number of fronts which are described in this paper.

Requirements for the modelling activity

Information on pore pressure history for formations forming seals is required when reconstructing the hydrocarbon charge histories of sedimentary basins. Excess pressure developments and their timing are important for hydrocarbon migration in sedimentary basins (Fig. 1). Such information is obtained from the permeability history of the formations

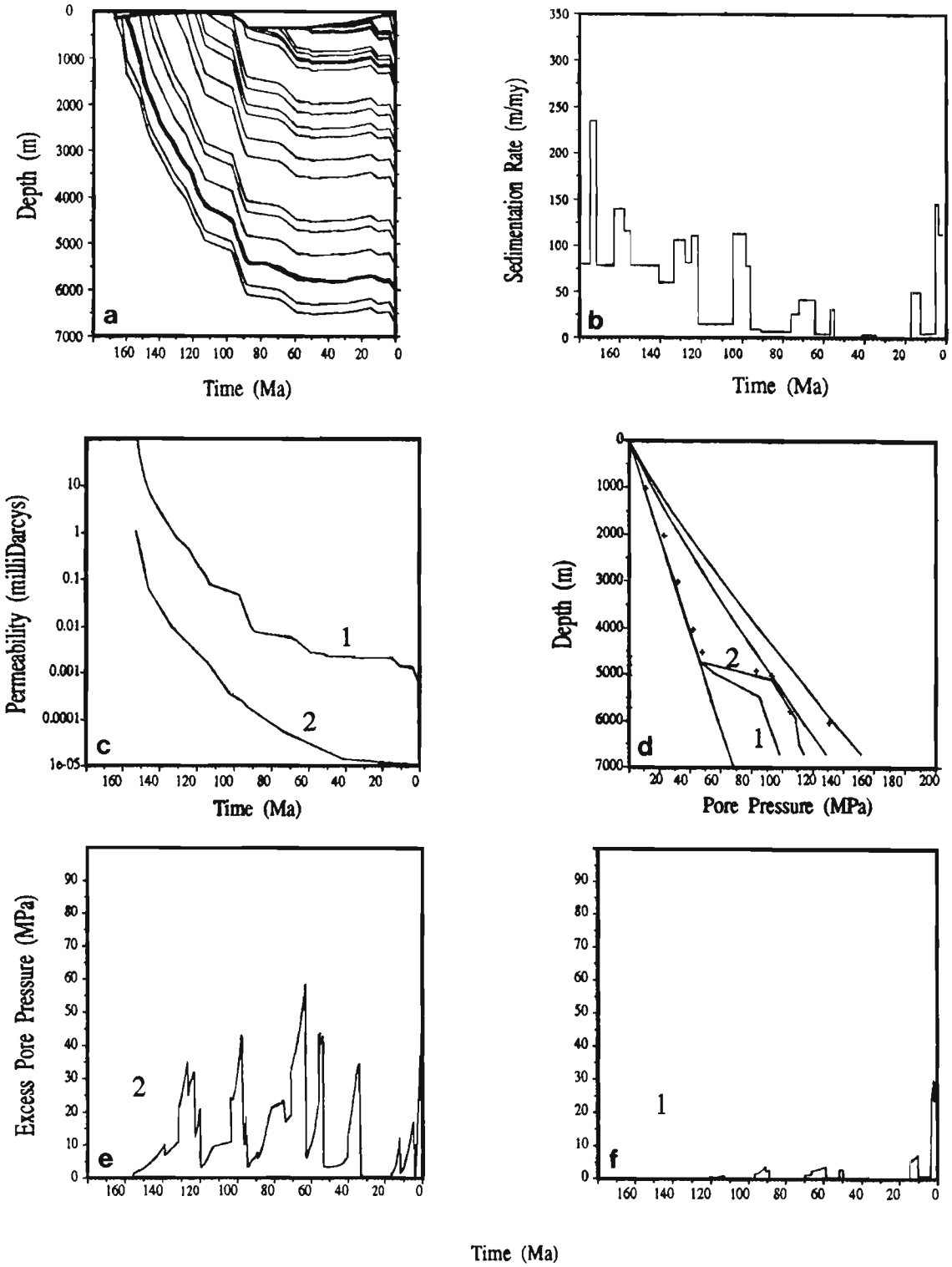

Figure 1. *Compaction corrected subsidence history (Williamson, 1992; Katsube and Williamson, 1993) for the Venture B-43 well, Venture Gas Field. (a) Compaction corrected burial history curve, bold line representing datum within the Jurassic Mic Mac Formation. (b) Sedimentation rate. (c) Model assumed permeability-time profiles (1 and 2). (d) Model predicted present day pore pressure-depth profiles (asterixes indicate actual measurements). (e) Modelled excess pressure-time profile for the 152 Ma datum, assuming curve 2 permeability profile. (f) Modelled excess pressure-time profile for the same datum, assuming curve 1 permeability profile.*

(Williamson, 1992; Williamson and Smyth, 1992). Currently for the Canadian east coast basins, that information (permeability-time curves) is derived indirectly from porosity-depth data being inserted into permeability-porosity equations (Williamson, 1992; Williamson and Smyth, 1992). The resulting permeabilities are verified by current day permeability values obtained from experimental measurements on shale samples from these formations. Figure 1 shows the effect of differing permeability-time assumptions on modelled excess pressure-time curves.

Confidence in the accuracy of the permeability-time curves may be increased by experimental measurements. Permeability-stress measurements for consolidated shales and unconsolidated muds are underway for this purpose (Coyner et al., 1993). Various measurement problems are being overcome for extremely low permeability shales and compacted muds. However, data analysis and interpretation problems still exist, such as the question of whether the permeability-stress relationship follows an exponential or power law (Mudford et al., 1991).

Analytical studies of shale and mud permeability-stress data are of high priority for this reason. These studies accompany porosity-stress, formation factor-stress, and pore-size distribution analysis to obtain a comprehensive understanding of shale petrophysical property evolution with increased burial depth. Katsube and Coyner (1994) suggested that permeability-stress curves consist of multiple exponential curves. Possible influence of undercompaction and overpressure on pore-size distribution (Katsube and Issler, in prep.) is another important study. Different subsidence rates could affect pore interconnectivity, permeability-stress and porosity-stress relationships (Issler and Katsube, 1994). In the future, information on shale relative permeability, wettability, capillary pressure, irreducible water saturation, and temperature effects could become pertinent.

QUESTIONS REGARDING PERMEABILITY-STRESS CURVES

Permeability generally decreases with increasing effective stress. Shi and Wang (1986) expressed the permeability (k) versus effective stress (P_e) relationship empirically by a power curve, using the experimental data by Morrow et al. (1984). The same relationship for tight shales has been expressed by an exponential curve (Katsube et al., 1991). Later studies (Katsube and Coyner, 1994) favour the exponential expression for tight shales. The shale permeability-stress curve is seldom a single exponential curve; it usually consists of at least two and possibly three separate exponential curves (Fig. 2a, b). Katsube and Coyner (1994) suggested that the effective stress at the transitional point (P_{et}) between the first two curves is related to the in situ effective stress. Under increasing stress at stresses below P_{et}, these samples undergo restoration of pores widened as a result of stress release caused by their removal from in situ condition. Similarly, at stresses above P_{et}, the original pores of the sample are reduced in size. Results of previous work on permeability-stress (Annor, 1986), non-linear stress-strain and crack porosity (Walsh, 1965; Brace, 1965; Annor and Katsube, 1983; Katsube and Mareschal, 1993) have been used to provide this explanation.

However, for tight shale samples, P_{et} is usually considerably smaller (Fig. 2a, Katsube and Coyner, 1994) than the in-situ effective stress calculated using hydrostatic and lithostatic stresses. Best and Katsube (1993) showed that this is due to the actual in situ effective stress being reduced by overpressure. These results suggest that permeability-stress

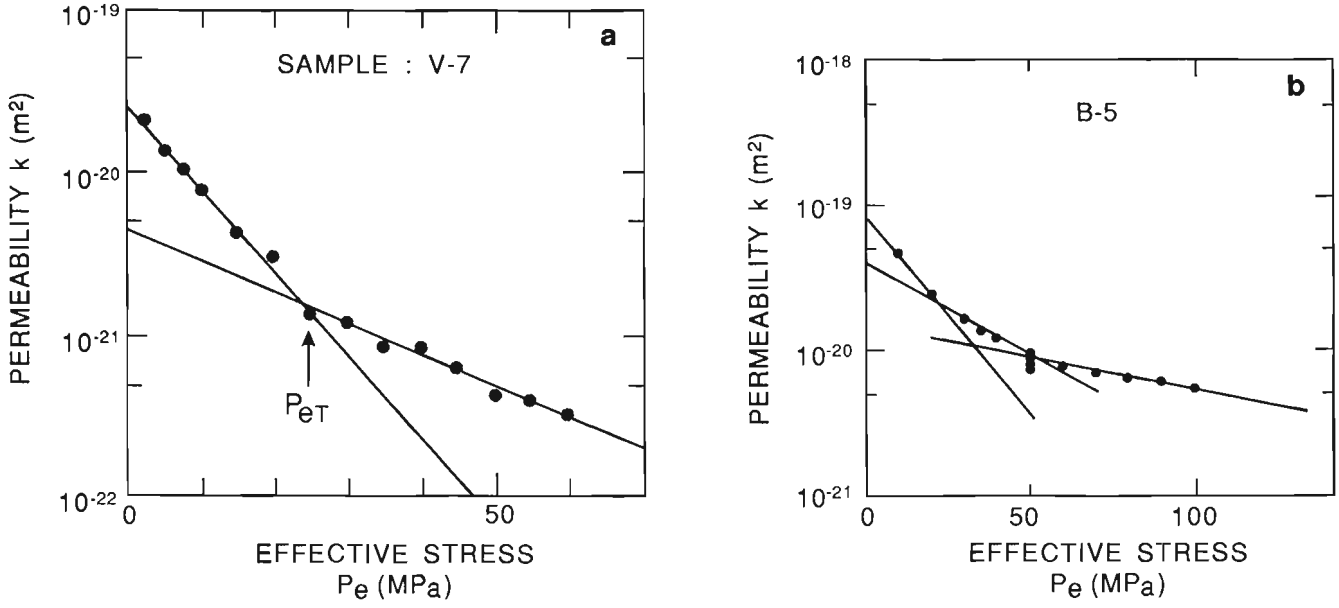

Figure 2. *Permeability (k) as a function of effective stress (P_e) for tight shale samples (Katsube and Coyner, 1994), from* ***(a)*** *Venture Gas Field, and from* ***(b)*** *the Beaufort-MacKenzie basin.*

curves reflect past historical events, and therefore, it is essential to extract the appropriate data from the complex curve system to improve accuracy and reliability of the permeability-time data.

BASIC SHALE PORE STRUCTURE AND CONNECTIVITY

Results of the petrophysical studies to date show that nano-pores, in the range of 3 to 14 nm (Fig. 3), constitute the main pore throats (Katsube et al., 1990, 1991, 1992b) or fluid flow paths of tight shales, and are the reason for extremely low shale permeabilities of 10^{-22}-$2x10^{-20}$ m^2 (Katsube et al., 1991; Coyner et al., 1993). These nano-pores are characterized by unimodal distributions (Fig. 3) of 0.3-60 nm (Katsube, 1992), with mean pore-sizes or modes (d_{np}) of 2.7-11.5 nm, values representing some of the smallest known pore-sizes for rocks. Pore-sizes above 25 nm do exist but do not significantly contribute to the flow paths, although they may be part of the inter-connected pore-structure network. They are either few in number or are blind (or pocket) pores.

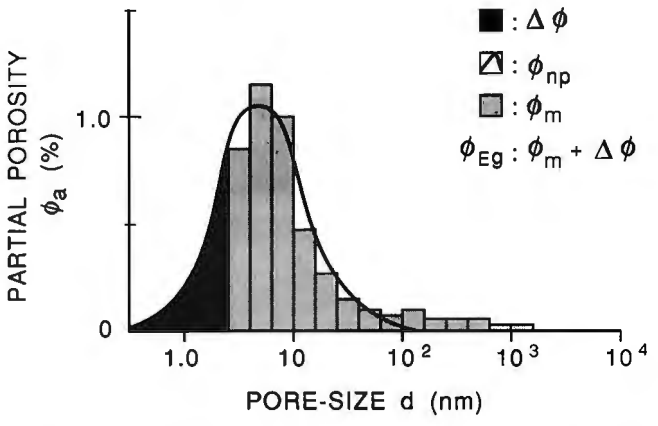

Figure 3. *Unimodal distribution of nano-pores (0.3-60 nm) characterizing tight shales (Katsube, 1992).*

Pore-size distribution analysis for a suite of tight shale samples (Katsube, 1992; Katsube et al., 1992b) has shown that their nano-pore porosities (ϕ_{np}) are 1.5-10.2%, which is about 83 ± 4% of their effective porosity (ϕ_E). There is evidence of water penetrating and being evacuated from extremely small pores of 0.3-3 nm for these shale. Analysis of the relationship between formation factor (F) and ϕ_{np} (Katsube et al., 1992a, b) for the same suite of samples has shown that these shales have two critical nano-pore porosities (Fig. 4), ϕ_{np1} and ϕ_{np2}, with values of 1.0-1.5% and about 6%, respectively. In Figure 4, ϕ_F=1/F. Above ϕ_{np2}, 50-60% of the nano-pore porosity (ϕ_{np}) is contained in interconnected paths. Between ϕ_{np1} and ϕ_{np2} that percentage is reduced, with an increase in pocket or blind pores. Below ϕ_{np1}, water or mercury may enter the rock but cannot completely flow through it.

A theoretical study of permeability calculated from pore-size distribution data (Katsube, 1993) shows agreement with experimental measurements, when using a tortuosity value of

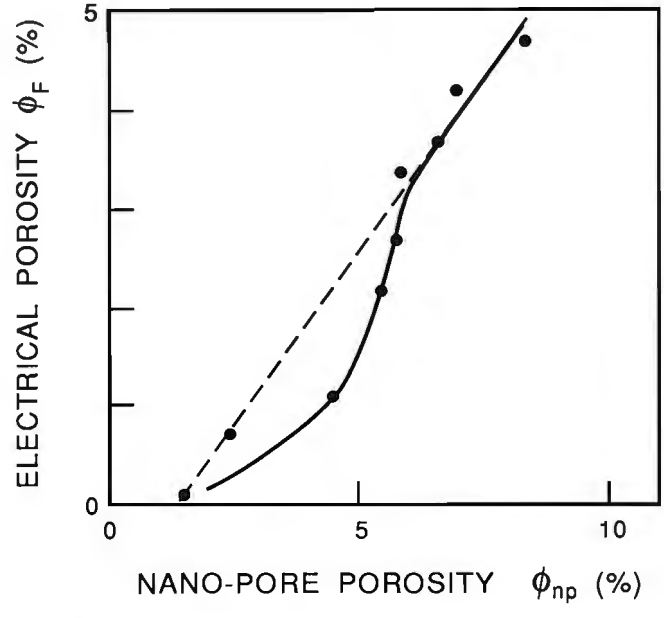

Figure 4. *Relationship between electrical porosity (ϕ_F) and nano-pore porosity (ϕ_{np}), showing the change in nano-pore interconnectivity with reduction in ϕ_{np} for a suite of tight shales (Katsube et al., 1992b).*

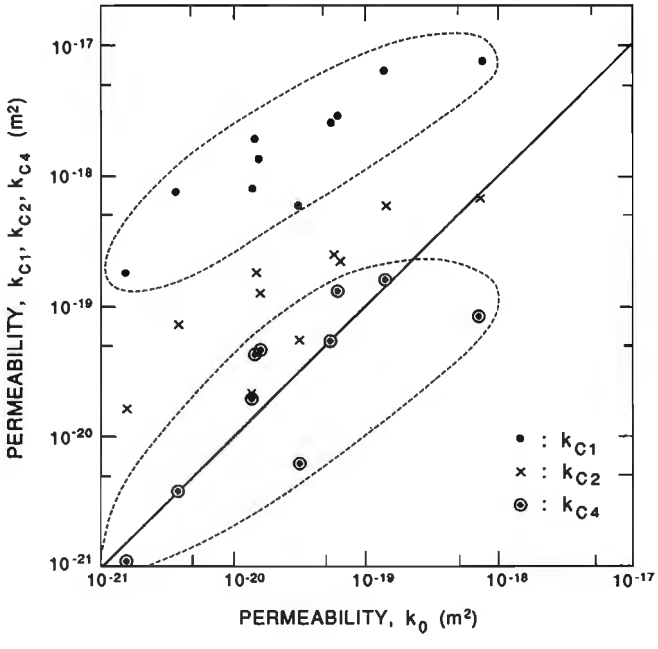

Figure 5. *Calculated permeability values versus the experimentally measured values. k_{C1} and k_{C2} represent the permeabilities for true tortuosities (τ) of 1 and 3.3. k_{C4} represents the permeabilities for τ = 3.3 and for partial porosities only above the critical partial porosity (ϕ_{acr}) of 0.39%.*

3.3 (Katsube et al., 1991) and partial porosities only above 0.39%. Partial porosity is the porosity of the pore-size ranges (e.g., 1.0 to 1.6 nm or 1.6 to 2.5 nm, see Fig. 3) constituting the pore-distribution. These results are compared with the case where a tortuosity of unity and partial porosity values for all nano-pores are used (Fig. 5). Similar results have been obtained for formation factor values (Katsube, 1993).

Petrophysical studies on tight shales have provided an insight into nano-pore interconnectivity and low permeability mechanisms in three areas: (1) water penetrates the smallest pores that are detected in these shales (Katsube, 1992), (2) the nano-pores form the main interconnected pore network and the major pore throats (Katsube et al., 1991, 1992a,b; Katsube, 1993), and (3) a critical nano-pore porosity exists, below which the availability of flow paths rapidly decrease with decreasing nano-pore porosity (Katsube et al., 1992a,b).

PORE STRUCTURE EVOLUTION (BURIAL DEPTH AND DIAGENESIS)

Burial depth

Shales have been characterized by unimodal pore-size distributions, with modes and porosities decreasing from about 120 nm and 30% at about 1000 m depth to 10-20 nm and 5-15% at greater depth (Katsube and Best, 1992; Katsube and

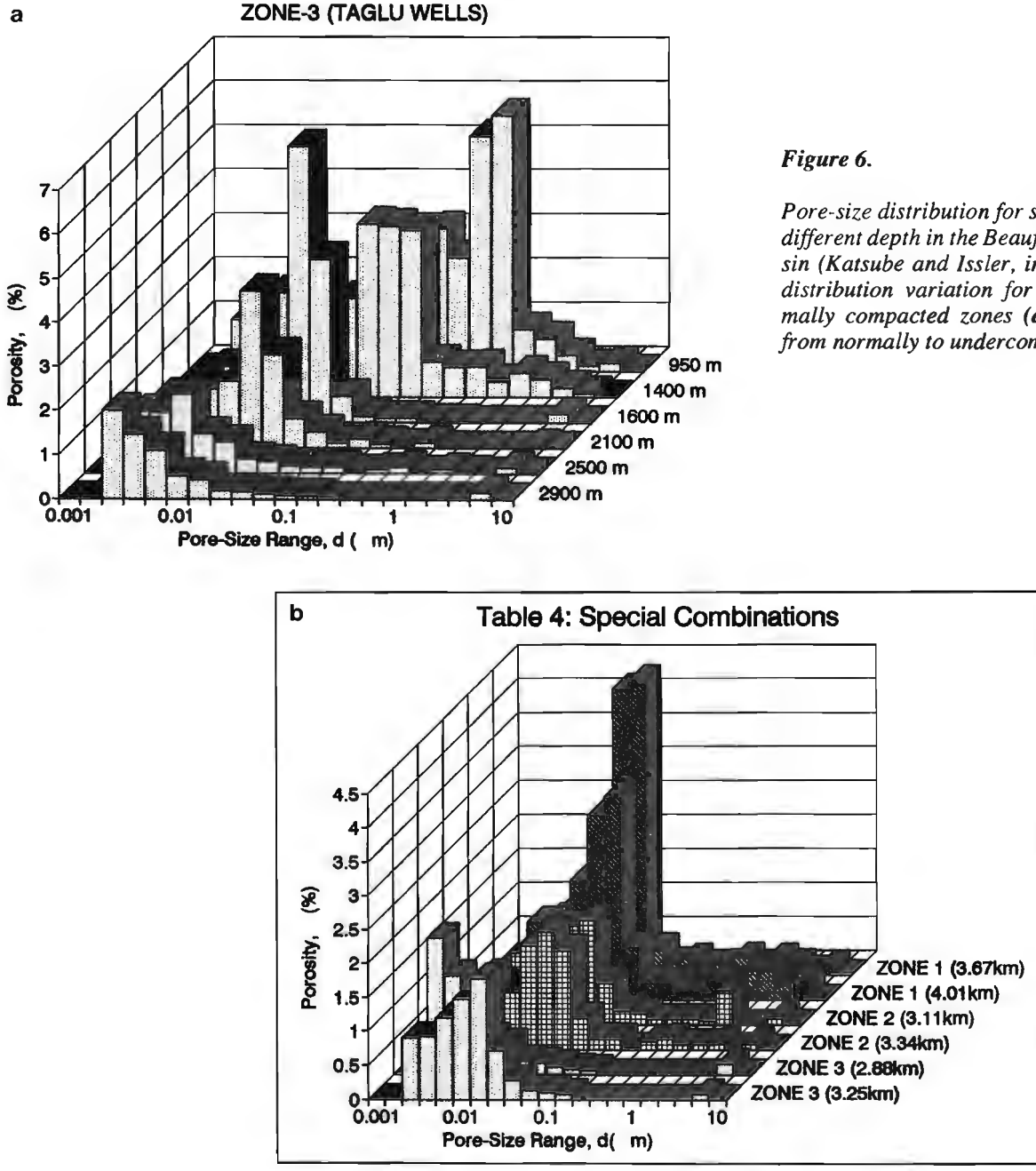

Figure 6.

Pore-size distribution for shale samples from different depth in the Beaufort-Mackenzie basin (Katsube and Issler, in prep.). Pore-size distribution variation for shales from normally compacted zones ***(a)****, and for shales from normally to undercompacted zones* ***(b)****.*

Issler, 1993) as a result of compaction (Fig. 6a). However, it has been indicated (Katsube and Issler, in prep.) that high subsidence rates tend to allow only a porosity decrease with burial, and delays the reduction of mean pore-sizes, resulting in little change in mean pore-size with depth (Fig. 6b). There are also indications that porosities of certain pore-sizes (e.g., 30 nm) show abnormal increases in overpressured zones. Considerable effort is being put into analysis of shale pore-size distribution patterns, because they likely reflect historical events during compaction.

Diagenesis

Texture analyses of a suite of tight shales (Katsube and Williamson, 1993) show that samples characterized by late-stage cementation have small effective porosities (ϕ_E) of 1.5-2.5%, with the majority of the larger pores filled with cement, and about 70-80% of the nano-pores being blocked (Katsube et al., 1992b). Samples characterized by late-stage dissolution have effective porosities of 8-12%, with contributions from larger pores. The nano-pores are thought to be associated with clay matrix minerals and microcrystalline pore-filling cement. The existence of the late dolomitic pore-filling cement has a striking effect (Katsube et al., 1992b) by blocking the nano-pores and thus reducing the values of ϕ_{np} and ϕ_E considerably. These results demonstrate the significance of diagenesis on shale pore structure.

THE CRITICAL DEPTH OF BURIAL (CDB) CONCEPT

Consolidation of muds into tight shales during burial can be divided into two stages (Katsube and Williamson, 1993) by the critical depth of burial, a depth ranging from 2.4 to 3.2 km (Fig. 7). Mechanical compaction is the main compacting mechanism in the first stage, and both mechanical compaction and diagenesis in the second. Shales seem to approach a maximum state of compaction at the critical depth of burial, with bulk densities (δ), porosities (ϕ) and permeabilities (k) ranging from 2.5-2.6 g/mL, 2.0-5.0% and $3x10^{-21}$-10^{-20} m^2, respectively (Katsube and Best, 1992; Katsube and Issler, 1993; Katsube and Coyner, 1994). At depths greater than the critical depth of burial, diagenetic phases of cementation and dissolution play a major role in determining the petrophysical characteristics of compacting shales.

Considerable effort is being made to obtain data on shale depth characteristics for permeability (k), porosity (ϕ), formation factor (F), and pore-size distribution, by k, F, ϕ as a function of pressure (P) measurements (k,F,ϕ/P) for both solid shales and unconsolidated mud samples from the ocean floor, and by pore-size distribution measurements of samples from various depths. All published and unpublished results, to date, point towards a critical depth of burial at the depth range stated above. For example, permeability for a shale sample from a depth of 2.6 km was 10^{-19} to $1.6x10^{-19}$ m^2, values approaching those from greater depths (Katsube et al., 1991; Coyner et al., 1993). Other measurements, such as those for F and ϕ (Loman et al., 1993) are also consistent with the critical depth of burial concept (Katsube and Williamson, 1993; Paxton et al., 1993).

Acquisition of information on the k/P relationship requires data from both above and below the critical depth of burial. For depths smaller than the critical depth of burial, compaction of loose sediments is the dominant consideration. For depths greater than the critical depth of burial, compaction of solid shales with different diagenetic characteristics is the dominant consideration. The petrophysical response to stress for shales of varied degrees between cementation and dissolution can vary considerably (Katsube et al., 1992b).

The expected effects of diagenesis on shale seal characteristics are shown diagrammatically in Figure 8 (Katsube and Williamson, 1993). At constant subsidence rates, shales with dissolution pores are characterized by high permeabilities that rapidly decrease. Shales with cemented pores are characterized by low permeabilities with smaller rates of decrease under compaction. This implies a reverse of permeabilities at greater depth, resulting in a tendency for an early stage excess pore pressure pulse for shales with cemented pores, and a delayed pulse for shales with dissolution pores.

THE GEOCHEMICAL BALANCE OF A SUBSIDING FORMATION

As muds of a subsiding formation are being transformed into shale, various geochemical and petrophysical events take place. In certain circumstances, fluids are forced through the formations. In others, precipitates from these fluids block the flow paths causing excessive pressure build up. These pressures can reach a level that could force fluids to flow again. Such events will be recorded in the shale petrography as remnants of various cementing and dissolution phases.

Accompanying the geochemical and textural changes with subsidence is a petrophysical evolution. A cementing phase will generally cause a reduction of permeability. However, there can be cases where porosity is reduced by cement filling the pores, and cases where porosity may be isolated but preserved by the cement. Dissolution generally can be considered to increase porosity and permeability. However, under compression, dissolution may have weakened the pore framework to the extent that fluid flow is blocked by collapsing pores (Katsube et al., 1992b). At extremely low permeability conditions, high temperatures could cause local fluid movements accompanied by dissolution and cementation.

The preceding discussion indicates close linkages between geochemical and petrophysical evolution. A cement is likely to contain foreign material if it is a result of precipitation from fluids flowing through the formation, for example, due to high permeabilities. If the cement is a result of local dissolution, an event due to low permeability, it is likely to contain only local material. This implies that the petrophysical history of a shale should be consistent with its geochemical history. Therefore, it should be possible, in principle, to verify petrophysical predictions by geochemical analysis.

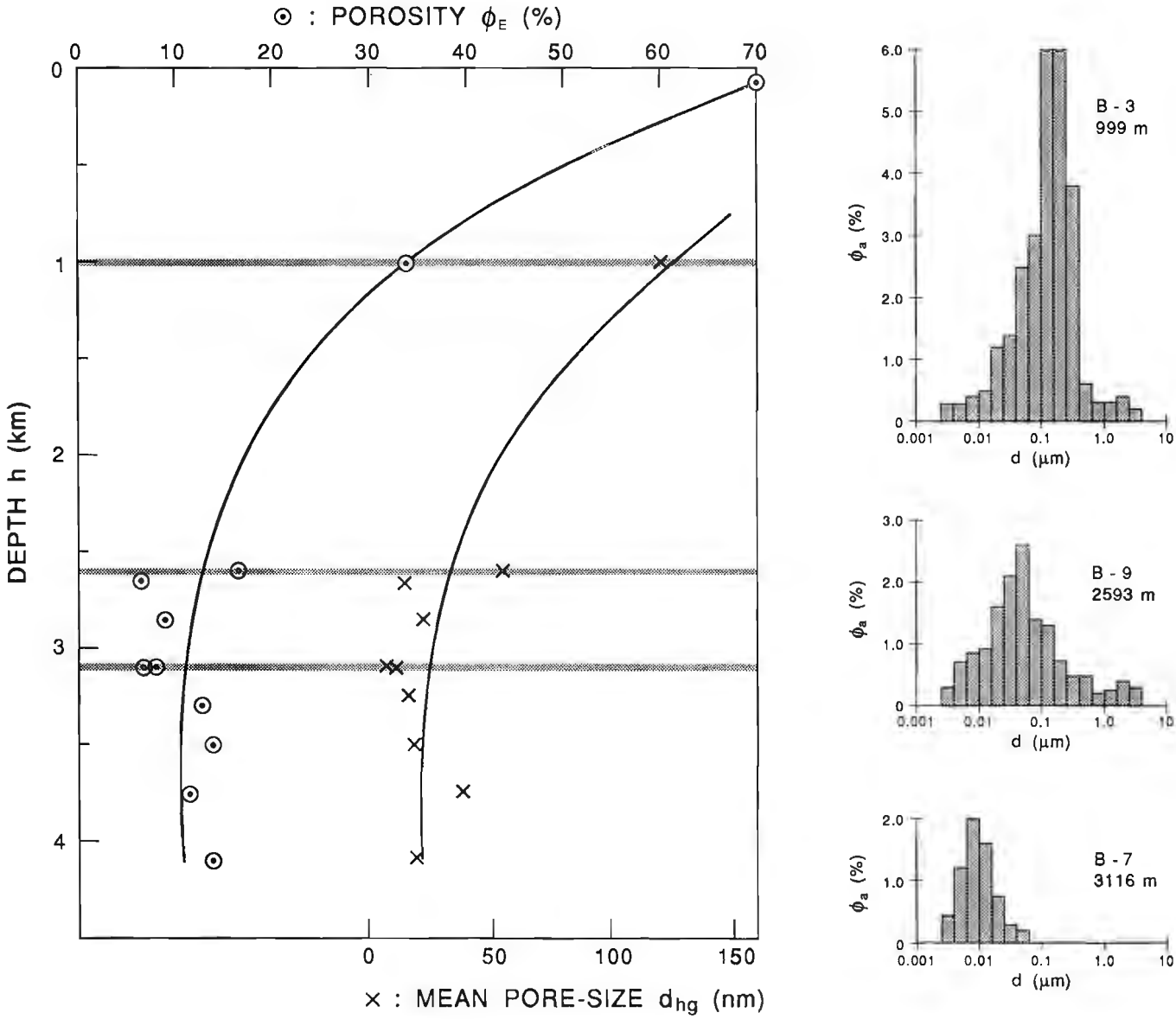

Figure 7. *Pore-size distribution variation with depth for the Beaufort-Mackenzie shale samples (Katsube and Best, 1992), showing effective porosity (ϕ_E) and mean pore-size (d_{hg}) decreasing (left-hand side) and pore-size distribution changing with increasing depth (right-hand side). The shaded lines (left-hand side) indicate sample locations for pore-size distributions displayed on*

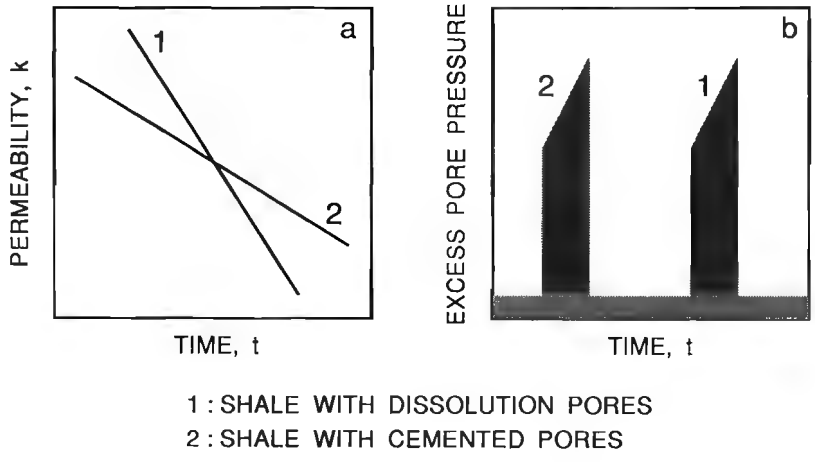

Figure 8.

*Influence of diagenesis on timing of excess pore pressure (Katsube and Williamson, 1993). (**a**) Typical curves for permeability as a function of pressure for shales with secondary dissolution pores and with cemented pores. (**b**) Excess pore pressure pulses for shales with cemented pores and with dissolution pores.*

Shale texture analyses consisting of petrographic thin section analysis (PTS), X-ray diffraction analysis (XRD) and scanning electron microscope analysis (SEM) are routinely conducted on all shale samples that are analyzed (Katsube et al., 1990, 1991, 1992b). The main focus is on determining the sequence of cementation and dissolution events that shales have undergone, and the geochemistry of the cements. One of the main objectives of this study is to develop the ability to verify predictions made on the petrophysical history or evolution of shales.

OTHER PETROPHYSICAL STUDIES

Besides the petrophysical studies already discussed, additional studies are planned or in progress that have significance for our future research efforts. Examples are shale wettability and relative permeability studies, occluded pore studies, anisotropy studies, critical permeable shale texture studies, and studies on the effect of heat on shale petrophysical characteristics.

For example, theoretical and experimental studies are being carried out to obtain shale relative permeability curves (Coyner et al., 1993). As part of this study, irreducible water saturation values in the range of 75-95% have been obtained using a high powered centrifuge. Katsube et al. (1992b) have suggested that significant amounts of occluded pores may exist in tight shales. Several tests are being carried out, including petrographic image analysis, to verify this suggestion. This information is required to understand the petrophysical history of a formation and to interpret geophysical data.

As the rock type varies from a sandstone to a shale, permeabilities show drastic changes, with variations exceeding nine orders of magnitude (Brace, 1980). Some shaly sands have permeabilities in the order of 10^{-20} m^2 or less (Katsube et al., 1991; Coyner et al., 1993), similar to a tight shale. Sandstone permeabilities are usually above 10^{-10} m^2. Therefore, questions are raised regarding the sand and clay content at which the permeability of a rock becomes extremely low. Studies are planned for obtaining answers to this question.

CONCLUSIONS

One of the most important objectives of these ongoing shale petrophysical studies is to provide accurate information on the rates and mechanisms of decreasing permeabilities in muds during their transformation to shales. This is key to understanding seal development and is information required for the hydrocarbon charge models. The problem of obtaining reliable experimental data for extremely low present day shale permeabilities has been overcome so that some of the required information is being provided. However, currently there is a problem in analysis and interpretation of the permeability-stress data which is key to understanding the permeability mechanisms of mud-shale transformation. For this reason, a wide range of petrophysical studies are being carried out. Basic shale pore structure and connectivity, pore structure evolution with burial depth and diagenesis, effect of overpressure and depth on petrophysical properties, and the geochemical balance of subsiding formations, are some of the main studies being performed.

An important finding in these studies is that extremely low permeabilities (10^{-22} to $2x10^{-20}$ m^2) are a result of shales having extremely small pore throats, in the range of 3-14 nm, some of the smallest pore-sizes reported for rocks. Another important finding is that there may be a critical depth of burial at 2.4-3.2 km, which is a transitional zone dividing the burial process into two major stages. Permeabilities and porosities rapidly decrease with burial at depths smaller than the critical depth of burial and tend to level off at greater depths. A pore structure model suggests that at depth greater than the critical depth of burial, the rate of permeability decrease varies according to the degree of cementation or dissolution of the pores, implying that shale diagenesis significantly affects the timing of excess pore pressure pulses. Although shales are characterized by unimodal pore-size distributions with mean pore-sizes decreasing with depth, rapid subsidence seems to delay the rate of decrease, suggesting that pore-size distribution patterns contain significant petrophysical history information. A "geochemical balance" concept under development is expected to link geochemical and petrophysical evolutions of subsiding formations.

ACKNOWLEDGMENTS

The authors thank M.E. Best (Pacific Geoscience Centre, Sydney, B.C.) for his valuable guidance and advice in this study. The authors also thank G. Gray and W. Shea (EXXON Production Research, U.S.A.) and S.T. Paxton (ESSO Exploration and Production, UK) for their valuable comments related to this study, and are grateful to A.C. Grant (AGC, Dartmouth) for critically reviewing this paper.

REFERENCES

Annor, A.
1986: The effects of pressure and temperature on the permeability and porosity of selected crystalline rock samples: CANMET (Canada Centre for Mineral and Energy Technology) Report, M&ET/MRL 86-8, 290 p.

Annor, A. and Katsube, T.J.
1983: Nonlinear elastic characteristics of granite rock samples from Lac du Bonnet batholith; in Current Research, Part A; Geological Survey of Canada, Paper 83-1A, p. 411-416.

Best, M.E. and Katsube, T.J.
1993: Possible effect of overpressure on shale permeabilities; in Society of Exploration Geophysicists Expanded Abstracts with Biographies, 1993 Technical Program, 63rd Annual Meeting and International Exhibition, p. 1237-1240.

Brace, W.F.
1965: Some new measurements of linear compressibility of rocks; Journal of Geophysical Research, v. 70, p. 391-398.
1980: Permeability of crystalline and argillaceous rocks; Int. J. Rock Mech. Min. Sci. & Geomech. Abstracts 17, p. 241-251.

Coyner, K., Katsube, T.J., Best, M.E., and Williamson, M.
1993: Gas and water permeability of tight shales from the Venture Gas Field offshore Nova Scotia; in Current Research, Part D; Geological Survey of Canada, Paper 93-1D, p. 129-136.

IRAS
1992: Industry Research Associates Scheme: Hydrocarbon Charge Modelling Project, Newsletter, v. 3, December 1992.
1993: Industry Research Associates Scheme: Hydrocarbon Charge Modelling Project, Newsletter, v. 4, June 1993.

Issler, D.R. and Katsube, T.J.
1994: Effective porosity of shale samples from the Beaufort-Mackenzie Basin, northern Canada; in Current Research 1994-B; Geological Survey of Canada.

Katsube, T.J.
1992: Statistical analysis of pore-size distribution data of tight shales from the Scotian Shelf; in Current Research, Part E; Geological Survey of Canada, Paper 92-1E, p. 365-372.
1993: Nano pore transport mechanism of tight shales from the Scotian Shelf; in Current Research, Part D; Geological Survey of Canada, Paper 93-1D, p. 121-127.

Katsube, T.J. and Best, M.E.
1992: Pore structure of shales from the Beaufort-MacKenzie Basin, Northwest Territories; in Current Research, Part E; Geological Survey of Canada, Paper 92-1E, p. 157-162.

Katsube, T.J. and K. Coyner, K.
1994: Determination of permeability(k)-compaction relationship from interpretation of k-stress data for shales from Eastern and Northern Canada; in Current Research 1994-D; Geological Survey of Canada.

Katsube, T.J. and Mareschal, M.
1993: Petrophysical model of deep electrical conductors; Graphite lining as a source and its disconnection due to uplift; Journal of Geophysical Research, v. 98, B5, p. 8019-8030.

Katsube, T.J. and Williamson, M.A.
1993: Effect of diagenesis on shale nano-pore structure and implications for sealing capacity; presented at the Conference on Diagenesis, Overpressure and Reservoir Quality, Cambridge, U.K., 25-26 March 1993.

Katsube, T.J., Best, M.E., and Mudford, B.S.
1991: Petrophysical characteristics of shales from the Scotian shelf; Geophysics, v. 56, p. 1681-1689.

Katsube, T.J., Murphy, T.B., Best, M.E., and Mudford, B.S.
1990: Pore structure characteristics of low permeability shales from deep formations; in Proceedings of the 1990 Society of Core Analysts 4th Annual Technical Conference, August, 1990, Dallas, Texas, SCA-9010, p. 1-21.

Katsube, T.J., Scromeda, N., and Williamson, M.
1992a: Effective porosity of tight shales from the Venture Gas Field, offshore Nova Scotia; in Current Research, Part D; Geological Survey of Canada, Paper 92-1D, p. 111-119.

Katsube, T.J., Williamson, M., and Best, M.E.
1992b: Shale pore structure evolution and its effect on permeability; in Symposium Volume III of the Thirty-Third Annual Symposium of the Society of Professional Well Log Analysts, The Society of Core Analysts Preprints, Oklahoma City, Oklahoma, June 15-17, 1992, Paper SCA-9214, p. 1-22.

Keen, M.J. and Williams, G.L.
1990: Geology of the Continental Margin of Eastern Canada, (ed.) M.J. Keen and G.L. Williams; Geological Survey of Canada, Geology of Canada no 2. (also Geological Society of America, Geology of North America Series, v. I-1, p. 853).

Loman, J.M., Katsube, T.J., Correia, J., Best, M.E., and Williamson, M.A.
1993: Effect of compaction on porosity and formation factor for tight shales from the Scotian Shelf; in Current Research, Part E; Geological Survey of Canada, Paper 93-1E, p. 331-335.

Morrow, C., Shi, L., and Byerlee, J.
1984: Permeability of fault gauge under confining pressure and shear stress; Journal of Geophysical Research, v. 89, p. 3193-3200.

Mudford, B.S.
1988: Modelling the occurrence of overpressures on the Scotian Shelf, offshore Eastern Canada; Journal of Geophysical Research, v. 93, p. 7845-7855.

Mudford, B.S. and Best, M.E.
1989: Venture Gas Field, offshore Nova Scotia; case study of over-pressuring in region of low sedimentation rate; American Association of Petroleum Geologists Bulletin, v. 73, p. 1383-1396.

Mudford, B.S., Gradstein, F.M., Katsube, T.J., and Best, M.E
1991: Modelling 1 D compaction - driven flow in sedimentary basins; a comparison of the Scotian Shelf, North Sea and Gulf Coast; in Petroleum Migration, (ed.) W.A. England and A.J. Fleet; Geological Society Special Publication, No 59, The Geological Society, London, p. 65-85.

Paxton, S.T., Nardin, T.R., Converse, D.R., and Cayley, G.T.
1993: North sea fluid pressure distribution and effects upon Brent Group reservoir quality; presented at the Conference on Diagenesis, Overpressure and Reservoir Quality of the Mineralogical Society, Cambridge (U.K.), 25-26 March 1993.

Shi, Y. and Wang, C-y.
1986: Pore pressure generation in sedimentary basins; overloading versus aquathermal; Journal of Geophysical Research, v. 91, p. 2153-2162.

Walsh, J.B.
1965: The effect of cracks on the compressibility of rock; Journal of Geophysical Research, v. 70(2), p. 381-389.

Williamson, M.A.
1992: The subsidence, compaction, thermal and maturation history of the Egret Member source rock, Jeanne D'Arc Basin, offshore Newfoundland; Bulletin of Canadian Petroleum Geology, v. 40, no. 2, p. 136-150.

Williamson, M.A. and Smyth, C
1992: Timing of gas and overpressure generation in the Sable Basin offshore Nova Scotia; Bulletin of Canadian Petroleum Geology, v. 40, no. 2, p. 151-169.

Geological Survey of Canada Projects 870057 and 920058

AUTHOR INDEX

NOTE TO CONTRIBUTORS

Submissions to the Discussion section of Current Research are welcome from both the staff of the Geological Survey of Canada and from the public. Discussions are limited to 6 double-spaced typewritten pages (about 1500 words) and are subject to review by the Chief Scientific Editor. Discussions are restricted to the scientific content of Geological Survey reports. General discussions concerning sector or government policy will not be accepted. All manuscripts must be computer word-processed on an IBM compatible system and must be submitted with a diskette using WordPerfect 5.0 or 5.1. Illustrations will be accepted only if, in the opinion of the editor, they are considered essential. In any case no redrafting will be undertaken and reproducible copy must accompany the original submissions. Discussion is limited to recent reports (not more than 2 years old) and may be in either English or French. Every effort is made to include both Discussion and Reply in the same issue. Current Research is published in January and July. Submissions should be sent to the Chief Scientific Editor, Geological Survey of Canada, 601 Booth Street, Ottawa, Canada, K1A 0E8.

AVIS AUX AUTEURS D'ARTICLES

Nous encourageons tant le personnel de la Commission géologique que le grand public à nous faire parvenir des articles destinés à la section discussion de la publication Recherches en cours. Le texte doit comprendre au plus six pages dactylographiées à double interligne (environ 1500 mots), texte qui peut faire l'objet d'un réexamen par le rédacteur scientifique en chef. Les discussions doivent se limiter au contenu scientifique des rapports de la Commission géologique. Les discussions générales sur le Secteur ou les politiques gouvernementales ne seront pas acceptées. Le texte doit être soumis à un traitement de texte informatisé par un système IBM compatible et enregistré sur disquette WordPerfect 5.0 ou 5.1. Les illustrations ne seront acceptées que dans la mesure où, selon l'opinion du rédacteur, elles seront considérées comme essentielles. Aucune retouche ne sera faite au texte et dans tous les cas, une copie qui puisse être reproduite doit accompagner le texte original. Les discussions en français ou en anglais doivent se limiter aux rapports récents (au plus de 2 ans). On s'efforcera de faire coïncider les articles destinés aux rubriques discussions et réponses dans le même numéro. La publication Recherches en cours paraît en janvier et en juillet. Les articles doivent être envoyés au rédacteur en chef scientifique, Commission géologique du Canada, 601, rue Booth, Ottawa, Canada, K1A 0E8.

Geological Survey of Canada Current Research, is released twice a year, in January and July. The four parts published in January 1994 (Current Research 1994- A to D) are listed below and can be purchased separately.

Recherches en cours, une publication de la Commission géologique du Canada, est publiée deux fois par année, en janvier et en juillet. Les quatre parties publiées en janvier 1994 (Recherches en cours 1994-A à D) sont énumérées ci-dessous et sont vendues séparément.

Part A: Cordillera and Pacific Margin
Partie A : Cordillère et marge du Pacifique

Part B: Interior Plains and Arctic Canada
Partie B : Plaines intérieures et région arctique du Canada

Part C: Canadian Shield
Partie C : Bouclier canadien

Part D: Eastern Canada and national and general programs
Partie D : Est du Canada et programmes nationaux et généraux